

**AUTOPHAGY AS A MASTER IMMUNOMETABOLIC REGULATOR IN T-CELL-MEDIATED PROTECTION AGAINST HIV-1 INFECTION**

By  
Hamza Loucif

A dissertation submitted in partial satisfaction of the requirements for the degree of  
*Philosophiae Doctor (Ph.D.) in Virology and Immunology*

**Evaluation Committee**

Committee President and  
Internal Examiner

Pr. Alain Lamarre  
INRS-Centre Armand-Frappier Santé  
Biotechnologie

External Examiner

Dr. Silvia Vidal  
Departments of Human Genetics,  
Microbiology and Immunology  
McGill University Research Centre on  
Complex Traits

External Examiner

Dr. Daniel Kaufmann  
Département de médecine, Centre de  
recherche du CHUM  
Université de Montréal

Thesis Supervisor

Dr. Julien van Grevenynghe  
INRS-Centre Armand-Frappier Santé  
Biotechnologie

## DEDICATION

To my dear and beloved parents, my father **Abdelaziz Loucif**, and my mother **Djamila Hadjaj** for their unconditional love and support.

To my precious siblings, the youngest **Aissa Loucif**, **Sara Loucif** and **Omar Loucif**.

Dedication to the loving memory of my father **Abdelaziz Loucif** (1956 – 2017).

"One never notices what has been done; one can only see what remains to be done."

"I was taught that the way of progress is neither swift nor easy."

**Marie Sklodowska Curie**



## ACKNOWLEDGMENTS

This memorable venture was accomplished thanks to many people for whom I am genuinely grateful to have in my life. My thesis supervisor, Dr. Julien van Grevenynghe, and his immeasurable support and perspicuous guidance throughout various phases of my Ph.D. project. It is your inspiration and intangible vision as a scientist that has helped develop me as a researcher. I am truly indebted to you and privileged for everything you have taught me.

I would like to especially thank the evaluation committee members; Professor Alain Lamarre (as the jury president), Dr. Silvia Vidal (as an external examiner), and Dr. Daniel Kaufmann (as an external examiner) for their time and effort in kindly accepting and critically examining my thesis.

I was blessed with a very friendly and interactive environment over the past 4 years. I had the opportunity to discuss beautiful science during lab meetings that shaped my growth as a scientist with each of the following INRS professors: Dr. Krista Heinonen, Dr. Simona Stäger, Dr. Laurent Chatel-Chaix, and Dr. Ian Gaël Rodrigue-Gervais. I would like to thank you all and your respective team members for being available and perceptive whenever I needed insight. I would like to thank my colleagues Xavier and Cherifa from van Grevenynghe's lab for all the convivial moments that we had, and your help and support throughout the most difficult times as well. I am also grateful for many people from various labs that made my journey animated: Privil, Merve, Maha, Mohamed Eisa, Mariem, Imene, Marwa, Roman, and Jihan.

I want to appreciate and acknowledge several people that made my journey special. I would like to sincerely thank my best friend Hicham Bessaiah for his unwavering support and his availability. Special thanks to my family and friends both in Algeria and here in Quebec for their unconditional support in every step that I have made throughout my journey.

I will be forever grateful to the many collaborators that played a significant role in my growth as a researcher and in expanding my network. I would like to thank Professor Jean-Pierre Routy, Professor William L Stanford, Dr. David Olnagier, Dr. Jörg H. Fritz, Daina Avizonis, Luc Choinière, and Hani Jrade for their valuable contributions in fulfilling my respective studies of this thesis. I am also grateful to all subjects who participated in my thesis studies, their physicians, and attending staff members from the Réseau SIDA/Maladies Infectieuses of the Fonds de la Recherche Québec-Santé. Special thanks to Mario Legault for technical and administrative assistance. I want to thank Professor Angela Pearson, Professor Charles Dozois, and Dr. Patrick Labonté for considering me to work in your projects as a collaborator, and for giving me a chance

to expand my expertise within your area of research. I am also indebted to the Fondation Armand-Frappier for their continuous support and belief in my academic progress throughout my journey.

Everyone was affected by the COVID-19 pandemic. I would like to thank all the staff members of the INRS that made working under very intense and unprecedented conditions possible. I would like to thank all the administrative staff that managed their tasks brilliantly and helped in the progress of my research activities. Finally, I want to thank all my colleagues, INRS staff, and friends that I worked with during the organization of the last 2 editions of Congrès Armand-Frappier 2019 and 2021, and during the INRS mentorship programs.



## ABSTRACT

Although there is no cure for HIV-1, patients can keep the infection at bay by taking a daily antiretroviral therapy (ART) regimen, consisting of the combination of several antiretroviral drugs (ARV). Unfortunately, life-long administration of ARV causes health complications profoundly affecting patient's quality of life. This therapeutic approach also exhibits a weak restoration of major immune functions, such as HIV-specific T cell immune responses. Therefore, it is of clinical importance to find new alternatives to potentiate and optimize anti-HIV-1 T cell responses in ART patients. To do so, we studied these mechanisms through Elite Controllers (EC), a rare subset of HIV-1 infected population who controls the infection and maintains effective immune features including T cell responses without ARV intervention. The mechanism(s) responsible for this feature is/are still unknown. Autophagy is a conserved catabolic process involved in the regulation of homeostasis and energy metabolism in T cells. It was reported to be highly active in EC. In addition, it was demonstrated that T cells in EC present plastic metabolic resources to fuel their mitochondrial oxidative metabolism. Therefore, we hypothesized that autophagy provides essential carbon sources to fuel the mitochondrial oxidative metabolism, which accommodate the bioenergetic requirements for protective anti-HIV-1 T cell immunity. Using multiple experimental platforms, our first set of findings revealed that autophagy mediates effective cytotoxic anti-HIV-1 CD8A T cells immunity in EC in comparison to ART patients following the engagement of T cell receptor. Interestingly, a significant positive correlation between the highly active autophagy and the presence of IL21-secreting CD4 T cells was observed in EC. Unlike ART patients, EC is characterized by strong production of IL21. We then established that IL21 rescue occurred due to the enhanced degradation of endogenous lipids via autophagy, referred to as lipophagy, fueling the cellular rates of mitochondrial beta-oxidation of fatty acids. Our first set of findings led us to unravel the possibility of a critical metabolic role of autophagy in protective IL21-secreting CD4 T cell in EC. Indeed, our second set of findings substantiate that autophagy-mediated proteolysis, not lipophagy, can fuel their mitochondrial respiration and ATP production through glutaminolysis to ensure optimal IL21 production in HIV-1-specific CD4 T cells from EC. We further revealed that autophagy was mediated via AMPK activation in IL21-secreting CD4 T cells in EC, and was rescued through AMPK-activator (AICAR) treatment in ART patients. In summary, autophagy-dependent metabolic reprogramming may be considered to enhance the antiviral potency of anti-HIV-1 T cells in patients under ARV.

**Keywords** : antiretroviral therapy, elite controllers, FAO, HIV-1, IL21, lipophagy, polyfunctionality. autophagy-mediated proteolysis, glutaminolysis, AMPK.

## RÉSUMÉ

Les traitements antirétroviraux (ART), consistant de plusieurs médicaments antirétroviraux (ARV), permettent aux patients de survivre à l'infection par le VIH-1 à long terme. Malheureusement, l'administration à vie d'ARV entraîne des complications de santé affectant profondément la qualité de vie des patients. Cette approche thérapeutique présente également une faible restauration des principales fonctions immunitaires, telles que les réponses immunitaires des lymphocytes T (LT). Par conséquent, il est d'une importance clinique de trouver de nouvelles alternatives pour optimiser les réponses LT anti-VIH-1 spécifiques chez les patients sous ART. Pour ce faire, nous avons étudié ces mécanismes via les élites contrôleurs (EC), ce sont des individus rares infectés par le VIH-1 qui contrôlent l'infection et maintiennent des caractéristiques immunitaires efficaces, notamment des réponses LT sans l'intervention d'ARV. Le(s) mécanisme(s) responsable(s) de cette fonctionnalité est/sont encore inconnu(s). L'autophagie est un processus catabolique conservé impliqué dans la régulation de l'homéostasie et du métabolisme énergétique des LT. Il a été démontré comme étant très actif chez les EC. De plus, il a été démontré que les LT des EC présentent diverses ressources métaboliques pour alimenter leur métabolisme oxydatif mitochondrial (MOM). Par conséquent, nous avons émis l'hypothèse que l'autophagie fournit des sources de carbone essentielles pour alimenter le MOM qui répond aux exigences bioénergétiques pour l'immunité protectrice des LT anti-VIH-1. Notre première série de résultats a révélé que l'autophagie confère une immunité efficace des LT CD8A cytotoxiques chez les EC par rapport aux patients sous ART. Il est intéressant de noter qu'une corrélation positive significative a été observée entre l'autophagie hautement active et la présence de LT CD4 sécrétant de l'interleukine 21 (IL21) chez les EC. Contrairement aux patients sous ART, les EC se caractérisent par une forte production d'IL21. Nous avons ensuite établi que le rétablissement fonctionnel via l'IL21 s'est produit en raison de la dégradation accrue des lipides endogènes via l'autophagie, appelée lipophagie, alimentant les taux cellulaires de la bêta-oxydation mitochondriale des acides gras. Notre première série de résultats nous a dirigé à élucider la possibilité d'un rôle métabolique critique de l'autophagie dans la sécrétion de l'IL21 des LT CD4. En effet, notre deuxième série de résultats confirme que la protéolyse médiée par l'autophagie via l'AMPK, est capable d'alimenter leur MOM par la glutaminolyse pour assurer une production optimale d'IL21. En résumé, une reprogrammation métabolique dépendante de l'autophagie peut être envisagée pour améliorer l'immunité des LT anti-VIH-1 chez les patients sous ART.

**Mots-clés :** thérapie antirétrovirale, élités contrôleurs, bêta-oxydation mitochondriale, VIH-1, IL21, lipophagie, polyfonctionnalité, protéolyse par l'autophagie, glutaminolyse, AMPK.

# SOMMAIRE RÉCAPITULATIF

## Mise en contexte du sujet de recherche

Bien qu'il n'y ait pas de traitement curatif contre le VIH-1, les patients peuvent survivre à l'infection en suivant un régime quotidien de la thérapie antirétrovirale (ART), consistant de plusieurs médicaments antirétroviraux (ARV). Malheureusement, l'administration à vie d'ARV entraîne des complications de santé affectant profondément la qualité de vie des patients (Haddad *et al.*, 2019; Loucif *et al.*, 2018). Cette approche thérapeutique présente également une faible restauration des principales fonctions immunitaires, telles que les réponses immunitaires des lymphocytes T (LT). Par conséquent, il est d'une importance clinique de trouver de nouvelles alternatives pour optimiser les réponses des lymphocytes T spécifiques au VIH-1 chez les patients sous ART. Afin d'atteindre cet objectif, il est nécessaire d'identifier d'abord tous les mécanismes défectueux qui peuvent fonctionner comme cibles thérapeutiques potentielles. Pour ce faire, nous avons étudié ces mécanismes par le biais des élites contrôleurs (EC), un groupe d'individus infecté par le VIH-1 rare, qui contrôlent l'infection et maintiennent des caractéristiques immunitaires efficaces, notamment des réponses cellulaires efficaces LT sans intervention d'ARV (Loucif *et al.*, 2018). Le(s) mécanisme(s) responsable(s) de cette fonctionnalité est/sont encore inconnu(s). L'autophagie est un processus catabolique conservé impliqué dans la régulation de l'homéostasie et du métabolisme énergétique des lymphocytes T (Hubbard *et al.*, 2010). Il a été montré comme étant très actif chez les EC comparé aux patients infectés non-traités et les contrôles de non-infecté (Nardacci *et al.*, 2014; Nardacci *et al.*, 2017). De plus, il a été démontré que les LT des EC présentent des ressources métaboliques plastiques pour alimenter leur métabolisme oxydatif mitochondrial (Angin *et al.*, 2019). Par conséquent, nous avons émis l'hypothèse que **l'autophagie fournit des sources de carbone essentielles pour alimenter le métabolisme oxydatif mitochondrial, qui répond aux exigences bioénergétiques pour l'immunité protectrice des LT anti-VIH-1.**

## Les objectifs de recherche

Notre objectif général est basé sur l'étude du rôle de l'autophagie sur la plasticité métabolique et l'immunité des LT CD8A et LT CD4 mémoire (Mem) des EC par rapport à ceux des patients traités (ART) et les contrôles de non-infection (HIV<sup>neg</sup>). Pour réaliser ceci, les étapes suivantes ont été entreprises :

**Objectif 1.** Mesurer l'activité autophagique dans les LT CD8A et LT CD4 Mem



**Objectif 2.** Caractériser la prise en charge des matériels lipidiques ou le métabolisme de la glutamine sur le métabolisme mitochondriale et l'immunité des LT CD8A et LT CD4 Mem

**Objectif 3.** Cibler les voies moléculaires subjacentes de la meilleure prise autophagique des EC, et étudier la possibilité de les rétablir chez les ART

### **Les méthodes et analyses**

**Objectif 1.** Afin d'étudier l'autophagie dans les LT, nous avons activé les cellules d'une manière polyclonale (anti-CD3/anti-CD28) ou spécifique aux antigènes du VIH-1, CMV, EBV et l'influenza (p55 Gag et peptides CEF respectivement) pendant 6h. L'activité autophagique/lipophagique a été mesurée via différentes plateformes expérimentales qui sont :

(1) Cytométrie en flux multiparamétrique (marqueurs d'autophagie classiques : BECN1, ULK1, ATG7, accumulation de SQSTM1/p62) ;

(2) ImageStreamX (l'Imagerie en flux de la localisation de LC3 lysosomal et matériels lipidiques lysosomal) ;

(3) Microscope électronique à transmission (visualisation des vésicules autophagiques qui contient des matériels lipidiques) ;

(4) le traçage de la <sup>14</sup>C-L-valine radio-marquée pour la dégradation protéolytique des protéines à long vie (l'autophagie active).

**Objectif 2.** Grâce à la culture cellulaire primaire des cellules mononuclées du sang périphériques (PBMC), nous pouvons étudier l'impact de l'autophagie sur l'immunité des LT chez les EC. Nous inhiberons l'autophagie soit pharmacologiquement (inhibiteurs de la dégradation lysosomale : Bafilomycin A1 ou chloroquine) ou par des particules lentivirales (LVP) siRNA-*BECN1* (inhibition de la phase initiale de l'autophagie). Puis nous évaluerons l'impact de l'inhibition de l'autophagie sur la fonctionnalité des LT CD8A (IL2, IFNG, TNFA, PRF1, GZMA et GZMB) et des LT CD4 Mem (sécrétion de l'IL21) via le marquage intracellulaire de la cytométrie en flux.

Nous avons deux aspects : fonctionnel (métabolisme mitochondriale) et mécanistique (autophagie/lipophagie). Nous utiliserons la mitochondriale des LT. Nous avons effectué plusieurs tests sous conditions inhibitrices ou non de l'autophagie et voir la capacité respiratoire mitochondriale et la production de l'ATP globales dans les LT activées. Nous allons évaluer l'impact de bloquer plusieurs voies métaboliques impliquées de métaboliser les sources

carbonées pour alimenter la mitochondrie telle que : L'oxydation des acides gras (l'etomoxir) et la glutaminolyse (BPTES).

**Objectif 3.** Des études ont montré que les gamma-chain cytokines, notamment l'IL21, sont impliqués dans plusieurs phénotypes immunitaires chez les EC. Nous allons évaluer le lien entre l'activité autophagique, et l'immunité des LT (CD8A et LT CD4 Mem) activées.

### Article 1

À l'aide de plusieurs plateformes expérimentales, notre première série de résultats a révélé que l'autophagie médie une immunité supérieure des LT CD8A cytotoxiques anti-VIH-1 chez les EC par rapport aux patients sous ART via l'activation polyclonale des récepteurs des LT (TCR). Nous avons confirmé nos résultats en inhibant spécifiquement l'autophagie via l'approche «post-transcriptionnel gene silencing» du gène *BECN1* avec le siRNA-*BECN1*, ou en inhibant chimiquement la digestion lysosomale des matériaux intracellulaires avec la Bafilomycine A1, la Chloroquine ou l'E64d/Pepstatine A. En fait, une corrélation positive significative a été observée entre l'autophagie hautement active et la présence des lymphocytes T CD4 sécrétant de l'IL21 chez les EC. Contrairement aux patients sous ART, les EC se caractérisent par une forte production d'IL21. Nous avons ensuite effectué des essais de restauration en utilisant l'IL21 recombinant humain sur des LT CD8A des patients sous ART. Le traitement à l'IL21 a entraîné une augmentation de l'activité d'autophagie suivie d'une amélioration des réponses efficaces des LT CD8A cytotoxiques. **Nous avons ensuite établi que la restauration via IL21 recombinant s'est produite en raison de la dégradation accrue des lipides endogènes via l'autophagie, appelée lipophagie, alimentant les taux cellulaires de bêta-oxydation mitochondriale des acides gras (Loucif et al., 2021b).**

### Article 2

Notre première série de résultats nous a conduits à élucider la possibilité d'un rôle métabolique critique de l'autophagie dans la protection des LT CD4 mémoires (Mem) sécrétant de l'IL21 chez les EC. En effet, notre deuxième série de résultats confirme que la protéolyse médiée par l'autophagie, et non la lipophagie, est capable d'alimenter leur respiration mitochondriale et leur production d'ATP par la glutaminolyse, pour assurer une production optimale d'IL21 dans les Mem spécifiques au VIH-1 chez les EC. Il est important de noter que pour l'ensemble des résultats, l'autophagie a été induite de manière indépendante de l'inactivation du MTOR. Nous avons en outre révélé que l'autophagie était médiée par l'activation de l'AMPK dans les Mem sécrétant de

l'IL21 des EC, et l'autophagie a été restaurée par le traitement en utilisant un activateur de l'AMPK (AICAR) chez les patients sous ART (Loucif *et al.*, 2021a).

### **Conclusion**

En résumé, une reprogrammation métabolique dépendante de l'autophagie peut être envisagée pour améliorer la puissance antivirale des lymphocytes T spécifique au VIH-1 chez les patients sous ART. En particulier, l'autophagie est un processus clé essentiel pour monter une réponse efficace des lymphocytes T et une aptitude métabolique en fournissant diverses sources de carbone dans un microenvironnement agressif lors d'une infection persistante par le VIH-1.

# TABLE OF CONTENTS

<b>DEDICATION.....</b>	<b>I</b>
<b>ACKNOWLEDGMENTS .....</b>	<b>II</b>
<b>ABSTRACT .....</b>	<b>V</b>
<b>RÉSUMÉ .....</b>	<b>VII</b>
<b>SOMMAIRE RÉCAPITULATIF .....</b>	<b>IX</b>
<b>TABLE OF CONTENTS .....</b>	<b>XIII</b>
<b>LIST OF FIGURES .....</b>	<b>XVII</b>
<b>LIST OF TABLES .....</b>	<b>XIX</b>
<b>LIST OF ABBREVIATIONS.....</b>	<b>XXIII</b>
<b>1 INTRODUCTION.....</b>	<b>1</b>
<b>2 LITERATURE REVIEW .....</b>	<b>2</b>
2.1 HIV-1 INFECTION IN A NUTSHELL .....	2
2.1.1 <i>HIV-1 life cycle</i> .....	2
2.1.2 <i>HIV-1 T cell immunopathogenesis</i> .....	4
2.2 HIV-1 INFECTION COUNTERMEASURES .....	5
2.2.1 <i>Antiretroviral therapy inception and limitations</i> .....	6
2.2.2 <i>Next generation HIV-1 therapy challenges</i> .....	7
2.3 THE CONUNDRUM OF HIV-1 NATURAL CONTROL.....	9
2.3.1 <i>Who are HIV-1 natural controllers?</i> .....	11
2.3.2 <i>Protective anti-HIV-1 T cell immunity</i> .....	14
2.4 T CELL METABOLISM .....	17
2.4.1 <i>Plastic metabolism is privileged in protective T cell immunity</i> .....	17
2.4.2 <i>T cell metabolic discrepancies during HIV-1 infection</i> .....	22
2.5 MACROAUTOPHAGY/AUTOPHAGY .....	26
2.5.1 <i>Autophagy regulation in T cell immunity</i> .....	28
2.5.2 <i>Autophagy as a novel immune correlate in HIV-1 natural immune protection</i> .....	29
<b>3 HYPOTHESIS AND OBJECTIVES .....</b>	<b>31</b>
<b>4 FIRST ARTICLE: IMPACT OF AUTOPHAGY-MEDIATED LIPID METABOLISM IN HIV-1-SPECIFIC CD8 T-CELLS IMMUNITY .....</b>	<b>32</b>
4.1 ABSTRACT.....	33
4.2 INTRODUCTION .....	35
4.3 RESULTS.....	36
4.3.1 <i>Confirmation of reduced autophagic activity in HIV-1-specific CD8A T-cells from ART...</i>	36
4.3.2 <i>Strong autophagy in EC drives their anti-HIV-1 CD8A T-cell polyfunctionality.</i> .....	42

4.3.3	<i>IL21 enhances antiviral CD8A T-cell responses from ART in an autophagy-dependent manner.</i>	45
4.3.4	<i>IL21 promotes the autophagy-dependent degradation of endogenous lipids in CD8A T-cells from ART.</i>	50
4.3.5	<i>IL21-induced lipophagy in ART leads to a better use of their mitochondrial respiration due to FAO.</i>	53
4.4	DISCUSSION	56
4.5	MATERIALS AND METHODS	59
4.6	REFERENCES	65
4.7	SUPPLEMENTARY MATERIALS	71
<b>5</b>	<b>SECOND ARTICLE: IMPACT OF GLUTAMINOLYSIS THROUGH AUTOPHAGY-MEDIATED PROTEIN CATABOLISM IN HIV-1-SPECIFIC MEMORY CD4 T-CELLS IMMUNITY</b>	<b>85</b>
5.1	ABSTRACT	86
5.2	INTRODUCTION	87
5.3	RESULTS	88
5.3.1	<i>Activated Mem from EC display enhanced PRKAA1-dependent autophagy when compared to ART.</i>	88
5.3.2	<i>Strong autophagy-mediated proteolysis is needed to ensure effective IL21 Mem production during HIV-1 infection.</i>	92
5.3.3	<i>Autophagy activity in Mem from EC favors the release of free glutamine rather than fatty acids, therefore promoting glutaminolysis.</i>	95
5.3.4	<i>Autophagy-dependent glutaminolysis in EC represents a new metabolic advantage required for strong IL21 production.</i>	100
5.3.5	<i>Stimulating PRKAA1 activity in Mem from ART rescues their autophagy-mediated mitochondrial respiration and IL21 production.</i>	104
5.4	DISCUSSION	107
5.5	METHODS	111
5.6	REFERENCES	118
5.7	SUPPLEMENTARY MATERIALS	124
<b>6</b>	<b>GENERAL DISCUSSION</b>	<b>147</b>
6.1	AUTOPHAGY AS A MAJOR REGULATOR OF T CELLS METABOLISM AND IMMUNITY DURING NATURAL CONTROL OF HIV-1 INFECTION	147
6.2	WHAT IS NEXT TO EXPLOIT? DEEP UNDERSTANDING OF AUTOPHAGY IN OTHER IMMUNE CELLS	148
6.3	THERAPEUTIC POTENTIAL AND PERSPECTIVES	149
6.3.1	<i>Targeting autophagy as a part of HIV-1 therapy regimen</i>	151
<b>7</b>	<b>CONCLUSION</b>	<b>154</b>

<b>8</b>	<b>BIBLIOGRAPHY.....</b>	<b>155</b>
<b>9</b>	<b>APPENDIX I.....</b>	<b>165</b>
<b>10</b>	<b>APPENDIX II.....</b>	<b>166</b>
<b>11</b>	<b>APPENDIX III.....</b>	<b>167</b>
<b>12</b>	<b>APPENDIX IV.....</b>	<b>169</b>
<b>13</b>	<b>APPENDIX V.....</b>	<b>170</b>
<b>14</b>	<b>APPENDIX VI.....</b>	<b>171</b>
<b>15</b>	<b>APPENDIX VII.....</b>	<b>172</b>



## LIST OF FIGURES

FIGURE 2.1	SCHEMATIC REPRESENTATION DESCRIBING THE DIFFERENT STAGES OF HIV-1 LIFE CYCLE (TAKEN FROM (DEEKS <i>ET AL.</i> , 2015)).....	3
FIGURE 2.2	SCHEMATIC REPRESENTATION REVEALING THE IMPACT OF HIV-1 INFECTION ON DIFFERENT KEY CELLS OF ADAPTIVE IMMUNE RESPONSE WITHIN LYMPHOID AND MUCOSAL SANCTUARY (TAKEN FROM (DEEKS <i>ET AL.</i> , 2015)). .....	5
FIGURE 2.3	SCHEMATIC REPRESENTATION OF THE CURRENT HIV-1 TREATMENT PROGRESS AND NEW THERAPEUTIC CONCEPTS TO ACHIEVE ART TERMINATION (TAKEN FROM (LOUCIF <i>ET AL.</i> , 2018)). .....	10
FIGURE 2.4	SCHEMATIC REPRESENTATION ILLUSTRATING THE MOLECULAR AND METABOLIC ADVANTAGES OF EC OVER PATIENTS UNDER ART THAT CONTRIBUTE TO THE MAINTENANCE OF EFFECTIVE ANTIVIRAL IMMUNITY (TAKEN FROM (LOUCIF <i>ET AL.</i> , 2018)).....	13
FIGURE 2.5	SCHEMATIC REPRESENTATION OF KEY CARBON-BASED SUBSTRATES AND THEIR CATABOLIC PATHWAYS THAT FUEL THE MITOCHONDRIAL RESPIRATION (TAKEN FROM (LOUCIF <i>ET AL.</i> , 2020)). .....	19
FIGURE 2.6	UP-REGULATED METABOLITES AND KEY METABOLIC REGULATORS THAT MAY CONFER BETTER ANTIVIRAL IMMUNITY IN HIV-1 CONTROLLERS (IN GREEN) WHEN COMPARED TO NON-CONTROLLERS PATIENTS (IN RED) (TAKEN FROM (LOUCIF <i>ET AL.</i> , 2020)).....	24
FIGURE 2.7	SCHEMATIC REPRESENTATION OF THE COMPLEXITY OF DESIGNING THERAPEUTIC STRATEGIES FOR T-CELL METABOLIC REPROGRAMMING DURING HIV-1 INFECTION (TAKEN FROM (LOUCIF <i>ET AL.</i> , 2020)).....	25
FIGURE 2.8	A GENERAL SCHEMATIC REPRESENTATION OF AUTOPHAGY PROCESS PHASES (TAKEN FROM (HANSEN <i>ET AL.</i> , 2018)). .....	27
FIGURE 4.1	REDUCED AUTOPHAGIC ACTIVITY IN ART AFTER CD8A T-CELL ACTIVATION. ....	38
FIGURE 4.2	LOWER AMOUNTS OF ALs IN ACTIVATED CD8A T-CELLS FROM ART. ....	41
FIGURE 4.3	ACTIVE AUTOPHAGY PLAYS A KEY ROLE IN ANTIVIRAL CD8A IMMUNITY DURING HIV-1 INFECTION. ....	44
FIGURE 4.4	CD4 T-CELL HELP IS REQUIRED TO ENSURE HIGH AUTOPHAGIC ACTIVITY IN EC. ....	47
FIGURE 4.5	RESCUE OF ANTIVIRAL CD8A IMMUNITY IN ART BY IL21 IS DRIVEN BY ENHANCED ACTIVE AUTOPHAGY. ....	49
FIGURE 4.6	ENHANCED LIPOPHAGY IN ART IN RESPONSE TO IL21 TREATMENT. ....	52
FIGURE 4.7	LIPOPHAGY-INDUCED IL21 IN ART IMPROVES THE CELLULAR RATES OF MITOCHONDRIAL BETA-OXIDATION. ....	55
FIGURE 5.1	ENHANCED AUTOPHAGY-MEDIATED PROTEOLYSIS IN MEM FROM EC AFTER CELL ACTIVATION..	90
FIGURE 5.2	ENHANCED PRKAA1-DEPENDENT AUTOPHAGY-MEDIATED PROTEOLYSIS IN MEM FROM EC AFTER CELL ACTIVATION.....	92
FIGURE 5.3	AUTOPHAGY-MEDIATED PROTEOLYSIS IS REQUIRED FOR OPTIMAL IL21 PRODUCTION IN MEM FROM EC. ....	94
FIGURE 5.4	SIMILAR LIPOPHAGY LEVELS IN ACTIVATED MEM. ....	97
FIGURE 5.5	MEM FROM EC RATHER USE AUTOPHAGY-MEDIATED PROTEOLYSIS TO SUPPORT THE RELEASE OF FREE GLUTAMINE. ....	100



FIGURE 5.6	BLOCKING AUTOPHAGY-MEDIATED PROTEOLYSIS OR GLUTAMINOLYSIS IN EC INHIBITS THEIR CELLULAR RATES OF MITOCHONDRIAL B-OXIDATION. ....	102
FIGURE 5.7	GLUTAMINOLYSIS IS REQUIRED TO PROVIDE OPTIMAL IL21 PRODUCTION IN MEM FROM EC ...	102
FIGURE 5.8	SCHEMATIC SUMMARY OF THE OVERALL AUTOPHAGY-MEDIATED PROTEOLYSIS METABOLIC ADVANTAGE DICTATING THE STRONG IL21 PRODUCTION IN HIV-1-SPECIFIC MEM FROM EC, WHICH CONFERS AN EFFECTIVE HIV-1-SPECIFIC CD8A T CELLS RESPONSE. ....	103
FIGURE 5.9	TRIGGERING THE PRKAA1 WITH AICAR ENHANCES AUTOPHAGY-MEDIATED PROTEOLYSIS AND GLUTAMINE/GLUTAMATE AVAILABILITY IN ART. ....	104
FIGURE 5.10	TRIGGERING THE PRKAA1-DEPENDENT AUTOPHAGY-MEDIATED PROTEOLYSIS WITH AICAR IN ART IMPROVES THEIR CELLULAR RATES OF MITOCHONDRIAL B-OXIDATION AND MEM-RELATED IL21 PRODUCTION. ....	106

## LIST OF TABLES

TABLEAU 2.1	PROFILES OF MOLECULAR/IMMUNE MARKERS IN PATIENTS UNDER ART AND HIV-1 CONTROLLERS, WHEN COMPARED TO THE UNINFECTED CONTROLS (BASELINE) (TAKEN FROM (LOUCIF <i>ET AL.</i> , 2018)).....	15
TABLEAU 2.2	LIST OF IMMUNE T-CELL FEATURES THAT ARE CONTROLLED BY DIFFERENT CATABOLIC PATHWAYS INCLUDING GLYCOLYSIS, GLUTAMINOLYSIS AND MITOCHONDRIAL FAO (TAKEN FROM (LOUCIF <i>ET AL.</i> , 2020)).....	20
TABLEAU 5.1	LIST OF ALL ANTIBODIES USED.....	110







## LIST OF ABBREVIATIONS

**AMPK:** Protein kinase AMP-activated

**ART:** Antiretroviral therapy

**ARV:** Antiretroviral drugs

**ATG:** Autophagy related genes/proteins

**BECN1:** Beclin 1

**CEF:** Cytomegalovirus, Epstein-Barr virus, and influenza virus) control peptide pool for immune cell activation

**CMV:** Cytomegalovirus

**EBV:** Epstein-Barr virus

**EC:** Elite controllers

**FAO:** Fatty acid beta-oxidation

**HIV-1:** Human immunodeficiency virus type 1

**HIV<sup>neg</sup>:** HIV-1-uninfected control donors

**IFNG/IFN- $\gamma$ :** Interferon gamma

**IL21:** Interleukine 21

**MAP1LC3/LC3:** Microtubule associated protein 1 light chain 3

**mTOR/MTOR:** Mechanistic target of rapamycin kinase

**OxPhos:** Oxidative phosphorylation

**PBMC:** Peripheral blood mononuclear cells

**SQSTM1:** Sequestosome 1

**TCR:** T cell receptor

**ULK1:** Unc-51 like autophagy activating kinase 1



# 1 INTRODUCTION

---

HIV-1 Infection continues to be a major global public issue, leading in most cases to persistent infections that represent substantial health, sociological and economic burdens. The World Health Organization estimated that 38 million people lived with HIV-1 by the end of 2019, with 80,000 infected patients throughout Canada (Haddad *et al.*, 2019). Although there is no cure for HIV-1, patients can keep the infection at bay by taking a daily antiretroviral therapy (ART) regimen, consisting of the combination of several antiretroviral drugs (ARV). Although this therapeutic approach has been highly effective in suppressing HIV-1 replication, life-long administration of ARV leads to numerous health complications including premature aging, insulin resistance, osteopenia, and hypertension in patients, all profoundly affecting their quality of life (Cazzaniga *et al.*, 2021; Mitchell *et al.*, 2020; Schank *et al.*, 2021). Despite recent patient care improvements (Cambou & Landovitz, 2020), ART still fails to cure HIV-1 infection due to the inability to counteract immune defects and metabolic disturbances that are associated with residual and stressful inflammation alongside viral persistence. This raised the urgent need for novel HIV curative strategies over the past decade. In this context, two cure strategies are commonly being proposed. The first one is a sterilizing cure, which aims towards the complete elimination of virus-containing cells (reservoir cells) throughout the body. The second one is a functional cure, which aims to provide a long-term control of HIV infection without ARV intervention. However, whether it is the sterilizing or the functional cure, they both share the same goal, which is to achieve ART termination in patients (Henrich & Lelievre, 2018; Li & Blankson, 2021b; Li & Gandhi, 2021). To succeed in such an endeavor, patients must rely on a strong T cell-based immunity against the virus to contain the infection once ART is terminated. Unfortunately, patients under ART are known to display not only dysfunctional anti-HIV-1 T cell responses, but also a progressive loss of their memory populations despite medical care (Cubas *et al.*, 2015; Loucif *et al.*, 2021a; Loucif *et al.*, 2021b; van Grevenynghe *et al.*, 2008). As such, these patients are expected to be poor candidates for successful HIV cures. Therefore, it is of clinical importance to find new alternatives to potentiate and optimize anti-HIV-1 T cell responses in ART patients before treatment regimen is terminated. We introduce two papers with extensive literature reviewing to demonstrate the goal of studying natural control of HIV-1 infection, and shedding light on metabolic features that reinvigorate T cells immunity (Loucif *et al.*, 2020; Loucif *et al.*, 2018).



## 2 LITERATURE REVIEW

---

The following literature review sheds light into the main key words by reading the thesis title backwards. Each sub-chapter highlights an important part of two published review articles during my PhD in appendix [I](#) and [II](#).

### 2.1 HIV-1 infection in a nutshell

Since its discovery in 1983 and labelled as the causal agent of acquired immunodeficiency syndrome (AIDS) in humans, the human immunodeficiency virus type 1 (HIV-1) is considered one of the major public health concern worldwide (Deeks *et al.*, 2015). It is believed to be transmitted initially from non-human primates' species via simian immunodeficiency virus (SIV) (Deeks *et al.*, 2015). According to the world health organization, the pandemic claimed almost 36.3 million lives by the end of 2020. Although HIV-1 infection is an incurable disease, efforts have been made for increasing access to effective preventive measures, treatment and diagnosis. HIV infection has become a manageable chronic health condition since the introduction of the antiretroviral therapy (ART), enabling a decent quality of life for infected patients (which are around 37.7 million people on average at the end of 2020) (de Mendoza, 2019). Research is continuing its progress towards finding a cure, or at least ways to better control the infection with less side effects caused by daily ART regimen (Kemnic & Gulick, 2021).

#### 2.1.1 HIV-1 life cycle

HIV-1 is a retrovirus (*Retroviridae* family) that is characterized by the possession of a unique enzyme called reverse transcriptase (Moir *et al.*, 2011). The latter converts the HIV's single stranded RNA to a complementary DNA; which integrates the host cell's DNA. HIV-1 mainly targets CD4 T cells in mucosal and lymphoid tissues as primary host for replication and maintaining latent reservoirs. Similarly, to all viruses, HIV-1 has specific proteins encoded by specific gene regions to perform various functions during its life cycle. Briefly, there are structural proteins (Gag, Pol, and Env), regulatory proteins (Tat and Rev), and accessory proteins (Vpu, Vpr, Vif, and Nef) located on the central parts of HIV-1 proviral genome (Deeks *et al.*, 2015). The main HIV-1 surface glycoproteins 120 and 41 (gp120 and gp41), form a glycoprotein complex that allows the virus to fuse with CD4; CCR5 and CXCR4 surface receptors of CD4 T cells. The

infectious HIV-1 life cycle will then be initiated (Figure 2.1). The integrated form of HIV-1, also known as the provirus, is approximately 9.8 kilobases (flanked by Long Terminal Repeats at both ends). Studying the different stages of HIV-1 life cycle was critical in the deep understanding of its pathophysiology and treatment design in order to halt its replication (Deeks *et al.*, 2015; Moir *et al.*, 2011). The main steps are attachment, penetration, reverse transcription, integration, transcription, assembly, and finally budding and maturation, which is the release of newly formed viruses outside the infected host cells (All illustrated in Figure 2.1).

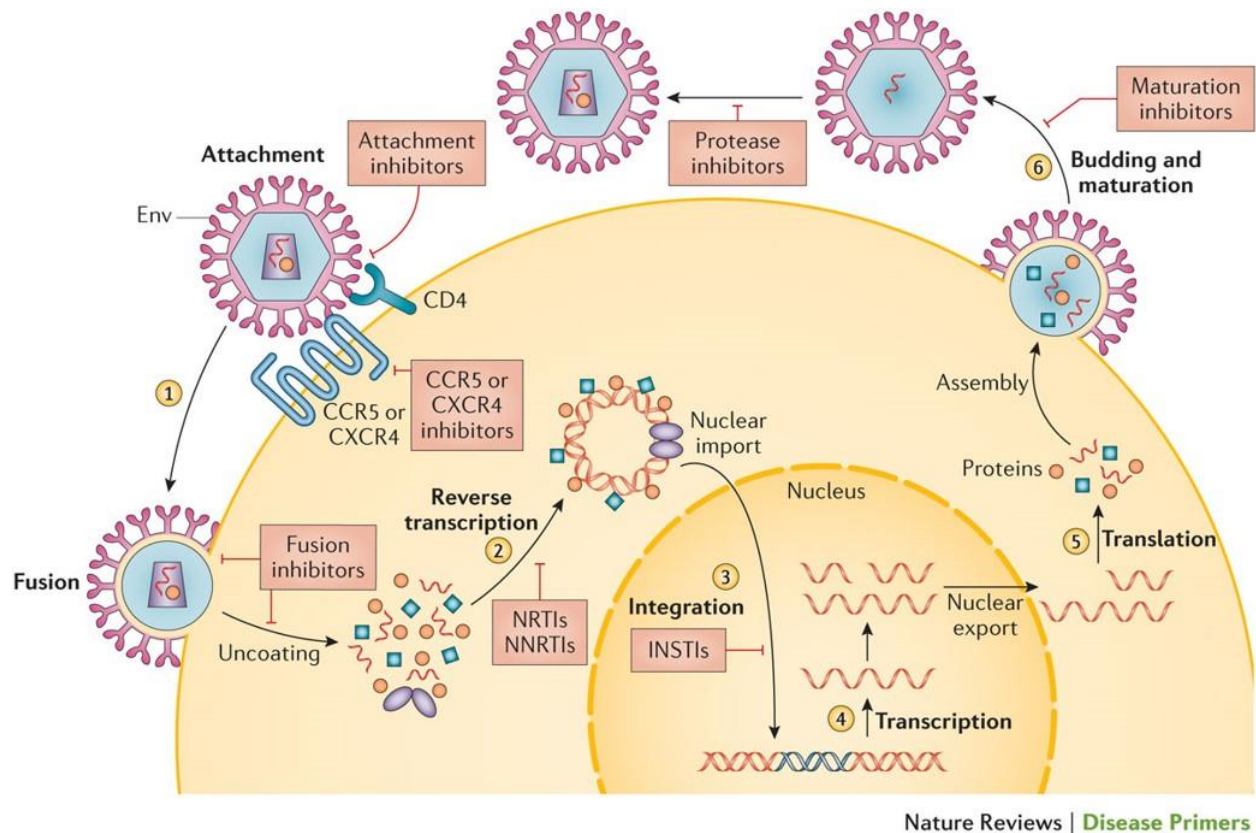


**Figure 2.1** Schematic representation describing the different stages of HIV-1 life cycle (taken from (Deeks *et al.*, 2015)).

The schematic demonstrates the results of the fundamental research of HIV-1 pathogenesis to design proper countermeasures for each phase of HIV-1 life cycle.

### 2.1.2 HIV-1 T cell immunopathogenesis

HIV-1 infection is a progressive and lethal disease if left untreated. Various physiological discrepancies caused by the continuous viral replication and CD4 T cells loss, which eventually leads to immunological abnormalities. For instance, an imminent progressive loss of CD4 T cell increases the risk of other health complications and emergence of opportunistic infections and cancer incidences (AIDS-related incidences). However, these AIDS-related incidences decreases significantly with the current ART regimen. HIV infection has a profound and complex effect on the immune system including T cell cellular and B cell humoral immune response (Deeks *et al.*, 2015; Moir *et al.*, 2011). In fact, CD4 T cell is the central immune cell, aka; adaptive immune response orchestrator, which helps other immune cells to perform their optimal functions via cytokines secretion. HIV-1 preferentially infects activated CD4 T cells and causes cell death via apoptosis and/or pyroptosis within the gut (including other mucosal tissues such as MALT), and lymphoid tissues (such as thymus and lymph nodes) (Deeks *et al.*, 2015; Moir *et al.*, 2011). These events lead to an immunodeficiency status due to T cell depletion (CD4/CD8 ratio) and dysfunction within the lymph nodes (where it occurs the maturation and differentiation of antigen-specific T cells). The chronic inflammation then stimulates a constant immunomodulatory feedback, which hinders proper T cell function (Figure 2.2). In chronic viral infection such as HIV-1 infection, T cells can also become progressively exhausted due to ongoing antigen exposure. Studies showed that cell exhaustion is positively correlated to reduced proliferation and cytokine production, leading to poor control of the infection. Exhaustion of T cells stems from the expression of multiple inhibitory transcription factors and receptors such as cytotoxic T lymphocyte-associated protein 4 (CTLA-4) and Programmed Death-1 (PD-1) expression during HIV infection (Barker & Evans, 2016; Deeks *et al.*, 2015; Kaufmann *et al.*, 2007; Mueller *et al.*, 2001; Quigley *et al.*, 2010). This phenotype is highly observed within CD8A T cells, weakening their maintenance, functionality and effective antiviral responses. It stands to reason why HIV-1 infection caused massive mortality rates since its outbreak in the 20<sup>th</sup> century. The complexity of HIV-1 pathogenesis, that includes insuring the longevity of latent reservoirs within tissue-resident CD4 T cell, require a complex therapeutic approach (Deeks *et al.*, 2015). On the one hand, the importance of eliminating the latent reservoirs and the virus from the body (Sterile Cure). On the other hand, the critical need to restore an effective HIV-1 specific immune response, especially, T cell immune responses to better control the infection (Functional Cure) (Davenport *et al.*, 2019; Loucif *et al.*, 2018).

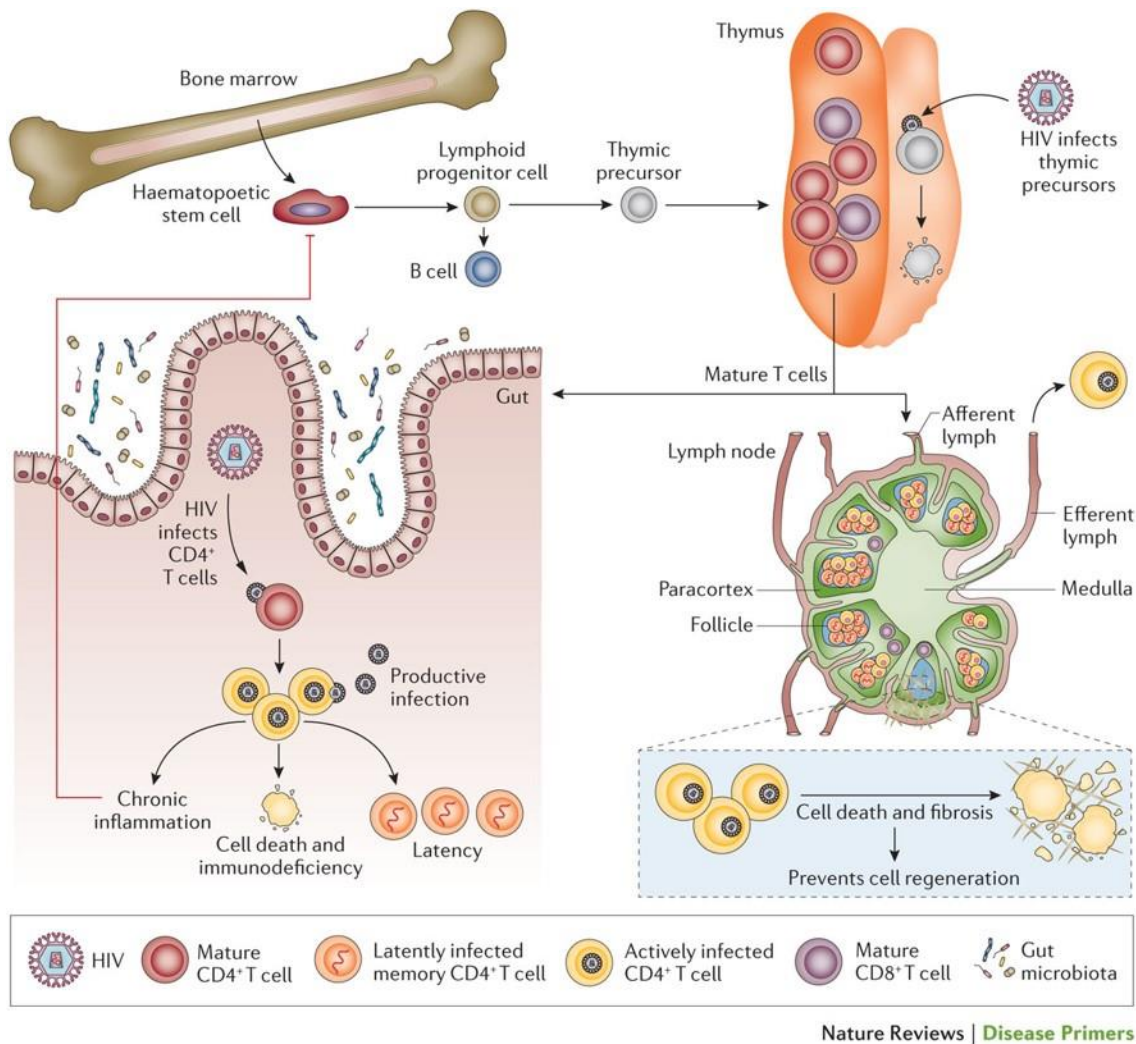


**Figure 2.2** Schematic representation revealing the impact of HIV-1 infection on different key cells of adaptive immune response within lymphoid and mucosal sanctuary (taken from (Deeks et al., 2015)).

HIV-1 infects activated CD4 T cells and causes severe collateral damage to other adaptive immune cells such as B cells and CD8A T cells.

## 2.2 HIV-1 infection countermeasures

The scientific community began to explore ways to abolish HIV-1 replication and a tentative plan to restore effective T cell responses. It started with several fundamental studies and clinical trials of Zidovudine, a nucleoside reverse transcriptase inhibitor (NRTI), establishing the highly active ART (or HAART) in 1987. The introduction of this therapy regimen led to a breakthrough in

suppressing the course of the disease towards AIDS, and substantially reducing its transmission. ART regimen is consisted of 2 to 3 antiretroviral drugs (ARV) combined in a single dosage (Deeks *et al.*, 2015). In the following two sub-chapters 2.2 and 2.3, we highlight the status report of the ART regimen, challenges to design an effective vaccine, and finally the use of a rare population called HIV-1 elite controllers (EC) in cure research. Furthermore, we highlight evidence illustrating the molecular and metabolic advantages of HIV-1 controllers over ART treated patients, which contribute to the maintenance of effective antiviral immunity (detailed in the [first review](#)).

### **2.2.1 Antiretroviral therapy inception and limitations**

The ART regimen was first introduced and initiated as a regular HIV-1 infection treatment in 1996. Indeed, ART has revolutionized the treatment for HIV-1 infection and successfully amended the life expectancy of infected individuals (Danforth *et al.*, 2017). The treatment consists of a daily dose of ARV to keep the systemic viral load less than 50 copies/ml, and the CD4 T cells count above 500 cells/mm<sup>3</sup>. Several ARV classes have been introduced throughout the years. The molecular nature of each ARV class differs from one to another, targeting different levels of HIV-1 life cycle mentioned in the previous sub-chapter (Kemnic & Gulick, 2021).

The research and development continued its progress in optimizing ART regimen throughout the years in order to overcome many hurdles that influence its efficacy, including drug-drug interactions and drug resistance (Collier *et al.*, 2019; Dionne, 2019). The goal was to ameliorate patients' care and sustain an optimal efficacy with less side effects. Nevertheless, the optimization of ART included the design of smaller pills without compromising its drug efficacy, adapted ARV combinations, and new classes of molecules such as integrase inhibitors (Pau & George, 2014). In addition, ARV encapsulation delivery systems were also considered as a new avenue in nanotherapy in the context of chronic HIV-1 infection (Dionne, 2019; Halling Folkmar Andersen & Tolstrup, 2020) (described in Figure 2.3).

Another critical finding that played a major role in changing ART regimen administration policy, which is its early initiation on primary infected individuals. Indeed, early ART administration is now recommended for all seropositive HIV-1 individuals regardless of CD4 counts. The benefits of early initiation of ART have been reported to be advantageous in sustaining a better control of infection, even after a short-term ART cessation for some individuals (called post-treatment

controllers; PTC) (Pasternak *et al.*, 2021). Interestingly, early ART initiation had a positive impact on protective T and B cells immunity, tissue inflammation (lower hyper immune activation markers), immuno-metabolism such as reduced tryptophan catabolism related to Treg/Th17 ratio, and finally the ability to reduce marginally the size of latent reservoirs (Loucif *et al.*, 2018; Pasternak *et al.*, 2021) (see Table 2.1). ART regimen could also be used as a prophylactic measure for exposure to high-risk sexual transmission (Deeks *et al.*, 2015). Although early ART initiation proved to be beneficial in some aspects, further evidence proved that ART is still far from ideal. Despite the success of ART in keeping the viral rebound at bay, many important points questioned the spectrum of its efficacy versus health, economic and sociological side effects. For example, ART regimen is unable to completely neutralize the latent reservoirs residing within lymphoid tissues. In addition, the life-long administration of ARV results in toxic effects and metabolic disorders such as lipodystrophy, insulin resistance and developing drug resistance (Loucif *et al.*, 2018; Pau & George, 2014). Although these concerns were mostly resolved with the novel ARV generation introduction (Cambou & Landovitz, 2020), patients under ART maintain chronic inflammation and lymphoid/mucosal tissue architecture disruption that negatively affects metabolism, survival and function of immune cells, loss of beneficial microbiota diversity (Loucif *et al.*, 2018) (see Figure 2.4). Other socio-economic burdens such as lifetime treatment, poor mental health, substance abuse, social isolation and care-related costs up to 48,000 per year (reported in 2012) for patients on ART regimen (McCann *et al.*, 2020).

Overall, the current ART regimen, regardless of its promising progress over the time, still fails to achieve Sterile Cure, to better control residual inflammation and fully restore immune function (Functional Cure). Thus, it is critical to find novel alternatives that achieve a potent antiviral immunity to ensure somehow a post treatment control phenotype.

### **2.2.2 Next generation HIV-1 therapy challenges**

Vaccinology in the context of HIV-1 infection faced multiple challenges over the years. Due to the high genetic diversity of HIV-1 mediated. Many studies and clinical trials were carried out but without a remarkable success to achieve long lasting cross-reactive humoral and cellular immune responses (Deeks *et al.*, 2015). Numerous efforts have been employed to develop novel therapeutic virus mediated by the strategies directed at achieving post-ART control or post-ART remission (Figure 2.3). Rare cases that successfully a Functional Cure such as the Berlin Patient

and the London Patient (participant 36 in the IciStem cohort), did raise so much interest in studying the utility of considering allogeneic stem cell transplantation with non-functional CCR5. However, this approach tends to be unrealistic due to its complexity and high risk of mortality involving full body radiation (Allers *et al.*, 2011; Gupta *et al.*, 2020; Loucif *et al.*, 2018). However, the recent EC patient from Esperanza in Argentina has recently made headlines, as the latter study showed the absence of replication-competent proviral genome without ART intervention. Therefore, these findings indicated the elimination of the viral reservoir, which is considered as a model for Sterile Cure (Turk *et al.*, 2022). Therefore, the scientific community focused on the possibility to find alternative less invasive approaches to achieve Functional Cure. The latter stands for the concept of boosting the HIV-1 specific immunity within patients under ART regimen, and attempting durable control over the infection after ART cessation (Li & Blankson, 2021a; Loucif *et al.*, 2018). This approach requires a deep understanding of the circumstances that achieves natural control over HIV-1 infection. Lessons could also be learned from several non-primates models such as SIV-1 macaque natural controllers for this endeavor (Mudd & Watkins, 2011). HIV-1 natural controllers are more likely to be the ideal research model to set up feasible therapeutic strategies. They constitute a small number of HIV-1 infected population that can live with the virus without ART regimen for several years (Davenport *et al.*, 2019; Loucif *et al.*, 2018). Most features that characterize this rare group is the ability to sustain highly effective antiviral immunity for years, thus providing crucial information to develop new generations of therapeutic and vaccines design (see Figure 2.3). The question remains to be asked: how HIV-1 controllers able to naturally sustain such effective anti-HIV-1 immunity? The answer for this question is within many fundamental-based studies in the last decade (Davenport *et al.*, 2019; Li & Blankson, 2021a; Loucif *et al.*, 2018). The main goal of these studies is to pinpoint and identify key molecular mechanisms that drive the long-term and highly effective immune control of HIV-1 infection. Collecting valuable information such the unique genetic and immunometabolic signature of HIV-1 controllers, is the first step towards achieving Functional Cure (see Figure 2.4). The second step would be to apply these findings to the current therapeutic strategies with more targeted approaches. One of these strategies called: Shock and Kill strategy. The strategy is a two-step approach: 1) "Shock" is to reactivate/reverse latency of the integrated proviral genome within quiescent reservoirs using chemical inhibitors or specific antibodies to against several latency players. For example, using histone deacetylase (HDAC) inhibitors, protein kinase C agonists or antibodies against PD-1 have already been established in several studies (Lichterfeld, 2020; Loucif *et al.*, 2018). 2) "Kill" is to neutralize the activated virus-specific cells detected by the immunosurveillance process via HIV-1-specific neutralizing antibodies or cytotoxic CD8A T cells.

HIV-1 controllers are characterized by a highly effective cytotoxic CD8A T cells Responses. In fact, most of studies correlates HIV-1 natural control with this particular feature. Determining the molecular and mechanistic signature of this feature could lead to accomplish not only Shock and Kill strategy, but also what is called chimeric antigen receptor (CAR) T cells approach (Mu *et al.*, 2020). As such, HIV-1 controllers display protective haplotypes and cytotoxic CD8A T cell responses of high functional avidity and broad variant cross-reactivity (Loucif *et al.*, 2018). Once again, it is a valuable information learned from HIV-1 controllers in order to achieve a successful CAR T cells approach. Finally, understanding the association of a diversified microbiota in HIV-1 controllers and the conserved metabolic signature may add additional information to complement the above-mentioned therapeutic strategies.

In summary, understanding the mechanisms that achieves natural control of HIV-1 infection without ART regimen is major step forward to improve the current treatment strategies. There are many valuable information that could be learned from HIV-1 controllers to help achieve a similar fate for patients under ART regimen by boosting their long-term antiviral protective T cell responses.

### **2.3 The conundrum of HIV-1 natural control**

Despite the difficulties for a successful next generation therapy and vaccine design, achieving a durable viral remission could be more realistic to apply for patients on ART regimen. It has been reported in a VISCONTI (Viro-immunological Sustained CONtrol after Treatment Interruption) study that it is possible to harness a long-term remission after interrupting 3 years of ART regimen during primary infection phase, as mentioned in the previous sub-chapter (Saez-Cirion *et al.*, 2013). Nonetheless, it's only possible for 5-15% of primary infected patients whose been diagnosed earlier rather than most of HIV-1 infected patients population in the chronic phase. For instance, the success and eligibility in what is called "Post-treatment control" depends on understanding the responsible mechanisms for such durable remission, keeping in mind the timing to initiate ART and its duration. In spite of a durable remission within "post-treatment controllers" which exhibits an efficient HIV-1 specific immune response and virological control reported by several studies, HIV-1 Elite Controllers (EC) might represent their other side of the mirror (Li & Blankson, 2021a; Loucif *et al.*, 2018). Indeed, it is critical to recall that the rare ability



of EC to naturally control HIV-1 infection despite residual inflammation could be exploited as a potential therapeutic model worth studying (see Figure 2.3) (Loucif *et al.*, 2018).

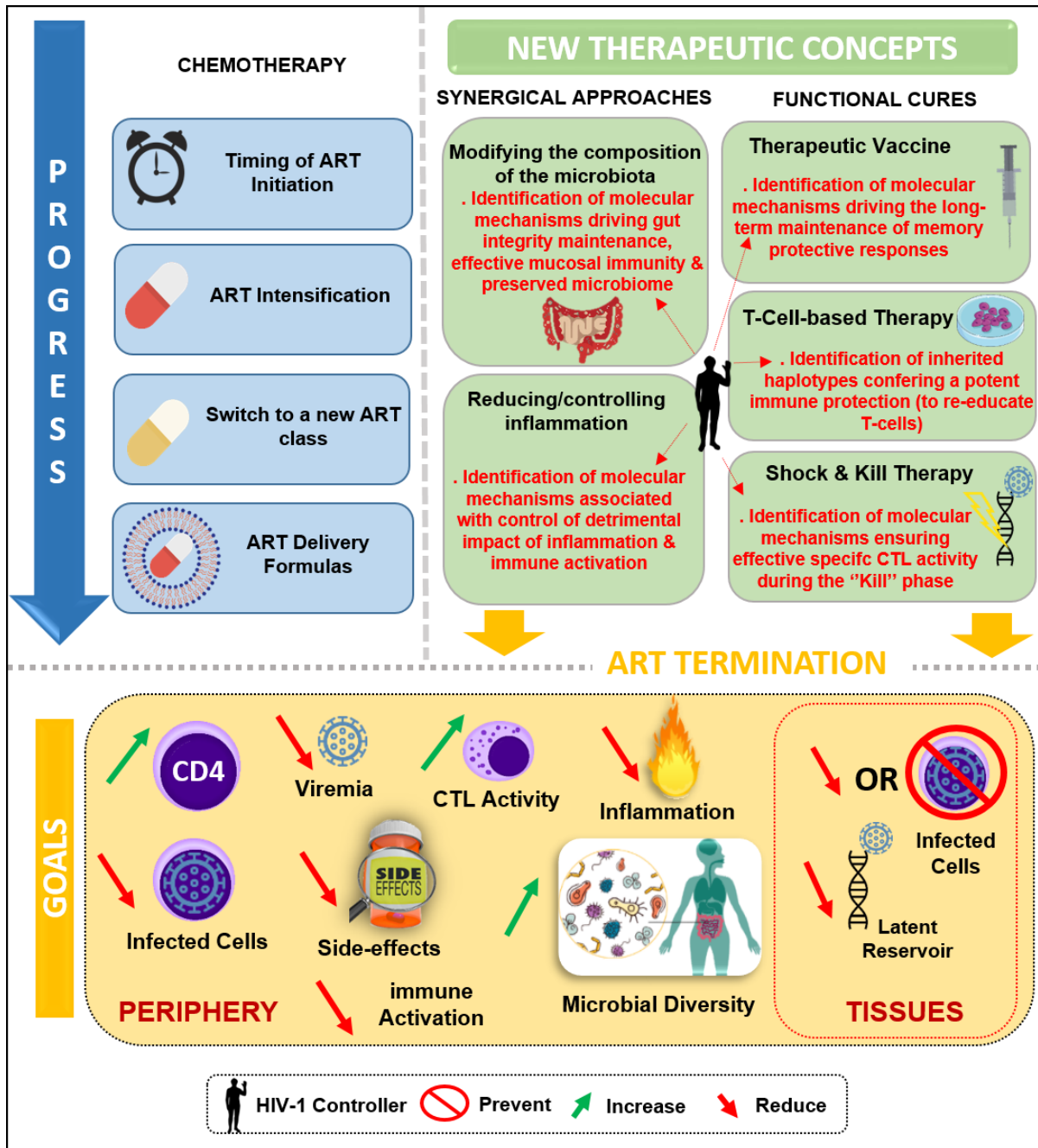


Figure 2.3 Schematic representation of the current HIV-1 treatment progress and new therapeutic concepts to achieve ART termination (Taken from (Loucif *et al.*, 2018)).

The schematic also includes the potential contribution of the observations collected from HIV-1 controllers (indicated in red), which may be critical for the development of the therapeutic concepts. Abbreviations: ART, antiretroviral therapy; CTL, cytotoxic T lymphocytes.

### 2.3.1 Who are HIV-1 natural controllers?

The rare ability of EC to naturally control HIV-1 infection without ART regimen intervention can be exploited to identify molecular mechanisms involved in host protection that may function as potential therapeutic targets. Our first step was to gather as much information regarding the unique immune protection features that characterize the EC. Unique immunometabolic features that allow them to suppress viremia and present effective HIV-1 specific immune responses characterize them. In fact, EC represent a small fraction (less than 1% of infected population) of the general population of HIV-1 Long Term Non-Progressors (Li & Blankson, 2021a; Loucif *et al.*, 2018). Several studies reported that some of the EC tend to lose their natural control features (see Figure 2.4). Some studies did characterize the natural control failure features including some immunological markers such as IL32 (El-Far *et al.*, 2016). Other inflammatory markers were reported which lead to the susceptibility of multiple comorbidities involving coronary atherosclerosis, cardiovascular and psychiatric disorders when compared to patients receiving ART (Crowell *et al.*, 2015; Hocini *et al.*, 2019). Nevertheless, the importance of the deep understanding on how HIV-1 natural controllers preserve effective immunity and tissue integrity despite inflammation is a valid goal. In Table 2.1, we characterized various immunometabolic features that confer highly effective HIV-1 specific immunity in HIV-1 natural controllers compared to patients on ART regimen. Of note, we also mentioned some reversible phenotypes even when considering early initiation of ART regimen. In comparison to HIV-1 natural controllers, ART regimen do not fully restore HIV-1-specific B cell responses and maintain it in long-term. Furthermore, patients under ART regimen display a high activity of the pro-apoptotic pathway FOXO3 in their memory B cells compared to HIV-1 natural controllers. This phenotype was also observed in their memory CD4 T cells within tissues such as gut associated lymphoid tissue (GALT). This proves that some natural control immune phenotypes are observed similarly in many key adaptive immune cells. HIV-1 controllers are also known to show potent innate phenotypes such as highly antiviral responses of Natural Killer cells (NK) and preserved plasmacytoid dendritic cells functionality (Dillon & Wilson, 2021).

As mentioned in the previous sub-chapters, HIV-1 infection is associated with chronic inflammation and immune defects that negatively affect microbiota diversity, gut integrity and cellular metabolism (Deeks *et al.*, 2015; Loucif *et al.*, 2020; Loucif *et al.*, 2018). However, HIV-1 controllers display a very rich and diversified (such as *Bacteroides* enrichment) of gut microbiota compared to healthy individuals that may help them to better keep an optimal control (see Figure

2.4) (Vesterbacka *et al.*, 2017). Such advantage is absent in patients on ART regimen. Tryptophan catabolism is also fairly studied in the context of HIV-1 infection (Jenabian *et al.*, 2015). It was reported that this pathway influence the gut integrity (See our review in the [appendix V](#)). Studies also confirm the higher Tryptophan catabolite levels, kynurenine, in patients under ART, even when treatment is administrated early (Gelpi *et al.*, 2017; Jenabian *et al.*, 2013). These observations also demonstrate the length of disturbed metabolism observed in patients on ART regimen compared to HIV-1 natural controllers. Finally, macroautophagy/autophagy is a conserved cellular catabolic process was reported to be highly activated in HIV-1 natural controllers within their peripheral blood mononuclear cells controls (Nardacci *et al.*, 2014; Nardacci *et al.*, 2017). This process will be detailed in the final sub-chapter. Altogether, studies showed a better preservation of memory B cells maintenance and functionality, sharper innate immune responses, better gut integrity and highly preserved anti-HIV-1 T cells immunity.

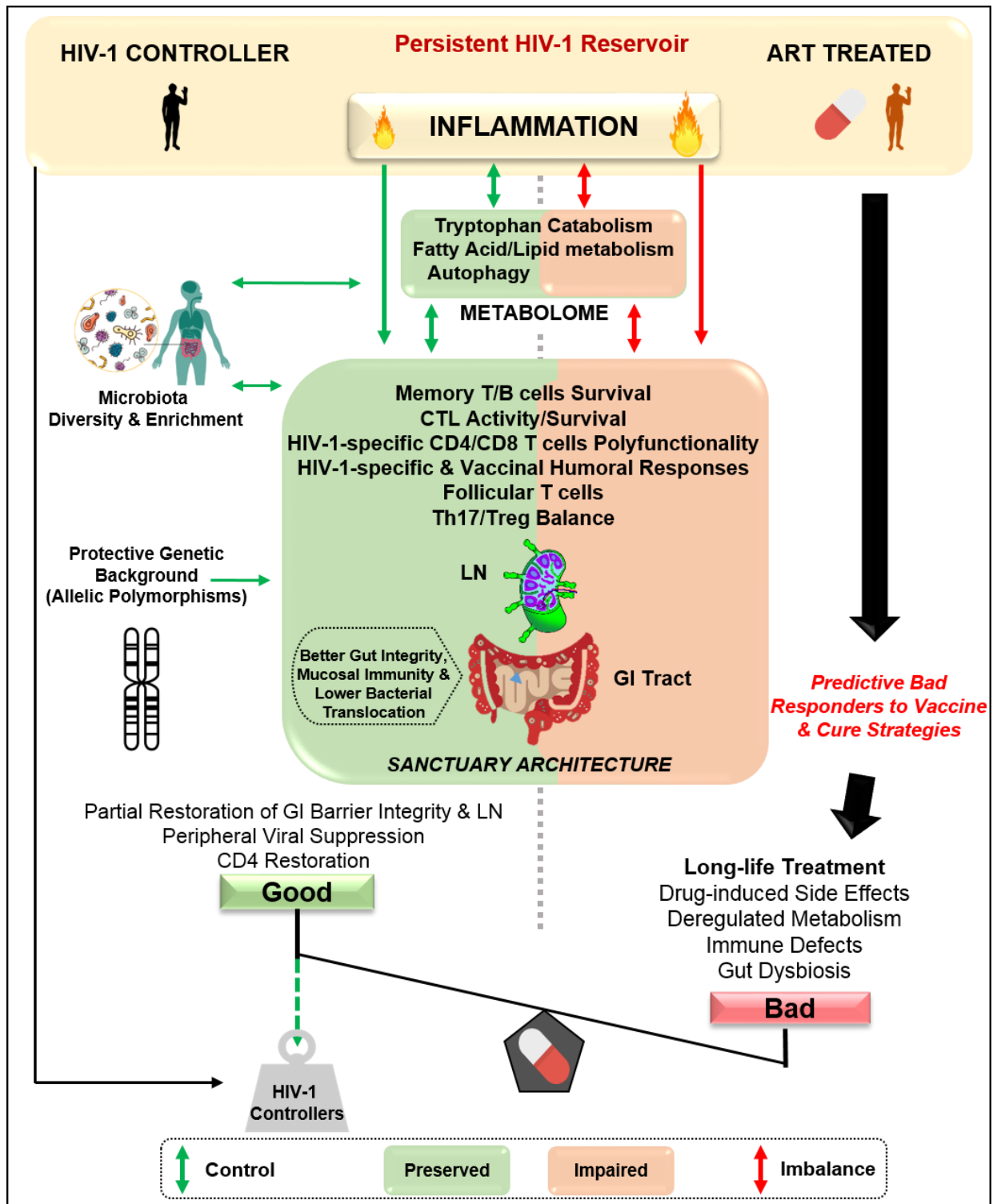


Figure 2.4 Schematic representation illustrating the molecular and metabolic advantages of EC over patients under ART that contribute to the maintenance of effective antiviral immunity (Taken from (Loucif *et al.*, 2018)).

Abbreviation: GI, gastrointestinal tract; LN, lymph node.

### 2.3.2 Protective anti-HIV-1 T cell immunity

T cells are the main troops of the adaptive immune response to fight microbial pathogens such as viruses. An antiviral response is initiated upon the first exposure to a virus, thus creating specialized T helper, T effector cell subsets, and memory T cell subsets. The latter recognize instantly the same virus during the second exposure and stimulates the virus-specific memory T cells subsets. Priming T helper cells, or CD4 T cells, upon T cell receptor engagement is induced during the interaction with the virus antigens on the surface of the antigen-presenting cells (such as dendritic cells). It is then followed by the release of a variety of cytokines that ultimately stimulate B cells to secrete specific neutralizing antibodies and cytotoxic CD8A T cells to eradicate virus-infected cells (Kumar *et al.*, 2018). In the context of HIV-1 infection, T cells survival, maintenance and functionality, are severely compromised even with ART intervention (described in the [first review](#)). A keen interest has been developed during the last decade for studies examining the key role for T cell immunity in the natural control of HIV-1 infection. In fact, some studies using EC provided some of the first clues of the cellular and molecular mechanism(s) of HIV-1 control. For example, studies have identified the role of transcriptional factor FOXO3 as a critical player in the long-term survival of memory CD4 T cells in EC. However, the majority of studies seeking to define the mechanism(s) of HIV-1 control have largely relied on the comparison of CD8A T cell responses from ECs compared to patients on ART regimen. In this context, qualitatively polyfunctional CD8A T-cell responses (which is the ability to secrete multiple cytokines simultaneously such as: IFNG/IFN- $\gamma$ , IL2, IL21, TNFA/TNF- $\alpha$ , and CCL4/MIP1- $\beta$ ), including high cytotoxic CD8A T cell activity (secretion of cytotoxic molecules such as: PRF1/perforin 1, GZMB/granzyme B and GZMA/granzyme A); have been most closely associated with natural control in these individuals. CD8A T cells in EC displayed a high survival rate and less exhaustion phenotype compared to patients on ART regimen. Collectively, these studies identify sustained CD8A T cell responses of high quality as primary correlates of immune protection in EC (Collins *et al.*, 2020; Loucif *et al.*, 2018).

EC are also known to preserve a high memory CD4 T-cells functionality and survival rates. They show a potent specific antiviral responses characterized by secreting key cytokines such as IL2 and IFNG upon HIV-1 specific activation (Table 2.1) (Potter *et al.*, 2007). Studies also reported that EC display preserved peripheral T-follicular helper CD4 T cells (pTfh) that confer HIV-1-specific broadly neutralizing antibodies (Buranapraditkun *et al.*, 2017). Furthermore, pTfh are

known to secrete a gamma chain cytokine IL21 that induces effective B cell responses observed in EC compared to patients under ART regimen (Claireaux *et al.*, 2018).

**Tableau 2.1** Profiles of molecular/immune markers in patients under ART and HIV-1 controllers, when compared to the uninfected controls (baseline) (Taken from (Loucif *et al.*, 2018)).

	Marker(s)	Compared to Baseline		Phenotype(s)	Ref(s)	
		ART	HIV Controllers			
IMMUNITY	<b>CD8</b>					
		TIGIT <sup>+</sup>	↗	≡	CD8 T-cells exhaustion	[74]
	HIV-specific	Perforin, Granzyme B, T-bet	↘	↗	CTL Activity	[52, 53]
		Cleaved Caspase-3 Bcl-2 <sup>high</sup>	↗	↘	Effector CD8 Survival	[54]
		IL-2, IFN-γ, CD107a, Perforin	↘	↗	CD8 Polyfunctionality	71
	<b>CD4</b>					
		Pro-apoptotic Foxo3a Pathway Protection (Fas, Bim)	↘	↗	Central Memory CD4 T-Cells Survival	[75, 76]
		IL-2, IFN-γ, CD127	↘	↗	Effector Memory CD4 T-cells Polyfunctionality	[76]
		TRAV24, TRBV2 motifs	↘	↗	T-cell Activation & Polyfunctionality upon TCR repertoire with High Affinity to Immunoprevalent Viral Epitopes	[78]
	<b>pTfh</b>					
		CCR5 <sup>+</sup> CCR3 <sup>+</sup> CD4 <sup>+</sup> IL21, Env-Specific IgG	↘	↗	B cells Help Antibodies Generation	[82, 83]
	<b>B-cells</b>					
		Foxo3a pro-apoptotic pathway (TRAL, Bim)	↗	≡	Memory B cells Survival	[86]
		STAT5 induced IL-2 pathway	↘	↗		
	CD21 <sup>high</sup> CD27 <sup>-</sup> IgG against common Vaccinal Ags (Tetanus, Measles, Pneumococcus)	↘	≡	Memory B-cell Frequency Vaccinal Humoral Response	[28, 85]	
	HIV-1 Specific IgG (Subclasses 1 & 3)	↘	↗	HIV-1 Specific Humoral Response Polyfunctional Ab Effector Activity	[85, 87, 88]	
<b>Innate System</b>						
	B2CA2 <sup>+</sup> CD123 <sup>+</sup> IFN-α induced TLR-9 pathway	↘	≡	pDC Count & Functionality	[92]	
	CD56 <sup>-</sup> CD16 <sup>+</sup> (NK) HLA-DR, CD38	↗	≡	Natural Killer Cells Activation	[89]	
INFLAMMATION	<b>Impact on Gut Microenvironment &amp; Immuno-Metabolism</b>					
		IL4, IL-10 (GALT iNKT)	↘	↗	Immune Activation	[103]
		<i>Bacteroides</i>	↘	≡	Microbiome Diversity & Enrichment	[35, 36, 95, 97, 103]
		sCD14	↗	↘	Microbial Translocation	[13, 101]
		CD3 <sup>+</sup> CD4 <sup>+</sup> (GALT) IL-17a	↘	≡	Mucosal CD4 T-cells Maintenance	[101, 102]
		Tryptophan Catabolism (Kynurenine)	↗	≡	Treg/Th17 balance	[17, 95, 98, 99]
		Atg-5, BECLIN-1 & AMBRA1	NA	↗	Increase Autophagic Activity as associated with Viral Containment	[104]

↘ Down-regulation ↗ Up-regulation ≡ Similar

Of course, HIV-specific responses in controllers are compared to those from patients under ART (yellow). This table also depicts the reversible phenotypes when ART is administered early or when the deregulated pathway is specifically targeted in "normal" patients (orange arrows).

A potent antiviral T cell response is believed to have what it takes to achieve the functional cure. The most critical component, which is required to ensure the success of the functional cures, is surely the restoration of a strong anti-HIV-1 immunity in patients on ART regimen. Indeed, a strong anti-HIV-1 immunity requires a steady regulation of T cell metabolism.

## **2.4 T cell metabolism**

Immunometabolism is a study field that links the metabolic regulation of broad-spectrum immune response. Metabolic regulation of these subsets brought a significant attention in the field of immunotherapy (Buck *et al.*, 2015; Steinert *et al.*, 2021). We have then decided to write a second review to highlight novel information regarding the necessity to provide mitochondrial energetic metabolism of HIV-1-infected patients with diverse sources of carbon substrates, a phenomenon referred to as metabolic plasticity (see our [second review](#) in the appendix II). In these two sub-chapters 2.4 and 2.5, we review previous and new pieces of evidence showing the metabolic profiles that are compatible with better cell survival and functions during persistent HIV-1 infection. In this regard, we point out the fact that cells from EC have a molecular singularity when compared to the other groups of infected patients. We also introduce what we believe to be a novel T cell immune protection correlate against HIV-1 infection. A molecular process called macroautophagy/autophagy. A special emphasis on the balance between metabolic plasticity and effective immunity that is impaired in the majority of HIV-1-infected patients, which may open the door for new ideas in the fight against this virus (Saez-Cirion & Sereti, 2021).

### **2.4.1 Plastic metabolism is privileged in protective T cell immunity**

It is well known that the cellular and mitochondrial metabolism dictate the maintenance and functionality of T cells (Buck *et al.*, 2015; Chapman *et al.*, 2020; Loucif *et al.*, 2020). Mitochondria is the cellular powerhouse that plays a key role in energy production within eukaryotic cells. Indeed, it produces almost 95% of the total cellular energetic yield in the form of adenosine triphosphate (ATP) (Spinelli & Haigis, 2018). The physiological process to produce energy within cells is due to two major metabolic processes (see Figure 2.5). The first metabolic cellular process



is called glycolysis. It breaks/convert the glucose into pyruvate or pyruvic acid to be oxidized within the mitochondria (aerobic glycolysis) (Ma & Zong, 2020). Glycolysis is a process that also does not require oxygen molecules (anaerobic glycolysis), which is known to be primarily utilized in an evolutionary point of view of living organisms (Melkonian & Schury, 2021). Anaerobic glycolysis is the fastest energetic source for all cells to produce two molecules of ATP per one molecule of glucose within few minutes. Depending on the physiological condition and the environmental stress, glycolysis could bypass pyruvate oxidation to a lactate fermentation pathway, a condition called glucose dependency or Warburg effect (Rabinowitz & Enerback, 2020).

The second metabolic process is the mitochondrial respiration or mitochondrial oxidative phosphorylation (OxPhos). Mitochondria is a potent cellular powerhouse organelle that solicit aerobic metabolic process. It produces up to 36 ATP molecules through the shuttling of electrons within the respiratory chain (34 ATP molecules) in tandem with the mitochondrial Krebs cycle (or tricarboxylic acid/TCA cycle) via incorporating acetyl coenzyme A (Acetyl-CoA) and reducing equivalents (2 ATP molecules). It starts with OxPhos where oxidizing multiple organic substrates including glycolysis-derived pyruvate, amino acid and fatty acids is taken place within the mitochondria. Various enzymes depending on the type of the substrates mediate these up-stream catabolic reactions. For instance, glutaminolysis, a process that catabolizes glutamine into glutamate mediated by glutaminase (GLS). Other key enzymes such as carnitine palmitoyltransferase 1A (CPT1A), which is essential for the beta-fatty acid oxidation (FAO), is also critical for catalyzing specifically long-chain fatty acids (C<sub>16</sub>) import into mitochondria. Overall, in the context of metabolic regulation, glycolysis, amino acids and fatty acid are key interconnected pathways, which confer optimal T cell metabolic plasticity.

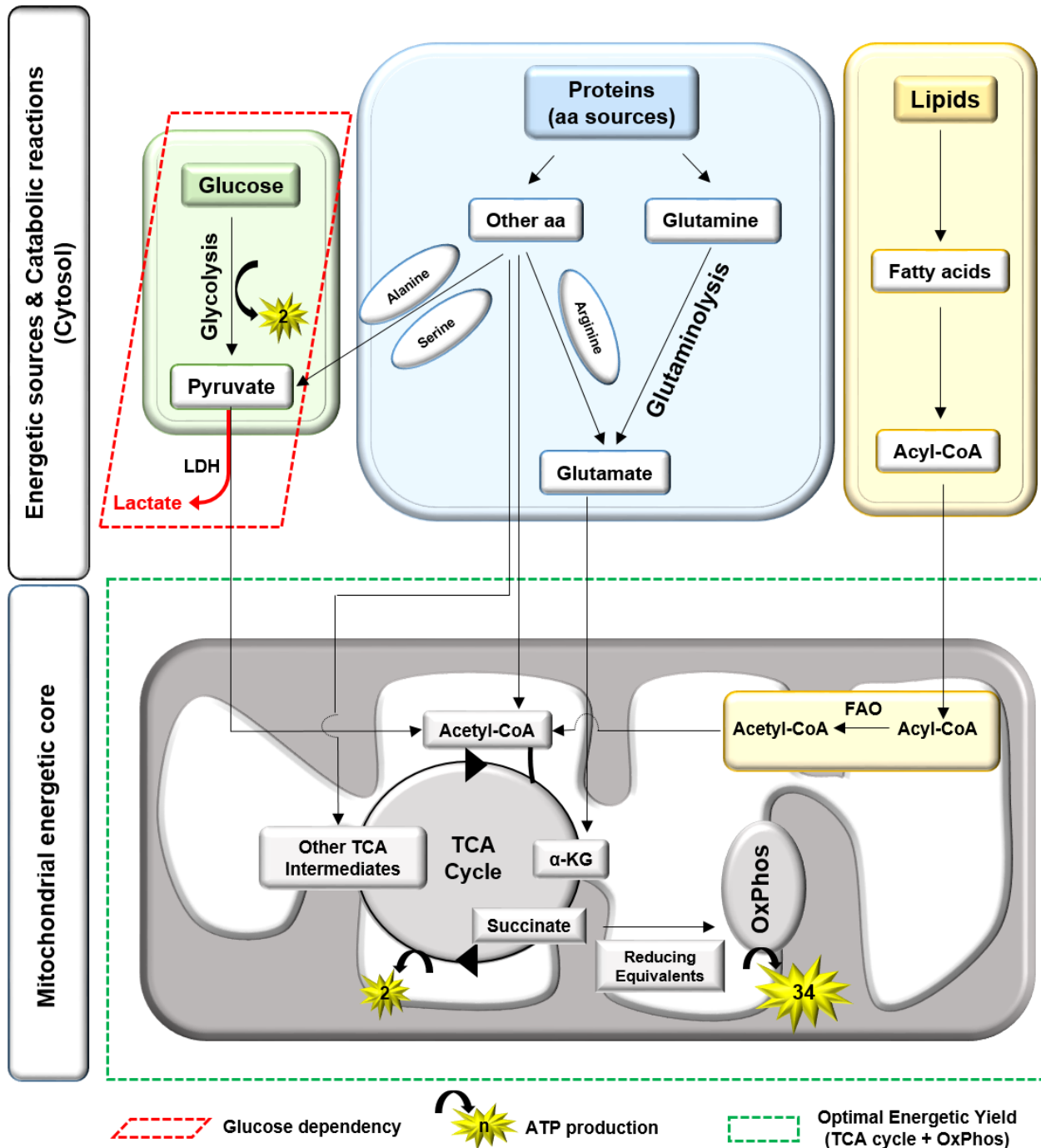


Figure 2.5 Schematic representation of key carbon-based substrates and their catabolic pathways that fuel the mitochondrial respiration (Taken from (Loucif *et al.*, 2020)).

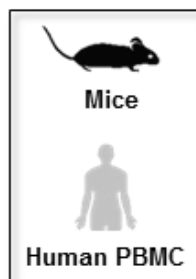
Abbreviations: Acetyl-CoA, acetyl coenzyme A; Acyl-CoA, acyl-coenzyme A; Aa, amino acids; ATP, adenosine triphosphate;  $\alpha$ -KG,  $\alpha$ -ketoglutarate; FAO, fatty acid oxidation; OxPhoS, oxidative phosphorylation; TCA, tricarboxylic acid.

The cell's ability to respond to energetic demand can be an indicator of cell fitness or flexibility. Indeed, glucose is one of the main nutrients from which cells extract energy. Nevertheless, studies showed that plastic mitochondrial metabolism and highly dynamic mitochondria is associated with a wide range of cellular specific functions (Klein Geltink *et al.*, 2017; Li *et al.*, 2020). It is well established that this criterion to use multiple carbon sources other than glucose is called metabolic plasticity. This ability of the cells to fuel mitochondrial metabolism also enables necessary adaptation to stress conditions (Loucif *et al.*, 2020). For instance, T cells immunity depends on a plastic metabolism to accommodate the required energetic needs for a specific function (described in details in Table 2.2).

Over the last decade, it is well established now that T cell activation solicit preferentially specific metabolic pathways in a context-dependent manner. Upon T cell receptor engagement, increased glycolytic rates is the hallmark of T cell activation, responding to the high energetic demands for T cells' functionality, proliferation and differentiation (Menk *et al.*, 2018). In addition to the glycolytic activity, increased mitochondrial mass and OxPhos is essential for oxidizing diverse energetic carbon sources to achieve metabolic plasticity (Buck *et al.*, 2015). Some key studies on mice and human PBMCs, unraveled the importance of the main metabolic pathways in CD4 and CD8A T cells immunity. For instance, glutamine, leucine, serine, alanine and arginine are important carbon sources for memory/effector phenotypes in CD4 (includes Treg and Th17 phenotypes), and CD8A T cells (Geiger *et al.*, 2016; Johnson *et al.*, 2018; Ma *et al.*, 2017; Ron-Harel *et al.*, 2019; Ron-Harel *et al.*, 2016). Furthermore, a study showed a differential metabolic programming and responsiveness within CD4 T cells subset themselves. The study demonstrated that quiescent memory subsets showed higher OxPhos compared to naïve subsets. In addition, Long- and Short-chain fatty acids are shown to be critical in producing IL2 and IFNG for proper memory T cell responses marked by elevated oxygen consumption rates and spare respiratory capacity (Jones *et al.*, 2019).

In summary, this metabolic plasticity during T cell activation allows the cells to cover their energetic needs for proliferation and cell division even in the context of glucose restriction. Glycolysis, amino acids, fatty acids are vital metabolic sources for activate T cells maintenance and functionality. It is important to have a deep understanding on how these pathways are being regulated/disturbed in the context of chronic viral infection such as HIV-1.

**Tableau 2.2** List of immune T-cell features that are controlled by different catabolic pathways including glycolysis, glutaminolysis and mitochondrial FAO (Taken from (Loucif *et al.*, 2020)).



Metabolite/ Catabolic player	T-cell phenotype	Experimental Model	Ref(s)
Glycolysis	Lck-dependent T cell activation Polyfunctionality (IFN- $\gamma$ +, TNF- $\alpha$ +) Effector memory CD8 T cells functionality, Cytolytic activity & proliferation		[16]
	Upregulation of IFN- $\gamma$ , GM-CSF, Granzym B, Cyclin D2 Increased Naive CD8 T cells CD89- frequency		[14, 15]
	Increased Effector memory CD8 T cells CD45RA-CD62L- IFN- $\gamma$ production		[17]
	Naive CD4 T cell IL-2 Production Akt Lck-dependent		[13]
Glutaminolysis	Enhanced Th1 polarisation & less Th17 Differentiation IL-17+ RoRyt+ Foxp+		[19]
	CTL potential CD8 T cells IFN- $\gamma$ + IL-2+ Granzym B+ Perforin+ Low expression of KLRG1 and inhibitory receptors PD-1, Tim3, and Lag3		
	Naive CD4 T cell IL-2 Production STAT5 Lck-dependent		[13]
Alanine	Exit from quiescence for: Naive T cell activation & Memory re-stimulation IFN- $\gamma$ , IL-6, IL17 secretion		[21]
Serine	Enhanced effector CD8 T cell reponse IFN- $\gamma$ + CD44+ T cells proliferation		[20]
Arginine	Naive CD8 & CD4 T cells survival & proliferation CD45RA+CCR7+ IFN- $\gamma$ production		[18]
	CD44 <sup>high</sup> CD4 T cells generation		
	Naive CD44 <sup>LOW</sup> & CD4 T cells survival under OVA257-264 peptide immunization		
OxPhos/FAO	CD8 T cell long-term memory survival		[25]
	Memory T cell IL-15 induced generation		[9]
	Prevent proinflammatory CD4 differentiation		[23]
	Naive CD4 T cell IL-2 Production STAT5 Lck-dependent		[13]
	effector CD4 T cell IFN- $\gamma$ + & Treg differentiation High Foxp3 expression & AMPK phosphorylation, low Glut1 expression		[26, 27]
	enhanced memory CD8 T cell TRAF+ Bcl-2low, Cpt1high		[29, 31]
	Downregulation of effector CD8 T cells response IFN- $\gamma$ +		
	Memory CD8+ T cell developement LA <sup>high</sup>		[28]

### 2.4.2 T cell metabolic discrepancies during HIV-1 infection

In the context of HIV-1 infection, emergent key studies during the last decade underlies the importance of considering the cellular and mitochondrial metabolism in sustaining an effective antiviral T cell response. Several key studies validate the importance to unravel the secrets behind the metabolic features within the highly conserved anti-HIV-1 T cell responses observed in EC (Angin *et al.*, 2019; Casado *et al.*, 2020; Kang & Tang, 2020). Many studies in the last decade depicted interesting concepts to define molecular mechanisms that are dysregulated in T cells during HIV-1 infection (see Figure 2.6). Indeed, a persistent inflammatory environment characterizes HIV-1 infection. This hostile environment causes a constant hyper immune activation; especially among T cells. This persistent immune activation places a high metabolic demand on T cells in HIV-1-infected patients. Thus, several metabolic pathways either are deemed either critical for the virus agenda (non-suppressive condition) or deleterious for specific T cell immunity under ART (suppressive condition) (Loucif *et al.*, 2020). For example, glycolysis in tandem with glutaminolysis are critical for the maintenance of HIV-1 fitness in CD4 T cells (Clerc *et al.*, 2019; Hegedus *et al.*, 2014). Whereas, under ART suppression of viral replication, T cells undergoes a high glycolytic activity associated with exhaustion phenotype (Rahman *et al.*, 2021). In fact, Angin *et al.* demonstrated that HIV-1 specific CD8A T cells displayed increased glycolysis associated with reduced mitochondrial respiratory capacity and lower fatty acid uptake from patients under ART regimen (Angin *et al.*, 2019). These results indicated T cells from ART exhibits a Warburg-effect like behavior and they are strictly dependent on glucose. Further studies showed that reduced mitochondrial mass and dysfunctional mitochondrial metabolism is associated with T cells exhaustion (PD-1<sup>+</sup> T cells) in patients under ART regimen (Maagaard *et al.*, 2008; Rahman *et al.*, 2021).

As mentioned in previous sub-chapters, HIV-1 natural controllers EC are living proof of sustained T cell-mediated immune control for HIV-1 that could be possible if we decipher the molecular and metabolic mechanisms responsible for it (see Figure 2.7). Angin *et al.* have also shown that CD8A T cells in EC, in contrast to patients under ART, preserve a potent polyfunctionality in glucose-independent manner (Angin *et al.*, 2019). The authors show that highly polyfunctional HIV-1-specific CD8A T cells require proper use of mitochondria to accommodate their bioenergetics needs. The authors hypothesize that CD8A T-cells in EC display a metabolic plasticity and rely on other metabolic sources, such as fatty acids. It was verified via Bodipy uptake assays that CD8A T cells from EC displayed higher fatty acids uptake than those from patients under ART

regimen. The study also revealed a diverse transcriptomic profiles that indicate several metabolic regulators up/down regulated within CD8A T cells from EC and patients under ART regimen. These findings could open new avenues into investigating the upstream pathways that regulated the metabolic plasticity observed in EC. In another study, Xu *et al.* transcriptomics indicated that autophagy might contribute to the metabolic plasticity within antigen-specific CD8A T cells during chronic lymphocytic choriomeningitis virus infection by providing other carbon substrates such as lipids (Xu *et al.*, 2014). Interestingly, a study indicated that EC showed an increased autophagic potential in their PBMC associated with viral containment (Nardacci *et al.*, 2014). Further studies are needed to confront the role of autophagy in providing diverse carbon sources to fuel the cellular rates of mitochondrial OxPhos.

In summary, persistent HIV-1 infection is associated with altered plasticity of T cell mitochondrial metabolism that is unfortunately not targeted by the current ART regimen. In contrast, metabolic plasticity may contribute to the effective antiviral immune response observed in EC via optimal mitochondrial respiration. Strong evidence points to the possible potential of autophagy in providing other carbon sources that mediates such plasticity.

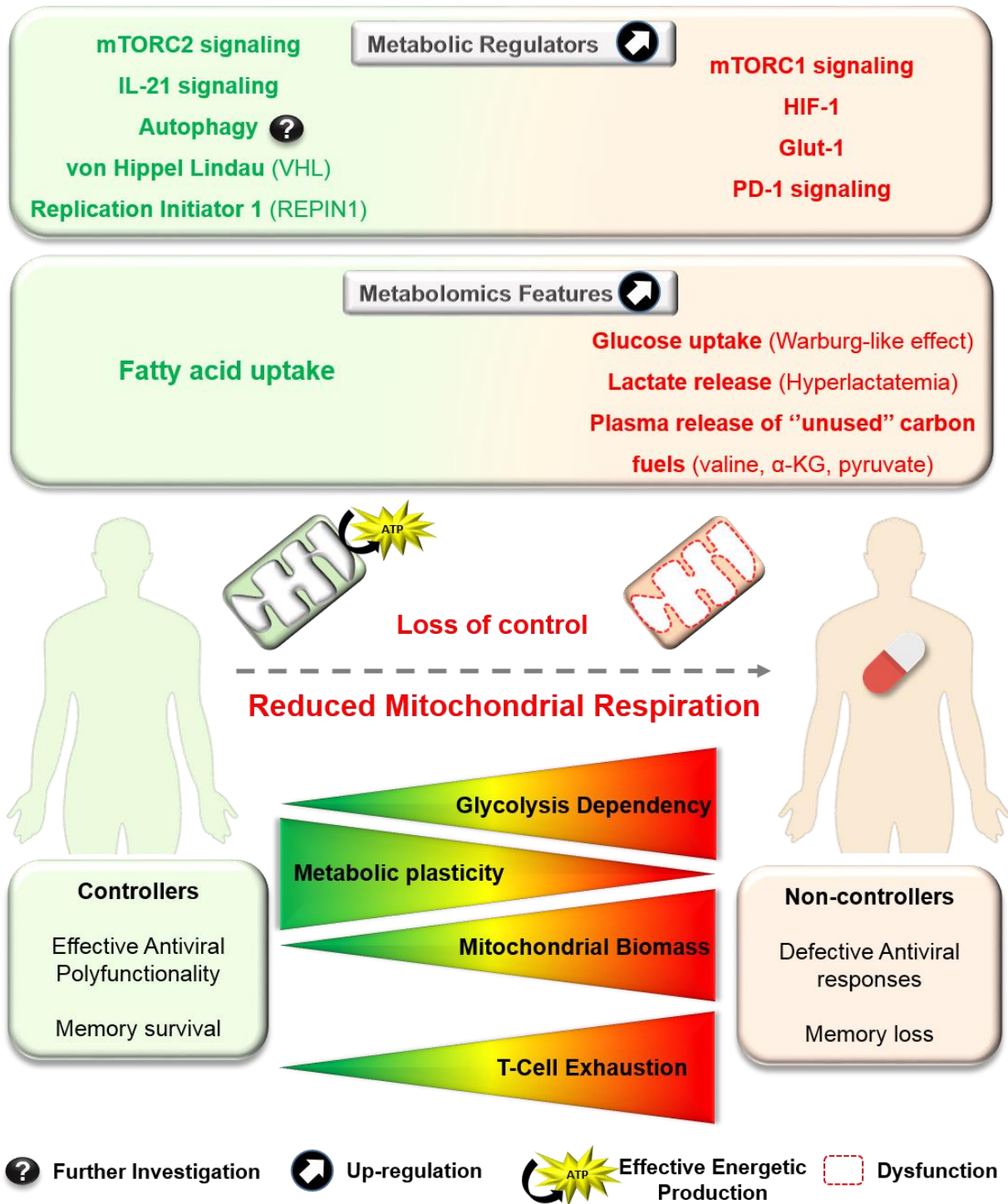


Figure 2.6 Up-regulated metabolites and key metabolic regulators that may confer better antiviral immunity in HIV-1 controllers (in green) when compared to non-controllers patients (in red) (Taken from (Loucif *et al.*, 2020)).

Abbreviations: ATP, adenosine triphosphate;  $\alpha$ -KG,  $\alpha$ -ketoglutarate; Glut-1, glucose Transporter type 1; HIF-1 $\alpha$ , hypoxia inducible factor 1-alpha; OxPhoS, oxidative phosphorylation; PD-1, programmed cell death 1; REPIN1, Replication Initiator 1; VHL: von Hippel Lindau.

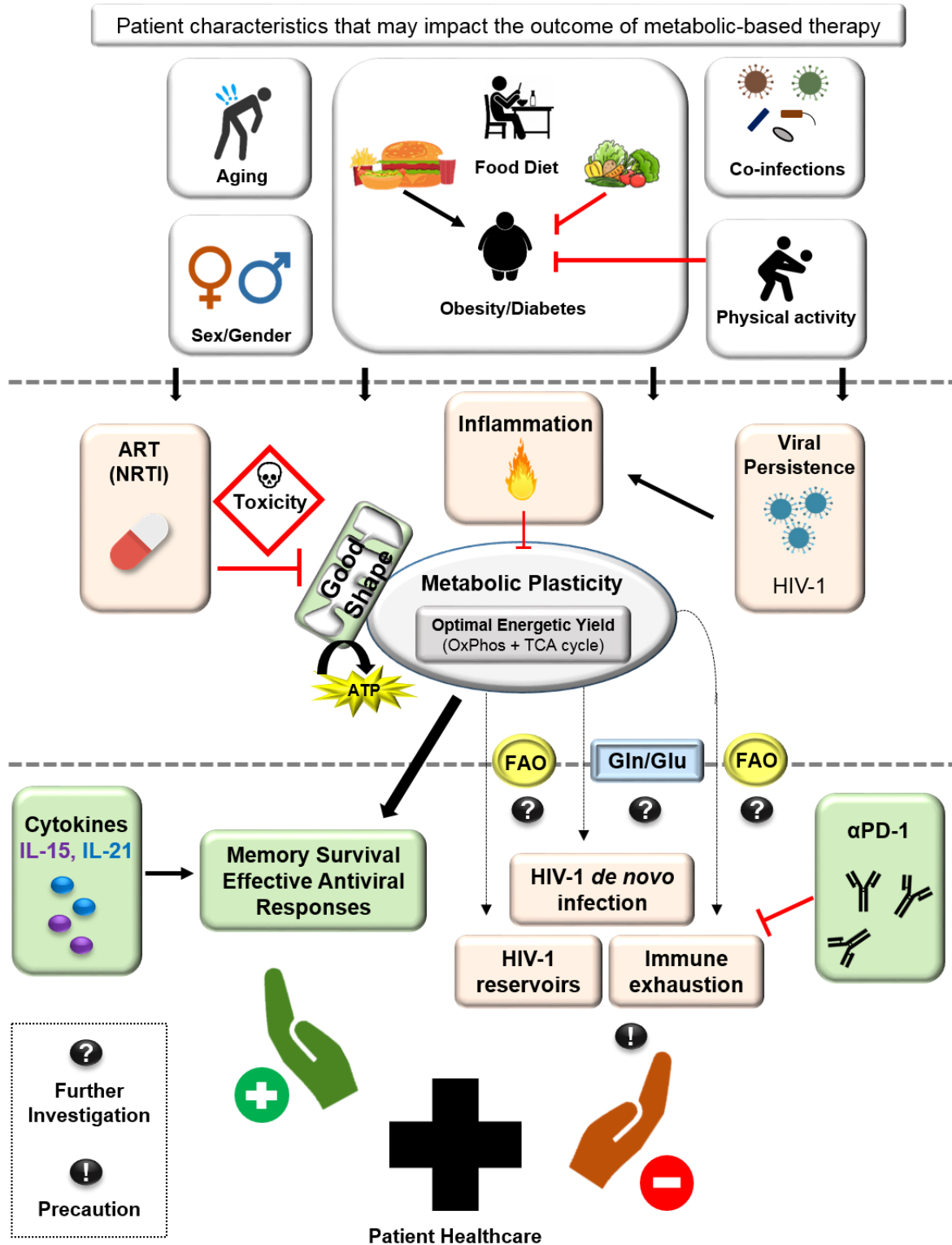


Figure 2.7 Schematic representation of the complexity of designing therapeutic strategies for T-cell metabolic reprogramming during HIV-1 infection (Taken from (Loucif *et al.*, 2020)).

Many factors may contribute or, conversely, prevent successful metabolic reprogramming in specific anti-HIV-1 T-cells. In some instances, patient conditions such as aging or obesity, and ART toxicity may impact



mitochondria integrity and prevent an effective metabolic reprogramming in patients. On the other hand, promoting metabolic plasticity in T-cells may enhance HIV-1 reservoir seeding and exhausted cell maintenance. Abbreviations: ART, antiretroviral therapy; ATP, adenosine triphosphate;  $\alpha$ PD-1, neutralizing anti-programmed cell death 1 antibodies; FAO, Fatty acid oxidation; Gln/Glu, glutamine/glutamate; NRTI, nucleoside reverse transcriptase inhibitor; OxPhoS, oxidative phosphorylation; TCA, tricarboxylic acid.

## 2.5 Macroautophagy/Autophagy

Finally, we were able to pinpoint a particular conserved molecular mechanism, macroautophagy/autophagy, as a potential candidate behind the maintenance of highly effective anti-HIV-1 T cell responses in EC. Autophagy is a conserved catabolic process throughout the eukaryotic cells that degrades damaged intracellular components (cargo) such as mitochondria (mitophagy), misfolded proteins (autophagy-mediated proteolysis) and lipid reserves or lipid droplets (lipophagy) (Doherty & Baehrecke, 2018; Hansen *et al.*, 2018). Briefly, it consists mainly of 5 phases (see Figure 2.8). Upon autophagy induction, a membrane nucleation process is launched to form bowl-like double-membrane structures called phagophores. The latter envelope the targeted intracellular cargos and complete the formation of the double-membrane vacuoles called autophagosomes. Afterward, autophagosome is fused with lysosomal vacuoles to form what is called autophagolysosomes/autolysosomes. The cargos are subsequently degraded via lysosomal lytic activity, and the degraded content is released to the cytoplasm to be processed for further metabolic- or anabolic-related purposes (Hansen *et al.*, 2018). Multiple autophagy-related proteins (ATG) between the different phases mainly regulate autophagic activity. Furthermore, it is induced/inhibited by the two major energy sensors, the mechanistic target of rapamycin kinase (mTOR/MTOR; as an inhibitor) and protein kinase AMP-activated (AMPK; as an activator). AMPK phosphorylates a variety of downstream catabolic and anabolic players, including glucose, fatty acid, and protein metabolism. For example, AMPK provides necessary support for metabolic requirements of hypoglycemic T cells by increasing glutamine uptake and glutaminolysis. It is important to understand the implication of these signaling pathways that regulates the T cell metabolism, which reflects potentially on their specific immunity functions, maintenance and survival.

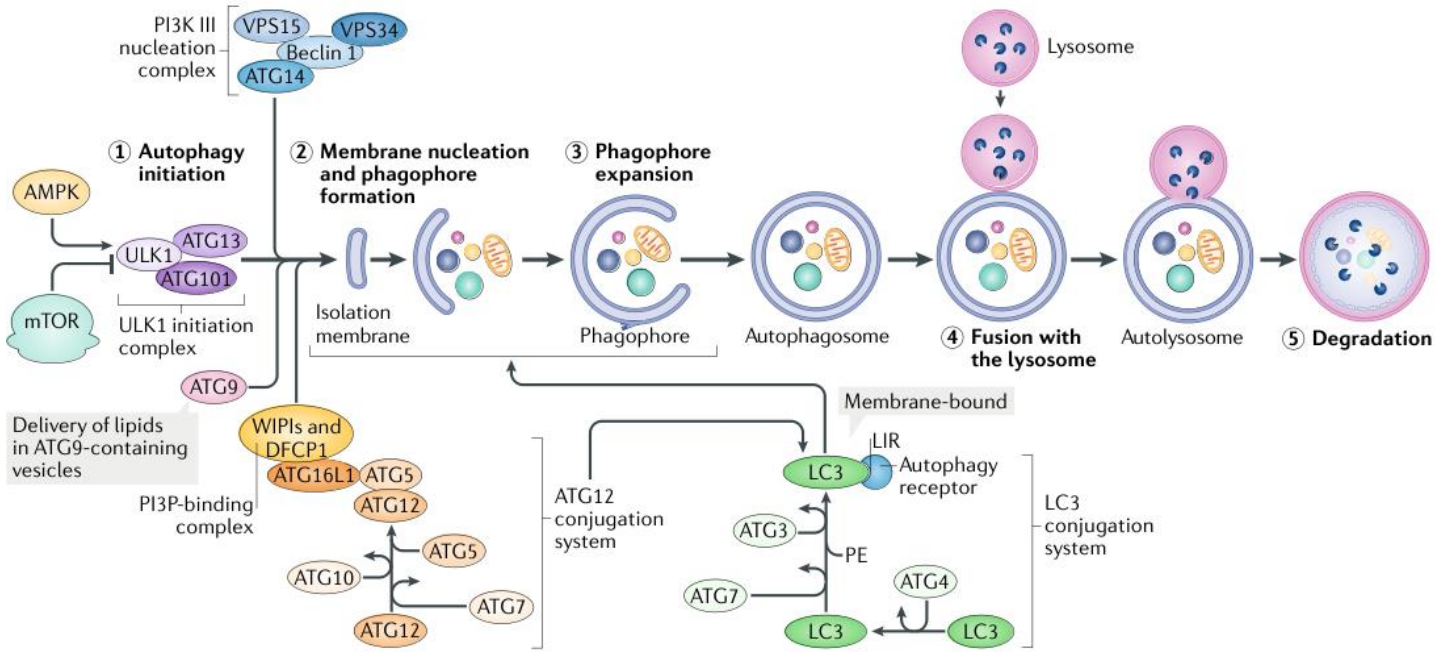


**Figure 2.8** A general schematic representation of autophagy process phases (Taken from (Hansen et al., 2018)).

**Abbreviations:** mTOR/MTOR, mechanistic target of rapamycin kinase; AMPK, protein kinase AMP-activated; ULK1, unc-51 like autophagy activating kinase 1; Beclin 1/BECN1; PI3K/PI3KC3 complex, the Beclin 1–class III phosphatidylinositol 3-kinase complex; ATG, autophagy related protein; LC3/MAP1LC3A, microtubule associated protein 1 light chain 3 alpha; WIPI/WIPI1, WD repeat domain, phosphoinositide interacting 1; DFCP1/ZFYVE1, zinc finger FYVE-type containing 1; PE, phosphatidylethanolamine; LIRs, LC3-interacting motifs; VPS34/PIK3C3, phosphatidylinositol 3-kinase catalytic subunit type 3; VPS15/PIK3R4, phosphoinositide-3-kinase regulatory subunit 4.

### 2.5.1 Autophagy regulation in T cell immunity

Upon TCR engagement, autophagy is an essential catabolic process with a massive metabolic entity that provides T cells homeostasis. The impact of autophagy in T cells survival, maintenance, functionality and differentiation was largely reviewed within the last decade's literature (Lunemann & Munz, 2009; Macian, 2019). Using various mice models with specific autophagy related genes deletions (such as: ATG3, ATG7, BECN1, etc.), studies were able to deduce that autophagy is a central process to maintain mature and antigen-specific T cells' abundance within lymphoid tissues (Puleston *et al.*, 2014a; Xu *et al.*, 2014). Reports further revealed the intricacy of autophagy in memory T cells generation. In addition, autophagy is highly effective as a countermeasure against mitochondrial apoptotic priming, hence apoptotic cell death confirmed using ATG-deficient mice (Arsov *et al.*, 2011). These findings indicate the crosstalk between mitochondrial homeostasis and autophagic activity within activated T cells. Thus, autophagy may play role in coordinating and regulating the mitochondrial metabolic reprogramming upon TCR activation.

In the previous sub-chapter, we indicated that T cells' metabolic plasticity is correlated with effective virus-specific CD8A T cells immunity. Dysfunctional autophagy is the hallmark of many chronic pathologies that involves a persistent inflamed environment, in which T cells are also dysregulated (Ren *et al.*, 2012). Further studies showed that specifically depleting an ATG in CD8A T cells reduces its memory and effector potential against viral infections such as influenza virus and CMV (Puleston *et al.*, 2014a). It is now became a legitimate question to investigate the central role of autophagy in regulating the metabolic program to execute an effective T cells antiviral responses. Further studies are needed to pinpoint the upstream molecular mechanisms that regulates autophagy in the context of T cell activation. The cross talk between conventional energy sensors and regulators of autophagy such as AMPK and MTOR should also be included (Kim *et al.*, 2011).

Finally, it is important to consider the circumstance behind the specific substrate selection for the lysosomal degradation in different context. Selective autophagy may appear to be context-dependent in accordance to the metabolic requirements for T cells immunity.

### **2.5.2 Autophagy as a novel immune correlate in HIV-1 natural immune protection**

As Nardacci *et al*, mentioned in their manuscript in 2014, that autophagy potential is upregulated and confers a steady viral containment in HIV-1 controllers compared to other infected groups (Nardacci *et al.*, 2014; Nardacci *et al.*, 2017). Although the study did not include patients under ART treatment, it is worth mentioning that it was the first study to indicate that autophagy could potentially represent a natural immune protection correlate against HIV-1 infection. Furthermore, their supplementary figure 1 pointed to a potential highly active autophagy within T cells populations. In another study showed that autophagy is activated upon T cell receptor (TCR) engagement (Botbol *et al.*, 2015). As a reminder, autophagy is well known to maintain T cells homeostasis and metabolism during chronic viral infections (Xu *et al.*, 2014). These pieces of evidence led us to investigate the versatile role of autophagy in regulating the mitochondrial metabolism leading to highly effective anti-HIV-1 T cell responses in EC.



### 3 HYPOTHESIS AND OBJECTIVES

---

In line with the extensive literature review, numerous pieces of evidence led us to convincingly hypothesize that **autophagy represents a potential and a novel immune correlate in HIV-1 natural controllers**. Furthermore, it confers a **versatile role in regulating the mitochondrial metabolism for protective antiviral T cell responses**.

It is important to investigate the levels of autophagy activity and its impact on the mitochondrial oxidative metabolism and T cell functionality in EC. Validating these findings will inform us to the ideal approach to the possibility to reinvigorate T cell dysfunctions observed in patients under ART treatment. We first need to investigate the most common feature of immune correlates in HIV-1 natural controllers, which is the highly functional CD8A T cells. Then, we aimed to look into the correlation of a possible cellular communication between highly functional CD8A T cells and IL21-secreting memory CD4 T cells (Mem). The latter might also depend on highly active autophagy in order to secrete IL21 efficiently. To succeed at such endeavor, we devised the study into the following several aims:

**Aim 1.** Measurement of autophagy activity in virus-specific (including HIV-1) and polyclonally activated CD8A T cells and Mem in Elite controllers (EC) compared to ART patients (ART) and non-infection controls (HIV<sup>neg</sup>).

**Aim 2.** Investigating the regulation of autophagy on the intracellular rates of mitochondrial oxidative metabolism and immunity in activated CD8A T cells and Mem.

**Aim 3.** Identifying the underlying upstream pathway(s).

## 4 FIRST ARTICLE: IMPACT OF AUTOPHAGY-MEDIATED LIPID METABOLISM IN HIV-1-SPECIFIC CD8 T-CELLS IMMUNITY

---

### **Lipophagy confers a key metabolic advantage that ensures protective CD8A T-cell responses against HIV-1**

La lipophagie confère un avantage métabolique clé qui assure des réponses protectrices des lymphocytes T CD8A contre le VIH-1

**Authors:** Hamza Loucif<sup>1</sup>, Xavier Dagenais-Lussier<sup>1</sup>, Cherifa Beji<sup>1</sup>, Léna Cassin<sup>1</sup>, Hani Jrade<sup>2-4</sup>, Roman Tellitchenko<sup>1</sup>, Jean-Pierre Routy<sup>5</sup>, David Olnagier<sup>6</sup>, and Julien van Grevenynghe<sup>1</sup>

<sup>1</sup> Institut national de la recherche scientifique (INRS)-Centre Armand-Frappier Santé Biotechnologie, 531 boulevard des Prairies, Laval, QC, Canada, H7V 1M7;

<sup>2</sup> Ottawa Hospital Research Institute, Regenerative Medicine Program, Ottawa ON, Canada, K1H 8L6;

<sup>3</sup> Department of Cellular and Molecular Medicine, University of Ottawa, Ottawa, ON, Canada, K1H 8M5;

<sup>4</sup> Ottawa Institute of Systems Biology, Ottawa, ON, Canada, K1H 8M5;

<sup>5</sup> Chronic Viral Illness Service and Division of Hematology, McGill University Health Centre, Glen site, Montreal, Quebec, Canada, H4A 3J1;

<sup>6</sup> Aarhus University; Department of Biomedicine, Research Center for Innate Immunology, Aarhus C, 8000, Denmark.

**Journal:** Autophagy

**Received** 18 Oct 2020, **Accepted** 06 Jan 2021, **Published online:** 18 Jan 2021

<https://doi.org/10.1080/15548627.2021.1874134>

**Authors' contribution:**

**H.L.** performed the experiments and analyzed the data. **X.D.L.**, **C.B.** and **L.C.** helped with a technical assistance for some experiments. **H.J.** helped with a technical assistance in ImageStreamX lipophagy validation experiment. **J-P.R.** contributed to the inclusion of study participants, obtaining clinical information and its validation. **J.V.G.** designed and supervised the

study. **H.L., X.D.L., R.T., O.D.** and **J.V.G.** drafted the article. All the authors critically reviewed the manuscript.

#### **4.1 Abstract**

Although macroautophagy/autophagy has been proposed as a critical defense mechanism against HIV-1 by targeting viral components for degradation, its contribution as a catabolic process in providing optimal anti-HIV-1 immunity has never been addressed. The failure to restore proper antiviral CD8A/CD8 T-cell immunity, especially against HIV-1, is still the major limitation of current antiretroviral therapies. Consequently, it is of clinical imperative to provide new strategies to enhance the function of HIV-1-specific CD8A T-cells in patients under antiretroviral treatments (ART). Here, we investigated whether targeting autophagy activity could be an optional solution to make this possible. Our data show that, after both polyclonal and HIV-1-specific activation, CD8A T-cells from ART displayed reduced autophagy-dependent degradation of lysosomal contents when compared to naturally HIV-1 protected elite controllers (EC). We further confirmed in EC, by using specific *BECN1* gene silencing and lysosomal inhibitors, the critical role of active autophagy in superior CD8A T-cell protection against HIV-1. More importantly, we found that an IL21 treatment was effective in rescuing the antiviral CD8A T-cell immunity from ART in an autophagy-dependent manner. Finally, we established that IL21-dependent rescue occurred due to the enhanced degradation of endogenous lipids via autophagy, referred to as lipophagy, which fueled the cellular rates of mitochondrial beta-oxidation. In summary, our data show that autophagy/lipophagy can be considered as a therapeutic tool to elicit functional antiviral CD8 T-cell responses. Our results also provide additional insights towards the development of improved T-cell-based prevention and cure strategies against HIV-1.





## 4.2 Introduction

The maintenance of polyfunctional CD8A/CD8 T-cell responses, especially against human immunodeficiency virus type-1 (HIV-1), is associated with better viral control and slower disease progression [1]. Polyfunctional CD8A T-cells are defined by their ability, upon activation, to secrete multiple cytokines simultaneously with cytotoxic molecules such as PRF1 (perforin 1) and GZMB (granzyme B) [2]. However, despite successful viral suppression, patients under antiretroviral therapies (ART) display defective antiviral CD8A T-cells with reduced polyfunctional responses when compared to elite controllers (EC) [3-7]. EC, who are able to maintain a natural control of HIV-1 due to strong antiviral CD8A T-cell responses, can help in the design of new strategies aiming at reinforcing CD8A T-cell immunity in ART [8].

Recently, Angin M. et al. have shown that antiviral CD8A T-cells from ART display a restrictive glucose dependency, which is a distinct metabolic defect not observed in EC [4]. In this study, the authors suggest that the superior CD8A T-cell immunity found in EC might be explained by their ability to use additional metabolic resources other than glucose. This consequently allows them to sustain effective mitochondrial respiration with high ATP production. This immune advantage, referred to as metabolic plasticity, has to be achieved in ART through the design of new strategies, but the molecular mechanisms responsible for it need to first be clarified among EC. In cancer, data show that the diverse metabolic fuel sources that can be produced by macroautophagy/autophagy, a lysosomal-dependent catabolic process, provide tumors with metabolic plasticity [9-11]. Since previous observations have proposed that autophagy may contribute to limiting HIV-1 pathogenesis in EC by targeting viral components for degradation, we raised the question of whether it could rather provide their CD8A T-cells with metabolic plasticity and superior antiviral immunity [12,13]. In the present study, we showed that following polyclonal and antigen-specific cell activation, CD8A T-cells from ART displayed reduced autophagic activity when compared to EC. Using specific gene silencing of *BECN1*, one major regulator of autophagic activity, we confirmed the critical role of this catabolic process in highly functional CD8A T-cell responses in EC [14]. We demonstrated that IL21 production by CD4 T-cells, which was lower in ART when compared to EC, was associated with the levels of autophagic activity in CD8A T-cells [15]. Our data further confirmed that IL21 addition in ART's cultures was effective in rescuing their antiviral CD8A T-cells in an autophagy-dependent manner. More precisely, we found that the IL21-mediated rescue was specifically provided due to increased lipophagy, which

describes the autophagic degradation of endogenous lipids [16-18]. Finally, we concluded our study by confirming in CD8A T-cells from ART that the enhanced lipophagy following IL21 treatment impacted the cellular energetic balance directly through lipid breakdown and fatty acid beta-oxidation (FAO).

Altogether, this study puts lipophagy at the center of the molecular pathway by which IL21 signaling leads to enhanced mitochondrial metabolism in protective CD8A T-cell immunity during persistent HIV-1 infection. Our results also provide new information to consider for the development of effective T cell-based vaccines and cure strategies against HIV-1, where effective HIV-1-specific CD8A T-cell responses are warranted [19-22].

### **4.3 Results**

#### **4.3.1 Confirmation of reduced autophagic activity in HIV-1-specific CD8A T-cells from ART.**

Autophagy is a highly dynamic intracellular degradative system that involves the capture, isolation and lysosomal digestion of intracellular materials in specialized structures called autolysosomes (ALs) [23]. Although previous findings suggest that autophagy in EC may be associated with virologic benefits by targeting HIV-1 components for degradation, no information is available regarding the potential immunological advantage that autophagy may provide in EC, especially in their antiviral CD8A T-cells [12,13].

We decided to use several complementary methods to assess autophagy in CD8A T-cells from all study groups such as multi-parameter and ImageStream flow cytometry, pulse-chase assay, and electron microscopy. First and foremost, we validated all methods by using CD8A T-cells from HIV<sup>neg</sup> donors (n = 10) that have been starved for 2 h, which is the most common way to increase autophagic activity in culture (Fig. S1A-D). As expected, we found significant increases in the expression levels for the autophagy-related protein BECN1 (beclin 1) and SQSTM1 (sequestosome 1) (Fig. S1A). Our data also showed increased autophagy-dependent lytic activity in starved CD8A T-cells by using a pulse-chase assay method that has previously been developed on macrophages (Fig. S1B) [24]. Then, by using Imaging flow cytometry, we evaluated the lysosomal content of MAP1LC3/LC3 (microtubule associated protein 1 light chain 3) protein [25], which was also shown increased under starvation. This was determined by the colocalization index of fluorescently labeled LC3 and lysosomal marker Lyso-ID, which is called bright detail similarity (BDS) (Fig. S1Ci-iii). However, in agreement with the previous observations that were also generated on CD8 T-cells [25], we did not find any difference in LC3 puncta counts after

cell starvation (Fig. S1Civ). This indicated that, due to the nature of lymphocytes (displaying almost no cytoplasm compartment) and the limitation of the Imaging-based assay, LC3 puncta counts could not be used as a quantitative and reproducible indicator values of CD8A T-cell-related autophagy.

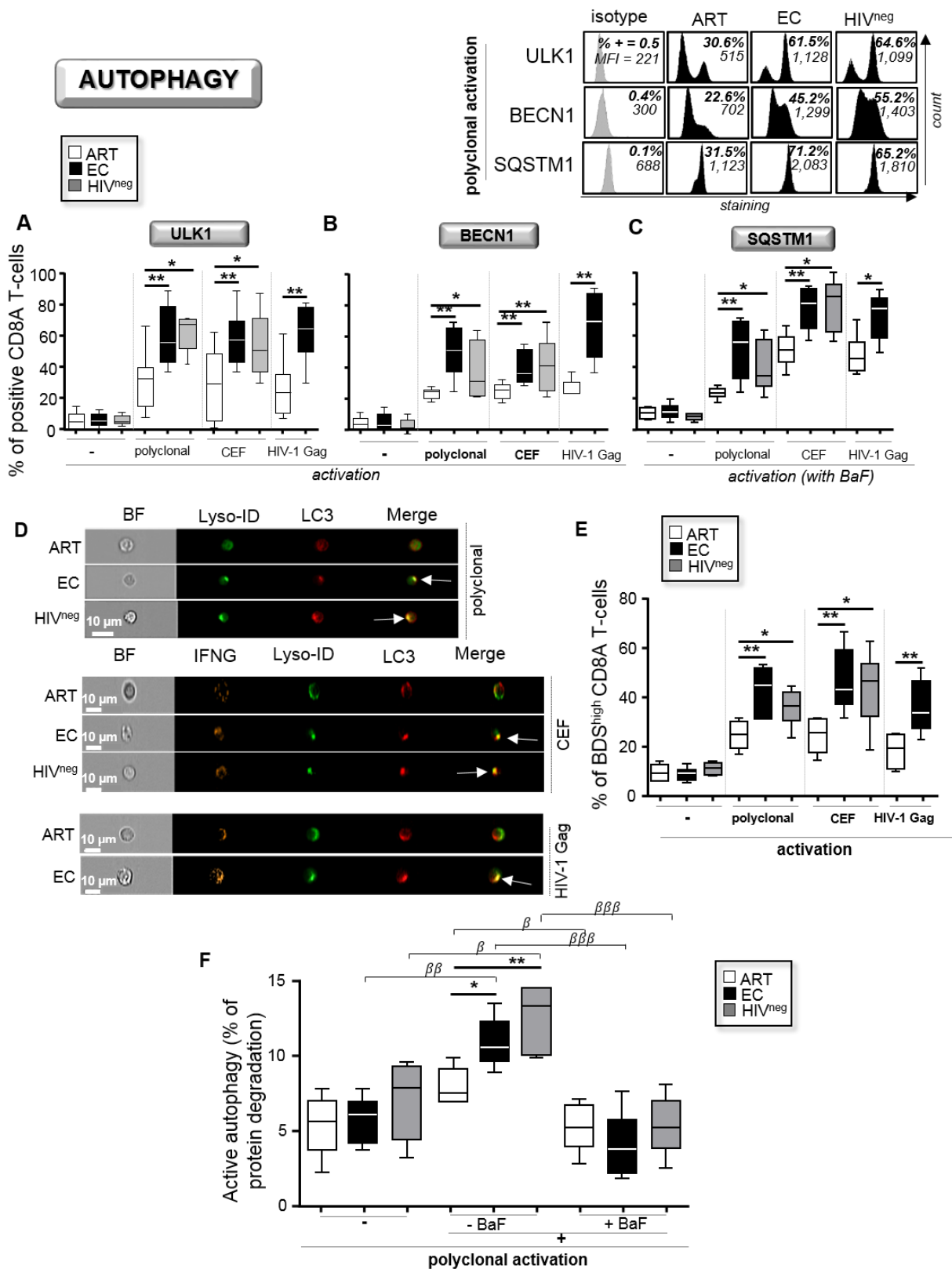


**Figure 4.1** Reduced autophagic activity in ART after CD8A T-cell activation.

(A-E) CD8A T-cells from ART, EC and HIV<sup>neg</sup> were either polyclonally or antigen-specifically (CEF peptides or Gag antigens) activated and cultured without activation for 6 h (n = 6). Of note, antigen-specific CD8A T-cells were identified at 6 h post-activation by positive staining for IFNG. The percentages of positive cells were then determined in CD8A T-cells for the autophagy-related players (A) ULK1 and (B) BECN1. (C) We also assessed the percentages of SQSTM1<sup>+</sup> CD8A T-cells when lysosomal activity was blocked by BaF during the culture. Representative histograms including isotype controls after 6 h of post-polyclonal activation are also shown above. (D and E) Lysosomal content of LC3 determined by Imaging flow cytometry. (D) Representative images of single CD3W<sup>+</sup> CD8A<sup>+</sup> (polyclonal activation) and CD3W<sup>+</sup> CD8A<sup>+</sup> IFNG<sup>+</sup> T-cells (CEF and HIV-1 activations) merged for fluorescent signals from LC3 and Lyso-ID. BF, bright field. (E) Percentages of BDS<sup>high</sup> LC3<sup>+</sup> Lyso-ID<sup>+</sup> CD8A T-cells in ART, EC and HIV<sup>neg</sup>. The colocalization index BDS stands for bright detail similarity. (F) Autophagy-dependent proteolytic degradation of long-lived proteins determined in purified CD8A T-cells after polyclonal activation in the presence or absence of BaF, by using a pulse-chase approach.  $\beta$ , symbol used for paired t test (comparison between treated CD8A T-cells and their untreated control). \*, symbol used for Mann-Whitney test (comparison between study groups). One symbol,  $0.05 > P > 0.01$ ; two symbols,  $0.01 > P > 0.001$ ; and three symbols,  $0.001 > P > 0.0001$ .

Once validated, we assessed the levels of protein expression of the two key autophagy-related genes, ULK1 and BECN1, in ART and compared them to those from age-matched EC and uninfected donor controls (HIV<sup>neg</sup>). The expression levels of ULK1 and BECN1 were determined by multiparameter flow cytometry in CD8 T-cells after 6 h of polyclonal and antiviral activations. To elicit antiviral activations, we used a combined CEF peptide pool (cytomegalo-virus with Epstein-Barr and flu viruses) or HIV-1 Gag. Antigen-specific CD8A T-cells were determined by their positive staining for IFNG/IFN- $\gamma$ , following the antiviral activations, as previously done [26]. Of note, we did not find any difference in the percentage of antigen-activated CD8A T-cells represented as IFNG<sup>+</sup> cells between ART and EC, and we used HIV<sup>neg</sup> as a negative control for HIV-1 Gag stimulation (Fig. S1E and S1F). In addition to ULK1 and BECN1, we decided to investigate intracellular accumulation of the SQSTM1, when cells were cultured with BaF. Our data showed that basal levels of ULK1, BECN1 and SQSTM1, as determined by the percentages of positive cells, were similar in non-activated CD8A T-cells for all study groups (Fig. 1A-C). In contrast, after both polyclonal and antiviral activations, we found that the expression levels for all molecules were significantly reduced in ART when compared to EC and HIV<sup>neg</sup>.

We next used an ImageStream-based autophagy assay. Our data showed reduced lysosomal content of LC3 in activated CD8A T-cells from ART (Fig. 1D and 1E). We further quantified the autophagy-dependent lytic activity as previously done in macrophages, but performed here in CD8A T-cells after 6 h of polyclonal activation with or without BaF [24]. Once again, our results showed that activated CD8A T-cells from ART displayed lower percentages of autophagy-dependent degradation when compared to EC and HIV<sup>neg</sup> (Fig. 1F). We decided to use this pulse-chase assay for the rest of our study to appreciate autophagic activity in CD8A T-cells. Indeed, not only did we confirm the efficacy of BaF in blocking autophagic activity with the assay (Fig. 1F),

but we also found that the results positively correlated with the expression levels of ULK1, BECN1 and SQSTM1, as well as with the lysosomal content of LC3 (Fig. S2).

Finally, we analyzed the polyclonally-activated CD8A T-cells for all study groups at the ultrastructural level. Similarly to others, we used electron microscopy to evaluate the number of both autophagic vacuoles (AV) and ALs [12]. In contrast to AV that were identified as a double-membrane-structure containing undigested cytoplasmic material, ALs were generated by the fusion (complete or in progress) of the autophagic vacuoles with the lysosomes and were limited by a single membrane (Fig. 2A). We validated the use of this method by starving CD8A T-cells from HIV<sup>neg</sup> donors (n = 3), which showed increased AL numbers (Fig. S1D). Our data showed that activated CD8A T-cells from ART displayed less AV and ALs than those of EC and HIV<sup>neg</sup> (as determined by both numbers and percentages of positivity per 40 cells) (Fig. 2B-E). Altogether, our results indicate that antiviral CD8A T-cells from ART, including those specific to HIV-1, display reduced autophagic activity along with lower numbers of ALs when compared to EC.

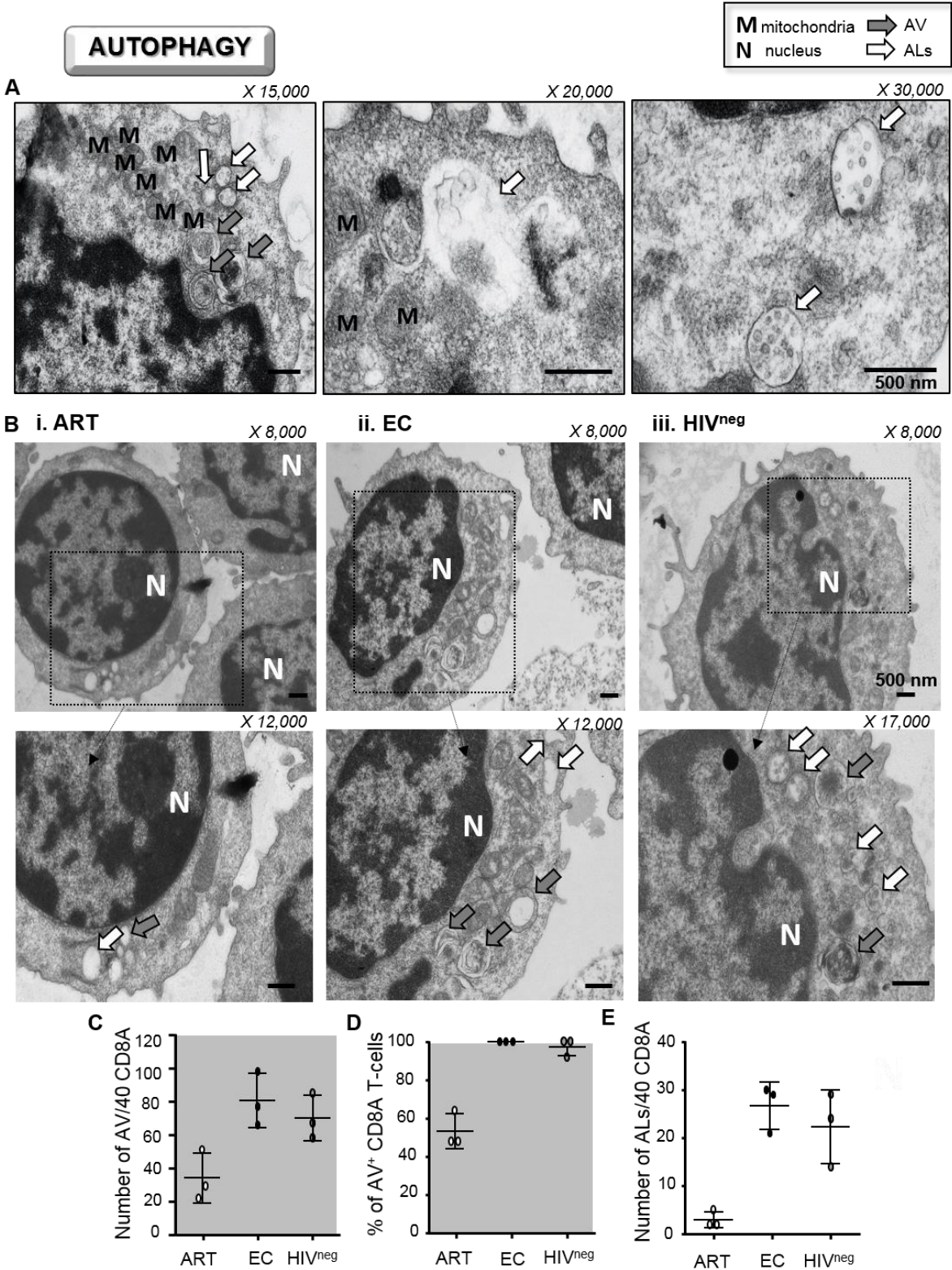


**Figure 4.2 Lower amounts of ALs in activated CD8A T-cells from ART.**

**(A-E) Ultrastructural analysis of purified CD8A T-cells from ART, EC and HIV<sup>neg</sup> after 6 h of polyclonal activation (n = 3). (A) Representative ultrastructural micrographs from uninfected controls to differentiate AV (autophagic**



vacuoles; gray arrows) from ALs (autolysosomes; white arrows). (B) Ultrastructural micrographs in i. ART, ii. EC and iii. HIV<sup>neg</sup> including strategic magnifications to appreciate the numbers of cellular vacuoles (X 8,000–17,000). Quantitative analysis of (C) the number and (D) percentages of positive CD8A T-cells for AV per 40 cells. (E) Number of ALs per 40 CD8A T-cells.

#### 4.3.2 Strong autophagy in EC drives their anti-HIV-1 CD8A T-cell polyfunctionality.

Given the key role that autophagy plays in protective CD8A T-cell immunity with mouse models of viral infection, it was reasonable to believe that it may be involved in natural immune protection against persistent HIV-1 infection as well [27].

To investigate whether autophagy was responsible for enhanced antiviral CD8A T-cell responses in EC, we specifically inhibited BECN1 expression using small interfering silencing RNAs (siRNA). Briefly, purified CD8A T-cells from all study groups were either electroporated or transfected with siRNA specific for *BECN1* or with negative control siRNA for 2 h. Then, cells were washed twice and cultured with their autologous CD8A-depleted PBMC (ratio CD8A:PBMC = 1:5). At 24 h post-transfection, cells were activated either polyclonally or specifically for an additional 6 h. At 6 h post-activation, we finally determined both the expression levels of BECN1 and cell apoptosis in CD8A T-cells by multi-parameter flow cytometry. Electroporation alone or transfection with negative siRNA did not affect BECN1 expression when compared to cells that were not electroporated. In contrast, CD8A T-cells that were transfected with *BECN1* siRNA displayed up to 86.1% and 82.5% reductions of BECN1 expression, respectively in EC and HIV<sup>neg</sup> (Fig. 3Ai and S3A-C). In fact, *BECN1* silencing in EC and HIV<sup>neg</sup> led to reductions of its protein expression to levels comparable to ART. Of note, we found similar percentages of cell apoptosis for all conditions of electroporation or transfection, regardless of the study groups (Fig. 3Aii). We further investigated whether specifically interfering with BECN1 expression in activated CD8A T-cells led to reduced autophagic activity. We also used the lysosomal inhibitors BaF and chloroquine (Chloro.), which are potent and well-acknowledged inhibitors of cellular autophagy by targeting lysosomal activity, as controls. Levels of active autophagy in activated CD8A T-cells that were electroporated or transfected with negative control siRNA were similar to those of cells that were not electroporated. Following polyclonal or antiviral activations, our data confirmed that both specific *BECN1* silencing and lysosomal inactivation led to significant reductions of active autophagy in EC and HIV<sup>neg</sup> to levels comparable to ART (Fig. 3B).

Next, using multi-parameter flow cytometry, we determined in activated CD8A T-cells from EC, ART, and HIV<sup>neg</sup> whether *BECN1* gene silencing and lysosomal inactivation could impact their antiviral immune responses. To this aim, we first analyzed the cells' ability to produce antiviral

cytokines (IFNG and IL2) and cytotoxic molecules (PRF1, GZMA and GZMB) with or without autophagy inhibition (Fig. S3D). When autophagy was untouched in CD8A T-cells, we found that both polyclonal and antiviral activations led to higher percentages of PRF1<sup>+</sup> and GZMB<sup>+</sup> cells in EC and HIV<sup>neg</sup> when compared to ART (Fig. 3C and 3D). In contrast, targeting active autophagy in activated CD8A T-cells from EC and HIV<sup>neg</sup>, by *BECN1* gene silencing or with lysosomal inhibitors, both led to significant reductions of both PRF1 and GZMB productions to levels comparable to ART (Fig. 3C and 3D). Of note, we did not find any differences between EC, ART and HIV<sup>neg</sup> for the single production of IFNG, IL2 and GZMA, even when autophagy was inhibited.

Finally, we assessed CD8A T-cell polyfunctionality including in HIV-1-specific cells for all study groups and treatments. Polyfunctional CD8A T-cells, which were characterized by their ability to produce multiple cytokines and cytotoxic molecules in addition to IFNG, are highly predictive of protective immunity against pathogens including HIV-1 [2-6]. In contrast, we characterized monofunctional CD8A T-cells by their single staining for IFNG. Our data showed that, when autophagy was untouched, activated CD8A T-cells in EC and HIV<sup>neg</sup> displayed superior cell polyfunctionality. This was illustrated by higher percentages of cells producing three or more molecules along with reduced percentages of monofunctional cells, when compared to ART (Fig. 3E). Once again, autophagy inhibition in EC and HIV<sup>neg</sup>, regardless of the method used, led to significant inhibition of CD8A T-cell polyfunctionality to levels that were comparable to ART. Overall, our results demonstrate a critical role of active autophagy in the superior CD8A anti-HIV-1 potential, as determined by cell polyfunctionality and production of cytotoxic molecules.

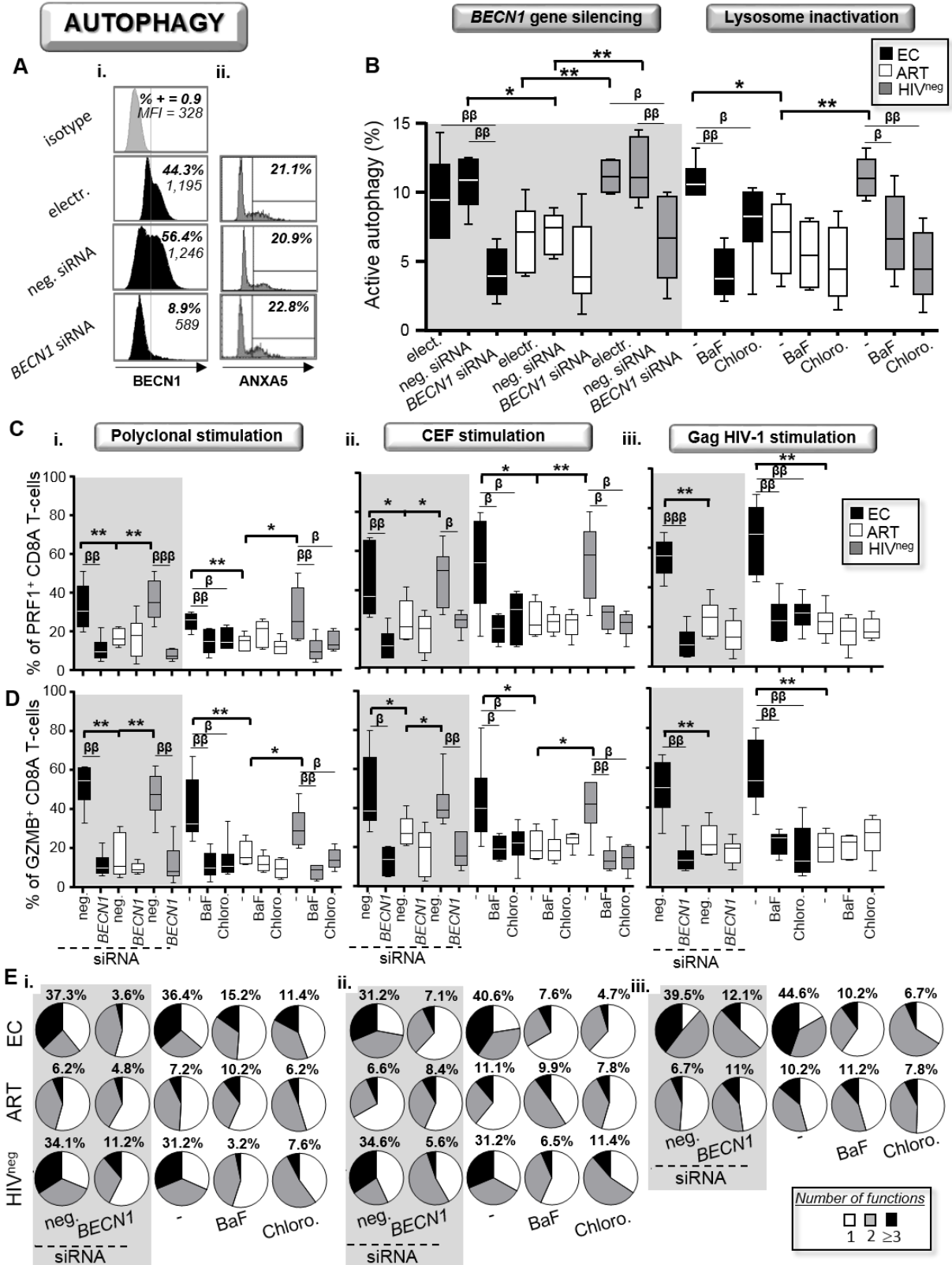


**Figure 4.3** Active autophagy plays a key role in antiviral CD8A immunity during HIV-1 infection.

(A-E) Active autophagy and effector function were both determined in activated CD8A T-cells under specific *BECN1* gene silencing or lysosomal inactivation with Baf or Chloro (n = 6). (A) Representative histograms of i. *BECN1* expression and ii. ANXA5 staining in transfected CD8A T-cells from EC at 6 h post-polyclonal activation. (B) Autophagy-dependent proteolytic degradation of long-lived proteins assessed in polyclonally activated CD8A T-cells when active autophagy was inhibited or not. Percentages of (C) PRF1<sup>+</sup> and (D) GZMB<sup>+</sup> CD8A T-cells in the context of autophagy blockade. Results were shown in the context of i. polyclonal, ii. CEF-specific and iii. HIV-1-specific activation. (E) Pie chart representations of CD8A T-cell polyfunctionality that were determined after i. polyclonal and ii and iii. antigen-specific activations with or without autophagy blockade. Percentages of highly functional CD8A T-cells (expressing three or more antiviral cytokines and cytotoxic molecules in addition to IFNG) were also indicated in bold for all study groups and conditions.  $\beta$ , symbol used for paired t test (comparison between treated CD8A T-cells and their untreated control). \*, symbol used for Mann-Whitney test (comparison between study groups). One symbol, 0.05 > P > 0.01; two symbols, 0.01 > P > 0.001; and three symbols, 0.001 > P > 0.0001.

#### 4.3.3 IL21 enhances antiviral CD8A T-cell responses from ART in an autophagy-dependent manner.

We investigated whether autophagy in activated CD8A T-cells during HIV-1 infection were controlled by intrinsic regulation or involved in cell cooperation with other immune key players such as CD4 helpers or CD14<sup>+</sup> monocytes. In this context, we first purified CD8A T-cells and activated them either alone or with autologous monocyte- and CD4 T-cell-depleted PBMC cultures for 6 h. Once again, we assessed both the expression levels of autophagy-related genes (ULK1, *BECN1* and *SQSTM1* in the context of lysosomal inactivation) and the autophagy-dependent lytic activity for all study groups and activation methods (polyclonal, CEF- and HIV-1 Gag-specific activations). Our data showed that activating CD8A T-cells alone or removing CD4 T-cells from cultures both led to significant inhibition of the expression levels of the autophagy-related genes along with reduced lytic activity in EC and HIV<sup>neg</sup> to levels comparable with ART (Fig. 4). In summary, our data confirmed that the strong autophagic activity found in activated CD8A T-cells from EC and HIV<sup>neg</sup> required the presence of CD4 T-cells in cultures. In this regard, we decided to investigate the role of IL21 (interleukin-21), which is a CD4-related cytokine known to promote antiviral CD8A T-cell responses [28].

First, our data showed that cultures from ART had lower percentages of IL21<sup>+</sup> CD4 T-cells when compared to those from EC and HIV<sup>neg</sup> after 6 h of polyclonal activation (Fig. 5A) [15,29]. Importantly, we found a positive and highly significant correlation between the percentages of IL21-producing CD4 T-cells and levels of autophagic activity in CD8A T-cells with all subjects (Fig. 5B). Altogether, these first sets of data strongly suggested an important role of IL21 in dictating the levels of active autophagy among antiviral CD8A T-cells during HIV-1 infection.

Therefore, we decided to add recombinant IL21 in cultures to confirm whether or not the treatment was effective in enhancing the autophagic activity among CD8A T-cells from ART. After 6 h of polyclonal and antiviral activations with or without IL21, we first assessed the levels of ULK1,

BECN1 and SQSTM1 by multi-parameter flow cytometry. Our data showed that IL21 treatment with ART was indeed effective in enhancing the percentages of CD8A T-cells positive for autophagy-related genes; however, they did not fully reach the levels observed in EC and HIV<sup>neg</sup> (Fig. 5C). Using electron microscopy, we also confirmed that IL21 treatment with ART increased the numbers of AVs and ALs in their activated CD8A T-cells (Fig. 5D). Furthermore, treating CD8A T-cells from ART with IL21 improved, although partially when compared to EC and HIV<sup>neg</sup> controls, their autophagic activity (Fig. 5E). In contrast, IL21 treatment with EC and HIV<sup>neg</sup> had no effect on their autophagy status (Fig. S4A and S4B).

# AUTOPHAGY

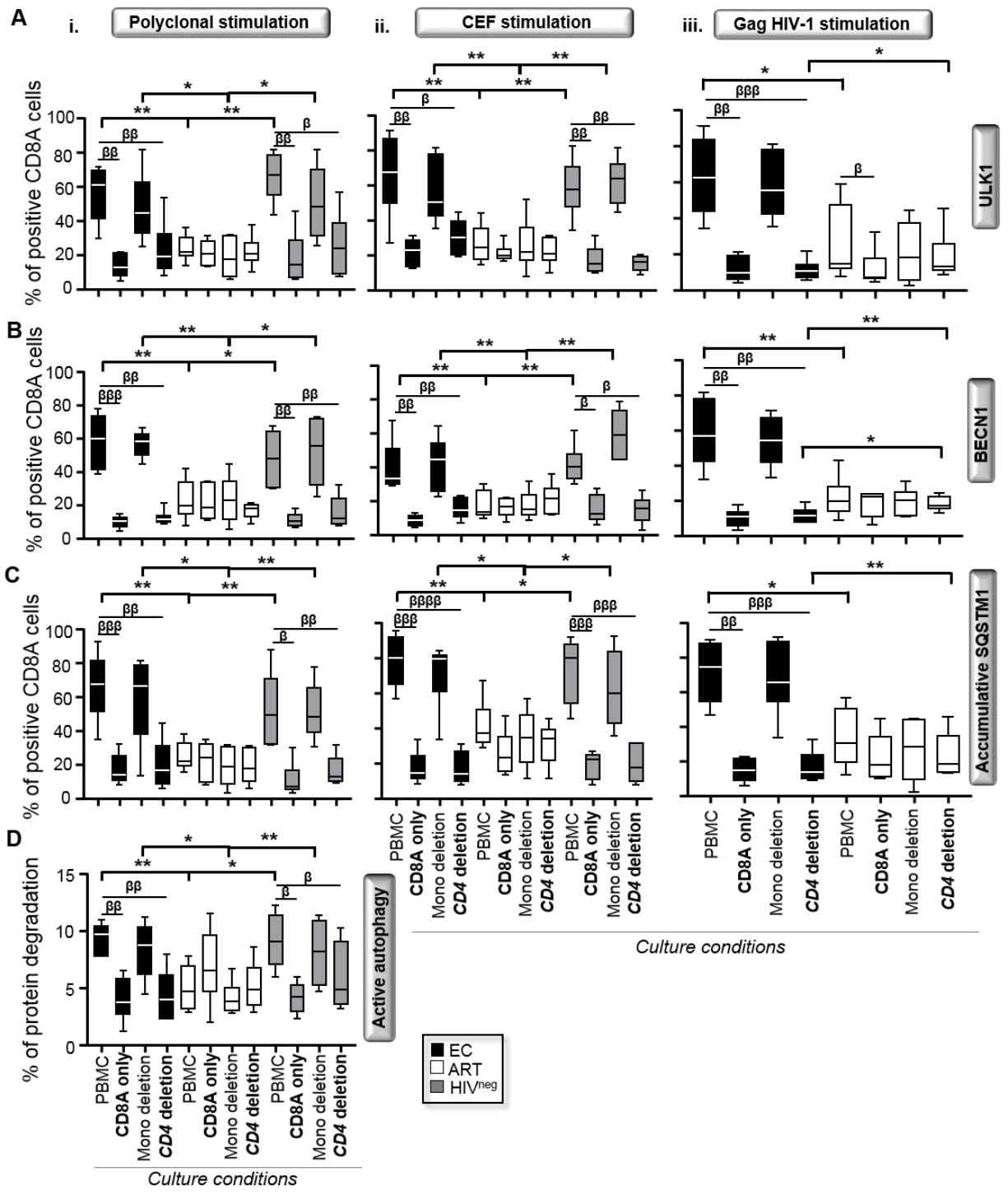


**Figure 4.4** CD4 T-cell help is required to ensure high autophagic activity in EC.

We first activated total PBMC, purified CD8A T-cells and PBMC whose CD4 T-cells or monocytes have been depleted either i. polyclonally, ii. CEF- or iii. HIV-1 Gag-specifically for 6 h (n = 6). Then, we assessed the percentages of (A) ULK1<sup>+</sup>, (B) BECN1<sup>+</sup> and (C) SQSTM1<sup>+</sup> (with BaF) in CD8A T-cells for all conditions by flow cytometry. (D) We also determined at 6 h post-polyclonal activation on purified CD8A T-cells the autophagy-

dependent proteolytic degradation of long-lived proteins using the pulse-chase approach.  $\beta$ , symbol used for paired *t* test (comparison between treated CD8A T-cells and their untreated control). \*, symbol used for Mann-Whitney test (comparison between study groups). One symbol,  $0.05 > P > 0.01$ ; two symbols,  $0.01 > P > 0.001$ ; and three symbols,  $0.001 > P > 0.0001$ .

Finally, we aimed to confirm that IL21 treatment in ART was effective in rescuing their antiviral CD8A T-cell responses, especially those against HIV-1, due to enhanced autophagic activity. To do so, we activated CD8A T-cells from ART (either polyclonally or antigen-specifically) with or without IL21, co-cultured them in the presence or absence of BaF, and assessed their antiviral polyfunctionality. In addition to increased expression levels of PRF1 and GZMB, IL21 treatment with ART led to significant enhancements of CD8A T-cell polyfunctionality including in cells specific for HIV-1 (Fig. 5F). IL21 rescue of antiviral CD8A T-cell responses in ART was autophagy-dependent, as co-treatment with BaF abrogated the enhancement of cell polyfunctionality (Fig. 5F). Once again, IL21 treatment with EC and HIV<sup>neg</sup> had no effect on their antiviral CD8A T-cell responses (Fig. S4C). In summary, our data indicate that endogenous IL21 was sufficient in eliciting optimal autophagic activity and related superior antiviral CD8A T-cell potential in EC. We further confirmed that IL21 treatment could be considered as a tool to rescue HIV-1-specific CD8A T-cell responses in ART in an autophagy-dependent manner.

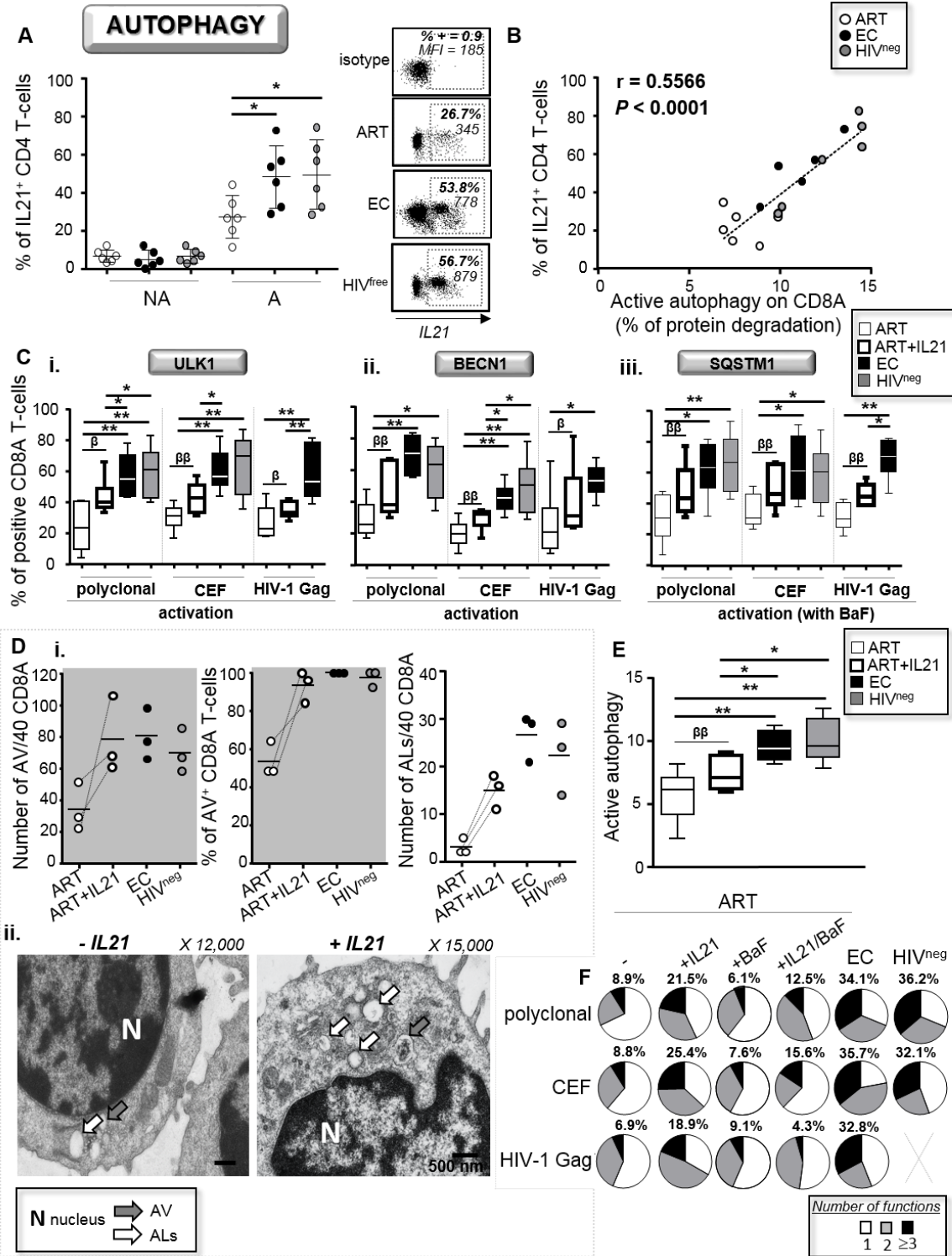


**Figure 4.5** Rescue of antiviral CD8A immunity in ART by IL21 is driven by enhanced active autophagy.

(A) Percentages of IL21-producing CD4 helpers from all study groups were determined after 6 h of polyclonal activation by flow cytometry. Representative dot plots are also shown including isotype control. (B) Correlation between the percentages of IL21-producing CD4 helpers and levels of active autophagy in activated CD8A T-cells for all participants. (C-F) 10 ng/mL recombinant IL21 was added in cultures from ART when their CD8A T-cells were activated either polyclonally or antigen-specifically. (C) Percentages of i. ULK1<sup>+</sup>, ii. BECN1<sup>+</sup> and iii.



SQSTM1<sup>+</sup> CD8A T-cells were then assessed by flow cytometry. (D) Ultrastructural analysis of purified CD8A T-cells following polyclonal activation including cells from ART that have been stimulated with or without IL21. i. Number and percentage of positivity for AV and ALs per 40 CD8A T-cells. ii. Representative micrographs with and without IL21. (E) Autophagy-dependent proteolytic degradation of long-lived protein determined in purified CD8A T-cells from ART with or without IL21. (F) CD8A T-cell polyfunctionality was assessed in activated CD8A T-cells from ART (with or without IL21 and BaF treatments), EC and HIV<sup>neg</sup>. Percentages of highly functional CD8A T-cells (expressing three or more antiviral cytokines and cytotoxic molecules in addition to IFNG) were also indicated in bold. n = 6, except for (B) n = 18 and (D) n = 3. β, symbol used for paired *t* test (comparison between treated CD8A T-cells and their untreated control). \*, symbol used for Mann-Whitney test (comparison between study groups). One symbol, 0.05 > P > 0.01; two symbols, 0.01 > P > 0.001; and three symbols, 0.001 > P > 0.0001.

#### 4.3.4 IL21 promotes the autophagy-dependent degradation of endogenous lipids in CD8A T-cells from ART.

Mounting an antiviral immune response against pathogens is an energetically demanding process. In this regard, autophagy can be essential for the maintenance of mitochondrial energetic function by providing metabolic substrates through lysosomal degradation. Since intrinsic lipolysis is critical for developing CD8A T-cell immunity after infection, we decided to investigate the levels of autophagy-mediated degradation of endogenous lipids, referred to as lipophagy, in our study groups [30].

By using electron microscopy with the osmium tetroxide negative-staining, we first confirmed the presence of lipid content within ALs from activated CD8A T-cells in ART (with or without IL21), EC and HIV<sup>neg</sup> (Fig. 6A). However, although we were able to detect lipid content for all study groups, we found higher numbers of ALs containing lipids per 40 cells in EC, HIV<sup>free</sup> and IL21-treated ART when compared to untreated ART (Fig. 6A and 6B). These data strongly indicated that IL21 treatment in ART could be associated with increased lipophagy.

Next, in order to measure the lipophagic activity among CD8A T-cells, we developed a novel ImageStream-based assay, which relies on the quantification of increased lipid content within lysosomes when cultures are conducted with BaF (Fig. 6C). Briefly, we cultured cells for each treatment condition with and without BaF. Then, we collected and stained cells with Lyso-ID and LipidTox, which are lysosomal and lipid dyes respectively. Finally, we determined their lipophagic activity by the formula:  $\Delta\text{BDS} = (\text{BDS}^{\text{high}} \text{ Lyso-ID}^+ \text{ LipidTox}^+ \text{ cells with BaF}) - (\text{BDS}^{\text{high}} \text{ Lyso-ID}^+ \text{ LipidTox}^+ \text{ cells without BaF})$ . First and foremost, to ascertain that this technique can measure the lipophagic activity in primary CD8A T-cells, we validated the protocol with hepatic Huh 7.5 cells which are starved for 2 h (Fig. S5). Indeed, nutrient starvation using hepatic cells is the most common way to increase lipophagy in culture [18]. Increases of lipophagy in starved Huh 7.5 cells were illustrated by higher  $\Delta\text{BDS}$  in comparison to those from cells that were cultured in complete DMEM (Fig. S5A and S5B). Similarly, we found higher mean LipidTox puncta per cell

with starved Huh 7.5 cells, when compared to cultures with complete media (Fig. S5C). Once validated, we assessed the lipophagic activity in activated CD8A T-cells from ART (with and without IL21), EC and HIV<sup>neg</sup>. Our data showed that, after polyclonal activation, CD8A T-cells from ART displayed less lipophagic activity than EC and HIV<sup>neg</sup> (Fig. 6D and 6E). We also found that IL21 treatment in ART led to increases in their lipophagic activity. Of note, although we found higher mean LipidTox puncta per cell in ART with IL21 treatment when compared to untreated ART, no significant differences were observed between study groups (Fig. S5D). Altogether, our data show that IL21 treatment of CD8A T-cells from ART enhanced their lipophagy. This indicates that metabolic reprogramming through IL21 treatment in ART is not out of reach and may abrogate their glucose dependency by providing cells with lipid substrates to fuel mitochondrial respiration.

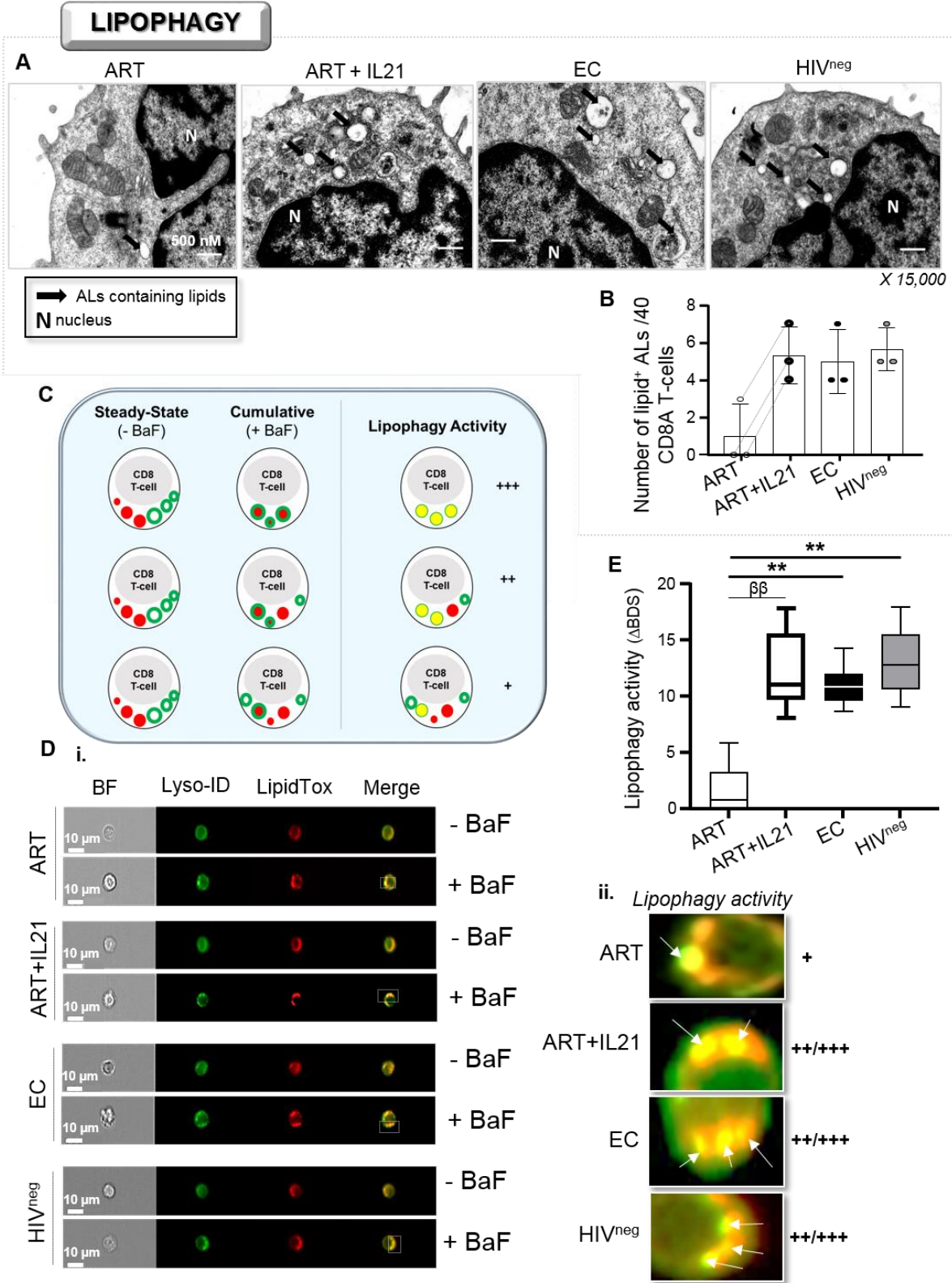


Figure 4.6 Enhanced lipophagy in ART in response to IL21 treatment.

(A and B) Visualization of ALs containing endogenous lipids using osmium tetroxide negative staining in activated CD8A T-cells (n = 3). (A) Magnified images showing ALs containing lipids (black arrows) for all study groups including ART that have been treated or not with IL21 (15,000 X). (B) Quantitative analysis of the number of ALs containing lipids per 40 cells. (C-E) Assessment of lipophagy activity by using a novel ImageStream-based lipophagy assay (n = 6). (C) Schematic representation for assessing lipophagy activity. (D) i. Representative images of single Lyso-ID<sup>+</sup>LipidTox<sup>+</sup> CD8A T-cells for all groups after 6 h of polyclonal activation in the presence or absence of BaF (“cumulative” and “steady-state” conditions, respectively). BF, bright field. ii. Magnified images showing increased lysosomal content of endogenous lipids in BaF-treated cells, which is an indicator of lipophagy activity when compared to cells without BaF. (E) Quantification of lipophagy activity determined in Lyso-ID<sup>+</sup>LipidTox<sup>+</sup> CD8A T-cells in ART (with or without IL-21), EC and HIV<sup>neg</sup>. Lipophagy activity was determined by the formula:  $\Delta\text{BDS} = (\% \text{ of BDS}^{\text{high}} \text{ cells with BaF}) - (\% \text{ of BDS}^{\text{high}} \text{ cells without BaF})$ .  $\beta$ , symbol used for paired *t* test (comparison between treated CD8A T-cells and their untreated control). \*, symbol used for Mann-Whitney test (comparison between study groups). One symbol, 0.05 > P > 0.01; two symbols, 0.01 > P > 0.001; and three symbols, 0.001 > P > 0.0001.

#### 4.3.5 IL21-induced lipophagy in ART leads to a better use of their mitochondrial respiration due to FAO.

The whole mitochondrial respiration, which can be enhanced in CD8A T-cells by IL15 treatment, is known to be critical to cover the energetic requirements for the effector and memory developments [4,31,32]. Therefore, we aimed to assess if IL21 treatment in polyclonally activated CD8A T-cells from ART was also associated with enhancement of their whole mitochondrial respiration. Following the manufacturer’s instruction, the respiratory kinetics that resulted from the sequential addition of pharmacological agents to the respiring cells allowed us to calculate the SRC and ATP-linked respiration. As expected, we found increases in both the whole mitochondrial SRC and ATP-linked respiration in ART when IL21 was added in culture (Fig. S6A).

Our next thought was to investigate whether IL21-induced lipophagy in ART provided free fatty acids to engage the mitochondrial fatty acid beta-oxidation (FAO). The protocol, developed to appreciate FAO, relies on the capacity of the cells to oxidize the fatty acid palmitate when other exogenous substrates are limited. Briefly, we polyclonally activated purified CD8A T-cells from ART for 6 h with or without IL21, BaF and the FAO inhibitor etomoxir. Cells were finally incubated with or without palmitate in substrate-limited media for an additional 45 min before assessing their mitochondrial respiration. Our data showed that IL21 treatment in ART led to increases of the FAO-mediated SRC and FAO ATP-linked respiration, which were both abrogated by BaF co-treatment (Fig. 7A-C). Of note, cells that were treated with BaF alone had similar respiratory kinetics compared to untreated cells. As expected, IL21-induced FAO was prevented by etomoxir pre-treatment, which validated our protocol as well (Fig. 7Aii). Finally, to assess the role of induced FAO on enhanced antiviral CD8A T-cells responses when IL21 was added in ART, we activated cells either polyclonally, CEF- or HIV-1- Gag-specifically for 6 h with or without IL21 and etomoxir. We found that the enhancements of PRF1 and GZMB expressions, as well as cell polyfunctionality that were mediated by IL21 were all prevented by etomoxir co-treatment (Fig. 7D

and 7E). In summary, our data show that IL21-mediated enhancement of antiviral CD8A T-cell responses in ART, including those against HIV-1, is driven by increased FAO.

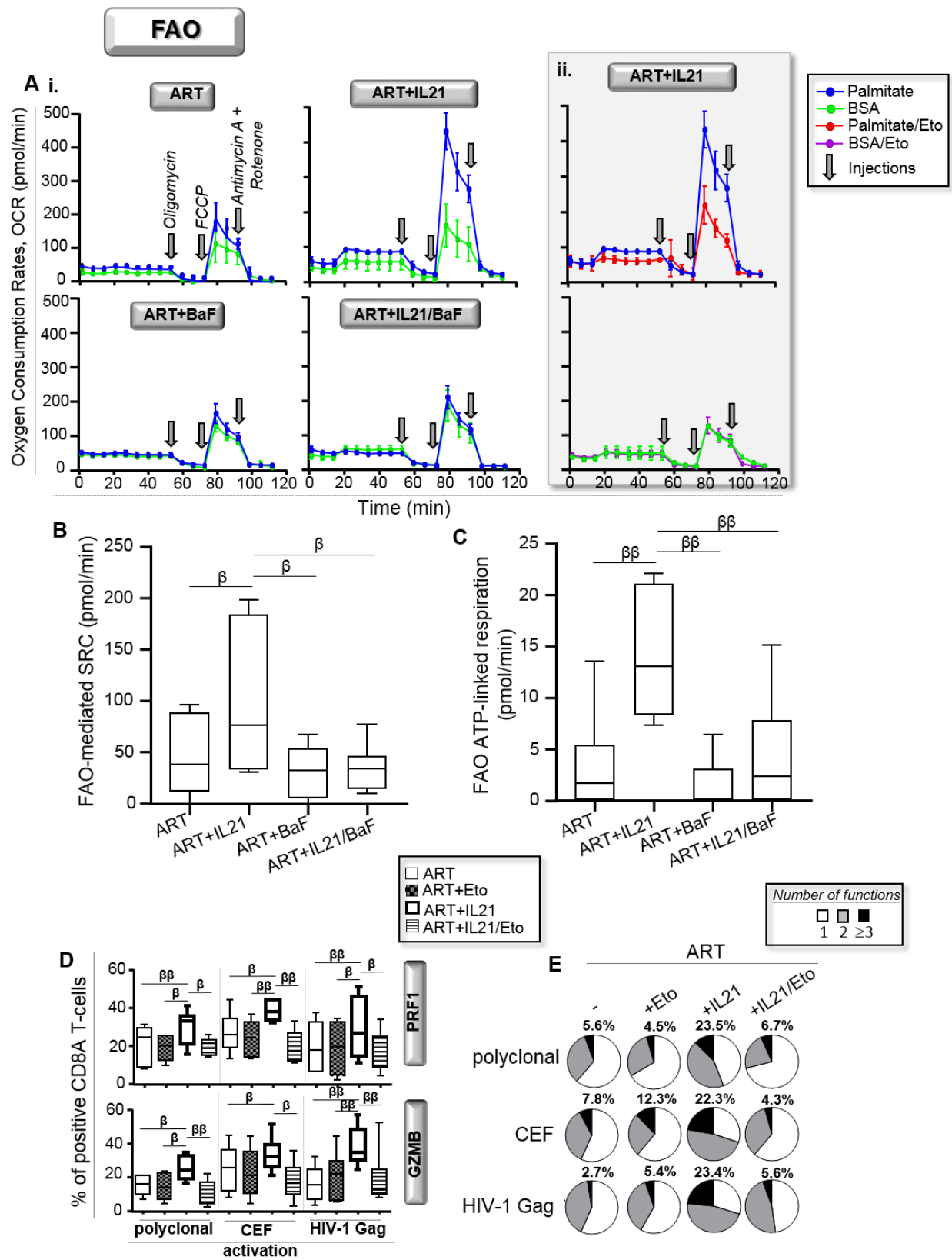


**Figure 4.7** Lipophagy-induced IL21 in ART improves the cellular rates of mitochondrial beta-oxidation.

(A-C) FAO determined in purified CD8A T-cells from ART at 6 h of polyclonal activation with or without IL21 and BaF (n = 6). (A) Representative graphs showing real-time oxygen consumption rates (OCR) in response to injections of mitochondrial respiration modulators, which are Oligomycin, Carbonyl cyanide 4-(trifluoromethoxy)-phenylhydrazone (FCCP) and Rotenone and Antimycin A, respectively in i. cells that have been incubated for the last 45 min with palmitate (blue kinetic) or BSA (green kinetic) and in ii. IL21-treated cells that have also been treated with the FAO inhibitor etomoxir (red and purple kinetics). Assessment of (B) FAO-mediated respiration and (C) related ATP-linked respiration for all conditions. Of note, FAO-mediated spare respiratory capacity (SRC) was determined with the formula: (SRC with palmitate) – (SRC with BSA). (D and E) CD8 T-cell polyfunctionality determined in CD8 T-cells from ART that have been polyclonally, CEF- and HIV-1 Gag- activated specifically in the presence or absence of IL21 and etomoxir (n = 6). (D) Percentages of PRF1<sup>+</sup> and GZMB<sup>+</sup> cells. (E) Pie chart representations of CD8A T-cell polyfunctionality. Percentages of highly functional CD8A T-cells were also indicated in bold.  $\beta$ , symbol used for paired *t* test (comparison between treated CD8 T-cells and their untreated control).  $\beta$ , 0.05 > P > 0.01;  $\beta\beta$ , 0.01 > P > 0.001 and  $\beta\beta\beta$ , 0.001 > P > 0.0001.

#### 4.4 Discussion

Although it is well-acknowledged that antiretroviral therapies fail to restore effective anti-HIV-1 CD8A T-cell responses, strategies aiming at rescuing them are limited in numbers [3-7]. EC, who control HIV-1 infection due to the maintenance of highly functional CD8A T-cells, represent a critical study group to identify which molecular mechanisms may be targeted to improve ART outcomes [3-5,8,33]. In a similar way, our previous works, which also included EC, have demonstrated the critical role of the transcription factor FOXO3/FOXO3a and its pro-apoptotic target genes on the loss of memory CD4 T- and B-cells in ART [34,35]. In the present study, we were interested in investigating the molecular mechanisms that were regulating the expression levels of both antiviral cytokines (IL2 and IFNG) and cytotoxic molecules (PRF1, GZMA and GZMB) in activated CD8A T-cells during chronic HIV-1 infection. Our data confirmed that antiviral CD8A T-cells from ART, including those specific to HIV-1, displayed both reduced expression of PRF1 and GZMB along with lower cell polyfunctionality. We also found that HIV-1-specific CD8A T-cells from ART had less autophagic activity along with lower numbers of ALs when compared to EC. We further confirmed that cytotoxic and polyfunctional HIV-1-specific CD8A T-cell responses in EC were autophagy-dependent. Altogether, the first sets of evidence pointed to a beneficial effect of stimulating autophagy-mediated lysosomal degradation in ART to potentiate their immune response to HIV-1. Of note, there is a possibility that the induction of autophagy, which is required for stimulating CD8A T-cell-related immune protection against HIV-1, might be transient and only found during the first hours of the antigen-stimulation. Indeed, although Xu X. et al. also confirmed that autophagy is essential for cytotoxic CD8A T-cell immune responses against the lymphocytic choriomeningitis virus, they showed that autophagy was finally found reduced in effector cells after 5 d of the viral infection [27]. In the context of HIV-1 infection, it will be interesting to investigate what is the status of autophagy activity in HIV-1-specific CD8A T-cells after a longer time of Gag stimulation.

Our study differs from others since autophagy has always been investigated in HIV-1 infection as a type of selective lytic process that targets the virus, referred to as xenophagy [12,36]. Another unique aspect of our study is based on the fact that the reduced autophagic activity in ART is not mediated by the productive HIV-1 infection and the expression of viral regulatory proteins such as Tat or Nef as reported in the past [13,37]. In contrast, our data showed that the reduced autophagy in ART was mediated by lower production of IL21, which is an immune defect reported after years of persistent HIV-1 infection despite antiretroviral therapy [15,29]. We showed that IL21-mediated rescue of antiviral CD8A T-cell responses in ART was driven by lipophagy, whose catabolic process of endogenous lipids has never been addressed in HIV-1 infection before. To do so, we have developed a high throughput, statistically robust method that quantifies lipophagic activity in primary human cells using the ImageStream cytometry. Several cytokines have been shown to promote autophagic activity, yet the role of IL21 in metabolic reprogramming through autophagy/lipophagy induction was unknown until now [38]. Altogether, our results showed that autophagy/lipophagy represents a new mechanism by which polyfunctional antiviral CD8A T-cells, including those specific to HIV-1, support mitochondrial respiration through FAO.

The efficiency of IL21-based therapy to promote effective HIV-1- and simian immunodeficiency virus (SIV)-specific CD8A T-cells has been repeatedly confirmed by in vitro and in vivo testing [39-42]. Besides HIV-1, IL21 can also serve as a critical factor that shapes the functional quality of antiviral CD8A T-cells against different viruses such as vaccinia virus, lymphocytic choriomeningitis virus, and hepatitis virus B [28,43,44]. Interestingly, IL21-based therapy, which has been proposed as a means of enhancing anti-tumor specific CD8A T-cell responses as well, led to a similar metabolic reprogramming towards FAO [45]. Therefore, our study, which reports how IL21 is mechanistically able to promote FAO, may provide useful information for designing therapies against viral infections as well as cancers. IL15 has also been proven effective in enhancing the antiviral capacity of HIV-1-specific CD8A T-cells in ART [4,46]. Enhancement by IL15 of HIV-1-specific CD8A T-cell responses has been associated with higher rates of oxidative metabolism as well [4]. However, recent data showed that the anti-HIV-1 capacity of IL21-stimulated CD8A T-cells exceeded that of IL15-stimulated cells [41,42]. This may be explained by the fact that, although IL15 enhanced the rates of oxidative metabolism, it failed to promote FAO in contrast to IL21 (Fig. S6B and S6C). Similar to IL15, IL21 was also found to enhance the rates of lipid uptake in ART (Fig. S6D) [4]. Although IL21-mediated rescue of antiviral CD8A T-cells in ART was driven by lipophagy, the fact remains that the rescue was only partial when compared to EC. This suggests that the highly functional CD8A T-cells from EC may not only depend on potent lipophagic activity, but also on other autophagy-dependent mechanisms. We



cannot rule out the involvement of the autophagy-dependent proteolysis, referred to as proteophagy, when it comes to EC. The pulse-chased assay, which was used here to uncover the reduced autophagic activity in ART when compared to EC, was based on protein degradation. Proteophagy may provide CD8A T-cells from EC with free amino-acids such as glutamine, leucine, serine, alanine, and arginine. These amino acids are all reported to fuel mitochondrial respiration and lay the foundation for effective T-cell immune protection, even in the context of glucose restriction [47-50].

Defective HIV-1-specific CD8A T-cells in ART have been characterized by other immune defects in addition to reduced polyfunctionality when compared to EC. For example, HIV-1-specific CD8A T-cells from ART may be prone to cell death due to high levels of CASP3 activation [51]. Although we found similar levels of basal apoptosis between ART and EC regardless of autophagy blockade, we cannot exclude the possibility that HIV-1-specific CD8A T-cells from ART display increased sensitivity to Fas-induced apoptosis [52]. HIV-1-specific CD8A T-cells from ART have also been shown to have a lower capacity than EC to eliminate both productively infected and latently infected CD4 T-cells [33,53,54]. Finally, HIV-1-specific CD8A T-cells from ART may display reduced expression levels for the CCL4/MIP-1 $\beta$  chemokine [3,5]. It would be of clinical imperative to investigate if each of these defects in ART can be rescued by IL21 and if enhanced autophagy/lipophagy is involved in the process.

In summary, we are just beginning to appreciate how and why autophagy is a fundamental mechanism by which CD8A T-cells adapt their energetic input under specific circumstances. Up until recently, the conventional view of CD8A T-cell metabolism was that, upon antigen-specific activation, antiviral CD8A T-cells primarily used glycolysis over mitochondrial respiration to support quick bioenergetic needs [32,55]. In contrast, it was established that, once an antigen is cleared, memory CD8A T-cells relied on FAO to fuel mitochondrial respiration in order to persist and be metabolically prepared for antigen recall [30-32,56]. We show that the metabolism of antiviral CD8A T-cells, which is induced upon antigen-specific activation, is more plastic than originally thought and can be promoted by the autophagy-lysosomal pathway. To conclude, our data provide the rationale for considering the IL21/lipophagy/FAO axis as a therapeutic target for boosting specific immunity against HIV-1. Our data may also aid in the development of HIV vaccine and cure strategies in ART, whose success depends mostly on their ability to induce protective CD8A T-cell responses [19-22].

## 4.5 Materials and Methods

### HIV-1-infected patients.

The experiments described in this study mainly rely on the comparison of total and HIV-1-specific CD8A T-cell features from patients under antiretroviral therapy (ART) to those from naturally protected EC. EC are unique patients displaying a long-term viral control with no treatments. All virus-infected patients were participants of the Montreal HIV infection study that received approval from the McGill University Health Centre Ethical Review Board (ethic reference number SL-00.069). All subjects provided an informed and written consent for participation. The inclusion criteria of untreated ECs and ART are: middle-aged subjects (31-51 years old), presumed to have HIV-1 infection for a minimum of 3.6 years (3.6-7.5 years), no protective gene polymorphisms such as CCR5  $\Delta$ 32 and B27/B57 haplotypes, with CD4 counts over 400 cells/ $\mu$ l in blood and undetectable viral loads (< 50 copies/ml) for 3 years or more. It is worth mentioning that ART patients in this study display years of chronic HIV- infection and antiretroviral therapy. Of note, we selected 6 age-matched and HIV-1-uninfected subjects as controls of non-infection.

### Media and Products.

RPMI-1640 media (Wisent, 350-000-EL) and DMEM media (Wisent, 319-005-CL), FBS (Wisent, 080-450), penicillin-streptomycin antibiotics (Wisent, 450-201-EL), and PBS (Wisent, 311-010-CL) were obtained from Wisent Inc. The starvation EBSS medium was purchased from ThermoFisher Scientific (ThermoFisher Scientific, 24010043). All monoclonal antibodies used for multi-parameter and Imaging flow cytometry such as anti-CD3W/CD3 (BD Biosciences, 557943) and anti-CD8A (BD Biosciences, 560347) were purchased in BD Biosciences, except for those against ULK1 (Santa Cruz Biotechnology, sc-390904 AF647), BECN1 (Abcam, ab246760), SQSTM1 (MBL Life Sciences, M162-A48), LC3 (MBL Life Sciences, M152-3), PRF1/perforin (Biolegend, 353314), and GZMA/granzyme A (ThermoFisher Scientific, 12-9177-42). Recombinant IL21 (Sigma Aldrich, SRP3087) and IL15 (Sigma Aldrich, I8648), lysosomal inhibitors bafilomycin A<sub>1</sub> (Sigma Aldrich, B1793) and chloroquine (Sigma Aldrich, C6628), and etomoxir (Sigma Aldrich, E1905) were all provided from Sigma Aldrich. Zenon labeling kits were purchased from Invitrogen (ThermoFisher Scientific, Z-25008). Concentrations for IL21, IL15, bafilomycin A<sub>1</sub>, chloroquine, and etomoxir were 10 ng/mL, 10 ng/mL, 100 nM, 100 nM and 5  $\mu$ M, respectively.

### **CD8A purification and cell subset removals.**

Some experiments required the purification of CD8A T-cells, or the removal of specific cell subsets such as CD4 T-cells and monocytes from the collected peripheral blood mononuclear cells (PBMC), before further analyses. **1. CD8A purification:** CD8A T-cells were isolated by using the EasySep human CD8A T-cell enrichment kit (StemCell Technologies, 17953). Our developed protocol allows for more than 95% purification without any cell stimulation or apoptosis. **2. Subset-depleted PBMC:** We removed CD4 T-cells and CD14<sup>+</sup> monocytes from the CD8A-depleted PBMC by using the EasySep human CD4 (StemCell Technologies, 17852) and CD14 (StemCell Technologies, 17858) positive selection kits II, respectively. The percentage of cell subset removal was determined at around 96.2% by using flow cytometry.

### **In-vitro activation assays.**

Total, cell subset-depleted PBMC and purified CD8A T-cells for all study groups were either polyclonally or antigen-specifically activated for 6 h in the presence of GolgiPlug (BD Biosciences, 555029) and GolgiStop (BD Biosciences, 554724) to assess autophagy and the intracellular production of effector molecules. For the polyclonal activation, we treated cells with 0.5 µg/mL of anti-CD3W (BioLegend, 317326) and of 1 µg/mL anti-CD28 Abs (BD Biosciences, 555726). To elicit the antigen-specific activations, we used either 2 µg/mL of CEF (cytomegalo- virus, with Epstein-Barr and flu viruses) peptide pool (Mabtech, 3616-1) or 5 µg/mL of HIV-1 p55 (Austral Biologicals, HI1A-730-5) and p24 Gag antigens (Austral Biologicals, HI1A-720-5) on PBMC. Of note, all cultures from ART were conducted with 10 µM of AZT (Sigma Aldrich, A2169-25MG) to prevent any de novo viral production (confirmed by the sensitive HIV-1 p24 ELISA (Abcam, ab218268) in culture supernatants).

### **BECN1-specific gene silencing.**

We first purified 10<sup>7</sup> CD8A T-cells from all tested groups and electroporated them using Nucleofector II technology according to the Amaxa Biosystems manufacturer's protocol. Specific *BECN1* siRNA (ThermoFisher Scientific, AM16708) and negative control siRNA (ThermoFisher Scientific, 4390843) were obtained from ThermoFisher Scientific. Of note, 7 µg of siRNA were either transfected for each condition for 2 h without antibiotics. Purified CD8A T-cells were washed three times thereafter to remove dead necrotic cells, counted and incubated 18 h with autologous CD8A-depleted PBMC (at ratio CD8A /PBMC = 1/5). Then, we activated cells for 6 h to assess

the autophagy activity and effector function in transfected CD8A T-cells. At 6 h post-activation, some cells were also collected to confirm BECN1 inhibition and to assess the percentages of cell apoptosis with ANXA5/annexin-V staining by flow cytometry.

### **Multi-parameter flow cytometry.**

**1. Intracellular staining:** To assess the expression levels of autophagy-related genes, cytokines and cytotoxic molecules, we subjected cells to intracellular staining assays as previously described [26]. Briefly, after surface staining with specific antibodies for CD8A T-cell phenotyping, we fixed and then permeabilized cells with 0.25% saponin (Sigma Aldrich, 47036) before the intracellular staining per se. After three washes, stained cells were finally ready for flow cytometry analyses. The viability marker 7-aminoactinomycin D or 7-AAD (ThermoFisher Scientific, 00-6993-50) was used to exclude dead cells from analyses. Of note, to assess the cumulative expression of the SQSTM1 during the 6 h-long cultures, we also cultured our cells with BaF. In order to appreciate the antiviral and cytotoxic programs on activated and viable 7-AADneg CD3W<sup>+</sup> CD8A<sup>+</sup> T-cell, we used the following multi-parameter antibody cocktail: anti-IL2-FITC (BD Biosciences, 561055) and anti-IFNG/IFN- $\gamma$ -AF647 (BD Biosciences, 563495) antibodies, and GZMA/granzyme A-PE, GZMB/granzyme B-PE-CF594 (BD Biosciences, 562462) and anti-PRF1/perforin-PerCP-Cy5.5 antibodies (Fig. S3D). **2. Palmitate uptake:** At 6 h post-activation, we incubated the cells for 5 min with 5  $\mu$ M of C<sub>16</sub> BODIPY<sup>TM</sup> (ThermoFisher Scientific, D3821). After three washes, lipid uptake was determined on gated CD8A T-cells and expressed as mean intensity fluorescence (MFI). Regarding the palmitate uptake assay, we did not perform any technical replicates. In fact, we only performed the palmitate BODIPY uptake in each single tube per condition. **3. Data analyses:** All samples were finally acquired using the BD LSRII Fortessa flow cytometer and analyzed with DIVA software (BD). 200,000-500,000 gated cells were analyzed for each sample.

### **Imaging flow cytometry.**

**1. Lysosomal content of LC3 (autophagy):** Lysosomal content of endogenous LC3 is a well-acknowledged marker for autophagy. In this context, we used a previously validated method to detect the lysosomal localization of LC3 in primary cells [25]. Briefly, after 6 h of cell activation with BaF, PBMC were first stained with the lysosomal Lyso-ID green dye according to the manufacturer's instructions (Enzo Life Sciences, ENZ-51005). Anti-CD3W-APC H7 (BD

Biosciences, 560176) and anti-CD8A-V450 Abs were used for surface staining. Cells were then fixed, permeabilized and finally labeled with anti-LC3-Alexa Fluor 647 Abs with or without anti-IFNG/IFN- $\gamma$ -PE (BD Biosciences, 559327) Abs. Lysosomal localization of LC3 was measured using a morphology mask to determine a similarity score, which quantifies the correlation of pixel values of the Lyso-ID and LC3 images on a per cell basis. A similarity score  $>1$  was used as a cutoff for nuclear localization. Cells in individual bins were visually inspected to confirm subcellular localization (values  $<$  or  $>1$ ). **2. Lysosomal content of endogenous lipids (lipophagy):** For the purpose of this study, we have developed a high throughput and statistically robust technique that quantitates lipophagy in primary human cells. The principle of this method consists in measuring the accumulation of lipid contents in ALs when cultures were performed with the lysosomal inhibitor BaF. This culture condition was referred as the "cumulative state" and compared to the BaF-free "steady-state" condition. At 6 h post-activation with or without BaF, cells were collected and co-stained with Lyso-ID green dye and the HCS LipidTox deep red neutral lipid dye (ThermoFisher Scientific, H34477) according to the manufacturer's instructions. Anti-CD3W-APC H7 and anti-CD8A-V450 Abs were used for surface staining. Our novel method to appreciate lipophagy activity was validated by using hepatic Huh 7.5 cell line that have been starved for 2 h (Fig. S5) [18]. **3. Data analyses:** Samples were acquired using the Image Stream X MKII flow cytometer and analyzed with IDEAS software (Amnis). 200,000-500,000 gated cell singlets were analyzed for each sample. Results were expressed as co-localization index BDS (for bright detail similarity) between the lysosomal dye Lyso-ID and the other fluorescently labeled marker of interest. Of note, we determined the lipophagy activity by the formula: (% of BDS<sup>high</sup> Lyso-ID<sup>+</sup> LipidTox<sup>+</sup> cells with BaF) – (% of BDS<sup>high</sup> Lyso-ID<sup>+</sup> LipidTox<sup>+</sup> cells without BaF). Finally, the Spot Wizard in IDEAS was used to create an algorithm to calculate the number of LC3 and LipidTox spots (referred as puncta). Two "truth population" were manually selected with 30 events per population: a positive population of cells, which have many spots, and a negative population of cells, which have no spots. The Wizard was then used to calculate the mean number of marker spots per cells.

### **Autophagy-dependent lytic assays.**

Autophagy-dependent lytic degradation of long-lived proteins in 106 purified CD8A T-cells was quantified as previously described [24]. The method is based on a pulse-chase approach, whereby cellular proteins are radiolabeled by [<sup>14</sup>C] valine (PerkinElmer, NEC291EU050UC). Briefly, 10<sup>6</sup> purified CD8A T-cells were seeded and incubated for 18 h in complete RPMI with 0.2

$\mu\text{Ci/ml}$  of L-[ $^{14}\text{C}$ ] valine in order to label intracellular proteins (Pulse media). Cells were then washed three times with PBS to eliminate any unincorporated radioactivity. The short-lived proteins are allowed to be degraded for 24 h in fresh RPMI (Chase media). After that, cells were polyclonally activated for 6 h in the presence or absence of BaF, and then seeded in 10% of trichloroacetic acid (TCA) containing RPMI overnight. After centrifugation, precipitated cells were washed twice with cold 10% TCA RPMI and dissolved in 0.2 M NaOH for 2 h. Of note, supernatants contained the acid-soluble radioactivity fraction. Radioactivity was finally quantified by liquid scintillation counting. The rate of autophagy-dependent degradation of long-lived proteins was calculated from the ratio of the acid-soluble radioactivity in the medium to the one in the acid-precipitable cell fraction.

### **Electron microscopy analysis.**

Electron microscopy analysis was done as previously reported, but with a few modifications [12]. Briefly, after 6 h of polyclonal activation with or without IL21, we purified  $2 \cdot 10^6$  CD8A T-cells for microscopic observation. Purified CD8A T-cells were first fixed overnight at  $4^\circ\text{C}$  with 2.5% glutaraldehyde (Mecalab, 1206) in 0.05 M cacodylate buffer (pH 7.4). Cells were then rinsed, post-fixed in 1.3% osmium tetroxide (Mecalab, 1605) in collidine buffer (pH 7.4), dehydrated, and embedded in two successive baths of SPURR (TedPella, 18300-4221). Grids were rinsed in distilled water, stained with aqueous 2% uranyl acetate for 15 min and finally photographed with a Hitachi H-7100 electron microscope fitted with an AMT XR111 camera (Hitachi High-Tech America Inc.). A number of 40 cells per slide were observed. We calculated the percentage of CD8A T-cells containing autophagic vacuoles (AV) and the total numbers of AV and autolysosomes (ALs) by using different magnifications. Finally, we also used osmium tetroxide negative-staining to visualize the presence of endogenous lipids in ALs for all study groups. Of note, lipid staining with osmium is characterized by bright areas.

### **Metabolic flux assay.**

At 6 h post-polyclonal activation with or without cytokines, we assessed both the overall and FAO-mediated mitochondrial respiration in purified CD8A T-cells from ART using a Seahorse XF96 metabolic analyzer. Of note,  $4 \cdot 10^5$  purified cells per condition were needed to ensure reproducible observations (in triplicate). **1. Whole mitochondrial respiration:** The oxygen consumption rates (OCR) were determined in ART by using the Seahorse XF Cell Mito Stress Test kit (Agilent

Technologies, 103015-100). Briefly,  $4 \cdot 10^5$  activated CD8A T-cells were seeded on XF96 well plates (Agilent Technologies, 102601-100) in complemented Agilent RPMI with glucose 10 mM, glutamine 2 mM and pyruvate 1 mM (Agilent Technologies, 103576-100). The XF Cell Mito Stress test kit was used according to the manufacturer protocol. OCR was determined under basal conditions and in response to modulators of respiration that were injected during the assay to reveal key parameters of mitochondrial functions. The modulators included in this assay were oligomycin (Agilent Technologies, 103015-100), carbonyl cyanide 4-(trifluoromethoxy) phenylhydrazone (FCCP; Agilent Technologies, 103015-100), rotenone (Agilent Technologies, 103015-100) and antimycin A (Agilent Technologies, 103015-100) (1.5  $\mu$ M, 2  $\mu$ M and 0.5  $\mu$ M, respectively). We determined the spare respiratory capacity (SRC) and ATP-linked respiration for each condition as follows: [(maximal OCR determined after FCCP treatment) – (basal OCR determined before oligomycin treatment)] and [(basal OCR) – (minimal OCR determined after Rotenone and Antimycin A treatment)], respectively. **2. Fatty acid beta-oxidation (FAO):** To determine the FAO status in ART, we used the Seahorse XF Palmitate Oxidation Stress Test kit (Agilent Technologies, 102720-100) protocol with a minor modification. Indeed, the  $4 \cdot 10^5$  activated CD8A T-cells were seeded on XF96 plates without going through the suggested nutrient restriction pre-step. This was made to keep a satisfying cell viability (superior to 90% of cell viability confirmed by flow cytometry). However, cells were still cultured under nutrient restriction, but at the end of culture and for 45 min. In this context, cells were cultured in a CO<sub>2</sub>-free incubator at 37°C with a pre-warmed XF FAO media containing only a necessary minimal content of glucose (2.5 mM) and 0.5 mM of L-carnitine (Sigma Aldrich, C0283). L-carnitine is an amino-acid derivative that transports fatty acids into cells to be processed for energy. The nutrient restriction step was also conducted in the presence of lipid substrate palmitate or bovine serum albumin (BSA; Agilent Technologies, 102720-100). Of note, 5  $\mu$ M of FAO inhibitor etomoxir was added or not at the onset of culture and during the first injection of the assay, as positive control for lipid metabolism. Once again, OCR values, that were determined under basal conditions and in response to modulators of respiration, were used to calculate SRC and ATP-linked respiration for each culture condition. FAO was determined according to the manufacturer's instructions and by the formula: (values with palmitate) – (values with BSA). **3. Data normalization:** All values were normalized to the number of viable cell events per seeded well thanks to the CytoFLEX benchtop flow cytometer (Beckman Coulter).

## Statistical analysis.

We used the non-parametric Mann-Whitney U test that assumes independent samples for all statistical analyses between study groups of subjects (\* symbol). On the other hand, statistical analyses between two different in vitro conditions were performed using two-sided Student paired *t* test ( $\beta$  symbol). Spearman's correlation test was used to identify association between two variables. P values of less than 0.05 were considered significant. One symbol,  $0.05 > P > 0.01$ ; two symbols,  $0.01 > P > 0.001$ ; three symbols,  $0.001 > P > 0.0001$ ; and four symbols,  $P < 0.0001$ .

## 4.6 References

1. Graw F, Regoes RR. Predicting the impact of CD8+ T cell polyfunctionality on HIV disease progression. *J Virol* 2014; 88:10134-45.
2. Boyd A, Almeida JR, Darrah PA, Sauce D, Seder RA, Appay V, et al. Pathogen-Specific T Cell Polyfunctionality Is a Correlate of T Cell Efficacy and Immune Protection. *PLoS One* 2015; 10:e0128714.
3. Almeida JR, Price DA, Papagno L, Arkoub ZA, Sauce D, Bornstein E, et al. Superior control of HIV-1 replication by CD8+ T cells is reflected by their avidity, polyfunctionality, and clonal turnover. *J Exp Med* 2007; 204:2473-85.
4. Angin M, Volant S, Passaes C, Lecuroux C, Monceaux V, Dillies MA, et al. Metabolic plasticity of HIV-specific CD8(+) T cells is associated with enhanced antiviral potential and natural control of HIV-1 infection. *Nat Metab* 2019; 1:704-16.
5. Betts MR, Nason MC, West SM, De Rosa SC, Migueles SA, Abraham J, et al. HIV nonprogressors preferentially maintain highly functional HIV-specific CD8+ T cells. *Blood* 2006; 107:4781-9.
6. Migueles SA, Weeks KA, Nou E, Berkley AM, Rood JE, Osborne CM, et al. Defective human immunodeficiency virus-specific CD8+ T-cell polyfunctionality, proliferation, and cytotoxicity are not restored by antiretroviral therapy. *J Virol* 2009; 83:11876-89.
7. Ndhlovu ZM, Proudfoot J, Cesa K, Alvino DM, McMullen A, Vine S, et al. Elite controllers with low to absent effector CD8+ T cell responses maintain highly functional, broadly directed central memory responses. *J Virol* 2012; 86:6959-69.



8. Loucif H, Gouard S, Dagenais-Lussier X, Murira A, Stager S, Tremblay C, et al. Deciphering natural control of HIV-1: A valuable strategy to achieve antiretroviral therapy termination. *Cytokine Growth Factor Rev* 2018; 40:90-8.
9. Guo JY, Teng X, Laddha SV, Ma S, Van Nostrand SC, Yang Y, et al. Autophagy provides metabolic substrates to maintain energy charge and nucleotide pools in Ras-driven lung cancer cells. *Genes Dev* 2016; 30:1704-17.
10. Perera RM, Stoykova S, Nicolay BN, Ross KN, Fitamant J, Boukhali M, et al. Transcriptional control of autophagy-lysosome function drives pancreatic cancer metabolism. *Nature* 2015; 524:361-5.
11. Strohecker AM, White E. Autophagy promotes BrafV600E-driven lung tumorigenesis by preserving mitochondrial metabolism. *Autophagy* 2014; 10:384-5.
12. Nardacci R, Amendola A, Ciccocanti F, Corazzari M, Esposito V, Vlassi C, et al. Autophagy plays an important role in the containment of HIV-1 in nonprogressor-infected patients. *Autophagy* 2014; 10:1167-78.
13. Nardacci R, Ciccocanti F, Marsella C, Ippolito G, Piacentini M, Fimia GM. Role of autophagy in HIV infection and pathogenesis. *J Intern Med* 2017; 281:422-32.
14. Kang R, Zeh HJ, Lotze MT, Tang D. The Beclin 1 network regulates autophagy and apoptosis. *Cell Death Differ* 2011; 18:571-80.
15. Iannello A, Boulassel MR, Samarani S, Debbeche O, Tremblay C, Toma E, et al. Dynamics and consequences of IL-21 production in HIV-infected individuals: a longitudinal and cross-sectional study. *J Immunol* 2010; 184:114-26.
16. Kounakis K, Chaniotakis M, Markaki M, Tavernarakis N. Emerging Roles of Lipophagy in Health and Disease. *Front Cell Dev Biol* 2019; 7:185.
17. Schulze RJ, Sathyanarayan A, Mashek DG. Breaking fat: The regulation and mechanisms of lipophagy. *Biochim Biophys Acta Mol Cell Biol Lipids* 2017; 1862:1178-87.
18. Singh R, Kaushik S, Wang Y, Xiang Y, Novak I, Komatsu M, et al. Autophagy regulates lipid metabolism. *Nature* 2009; 458:1131-5.
19. Collins DR, Gaiha GD, Walker BD. CD8(+) T cells in HIV control, cure and prevention. *Nat Rev Immunol* 2020; 20:471-82.

20. Excler JL, Robb ML, Kim JH. HIV-1 vaccines: challenges and new perspectives. *Hum Vaccin Immunother* 2014; 10:1734-46.
21. Jones RB, Walker BD. HIV-specific CD8(+) T cells and HIV eradication. *J Clin Invest* 2016; 126:455-63.
22. Perdomo-Celis F, Taborda NA, Rugeles MT. CD8(+) T-Cell Response to HIV Infection in the Era of Antiretroviral Therapy. *Front Immunol* 2019; 10:1896.
23. Parzych KR, Klionsky DJ. An overview of autophagy: morphology, mechanism, and regulation. *Antioxid Redox Signal* 2014; 20:460-73.
24. Roberts EA, Deretic V. Autophagic proteolysis of long-lived proteins in nonliver cells. *Methods Mol Biol* 2008; 445:111-7.
25. Phadwal K, Alegre-Abarrategui J, Watson AS, Pike L, Anbalagan S, Hammond EM, et al. A novel method for autophagy detection in primary cells: impaired levels of macroautophagy in immunosenescent T cells. *Autophagy* 2012; 8:677-89.
26. Dagenais-Lussier X, Loucif H, Cadorel H, Blumberger J, Isnard S, Bego MG, et al. USP18 is a significant driver of memory CD4 T-cell reduced viability caused by type I IFN signaling during primary HIV-1 infection. *PLoS Pathog* 2019; 15:e1008060.
27. Xu X, Araki K, Li S, Han JH, Ye L, Tan WG, et al. Autophagy is essential for effector CD8(+) T cell survival and memory formation. *Nat Immunol* 2014; 15:1152-61.
28. Novy P, Huang X, Leonard WJ, Yang Y. Intrinsic IL-21 signaling is critical for CD8 T cell survival and memory formation in response to vaccinia viral infection. *J Immunol* 2011; 186:2729-38.
29. Cubas R, van Grevenynghe J, Wills S, Kardava L, Santich BH, Buckner CM, et al. Reversible Reprogramming of Circulating Memory T Follicular Helper Cell Function during Chronic HIV Infection. *J Immunol* 2015; 195:5625-36.
30. O'Sullivan D, van der Windt GJ, Huang SC, Curtis JD, Chang CH, Buck MD, et al. Memory CD8(+) T cells use cell-intrinsic lipolysis to support the metabolic programming necessary for development. *Immunity* 2014; 41:75-88.
31. van der Windt GJ, Everts B, Chang CH, Curtis JD, Freitas TC, Amiel E, et al. Mitochondrial respiratory capacity is a critical regulator of CD8+ T cell memory development. *Immunity* 2012; 36:68-78.

32. van der Windt GJ, Pearce EL. Metabolic switching and fuel choice during T-cell differentiation and memory development. *Immunol Rev* 2012; 249:27-42.
33. Saez-Cirion A, Sinet M, Shin SY, Urrutia A, Versmisse P, Lacabaratz C, et al. Heterogeneity in HIV suppression by CD8 T cells from HIV controllers: association with Gag-specific CD8 T cell responses. *J Immunol* 2009; 182:7828-37.
34. van Grevenynghe J, Cubas RA, Noto A, DaFonseca S, He Z, Peretz Y, et al. Loss of memory B cells during chronic HIV infection is driven by Foxo3a- and TRAIL-mediated apoptosis. *J Clin Invest* 2011; 121:3877-88.
35. van Grevenynghe J, Procopio FA, He Z, Chomont N, Riou C, Zhang Y, et al. Transcription factor FOXO3a controls the persistence of memory CD4(+) T cells during HIV infection. *Nat Med* 2008; 14:266-74.
36. Sagnier S, Daussy CF, Borel S, Robert-Hebmann V, Faure M, Blanchet FP, et al. Autophagy restricts HIV-1 infection by selectively degrading Tat in CD4+ T lymphocytes. *J Virol* 2015; 89:615-25.
37. Dinkins C, Pilli M, Kehrl JH. Roles of autophagy in HIV infection. *Immunol Cell Biol* 2015; 93:11-7.
38. Botbol Y, Patel B, Macian F. Common gamma-chain cytokine signaling is required for macroautophagy induction during CD4+ T-cell activation. *Autophagy* 2015; 11:1864-77.
39. Chevalier MF, Julg B, Pyo A, Flanders M, Ranasinghe S, Soghoian DZ, et al. HIV-1-specific interleukin-21+ CD4+ T cell responses contribute to durable viral control through the modulation of HIV-specific CD8+ T cell function. *J Virol* 2011; 85:733-41.
40. Mendez-Lagares G, Lu D, Merriam D, Baker CA, Villinger F, Van Rompay KKA, et al. IL-21 Therapy Controls Immune Activation and Maintains Antiviral CD8(+) T Cell Responses in Acute Simian Immunodeficiency Virus Infection. *AIDS Res Hum Retroviruses* 2017; 33:S81-S92.
41. White L, Krishnan S, Strbo N, Liu H, Kolber MA, Lichtenheld MG, et al. Differential effects of IL-21 and IL-15 on perforin expression, lysosomal degranulation, and proliferation in CD8 T cells of patients with human immunodeficiency virus-1 (HIV). *Blood* 2007; 109:3873-80.
42. Wu K, Zhang S, Zhang X, Li X, Hong Z, Yu F, et al. IL-21 Expands HIV-1-Specific CD8(+) T Memory Stem Cells to Suppress HIV-1 Replication In Vitro. *J Immunol Res* 2019; 2019:1801560.

43. Tang L, Chen C, Gao X, Zhang W, Yan X, Zhou Y, et al. Interleukin 21 Reinvigorates the Antiviral Activity of Hepatitis B Virus (HBV)-Specific CD8+ T Cells in Chronic HBV Infection. *J Infect Dis* 2019; 219:750-9.
44. Yi JS, Du M, Zajac AJ. A vital role for interleukin-21 in the control of a chronic viral infection. *Science* 2009; 324:1572-6.
45. Loschinski R, Bottcher M, Stoll A, Bruns H, Mackensen A, Mougiakakos D. IL-21 modulates memory and exhaustion phenotype of T-cells in a fatty acid oxidation-dependent manner. *Oncotarget* 2018; 9:13125-38.
46. Mueller YM, Bojczuk PM, Halstead ES, Kim AH, Witek J, Altman JD, et al. IL-15 enhances survival and function of HIV-specific CD8+ T cells. *Blood* 2003; 101:1024-9.
47. Geiger R, Rieckmann JC, Wolf T, Basso C, Feng Y, Fuhrer T, et al. L-Arginine Modulates T Cell Metabolism and Enhances Survival and Anti-tumor Activity. *Cell* 2016; 167:829-42 e13.
48. Ma EH, Bantug G, Griss T, Condotta S, Johnson RM, Samborska B, et al. Serine Is an Essential Metabolite for Effector T Cell Expansion. *Cell Metab* 2017; 25:345-57.
49. Ron-Harel N, Ghergurovich JM, Notarangelo G, LaFleur MW, Tsubosaka Y, Sharpe AH, et al. T Cell Activation Depends on Extracellular Alanine. *Cell Rep* 2019; 28:3011-21 e4.
50. Ron-Harel N, Santos D, Ghergurovich JM, Sage PT, Reddy A, Lovitch SB, et al. Mitochondrial Biogenesis and Proteome Remodeling Promote One-Carbon Metabolism for T Cell Activation. *Cell Metab* 2016; 24:104-17.
51. Yan J, Sabbaj S, Bansal A, Amatya N, Shacka JJ, Goepfert PA, et al. HIV-specific CD8+ T cells from elite controllers are primed for survival. *J Virol* 2013; 87:5170-81.
52. Mueller YM, De Rosa SC, Hutton JA, Witek J, Roederer M, Altman JD, et al. Increased CD95/Fas-induced apoptosis of HIV-specific CD8(+) T cells. *Immunity* 2001; 15:871-82.
53. Migueles SA, Osborne CM, Royce C, Compton AA, Joshi RP, Weeks KA, et al. Lytic granule loading of CD8+ T cells is required for HIV-infected cell elimination associated with immune control. *Immunity* 2008; 29:1009-21.
54. Shan L, Deng K, Shroff NS, Durand CM, Rabi SA, Yang HC, et al. Stimulation of HIV-1-specific cytolytic T lymphocytes facilitates elimination of latent viral reservoir after virus reactivation. *Immunity* 2012; 36:491-501.

55. Buck MD, O'Sullivan D, Klein Geltink RI, Curtis JD, Chang CH, Sanin DE, et al. Mitochondrial Dynamics Controls T Cell Fate through Metabolic Programming. *Cell* 2016; 166:63-76.
56. Pearce EL, Walsh MC, Cejas PJ, Harms GM, Shen H, Wang LS, et al. Enhancing CD8 T-cell memory by modulating fatty acid metabolism. *Nature* 2009; 460:103-7.

## 4.7 Supplementary materials

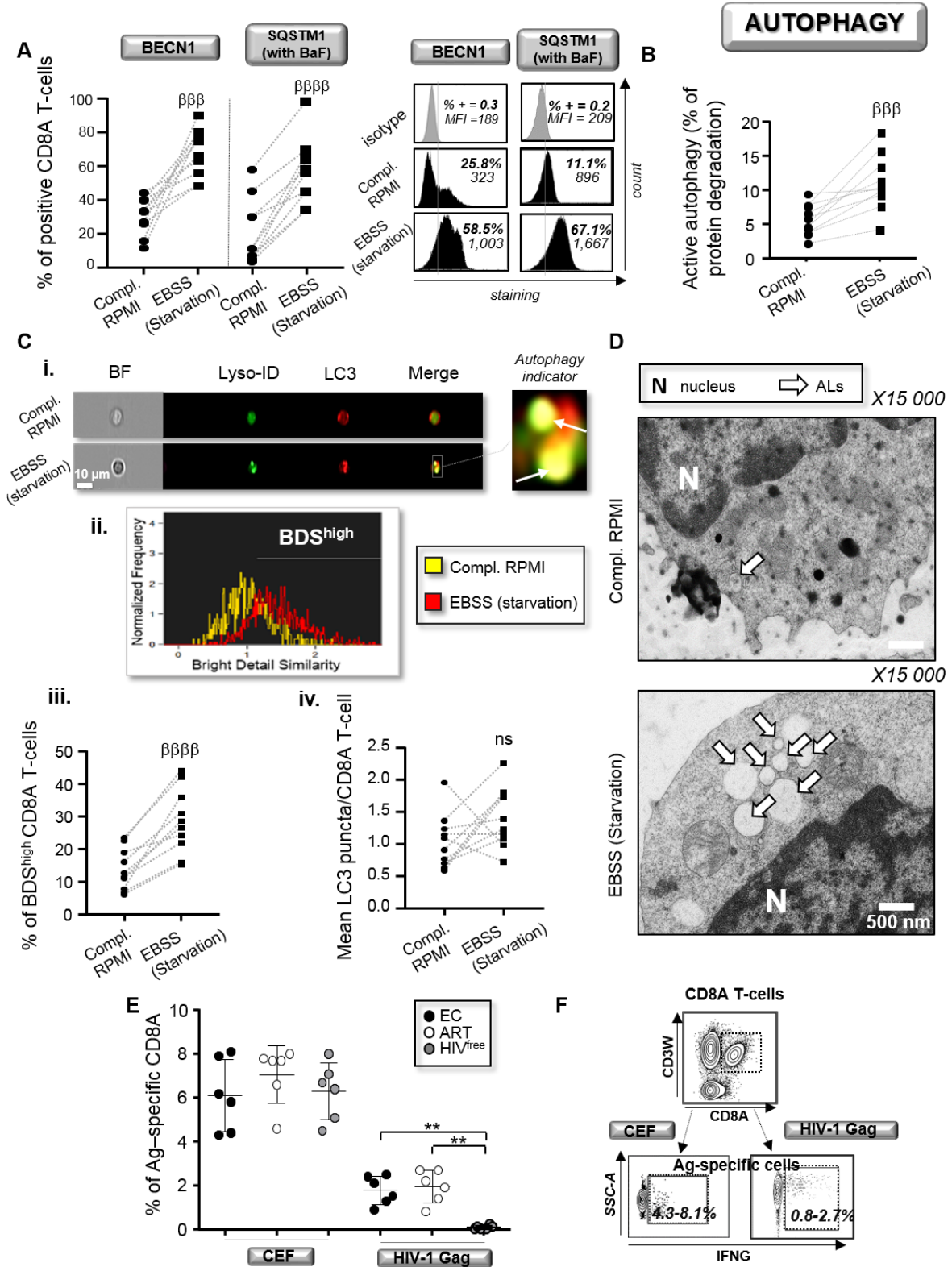


**Figure S1.** Validation of methods for autophagy detection using primary CD8A T-cells. (A-D) Autophagy induction was confirmed with several conventional autophagy detection techniques in CD8A T-cells that have been starved for 2 h in nutrient-depleted EBSS medium. n = 10, except for (D) n = 3. (A) Assessment of BECN1 and SQSTM1 cargo (when cells are cultured with BaF) expressions in CD8A T-cells that have been starved or not. Representative histograms including isotype control are also shown on the right side. (B) Autophagy-dependent lytic degradation determined in purified CD8A T-cells with or without cell starvation, by using the pulse-chase approach. (C) Lysosomal content of LC3 determined by Imaging flow cytometry. i. Representative images of single CD3W<sup>+</sup> CD8A<sup>+</sup> T-cells merged for fluorescent signals from LC3 and Lyso-ID. BF, bright field. ii. Representative BDS overlay of CD8A T-cells cultured in complete RPMI (yellow) or starved in EBSS medium (red line). The colocalization index BDS stands for bright detail similarity. iii. Percentages of BDS<sup>high</sup> LC3<sup>+</sup>Lyso-ID<sup>+</sup> cells and assessment of iv. Mean LC3 puncta per cells in primary CD8AT-cells. Ns, non-significant. (D) Representative ultrastructural micrographs from purified CD8A T-cells at 2 h post-starvation with autolysosomes (ALs) that are indicated by white arrows. (E, F) Assessment of antigen-specific CD8A T-cells at 6 h post-stimulation (n = 6). (E) Percentages of IFNG-producing CD8A T-cells from all study groups were determined after 6 h of CEF- and HIV-1 Gag-specific activation by flow cytometry. Their representative contour plots are also shown in (F).  $\beta$ , symbol used for paired *t* test (comparison between treated CD8A T-cells and their untreated control). \*, symbol used for Mann-Whitney test (comparison between study groups). One symbol, 0.05 > P > 0.01; two symbols, 0.01 > P > 0.001; and three symbols, 0.001 > P > 0.0001.

# AUTOPHAGY

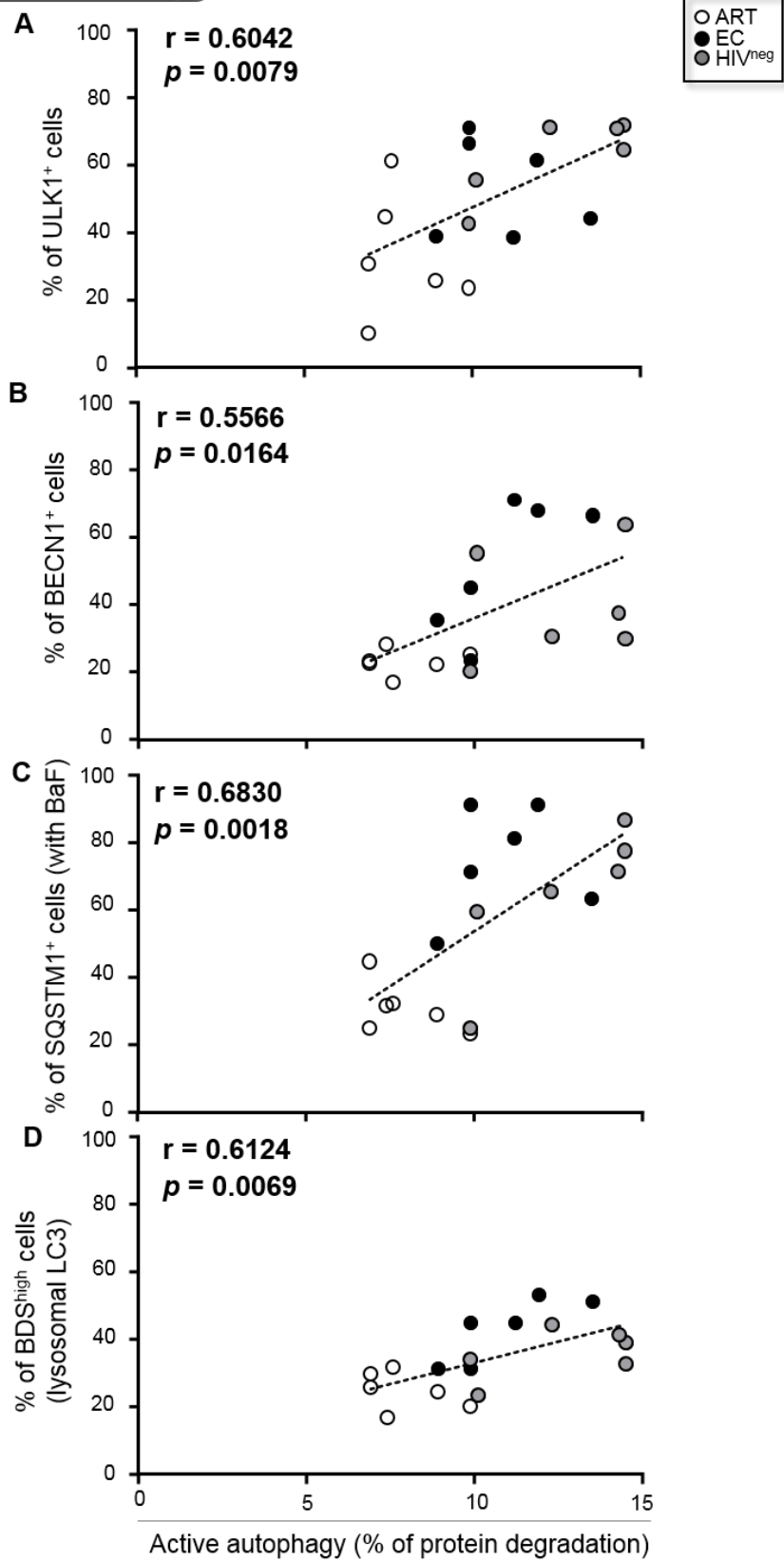




**Figure S2.** Validation of the pulse-chase approach as a good indicator of CD8A T-cell autophagic activity. We confirmed in polyclonally activated CD8A T-cells from EC (black), ART (white) and HIV<sup>neg</sup> (grey dots), the highly significant correlations between the levels of proteolytic degradation of long-lived proteins and percentages of (A) ULK1<sup>+</sup>, (B) BECN1<sup>+</sup>, (C) SQSTM1<sup>+</sup> (with BaF) and (D) BDS<sup>high</sup> LC3<sup>+</sup>Lyso-ID<sup>+</sup> CD8A T-cells. n = 18. Spearman's correlation test was used to assess side-side association between two variables.

# AUTOPHAGY

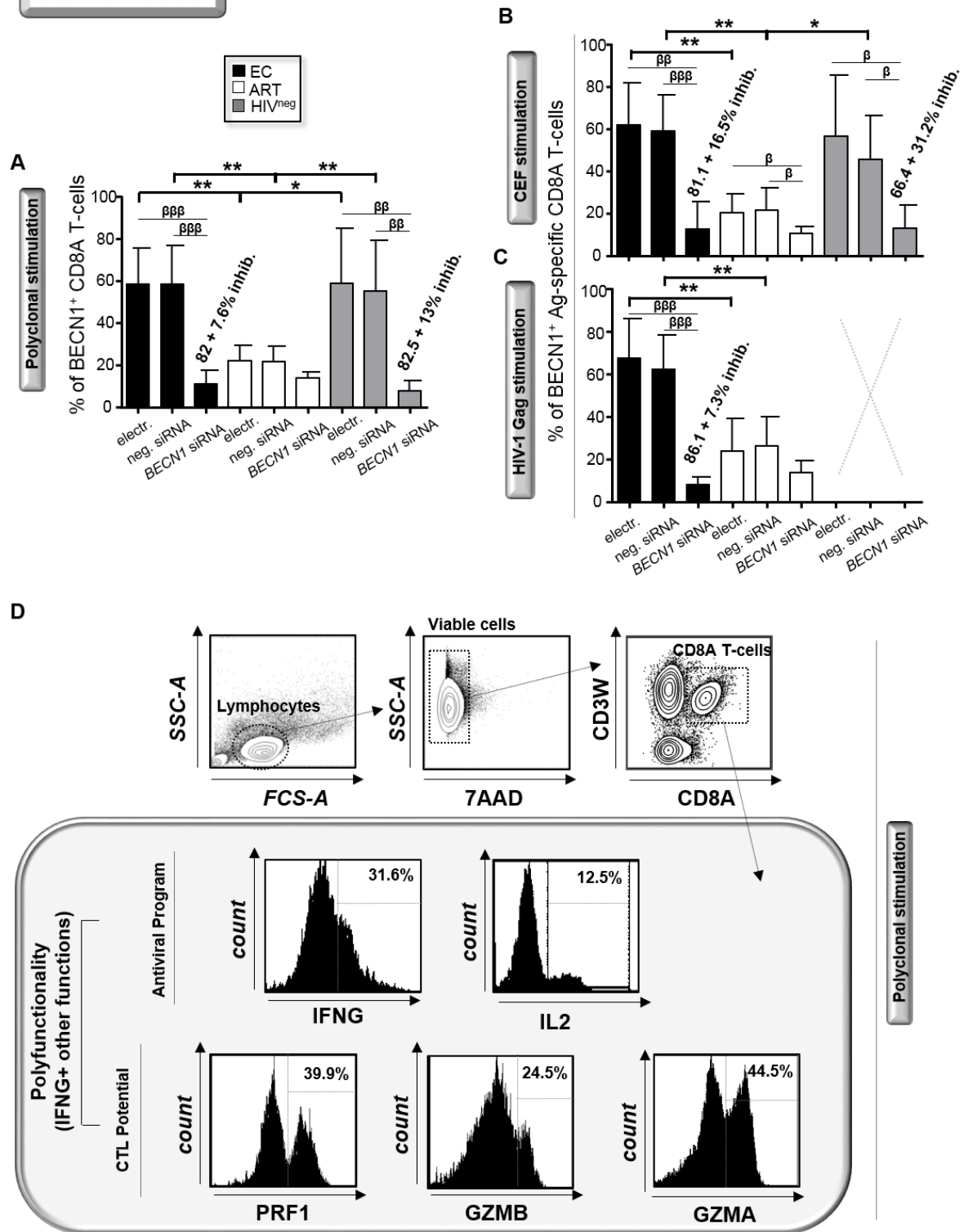


**Figure S3.** Confirmation of BECN1 inhibition in CD8A T-cells with specific gene silencing. We assessed the percentages of BECN1<sup>+</sup> cells in CD8A T-cells with or without specific *BECN1*

silencing after 6 h of (A) polyclonal, (B) CEF- and (C) HIV-1 Gag-specific activation for all study groups (n = 6). (D) Gating strategy to appreciate the antiviral (IFNG and IL2) and cytotoxic (GZMA and GZMB, and PRF1) programs in polyclonally activated CD8A T-cells from HIV<sup>neg</sup>. Of note, we determined the percentages of single positive cells for each molecule according to the respective isotype controls (indicated in bold on the histograms).  $\beta$ , symbol used for paired *t* test (comparison between treated CD8A T-cells and their untreated control). \*, symbol used for Mann-Whitney test (comparison between study groups). One symbol,  $0.05 > P > 0.01$ ; two symbols,  $0.01 > P > 0.001$ ; and three symbols,  $0.001 > P > 0.0001$ .

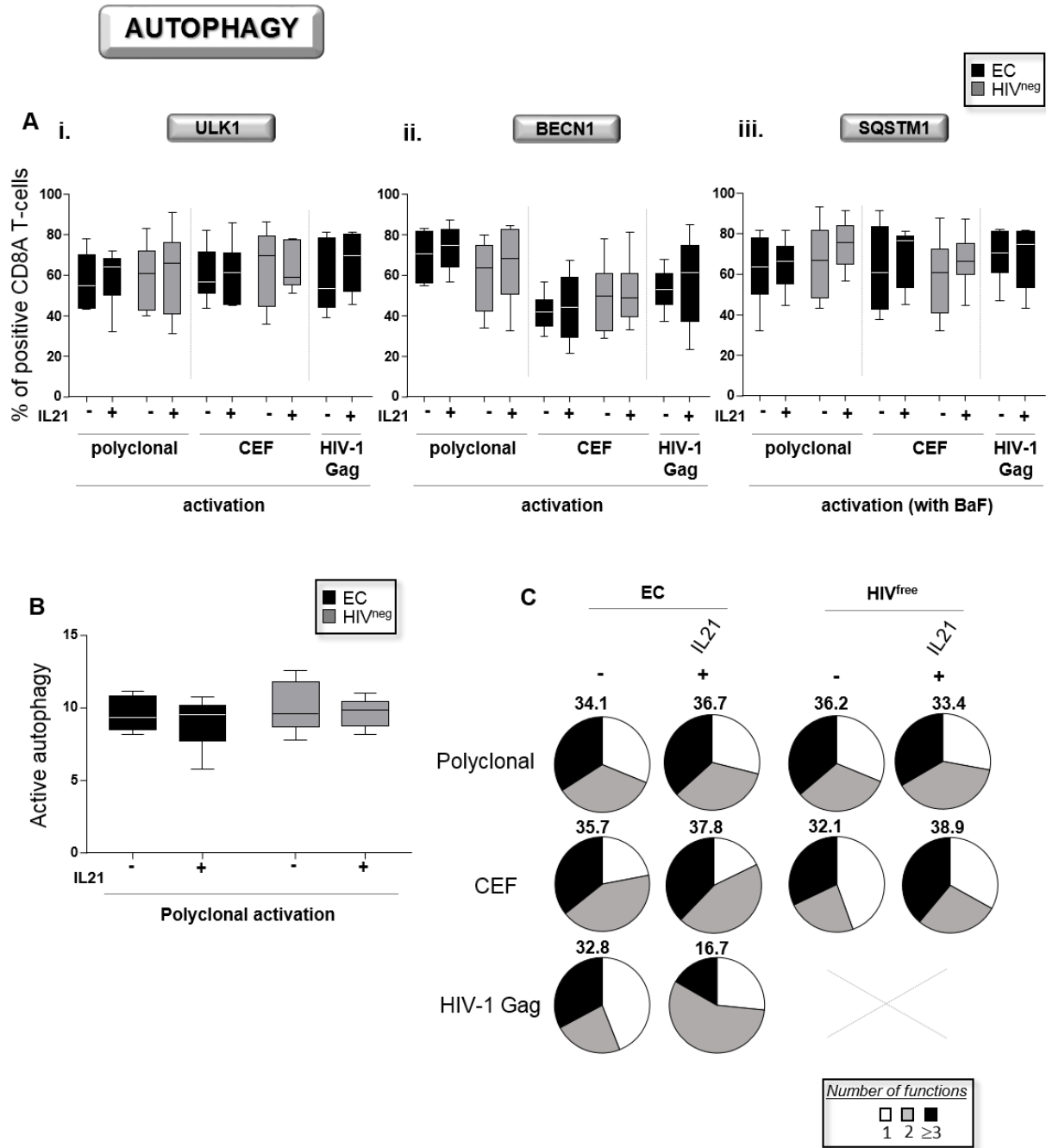


**Figure S4.** IL21 treatment of CD8A T-cells from EC did not impact their autophagy and cell polyfunctionality. (A-C), n = 6. After 6 h of cell activation with or without IL21 treatment, we assessed (A) the percentages of i. ULK1<sup>+</sup>, ii. BECN1<sup>+</sup> and iii. SQSTM1<sup>+</sup> (with BaF) CD8A T-cells in EC and HIV<sup>free</sup>. (B) Levels of active autophagy after 6 h of polyclonal activation by using the pulse-chase approach. (C) CD8A T-cell polyfunctionality determined in activated cells by flow cytometry. Results shown are representative pie charts of 6 subjects. Percentages of highly

polyfunctional CD8A T-cells are also indicated in bold. The error bars indicate standard deviations from the means.

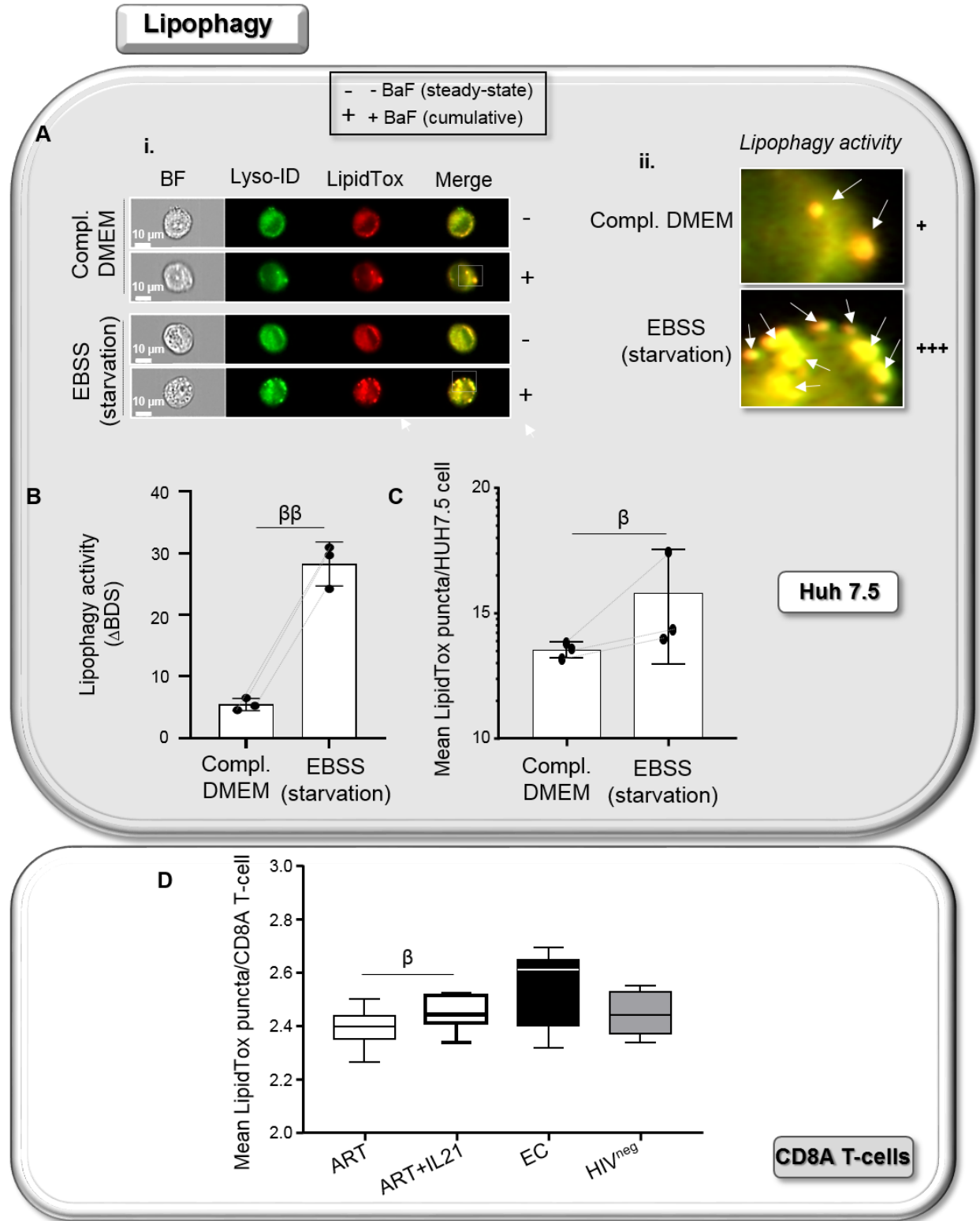


**Figure S5.** Validation of the novel ImageStream-based lipophagy assay. (A-C) Hepatic Huh 7.5 cell line was cultured either in complete DMEM or in starvation EBSS medium for 2 h in the

presence (cumulative) or absence (steady-state condition) of BaF (n = 3). (A) i. Representative images of single Huh 7.5 cells merged for fluorescent signals from Lyso-ID and LipidTox. BF, bright field. ii. Magnified images showing increased lysosomal content of lipid materials in BaF-treated Huh 7.5 cells, which is indicative of lipophagy activity when compared to cells without BaF. (B) Quantitation of lipophagy activity determined in Lyso-ID<sup>+</sup>LipidTox<sup>+</sup> Huh 7.5 cells (with or without cell starvation). Lipophagy activity was determined by the formula: (% of BDS<sup>high</sup> cells with BaF) – (% of BDS<sup>high</sup> cells without BaF). (C) Mean LipidTox puncta per Huh7.5 cells in cumulative state (after normalization with the related steady-state condition). (D) At 6 h of polyclonal activation, lipophagy activity was assessed in CD8A T-cells from ART (with or without IL21 treatment), EC and HIV<sup>neg</sup> (n = 6). Results shown are the mean LipidTox puncta per CD8A T-cells in cumulative state (after normalization with the related steady-state condition).  $\beta$ , symbol used for paired *t* test (comparison between treated CD8 T-cells and their untreated control).  $\beta$ ,  $0.05 > P > 0.01$  and  $\beta\beta$ ,  $0.01 > P > 0.001$ .

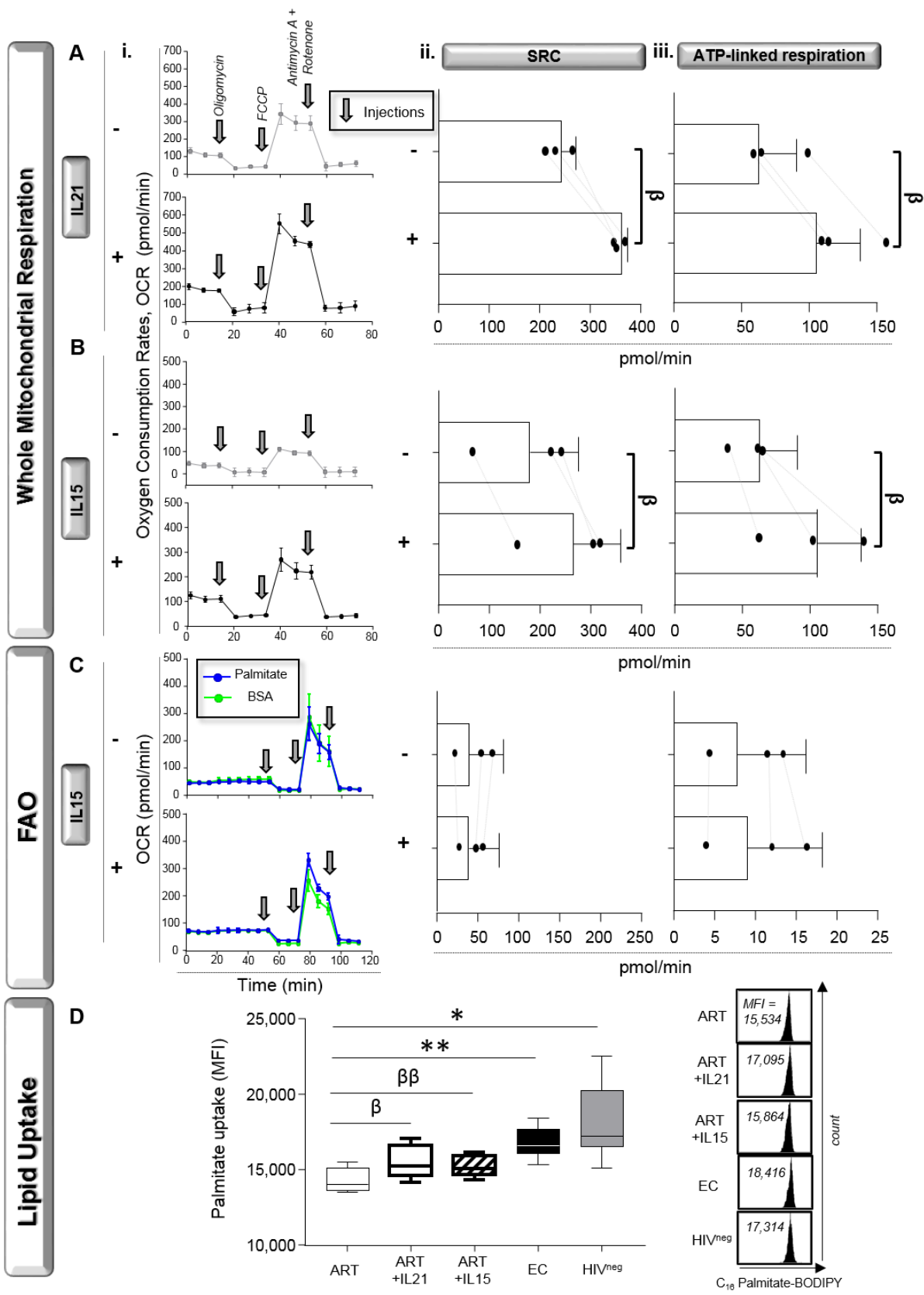




**Figure S6.** Both IL21 and IL15 treatments in ART enhance the whole mitochondrial respiration, however only IL15 fails in inducing FAO. (A-C) Briefly, we activated polyclonally purified CD8A T-cells from ART for 6 h in the presence or absence of IL21 or IL15 before assessing their (A and B) whole mitochondrial respiration and (C) FAO (n = 3). Results shown are i. Representative graphs showing real-time oxygen consumption rates (OCR) in response to injections of mitochondrial respiration modulators, which are oligomycin, carbonyl cyanide 4-(trifluoromethoxy)phenylhydrazone (FCCP) and rotenone and antimycin A respectively. Calculations of both ii. SRC and iii. ATP-linked respiration for all conditions of culture. (D) Flow cytometry analyses of C<sub>16</sub> palmitate-BODIPY uptake by CD8A T-cells in ART (with or without IL21), EC, and HIV<sup>neg</sup> at 6 h post-polyclonal activation (n = 6).  $\beta$ , symbol used for paired *t* test (comparison between treated CD8A T-cells and untreated control). \*, symbol used for Mann-Whitney test (comparison between study groups). One symbol, 0.05 > P > 0.01 and two symbols, 0.01 > P > 0.001.





## 5 SECOND ARTICLE: IMPACT OF GLUTAMINOLYSIS THROUGH AUTOPHAGY-MEDIATED PROTEIN CATABOLISM IN HIV-1-SPECIFIC MEMORY CD4 T-CELLS IMMUNITY

---

### Autophagy-dependent glutaminolysis drives superior IL21 production in HIV-1-specific CD4 T cells

La glutaminolyse médiée par l'autophagie entraîne une production supérieure d'IL21 dans les lymphocytes T CD4 spécifiques au VIH-1

**Authors :** Hamza Loucif<sup>1</sup>, Xavier Dagenais-Lussier<sup>1</sup>, Daina Avizonis<sup>2</sup>, Luc Choinière<sup>2</sup>, Cherifa Beji<sup>1</sup>, Léna Cassin<sup>3</sup>, Jean-Pierre Routy<sup>4</sup>, Jörg H. Fritz<sup>5</sup>, David OLAGNIER<sup>3</sup>, and Julien van Grevenynghe<sup>1</sup>

<sup>1</sup> Institut national de la recherche scientifique (INRS)-Centre Armand-Frappier Santé Biotechnologie, 531 boulevard des Prairies, Laval, QC, Canada, H7V 1M7;

<sup>2</sup> Metabolomics Innovation Resource, Rosalind and Morris Goodman Cancer Center, McGill University, 1160 Pine Avenue West, Montreal QC H3A 1A3, Canada

<sup>3</sup> Aarhus University; Department of Biomedicine, Research Center for Innate Immunology, Aarhus C, 8000, Denmark.

<sup>4</sup> Chronic Viral Illness Service and Division of Hematology, McGill University Health Centre, Glen site, Montreal, Quebec, Canada, H4A 3J1;

<sup>5</sup> Department of Microbiology and Immunology, McGill University, Montreal, Quebec, Canada H3G 0B1.

**Journal:** Autophagy

**Received** 05 Apr 2021, **Accepted** 20 Aug 2021, **Published online:** 06 Oct 2021

<https://doi.org/10.1080/15548627.2021.1972403>

**Authors' contribution:**

**H.L.** performed the experiments and analyzed the data. , **X.D.L.**, **C.B.** and **L.C.** contributed with a technical assistance in some experiments. **J-P.R.** contributed to the inclusion of study participants, obtaining clinical information and its validation. **J.H.F.**, **D.V.** and **Luc. C.** managed

and performed the GC/MS experiments including all sample analyses. **J.V.G.** designed and supervised the study with some help from **H.L.**

**J.V.G.**, **H.L.** and **D.O.** drafted the article. All the authors critically reviewed the manuscript.

### **Link to the previous paper:**

This study is a complementary piece of evidence that validates the intricacy of autophagy in not only conferring a highly cytotoxic CD8A T cells responses, but also sustaining an effective IL21 production in HIV-1-specific memory CD4 T-cell. In addition to confirming our hypothesis in the previous paper, we found a striking indication that autophagy activity is selective to the type of substrate provided to fuel the rates of mitochondrial oxidative metabolism in T cells (See the schematic presentation that summarizes the entire ultimatum; [Figure 8](#)).

## **5.1 Abstract**

The maintenance of a strong IL21 production in memory CD4 T cells, especially in HIV-1-specific cells, represents a major correlate of natural immune protection against the virus. However, the molecular mechanisms underlying IL21 production during HIV-1 infection, which is only elevated among the naturally protected elite controllers (EC), are still unknown. We recently found out that lipophagy is a critical immune mediator that control an antiviral metabolic state following CD8A T cell receptor engagement, playing an important role in the natural control of HIV-1 infection. This led us to investigate whether the beneficial role of a strong macroautophagy/autophagy, could also be used to ensure effective IL21 production as well. Herein, we confirm that after both polyclonal and HIV-1-specific activation, memory CD4 T cells (Mem) from EC display enhanced activity of the autophagy-mediated proteolysis compared to ART. Our results indicate that the enhanced autophagy activity in EC was controlled by the energy-sensing PRKAA1 (protein kinase AMP-activated catalytic subunit alpha 1). We further confirmed the critical role of the autophagy-mediated proteolysis in the strong IL21 production in EC by using *BECN1* gene silencing as well as protease, PRKAA1, and lysosomal inhibitors. Finally, we established that high autophagy-mediated proteolysis in EC fuels their cellular rates of mitochondrial respiration due to glutaminolysis. Our data confirm the critical role of autophagy in dictating the metabolic input, which is required not only to ensure protective cytotoxic CD8A T cell responses, but also to provide strong IL21 production among antiviral CD4 T cells.

## 5.2 Introduction

Despite the fact that antiretroviral therapy has substantially improved the life expectancy of HIV-1-infected patients, they are still associated with a number of health complications, metabolic disorders, drug resistances, and the inability to fully restore anti-HIV-1 immunity [1-3]. Therefore, a cure for HIV-1 is still highly required and has become a global research priority. Among all of the strategies that have been developed for this purpose, the most feasible ones are referred to as functional cures. These strategies consist of finding a way to coexist with the virus in the long run. The functional cures share a common goal of inducing antiretroviral therapy-free remission of HIV-1 pathogenesis and disease progression. The most critical component, which is required to ensure the success of these functional cures, is the restoration of a strong anti-HIV-1 immunity in patients [4]. Indeed, a strong anti-HIV-1 immunity is key to avoid or delay any viral rebound after medical interruption, which is needed to pave the way to a natural, long-lasting immune-based control of HIV-1 replication.

Elite controllers (EC) are a unique group of chronically HIV-1-infected patients who display a full drug-free control of HIV-1 infection for years [5, 6]. The fact that EC also maintain a strong anti-HIV-1 immune response despite persistent HIV-1 infection provided the evidence that a functional cure could eventually be achieved. However, we first have to identify the genetic, molecular, and metabolic mechanisms that are responsible for providing such protective immunity in EC [7-9]. For instance, in contrast to patients under therapy (ART), EC maintain an effective peripheral CD4 T-follicular cell function with untouched IL21 (interleukin 21) production [10-12] along with highly functional cell responses [7, 13]. In addition, we have previously demonstrated that memory CD4 T cells (Mem) from EC were more resistant to FAS-mediated apoptosis and were able to persist longer in culture after multiple rounds of T cell receptor triggering when compared to ART [14]. We further showed that higher Mem survival in EC was a direct consequence of enhanced suppression of the pro-apoptotic activity of the transcription factor FOXO3/FOXO3a.

However, besides Mem survival, the mechanisms responsible for the superior immunity found in Mem from EC, especially in their IL21-producing and HIV-1-specific CD4 T cells, are unknown.

In the present study, we confirmed that following polyclonal and HIV-1 Gag-specific cell activations, Mem from EC displayed increased expression of IL21. Our data showed that activated Mem from EC, including specific HIV-1 clones, displayed enhanced macroautophagy/autophagy activity when compared to Mem from ART. Autophagy is a housekeeping stress-induced

lysosomal degradation pathway, which regulates cellular homeostasis by clearing damaged proteins or organelles. Autophagy can also recycle macromolecules and metabolites for energy production under specific conditions [15-17]. For instance, autophagy, which is induced in CD4 T cells in response to T-cell receptor engagement [18], is a key catabolic process that regulates energy metabolism, cell proliferation, cytokine production, and Mem maintenance during effector T-cell activation [19-21]. Although previous observations have proposed that autophagy may contribute to limiting HIV-1 pathogenesis in EC by targeting viral components for degradation [22], we raised the question of whether it could also provide their Mem with energetic support and superior immunity. Using specific gene silencing of BECN1 (beclin 1), a major regulator of autophagic activity, we confirmed the critical role of this catabolic process in IL21-producing Mem. We further found that both lysosomal and protease activities were required for optimal IL21 expression during HIV-1 infection. Mechanistically speaking, we found that the energy-sensing PRKAA1 (protein kinase AMP-activated catalytic subunit alpha 1) activity regulated autophagy-mediated proteolysis in Mem from EC, rather than the MTOR (mechanistic target of rapamycin kinase). Finally, we concluded our study by confirming that the enhanced autophagy-mediated proteolysis impacted the cellular energetic balance directly through protein breakdown and glutaminolysis.

Overall, our study unveiled a new molecular and metabolic advantage in EC, which must be considered in the design of next generation functional cures for the treatment of HIV-1-infected patients, whose control of viral replication is solely mediated by their medication.

## **5.3 Results**

### **5.3.1 Activated Mem from EC display enhanced PRKAA1-dependent autophagy when compared to ART.**

In contrast to ART, we have recently shown that HIV-1-specific cytotoxic CD8A T cells from EC display a unique metabolic advantage involving the autophagy-dependent lytic activity [23]. Our data further demonstrated that this was possible because of memory CD4 T cell help via their IL21 production. Since the mechanisms governing the maintenance of strong IL21 production

during HIV-1 infection are still unknown, we sought to investigate whether HIV-1-specific Mem from EC could similarly display enhanced autophagy when compared to ART.

As a reminder, autophagy is a conserved catabolic process involved in the regulation of homeostasis and energy metabolism in T cells [19, 24]. It is basically a process that involves the capture, isolation, and lysosomal digestion of intracellular materials in autolysosomes or ALs [25]. Since autophagy is induced at early stages in CD4 T cells following their activation [18], we performed a 6 h-long polyclonal or HIV-1 Gag activation to evaluate autophagy in Mem for all study groups (EC, ART and HIV<sup>neg</sup> control donors). First, we thought it was necessary to characterize additional Mem features for all study groups at 6 h of cell activation (such as the levels of cell activation and survival) before assessing their autophagy. Our data confirmed that all HIV-1-specific CD4 T cells, which were characterized by IFNG/IFN- $\gamma$  expression after Gag-specific stimulation (Fig. S1A), had a CD45RA<sup>neg</sup> memory phenotype (Fig. S1B). At 6 h of polyclonal or HIV-1-specific stimulations, we did not find any differences in the levels of both Mem activation (as determined by the percentages of IFNG<sup>+</sup> cells) and apoptosis (as determined by the percentages and absolute numbers of viable ANXA5<sup>neg</sup> cells) between all study groups (Fig. S1C-E).

We then used several methods to ensure a controlled assessment of autophagy in viable Mem after cell activation and avoid any misinterpreted conclusions on collected data. In this context, we decided to assess in Mem from all study groups the expression levels of several autophagy-related genes by flow cytometry (gating strategy shown in Fig. S2), the numbers of both autophagic vacuoles (AVs) and active autolysosomes (ALs) using ultrastructural microscopy analysis (micrographs shown in Fig. S3A to discriminate between AV and AL structures), and the measurement of autophagy-mediated proteolysis with a radiometric assay. First, at 6 h of both polyclonal and HIV-1-specific activation, we found enhanced expression for several autophagy-related players (ATGs) in Mem from EC and HIV<sup>neg</sup> controls when compared to ART (as determined by both the percentage of BECN1<sup>+</sup>ULK1<sup>+</sup>ATG7<sup>+</sup> and SQSTM1<sup>+</sup> cells when bafilomycin A1 (BaF) was added in culture) (Fig. 1A,B). Of note, the low expression levels of the ATGs were found similar between all groups when considering non-activated cells. Our microscopic analysis further showed that activated Mem from EC and HIV<sup>neg</sup> displayed higher numbers of both AVs and ALs per cell when compared to ART (Fig. 1C, Fig. S3B,C and Table S2). Similarly, the activity of autophagy-mediated proteolysis in Mem, which was induced with 6 h-long T cell activation, was confirmed to be higher in EC and HIV<sup>neg</sup> when compared to ART (Fig. 1D). We also found that the activity of autophagy-mediated proteolysis in activated Mem from EC



and HIV<sup>neg</sup> was prevented by blocking the autophagy-related lytic (BaF and Chloro.) and protease (E64d-PepA) activity (Fig. 1D). Since the autophagy-mediated proteolysis represents a functional assessment of the autophagic activity in Mem and was tightly correlated with the expression of ATGs (Fig. 1E), we decided to use this radiometric assay for the rest of our study every time we had to determine the status of autophagy in culture.

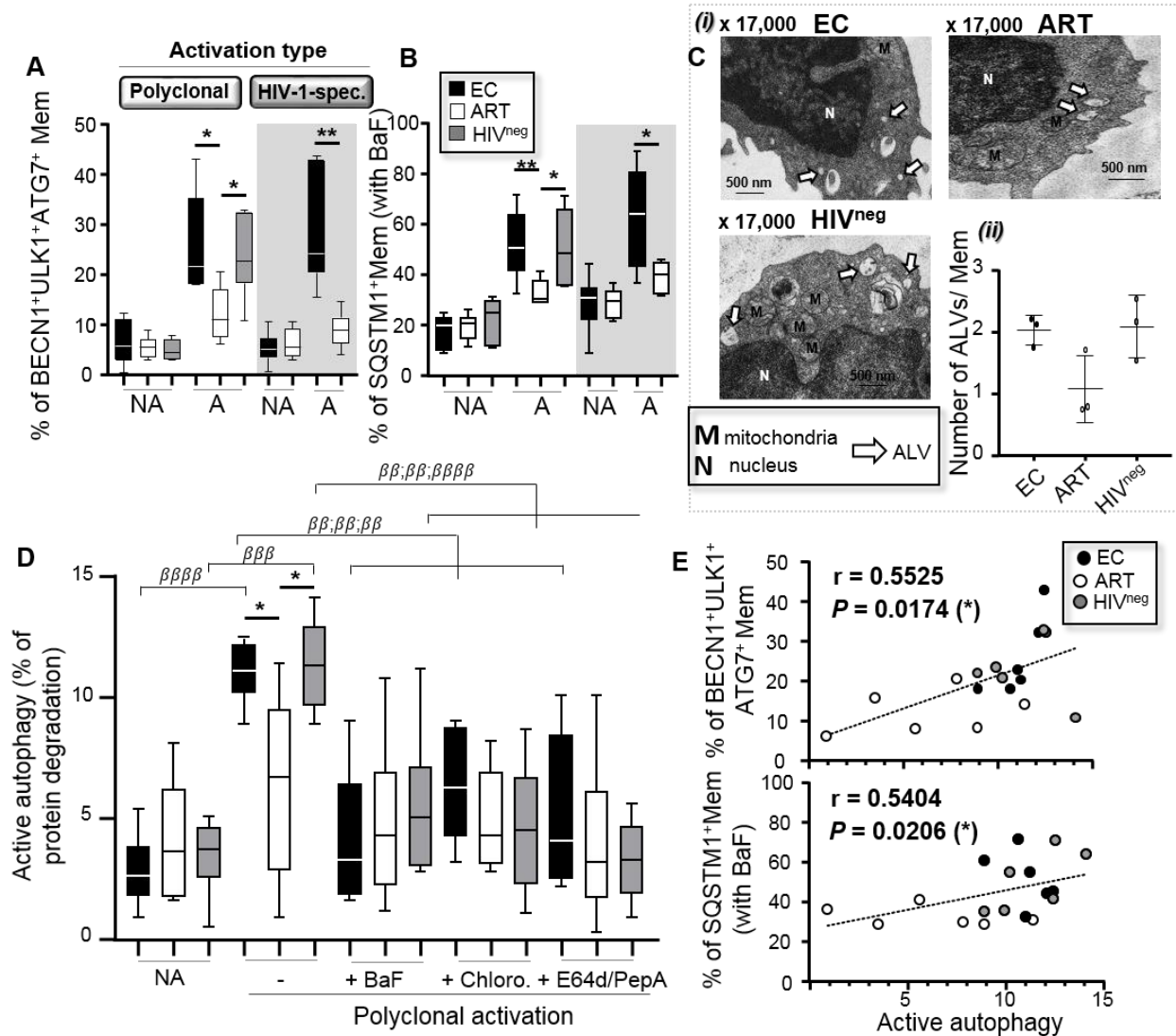


**Figure 5.1** Enhanced autophagy-mediated proteolysis in Mem from EC after cell activation.

Mem from EC, ART, and HIV<sup>neg</sup> were either polyclonally or HIV-1 Gag-specifically activated for 6 h. Of note, HIV-1-specific Mem were identified at 6 h post-activation by their positive staining for IFNG. (A) The percentages of Mem, which expressed autophagic players such as BECN1, ULK1 and ATG7, were then determined by flow cytometry. (B) We also assessed the percentages of SQSTM1<sup>+</sup> Mem when lysosomal activity was blocked by BaF during culture. A, activated and NA, non-activated culture condition. (C) Ultrastructural analysis of purified Mem from EC, ART, and HIV<sup>neg</sup> after 6 h of polyclonal activation. i. Representative micrographs to appreciate the numbers of active autophagolysosomes (ALs) (X 17,000). ii. Quantitative analysis of the number of ALs per Mem for all study groups. (D) Autophagy-mediated proteolysis determined in purified Mem after polyclonal

activation (PA) or not (NA), and in the presence or absence of BaF, Chloro., or E64d/PepA, by using a pulse-chase approach. (E) We assessed in polyclonally activated Mem from all study participants the correlation between the levels of proteolytic degradation of long-lived proteins with the percentages of BECN1<sup>+</sup> ULK1<sup>+</sup> ATG7<sup>+</sup> or SQSTM1<sup>+</sup> cells. N = 6 for all experiments, except for (C) and (E) with n = 3 and 18 respectively. The error bars indicate standard deviations from the means.  $\beta$ , symbol used for paired *t*-test (comparison between treated Mem and untreated control), \*, symbol used for Mann-Whitney test (comparison between study groups).

Finally, we aimed to identify the upstream cell mechanisms that drove the enhanced autophagy-mediated proteolysis in Mem from EC when compared to ART that follows T cell activation (Fig. 1D; NA versus A). Autophagy is known to be regulated by two major energy-sensors, MTOR and PRKAA1 [26]. In this context, we were interested to first investigate the impact of MTOR activity, since it is considered as the main negative regulator of autophagy [26, 27]. In addition to similar levels of MTOR activity for all study groups after Mem activation (as determined by the percentage of active p-S4228 MTOR<sup>+</sup> cells and its downstream target p-Thr36/45 EIF4EBP1<sup>+</sup> cells) (Fig. S4A-D) [18], we found that the addition of MTOR inhibitors (torin-1 and rapamycin) in culture had no impact on the levels of autophagy-mediated proteolysis (Fig. S4E,F). Similar and low levels of PRKAA1 activity (as determined by the relative protein expression levels of active p-Thr172 PRKAA1 and calculated as follows: p-Thr172 PRKAA1:total PRKAA1 in %) were found in non-activated Mem for all study groups (Fig. 2A). In contrast, we found higher increases in relative PRKAA1 activity with activated Mem from EC and HIV<sup>neg</sup> when compared to ART (Fig. 2A) [28]. Furthermore, the adding of the PRKAA1 inhibitor compound C in culture with activated Mem confirms the role of the kinase in regulating their autophagy-mediated proteolysis after T cell receptor engagement (Fig. 2B).

Overall, our data confirmed a superior autophagy-mediated proteolysis activity in activated Mem, including in HIV-1-specific cells, from EC when compared to ART. Mechanistically speaking, the results also showed that the activity of autophagy-mediated proteolysis during natural protection of HIV-1 infection was regulated through a PRKAA1-dependent control.

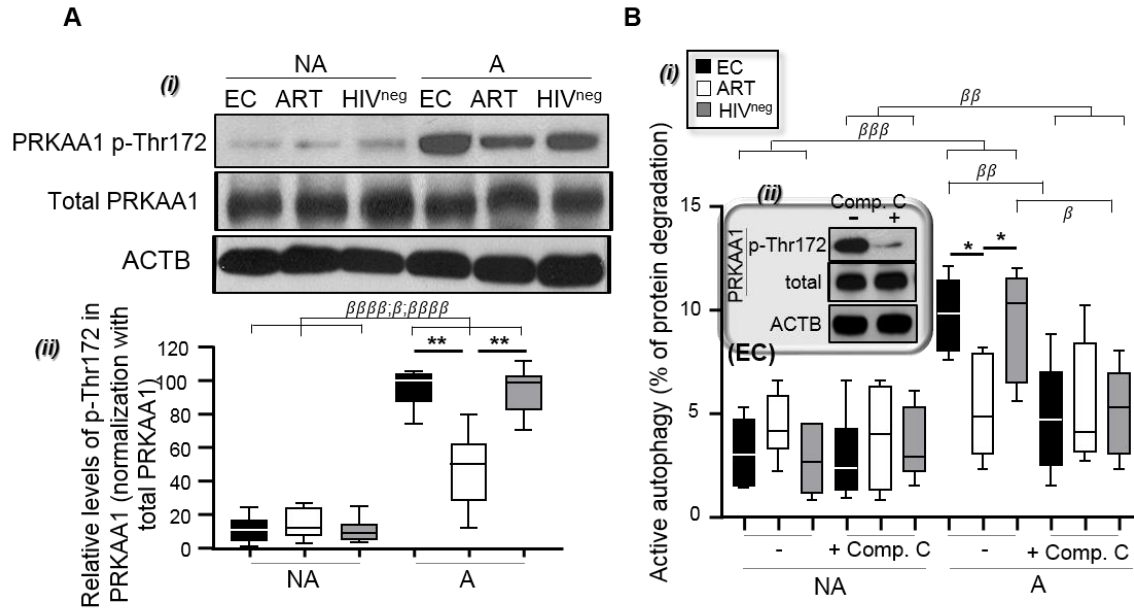


**Figure 5.2 Enhanced PRKAA1-dependent autophagy-mediated proteolysis in Mem from EC after cell activation.**

Mem from EC, ART, and HIV<sup>neg</sup> were polyclonally activated for 6 h. (A) Levels of total and p-Thr172 PRKAA1 were determined on non-activated (NA) and polyclonally activated (PA) Mem by western blotting. i. Representative blots for all study groups. ii. Densitometric quantification of 6 independent experiments was performed using ImageQuant software (mean  $\pm$  SD). Results shown represent the relative levels of p-Thr172 in PRKAA1 and were determined as follows: values for p-Thr172 PRKAA1/values in % of total PRKAA1. (B) i. Autophagy-dependent proteolysis determined in purified Mem from EC, ART and HIV<sup>neg</sup> with or without PRKAA1 inhibition (using compound C [comp. C]), and after 6 h of polyclonal activation (PA) or not (NA). ii. Confirmation of AMPK inhibition by compound C was determined by western blotting using polyclonally activated Mem from EC (representative blots of 3 independent confirmations). N = 6 for all experiments. The error bars indicate standard deviations from the means.  $\beta$ , symbol used for paired *t*-test (comparison between treated Mem and untreated control). \*, symbol used for Mann-Whitney test (comparison between study groups).

### 5.3.2 Strong autophagy-mediated proteolysis is needed to ensure effective IL21 Mem production during HIV-1 infection.

Studies based on the comparison between EC and ART led to the identification of several key correlates of natural immune protection against HIV-1 [9]. Among them, the superior IL21 production in EC is a well-acknowledged Mem-related advantage, since it provides critical help to CD8A T cell, natural killer, and B-cell-mediated antiviral responses during chronic HIV-1 infection [11, 12, 23, 29].

To investigate whether autophagy-mediated proteolysis was responsible for superior IL21 production in Mem during HIV-1 infection, we specifically inhibited BECN1 expression using small interfering silencing RNAs (siRNA) before cell activation. Briefly, purified Mem from all study groups were either electroporated or transfected with siRNAs specific for *BECN1* or with negative

control siRNA for 2 h. Then, cells were washed twice and cultured with their autologous CD4-depleted PBMC. At 24 h post-transfection, we confirmed by flow cytometry around 80% protein decrease of BECN1 expression in both EC and HIV<sup>neg</sup> (Fig. 3A). Of note, *BECN1* silencing in EC and HIV<sup>neg</sup> led to reductions of its protein expression to levels comparable to ART. Silencing *BECN1* had no impact on Mem survival as determined by the percentage of apoptotic ANXA5<sup>+</sup> Mem at 24 h post cell transfection (Fig. S5A). As expected, we found that pre-silencing BECN1 expression in EC and HIV<sup>neg</sup> led to potent blockade of autophagy-mediated proteolysis after 6 h of Mem activation (Fig. 3B and Fig. S5B). In addition to specific *BECN1* gene pre-silencing, we also treated our cultures with chemical inhibitors to block the autophagy-related lytic (BaF and Chloro.), protease (E64d-PepA) and PRKAA1 (compound C) activities before assessing IL21 expression levels. Of note, we confirmed the efficacy of all chemical inhibitors in blocking the autophagy-mediated proteolysis in 6 h-long polyclonally activated Mem from EC. Neither *BECN1* gene silencing nor the treatment with chemical inhibitors affected the percentage of IFNG<sup>+</sup> Mem at 6 h of cell activation for all study groups (Fig. S6A,B). In contrast, we found that blocking autophagy-mediated proteolysis with *BECN1* silencing or chemical inhibitors in EC and HIV<sup>neg</sup> led to potent decreases of the percentage of IL21<sup>+</sup> Mem to levels that were comparable to ART (Fig. 3C,D and Fig. S5C).

Overall, our results demonstrate a critical role of autophagy-mediated proteolysis in the superior IL21 production found in Mem from EC, including in HIV-1-specific cells.

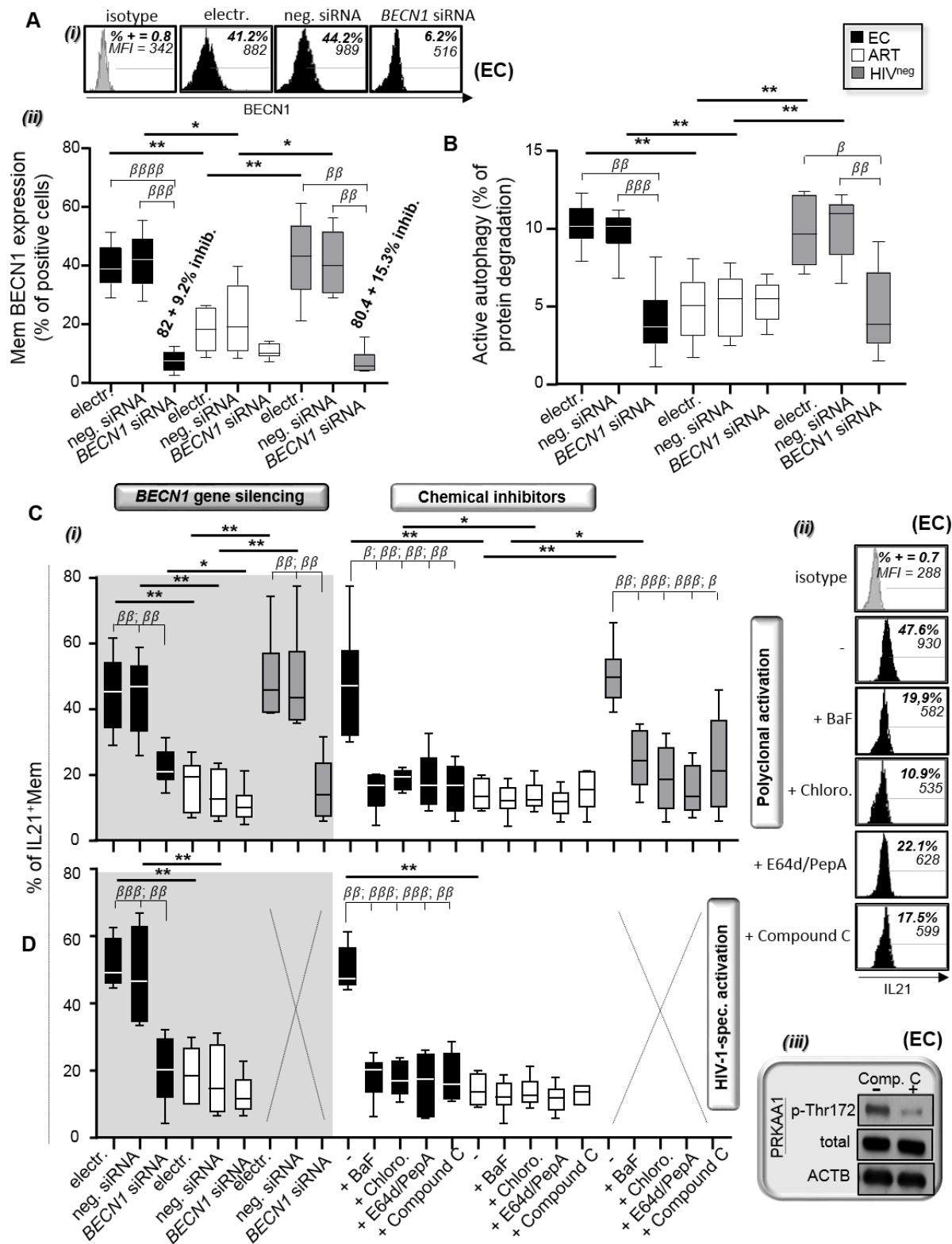


**Figure 5.3** Autophagy-mediated proteolysis is required for optimal IL21 production in Mem from EC.

Autophagy-mediated proteolysis and IL21 production were both determined in activated Mem under specific *BECN1* gene silencing (siRNA IDs: 137198), or PRKAA1 (compound C), lysosomal (BaF or Chloro.), and

protease (E64d-PepA) inactivation. (A) Levels of BECN1 were determined on Mem after 24 h of cell transfection with negative or *BECN1* siRNAs by flow cytometry. i. Representative histograms of BECN1 expression in transfected Mem from EC. ii. Percentages of BECN1<sup>+</sup> cells in Mem with or without specific *BECN1* silencing for all study groups. % of BECN1 decrease was also indicated in bold for the EC' and HIV<sup>neg</sup>'s groups. (B) Autophagy-mediated proteolysis assessed in polyclonally activated Mem with or without specific *BECN1* gene silencing or chemical inhibitors. Levels of IL21 production in Mem that have then been either (C) i. polyclonally or (D) HIV-1-specifically activated for 6 h with or without specific *BECN1* gene silencing or chemical inhibitors. (C) ii. Representative histograms of IL21 expression in polyclonally-activated Mem from EC with or without autophagy blockade. iii. Confirmation of PRKAA1 inhibition by compound C was determined by western blotting using polyclonally activated Mem from EC (representative blots of 3 independent confirmations). N = 6. The error bars indicate standard deviations from the means.  $\beta$ , symbol used for paired *t*-test (comparison between treated Mem and untreated control). \*, symbol used for Mann-Whitney test (comparison between study groups).

### 5.3.3 Autophagy activity in Mem from EC favors the release of free glutamine rather than fatty acids, therefore promoting glutaminolysis.

Mounting an antiviral immune response against pathogens is always an energetically demanding process. In this regard, under specific circumstances such as T cell activation, autophagy can be essential for the maintenance of mitochondrial energetic function by providing metabolic substrates through lysosomal degradation [19, 24].

We have recently shown that HIV-1-specific cytotoxic CD8A T cells from EC displayed a unique metabolic advantage involving the autophagy-dependent lytic activity [23]. In fact, we have determined that enhanced autophagy in CD8A T cells from EC was directed towards the degradation of intracellular lipid content and the release of free fatty acids, referred to as lipophagy, to fuel mitochondrial energy production. Although our current data on Mem indicated that EC used autophagy to degrade protein content and release free amino acids to support their strong IL21 production (Fig. 3C and D), we could not exclude a potential use of lipophagy as well. Therefore, we first assessed the levels of Mem lipophagy with a recently developed ImageStream-based assay, which relies on the quantification of increased lipid content within lysosomes when cultures are conducted with BaF (Fig. 4A and B) [23]. First and foremost, we validated our assay by using Huh7.5 hepatic cells, which have been starved or not for 2 h. In this regard, we confirmed higher lipophagic activity, as determined by the  $\Delta$ BDS value and mean LipidTox puncta per cells, in starved Huh7.5 cells when compared to those cultured in complete DMEM (Fig. 4C and D). Our data further showed no differences between EC and ART, both for Mem that have been activated or not. Similarly, we found no differences for the mean LipidTox puncta per Mem between EC and ART after cell activation (Fig. 4E). Of note, although mean LipidTox puncta were similar between all study groups, higher lipophagic activity determined with  $\Delta$ BDS value was found in HIV<sup>neg</sup> when compared to EC (Figs. 4C and E). Overall, our data confirm that higher

autophagy in Mem from EC after T cell activation is not associated with increased lipophagic activity when compared to ART.

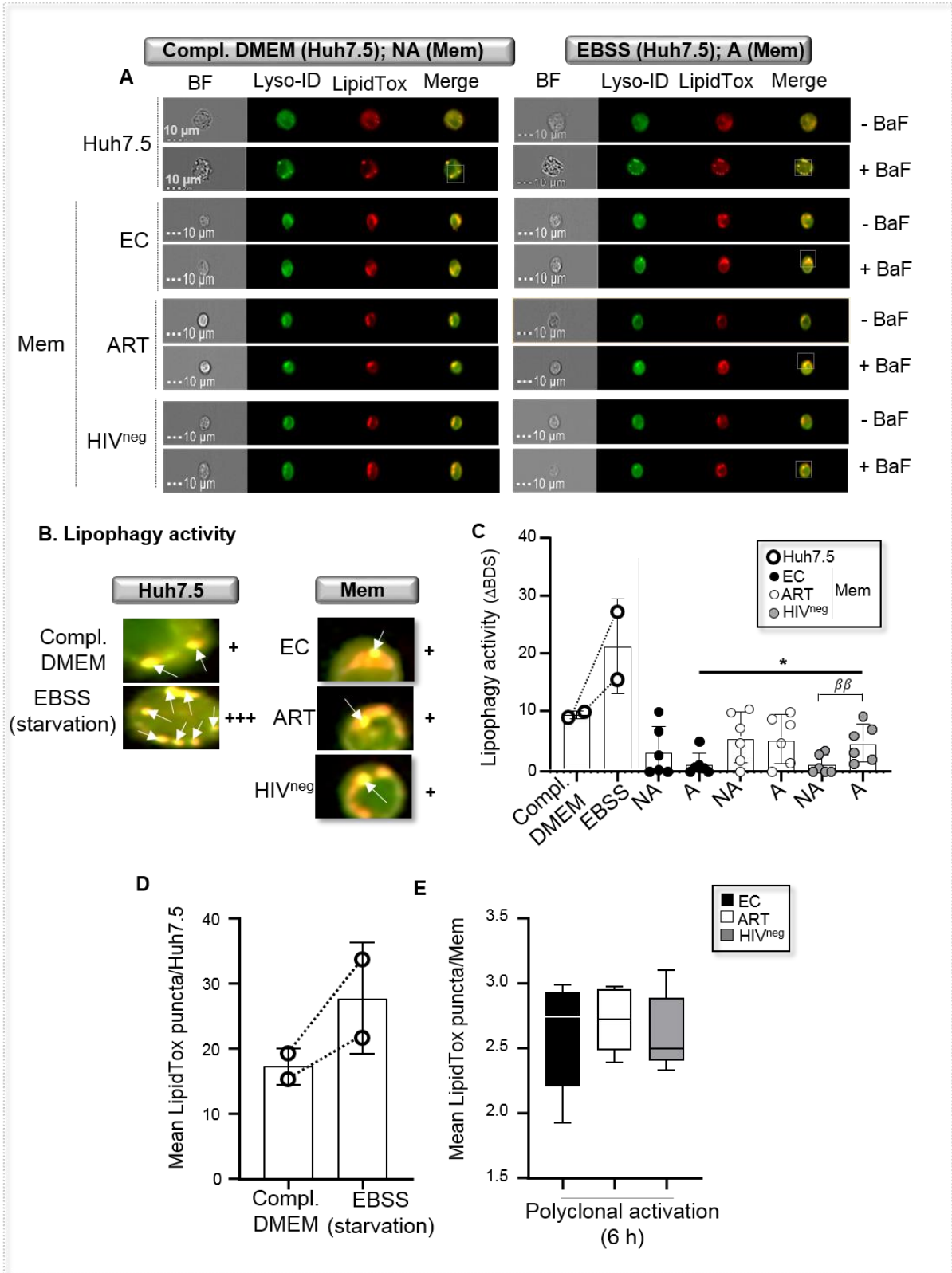


Figure 5.4 Similar lipophagy levels in activated Mem.



(A-C) Assessment of lipophagy activity for all study groups by using our recently developed ImageStream-based lipophagy assay. Of note, we included lipophagy induction in starved Huh7.5 hepatic cells as the experimental control. (A) Representative images of single Lyso-ID<sup>+</sup> LipidTox<sup>+</sup> Huh7.5 cells (with or without cell starvation) and Mem for all groups that have been polyclonally activated or not for 6 h. All culture conditions were conducted in the presence or absence of BaF ("cumulative" and "steady-state" conditions, respectively). BF, bright field. (B) Magnified images showing increased lysosomal content of endogenous lipids in BaF-treated cells, which is an indicator of lipophagy activity when compared to cells without BaF. (C) Quantification of lipophagy activity determined in Lyso-ID<sup>+</sup> LipidTox<sup>+</sup> Huh7.5 cells and Mem in EC, ART, and HIV<sup>neg</sup>. Lipophagy activity was determined by the formula:  $\Delta\text{BDS} = (\% \text{ of BDS}^{\text{high}} \text{ cells with BaF}) - (\% \text{ of BDS}^{\text{high}} \text{ cells without BaF})$ . (D, E) Imaging-based assay to assess lipophagy activity. (D) Mean LipidTox puncta per Huh7.5 cells in cumulative state (after normalization with the related steady-state condition). (E) At 6 h of polyclonal activation, lipophagy activity was assessed in Mem from EC, ART and HIV<sup>neg</sup>. Results shown are the mean LipidTox puncta per activated Mem in cumulative state (after normalization with the related steady-state condition). N = 6, except for n = 2 for Huh7.5 controls. The error bars indicate standard deviations from the means.  $\beta$ , symbol used for paired *t*-test (comparison between treated Mem and untreated control). \*, symbol used for Mann-Whitney test (comparison between study groups).

Next, we hypothesized that enhanced PRKAA1 and autophagic activities found in Mem from EC after 6 h-long T cell receptor stimulation could rather be used to degrade protein content and provide free glutamine. Indeed, a large body of literature vouch for the critical role of glutaminolysis, which is a two-step catabolic process starting with the conversion of free glutamine into glutamate, to meet CD4 T cell bioenergetic demands during cell activation [30, 31]. In this context, we first assessed the intracellular concentrations of total glutamine, which was converted into its downstream metabolite glutamate, by using a bioluminescence-based assay. Mem from EC have been activated or not for 6 h in the presence or absence of autophagy-mediated proteolysis (using BaF and E64d-PepA) or PRKAA1 (using compound C) blockade before assessing the intracellular concentrations of total glutamine. As expected, our data confirmed increases of total intracellular glutamine levels in EC after Mem activation, which were prevented when both of autophagy-mediated proteolysis and PRKAA1 were blocked in culture (Fig. 5A).

Then, we activated purified Mem for 6 h and for all study groups with or without PRKAA1-dependent autophagy blockade, before assessing in all study groups the intracellular levels of glutamate. First and foremost, we validated the assay on Mem from HIV<sup>neg</sup> control donors by confirming the increase of intracellular glutamate during T cell activation, which was unsurprisingly prevented when BPTES was added in culture (Fig. 5B). Of note, BPTES prevents glutamate formation from free glutamine by selectively blocking the enzymatic activity of GLS (glutaminase). At 6 h post-cell activation, our data showed that Mem from EC and HIV<sup>neg</sup> displayed increased levels of intracellular glutamate when compared to ART (Fig. 5C). We also found that, blocking autophagy-related lytic (BaF), protease (E64d-PepA) and PRKAA1 (compound C) activities in Mem from EC and HIV<sup>neg</sup> during cell activation all led to significant reduction of their glutamate production to levels comparable in ART (Fig. 5C). Finally, we validated higher presence of both

intracellular glutamine and glutamate only in activated Mem from EC and HIV<sup>neg</sup> when compared to those of ART (Fig. 5D-F).

In summary, our findings show that activated Mem from EC and HIV<sup>neg</sup>, when compared to ART, better support glutaminolysis in an autophagy-dependent manner.

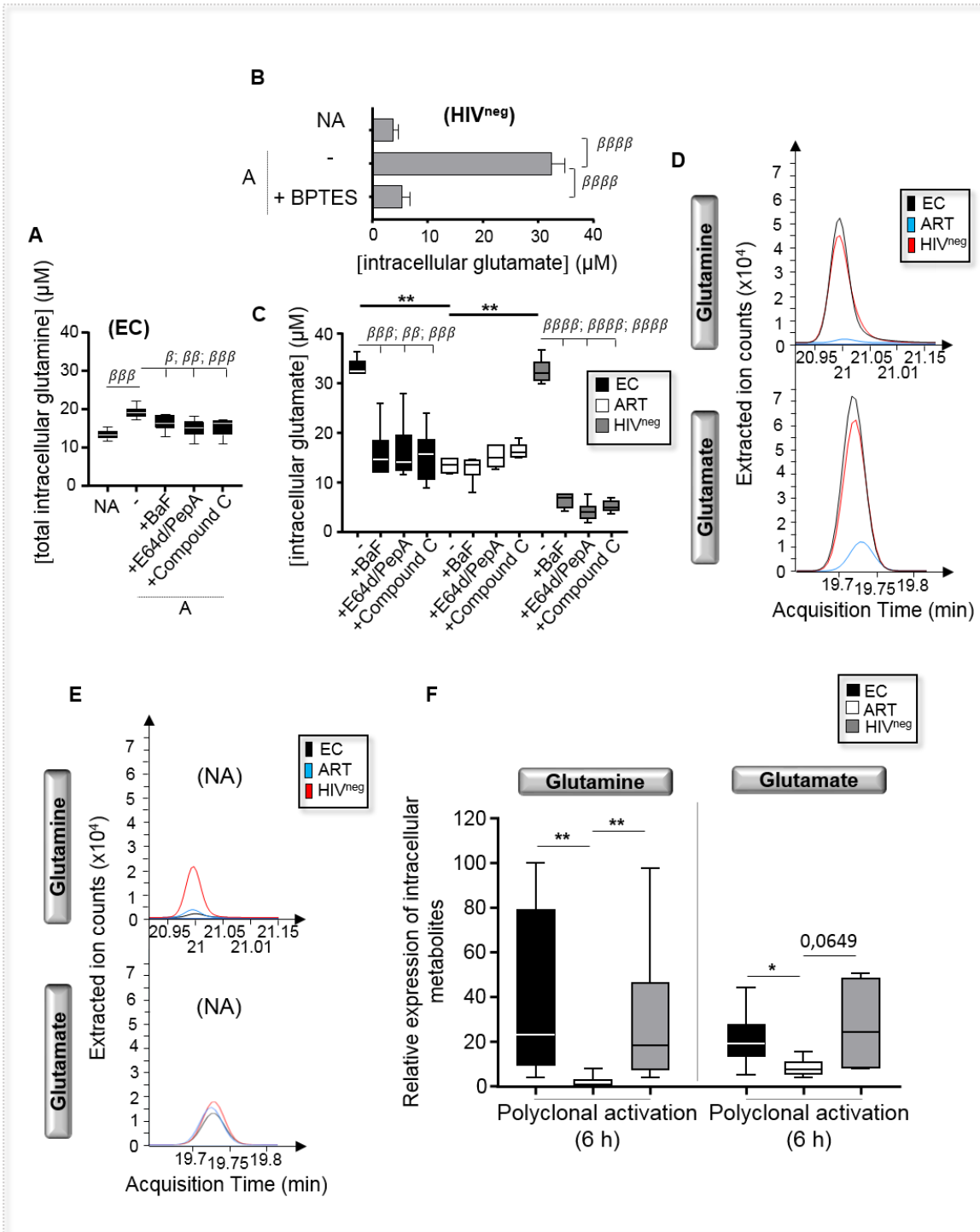


**Figure 5.5 Mem from EC rather use autophagy-mediated proteolysis to support the release of free glutamine.**

(A-D) Intracellular levels of (A) total converted glutamine and (B,C) glutamate only in Mem at 6 h of cell activation. (A) Levels of total converted glutamine within Mem from EC, which have been or not polyclonally activated with or without PRKAA1-dependent autophagy-mediated proteolysis blockade (BaF, E64d-PepA, or compound C). (B) Validation of the glutamate bioluminescence-based measurement by using Mem from HIV<sup>neg</sup> that have been treated with BPTES to block any glutamate conversion during their cell activation. (C) Levels of glutamate in polyclonally activated Mem for all study groups with or without PRKAA1-dependent autophagy-mediated proteolysis blockade (BaF, E64d-PepA, or compound C). (D) Chromatograms of extracted ion counts representing area under the curve quantification of glutamate and glutamine in polyclonally activated Mem in all study groups. (E) Chromatograms of extracted ion counts representing area under the curve quantification of glutamate and glutamine in non-activated (NA) Mem in all study groups. (F) Relative expression of intracellular glutamine and glutamate in activated Mem in all study groups. Of note, polyclonally activated Mem from EC and HIV<sup>neg</sup> counts required 10x dilution to avoid saturating signals. N = 6.  $\beta$ , symbol used for paired *t*-test (comparison between treated Mem and untreated control). \*, symbol used for Mann-Whitney test (comparison between study groups).

#### **5.3.4 Autophagy-dependent glutaminolysis in EC represents a new metabolic advantage required for strong IL21 production.**

Our next step was to investigate whether the enhanced autophagy-dependent glutaminolysis found in Mem from EC was associated with higher rates of energy production. To do so, we polyclonally activated Mem from EC for 6 h with or without blockade of PRKAA1-dependent and autophagy-mediated proteolysis (BaF, E64d-PepA, and compound C) or of glutaminolysis (BPTES and R162), before evaluating their mitochondrial respiration with the Agilent flux analyzer. Of note, the R162 inhibitor prevents the enzymatic conversion of glutamate into  $\alpha$ -ketoglutarate, which is the second step of the glutaminolysis. Following the manufacturer's instruction, the respiratory kinetics that resulted from the sequential addition of pharmacological agents to the respiring Mem allowed us to calculate both their mitochondrial spare respiratory capacity (SRC) and ATP-linked respiration. As expected, we found significant decrease of the whole mitochondrial SRC and ATP-linked respiration in EC when PRKAA1-dependent and autophagy-dependent proteolysis, and glutaminolysis were all blocked in culture (Fig. 6A-C). In contrast, the levels of mitochondrial respiration in non-activated Mem from EC were much lower and were not impacted by any of our chemical inhibitors (Fig S7). This indicated that only the elevated levels of mitochondrial respiration found in EC under activated conditions were suppressed by the inhibitors. We further confirmed that both specific gene silencing of PRKAA1 and GLS led to similar decreases of mitochondrial respiration in polyclonally activated Mem from EC (Fig. S8A-C).

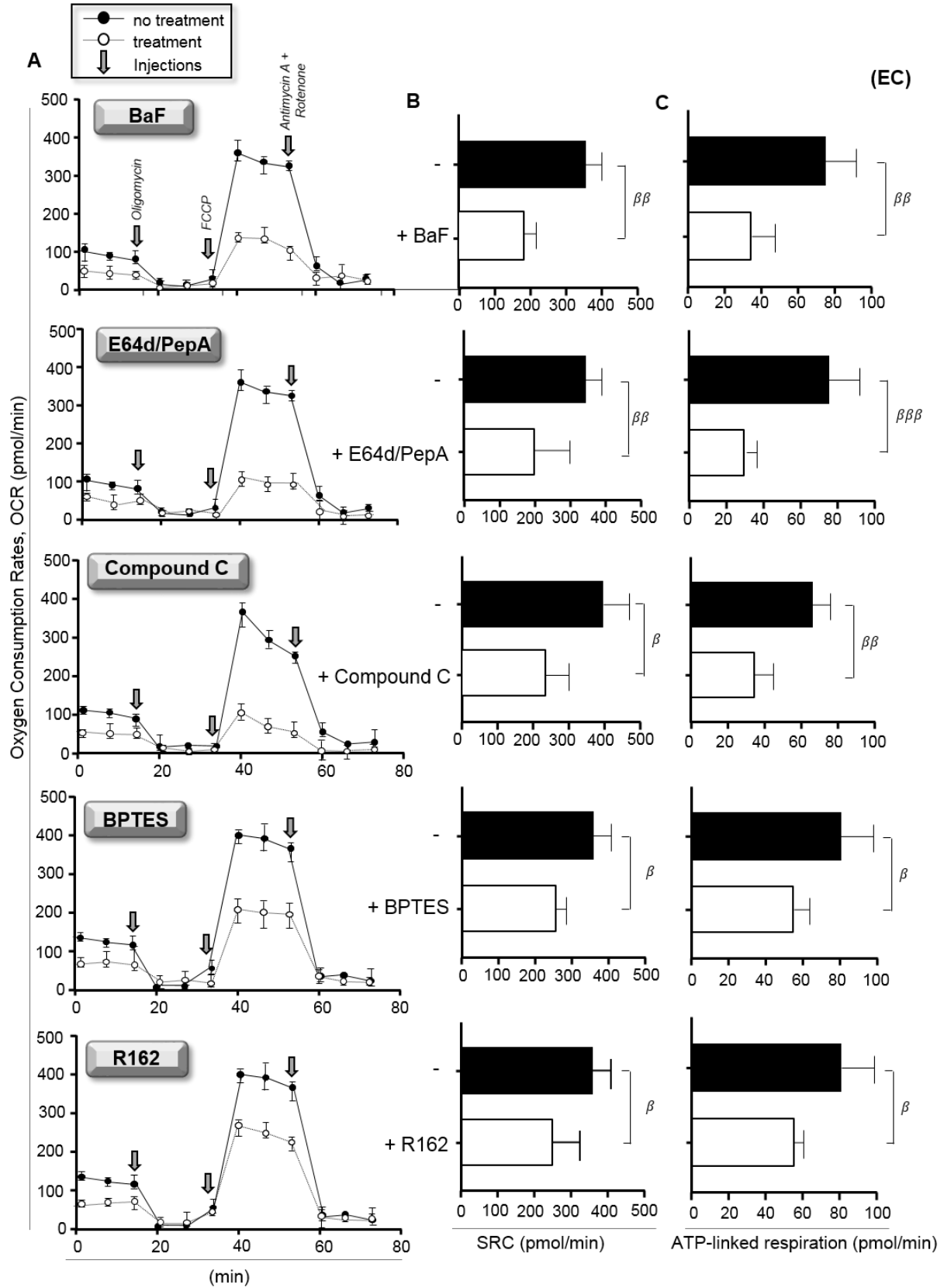


**Figure 5.6 Blocking autophagy-mediated proteolysis or glutaminolysis in EC inhibits their cellular rates of mitochondrial  $\beta$ -oxidation.**

We polyclonally activated Mem from EC in the presence or absence of PRKAA1-dependent autophagy-mediated proteolysis (BaF, E64d-PepA, and compound C) or glutaminolysis (BPTES, and R162) blockade before assessing their mitochondrial respiration. (A) Representative respiratory kinetics of Mem from EC at 6 h post-polyclonal activation when cells have been treated with or without chemical inhibitors. OCR, oxygen consumption rate. (B) SRC and (C) ATP-linked respiration were determined for all culture conditions. N = 6. The error bars indicate standard deviations from the means.  $\beta$ , symbol used for paired *t*-test (comparison between treated Mem and untreated control).

Finally, to confirm the positive impact of glutamine catabolism on the strong IL21 production during HIV-1 infection, we activated Mem from EC, ART, and HIV<sup>neg</sup> either polyclonally or HIV-1 Gag-specifically for 6 h in the presence or absence of glutaminolysis blockade (BPTES and R162) before assessing their IL21 production by flow cytometry. Our data showed that, unlike ART who displayed reduced IL21 production regardless of glutaminolysis blockade, the strong IL21 expression in EC and HIV<sup>neg</sup> was significantly reduced when BPTES and R162 were added in culture (Fig. 7A and B). Once again, we confirmed in EC that specific gene silencing of PRKAA1 and GLS both resulted in decreased IL21 production in activated Mem (Fig. S8D).

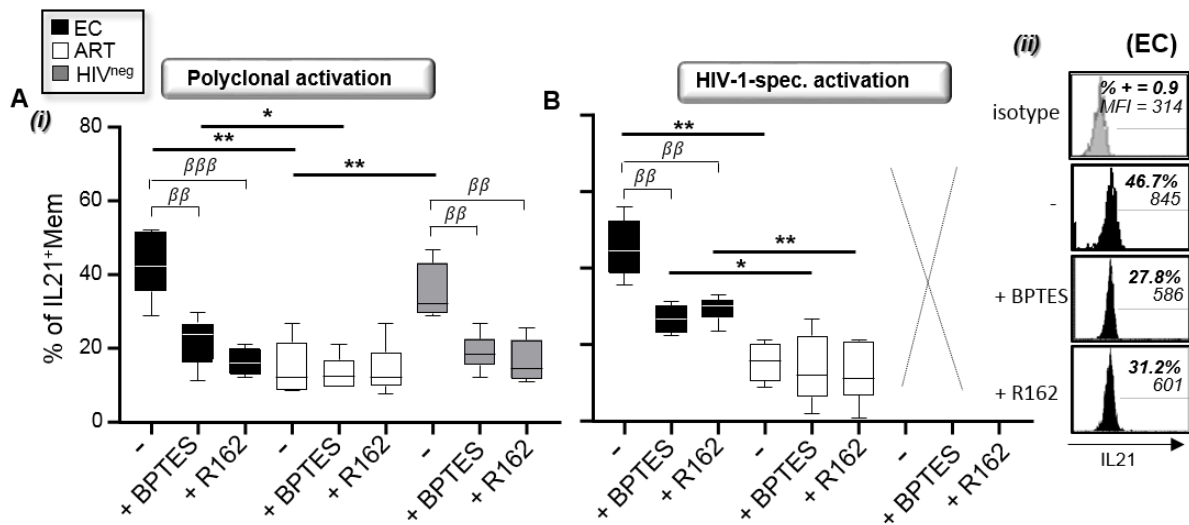


**Figure 5.7 Glutaminolysis is required to provide optimal IL21 production in Mem from EC**

We polyclonally or HIV-1-specifically activated Mem from all study groups for 6 h in the presence or absence of glutaminolysis blockade (BPTES, and R162). Levels of IL21 production at 6 h of (A) polyclonal and (B) HIV-1 Gag-specific activation. Representative histograms of IL21 expression in EC were also shown on the right side for all culture conditions (polyclonal activation). N = 6. The error bars indicate standard deviations from the means.  $\beta$ , symbol used for paired *t*-test (comparison between treated Mem and untreated control). \*, symbol used for Mann-Whitney test (comparison between study groups).

Overall, our data show that strong IL21 production among Mem from EC, including in HIV-1-specific cells, is potentially driven by increased PRKAA1- and autophagy-dependent glutaminolysis (Fig. 8).

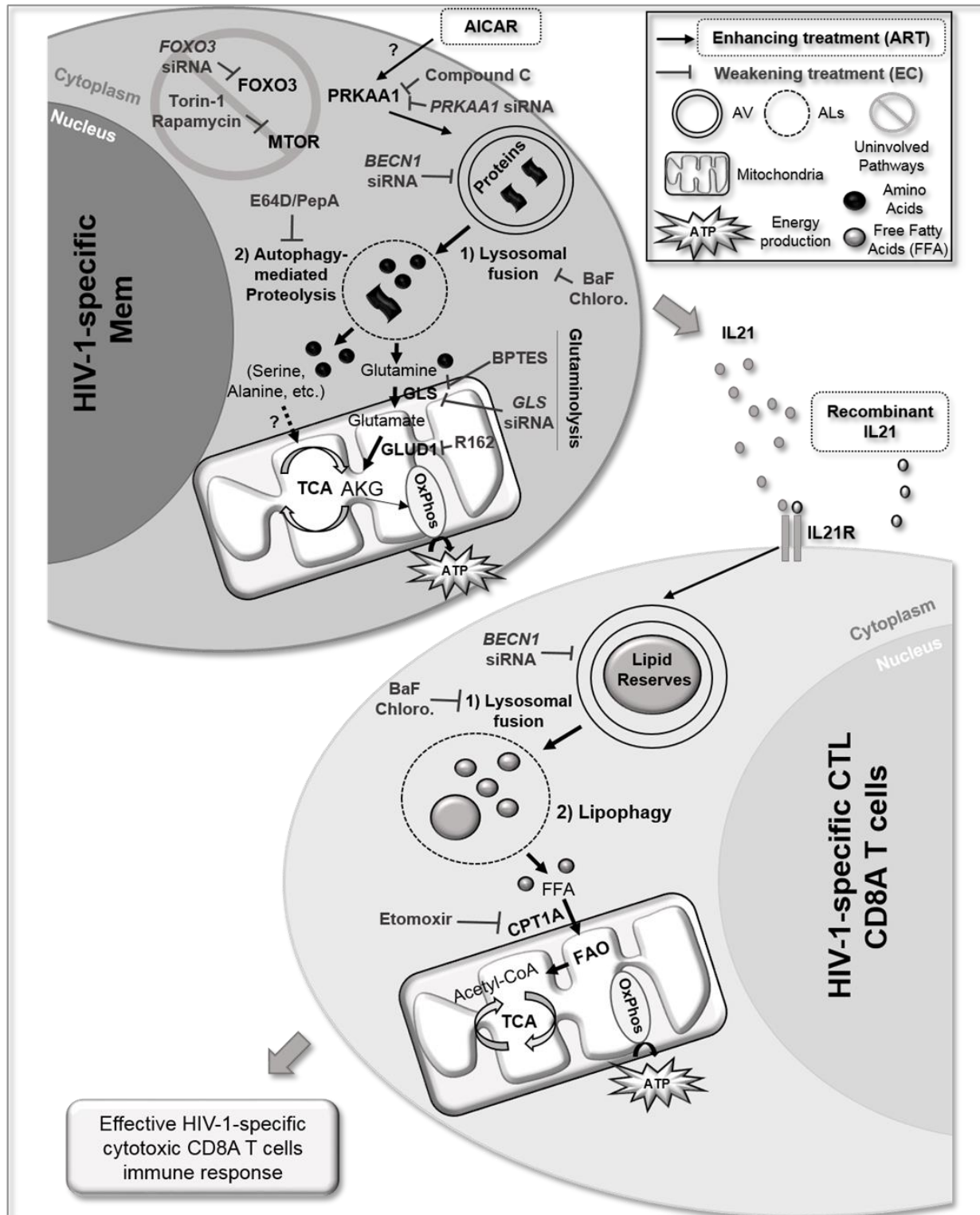


**Figure 5.8** Schematic summary of the overall autophagy-mediated proteolysis metabolic advantage dictating the strong IL21 production in HIV-1-specific Mem from EC, which confers an effective HIV-1-specific CD8A T cells response.

AKG, alpha-ketoglutarate; ALs, autolysosomes; AV, autophagic vacuoles; GLUD1, glutamate dehydrogenase 1; GLS, glutaminase; TCA, tricarboxylic acid cycle; OxPhos, oxidative phosphorylation; FAO, fatty acid beta-oxidation; CPT1A, carnitine palmitoyltransferase 1A).

### 5.3.5 Stimulating PRKAA1 activity in Mem from ART rescues their autophagy-mediated mitochondrial respiration and IL21 production.

Since our data on EC showed that the PRKAA1-dependent activity is critical for ensuring a strong Mem-related and autophagy-mediated proteolysis (Fig. 2A and B and Fig. 8), we decided to investigate whether treating Mem from ART with the PRKAA1 activator AICAR is effective in rescuing their low autophagy proteolytic activity and intracellular glutamine/glutamate levels. Therefore, we first polyclonally activated Mem from ART, EC, and HIV<sup>neg</sup> for 6 h with or without AICAR in the presence or absence of protease inhibitors co-treatment, and then assessed their autophagy-mediated proteolysis. Our data showed that AICAR treatment of Mem from ART led to a significant enhancement of their autophagy activity in the range of EC, which was prevented when cells were co-cultured with the protease inhibitors E64d-PepA (Fig. 9A). Of note, AICAR alone did not impact the autophagy activity in Mem from EC and HIV<sup>neg</sup>. We confirmed that AICAR treatment of Mem from ART also led to significant increases of both total glutamine and glutamate intracellular levels during their T cell activation, in a PRKAA1 and autophagy-dependent manner, not only with the bioluminescence assay, but also with the GC/MS approach (Fig. 9B and C).

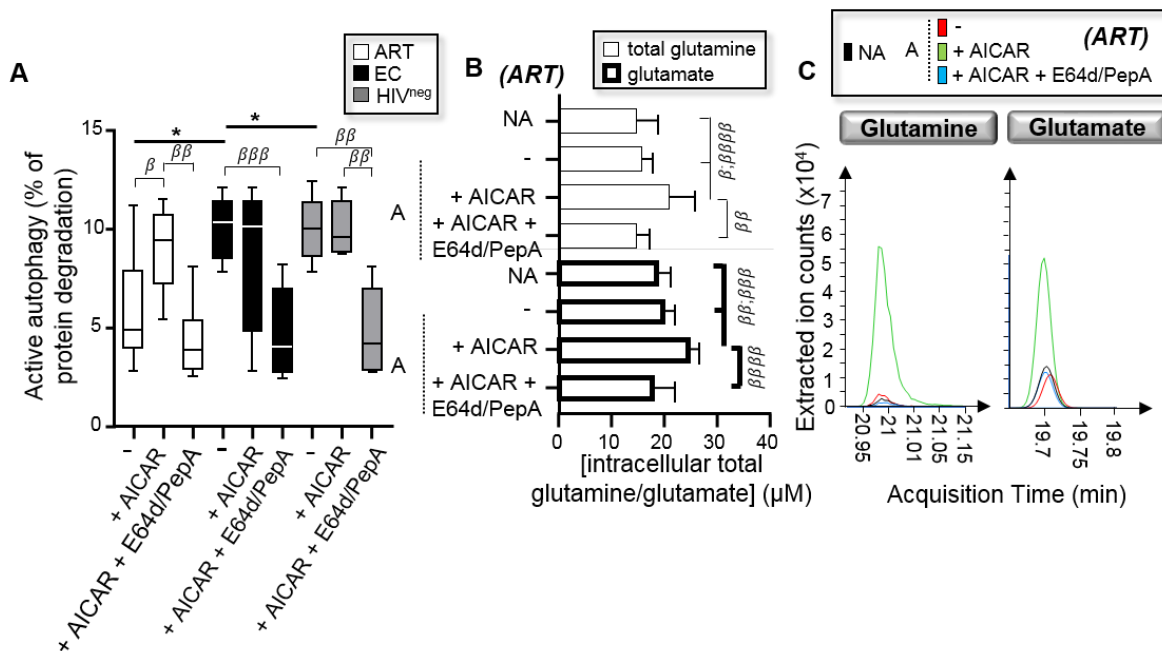


**Figure 5.9** Triggering the PRKAA1 with AICAR enhances autophagy-mediated proteolysis and glutamine/glutamate availability in ART.

(A) Autophagy-mediated proteolysis assessed in polyclonally activated Mem for all study groups with or without the PRKAA1 activator AICAR. We also co-cultured Mem with AICAR and protease inhibitors E64d-

**PepA. (B) Levels of total glutamine/glutamate were determined within Mem from ART, which have been or not polyclonally activated with or without AICAR and AICAR + E64d-PepA (co-)treatments. (C) Chromatograms of extracted ion counts representing area under the curve quantification of glutamate and glutamine in polyclonally activated or not Mem, with/without AICAR or AICAR + E64d-PepA in ART patients. Of note, polyclonally activated Mem treated with AICAR only counts required 10x dilution to avoid saturating signals. N = 6. The error bars indicate standard deviations from the means.  $\beta$ , symbol used for paired *t*-test (comparison between treated Mem and untreated control). \*, symbol used for Mann-Whitney test (comparison between study groups).**

Our next step was to assess whether AICAR treatment of ART's Mem culture further led to increased mitochondrial respiration in a proteolysis-dependent manner. To do so, we polyclonally activated Mem from ART with or without AICAR in the presence or absence of protease inhibitors (E64d-PepA), before evaluating their mitochondrial respiration with the Agilent metabolic flux cell analyzer. We found significant enhancement of the whole mitochondrial SRC and ATP-linked respiration in ART when AICAR was added in culture (Fig. 10A-C). We also confirmed the role of the proteolysis on the AICAR-induced enhancement of mitochondrial respiration, since co-adding E6d-PepA in culture significantly decreased the benefit caused by AICAR.

Finally, to confirm the positive impact of AICAR treatment on IL21 production in ART, we activated Mem from ART, EC, and HIV<sup>neg</sup> either polyclonally or HIV-1 Gag-specifically for 6 h in the presence or absence of AICAR and E64d-PepA before assessing their IL21 production by flow cytometry. Of note, we did not find any differences for IFNG expression in activated Mem regardless of study groups and treatments (Fig. S9A). In contrast, our results confirmed that AICAR treatment in ART was effective in rescuing IL21 production in the range of EC and involved the autophagy proteolytic activity in the process (Fig. 10D). As expected, AICAR alone had no impact on IL21 production with EC and HIV<sup>neg</sup>.

In summary, our last sets of experiments vouch for our ability to rescue both energetic input and related IL21 production in ART to levels comparable to those of EC, when the PRKAA1 activity is chemically induced during culture.



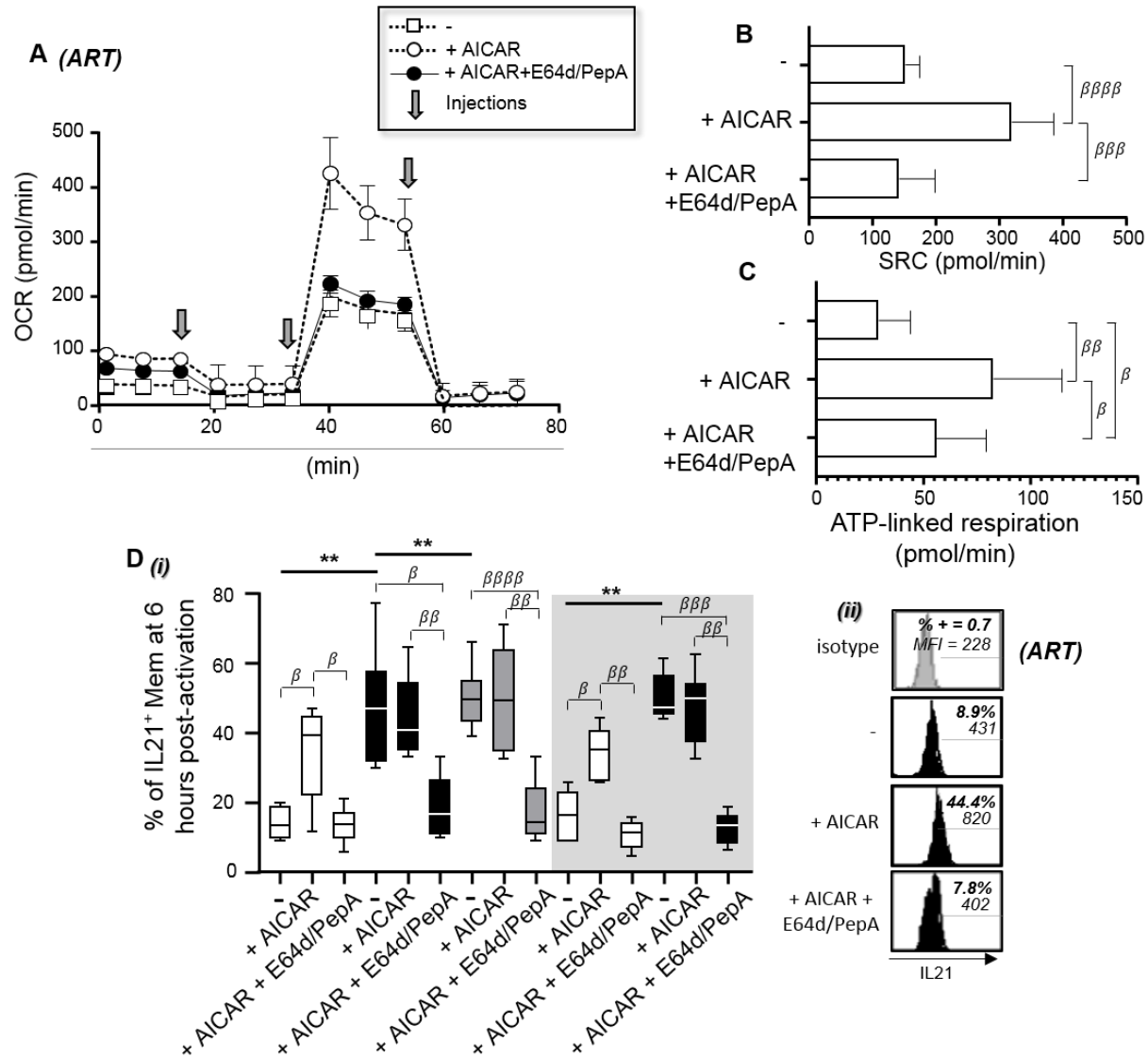


**Figure 5.10** Triggering the PRKAA1-dependent autophagy-mediated proteolysis with AICAR in ART improves their cellular rates of mitochondrial  $\beta$ -oxidation and Mem-related IL21 production.

(A-C) We polyclonally activated Mem from ART in the presence or absence of PRKAA1-dependent autophagy-mediated proteolysis (AICAR with or without BaF, and E64d-PepA) induction, before assessing their mitochondrial respiration. (A) Representative respiratory kinetics of Mem from ART at 6 h post-polyclonal activation when cells have been treated with or without PRKAA1-dependent autophagy-mediated proteolysis. OCR, oxygen consumption rate. (B) SRC and (C) ATP-linked respiration were determined for all culture conditions. (D) At 6 h of polyclonal and HIV-1-specific activation, we also monitored the intracellular levels of IL21 with or without AICAR and E64d-PepA treatments. N = 6. The error bars indicate standard deviations from the means.  $\beta$ , symbol used for paired *t*-test (comparison between treated Mem and untreated control). \*, symbol used for Mann-Whitney test (comparison between study groups).

## 5.4 Discussion

How do EC do what they do? This is the million-dollar question. In fact, understanding the mechanisms associated with natural control of HIV-1 infection is the first step towards improving the current treatment and/or achieving antiretroviral therapy termination [8, 9, 32]. EC are therefore important for the identification of long-term antiviral protective mechanisms that could then potentially be reproduced for treatment strategies. In this regard, previous observations confirm that CD4 T cells, especially Mem, from EC display not only better immune function such as IL21 production, but also higher cell survival, when compared to ART.

Thanks to EC, we have previously shown that effective Mem persistence to multiple rounds of T cell activation and cell resistance to a 24 h-long FAS-induced apoptosis was permitted due to a better control of the FOXO3 pro-apoptotic activity [14]. In contrast, at 6 h post-activation, we did not find any differences in apoptosis levels among Mem between EC and ART, regardless of the activation type (Fig. S1D,E). However, it also is acknowledged that the progressive loss of Mem during chronic HIV-1 infection is not attributed to apoptosis alone, but may also involve other death-related mechanisms such as pyroptosis. Pyroptosis is a highly inflammatory mode of regulated cell death, which involves the activation of CASP1 (caspase 1) and is known to be significantly decreased, but not fully suppressed, following ART when compared to HIV<sup>neg</sup> control donors [33]. Although it has been recently shown no significant differences between CD4 T cells from EC and ART for CASP1 activity, it would be interesting to investigate the levels of pyroptosis in activated Mem, especially in HIV-1-specific cells, from EC and ART and, in the case of lower levels in EC, to assess if autophagy is involved in the process.

In this study, we decided to emphasize on the molecular mechanisms responsible for the strong Mem-related IL21 production during HIV-1 infection, which is only found in EC and not fully restored by current treatments [11, 12, 29, 34]. In fact, a large body of literature confirm that IL21 is a potent immune mediator against HIV-1 endowed with pleotropic effects on antiviral immunity. We, and others, have shown that IL21 enhances the cytotoxic activity of HIV-1-specific CD8A T cell by inducing their lipid catabolism and mitochondrial respiration [23, 35-38]. Aside from potentiating HIV-1-specific CD8A T cell immunity and metabolism, IL21 can also enhance virus-specific antibody responses [11], and natural killer cell survival [39] in infected patients. By using specific FOXO3 gene silencing, we found no impact of FOXO3 protein decrease, regardless of study group, on both Mem survival and IL21 production at 6 h of polyclonal or HIV-1-specific activation (Fig. S10). Instead, when considering the strong IL21 production in EC, our data

revealed not a FOXO3-dependent, but rather autophagy- and metabolism-dependent mechanism responsible for it. In fact, our results showed that HIV-1-specific Mem from EC displayed higher expression levels of several autophagy-related proteins, high AVs and ALs numbers, and increased autophagy-mediated proteolysis activity when compared to ART (Fig. 1A-E). We further confirmed that the strong IL21 production in EC was driven by the autophagy-mediated proteolysis and involved PRKAA1 control in the process (Fig. 3). Altogether, our first set of data revealed a cell-intrinsic role for MTOR-independent and PRKAA1-dependent autophagy in ensuring strong Mem responses in EC (Fig. 8).

Our study differs from the others, since autophagy has usually been investigated in HIV-1 infection as a type of selective lytic process that targets the virus, referred to as xenophagy [22, 40, 41]. In fact, the rationale for comparing EC to ART, which maintain undetectable viral loads for years, and conducting all of ART's cultures with AZT is to focus on the host mechanisms and eliminate the side effects that could be caused by high viremia and viral protein production [9]. Several HIV-1 proteins, which are produced in ART-free patients, can inhibit by themselves the final stage of autophagy to prevent viral degradation [42]. Herein, we showed that highly IL21 expressing HIV-1-specific Mem in EC were driven by autophagy-mediated proteolysis, whose catabolic process of endogenous proteins has never been addressed in HIV-1 infection before in the context of host immune protection.

In this context, our next sets of experiments confirmed that autophagy-mediated proteolysis represents a new energetic process by which IL21-secreting Mem from EC, including those specific to HIV-1, support mitochondrial respiration and energy production through glutaminolysis (Fig. 6 and 7). Although all Mem treatments with chemical inhibitors led to significant reductions of EC's mitochondrial respiration, those found with glutaminolysis blockade (BPTES and R162) were less pronounced in comparison to the ones when PRKAA1-dependent and autophagy-mediated proteolysis was prevented in culture (BaF, E64d-PepA, and compound C) (Fig. 6). These results indicate that, during T cell activation, Mem from EC may use lytic autophagy activity not only to provide free glutamine, but also other essential amino-acids such as serine, alanine and arginine to fuel their energetic mitochondrial input [43-47] (Fig. 8). In addition to IL21 production, it would be interesting to investigate whether similar molecular and catabolic mechanisms could also be used by EC to ensure additional CD4 T cell-related correlates of immune protection against HIV-1. These include Mem cytotoxic activity, IL2 (interleukin 2) production, cell polyfunctionality (i.e. ability to produce multiple cytokines and cytotoxic molecules) and Gag antigen avidity [48-52].

Finally, our data provide the rationale for considering the PRKAA1 activity/autophagy-mediated proteolysis/glutaminolysis axis as a therapeutic target for boosting specific immune responses against HIV-1 among ART (Fig. 8). Interestingly, our last sets of results collected on ART confirm our ability to enhance their autophagy-mediated proteolytic activity along with IL21 production with the PRKAA1 activator AICAR (Fig. 9A and 10D). Aside from directly targeting PRKAA1 activity with AICAR, improvements of anti-HIV-1 Mem responses among ART could be achieved with cytokine-based immunotherapy combined with medically induced HIV-1 suppression. Indeed, it has been shown that the common gamma-chain cytokine signaling is required for optimal autophagy induction during CD4 T cell activation [18]. This cytokine family has several critical cytokines such as IL2 and IL21, known to potentiate HIV-1-specific CD4 T cell function [53, 54]. Although IL2 has been proposed as a potential immune modulator to reverse HIV-specific CD4 T cell dysfunction in HIV-1-infected patients [53-55], this cytokine negatively impacts peripheral CD4 T-follicular cell function and anti-HIV-1 antibody production in EC [11]. Taking this into account, it may be plausible that the overall IL2-based immunotherapy in ART may be ineffective in enhancing IL21 production. It may be interesting to rather focus on IL21 itself for Mem enhancement in ART, since IL21 not only promotes CD4 T cell survival and effector function during HIV-1 infection [12, 29, 56], but also cell-intrinsic resistance to HIV-1 de novo infection [57]. In fact, our preliminary data seemed to confirm that the addition of recombinant IL21 in ART's culture led to significant improvements of their Mem-related mitochondrial respiration (Fig. S9B,C).

To conclude, we are only beginning to appreciate the extent to which cytoplasmic autophagy and mitochondria work together as a fundamental catabolic process by which T cells, including Mem, regulate their energetic metabolism, thereby controlling a proper and protective antigen-specific immune response. Emerging evidence, including ours, show that the regulation of T cell metabolism is context-dependent and can be autophagy-dependent under certain stressful conditions such as a persistent HIV-1 infection. In fact, our results confirm for the first time that EC, who maintain the strongest IL21 expressing and anti-HIV-1 Mem among all study groups of infected patients, display the highest use of mitochondrial respiration via glutaminolysis in those same cells.

Tableau 5.1 List of all antibodies used.

**Multi-parameter antibody cocktails developed.**

**a. For the autophagy assessment**

	Immunogen	clone ID	fluorophore	Catalog number	vendor
Surface	CD3W	UCHT-1	Alexa Fluor 700	557943	BD Biosciences
	CD4	RPA-T8	V450	560346	BD Biosciences
	CD45RA	RPA-T4	APC H7	561212	BD Biosciences
IC	ULK1	F-4	PE	sc-390904	Santa Cruz Biotechnology
	BECN1	EPR 20473	Alexa Fluor 647	ab246760	Abcam
	ATG7	B-9	Alexa 488	sc-376212	Santa Cruz Biotechnology

	Immunogen	clone ID	fluorophore	Catalog number	vendor
Surface	CD3W	UCHT-1	Alexa Fluor 700	557943	BD Biosciences
	CD4	RPA-T8	V450	560346	BD Biosciences
	CD45RA	RPA-T4	APC H7	561212	BD Biosciences
IC	SQSTM1	5F2	Alexa Fluor 488	M162-A48	MBL Life Sciences

**b. For MTOR assessment**

(i)	Immunogen	clone ID	fluorophore	Catalog number	vendor
Surface	CD3W	UCHT-1	Alexa Fluor 700	557943	BD Biosciences
	CD4	RPA-T8	V450	560346	BD Biosciences
	CD45RA	RPA-T4	APC H7	561212	BD Biosciences
IC	MTOR p-S2448	MRRBY	PE	215Q18	Invitrogen (ThermoFisher)
	Total MTOR	EPR 20473	unconjugated*	12-9718-42	Invitrogen (ThermoFisher)

\*Abs were conjugated to AlexaFluor 647dye using the Zenon mouse IgG1 labeling kit (ThermoFisher Scientific, Z25008)

(ii)	Immunogen	clone ID	fluorophore	Catalog number	vendor
Surface	CD3W	UCHT-1	Alexa Fluor 700	557943	BD Biosciences
	CD4	RPA-T8	V450	560346	BD Biosciences
	CD45RA	RPA-T4	APC H7	561212	BD Biosciences
IC	EIF4BP1 p-Thr36/45	V3NTY24	PE	12-9107-42	Invitrogen (ThermoFisher)

**c. For the immune function assessment**

	Immunogen	clone ID	fluorophore	Catalog number	vendor
Surface	CD3W	UCHT-1	Alexa Fluor 700	557943	BD Biosciences
	CD4	RPA-T8	V450	560346	BD Biosciences
	CD45RA	RPA-T4	APC H7	561212	BD Biosciences
IC	IFNG	4S.B3	Alexa Fluor 647	563495	BD Biosciences
	IL21	3A3-N2	PE	560463	BD Biosciences

The Table includes information about the vendor, clone and fluorophore as well as our antibody cocktail to characterize Mem signaling and immune function.

## 5.5 Methods

### Study groups and Ethics statement.

The experiments described in this study mainly rely on the comparison of Mem features between naturally HIV-1 protected EC and patients under antiretroviral therapy (ART). Of note, EC are unique patients displaying a long-term viral control and strong anti-HIV-1 immunity without any medical intervention. All virus-infected patients were participants of the Montreal HIV infection study that received approval from the McGill University Health Centre Ethical Review Board (ethic reference number SL-00.069). All subjects provided an informed and written consent for participation. The inclusion criteria of untreated EC and ART are: middle-aged subjects (31-45 years old), presumed to have HIV-1 infection for a minimum of 3.4 years (3.4-9.8 years), no protective gene polymorphisms such as CCR5  $\Delta$ 32, with CD4 counts over 400 cells/ $\mu$ l in blood and undetectable viral loads (< 50 copies/ml) for 2.8 years or more. We also selected 6 age-matched and HIV-1-uninfected subjects as controls of non-infection. All clinical information regarding EC and ART including their Mem counts are summarized in Table S1.

### Media and Products.

RPMI-1640 (Wisent, 350-000-EL), DMEM (Wisent, 319-005-CL), FBS (Wisent, 080-450), penicillin-streptomycin antibiotics (Wisent, 450-201-EL), and PBS (Wisent, 311-010-CL) were obtained from Wisent Inc. All monoclonal antibody used for multi-parameter and Imaging flow cytometry such as anti-CD3W/CD3 (BD Biosciences, 557943), anti-CD4 (BD Biosciences, 560346) and anti-CD45RA (BD Biosciences, 561212) were purchased in BD Biosciences, except for those against ULK1 (Santa Cruz Biotechnology, sc-390904 PE) and ATG7 (Santa Cruz Biotechnology, sc-376212 AF488), total MTOR (ThermoFisher, 12-9718-42) and p-S2448 MTOR (ThermoFisher, 215Q18), BECN1 (Abcam, ab246760), and SQSTM1 (MBL Life Sciences, M162-A48). Lysosomal protease inhibitors bafilomycin A1 (BaF; Sigma Aldrich, B1793) and chloroquine (Chloro.; Sigma Aldrich, C6628), E64d (Sigma Aldrich, E8640-250UG) and pepstatin A (PepA; Sigma Aldrich, P5318-5MG), PRKAA1 inhibitor (compound C; Sigma Aldrich, 171260-1MG), GLS inhibitor (BPTES; Sigma Aldrich, SML0601-5MG), GLUD1/glutamate dehydrogenase 1 inhibitor

(R162; Sigma Aldrich, 5380980001), and recombinant IL21 (Sigma Aldrich, SRP3087) were all provided from Sigma Aldrich. The PRKAA1 activator AICAR (Sigma Aldrich, A9978-5MG) also came from Sigma Aldrich. The primary antibodies against FOXO3 (Cell Signaling Technology, 12829S), total PRKAA1 (Cell Signaling Technology, 2532S) and p-Thr172 PRKAA1 (Cell Signaling Technology, 2531S), and ACTB/ $\beta$ -actin (Cell Signaling Technology, 4967S) used in western blots came from Cell Signaling Technology. The culture concentrations for bafilomycin A1, chloroquine, E64d-PepA, compound C, AICAR, BPTES, R162 and IL21 were 10 ng/mL, 10 ng/mL, 2  $\mu$ g/mL, 10  $\mu$ M, 50  $\mu$ M, 30  $\mu$ M, 30  $\mu$ M and 10 ng/mL, respectively.

### **Purification of Mem.**

Mem were purified using the untouched memory CD4 isolation kit (EasySep human memory CD4<sup>+</sup> T cell Enrichment Kit; StemCell Technologies, 19157) allowing for more than 94.6% purification without any cell stimulation and apoptosis [58].

### **Activation methods.**

PBMC and purified Mem for all study groups were either polyclonally or HIV-1 Gag-specifically activated for 6 h with GolgiPlug (BD Biosciences, 555029) and GolgiStop (BD Biosciences, 554724) and in the presence or absence of chemical inhibitors. For the polyclonal activation, we treated cells with 0.5  $\mu$ g/mL of anti-CD3W (BioLegend, 317326) and of 1  $\mu$ g/mL anti-CD28 Abs (BD Biosciences, 555726). To elicit the HIV-1-specific activations, we used 5  $\mu$ g/mL of HIV-1 p55 (Austral Biologicals, HI1A-730-5) and p24 Gag antigens (Austral Biologicals, HI1A-720-5) with 1  $\mu$ g/mL of anti-CD28 Abs on PBMC [58]. Of note, all cultures from ART were conducted with 10  $\mu$ M of AZT (Sigma Aldrich, A2169-25MG) to prevent any de novo viral production (confirmed by the sensitive Abcam HIV-1 p24 ELISA (Abcam, ab218268) in culture supernatants).

### **Specific gene silencing using siRNA.**

We first purified 10<sup>7</sup> Mem from all tested groups and electroporated them using Nucleofector II technology according to the Amaxa Biosystems manufacturer's protocol. Specific siRNA for *FOXO3* (ThermoFisher Scientific, siRNA ID: 115208), for *BECN1* (ThermoFisher Scientific, siRNA IDs: 137198 [siRNA 1] and 137200 [siRNA 2]), for *PRKAA1* (ThermoFisher Scientific, siRNA IDs: 143192 [siRNA 1] and 143193 [siRNA 2]), for *GLS* (ThermoFisher, siRNA IDs: 145342 [siRNA 1] and 145344 [siRNA 2]) and their negative control siRNA (ThermoFisher Scientific, 4390843) were

all obtained from ThermoFisher Scientific. Of note, 5 µg of siRNA were transfected or not for 2 h without antibiotics. Purified Mem were washed three times thereafter, to remove dead necrotic cells, counted and incubated for 48 h (for FOXO3 silencing) or 24 h (for *BECN1*, *PRKAA1* and *GLS* silencing) with autologous CD4-depleted PBMC (at ratio Mem/PBMC = 1/4 [58]). The efficacy of protein decrease and levels of cell apoptosis in Mem were determined by western blotting and flow cytometry for FOXO3, PRKAA1, GLS, and BECN1 respectively. Ultimately, we activated cells for an additional 6 h to assess both autophagy, mitochondrial respiration and effector function in transfected Mem.

### **Multi-parameter flow cytometry.**

Table 1 shows the multi-parameter antibody cocktails that we developed in our study. a. Intracellular staining. To assess the expression levels of autophagy-related genes, total MTOR, anti-IFNG/IFN-γ-AF647 (BD Biosciences, 563495) and IL21 cytokine (BD Biosciences, 560463), we subjected cells to intracellular staining assays as previously described [58]. Briefly, after surface staining with specific antibodies for Mem phenotyping, we fixed and then permeabilized cells with 0.25% saponin (Sigma Aldrich, 47036) before the intracellular staining per se. After three washes, stained cells were finally ready for flow cytometry analyses. The viability marker 7-aminoactinomycin D or 7-AAD (ThermoFisher Scientific, 00-6993-50) was used to exclude dead cells from analyses. Of note, to assess the cumulative expression of the autophagy-related SQSTM1 protein cargo during the 6 h-long cultures, lysosomal inhibitor BaF was added in our cultured cells. b. PhosFlow assays. PhosFlow assays were performed to assess the intracellular expression levels of MTOR p-S2448 and EIF4EBP1 p-Thr36/45 (ThermoFisher Scientific, 12-9107-42) in activated Mem. Briefly, cellular fixation was done using 4% PFA for 10 min at 36 °C followed by surface staining for 10 min at 4 °C. Afterwards, the cellular permeabilization was done using 90% ice cold methanol for 30 min at 4 °C followed by 30 min of intracellular staining in PBS + 2% FBS at room temperature. The viability marker 7-AAD was also used to exclude dead cells from analyses. c. Data analyses. BD LSR II Fortessa flow cytometer (BD) was used to collect the data which were analyzed using the DIVA software. 200,000-500,000 gated cells were analyzed for each sample.



### **Electron microscopy.**

Electron microscopy analysis was done as previously reported [22], but with a few modifications. Briefly, we first polyclonally activated  $10^6$  purified Mem for 6 h and then fixed them overnight at 4°C with 2.5% glutaraldehyde (Mecalab, 1206) in 0.05 M cacodylate buffer (pH 7.4). Cells were thereafter rinsed, post-fixated in 1.3 % osmium tetroxide (Mecalab, 1605) in collidine buffer (pH 7.4), dehydrated, and embedded in two successive baths of SPURR (TedPella, 18300-4221). Grids were rinsed in distilled water, stained with aqueous 2% uranyl acetate for 15 min and finally photographed with a Hitachi H-7100 electron microscope fitted with an AMT XR111 camera (Hitachi High-Tech America Inc.). A number of 24 cells per slide were observed (Table S2). We calculated the total numbers of autophagic vacuoles (AVs) and autolysosomes (ALs) per Mem by using different magnifications. We included representative micrographs showing the visual differences between AV and AL structures (Fig. S3A). Of note, AVs were identified as a double-membrane-structure containing undigested cytoplasmic material, ALs were characterized by the autophagic vacuoles limited by a single membrane.

### **Autophagy-mediated proteolysis assays.**

Autophagy-dependent lytic degradation of long-lived proteins in  $10^6$  purified Mem was quantified as previously described [59]. The method is based on a pulse-chase approach, whereby cellular proteins are radiolabeled by [ $^{14}\text{C}$ ] valine (PerkinElmer, NEC291EU050UC). Briefly,  $10^6$  purified Mem were seeded and incubated for 18 h in complete RPMI with 0.2 $\mu\text{Ci/ml}$  of L-[ $^{14}\text{C}$ ] valine in order to label intracellular proteins (Pulse media). Cells were then washed three times with PBS to eliminate any unincorporated radioactivity. The short-lived proteins are allowed to be degraded for 24 h in fresh RPMI (Chase media). After that, cells were polyclonally activated for 6 h in the presence or absence of chemical inhibitors, and then seeded in 10% of trichloroacetic acid (TCA) containing RPMI overnight. After centrifugation, precipitated cells were washed twice with cold 10% TCA RPMI and dissolved in 0.2M NaOH for 2 h. Of note, the supernatants contained the acid-soluble radioactivity fraction. Radioactivity was finally quantified by liquid scintillation counting. The rate of autophagy-dependent degradation of long-lived proteins was calculated from the ratio of the acid-soluble radioactivity in the medium to the one in the acid-precipitable cell fraction.

### **Imaging flow cytometry.**

We have recently developed a high throughput and statistically robust technique that quantitates lipophagy in primary human T cells including starved hepatic Huh7.5 cells as experimental control [23]. The principle of this method consists in measuring the accumulation of lipid contents in ALs when cultures were performed with the lysosomal inhibitor BaF. This culture condition was referred as the "cumulative state" and compared to the BaF-free "steady-state" condition. At 6 h post-activation with or without BaF, cells were collected and co-stained with Lyso-ID green dye (Enzo Life Sciences, ENZ-51005) and the HCS LipidTox deep red neutral lipid dye (ThermoFisher Scientific, H34477) according to the manufacturer's instructions. Anti-CD3W-APC H7 (BD Biosciences, 560176), anti-CD45RA-ECD (Beckman Coulter, IM2711U) and anti-CD4-PE (BD Biosciences, 555347) monoclonal antibodies were used for surface staining. Data analyses. Samples were acquired using the Image Stream X MKII flow cytometer and analyzed with IDEAS software (Amnis). 200,000-500,000 gated cell singlets were analyzed for each sample. Results were expressed as co-localization index BDS (for bright detail similarity) between the lysosomal dye Lyso-ID and the other fluorescently labeled marker of interest. We determined the lipophagy activity by the formula: (% of BDS<sup>high</sup> Lyso-ID<sup>+</sup> LipidTox<sup>+</sup> cells with BaF) – (% of BDS<sup>high</sup> Lyso-ID<sup>+</sup> LipidTox<sup>+</sup> cells without BaF).

### **Intracellular levels of total glutamine/glutamate.**

In order to measure the intracellular concentrations of total glutamine and glutamate, we used a bioluminescence-based assay Glutamine/Glutamate-Glo assay kit (Promega, J8021). Briefly, Mem from each of the study groups were polyclonally activated with or without inhibitors (BaF, E64d-PepA, compound C, and BPTES), or AICAR for 6 h in the presence of GolgiPlug/GolgiStop. Following the manufacturer protocol, cells were then washed with PBS and lysed with the inactivation solution (0.6 N HCl) followed by a neutralization solution (1 M Tris Base). An equivalent of  $15 \cdot 10^4$  Mem per well were plated in clear bottom 96-well plate (in duplicate). GLS reagent was added in wells to measure the total converted glutamine levels, whereas adding GLS buffer only on wells to measure total glutamate only. Glutamate detection reagent was then added in all wells. The principal of the assay is based on the conversion of glutamine to glutamate by GLS. Afterwards, glutamate dehydrogenase catalyzes the oxidation of glutamate with concomitant reduction of NAD<sup>+</sup> to NADH. In the presence of NADH, Reductase enzymatically reduces a pro-luciferin Reductase Substrate to luciferin. Luciferin is detected in a luciferase reaction using Ultra-Glo™ Luciferase and ATP, and the amount of light produced is proportional

to the amount of glutamate presented within the Mem lysate. The luminescent signal was measured by Cytation™ 5 Cell Imaging Multi-Mode Reader (Biotek). All values were normalized to control PBS only. To determine the intracellular levels for both total glutamine and glutamate, we followed the manufacturer's instruction.

### **Metabolomics: Gas Chromatography/Mass Spectrometry (GC/MS)**

Glutamine and glutamate measurements were performed using GC/MS. ( $1 \times 10^6$ ) Mem were gently centrifuged at 21,000 x g and spent media collected for Nova Bioprofil analysis. The cells were rinsed three times with ice-cold normal saline solution 0.9% (Sigma-Aldrich, S8776-100ML), after centrifugation, supernatant was removed and discarded. Metabolism was then quenched with 80% HPLC-grade methanol (-20°C). Samples were then sonicated to ensure lysis followed by centrifugation for 10 min at 1°C and 21,000 x g. The supernatants were transferred to fresh tubes containing 800 ng of 2H27-myristic acid (CDN isotopes Inc., D-1711) retention time locking and quality control internal standard. Samples were dried in a temperature-controlled vacuum centrifuge with sample temperature maintained at -4°C (Labconco). Dried extracts were solubilized in 15 µl of methoxyamine-HCl (Sigma-Aldrich, 226904) freshly prepared 10 mg/mL in pyridine (Sigma-Aldrich, 270970), incubated at room temperature for 1 h followed by derivatization with 35 µl N-tert-butyltrimethylsilyl-N-methyltrifluoroacetamide (MTBSTFA; Sigma-Aldrich, 394882) at 70°C for 1 h.

Immediately after derivatization, samples were subjected to GC/MS analysis. A volume of 1 µL per sample was injected into an Agilent 5975C GC/MS equipped with a DB-5MS+DG (30 m x 250 µm x 0.25 µm) capillary column (Agilent J&W, 122-5532G). Data were collected in both scan (50-1000 m/z) and in single ion monitoring (5 ms well time per ion) where the M-57 ion,  $[M+•-C_4H_9•]^+$ , 432 and 431 for glutamate (retention time 19.711 min) and glutamine (retention time 20.987 min) respectively. Compound spectra and retention times were validated using authentic standards. The extracted ion chromatogram was used for area under the curve quantification using Mass Hunter Quant (Agilent Technologies). Polyclonally activated Mem (Except for ART samples) and those of ART samples co-treated with AICAR, required 1:9 dilution due to saturating signals. Other treatment samples were not diluted due to their comparatively low levels of glutamine and glutamate. Dilution of these samples would have resulted in signals below our detection limit. Results shown in Supplementary materials represent the relative levels of extraction ion counts of glutamine and glutamate. Relative ion counts % levels were determined by normalizing the highest ion counts value of glutamine (Activated Mem from EC) and glutamate

(Activated + AICAR Mem from ART), and then calculated as follows: (ion counts value glutamine/glutamate/highest ion counts value glutamine/glutamate) x 100.

### **Evaluation of mitochondrial respiration.**

At 6 h post-polyclonal activation or not, and with or without chemical inhibitors (BaF, E64d-PepA, compound C, AICAR, BPTES and R162) or recombinant IL21, we assessed the overall mitochondrial respiration in purified Mem from EC and ART using a Seahorse XF96 metabolic analyzer and the XF Cell Mito Stress Test kit. Briefly,  $4 \cdot 10^5$  activated Mem per culture condition were seeded on XF96 well plates (Agilent Technologies, 102601-100) in complemented Agilent RPMI with glucose 10 mM, glutamine 2 mM and pyruvate 1 mM (Agilent Technologies, 103576-100). Of note, the XF Cell Mito Stress test kit was used strictly according to manufacturer protocol. The oxygen consumption rates (OCR) were determined under basal conditions and in response to modulators of respiration that were injected during the assay to reveal key parameters of mitochondrial functions. The modulators included in this assay were oligomycin (Agilent Technologies, 103015-100), carbonyl cyanide 4-(trifluoromethoxy) phenylhydrazone (FCCP; Agilent Technologies, 103015-100), rotenone (Agilent Technologies, 103015-100) and antimycin A (Agilent Technologies, 103015-100; 1.5  $\mu$ M, 2  $\mu$ M and 0.5  $\mu$ M, respectively). We determined the spare respiratory capacity (SRC) and ATP-linked respiration for each culture condition as follows: [(maximal OCR determined after FCCP treatment) – (basal OCR determined before oligomycin treatment)] and [(basal OCR) – (minimal OCR determined after Rotenone and Antimycin A treatment)], respectively. All values were finally normalized to the number of viable cell events per seeded well thanks to the CytoFLEX benchtop flow cytometer (Beckman Coulter).

### **Statistical analysis.**

In the study, we systematically used the non-parametric Mann-Whitney U test that assumes independent samples for all statistical analyses between those groups (\* symbol). A sample size of 6 subjects per study group was sufficient to achieve a significant statistical power based on the observed changes. Statistical analyses between two different in vitro conditions were performed using two-sided Student's paired t-test ( $\beta$  symbol). P values of less than 0.05 were considered significant. One symbol,  $0.05 > P > 0.01$ ; two symbols,  $0.01 > P > 0.001$ ; three symbols,  $0.001 > P > 0.0001$ ; and four symbols,  $P < 0.0001$ .

## 5.6 References

- [1] C.A. Boucher, M.R. Bobkova, A.M. Geretti, C.C. Hung, R. Kaiser, A.G. Marcelin, A. Streinu-Cercel, J. van Wyk, P. Dorr, A.M. Vandamme, State of the Art in HIV Drug Resistance: Science and Technology Knowledge Gap, *AIDS Rev* 20(1) (2018) 27-42.
- [2] M.P. Dube, F.R. Sattler, Inflammation and complications of HIV disease, *J Infect Dis* 201(12) (2010) 1783-5.
- [3] A.H. Warriner, G.A. Burkholder, E.T. Overton, HIV-related metabolic comorbidities in the current ART era, *Infect Dis Clin North Am* 28(3) (2014) 457-76.
- [4] M.P. Davenport, D.S. Khoury, D. Cromer, S.R. Lewin, A.D. Kelleher, S.J. Kent, Functional cure of HIV: the scale of the challenge, *Nat Rev Immunol* 19(1) (2019) 45-54.
- [5] S.G. Fonseca, F.A. Procopio, J.P. Goulet, B. Yassine-Diab, P. Ancuta, R.P. Sekaly, Unique features of memory T cells in HIV elite controllers: a systems biology perspective, *Curr Opin HIV AIDS* 6(3) (2011) 188-96.
- [6] E. Gonzalo-Gil, U. Ikediobi, R.E. Sutton, Mechanisms of Virologic Control and Clinical Characteristics of HIV+ Elite/Viremic Controllers, *Yale J Biol Med* 90(2) (2017) 245-259.
- [7] C. Casado, C. Galvez, M. Pernas, L. Tarancon-Diez, C. Rodriguez, V. Sanchez-Merino, M. Vera, I. Olivares, R. De Pablo-Bernal, A. Merino-Mansilla, J. Del Romero, R. Lorenzo-Redondo, E. Ruiz-Mateos, M. Salgado, J. Martinez-Picado, C. Lopez-Galindez, Permanent control of HIV-1 pathogenesis in exceptional elite controllers: a model of spontaneous cure, *Sci Rep* 10(1) (2020) 1902.
- [8] C. Lopez-Galindez, M. Pernas, C. Casado, I. Olivares, R. Lorenzo-Redondo, Elite controllers and lessons learned for HIV-1 cure, *Curr Opin Virol* 38 (2019) 31-36.
- [9] H. Loucif, S. Gouard, X. Dagenais-Lussier, A. Murira, S. Stager, C. Tremblay, J. Van Grevenynghe, Deciphering natural control of HIV-1: A valuable strategy to achieve antiretroviral therapy termination, *Cytokine Growth Factor Rev* 40 (2018) 90-98.
- [10] S. Buranapraditkun, F. Pissani, J.E. Teigler, B.T. Schultz, G. Alter, M. Marovich, M.L. Robb, M.A. Eller, J. Martin, S. Deeks, N.L. Michael, H. Streeck, Preservation of Peripheral T Follicular Helper Cell Function in HIV Controllers, *J Virol* 91(14) (2017).

- [11] R. Cubas, J. van Grevenynghe, S. Wills, L. Kardava, B.H. Santich, C.M. Buckner, R. Muir, V. Tardif, C. Nichols, F. Procopio, Z. He, T. Metcalf, K. Ghneim, M. Locci, P. Ancuta, J.P. Routy, L. Trautmann, Y. Li, A.B. McDermott, R.A. Koup, C. Petrovas, S.A. Migueles, M. Connors, G.D. Tomaras, S. Moir, S. Crotty, E.K. Haddad, Reversible Reprogramming of Circulating Memory T Follicular Helper Cell Function during Chronic HIV Infection, *J Immunol* 195(12) (2015) 5625-36.
- [12] A. Iannello, M.R. Boulassel, S. Samarani, O. Debbeche, C. Tremblay, E. Toma, J.P. Routy, A. Ahmad, Dynamics and consequences of IL-21 production in HIV-infected individuals: a longitudinal and cross-sectional study, *J Immunol* 184(1) (2010) 114-26.
- [13] R.E. Owen, J.W. Heitman, D.F. Hirschhorn, M.C. Lanteri, H.H. Biswas, J.N. Martin, M.R. Krone, S.G. Deeks, P.J. Norris, N.C.f.H.A.V. Immunology, HIV+ elite controllers have low HIV-specific T-cell activation yet maintain strong, polyfunctional T-cell responses, *AIDS* 24(8) (2010) 1095-105.
- [14] J. van Grevenynghe, F.A. Procopio, Z. He, N. Chomont, C. Riou, Y. Zhang, S. Gimmig, G. Boucher, P. Wilkinson, Y. Shi, B. Yassine-Diab, E.A. Said, L. Trautmann, M. El Far, R.S. Balderas, M.R. Boulassel, J.P. Routy, E.K. Haddad, R.P. Sekaly, Transcription factor FOXO3a controls the persistence of memory CD4(+) T cells during HIV infection, *Nat Med* 14(3) (2008) 266-74.
- [15] T. Riffelmacher, F.C. Richter, A.K. Simon, Autophagy dictates metabolism and differentiation of inflammatory immune cells, *Autophagy* 14(2) (2018) 199-206.
- [16] A. Rocchi, C. He, Emerging roles of autophagy in metabolism and metabolic disorders, *Front Biol (Beijing)* 10(2) (2015) 154-164.
- [17] S.W. Ryter, D. Bhatia, M.E. Choi, Autophagy: A Lysosome-Dependent Process with Implications in Cellular Redox Homeostasis and Human Disease, *Antioxid Redox Signal* 30(1) (2019) 138-159.
- [18] Y. Botbol, B. Patel, F. Macian, Common gamma-chain cytokine signaling is required for macroautophagy induction during CD4+ T-cell activation, *Autophagy* 11(10) (2015) 1864-77.
- [19] V.M. Hubbard, R. Valdor, B. Patel, R. Singh, A.M. Cuervo, F. Macian, Macroautophagy regulates energy metabolism during effector T cell activation, *J Immunol* 185(12) (2010) 7349-57.
- [20] E. Jacquin, L. Apetoh, Cell-Intrinsic Roles for Autophagy in Modulating CD4 T Cell Functions, *Front Immunol* 9 (2018) 1023.
- [21] D. Murera, F. Arbogast, J. Arnold, D. Bouis, S. Muller, F. Gros, CD4 T cell autophagy is integral to memory maintenance, *Sci Rep* 8(1) (2018) 5951.

- [22] R. Nardacci, A. Amendola, F. Ciccocanti, M. Corazzari, V. Esposito, C. Vlassi, C. Taibi, G.M. Fimia, F. Del Nonno, G. Ippolito, G. D'Offizi, M. Piacentini, Autophagy plays an important role in the containment of HIV-1 in nonprogressor-infected patients, *Autophagy* 10(7) (2014) 1167-78.
- [23] H. Loucif, X. Dagenais-Lussier, C. Beji, L. Cassin, H. Jrade, R. Tellitchenko, J.P. Routy, D. Olganier, J. van Grevenynghe, Lipophagy confers a key metabolic advantage that ensures protective CD8 T-cell responses against HIV-1, *Autophagy* 18 (2021) 1-16.
- [24] S.D. Dowling, F. Macian, Autophagy and T cell metabolism, *Cancer Lett* 419 (2018) 20-26.
- [25] K.R. Parzych, D.J. Klionsky, An overview of autophagy: morphology, mechanism, and regulation, *Antioxid Redox Signal* 20(3) (2014) 460-73.
- [26] J. Kim, M. Kundu, B. Viollet, K.L. Guan, AMPK and mTOR regulate autophagy through direct phosphorylation of Ulk1, *Nat Cell Biol* 13(2) (2011) 132-41.
- [27] E.A. Dunlop, A.R. Tee, mTOR and autophagy: a dynamic relationship governed by nutrients and energy, *Semin Cell Dev Biol* 36 (2014) 121-9.
- [28] P. Tamas, S.A. Hawley, R.G. Clarke, K.J. Mustard, K. Green, D.G. Hardie, D.A. Cantrell, Regulation of the energy sensor AMP-activated protein kinase by antigen receptor and Ca<sup>2+</sup> in T lymphocytes, *J Exp Med* 203(7) (2006) 1665-70.
- [29] A. Iannello, C. Tremblay, J.P. Routy, M.R. Boulassel, E. Toma, A. Ahmad, Decreased levels of circulating IL-21 in HIV-infected AIDS patients: correlation with CD4<sup>+</sup> T-cell counts, *Viral Immunol* 21(3) (2008) 385-8.
- [30] L. Araujo, P. Khim, H. Mkhikian, C.L. Mortales, M. Demetriou, Glycolysis and glutaminolysis cooperatively control T cell function by limiting metabolite supply to N-glycosylation, *Elife* 6 (2017).
- [31] J.A. Shyer, R.A. Flavell, W. Bailis, Metabolic signaling in T cells, *Cell Res* 30(8) (2020) 649-659.
- [32] M. Saag, S.G. Deeks, How do HIV elite controllers do what they do?, *Clin Infect Dis* 51(2) (2010) 239-41.
- [33] C. Zhang, J.W. Song, H.H. Huang, X. Fan, L. Huang, J.N. Deng, B. Tu, K. Wang, J. Li, M.J. Zhou, C.X. Yang, Q.W. Zhao, T. Yang, L.F. Wang, J.Y. Zhang, R.N. Xu, Y.M. Jiao, M. Shi, F. Shao, R.P. Sekaly, F.S. Wang, NLRP3 inflammasome induces CD4<sup>+</sup> T cell loss in chronically HIV-1-infected patients, *J Clin Invest* 131(6) (2021).

- [34] L.D. Williams, A. Bansal, S. Sabbaj, S.L. Heath, W. Song, J. Tang, A.J. Zajac, P.A. Goepfert, Interleukin-21-producing HIV-1-specific CD8 T cells are preferentially seen in elite controllers, *J Virol* 85(5) (2011) 2316-24.
- [35] M.F. Chevalier, B. Julg, A. Pyo, M. Flanders, S. Ranasinghe, D.Z. Soghoian, D.S. Kwon, J. Rychert, J. Lian, M.I. Muller, S. Cutler, E. McAndrew, H. Jessen, F. Pereyra, E.S. Rosenberg, M. Altfeld, B.D. Walker, H. Streeck, HIV-1-specific interleukin-21+ CD4+ T cell responses contribute to durable viral control through the modulation of HIV-specific CD8+ T cell function, *J Virol* 85(2) (2011) 733-41.
- [36] G. Mendez-Lagares, D. Lu, D. Merriam, C.A. Baker, F. Villinger, K.K.A. Van Rompay, J.M. McCune, D.J. Hartigan-O'Connor, IL-21 Therapy Controls Immune Activation and Maintains Antiviral CD8(+) T Cell Responses in Acute Simian Immunodeficiency Virus Infection, *AIDS Res Hum Retroviruses* 33(S1) (2017) S81-S92.
- [37] K. Wu, S. Zhang, X. Zhang, X. Li, Z. Hong, F. Yu, B. Liu, T. Pan, Z. Huang, X.P. Tang, W. Cai, J. Xia, X. Li, H. Zhang, Y. Zhang, L. Li, IL-21 Expands HIV-1-Specific CD8(+) T Memory Stem Cells to Suppress HIV-1 Replication In Vitro, *J Immunol Res* 2019 (2019) 1801560.
- [38] J.S. Yi, M. Du, A.J. Zajac, A vital role for interleukin-21 in the control of a chronic viral infection, *Science* 324(5934) (2009) 1572-6.
- [39] A. Iannello, M.R. Boulassel, S. Samarani, C. Tremblay, E. Toma, J.P. Routy, A. Ahmad, IL-21 enhances NK cell functions and survival in healthy and HIV-infected patients with minimal stimulation of viral replication, *J Leukoc Biol* 87(5) (2010) 857-67.
- [40] R. Nardacci, F. Ciccocanti, C. Marsella, G. Ippolito, M. Piacentini, G.M. Fimia, Role of autophagy in HIV infection and pathogenesis, *J Intern Med* 281(5) (2017) 422-432.
- [41] S. Sagnier, C.F. Daussy, S. Borel, V. Robert-Hebmann, M. Faure, F.P. Blanchet, B. Beaumelle, M. Biard-Piechaczyk, L. Espert, Autophagy restricts HIV-1 infection by selectively degrading Tat in CD4+ T lymphocytes, *J Virol* 89(1) (2015) 615-25.
- [42] C. Dinkins, M. Pilli, J.H. Kehrl, Roles of autophagy in HIV infection, *Immunol Cell Biol* 93(1) (2015) 11-7.
- [43] R. Geiger, J.C. Rieckmann, T. Wolf, C. Basso, Y. Feng, T. Fuhrer, M. Kogadeeva, P. Picotti, F. Meissner, M. Mann, N. Zamboni, F. Sallusto, A. Lanzavecchia, L-Arginine Modulates T Cell Metabolism and Enhances Survival and Anti-tumor Activity, *Cell* 167(3) (2016) 829-842 e13.



- [44] M.O. Johnson, M.M. Wolf, M.Z. Madden, G. Andrejeva, A. Sugiura, D.C. Contreras, D. Maseda, M.V. Liberti, K. Paz, R.J. Kishton, M.E. Johnson, A.A. de Cubas, P. Wu, G. Li, Y. Zhang, D.C. Newcomb, A.D. Wells, N.P. Restifo, W.K. Rathmell, J.W. Locasale, M.L. Davila, B.R. Blazar, J.C. Rathmell, Distinct Regulation of Th17 and Th1 Cell Differentiation by Glutaminase-Dependent Metabolism, *Cell* 175(7) (2018) 1780-1795 e19.
- [45] E.H. Ma, G. Bantug, T. Griss, S. Condotta, R.M. Johnson, B. Samborska, N. Mainolfi, V. Suri, H. Guak, M.L. Balmer, M.J. Verway, T.C. Raissi, H. Tsui, G. Boukhaled, S. Henriques da Costa, C. Frezza, C.M. Krawczyk, A. Friedman, M. Manfredi, M.J. Richer, C. Hess, R.G. Jones, Serine Is an Essential Metabolite for Effector T Cell Expansion, *Cell Metab* 25(2) (2017) 345-357.
- [46] N. Ron-Harel, J.M. Ghergurovich, G. Notarangelo, M.W. LaFleur, Y. Tsubosaka, A.H. Sharpe, J.D. Rabinowitz, M.C. Haigis, T Cell Activation Depends on Extracellular Alanine, *Cell Rep* 28(12) (2019) 3011-3021 e4.
- [47] N. Ron-Harel, D. Santos, J.M. Ghergurovich, P.T. Sage, A. Reddy, S.B. Lovitch, N. Dephoure, F.K. Satterstrom, M. Sheffer, J.B. Spinelli, S. Gygi, J.D. Rabinowitz, A.H. Sharpe, M.C. Haigis, Mitochondrial Biogenesis and Proteome Remodeling Promote One-Carbon Metabolism for T Cell Activation, *Cell Metab* 24(1) (2016) 104-17.
- [48] D. Benati, M. Galperin, O. Lambotte, S. Gras, A. Lim, M. Mukhopadhyay, A. Nouel, K.A. Campbell, B. Lemercier, M. Claireaux, S. Hendou, P. Lechat, P. de Truchis, F. Boufassa, J. Rossjohn, J.F. Delfraissy, F. Arenzana-Seisdedos, L.A. Chakrabarti, Public T cell receptors confer high-avidity CD4 responses to HIV controllers, *J Clin Invest* 126(6) (2016) 2093-108.
- [49] S. Kannanganat, B.G. Kapogiannis, C. Ibegbu, L. Chennareddi, P. Goepfert, H.L. Robinson, J. Lennox, R.R. Amara, Human immunodeficiency virus type 1 controllers but not noncontrollers maintain CD4 T cells coexpressing three cytokines, *J Virol* 81(21) (2007) 12071-6.
- [50] C. Phetsouphanh, D. Aldridge, E. Marchi, C.M.L. Munier, J. Meyerowitz, L. Murray, C. Van Vuuren, D. Goedhals, S. Fidler, A. Kelleher, P. Klenerman, J. Frater, Maintenance of Functional CD57+ Cytolytic CD4+ T Cells in HIV+ Elite Controllers, *Front Immunol* 10 (2019) 1844.
- [51] S.J. Potter, C. Lacabaratz, O. Lambotte, S. Perez-Patrigeon, B. Vingert, M. Sinet, J.H. Colle, A. Urrutia, D. Scott-Algara, F. Boufassa, J.F. Delfraissy, J. Theze, A. Venet, L.A. Chakrabarti, Preserved central memory and activated effector memory CD4+ T-cell subsets in human immunodeficiency virus controllers: an ANRS EP36 study, *J Virol* 81(24) (2007) 13904-15.

- [52] B. Vingert, S. Perez-Patrigéon, P. Jeannin, O. Lambotte, F. Boufassa, F. Lemaitre, W.W. Kwok, I. Theodorou, J.F. Delfraissy, J. Theze, L.A. Chakrabarti, A.E.H.C.S. Group, HIV controller CD4+ T cells respond to minimal amounts of Gag antigen due to high TCR avidity, *PLoS Pathog* 6(2) (2010) e1000780.
- [53] M.L. Gougeon, F. Chiodi, Impact of gamma-chain cytokines on T cell homeostasis in HIV-1 infection: therapeutic implications, *J Intern Med* 267(5) (2010) 502-14.
- [54] X.X. Gu, F.Y. Yue, C.M. Kovacs, M.A. Ostrowski, The role of cytokines which signal through the common gamma chain cytokine receptor in the reversal of HIV specific CD4(+) and CD8(+) T cell anergy, *PLoS One* 2(3) (2007) e300.
- [55] K. Nakayama-Hosoya, T. Ishida, B. Youngblood, H. Nakamura, N. Hosoya, M. Koga, T. Koibuchi, A. Iwamoto, A. Kawana-Tachikawa, Epigenetic repression of interleukin 2 expression in senescent CD4+ T cells during chronic HIV type 1 infection, *J Infect Dis* 211(1) (2015) 28-39.
- [56] M. Strengell, T. Sareneva, D. Foster, I. Julkunen, S. Matikainen, IL-21 up-regulates the expression of genes associated with innate immunity and Th1 response, *J Immunol* 169(7) (2002) 3600-5.
- [57] S. Adoro, J.R. Cubillos-Ruiz, X. Chen, M. Deruaz, V.D. Vrbanac, M. Song, S. Park, T.T. Murooka, T.E. Dudek, A.D. Luster, A.M. Tager, H. Streeck, B. Bowman, B.D. Walker, D.S. Kwon, V. Lazarevic, L.H. Glimcher, IL-21 induces antiviral microRNA-29 in CD4 T cells to limit HIV-1 infection, *Nat Commun* 6 (2015) 7562.
- [58] X. Dagenais-Lussier, H. Loucif, H. Cadorel, J. Blumberger, S. Isnard, M.G. Bego, E.A. Cohen, J.P. Routy, J. van Grevenynghe, G. Montreal Primary Infection Study, USP18 is a significant driver of memory CD4 T-cell reduced viability caused by type I IFN signaling during primary HIV-1 infection, *PLoS Pathog* 15(10) (2019) e1008060.
- [59] E.A. Roberts, V. Deretic, Autophagic proteolysis of long-lived proteins in nonliver cells, *Methods Mol Biol* 445 (2008) 111-7.

## 5.7 Supplementary materials

**Table S1.** Clinical data of all selected HIV-1-infected subjects.

### A. Patients under therapy (ART)

	Plasma HIV RNA <sup>1</sup> (copies/mL)	Age <sup>1</sup> (years)	Gender	Duration of presumed HIV infection <sup>2</sup> (years)	Time of aviremia <sup>2</sup> (years)	CD4 cell count <sup>1</sup> (cells/mm <sup>3</sup> )	Mem count <sup>2</sup> (cells/mm <sup>3</sup> )	CD8 cell count <sup>1</sup> (cells/mm <sup>3</sup> )	CCR5 genotype
1	< 50	31	F	5.6	4.2	601	210	345	WT/WT
2	< 50	45	M	7.2	5.6	444	173	555	WT/WT
3	< 50	33	M	3.4	2.8	657	170	359	WT/WT
4	< 50	36	M	5.6	4.9	778	342	601	WT/WT
5	< 50	42	M	8.2	7.5	501	120	421	WT/WT
6	< 50	44	M	4.1	2.8	669	241	457	WT/WT
	<b>&lt; 50</b>	<b>39</b>	<b>M (84%)</b>	<b>5.7</b>	<b>4.6</b>	<b>608</b>	<b>209</b>	<b>456</b>	<b>WT (100%)</b>

### B. Elite controllers (EC)

	Plasma HIV RNA <sup>1</sup> (copies/mL)	Age <sup>1</sup> (years)	Gender	Duration of presumed HIV infection <sup>2</sup> (years)	CD4 cell count <sup>1</sup> (cells/mm <sup>3</sup> )	Mem count <sup>2</sup> (cells/mm <sup>3</sup> )	CD8 cell count <sup>1</sup> (cells/mm <sup>3</sup> )	CCR5 genotype	Treatment <sup>2</sup>
1	< 50	42	M	6.1	589	247	551	WT/WT	no
2	< 50	35	M	5.6	888	222	721	WT/WT	no
3	< 50	39	M	4.3	432	112	421	WT/WT	no
4	< 50	45	M	3.9	569	199	339	WT/WT	no
5	< 50	31	M	5.1	668	294	561	WT/WT	no
6	< 50	33	M	9.8	705	226	666	WT/WT	no
	<b>&lt; 50</b>	<b>38</b>	<b>M (100%)</b>	<b>5.8</b>	<b>642</b>	<b>217</b>	<b>543</b>	<b>WT (100%)</b>	<b>no</b>

<sup>1</sup> Clinic data collected at leukapheresis time

<sup>2</sup> Since inclusion of the patient

Data include viral loads as well as the absolute numbers of CD4 and Mem counts for all 6 EC and 6 ART.

**Table S2.** Detailed autophagic vacuole (AV) and autolysosome (AL) counting per activated Mem.

Cell Number	EC						ART						HIV <sup>neg</sup>						
	1		2		3		1		2		3		1		2		3		
	AV	AL	AV	AL	AV	AL	AV	AL	AV	AL	AV	AL	AV	AL	AV	AL	AV	AL	
1	0	2	0	3	0	4	0	0	0	1	5	0	0	0	1	2	1	0	2
2	2	2	1	1	0	0	0	0	0	1	8	0	0	0	2	1	8	0	1
3	1	2	3	0	1	3	0	0	0	1	0	0	4	0	0	3	1	1	1
4	0	1	2	0	1	5	0	1	0	8	0	2	0	1	0	3	0	1	1
5	1	2	2	1	2	2	0	1	0	2	0	0	0	1	1	0	1	2	1
6	1	0	1	1	3	1	0	0	0	0	0	2	1	0	1	3	0	1	1
7	0	2	3	4	1	4	1	0	0	0	0	0	0	1	3	2	1	0	1
8	1	2	2	4	1	1	1	0	0	2	1	0	0	3	1	6	0	2	2
9	1	0	2	4	1	6	0	1	0	0	1	2	2	7	0	2	1	3	3
10	0	0	0	5	0	0	1	1	0	1	0	0	0	2	0	1	0	3	3
11	0	0	1	0	1	1	0	1	1	1	0	1	0	2	0	6	2	2	2
12	1	2	2	2	3	3	0	0	0	3	2	0	2	2	0	0	1	1	1
13	0	1	0	9	1	0	2	2	0	2	2	0	2	3	1	0	0	1	1
14	0	2	1	2	3	3	0	3	1	2	0	0	2	2	2	4	0	2	2
15	1	2	1	1	1	2	0	1	1	0	0	0	0	1	0	5	1	0	0
16	0	4	3	4	1	6	0	1	0	2	1	0	1	0	1	4	0	1	1
17	1	1	0	0	0	3	0	0	0	1	0	2	0	0	1	1	1	2	2
18	1	2	0	0	1	0	1	0	0	2	0	1	0	5	0	5	1	1	1
19	2	3	1	1	1	1	0	0	1	0	0	3	1	2	0	0	0	1	1
20	1	5	1	0	1	3	2	2	0	2	0	2	0	4	1	0	0	1	1
21	2	1	2	3	0	1	0	2	0	1	0	0	1	0	1	1	1	1	1
22	1	2	0	0	0	1	1	0	0	0	0	0	0	2	0	4	0	3	3
23	1	1	0	6	0	1	0	0	0	2	0	0	0	0	1	1	0	3	3
24	2	3	1	0	2	2	3	2	0	3	0	0	0	1	1	1	1	2	2
Total	20	42	29	51	25	53	12	18	8	41	12	19	18	52	16	61	12	37	37
Mean/Cell	1	2	1	2	1	2	1	1	0	2	1	1	1	2	1	3	1	1	2

Data includes AV and AL counts including their mean per one cell for all 3 EC, 3 ART, and 3 HIV<sup>neg</sup> (determined on 24 cells).

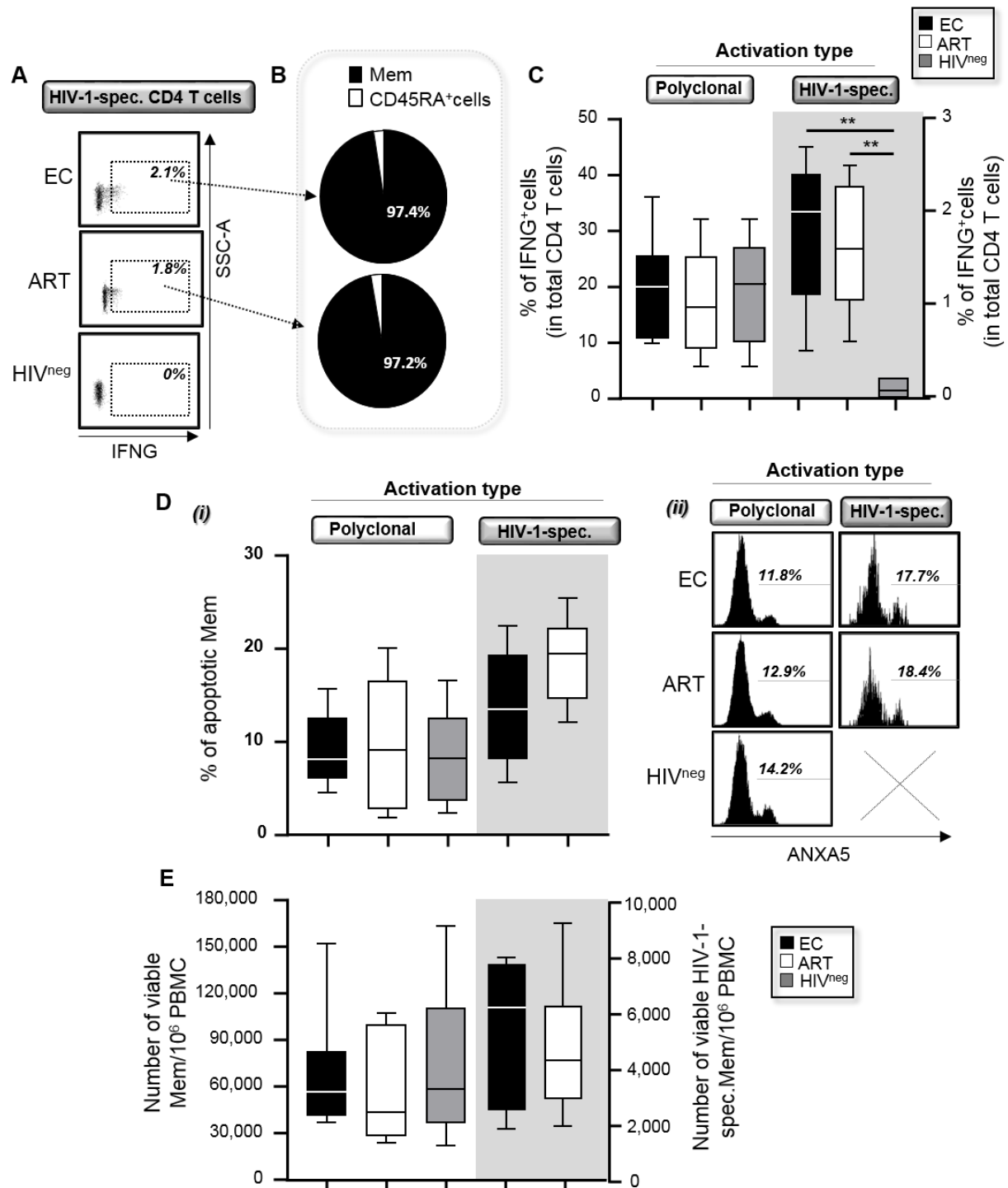


**Figure S1.** Characterization of HIV-1-specific CD4 T cells at 6 h post-activation. (A) Gating strategy in EC, ART, and HIV<sup>neg</sup> for antigen-specific CD4 T cells after 6 h of HIV-1 Gag-specific activations. (B) Percentages of CD45RA<sup>neg</sup> Mem within HIV-1-specific CD4 T cells in EC and ART. (C) Percentages of stimulated IFNG<sup>+</sup> Mem determined among total CD4 T cells in ART, EC, and HIV<sup>neg</sup> at 6 h of polyclonal and HIV-1-specific activation. (D) i. Levels of cell survival determined

on total Mem (polyclonal) or HIV-1-specific Mem (HIV-1-specific activation). Cell survival was determined by the percentages of ANXA5<sup>neg</sup> Mem. We also included ii. Representative histograms for all study groups that show percentages of apoptotic Mem. (E) Calculation at 6 h of cell activation of the absolute number of viable Mem for all study groups. We calculated the numbers according to the formulas: Number [for polyclonal activation] =  $10^6$  PBMC \* (% of Mem among PBMC) \* (% of ANXA5<sup>neg</sup> Mem). Number [for HIV-1-specific activation] =  $10^6$  PBMC \* (% of IFNG<sup>+</sup> Mem among PBMC) \* (% of ANXA5<sup>neg</sup> IFNG<sup>+</sup> Mem). N = 6. The error bars indicate standard deviations from the means.

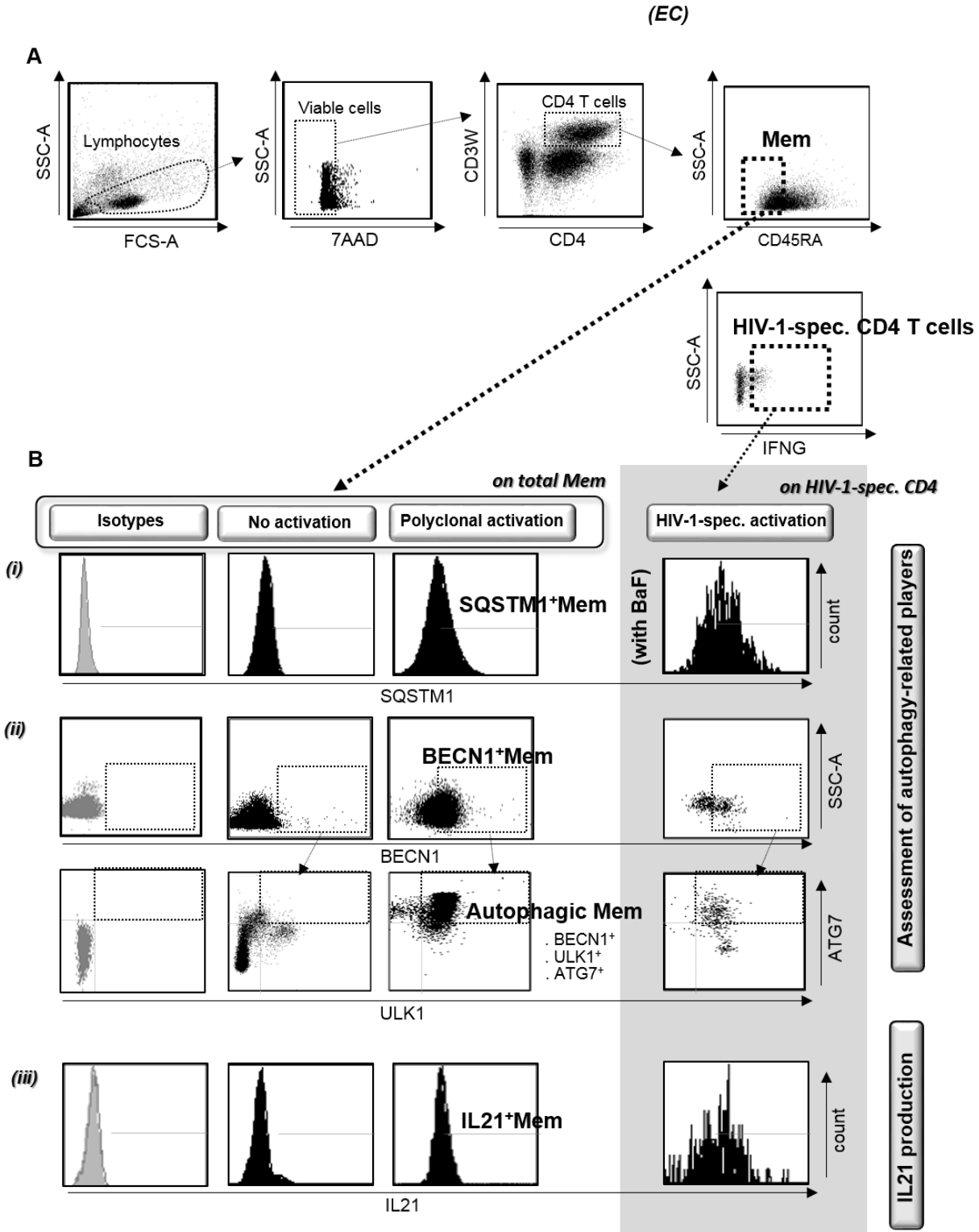


**Figure S2.** Gating strategy for assessing autophagy related gene (ATG) and IL21 production in Mem. Representative histograms and contour plots of Mem from one EC that have been polyclonally or HIV-1-specifically activated or not for 6 h. (A) Surface staining to characterize total

viable (for polyclonal) and Gag-specific (for HIV-1-specific activation) Mem. We then assessed in Mem and for both activation types (B) i. the intracellular levels of SQSTM1 (when cells were treated with BaF), ii. the percentages of BECN1<sup>+</sup> ULK1<sup>+</sup> ATG7<sup>+</sup> cells, and iii. the intracellular levels of IL21. Of note, we also included isotype controls and the non-activation condition as well. Of note, in order to determine the percentages of BECN1<sup>+</sup> ULK1<sup>+</sup> ATG7<sup>+</sup> cells, we first gated on populations that were positively stained for anti-BECN1 Abs, and then assessed the proportion of cells that displayed the triple staining for BECN1 including ULK1 and ATG7.



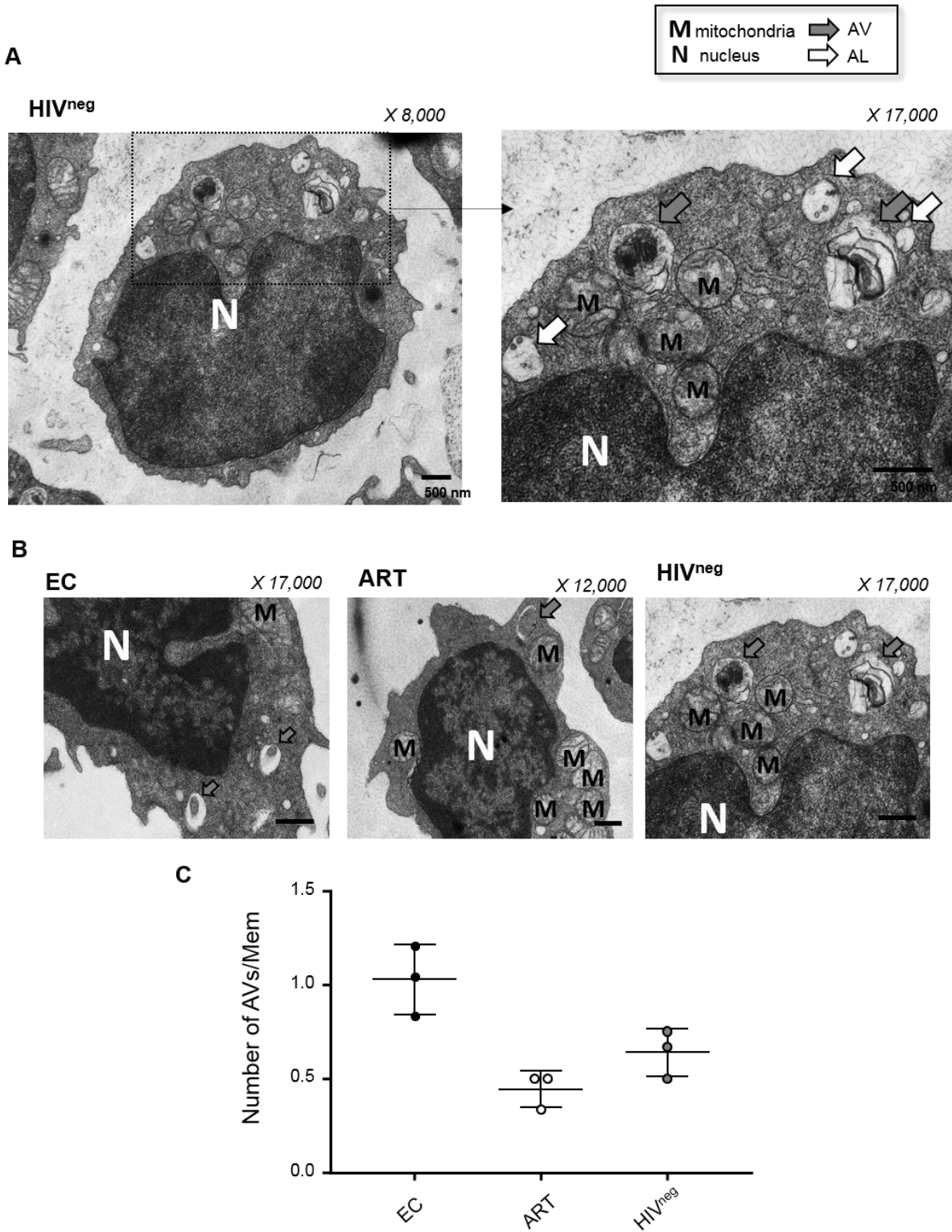


**Figure. S3.** Activated Mem from EC and HIV<sup>neg</sup> displayed higher numbers of AVs per cells when compared to ART. (A-C) Ultrastructural analysis of purified Mem from ART, EC and HIV<sup>neg</sup> after 6 h of polyclonal activation (n = 3). (A) Representative ultrastructural micrographs from uninfected

controls to differentiate AV (autophagic vacuoles; gray arrows) from ALs (autolysosomes; white arrows). Of note, AV were identified as a double-membrane-structure containing undigested cytoplasmic material, ALs were characterized by the autophagic vacuoles limited by a single membrane. (B) Magnified ultrastructural micrographs in ART, EC and HIV<sup>neg</sup> to appreciate the numbers of cellular vacuoles (X 12,000-17,000). Quantitative analysis of (C) the number of AVs per Mem.

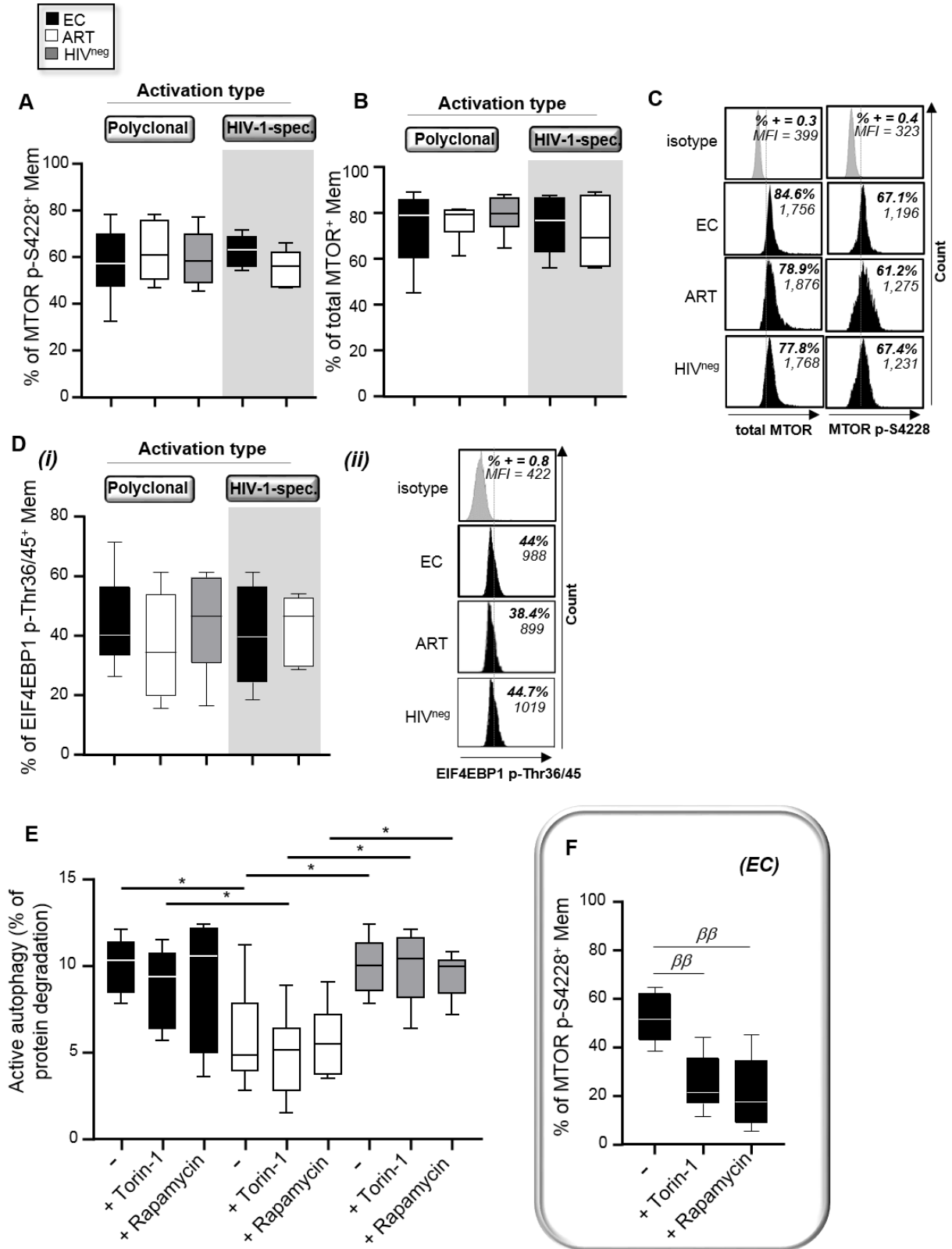


**Figure S4.** Enhanced autophagy-mediated proteolysis in Mem from EC does not involve MTOR activity. At 6 h of both polyclonal and HIV-1-specific activation, we monitored the intracellular levels of (A) i. activated (p-S2448), (B) i. total MTOR and (C) its target EIF4BP1 (p-Thr36/45) in Mem from EC, ART, and HIV<sup>neg</sup>. ii. Representative histograms are also shown including isotype controls. (C) Autophagy-mediated proteolysis determined in purified Mem after polyclonal activation in the presence or absence of the MTOR inhibitors torin-1 and rapamycin. (E) Confirmation of torin-1 and rapamycin efficacy on decreasing MTOR activity. Results shown represent the percentage of MTOR p-S4228<sup>+</sup> Mem from EC with cells that have been polyclonally activated in the presence or absence of inhibitors. N = 6. The error bars indicate standard deviations from the means.  $\beta$ , symbol used for paired *t*-test (comparison between treated Mem and untreated control). \*, symbol used for Mann-Whitney test (comparison between study groups).

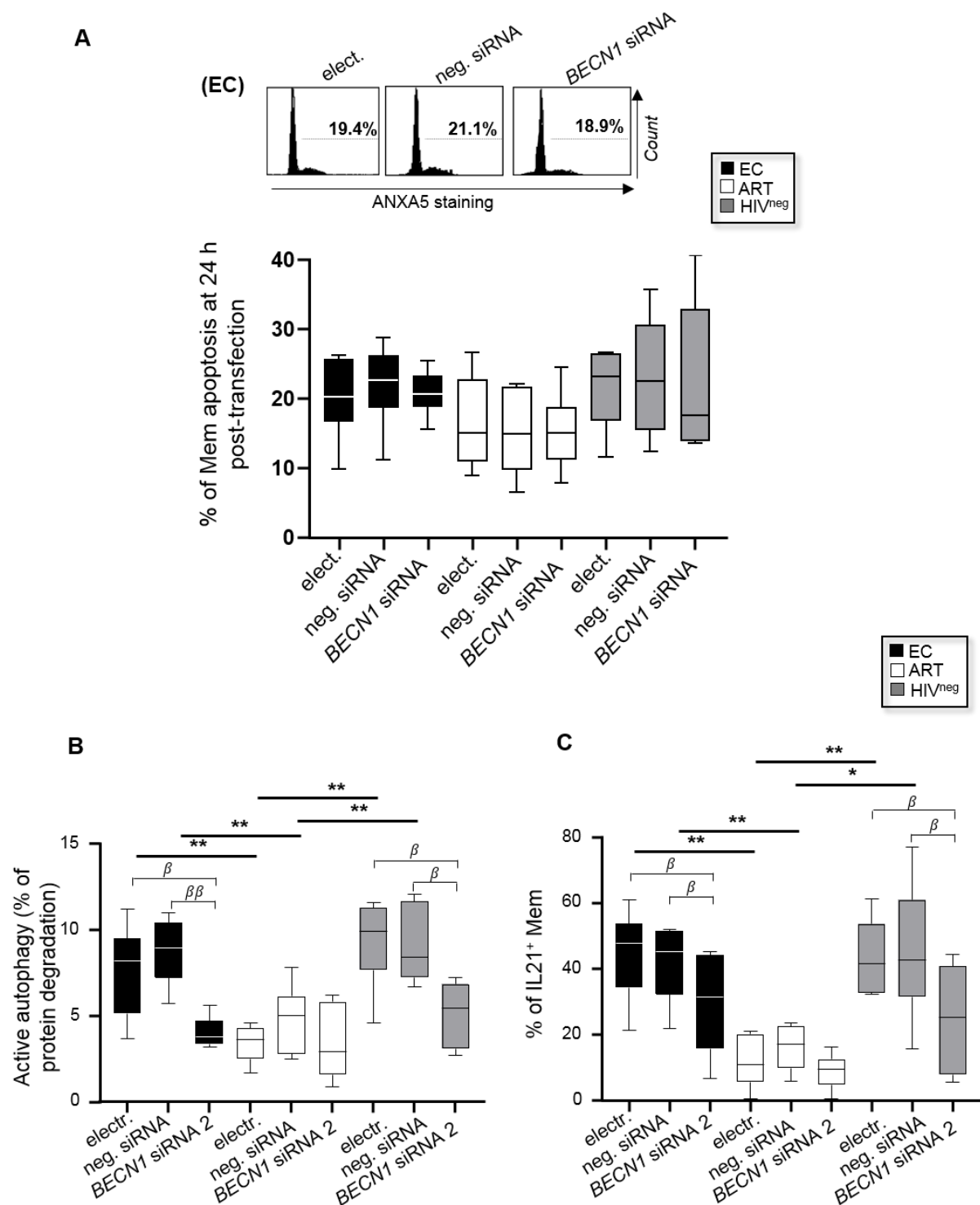


**Figure S5.** Silencing the expression of BECN1 in Mem does not affect the levels of apoptosis and results in autophagy and IL21 production in activated Mem from EC (confirmation with a second *BECN1* siRNA). (A) We assessed in transfected Mem from all study groups at 24 h of specific

*BECN1* gene silencing the levels of apoptosis by flow cytometry. Representative ANXA5 staining are also shown in EC. (B, C) Autophagy-mediated proteolysis and IL21 production were both determined in 6-h-long polyclonally activated Mem under specific *BECN1* gene silencing (siRNA IDs: 137200 [siRNA 2]). Of note, we found  $69\% \pm 25.1\%$  decrease of *BECN1* protein expression in Mem from EC, which have been transfected with *BECN1* siRNA 2. (B) Autophagy-mediated proteolysis assessed in polyclonally activated Mem with or without specific *BECN1* gene silencing. (C) Levels of IL21 production in Mem that have then been polyclonally activated for 6 h with or without specific *BECN1* gene silencing (*BECN1* siRNA 2). N = 6. The error bars indicate standard deviations from the means.  $\beta$ , symbol used for paired *t*-test (comparison between treated Mem and untreated control). \*, symbol used for Mann-Whitney test (comparison between study groups).

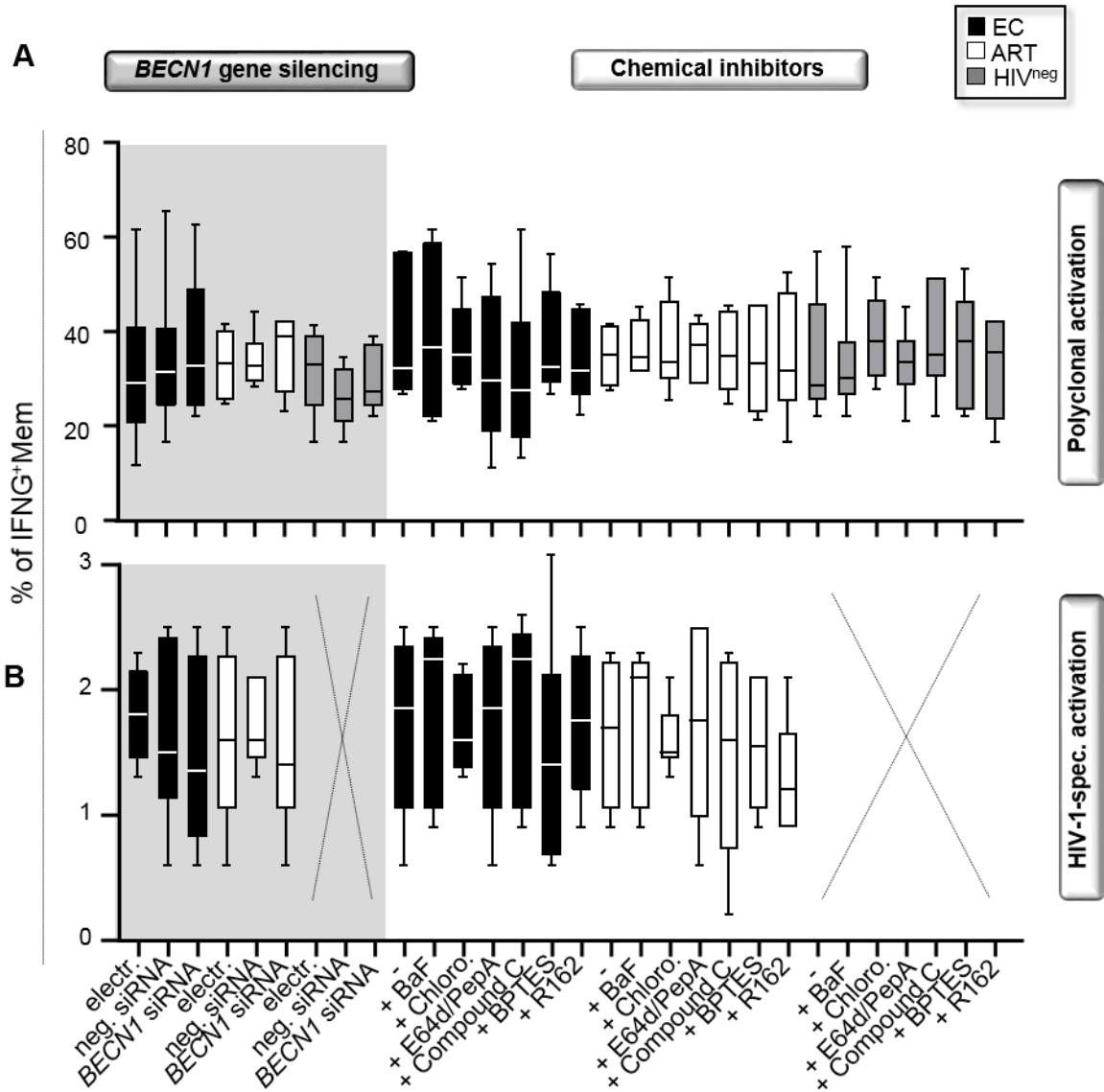


**Figure S6.** Confirmation in polyclonally activated Mem from EC that all chemical inhibitors used in Fig. 3C are blocking autophagy. (A, B) Characterization of similar IFNG expression in Mem for all culture conditions. At 6 h of (A) polyclonal and (B) HIV-1-specific activation the percentages of IFNG<sup>+</sup> Mem in the context of specific *BECN1* gene silencing, PRKAA1-dependent autophagy-mediated proteolysis (BaF, Chloro., E64d/PepA, and compound C), and glutaminolysis (BPTES, and R162) blockade. N = 6. The error bars indicate standard deviations from the means.  $\beta$ , symbol used for paired *t*-test (comparison between treated Mem and untreated control).

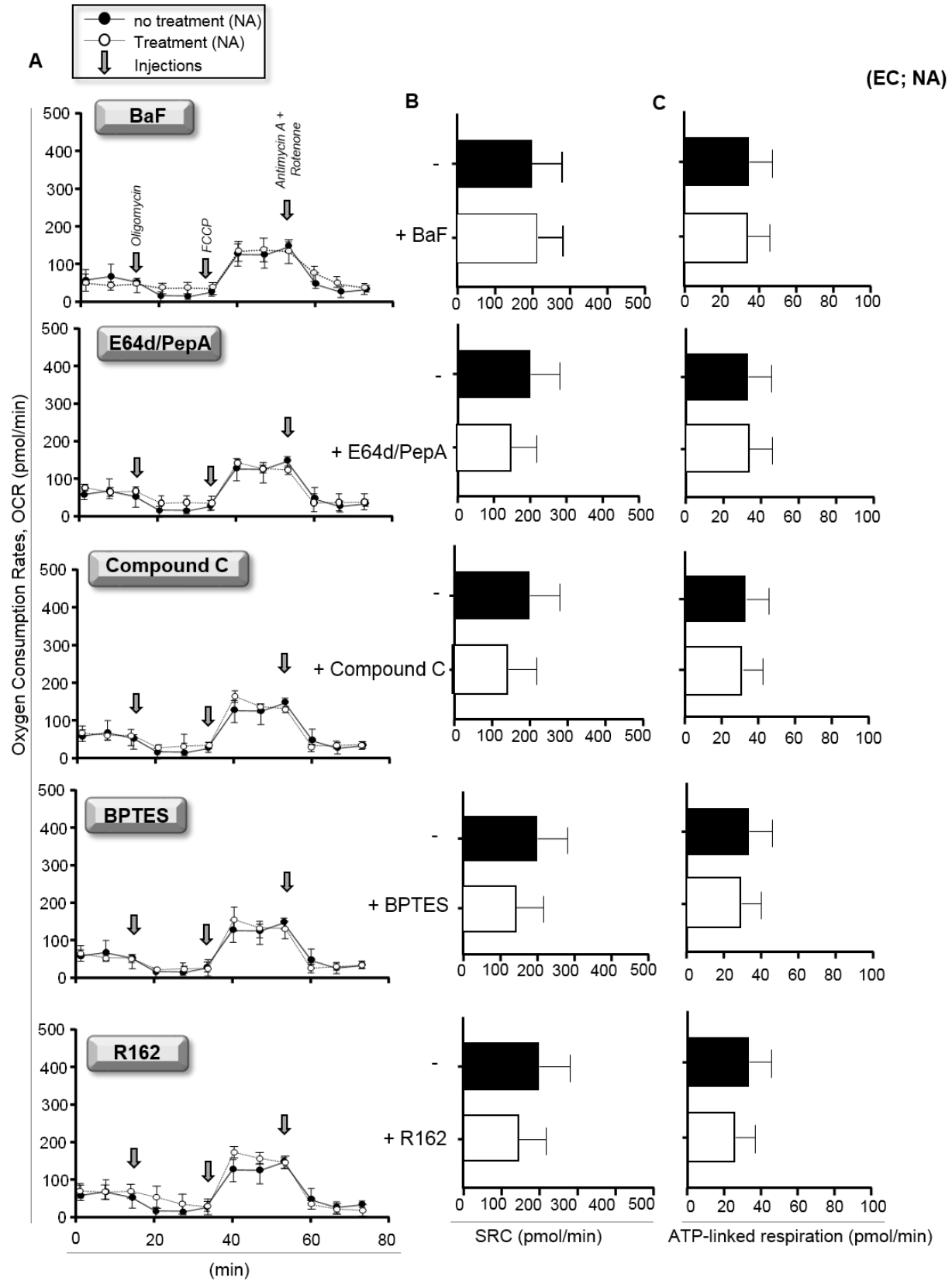




**Figure S7.** The low levels of mitochondrial respiration found in non-activated Mem were not modulated by any of the chemical inhibitors. We cultured Mem from EC for 6 h without T cell activation and in the presence or absence of PRKAA1-dependent autophagy-mediated proteolysis (BaF, E64d-PepA, and compound C) or glutaminolysis (BPTES, and R162) blockade before assessing their mitochondrial respiration. (A) Representative respiratory kinetics of non-activated Mem from EC when cells have been treated with or without chemical inhibitors. OCR, oxygen consumption rate. (B) SRC and (C) ATP-linked respiration were determined for all culture conditions. N = 6. The error bars indicate standard deviations from the means.

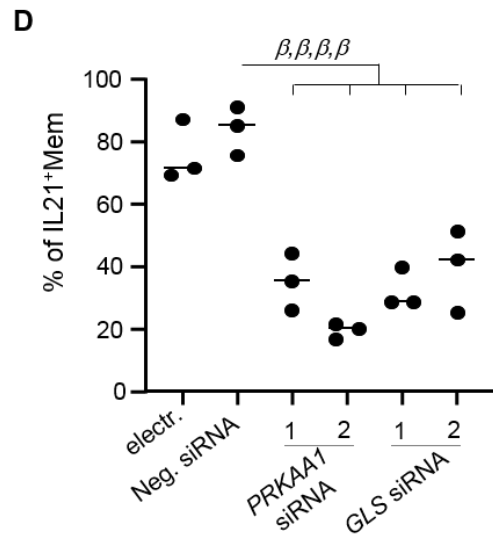
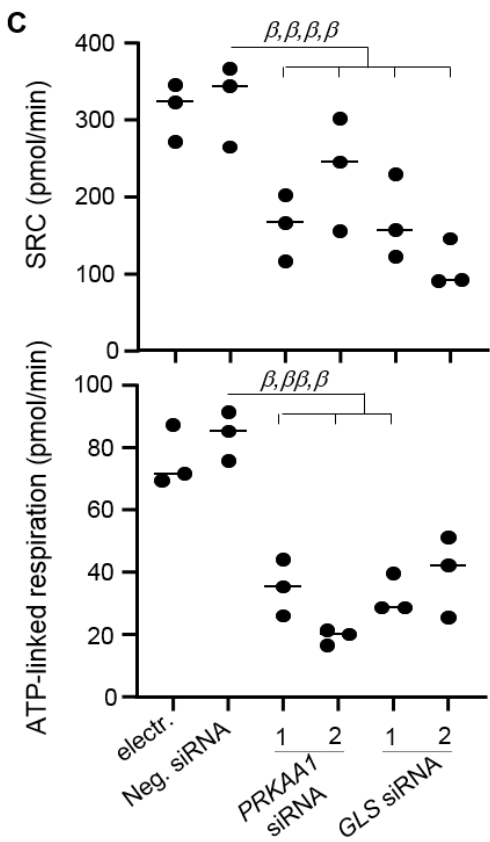
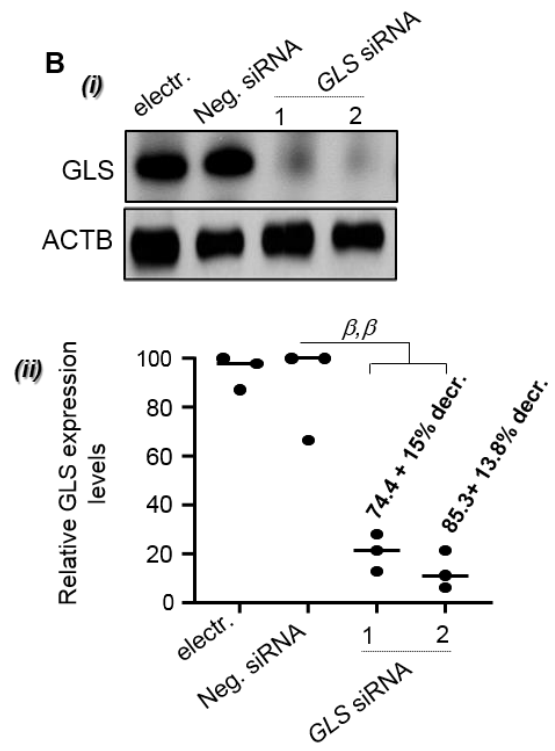
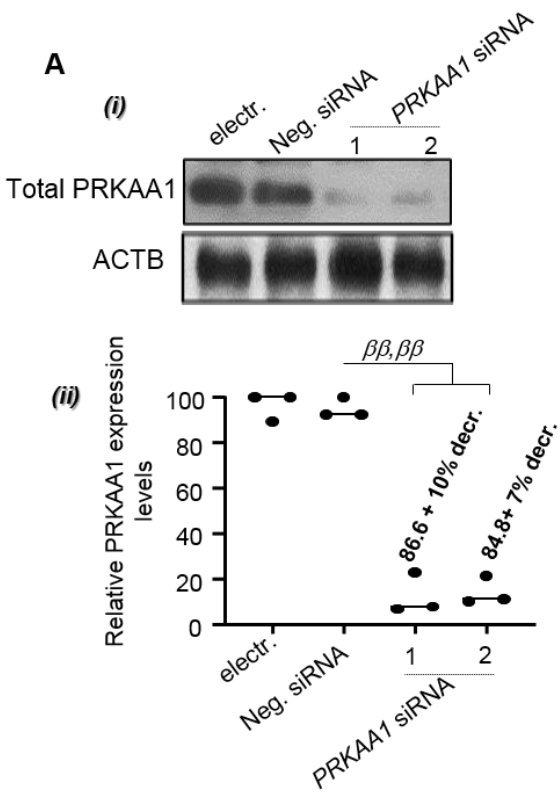


**Figure S8.** *PRKAA1* and *GLS* silencing both led to reduced mitochondrial respiration and IL21 production. Protein abundances for *PRKAA1* (A) and *GLS* (B) in purified Mem were assessed at 24 h post-transfection with or without their specific siRNAs by western blotting. i. Representative blots for *PRKAA1*, *GLS* and *ACTB*/ $\beta$ -actin expressions in EC. ii. Densitometric quantifications of specific *PRKAA1* and *GLS* bands were performed using ImageQuant software. Results shown represent the mean relative expression  $\pm$  SD of 3 independent experiments. Of note, percentages of protein inhibition under specific gene silencing were also included in bold. (C) At 6 h of polyclonal activation, we evaluated in Mem their levels of mitochondrial spare respiratory capacity (SRC) and ATP-linked respiration. (D) We also determined the percentages of IL21<sup>+</sup>Mem with or without *PRKAA1* and *GLS* gene silencing by flow cytometry. N = 3.  $\beta$ , symbol used for paired *t*-test (comparison between treated Mem and untreated control).

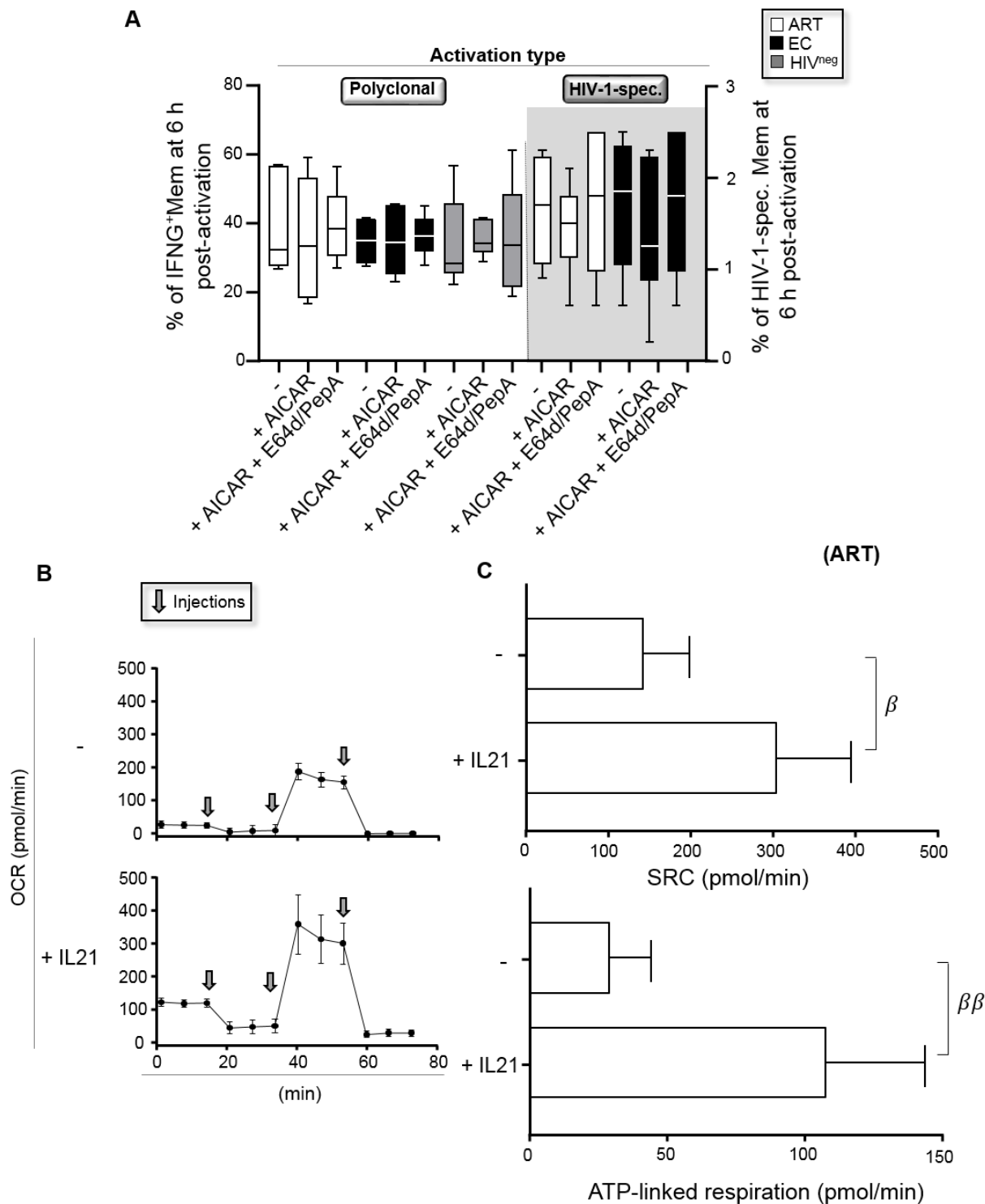


**Figure S9.** AICAR does not influence IFNG production, regardless of study group. (A) At 6 h of polyclonal and HIV-1-specific activation, we monitored in Mem from ART, EC, and HIV<sup>neg</sup> their intracellular levels of IFNG when AICAR and E64d-PepA were added or not in culture. (B, C) IL21 treatment of Mem from ART results in enhanced mitochondrial respiration. We polyclonally

activated Mem from ART in the presence or absence of recombinant IL21, before assessing their mitochondrial respiration. (B) Representative respiratory kinetics of Mem from ART at 6 h post-polyclonal activation when cells have been treated with or without IL21. OCR, oxygen consumption rate. (C) SRC and ATP-linked respiration rates were determined for all culture conditions. N = 6. The error bars indicate standard deviations from the means.  $\beta$ , symbol used for paired *t*-test (comparison between treated Mem and untreated control).

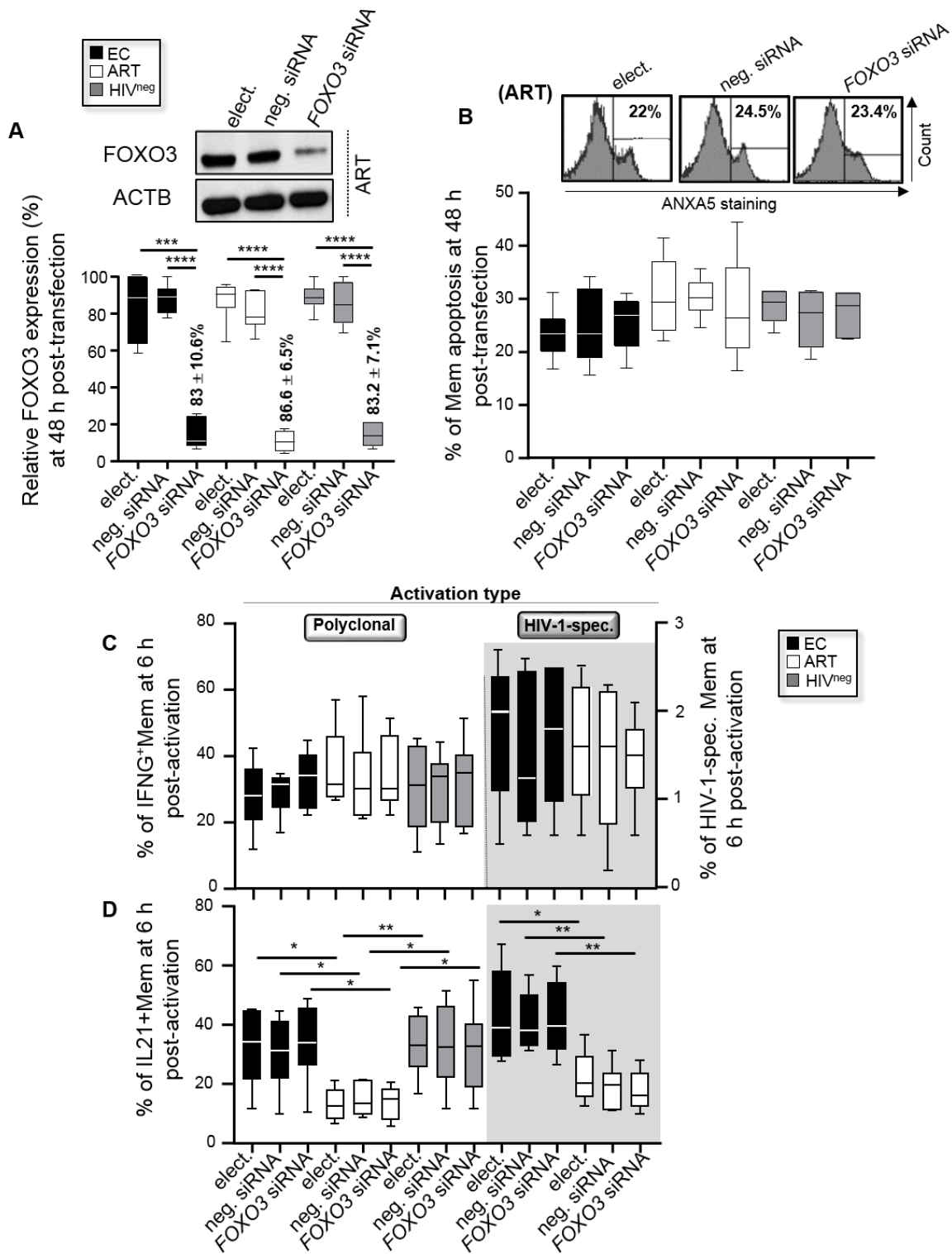




**Figure S10.** FOXO3 is not involved in IL21 production in Mem after cell activation. (A) FOXO3 protein abundance in purified Mem was assessed at 48 h post-transfection with or without specific siRNA for *FOXO3* by western blotting. i. Representative blots for FOXO3 and  $\beta$ -actin expressions in ART. ii. Densitometric quantification of specific FOXO3 bands was performed using ImageQuant software for all study groups and culture conditions. Results shown represent the mean relative expression  $\pm$  SD of 6 independent experiments. Of note, percentages of FOXO3 inhibition under specific gene silencing were also included in bold. (B) We assessed in transfected Mem from all study groups at 48 h of specific *FOXO3* gene silencing the levels of apoptosis by flow cytometry. Representative ANXA5 staining are also shown in ART. At 6 h of polyclonal and HIV-1-specific activation, we also monitored the intracellular levels of (C) IFNG and (D) IL21 with or without specific *FOXO3* gene silencing. N = 6. The error bars indicate standard deviations from the means. \*, symbol used for Mann-Whitney test (comparison between study groups).





## 6 GENERAL DISCUSSION

---

It is important to unravel a new insight into all mechanisms that control highly active T cell responses during persistent HIV-1 infection, since these cells are not only associated with natural viral control, but also are critical to ensure the success of next generation T cell-based therapy. In this thesis, we indicate that enhanced autophagy has the potential to promote HIV-1-specific T cell responses, hence contributing to a better control of the infection in the long run. In fact, understanding how we could enhance antiviral T cell immune protection in patients is not only important to fight HIV-1 in the era of antiretroviral therapy (ART), but will also be helpful for clearing other persistent infections such as herpesviruses including cytomegalovirus (Lepone *et al.*, 2010; Snyder *et al.*, 2016), and hepatitis viruses among others (Abdel-Hakeem *et al.*, 2014; Boni *et al.*, 2012; Boyd *et al.*, 2015a; Boyd *et al.*, 2015b). In the context of HIV-1 infection, it has recently been shown that only HIV-1-specific CD8A T cells from Elite Controllers (EC) displayed the ability to use carbon sources other than glucose to provide the energetic background for optimal T cell protection (Angin *et al.*, 2019; Loucif *et al.*, 2020). Although this advantage, referred to as metabolic plasticity, was clearly responsible for better CD8A T cell antiviral potential, the upstream mechanisms responsible for this are unknown and need to be unveiled. Interestingly, we found that IL21-mediated autophagy plays a major role in regulating the metabolic plasticity not only within highly functional CD8A T cells response, but also in memory CD4 T cells (Mem) to secrete IL21. Furthermore, we found a certain preference in the type of the degraded substrate within the autolysosomes (ALs) in activated CD8A T-cells (lipid catabolism) and Mem (protein catabolism). Each has yet to elucidate that autophagy regulates mitochondrial metabolism by providing a specific type of organic substrate depending on T cell subset and its functionality.

### 6.1 Autophagy as a major regulator of T cells metabolism and immunity during natural control of HIV-1 infection

In this thesis, the rationale for comparing EC to patients under ART, which both maintain undetectable viral loads for years, is to focus on the host mechanisms and eliminate the side effects that could be caused by high viremia and viral protein production, that eventually would influence autophagy (Loucif *et al.*, 2018). Although autophagy is often defined as a housekeeping mechanism used in removing either misfolded or aggregated proteins (macroautophagy), clearing damaged organelles such as mitochondria (mitophagy), or invading pathogens (xenophagy), it can also contribute to the mobilization of diverse cellular energy stores (Poillet-Perez *et al.*, 2021; Rabinowitz & White, 2010; Singh, 2010; Singh & Cuervo, 2011). In this context, *in vivo* T cell-

targeted genetic deletion of the autophagy related protein ATG7 is associated with a reduced ATP production that drives effector T cell dysfunction (Hubbard *et al.*, 2010). Metabolomics analysis, further conducted with the same *in vivo* model of autophagy blockade, has also shown profound alterations of several metabolic pathways in effector T cells, especially in their lipid catabolism (Xu *et al.*, 2014). In fact, there are several clues in the literature supporting a potential role of the autophagy-dependent lipolysis, referred to as lipophagy, in promoting memory CD8A T-cell immunity against viruses (O'Sullivan *et al.*, 2014; O'Sullivan *et al.*, 2018; Puleston *et al.*, 2014b). Interestingly, it has been shown in the context of persistent HIV-1 infection that the enhancement of bulk CD8A T cell immunity in ART was associated with higher rates of fatty acid uptake along with increased mitochondrial respiration (Angin *et al.*, 2019). In our first study, we confirmed the critical role of the mitochondrial fatty acid beta-oxidation (FAO) in improving CD8A T cell polyfunctional responses in ART, including against HIV-1 Gag, when cells were co-stimulated with IL21. We further showed that these higher rates of FAO in ART were dependent on autophagic activity since they were abolished by BaF treatment despite IL21 presence in cultures. The metabolic plasticity in EC may not only be explained by the autophagic degradation of intracellular lipid stores, but also by additional and synergic mechanisms. For instance, we cannot rule out an autophagy-dependent proteolysis in T cell responses observed in EC. Indeed, we proved in our second study, that autophagy-mediated proteolysis provides Mem from EC with an essential amino acid such as glutamine. The metabolism of glutamine, also known as glutaminolysis, was found to be imminent to fuel the high rates of mitochondrial oxidative metabolism and ATP production in activated Mem. Finally, the notion of metabolic plasticity in EC does not imply that glycolysis-derived products, such as pyruvate, are not used as well to fuel their mitochondria. Upon antigen recognition, when T cells rapidly upregulate both autophagy and aerobic glycolysis (the metabolic hallmark of T cell activation) (Cham *et al.*, 2008; Chapman *et al.*, 2020; Jacobs *et al.*, 2008; Menk *et al.*, 2018), it is likely that the ability of autophagy to degrade glycogen, the readily mobilized storage form of glucose, may also provide energy substrates to support cell activation (Dowling & Macian, 2018; Singh & Cuervo, 2011).

## **6.2 What is next to exploit? Deep understanding of autophagy in other immune cells.**

Although our findings led to a straightforward mechanism behind the deleterious effects of reduced autophagy activity on reduced CD8A T cell polyfunctionality or IL21 secretion from Mem, there are still other factors to consider if we want to thoroughly map out the molecular network involved during this signaling as well as its full impact. (i) One such aspect is the extent at which

autophagy is reduced in ART. Autophagy could be also potentially dysfunctional for other adaptive and innate immune populations such as B cells, dendritic cells and monocytes. This potential future investigation may place autophagy as a potential key component of the immune system's critical function as it could affect a broad spectrum of cell populations during HIV-1 infection (Nardacci *et al.*, 2014). (ii) It is worth noting that the information provided by this study is based on the comparison of EC to ART with participants that are almost exclusively men. Since cells obtained from either men and women have been reported to act differently when it comes to autophagy (Koenig *et al.*, 2014; Oliván *et al.*, 2014), further investigations, which take into account sex/gender as biological variables, may be required. It is not surprising that autophagy needs to be finely regulated to avoid either excessive or insufficient activity and to provide long-lasting immunity. Finally, *in-vivo* investigations using HIV-1 humanized mice and macaque models are necessary to consolidate our findings (Berges & Rowan, 2011; Klein *et al.*, 2012; Thippeshappa *et al.*, 2020).

### **6.3 Therapeutic potential and perspectives**

During T cell activation, when cells are reported to switch their metabolic programming to glycolysis over mitochondrial respiration, recent evidence, including ours, indicate that the regulation of T cell metabolism is context-dependent and can involve autophagic activity under certain stressful conditions such as persistent HIV-1 infection. Unveiling the role of lipophagy-mediated metabolic plasticity in highly functional CD8 T cells and autophagy-mediated proteolysis glutaminolysis in Mem, may be helpful in designing the next generation of combinatorial treatments, which include IL21-based immunotherapy, in order to promote CD8A T cell metabolic reprogramming in non-controllers towards a FAO-dependent mitochondrial metabolism.

Finally, in order to design these proper T cell metabolic reprogramming strategies in HIV-1-infected patients, it is critical to consider other parameters that could impede the safety and the clinical outcome of such treatments. For example, although our data confirmed the efficacy of IL21 treatment in non-controllers in re-educating their CD8A T cells towards better anti-HIV-1 protection, the treatment may promote the maintenance of viral reservoirs. Indeed, HIV-1 reservoirs are mainly located in memory CD4 T-cells (Chomont *et al.*, 2009), which rely on mitochondria FAO for ensuring their long-term maintenance (Taub *et al.*, 2013). The enhancement of fatty acid use may also lead to the maintenance of exhausted CD4/CD8A T cells in patients, which is another HIV-1-related immune T-cell dysfunction, here illustrated by the

progressive loss of antigen-specific T cell immunity (Day *et al.*, 2006; El-Far *et al.*, 2008; Trautmann *et al.*, 2006). Similarly, to long-lasting Mem, evidence shows that exhausted cells rely on mitochondrial FAO for energy production and cell maintenance (Bettonville *et al.*, 2018; Patsoukis *et al.*, 2015). To conclude, although it is critical to ensure that T cell metabolic reprogramming towards FAO-dependent mitochondrial metabolism provide more benefits for the host rather than for the virus, our data will surely be helpful to facilitate the translation of this therapeutic concept into a successful treatment against HIV-1 infection in the final attempt to boost antiviral immunity. In cancer, data show that the diverse metabolic fuel sources that can be produced by autophagy, a lysosomal-dependent catabolic process, provide tumors with metabolic plasticity (Guo *et al.*, 2013; Perera *et al.*, 2015; Strohecker *et al.*, 2013; Strohecker & White, 2014).

### **6.3.1 Targeting autophagy as a part of HIV-1 therapy regimen**

#### **6.3.1.1 Via targeting AMPK/PRKAA1 and MTOR**

Targeting AMPK and MTOR pathways piqued interests of the scientific community in the last 3 decades. The key role of AMPK in the metabolic homeostasis in various tissues of the body is critical to overcome energy imbalance (EI). This EI leads to multiple comorbidities such as type 2 diabetes, cancer and cardiovascular diseases (Chomanicova *et al.*, 2021; Steinberg & Carling, 2019). EI is the inability for the cells to maintain a steady energy demand/intake, which is represented by the intracellular ratio of adenine nucleotides such as Adenosine monophosphate (AMP)/Adenosine diphosphate (ADP) to ATP. This loss of ability is mainly due to the various environmental and physiological stresses that lead to disturbed cellular functions and energetic metabolism (such a chronic inflammation, imbalanced diet, starvation, etc.). AMPK is a vital energy sensor enzyme that regulates main energy sources and processes such as gluconeogenesis, lipogenesis, mitochondrial biogenesis, glycolysis, mitochondrial OxPhos and FAO (Steinberg & Carling, 2019). Therefore, various pharmacological and clinical studies aimed to understand and target AMPK activation in order to manage the EI in several disease contexts. The activation of AMPK can be inferred by its phosphorylation at the catalytic site such as Thr172  $\alpha$ -subunit (PRKAA1) as shown in our study. Other important subunits such as  $\beta$ - and  $\gamma$ -subunits are implicated in the autoregulation of AMPK and binding sites for the adenine nucleosides. Understanding the AMPK activation dynamics and its domain structure led to the discovery of multiple prodrugs and compounds used in *in-vivo* and *in-vitro* studies as well as in pre-clinical trials. Steinberg and Carling latest review summarized the potential direct/indirect AMPK activators currently available in various development stages (Steinberg & Carling, 2019). For instance, Metformin is an indirect AMPK activator, which reduces the ATP-linked mitochondrial respiration production. It also known to possess an anti-cancer activity features through AMPK/MTOR pathways (Chomanicova *et al.*, 2021). Other indirect activators such as berberin and resveratrol, natural occurring products (aka, nutraceutical molecules), also studied to treat type 2 diabetes and neurodegenerative diseases. In this thesis, we used the direct AMPK activator compound AICAR, which is a non-specific activator that mimics AMPK-nucleotide-dependent activation. Studies showed AICAR treatment increases glucose uptake, FAO, autophagy and exercise capacity in some rodent models.

It is well-known that autophagy can also be regulated and promoted by AMPK (Kim & Guan, 2011; Kim *et al.*, 2011; Lee *et al.*, 2010). In T cells, AMPK is activated by the T cell receptor signaling events (Tamas *et al.*, 2006). Our results showed that superior autophagy activity found in Mem of EC could not be explained by MTOR inactivation but rather dependent on the PRKAA1 activity. On the contrary, we found that activation-induced autophagy in Mem for all study groups was systematically associated with increased MTOR activity (Botbol *et al.*, 2015). Therefore, we cannot exclude an autophagy-independent role of MTOR signaling on HIV-1-specific T cell immunity during HIV-1 infection, especially when recent transcription analyses showed that cells from EC displayed distinct MTOR-related gene programs when compared to ART (Angin *et al.*, 2019; Loucif *et al.*, 2020). It will be interesting in the future to consolidate our results by using other direct AMPK activators on HIV-1 murine and primate models and assess their safety. It is also important to note that antiretroviral drugs (ARV) can also affect the AMPK-mediated molecular mechanisms of lipid metabolism and neuroprotection (Tsai *et al.*, 2018). These are indications of the challenges that should be outlooked in future studies to therapeutically target AMPK in the context of HIV-1 infection.

#### **6.3.1.2 Via IL21-based immunotherapy**

We found that CD4 cooperation was a key component for providing high autophagy induction in EC. CD4 T cells are known to interact with other immune cells by several mechanisms that include the release of cytokines. In this context, we were particularly interested in the potential involvement of IL21, which is part of a group of cytokines that include IL2, IL4, IL7 and IL15 whose receptor complexes share the common  $\gamma$  chain. Indeed, IL21 is known to play an important role in promoting memory and effector CD8A T-cell immunity to various pathogens including HIV-1 (Novy *et al.*, 2011; Pallikkuth *et al.*, 2012; Shen *et al.*, 2019; Wu *et al.*, 2019; Zander *et al.*, 2019). Interestingly, our results showed the possibility to rescue the autophagic activity in CD8A T cells from ART, including HIV-1-specific cells, when they were co-stimulated with recombinant IL21 during cell activation. We further confirmed that IL21-mediated rescue of cellular autophagy in ART was crucial to improve their antiviral CD8A T-cell potential following HIV-1 Gag stimulation. Unveiling a new autophagy-related mechanism that is promoted by the IL21 signaling intrinsic to CD8A T cells may be informative for other human diseases and complications. For example, it is now well-established that IL21 is also a potent stimulator of antitumor T cell immunity by supporting polyfunctionality of cytotoxic CD8A T cells (Novy *et al.*, 2011; Pallikkuth *et al.*, 2012; Shen *et al.*, 2019; Wu *et al.*, 2019; Zander *et al.*, 2019). Several authors have reported the critical

role of another key cytokine, IL15, in shaping protective CD8A T cell immunity against HIV-1 (Angin *et al.*, 2019; Mueller *et al.*, 2003; Younes *et al.*, 2016). Recent data have also shown that IL15 treatment of non-controllers provides the metabolic plasticity in HIV-1-specific CD8A T cells that is required for eliciting their antiviral immune responses (Angin *et al.*, 2019). Although IL15-based immunotherapy appears to be a strategic tool to improve both CD8A T cells metabolism and immune function in HIV-1-infected patients, it may bring some harmful side effects. For instance, in addition to exacerbating T cell activation and proliferation during the time course of HIV-1 infection (White *et al.*, 2007; Younes *et al.*, 2016), IL15 is also known to increase the susceptibility of CD4 T cells to viral infection (Manganaro *et al.*, 2018). Since IL21 has been shown to enhance cytotoxic molecules in CD8A T cells without undergoing cellular activation (White *et al.*, 2007), our data along with evidence found in the literature indicate that IL21 may be an immunotherapeutic agent potentially capable of improving overall viral containment in combination with ART treatment. However, it would be interesting to investigate whether the IL15-mediated enhancement of CD8A T cell immunity against HIV-1 is also driven by higher autophagic activity. Finally, beyond IL21 and IL15, there are other immune cytokines that have to be taken into consideration such as IL7, whose treatment not only enhances specific T cell immunity in ART (Sortino *et al.*, 2018), but also has been found to increase cellular autophagy during CD4 T cell activation (Botbol *et al.*, 2015; Hubbard *et al.*, 2010). Overall, our findings indicate that immunotherapy may be considered as a therapeutic tool that could be used for stimulating anti-HIV-1 T cell immunity against persistent viral infections, when autophagy induction is involved in the process.



## **7 CONCLUSION**

---

We are just beginning to appreciate how and why autophagy is a fundamental mechanism by which T cells regulate metabolism, and thereby modulate differentiation and function. Lessons could be learned from key studies in better understanding the interplay between autophagy-mediated metabolic plasticity and antitumor T cells immune responses. It was indeed proven that autophagy regulation is cell type and context dependent. This knowledge is required in order to correctly use autophagy as an effective therapy in combination with conventional treatments against HIV-1 infection.

## 8 BIBLIOGRAPHY

---

- Abdel-Hakeem MS, Bedard N, Murphy D, Bruneau J, Shoukry NH (2014) Signatures of protective memory immune responses during hepatitis C virus reinfection. *Gastroenterology* 147(4):870-881 e878.
- Allers K, Hutter G, Hofmann J, Loddenkemper C, Rieger K, Thiel E, Schneider T (2011) Evidence for the cure of HIV infection by CCR5Delta32/Delta32 stem cell transplantation. *Blood* 117(10):2791-2799.
- Angin M, Volant S, Passaes C, Lecuroux C, Monceaux V, Dillies MA, Valle-Casuso JC, Pancino G, Vaslin B, Le Grand R, Weiss L, Goujard C, Meyer L, Boufassa F, Muller-Trutwin M, Lambotte O, Saez-Cirion A (2019) Metabolic plasticity of HIV-specific CD8(+) T cells is associated with enhanced antiviral potential and natural control of HIV-1 infection. *Nat Metab* 1(7):704-716.
- Arsov I, Adebayo A, Kucerova-Levisohn M, Haye J, MacNeil M, Papavasiliou FN, Yue Z, Ortiz BD (2011) A role for autophagic protein beclin 1 early in lymphocyte development. *J Immunol* 186(4):2201-2209.
- Barker E & Evans DT (2016) HLA-C Downmodulation by HIV-1 Vpu. *Cell Host Microbe* 19(5):570-571.
- Berges BK & Rowan MR (2011) The utility of the new generation of humanized mice to study HIV-1 infection: transmission, prevention, pathogenesis, and treatment. *Retrovirology* 8:65.
- Bettonville M, d'Aria S, Weatherly K, Porporato PE, Zhang J, Bousbata S, Sonveaux P, Braun MY (2018) Long-term antigen exposure irreversibly modifies metabolic requirements for T cell function. *Elife* 7.
- Boni C, Laccabue D, Lampertico P, Giuberti T, Vigano M, Schivazappa S, Alfieri A, Pesci M, Gaeta GB, Brancaccio G, Colombo M, Missale G, Ferrari C (2012) Restored function of HBV-specific T cells after long-term effective therapy with nucleos(t)ide analogues. *Gastroenterology* 143(4):963-973 e969.
- Botbol Y, Patel B, Macian F (2015) Common gamma-chain cytokine signaling is required for macroautophagy induction during CD4+ T-cell activation. *Autophagy* 11(10):1864-1877.
- Boyd A, Almeida JR, Darrah PA, Sauce D, Seder RA, Appay V, Gorochov G, Larsen M (2015a) Correction: Pathogen-Specific T Cell Polyfunctionality Is a Correlate of T Cell Efficacy and Immune Protection. *PLoS One* 10(9):e0138395.
- Boyd A, Almeida JR, Darrah PA, Sauce D, Seder RA, Appay V, Gorochov G, Larsen M (2015b) Pathogen-Specific T Cell Polyfunctionality Is a Correlate of T Cell Efficacy and Immune Protection. *PLoS One* 10(6):e0128714.
- Buck MD, O'Sullivan D, Pearce EL (2015) T cell metabolism drives immunity. *J Exp Med* 212(9):1345-1360.
- Buranapraditkun S, Pissani F, Teigler JE, Schultz BT, Alter G, Marovich M, Robb ML, Eller MA, Martin J, Deeks S, Michael NL, Streeck H (2017) Preservation of Peripheral T Follicular Helper Cell Function in HIV Controllers. *J Virol* 91(14).
- Cambou MC & Landovitz RJ (2020) Novel Antiretroviral Agents. *Curr HIV/AIDS Rep* 17(2):118-124.

- Casado C, Galvez C, Pernas M, Tarancon-Diez L, Rodriguez C, Sanchez-Merino V, Vera M, Olivares I, De Pablo-Bernal R, Merino-Mansilla A, Del Romero J, Lorenzo-Redondo R, Ruiz-Mateos E, Salgado M, Martinez-Picado J, Lopez-Galindez C (2020) Permanent control of HIV-1 pathogenesis in exceptional elite controllers: a model of spontaneous cure. *Sci Rep* 10(1):1902.
- Cazzaniga A, Scrimieri R, Galli M, Maier J, Rusconi S (2021) Unveiling the basis of antiretroviral therapy-induced osteopenia: the effects of Dolutegravir, Darunavir and Atazanavir on osteogenesis. *AIDS* 35(2):213-218.
- Cham CM, Driessens G, O'Keefe JP, Gajewski TF (2008) Glucose deprivation inhibits multiple key gene expression events and effector functions in CD8+ T cells. *Eur J Immunol* 38(9):2438-2450.
- Chapman NM, Boothby MR, Chi H (2020) Metabolic coordination of T cell quiescence and activation. *Nat Rev Immunol* 20(1):55-70.
- Chomanicova N, Gazova A, Adamickova A, Valaskova S, Kyselovic J (2021) The role of AMPK/mTOR signaling pathway in anticancer activity of metformin. *Physiol Res* 70(4):501-508.
- Chomont N, El-Far M, Ancuta P, Trautmann L, Procopio FA, Yassine-Diab B, Boucher G, Boulassel MR, Ghattas G, Brenchley JM, Schacker TW, Hill BJ, Douek DC, Routy JP, Haddad EK, Sekaly RP (2009) HIV reservoir size and persistence are driven by T cell survival and homeostatic proliferation. *Nat Med* 15(8):893-900.
- Claireaux M, Galperin M, Benati D, Nouel A, Mukhopadhyay M, Klingler J, de Truchis P, Zucman D, Hendou S, Boufassa F, Moog C, Lambotte O, Chakrabarti LA (2018) A High Frequency of HIV-Specific Circulating Follicular Helper T Cells Is Associated with Preserved Memory B Cell Responses in HIV Controllers. *mBio* 9(3).
- Clerc I, Moussa DA, Vahlas Z, Tardito S, Oburoglu L, Hope TJ, Sitbon M, Dardalhon V, Mongellaz C, Taylor N (2019) Entry of glucose- and glutamine-derived carbons into the citric acid cycle supports early steps of HIV-1 infection in CD4 T cells. *Nat Metab* 1(7):717-730.
- Collier DA, Monit C, Gupta RK (2019) The Impact of HIV-1 Drug Escape on the Global Treatment Landscape. *Cell Host Microbe* 26(1):48-60.
- Collins DR, Gaiha GD, Walker BD (2020) CD8(+) T cells in HIV control, cure and prevention. *Nat Rev Immunol* 20(8):471-482.
- Crowell TA, Gebo KA, Blankson JN, Korthuis PT, Yehia BR, Rutstein RM, Moore RD, Sharp V, Nijhawan AE, Mathews WC, Hanau LH, Corales RB, Beil R, Somboonwit C, Edelstein H, Allen SL, Berry SA, Network HIVR (2015) Hospitalization Rates and Reasons Among HIV Elite Controllers and Persons With Medically Controlled HIV Infection. *J Infect Dis* 211(11):1692-1702.
- Cubas R, van Grevenynghe J, Wills S, Kardava L, Santich BH, Buckner CM, Muir R, Tardif V, Nichols C, Procopio F, He Z, Metcalf T, Ghneim K, Locci M, Ancuta P, Routy JP, Trautmann L, Li Y, McDermott AB, Koup RA, Petrovas C, Migueles SA, Connors M, Tomaras GD, Moir S, Crotty S, Haddad EK (2015) Reversible Reprogramming of Circulating Memory T Follicular Helper Cell Function during Chronic HIV Infection. *J Immunol* 195(12):5625-5636.
- Danforth K, Granich R, Wiedeman D, Baxi S, Padian N (2017) Global Mortality and Morbidity of HIV/AIDS. *Major Infectious Diseases*, Rd, Holmes KK, Bertozzi S, Bloom BR, Jha P (Édit.) Washington (DC) 10.1596/978-1-4648-0524-0\_ch2.

- Davenport MP, Khoury DS, Cromer D, Lewin SR, Kelleher AD, Kent SJ (2019) Functional cure of HIV: the scale of the challenge. *Nat Rev Immunol* 19(1):45-54.
- Day CL, Kaufmann DE, Kiepiela P, Brown JA, Moodley ES, Reddy S, Mackey EW, Miller JD, Leslie AJ, DePierres C, Mncube Z, Duraiswamy J, Zhu B, Eichbaum Q, Altfeld M, Wherry EJ, Coovadia HM, Goulder PJ, Klenerman P, Ahmed R, Freeman GJ, Walker BD (2006) PD-1 expression on HIV-specific T cells is associated with T-cell exhaustion and disease progression. *Nature* 443(7109):350-354.
- de Mendoza C (2019) UNAIDS Update Global HIV Numbers. *AIDS Rev* 21(3):170-171.
- Deeks SG, Overbaugh J, Phillips A, Buchbinder S (2015) HIV infection. *Nat Rev Dis Primers* 1:15035.
- Dillon SM & Wilson CC (2021) Gut Innate Immunity and HIV Pathogenesis. *Curr HIV/AIDS Rep* 18(2):128-138.
- Dionne B (2019) Key Principles of Antiretroviral Pharmacology. *Infect Dis Clin North Am* 33(3):787-805.
- Doherty J & Baehrecke EH (2018) Life, death and autophagy. *Nat Cell Biol* 20(10):1110-1117.
- Dowling SD & Macian F (2018) Autophagy and T cell metabolism. *Cancer Lett* 419:20-26.
- El-Far M, Halwani R, Said E, Trautmann L, Doroudchi M, Janbazian L, Fonseca S, van Grevenynghe J, Yassine-Diab B, Sekaly RP, Haddad EK (2008) T-cell exhaustion in HIV infection. *Curr HIV/AIDS Rep* 5(1):13-19.
- El-Far M, Kouassi P, Sylla M, Zhang Y, Fouda A, Fabre T, Goulet JP, van Grevenynghe J, Lee T, Singer J, Harris M, Baril JG, Trottier B, Ancuta P, Routy JP, Bernard N, Tremblay CL, Investigators of the Canadian HIVSPC (2016) Proinflammatory isoforms of IL-32 as novel and robust biomarkers for control failure in HIV-infected slow progressors. *Sci Rep* 6:22902.
- Geiger R, Rieckmann JC, Wolf T, Basso C, Feng Y, Fuhrer T, Kogadeeva M, Picotti P, Meissner F, Mann M, Zamboni N, Sallusto F, Lanzavecchia A (2016) L-Arginine Modulates T Cell Metabolism and Enhances Survival and Anti-tumor Activity. *Cell* 167(3):829-842 e813.
- Gelpi M, Hartling HJ, Ueland PM, Ullum H, Troseid M, Nielsen SD (2017) Tryptophan catabolism and immune activation in primary and chronic HIV infection. *BMC Infect Dis* 17(1):349.
- Guo JY, Xia B, White E (2013) Autophagy-mediated tumor promotion. *Cell* 155(6):1216-1219.
- Gupta RK, Peppas D, Hill AL, Galvez C, Salgado M, Pace M, McCoy LE, Griffith SA, Thornhill J, Alrubayyi A, Huyvener LEP, Nastouli E, Grant P, Edwards SG, Innes AJ, Frater J, Nijhuis M, Wensing AMJ, Martinez-Picado J, Olavarria E (2020) Evidence for HIV-1 cure after CCR5Delta32/Delta32 allogeneic haemopoietic stem-cell transplantation 30 months post analytical treatment interruption: a case report. *Lancet HIV* 7(5):e340-e347.
- Haddad N, Robert A, Weeks A, Popovic N, Siu W, Archibald C (2019) HIV in Canada-Surveillance Report, 2018. *Can Commun Dis Rep* 45(12):304-312.
- Halling Folkmar Andersen A & Tolstrup M (2020) The Potential of Long-Acting, Tissue-Targeted Synthetic Nanotherapy for Delivery of Antiviral Therapy Against HIV Infection. *Viruses* 12(4).
- Hansen M, Rubinsztein DC, Walker DW (2018) Autophagy as a promoter of longevity: insights from model organisms. *Nat Rev Mol Cell Biol* 19(9):579-593.

- Hegedus A, Kavanagh Williamson M, Huthoff H (2014) HIV-1 pathogenicity and virion production are dependent on the metabolic phenotype of activated CD4+ T cells. *Retrovirology* 11:98.
- Henrich TJ & Lelievre JD (2018) Progress towards obtaining an HIV cure: slow but sure. *Curr Opin HIV AIDS* 13(5):381-382.
- Hocini H, Bonnabau H, Lacabaratz C, Lefebvre C, Tisserand P, Foucat E, Lelievre JD, Lambotte O, Saez-Cirion A, Versmisse P, Thiebaut R, Levy Y (2019) HIV Controllers Have Low Inflammation Associated with a Strong HIV-Specific Immune Response in Blood. *J Virol* 93(10).
- Hubbard VM, Valdor R, Patel B, Singh R, Cuervo AM, Macian F (2010) Macroautophagy regulates energy metabolism during effector T cell activation. *J Immunol* 185(12):7349-7357.
- Jacobs SR, Herman CE, Maciver NJ, Wofford JA, Wieman HL, Hammen JJ, Rathmell JC (2008) Glucose uptake is limiting in T cell activation and requires CD28-mediated Akt-dependent and independent pathways. *J Immunol* 180(7):4476-4486.
- Jenabian MA, El-Far M, Vyboh K, Kema I, Costiniuk CT, Thomas R, Baril JG, LeBlanc R, Kanagaratham C, Radzioch D, Allam O, Ahmad A, Lebouche B, Tremblay C, Ancuta P, Routy JP, Montreal Primary i, Slow Progressor Study G (2015) Immunosuppressive Tryptophan Catabolism and Gut Mucosal Dysfunction Following Early HIV Infection. *J Infect Dis* 212(3):355-366.
- Jenabian MA, Patel M, Kema I, Kanagaratham C, Radzioch D, Thebault P, Lapointe R, Tremblay C, Gilmore N, Ancuta P, Routy JP (2013) Distinct tryptophan catabolism and Th17/Treg balance in HIV progressors and elite controllers. *PLoS One* 8(10):e78146.
- Johnson MO, Wolf MM, Madden MZ, Andrejeva G, Sugiura A, Contreras DC, Maseda D, Liberti MV, Paz K, Kishton RJ, Johnson ME, de Cubas AA, Wu P, Li G, Zhang Y, Newcomb DC, Wells AD, Restifo NP, Rathmell WK, Locasale JW, Davila ML, Blazar BR, Rathmell JC (2018) Distinct Regulation of Th17 and Th1 Cell Differentiation by Glutaminase-Dependent Metabolism. *Cell* 175(7):1780-1795 e1719.
- Jones N, Vincent EE, Cronin JG, Panetti S, Chambers M, Holm SR, Owens SE, Francis NJ, Finlay DK, Thornton CA (2019) Akt and STAT5 mediate naive human CD4+ T-cell early metabolic response to TCR stimulation. *Nat Commun* 10(1):2042.
- Kang S & Tang H (2020) HIV-1 Infection and Glucose Metabolism Reprogramming of T Cells: Another Approach Toward Functional Cure and Reservoir Eradication. *Front Immunol* 11:572677.
- Kaufmann DE, Kavanagh DG, Pereyra F, Zaunders JJ, Mackey EW, Miura T, Palmer S, Brockman M, Rathod A, Piechocka-Trocha A, Baker B, Zhu B, Le Gall S, Waring MT, Ahern R, Moss K, Kelleher AD, Coffin JM, Freeman GJ, Rosenberg ES, Walker BD (2007) Upregulation of CTLA-4 by HIV-specific CD4+ T cells correlates with disease progression and defines a reversible immune dysfunction. *Nat Immunol* 8(11):1246-1254.
- Kemnic TR & Gulick PG (2021) HIV Antiretroviral Therapy. *StatPearls*, Treasure Island (FL).
- Kim J & Guan KL (2011) Regulation of the autophagy initiating kinase ULK1 by nutrients: roles of mTORC1 and AMPK. *Cell Cycle* 10(9):1337-1338.
- Kim J, Kundu M, Viollet B, Guan KL (2011) AMPK and mTOR regulate autophagy through direct phosphorylation of Ulk1. *Nat Cell Biol* 13(2):132-141.
- Klein F, Halper-Stromberg A, Horwitz JA, Gruell H, Scheid JF, Bournazos S, Mouquet H, Spatz LA, Diskin R, Abadir A, Zang T, Dorner M, Billerbeck E, Labitt RN, Gaebler C,

- Marcovecchio P, Incesu RB, Eisenreich TR, Bieniasz PD, Seaman MS, Bjorkman PJ, Ravetch JV, Ploss A, Nussenzweig MC (2012) HIV therapy by a combination of broadly neutralizing antibodies in humanized mice. *Nature* 492(7427):118-122.
- Klein Geltink RI, O'Sullivan D, Corrado M, Bremser A, Buck MD, Buescher JM, Firat E, Zhu X, Niedermann G, Caputa G, Kelly B, Warthorst U, Rensing-Ehl A, Kyle RL, Vandersarren L, Curtis JD, Patterson AE, Lawless S, Grzes K, Qiu J, Sanin DE, Kretz O, Huber TB, Janssens S, Lambrecht BN, Rambold AS, Pearce EJ, Pearce EL (2017) Mitochondrial Priming by CD28. *Cell* 171(2):385-397 e311.
- Koenig A, Sateriale A, Budd RC, Huber SA, Buskiewicz IA (2014) The role of sex differences in autophagy in the heart during coxsackievirus B3-induced myocarditis. *J Cardiovasc Transl Res* 7(2):182-191.
- Kumar BV, Connors TJ, Farber DL (2018) Human T Cell Development, Localization, and Function throughout Life. *Immunity* 48(2):202-213.
- Lee JW, Park S, Takahashi Y, Wang HG (2010) The association of AMPK with ULK1 regulates autophagy. *PLoS One* 5(11):e15394.
- Lepone L, Rappocciolo G, Knowlton E, Jais M, Piazza P, Jenkins FJ, Rinaldo CR (2010) Monofunctional and polyfunctional CD8+ T cell responses to human herpesvirus 8 lytic and latency proteins. *Clin Vaccine Immunol* 17(10):1507-1516.
- Li JZ & Blankson JN (2021a) How elite controllers and posttreatment controllers inform our search for an HIV-1 cure. *The Journal of Clinical Investigation* 131(11).
- Li JZ & Blankson JN (2021b) How elite controllers and posttreatment controllers inform our search for an HIV-1 cure. *J Clin Invest* 131(11).
- Li JZ & Gandhi RT (2021) The Search for an HIV Cure: Where Do We Go From Here? *J Infect Dis* 223(12 Suppl 2):1-3.
- Li W, Cheng H, Li G, Zhang L (2020) Mitochondrial Damage and the Road to Exhaustion. *Cell Metab* 32(6):905-907.
- Lichterfeld M (2020) Reactivation of latent HIV moves shock-and-kill treatments forward. *Nature* 578(7793):42-43.
- Loucif H, Dagenais-Lussier X, Avizonis D, Choiniere L, Beji C, Cassin L, Routy JP, Fritz JH, Olganier D, van Grevenynghe J (2021a) Autophagy-dependent glutaminolysis drives superior IL21 production in HIV-1-specific CD4 T cells. *Autophagy* 10.1080/15548627.2021.1972403:1-18.
- Loucif H, Dagenais-Lussier X, Beji C, Cassin L, Jrade H, Tellitchenko R, Routy JP, Olganier D, van Grevenynghe J (2021b) Lipophagy confers a key metabolic advantage that ensures protective CD8A T-cell responses against HIV-1. *Autophagy* 10.1080/15548627.2021.1874134:1-16.
- Loucif H, Dagenais-Lussier X, Beji C, Tellitchenko R, Routy JP, van Grevenynghe J (2020) Plasticity in T-cell mitochondrial metabolism: A necessary peacekeeper during the troubled times of persistent HIV-1 infection. *Cytokine Growth Factor Rev* 55:26-36.
- Loucif H, Gouard S, Dagenais-Lussier X, Murira A, Stager S, Tremblay C, Van Grevenynghe J (2018) Deciphering natural control of HIV-1: A valuable strategy to achieve antiretroviral therapy termination. *Cytokine Growth Factor Rev* 40:90-98.
- Lunemann JD & Munz C (2009) Autophagy in CD4+ T-cell immunity and tolerance. *Cell Death Differ* 16(1):79-86.

- Ma EH, Bantug G, Griss T, Condotta S, Johnson RM, Samborska B, Mainolfi N, Suri V, Guak H, Balmer ML, Verway MJ, Raissi TC, Tsui H, Boukhaled G, Henriques da Costa S, Frezza C, Krawczyk CM, Friedman A, Manfredi M, Richer MJ, Hess C, Jones RG (2017) Serine Is an Essential Metabolite for Effector T Cell Expansion. *Cell Metab* 25(2):482.
- Ma L & Zong X (2020) Metabolic Symbiosis in Chemoresistance: Refocusing the Role of Aerobic Glycolysis. *Front Oncol* 10:5.
- Maagaard A, Holberg-Petersen M, Lovgarden G, Holm M, Pettersen FO, Kvale D (2008) Distinct mechanisms for mitochondrial DNA loss in T and B lymphocytes from HIV-infected patients exposed to nucleoside reverse-transcriptase inhibitors and those naive to antiretroviral treatment. *J Infect Dis* 198(10):1474-1481.
- Macian F (2019) Autophagy in T Cell Function and Aging. *Front Cell Dev Biol* 7:213.
- Manganaro L, Hong P, Hernandez MM, Argyle D, Mulder LCF, Potla U, Diaz-Griffero F, Lee B, Fernandez-Sesma A, Simon V (2018) IL-15 regulates susceptibility of CD4(+) T cells to HIV infection. *Proc Natl Acad Sci U S A* 115(41):E9659-E9667.
- McCann NC, Horn TH, Hyle EP, Walensky RP (2020) HIV Antiretroviral Therapy Costs in the United States, 2012-2018. *JAMA Intern Med* 180(4):601-603.
- Melkonian EA & Schury MP (2021) Biochemistry, Anaerobic Glycolysis. *StatPearls*, Treasure Island (FL).
- Menk AV, Scharping NE, Moreci RS, Zeng X, Guy C, Salvatore S, Bae H, Xie J, Young HA, Wendell SG, Delgoffe GM (2018) Early TCR Signaling Induces Rapid Aerobic Glycolysis Enabling Distinct Acute T Cell Effector Functions. *Cell Rep* 22(6):1509-1521.
- Mitchell BI, Laws EI, Chow DC, SahBandar IN, Gangcuangco LMA, Shikuma CM, Ndhlovu LC (2020) Increased Monocyte Inflammatory Responses to Oxidized LDL Are Associated with Insulin Resistance in HIV-Infected Individuals on Suppressive Antiretroviral Therapy. *Viruses* 12(10).
- Moir S, Chun TW, Fauci AS (2011) Pathogenic mechanisms of HIV disease. *Annu Rev Pathol* 6:223-248.
- Mu W, Carrillo MA, Kitchen SG (2020) Engineering CAR T Cells to Target the HIV Reservoir. *Front Cell Infect Microbiol* 10:410.
- Mudd PA & Watkins DI (2011) Understanding animal models of elite control: windows on effective immune responses against immunodeficiency viruses. *Curr Opin HIV AIDS* 6(3):197-201.
- Mueller YM, Bojczuk PM, Halstead ES, Kim AH, Witek J, Altman JD, Katsikis PD (2003) IL-15 enhances survival and function of HIV-specific CD8+ T cells. *Blood* 101(3):1024-1029.
- Mueller YM, De Rosa SC, Hutton JA, Witek J, Roederer M, Altman JD, Katsikis PD (2001) Increased CD95/Fas-induced apoptosis of HIV-specific CD8(+) T cells. *Immunity* 15(6):871-882.
- Nardacci R, Amendola A, Ciccocanti F, Corazzari M, Esposito V, Vlassi C, Taibi C, Fimia GM, Del Nonno F, Ippolito G, D'Offizi G, Piacentini M (2014) Autophagy plays an important role in the containment of HIV-1 in nonprogressor-infected patients. *Autophagy* 10(7):1167-1178.
- Nardacci R, Ciccocanti F, Marsella C, Ippolito G, Piacentini M, Fimia GM (2017) Role of autophagy in HIV infection and pathogenesis. *J Intern Med* 281(5):422-432.

- Novy P, Huang X, Leonard WJ, Yang Y (2011) Intrinsic IL-21 signaling is critical for CD8 T cell survival and memory formation in response to vaccinia viral infection. *J Immunol* 186(5):2729-2738.
- O'Sullivan D, van der Windt GJ, Huang SC, Curtis JD, Chang CH, Buck MD, Qiu J, Smith AM, Lam WY, DiPlato LM, Hsu FF, Birnbaum MJ, Pearce EJ, Pearce EL (2014) Memory CD8(+) T cells use cell-intrinsic lipolysis to support the metabolic programming necessary for development. *Immunity* 41(1):75-88.
- O'Sullivan D, van der Windt GJ, Huang SC, Curtis JD, Chang CH, Buck MD, Qiu J, Smith AM, Lam WY, DiPlato LM, Hsu FF, Birnbaum MJ, Pearce EJ, Pearce EL (2018) Memory CD8(+) T Cells Use Cell-Intrinsic Lipolysis to Support the Metabolic Programming Necessary for Development. *Immunity* 49(2):375-376.
- Olivan S, Calvo AC, Manzano R, Zaragoza P, Osta R (2014) Sex differences in constitutive autophagy. *Biomed Res Int* 2014:652817.
- Pallikkuth S, Parmigiani A, Silva SY, George VK, Fischl M, Pahwa R, Pahwa S (2012) Impaired peripheral blood T-follicular helper cell function in HIV-infected nonresponders to the 2009 H1N1/09 vaccine. *Blood* 120(5):985-993.
- Pasternak AO, Psomas CK, Berkhout B (2021) Predicting Post-treatment HIV Remission: Does Size of the Viral Reservoir Matter? *Front Microbiol* 12:648434.
- Patsoukis N, Bardhan K, Chatterjee P, Sari D, Liu B, Bell LN, Karoly ED, Freeman GJ, Petkova V, Seth P, Li L, Boussiotis VA (2015) PD-1 alters T-cell metabolic reprogramming by inhibiting glycolysis and promoting lipolysis and fatty acid oxidation. *Nat Commun* 6:6692.
- Pau AK & George JM (2014) Antiretroviral therapy: current drugs. *Infect Dis Clin North Am* 28(3):371-402.
- Perera RM, Stoykova S, Nicolay BN, Ross KN, Fitamant J, Boukhali M, Lengrand J, Deshpande V, Selig MK, Ferrone CR, Settleman J, Stephanopoulos G, Dyson NJ, Zoncu R, Ramaswamy S, Haas W, Bardeesy N (2015) Transcriptional control of autophagy-lysosome function drives pancreatic cancer metabolism. *Nature* 524(7565):361-365.
- Poillet-Perez L, Sarry JE, Joffre C (2021) Autophagy is a major metabolic regulator involved in cancer therapy resistance. *Cell Rep* 36(7):109528.
- Potter SJ, Lacabaratz C, Lambotte O, Perez-Patrigeon S, Vingert B, Sinet M, Colle JH, Urrutia A, Scott-Algara D, Boufassa F, Delfraissy JF, Theze J, Venet A, Chakrabarti LA (2007) Preserved central memory and activated effector memory CD4+ T-cell subsets in human immunodeficiency virus controllers: an ANRS EP36 study. *J Virol* 81(24):13904-13915.
- Puleston DJ, Zhang H, Powell TJ, Lipina E, Sims S, Panse I, Watson AS, Cerundolo V, Townsend AR, Klenerman P (2014a) Autophagy is a critical regulator of memory CD8+ T cell formation. *Elife* 3:e03706.
- Puleston DJ, Zhang H, Powell TJ, Lipina E, Sims S, Panse I, Watson AS, Cerundolo V, Townsend AR, Klenerman P, Simon AK (2014b) Autophagy is a critical regulator of memory CD8(+) T cell formation. *Elife* 3.
- Quigley M, Pereyra F, Nilsson B, Porichis F, Fonseca C, Eichbaum Q, Julg B, Jesneck JL, Brosnahan K, Imam S, Russell K, Toth I, Piechocka-Trocha A, Dolfi D, Angelosanto J, Crawford A, Shin H, Kwon DS, Zupkosky J, Francisco L, Freeman GJ, Wherry EJ, Kaufmann DE, Walker BD, Ebert B, Haining WN (2010) Transcriptional analysis of HIV-specific CD8+ T cells shows that PD-1 inhibits T cell function by upregulating BATF. *Nat Med* 16(10):1147-1151.



- Rabinowitz JD & Enerback S (2020) Lactate: the ugly duckling of energy metabolism. *Nat Metab* 2(7):566-571.
- Rabinowitz JD & White E (2010) Autophagy and metabolism. *Science* 330(6009):1344-1348.
- Rahman AN, Liu J, Mujib S, Kidane S, Ali A, Szep S, Han C, Bonner P, Parsons M, Benko E, Kovacs C, Yue FY, Ostrowski M (2021) Elevated glycolysis imparts functional ability to CD8(+) T cells in HIV infection. *Life Sci Alliance* 4(11).
- Ren T, Dong W, Takahashi Y, Xiang D, Yuan Y, Liu X, Loughran TP, Jr., Sun SC, Wang HG, Cheng H (2012) HTLV-2 Tax immortalizes human CD4+ memory T lymphocytes by oncogenic activation and dysregulation of autophagy. *J Biol Chem* 287(41):34683-34693.
- Ron-Harel N, Ghergurovich JM, Notarangelo G, LaFleur MW, Tsubosaka Y, Sharpe AH, Rabinowitz JD, Haigis MC (2019) T Cell Activation Depends on Extracellular Alanine. *Cell Rep* 28(12):3011-3021 e3014.
- Ron-Harel N, Santos D, Ghergurovich JM, Sage PT, Reddy A, Lovitch SB, Dephore N, Satterstrom FK, Sheffer M, Spinelli JB, Gygi S, Rabinowitz JD, Sharpe AH, Haigis MC (2016) Mitochondrial Biogenesis and Proteome Remodeling Promote One-Carbon Metabolism for T Cell Activation. *Cell Metab* 24(1):104-117.
- Saez-Cirion A, Bacchus C, Hocqueloux L, Avettand-Fenoel V, Girault I, Lecuroux C, Potard V, Versmisse P, Melard A, Prazuck T, Descours B, Guergnon J, Viard JP, Boufassa F, Lambotte O, Goujard C, Meyer L, Costagliola D, Venet A, Pancino G, Autran B, Rouzioux C, Group AVS (2013) Post-treatment HIV-1 controllers with a long-term virological remission after the interruption of early initiated antiretroviral therapy ANRS VISCONTI Study. *PLoS Pathog* 9(3):e1003211.
- Saez-Cirion A & Sereti I (2021) Immunometabolism and HIV-1 pathogenesis: food for thought. *Nat Rev Immunol* 21(1):5-19.
- Schank M, Zhao J, Moorman JP, Yao ZQ (2021) The Impact of HIV- and ART-Induced Mitochondrial Dysfunction in Cellular Senescence and Aging. *Cells* 10(1).
- Shen Z, Liu J, Wu J, Zhu Y, Li G, Wang J, Luo M, Deng Q, Zhang J, Xie Y (2019) IL-21-based therapies induce clearance of hepatitis B virus persistence in mouse models. *Theranostics* 9(13):3798-3811.
- Singh R (2010) Autophagy and regulation of lipid metabolism. *Results Probl Cell Differ* 52:35-46.
- Singh R & Cuervo AM (2011) Autophagy in the cellular energetic balance. *Cell Metab* 13(5):495-504.
- Snyder LD, Chan C, Kwon D, Yi JS, Martissa JA, Copeland CA, Osborne RJ, Sparks SD, Palmer SM, Weinhold KJ (2016) Polyfunctional T-Cell Signatures to Predict Protection from Cytomegalovirus after Lung Transplantation. *Am J Respir Crit Care Med* 193(1):78-85.
- Sortino O, Richards E, Dias J, Leeansyah E, Sandberg JK, Sereti I (2018) IL-7 treatment supports CD8+ mucosa-associated invariant T-cell restoration in HIV-1-infected patients on antiretroviral therapy. *AIDS* 32(6):825-828.
- Spinelli JB & Haigis MC (2018) The multifaceted contributions of mitochondria to cellular metabolism. *Nat Cell Biol* 20(7):745-754.
- Steinberg GR & Carling D (2019) AMP-activated protein kinase: the current landscape for drug development. *Nat Rev Drug Discov* 18(7):527-551.

- Steinert EM, Vasan K, Chandel NS (2021) Mitochondrial Metabolism Regulation of T Cell-Mediated Immunity. *Annu Rev Immunol* 39:395-416.
- Strohecker AM, Guo JY, Karsli-Uzunbas G, Price SM, Chen GJ, Mathew R, McMahon M, White E (2013) Autophagy sustains mitochondrial glutamine metabolism and growth of BrafV600E-driven lung tumors. *Cancer Discov* 3(11):1272-1285.
- Strohecker AM & White E (2014) Autophagy promotes BrafV600E-driven lung tumorigenesis by preserving mitochondrial metabolism. *Autophagy* 10(2):384-385.
- Tamas P, Hawley SA, Clarke RG, Mustard KJ, Green K, Hardie DG, Cantrell DA (2006) Regulation of the energy sensor AMP-activated protein kinase by antigen receptor and Ca<sup>2+</sup> in T lymphocytes. *J Exp Med* 203(7):1665-1670.
- Taub DD, Hesdorffer CS, Ferrucci L, Madara K, Schwartz JB, Goetzl EJ (2013) Distinct energy requirements for human memory CD4 T-cell homeostatic functions. *FASEB J* 27(1):342-349.
- Thippeshappa R, Kimata JT, Kaushal D (2020) Toward a Macaque Model of HIV-1 Infection: Roadblocks, Progress, and Future Strategies. *Front Microbiol* 11:882.
- Trautmann L, Janbazian L, Chomont N, Said EA, Gimmig S, Bessette B, Boulassel MR, Delwart E, Sepulveda H, Balderas RS, Routy JP, Haddad EK, Sekaly RP (2006) Upregulation of PD-1 expression on HIV-specific CD8+ T cells leads to reversible immune dysfunction. *Nat Med* 12(10):1198-1202.
- Tsai FJ, Ho MW, Lai CH, Chou CH, Li JP, Cheng CF, Wu YC, Liu X, Tsang H, Lin TH, Liao CC, Huang SM, Lin JC, Lin CC, Hsieh CL, Liang WM, Lin YJ (2018) Evaluation of Oral Antiretroviral Drugs in Mice With Metabolic and Neurologic Complications. *Front Pharmacol* 9:1004.
- Turk G, Seiger K, Lian X, Sun W, Parsons EM, Gao C, Rassadkina Y, Polo ML, Czernikier A, Ghiglione Y, Vellicce A, Varriale J, Lai J, Yuki Y, Martin M, Rhodes A, Lewin SR, Walker BD, Carrington M, Siliciano R, Siliciano J, Lichtenfeld M, Laufer N, Yu XG (2022) A Possible Sterilizing Cure of HIV-1 Infection Without Stem Cell Transplantation. *Ann Intern Med* 175(1):95-100.
- van Grevenynghe J, Procopio FA, He Z, Chomont N, Riou C, Zhang Y, Gimmig S, Boucher G, Wilkinson P, Shi Y, Yassine-Diab B, Said EA, Trautmann L, El Far M, Balderas RS, Boulassel MR, Routy JP, Haddad EK, Sekaly RP (2008) Transcription factor FOXO3a controls the persistence of memory CD4(+) T cells during HIV infection. *Nat Med* 14(3):266-274.
- Vesterbacka J, Rivera J, Noyan K, Parera M, Neogi U, Calle M, Paredes R, Sonnerborg A, Noguera-Julian M, Nowak P (2017) Richer gut microbiota with distinct metabolic profile in HIV infected Elite Controllers. *Sci Rep* 7(1):6269.
- White L, Krishnan S, Strbo N, Liu H, Kolber MA, Lichtenheld MG, Pahwa RN, Pahwa S (2007) Differential effects of IL-21 and IL-15 on perforin expression, lysosomal degranulation, and proliferation in CD8 T cells of patients with human immunodeficiency virus-1 (HIV). *Blood* 109(9):3873-3880.
- Wu Q, Liu B, Yuan L, Peng Q, Cheng L, Zhong P, Yang X, Yu H (2019) Dysregulations of follicular helper T cells through IL-21 pathway in age-related macular degeneration. *Mol Immunol* 114:243-250.

- Xu X, Araki K, Li S, Han JH, Ye L, Tan WG, Konieczny BT, Bruinsma MW, Martinez J, Pearce EL, Green DR, Jones DP, Virgin HW, Ahmed R (2014) Autophagy is essential for effector CD8(+) T cell survival and memory formation. *Nat Immunol* 15(12):1152-1161.
- Younes SA, Freeman ML, Mudd JC, Shive CL, Reynaldi A, Panigrahi S, Estes JD, Deleage C, Lucero C, Anderson J, Schacker TW, Davenport MP, McCune JM, Hunt PW, Lee SA, Serrano-Villar S, Debernardo RL, Jacobson JM, Canaday DH, Sekaly RP, Rodriguez B, Sieg SF, Lederman MM (2016) IL-15 promotes activation and expansion of CD8+ T cells in HIV-1 infection. *J Clin Invest* 126(7):2745-2756.
- Zander R, Schauder D, Xin G, Nguyen C, Wu X, Zajac A, Cui W (2019) CD4(+) T Cell Help Is Required for the Formation of a Cytolytic CD8(+) T Cell Subset that Protects against Chronic Infection and Cancer. *Immunity* 51(6):1028-1042 e1024.



Contents lists available at ScienceDirect

### Cytokine and Growth Factor Reviews

journal homepage: [www.elsevier.com/locate/cytogfr](http://www.elsevier.com/locate/cytogfr)



## Deciphering natural control of HIV-1: A valuable strategy to achieve antiretroviral therapy termination



Hamza Loucif<sup>a</sup>, Steven Gouard<sup>a</sup>, Xavier Dagenais-Lussier<sup>a</sup>, Armstrong Murira<sup>a</sup>, Simona Stäger<sup>a</sup>,  
Cécile Tremblay<sup>b</sup>, Julien Van Grevenynghe<sup>a,\*</sup>

<sup>a</sup> Institut National de la Recherche Scientifique (INRS)-Institut Armand-Prappier, 531 Boulevard des Prairies, Laval, H7V 1B7, QC, Canada

<sup>b</sup> Centre de Recherche de l'Université de Montréal, Montréal, QC, Canada

---



## Deciphering natural control of HIV-1: A valuable strategy to achieve antiretroviral therapy termination

Hamza Loucif<sup>a</sup>, Steven Gouard<sup>a</sup>, Xavier Dagenais-Lussier<sup>a</sup>, Armstrong Murira<sup>a</sup>, Simona Stäger<sup>a</sup>, Cécile Tremblay<sup>b</sup>, Julien Van Grevenynghe<sup>a,\*</sup>

<sup>a</sup> Institut National de la Recherche Scientifique (INRS)-Institut Armand-Frappier, 531 Boulevard des Prairies, Laval, H7V 1B7, QC, Canada

<sup>b</sup> Centre de Recherche de l'Université de Montréal, Montréal, QC, Canada



### ARTICLE INFO

#### Keywords:

HIV-1  
Cure  
ART  
Controllers  
Inflammation  
Metabolism  
Antiviral immunity  
Microbiota

### ABSTRACT

Antiretroviral therapy (ART) has dramatically reduced HIV-1-associated morbidity and mortality, and has transformed HIV-1 infection into a manageable chronic condition by suppressing viral replication. However, despite recent patient care improvements, ART still fails to cure HIV-1 infection due to the inability to counteract immune defects and metabolic disturbances that are associated with residual inflammation alongside viral persistence. Life-long drug administration also results in multiple side-effects in patients including lipodystrophy and insulin resistance. Thus, it is critical to find new ways to reduce the length of treatment and facilitate the termination of ART, for example by boosting protective immunity. The rare ability of some individuals to naturally control HIV-1 infection despite residual inflammation could be exploited to identify molecular mechanisms involved in host protection that may function as potential therapeutic targets. In this review, we highlight evidence illustrating the molecular and metabolic advantages of HIV-1 controllers over ART treated patients that contribute to the maintenance of effective antiviral immunity.

### 1. The need to achieve ART termination

#### 1.1. Introduction to ART and progress since its inception

The introduction of antiretroviral therapy (ART) since 1996 has revolutionized the treatment against human immunodeficiency virus type 1 (HIV-1) infection. ART consists of a combination of antiretroviral drugs (ARV) targeting different stages of HIV-1 life cycle to achieve maximal virus suppression and stop disease progression in infected patients [1]. Early versions of ARV required frequent dosing, and were also associated with drug-drug interactions that are defined by the change in a drug's effect on the body when the drug is taken together with other drugs. In the attempt to ensure life-long HIV-1 suppression and CD4 recovery along with better drug tolerability, some ART advancements have been provided to improve patient care (Fig. 1); these include smaller pills without compromising drug efficacy, adapted ARV combinations, as well as new classes of molecules such as integrase inhibitors [2,3]. Efforts have also been directed toward developing personalized ARV encapsulation delivery systems. For example, a nanomedicine-based drug delivery system has been recently designed to distribute ARV more effectively [4–6].

#### 1.2. Advantages of early ART administration

Today, ART is recommended for all individuals with HIV-1 regardless of CD4 counts, and has to be initiated as soon as possible following HIV-1 infection (Fig. 1). Early initiation of ART has been associated with beneficial effects on disease outcome, which are independent of the clinical features of enrolled patients (e.g. age, sex, race, CD4 counts and viral load) [7,8]. Interestingly, evidence shows that the prompt initiation of ART can lead to durable viral control after cessation of prolonged treatment (French cohort VISCONTI, Mississippi Child) [9–11]. These patients are called post-treatment controllers (PTC). A recently proposed mathematical model to characterize PTC takes into account natural protection of HIV-1 controllers and highlight the critical need of strong antiviral immunity to avoid viral rebound after treatment cessation [12]. These lines of evidence illustrate the beneficial impact of early ART on protective immunity, tissue inflammation and immuno-metabolism. This includes (i) increased number and function of memory CD4 T-cells, mucosal Th<sub>17</sub> cells, CD8 T-cells and memory B-cells, (ii) preservation of HIV-1-specific humoral responses, and (iii) reduced tryptophan catabolism [13–21] (Table 1). Lastly, initiation of ART within 6 months of HIV-1 infection is also associated with lower hyper immune activation (IA) [22].

\* Corresponding author.

E-mail address: [julien.vangrevenynghe@iaf.inrs.ca](mailto:julien.vangrevenynghe@iaf.inrs.ca) (J. Van Grevenynghe).

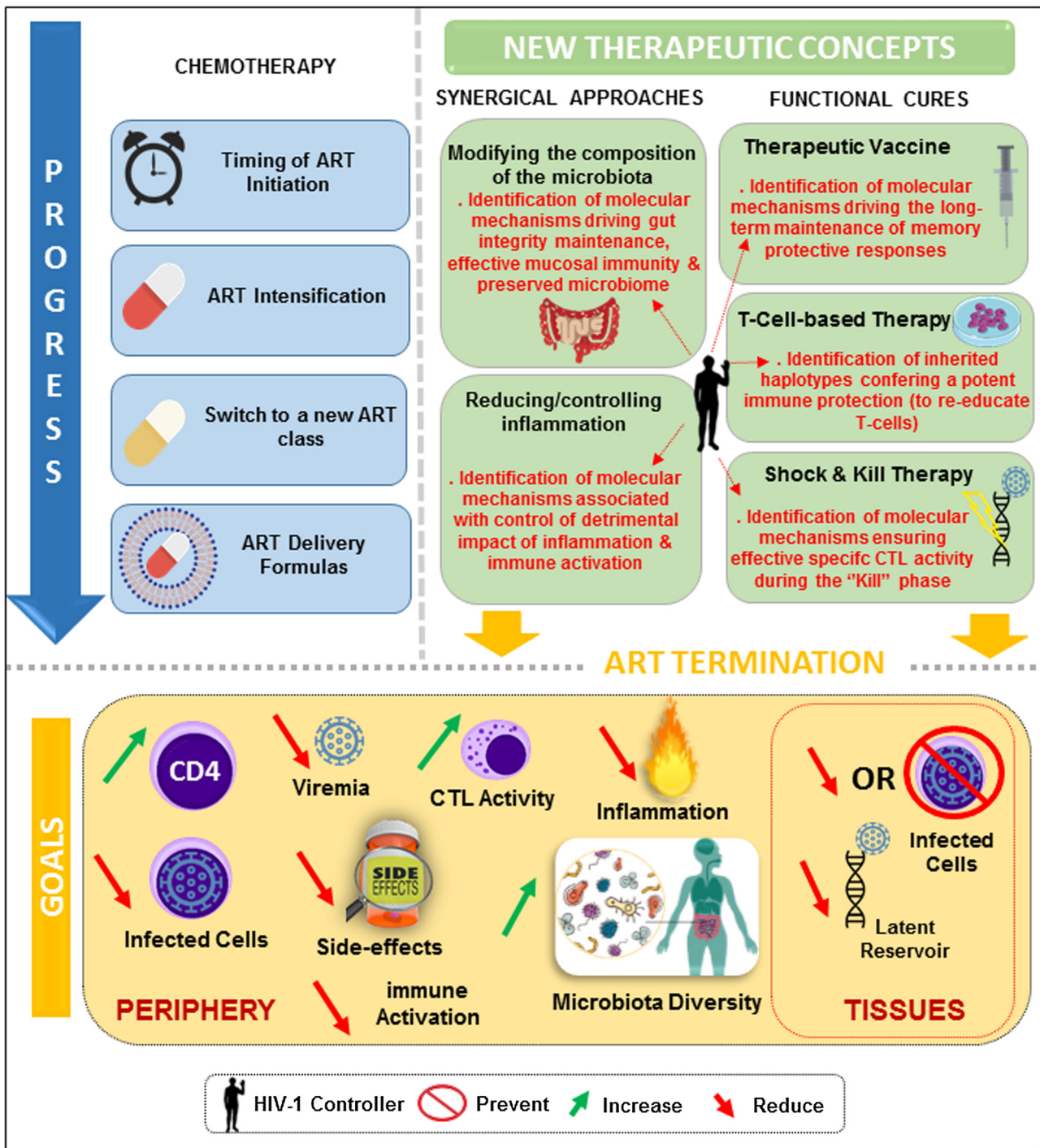


Fig. 1. Schematic representation of the current HIV-1 treatment progress and new therapeutic concepts to achieve ART termination. The schematic also includes the potential contribution of the observations collected from HIV-1 controllers (indicated in red), which may be critical for the development of the therapeutic concepts. Abbreviations: ART, antiretroviral therapy; CTL, cytotoxic T lymphocytes.

1.3. Modern ART is far from ideal

Despite the success of ART in fully suppressing viral replication, HIV-1 remains an incurable viral infection due to inherent limitations in the therapy:

(i) ART fails to eradicate the pool of latently HIV-1-infected long-lived cells, called the viral reservoir [23]. Of note, early initiation of ART partially reduces the size and decay kinetics of HIV-1 reservoir, but fails to achieve complete viral clearance [22,24].

- (ii) Except for rare PTC, the majority of patients must maintain a life-long treatment to prevent viremia rebound. Indeed, recent study show that the prompt initiation of treatment does not guarantee a post treatment control of HIV-1 after treatment cessation [25].
- (iii) Life-long administration of ARV results in toxic effects and metabolic disorders that some patients cannot tolerate, such as lipodystrophy, insulin resistance and dyslipidemia [26,27].
- (iv) Finally, patients under ART display chronic inflammation and tissue architecture disruption that negatively impact metabolism, survival and function of immune cells [28] (Fig. 2). For instance,

**Table 1**

**Profiles of molecular/immune markers in patients under ART and HIV-1 controllers, when compared to the uninfected controls (baseline).** Of course, HIV-specific responses in controllers are compared to those from patients under ART (yellow). This table also depicts the reversible phenotypes when ART is administrated early or when the deregulated pathway is specifically targeted in "normal" patients (orange arrows). (For interpretation of the references to colour in this table legend, the reader is referred to the web version of this article.)

	Marker(s)	Compared to Baseline		Phenotype(s)	Ref(s)	
		ART	HIV Controllers			
IMMUNITY	<b>CD8</b>					
		TIGIT <sup>+</sup>	↗	≡	CD8 T-cells exhaustion	[71]
	HIV-specific	Perforin, Granzyme B, T-bet	↘	↗	CTL Activity	[49, 50]
		Cleaved Caspase-3 Bcl-2 <sup>high</sup>	↗	↘	Effector CD8 Survival	[51]
		IL-2, IFN-γ, CD107a, Perforin	↘	↗	CD8 Polyfunctionality	[68]
	<b>CD4</b>					
		Pro-apoptotic Foxp3a Pathway Protection (Fas, Bim)	↘	↗	Central Memory CD4 T-Cells Survival	[72, 73]
		IL-2, IFN-γ, CD127	↘	↗	Effector Memory CD4 T-cells Polyfunctionality	[73]
		TRAV24, TRBV2 motifs	↘	↗	T-cell Activation & Polyfunctionality upon TCR repertoire with High Affinity to Immunoprevalent Viral Epitopes	[75]
	<b>pTfh</b>					
	CCR5 <sup>+</sup> CCR3 <sup>+</sup> CD4 <sup>+</sup> IL21, Env-Specific IgG	↘	↗	B cells Help Antibodies Generation	[79, 80]	
<b>B cells</b>						
	Foxp3a pro-apoptotic pathway (TRAIL, Bim)	↗	≡	Memory B cells Survival	[84]	
	STAT5 induced IL-2 pathway	↘	↗			
	IgG against common Vaccinal Ags (Tetanus, Measles, Pneumococcus)	↘	≡	Vaccinal Humoral Response	[82, 83]	
	HIV-1 Specific IgG (Subclasses 1 & 3)	↘	↗	HIV-1 Specific Humoral Response Polyfunctional Ab Effector Activity	[83, 85, 86]	
<b>Innate System</b>						
	BDC A2 <sup>+</sup> CD123 <sup>+</sup> IFN-α induced TLR-9 pathway	↘	≡	pDC Count & Functionality	[90]	
	CD56 <sup>+</sup> CD16 <sup>+</sup> (NK) HLA-DR, CD38	↗	≡	Natural Killer Cells Activation	[87]	
INFLAMMATION	<b>Impact on Gut Microenvironment &amp; Immuno-Metabolism</b>					
		IL4, IL-10 (GALT INKT)	↘	↗	Immune Activation	[101]
		<i>Bacteroides</i>	↘	≡	Microbiota Diversity & Enrichment	[34, 35, 93, 101]
		sCD14	↗	↘	Microbial Translocation	[13, 99]
		CD3 <sup>+</sup> CD4 <sup>+</sup> (GALT) IL-17a	↘	≡	Mucosal CD4 T-cells Maintenance	[99, 100]
		Tryptophan Catabolism (Kynurenine)	↗	≡	Treg/Th17 balance	[17, 93, 96, 97]
		Atg-5, BECLIN-1 & AMBRA1	N/A	↗	Increased Autophagic Activity associated with Viral Containment	[102]

↘ Down-regulation ↗ Up-regulation ≡ Similar N/A Not Available



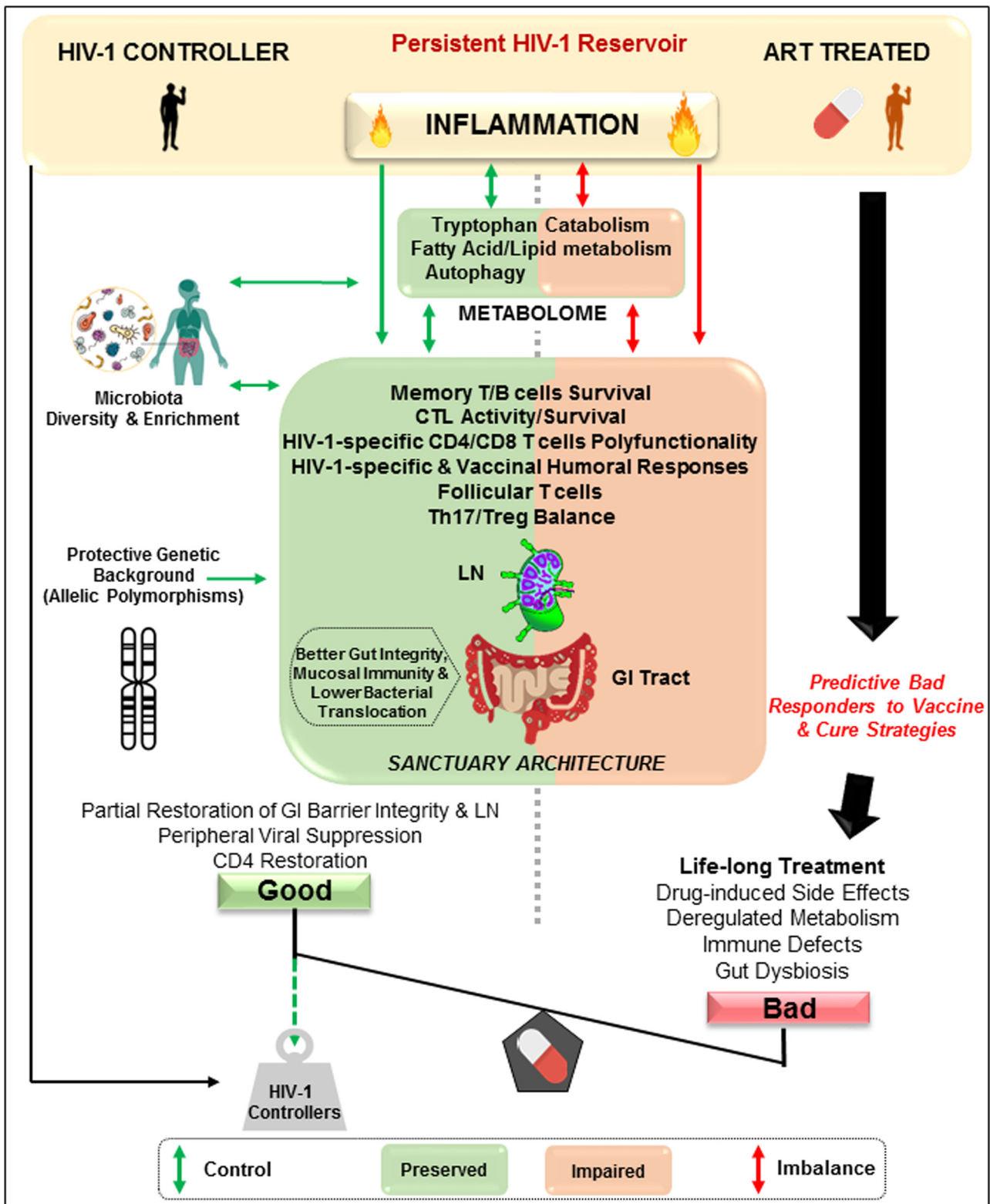


Fig. 2. Interplay between immuno-metabolism and residual inflammation caused by persistent reservoir in HIV-1 controllers and patients under ART. HIV-1 controllers represent a typical model for vaccine development and new therapeutic strategies, since they are characterized by a "better" genetic and immuno-metabolic features to balance the systemic inflammation and immune activation. Abbreviation: GI, gastrointestinal tract; LN, lymph node.

ART is unable to fully restore lymph node and gastro-intestinal (GI) tract reconstitution, as well as reduce adipose tissue inflammation [13,28–32]. Therapy also leads to gut dysbiosis, which is illustrated by the alteration of the microbial composition (or microbiota), therefore contributing to inflammation by the release

of several specific pro-inflammatory bacterial products [33–35].

In summary, modern ART even when administrated early still fails to achieve sterile cure, and to reduce immune defects and metabolic disturbances that are associated with residual inflammation and viral



persistence. In fact, it is widely accepted that HIV-1 infection, despite effective ART, causes sustained IA that leads to premature immune senescence (phenomena described as "premature aging") [36]. Resultantly, ART termination is not a viable option, since it will lead to viral rebound in the majority of patients, who display a weakened immune system. It is critical to find new therapeutic strategies to be able to boost antiviral immune protection to ensure post treatment control.

#### 1.4. HIV-1 controllers and how they can help to achieve ART termination?

There have been a number of efforts to develop therapeutic strategies directed at achieving ART termination (Fig. 1). In fact, there are two possible ways to achieve it. On one hand, by purging the persistent viral reservoir ("sterilizing" or "eradication" cure), which has been achieved only once with the "Berlin Patient" [39–41]. However, this strategy cannot guarantee viral eradication and is associated with high morbidity and mortality due to allogeneic transplantation in the infected receivers [39,42]. As a consequence, most strategies to achieve a cure of HIV-1 are based on the ability to "co-exist" with the virus and be able to permanently control HIV-1 infection without ART. Of course, these therapeutic approaches (or "functional" cures) aiming to achieve long-term HIV-1 control in the absence of medication depend on their ability to maintain effective HIV-specific immunity and to counteract the detrimental impact of residual inflammation that is associated with viral persistence. Functional cures are more likely to be feasible by using HIV-1 controllers as a strategic model for engineering robust genetically or immunologically based therapeutic approaches [43]. This cohort of patients constitutes a small number of people who contract HIV-1 can live with the virus without needing treatment for many years. These individuals are known as HIV-1 controllers (elite controllers; EC) or long-term non progressors (LTNP) depending on whether the viral load or CD4 is being examined. In fact, HIV-1 controllers represent a small fraction of LTNP (less than 1% of infected population) and are specifically characterized by long-term undetectable viral loads in addition of preserved CD4 counts [43,44].

For instance, HIV-1 controllers, who naturally control HIV-1 infection without the need for ART, are able to maintain effective host-mediated antiviral immunity for decades, thus providing crucial information to develop the new generations of therapeutic vaccines (Fig. 1). Indeed, the challenge for developing a therapeutic vaccine lies in the ability to generate effective and sustained anti-HIV-1 immunity in infected patients [44]. The identification of molecular mechanisms that drive the long-term immune control of HIV-1 infection and memory cell persistence in naturally-protected controllers may be crucial to ensure the design of successful vaccines in other patients. It is worth noting that the natural viral control stems from the unique genetic and immuno-metabolic background of controllers (Fig. 2). Delineating the inherited and molecular parameters characterizing HIV-1 controllers may also be useful for other therapeutic approaches that include the "Shock and Kill" and the chimeric antigen receptor (CAR) expressing T-cell therapies [40,42,45]. The "Shock and Kill" therapy, which targets the latent HIV-1 reservoir, aims to "shock" latently infected cells in patients by inducing HIV-1 viral expression through latency reversing agents [46]. Upon reactivation, the "kill" method refers to the termination of virus-infected cells by employing strategies involving HIV-specific CD8 T-cells. As such, HIV-1 controllers, who display reduced HIV-1 reservoir size [47,48] and effective specific cytotoxic T-lymphocytes (CTL) [49–51], are strategic candidates to provide crucial information to advance the technique. The T-cell therapy consists in re-directing CD8 activity to HIV-1 in patients by the introduction of CAR expressing effector CTL targeting HIV-1 epitopes on HLA type I or cell-surface HIV-1 envelop [45]. Once again, HIV-1 controllers who display protective haplotypes and CTL responses of high functional avidity and broad variant cross-reactivity are surely useful to improve the method [52–54]. Finally, understanding the association of natural

control of HIV-1 with conserved metabolism and microbiota may lead to novel synergic therapies to decrease inflammation and IA, and impact HIV-1 reservoir and vaccine responses [55–57].

In summary, understanding mechanisms associated with natural control of HIV-1 infection is the first step towards improving the current treatment. HIV-1 controllers can be considered as a probe into the strategies to reproduce their long-term antiviral protective mechanisms.

## 2. What is to learn from HIV-1 controllers?

### 2.1. Controllers do not fully handle long-term inflammation

There is no doubt that natural HIV-1 controllers are able to preserve effective immunity and tissue structures for decades, even with residual inflammation (Fig. 2). Although they display an appearance of long-term immune control, this is not guaranteed for life. These individuals will eventually display disease progression and control failure, which have been recently associated with pro-inflammatory markers [58,59]. In addition, HIV-1 controllers have high incidences of inflammation-related diseases that are illustrated by a significant degree of coronary atherosclerosis and monocyte activation, as well as increased hospitalization rate for cardiovascular and psychiatric diseases when compared to patients receiving ART [60–63]. It is for this reason that HIV-1 controllers are also included in the current panel's recommendations for initiating ART in treatment-naïve patients. Therefore, it has been a difficult task to recruit untreated HIV-1 controllers in the last decade.

### 2.2. Controllers preserve effective immunity and tissue integrity despite inflammation

#### 2.2.1. High quality of HIV-1-specific CD8 T-cell functions

A handful of studies examining HIV-1 controllers, have demonstrated the key role for CD8 T-cell immunity in the natural control of HIV-1 infection. In fact, some studies using this specific group of subjects provided some of the first clues of the cellular and molecular mechanisms of natural HIV-1 control. The majority of studies seeking to define the mechanism(s) of HIV-1 control have largely relied on the comparison of memory CD8 T-cell responses, especially virus-specific ones, from HIV-1 controllers to those of other patients. For example, some HIV-1 controllers are enriched for certain protective HLA type I alleles, such as B<sub>27</sub>/<sub>57</sub>, and particular killer-cell immunoglobulin-like receptors (KIR) [37 54,64,65]. Other studies show that controllers contain a greater fraction of HIV-1-specific CD8 T-cell that (i) expressed higher perforin and granzyme B levels, (ii) produce multiple functional cytokines and chemokines such as IFN- $\gamma$ , IL-2, IL-21, TNF- $\alpha$ , and MIP-1 $\alpha$ / $\beta$ , and (iii) display markedly better proliferative potential upon HIV-1 peptide stimulation, when compared to other groups of infected people including patients under ART [49,50,66–70] (Table 1). HIV-1-specific CD8 T-cells in ECs are more primed to survival when compared to ART treated subjects by down-regulating cleaved caspase-3 [51]. CD8 T-cell responses in HIV-1 controllers react to lower HIV-1 antigen concentrations and recognize more epitope variants than responses in non-controller patients [52]. Finally, recent data show increased exhausted phenotype in CD8 T-cells from patients under ART, regardless of timing of ART initiation, which is not observed in controllers [71].

Collectively, these findings confirm sustained HIV-1 specific CD8 T-cell responses of higher quality and functional avidity in HIV-1 controllers compared to other groups of infected people, even those under ART.

#### 2.2.2. Preservation of memory and pTfh CD4 T-cells

The persistence of memory CD4 T-cells, especially the long-lasting central memory CD4 T-cells (T<sub>CM</sub>), is a major correlate of immunological protection in HIV-1 infection, as the rate of T<sub>CM</sub> decline predicts HIV-1 disease progression [38]. In contrast to patient under ART, HIV-1 controllers show a preserved T<sub>CM</sub> compartment that

maintain the capacity to produce antiviral cytokines such as IL-2 and IFN- $\gamma$  upon HIV-1 peptide stimulation, as well as signs of potent functional activation in effector memory CD4 T-cells ( $T_{EM}$ ) [73] (Table 1). The persistence of memory CD4 T-cells in HIV-1 controllers has been attributed to higher protection against the pro-apoptotic activity of the transcription factor Foxo3a [72,74]. In addition, recent study show that HIV-1 controllers display higher avidity Gag<sub>293</sub>-specific CD4 responses when compared to patients under ART [75]. Finally, a large body of literature reports that HIV-1 controllers, especially those called "neutralizers" because of their ability to generate HIV-1-specific broadly neutralizing antibodies, display preserved peripheral T-follicular helper CD4 T-cells (pTfh) [76–78]. pTfh, which are able to secrete IL-21 and support B-cell responses, are functionally defective in patients under ART, when compared to both HIV-1 controllers and HIV-1-uninfected controls [79,80]. Finally, using a whole-genome transcriptional profiling approach, Vigneault et al. have identify a specific subgroup of controllers, whose immunological and gene expression characteristics approximate those of uninfected controls [81].

### 2.2.3. Maintenance of vaccine- and HIV-1-specific B-cell responses

Although the acute initiation of ART helps in preserving the integrity of memory B-cells and longevity of specific humoral responses, it does not guarantee full normalization of B-cell immunity. This includes the protective antibody memory against common vaccination antigens [19,20,82]. In contrast, HIV-1 controllers have memory B-cell frequencies and levels of antigen-specific antibodies comparable with uninfected controls [82,83]. Similarly to memory CD4 T-cells, memory B-cell survival in HIV-1 controllers depends on effective protection against pro-apoptotic activity of Foxo3a [84] (Table 1). In addition, HIV-1 controllers display higher HIV-specific B-cell responses, which are also able to harness the potent antiviral activities of innate cells including natural killer (NK) cells and phagocytic cells, when compared to patients under ART [83,85,86].

### 2.2.4. Low levels of NK activation and preserved pDC

Specific features among innate cells also differ in HIV-1 controllers compared to other patients, even those under ART. For example, the activation of NK cells, which is associated with HIV-1 disease progression, is increased in patients under ART when compared to both HIV-1 controllers and uninfected controls [87] (Table 1). Of note, the inheritance of specific protective KIR haplotypes such as KIR<sub>3DL1</sub> among controllers is associated with heightened anti-HIV NK function [88,89]. In addition, when compared to HIV-1 uninfected controls, evidence shows the preservation of plasmacytoid dendritic cells (pDC) counts with similar IFN- $\alpha$  production only in the controller group [90].

### 2.2.5. Preservation of microbiota and metabolism

As previously reviewed, HIV-1 infection is associated with persistent immune inflammation that negatively impact microbiota diversity, gut integrity and cellular metabolism [31,91,92].

Despite prolonged tissue inflammation, HIV-1 controllers display similar richness, bacterial metabolism, and diversity of gut microbiota to uninfected controls [93] (Fig. 2). In contrast, other studies revealed an altered metabolism and diversity of gut microbiota in patients under ART [34,35,94]. Data also indicate that microbiota richness and gut environment during HIV-1 infection is inversely associated with the kynurenine pathway of the tryptophan catabolism [93,95]. Jenabian and colleagues have shown that HIV-1 controllers display a distinct tryptophan catabolism, which is mainly characterized by kynurenine levels similar to those in uninfected controls. In contrast, data confirm higher kynurenine levels in patients under ART, even when treatment is administrated early [15,17,96,97]. Interestingly, recent data suggest that the low kynurenine levels may also participate in maintaining the memory CD4 T-cell pool in HIV-1 controllers [15].

In addition of gut dysbiosis, progressive HIV-1 infection is also characterized by microbial translocation from the gastro-intestinal (GI)

tract to portal and systemic circulation, which is not fully suppressed by ART and is a major driver of the chronic IA [13,98]. One the other hand, HIV-1 controllers display moderate differences, if any, when compared to uninfected controls with respect to microbial translocation [13,99]. It was shown that the preservation of gut mucosal immunity is critical to ensure lower bacterial translocation and IA in HIV-1 controllers. For example, the maintenance of mucosal T-cells including CD4 subsets and effective virus-specific responses in the gut associated lymphoid tissue (GALT) correlate with clinical outcome of controllers [99,100]. In GALT, HIV-1 controllers also show a higher frequency of invariant NK T-cells, which are associated with less IA and lower markers of microbial translocation compared to both uninfected controls and patients under ART [101].

Finally, although there are no transactional comparison with patients under ART, it was recently reported that autophagy, which is a critical and conserved catabolic process that degrades cytoplasmic constituents and organelles in the lysosomes, is up-regulated in peripheral blood mononuclear cells in HIV-1 controllers when compared to both normal patients and uninfected controls [102,103]. The data suggest that this distinct catabolic feature in controllers may participate in viral containment along with immune advantages.

Altogether, the data show a better preservation of gut integrity and local anti-HIV-1 immunity in controllers, which is associated with less metabolic disturbance.

## 3. Concluding remarks

HIV-1 controllers, who display effective anti-HIV-1 immunity despite sustained inflammation (Fig. 2), could be exploited to identify molecular mechanisms involved in host protection that may function as potential therapeutic targets. Currently, there is a general consensus that sterile cure is not a viable option. Hence, learning to "co-exist" with the virus, but with less clinical costs, is more likely to be the preferred alternative for improving the current treatment against HIV-1 infection. As our knowledge of HIV-1 controllers is still improving, the scientific community realizes that they are an example of co-existence with the virus. Therefore, there is no doubt that information gained from studying protective immunity in the controllers will be helpful to facilitate the translation of those therapeutic concepts into successful treatment in HIV-1 infection to finally achieve ART termination.

## Conflict of interest

The authors declare no conflict of financial and personal interests.

## References

- [1] F. Barre-Sinoussi, A.L. Ross, J.F. Delfraissy, Past, present and future: 30 years of HIV research, *Nat. Rev. Microbiol.* 11 (12) (2013) 877–883.
- [2] E.S. Daar, Novel approaches to HIV therapy, *F1000Research* 6 (2017) 759.
- [3] B. Edagwa, J. McMillan, B. Sillman, H.E. Gendelman, Long-acting slow effective release antiretroviral therapy, *Expert Opin. Drug Deliv.* 14 (11) (2017) 1281–1291.
- [4] M.K. Das, A. Sarma, T. Chakraborty, Nano-ART and NeuroAIDS, *Drug Deliv. Transl. Res.* 6 (5) (2016) 452–472.
- [5] L. Fiandra, A. Capetti, L. Sorrentino, F. Corsi, Nanoformulated antiretrovirals for penetration of the Central nervous system: State of the art, *J. Neuroimmune Pharmacol.* 12 (1) (2017) 17–30.
- [6] A.R. Kirtane, O. Abouzid, D. Minahan, T. Bensen, A.L. Hill, C. Selinger, A. Bershteyn, M. Craig, S.S. Mo, H. Mazdiyasi, C. Cleveland, J. Rogner, Y.L. Lee, L. Booth, F. Javid, S.J. Wu, T. Grant, A.M. Bellinger, B. Nikolic, A. Hayward, L. Wood, P.A. Eckhoff, M.A. Nowak, R. Langer, G. Traverso, Development of an oral once-weekly drug delivery system for HIV antiretroviral therapy, *Nat. Commun.* 9 (1) (2018) 2.
- [7] S.J. Krebs, J. Ananworanich, Immune activation during acute HIV infection and the impact of early antiretroviral therapy, *Curr. Opin. HIV AIDS* 11 (2) (2016) 163–172.
- [8] J.D. Lundgren, A.H. Borges, J.D. Neaton, Serious non-AIDS conditions in HIV: benefit of early ART, *Curr. HIV/AIDS Rep.* 15 (2) (2018) 162–171.
- [9] A. Saez-Cirion, C. Bacchus, L. Hocqueloux, V. Avettand-Fenoel, I. Girault, C. Lecroux, V. Potard, P. Versmisse, A. Melard, T. Prazuck, B. Descours,

- J. Guernon, J.P. Viard, F. Boufassa, O. Lambotte, C. Goujard, L. Meyer, D. Costagliola, A. Venet, G. Pancino, B. Autran, C. Rouzioux, the ANRS VISCONTI Study Group, Post-treatment HIV-1 controllers with a long-term virological remission after the interruption of early initiated antiretroviral therapy ANRS VISCONTI study, *PLoS Pathog.* 9 (3) (2013) e1003211.
- [10] S.T. Investigators, S. Fidler, K. Porter, F. Ewings, J. Frater, G. Ramjee, D. Cooper, H. Rees, M. Fisher, M. Schechter, P. Kaleebu, G. Tambussi, S. Kinloch, J.M. Miro, A. Kelleher, M. McClure, S. Kaye, M. Gabriel, R. Phillips, J. Weber, A. Babiker, Short-course antiretroviral therapy in primary HIV infection, *N. Engl. J. Med.* 368 (3) (2013) 207–217.
- [11] K. Rainwater-Lovett, K. Luzuriaga, D. Persaud, Very early combination antiretroviral therapy in infants: prospects for cure, *Curr. Opin. HIV AIDS* 10 (1) (2015) 4–11.
- [12] J.M. Conway, A.S. Perelson, Post-treatment control of HIV infection, *Proc. Natl. Acad. Sci. U. S. A.* 112 (17) (2015) 5467–5472.
- [13] J.M. Brenchley, D.A. Price, T.W. Schacker, T.E. Asher, G. Silvestri, S. Rao, Z. Kazzaz, E. Bornstein, O. Lambotte, B. Altmann, B.R. Blazar, B. Rodriguez, L. Teixeira-Johnson, A. Landay, J.N. Martin, F.M. Hecht, L.J. Picker, M.M. Lederman, S.G. Deeks, D.C. Douek, Microbial translocation is a cause of systemic immune activation in chronic HIV infection, *Nat. Med.* 12 (12) (2006) 1365–1371.
- [14] W. Cao, V. Mehraj, B. Trottier, J.G. Baril, R. Leblanc, B. Lebouche, J. Cox, C. Tremblay, W. Lu, J. Singer, T. Li, J.P. Routy, Montreal Primary HIV Infection Study Group, S. Vezina, L. Charest, M. Milne, E. Huchet, S. Lavoie, J. Friedman, M. Duchastel, F. Villielm, P. Cote, M. Potter, B. Lessard, M.A. Charron, S. Dufresne, M.E. Turgeon, D. Rouleau, L. Labrecque, C. Fortin, A. de Pokomandy, V. Hal-Gagne, M. Munoz, B. Deligne, V. Martel-Laferriere, N. Gilmore, M. Fletcher, J. Szabo, Early initiation rather than prolonged duration of antiretroviral therapy in HIV infection contributes to the normalization of CD8 T-cell counts, *Clin. Infect. Dis.* 62 (2) (2016) 250–257.
- [15] X. Dagenais-Lussier, M. Aounallah, V. Mehraj, M. El-Far, C. Tremblay, R.P. Sekaly, J.P. Routy, J. van Grevenynghe, Kynurenine reduces memory CD4 T-cell survival by interfering with interleukin-2 signaling early during HIV-1 infection, *J. Virol.* 90 (17) (2016) 7967–7979.
- [16] M. Gelpi, H.J. Hartling, P.M. Ueland, H. Ullum, M. Troseid, S.D. Nielsen, Tryptophan catabolism and immune activation in primary and chronic HIV infection, *BMC Infect. Dis.* 17 (1) (2017) 349.
- [17] M.A. Jenabian, M. Patel, I. Kema, C. Kanagaratham, D. Radzioch, P. Thebault, R. Lapointe, C. Tremblay, N. Gilmore, P. Ancuta, J.P. Routy, Distinct tryptophan catabolism and Th17/Treg balance in HIV progressors and elite controllers, *PLoS One* 8 (10) (2013) e78146.
- [18] G.R. Kaufmann, J.J. Zaunders, P. Cunningham, A.D. Kelleher, P. Grey, D. Smith, A. Carr, D.A. Cooper, Rapid restoration of CD4 T cell subsets in subjects receiving antiretroviral therapy during primary HIV-1 infection, *Aids* 14 (17) (2000) 2643–2651.
- [19] S. Pensiero, A. Cagigi, P. Palma, A. Nilsson, C. Capponi, E. Freda, S. Bernardi, R. Thorstenson, F. Chiodi, P. Rossi, Timing of HAART defines the integrity of memory B cells and the longevity of humoral responses in HIV-1 vertically-infected children, *Proc. Natl. Acad. Sci. U. S. A.* 106 (19) (2009) 7939–7944.
- [20] M. Pogliaghi, M. Ripa, S. Pensiero, M. Tolazzi, S. Chiappetta, S. Nozza, A. Lazzarin, G. Tambussi, G. Scarlatti, Beneficial effects of cART initiated during primary and chronic HIV-1 infection on immunoglobulin-expression of memory B-cell subsets, *PLoS One* 10 (10) (2015) e0140435.
- [21] A. Schuetz, C. Deleage, I. Sereti, R. Rerkinmimit, N. Phanuphak, Y. Phuang-Ngern, J.D. Estes, N.G. Sandler, S. Sukhumvittaya, M. Marovich, Initiation of ART during early acute HIV infection preserves mucosal Th17 function and reverses HIV-related immune activation, *PLoS Pathog.* 10 (12) (2014) e1004543.
- [22] V. Jain, W. Hartogensis, P. Bacchetti, P.W. Hunt, H. Hatano, E. Sinclair, L. Epling, T.H. Lee, M.P. Busch, J.M. McCune, C.D. Pilcher, F.M. Hecht, S.G. Deeks, Antiretroviral therapy initiated within 6 months of HIV infection is associated with lower T-cell activation and smaller HIV reservoir size, *J. Infect. Dis.* 208 (8) (2013) 1202–1211.
- [23] M.L. Mzingwane, C.T. Tiemessen, Mechanisms of HIV persistence in HIV reservoirs, *Rev. Med. Virol.* 27 (2) (2017).
- [24] M.J. Buzon, E. Martin-Gayo, F. Pereyra, Z. Ouyang, H. Sun, J.Z. Li, M. Piovoso, A. Shaw, J. Dalmau, N. Zangger, J. Martinez-Picado, R. Zurakowski, X.G. Yu, A. Telenti, B.D. Walker, E.S. Rosenberg, M. Lichterfeld, Long-term antiretroviral treatment initiated at primary HIV-1 infection affects the size, composition, and decay kinetics of the reservoir of HIV-1-infected CD4 T cells, *J. Virol.* 88 (17) (2014) 10056–10065.
- [25] J. Maenza, K. Tapia, S. Holte, J.D. Stekler, C.E. Stevens, J.I. Mullins, A.C. Collier, How often does treatment of primary HIV lead to post-treatment control? *Antivir. Ther.* 20 (8) (2015) 855–863.
- [26] S.J. Souza, L.A. Luzia, S.S. Santos, P.H. Rondo, Lipid profile of HIV-infected patients in relation to antiretroviral therapy: a review, *Rev. Assoc. Med. Bras.* (1992) 59 (2) (2013) 186–198.
- [27] K. Yoshimura, Current status of HIV/AIDS in the ART era, *J. Infect. Chemother.* 23 (1) (2017) 12–16.
- [28] J. van Grevenynghe, R. Halwani, N. Chomont, P. Ancuta, Y. Peretz, A. Tanel, F.A. Procopio, Y. Shi, E.A. Said, E.K. Haddad, R.P. Sekaly, Lymph node architecture collapse and consequent modulation of FOXO3a pathway on memory T- and B-cells during HIV infection, *Semin. Immunol.* 20 (3) (2008) 196–203.
- [29] J.C. Mudd, P. Murphy, M. Manion, R. Debernardo, J. Hardacre, J. Ammori, G.A. Hardy, C.V. Harding, G.H. Mahabaleswar, M.K. Jain, J.M. Jacobson, A.D. Brooks, S. Lewis, T.W. Schacker, J. Anderson, E.K. Haddad, R.A. Cubas, B. Rodriguez, S.F. Sieg, M.M. Lederman, Impaired T-cell responses to sphingosine-1-phosphate in HIV-1 infected lymph nodes, *Blood* 121 (15) (2013) 2914–2922.
- [30] J.C. Mudd, J.M. Brenchley, Gut mucosal barrier dysfunction, microbial dysbiosis, and their role in HIV-1 disease progression, *J. Infect. Dis.* 214 (Suppl. 2) (2016) S58–S66.
- [31] X. Dagenais-Lussier, A. Mouna, J.P. Routy, C. Tremblay, R.P. Sekaly, M. El-Far, J. Grevenynghe, Current topics in HIV-1 pathogenesis: the emergence of deregulated immuno-metabolism in HIV-infected subjects, *Cytokine Growth Factor Rev.* 26 (6) (2015) 603–613.
- [32] M.L. Morieri, V. Guardigni, J.M. Sanz, E. Dalla Nora, C. Soavi, G. Zuliani, L. Sighinolfi, A. Passaro, Adipokines levels in HIV infected patients: lipocalin-2 and fatty acid binding protein-4 as possible markers of HIV and antiretroviral therapy-related adipose tissue inflammation, *BMC Infect. Dis.* 18 (1) (2018) 10.
- [33] M. El-Far, C.L. Tremblay, Gut microbial diversity in HIV infection post combined antiretroviral therapy: a key target for prevention of cardiovascular disease, *Curr. Opin. HIV AIDS* 13 (1) (2018) 38–44.
- [34] P. Nowak, M. Troseid, E. Avershina, B. Barqasho, U. Neogi, K. Holm, J.R. Hov, K. Noyan, J. Vesterbacka, J. Svard, K. Rudi, A. Sonnerborg, Gut microbiota diversity predicts immune status in HIV-1 infection, *AIDS* 29 (18) (2015) 2409–2418.
- [35] J.F. Vazquez-Castellanos, S. Serrano-Villar, A. Latorre, A. Artacho, M.L. Ferrus, N. Madrid, A. Vallejo, T. Sainz, J. Martinez-Botas, S. Ferrando-Martinez, M. Vera, F. Dronda, M. Leal, J. Del Romero, S. Moreno, V. Estrada, M.J. Gosalbes, A. Moya, Altered metabolism of gut microbiota contributes to chronic immune activation in HIV-infected individuals, *Mucosal Immunol.* 8 (4) (2015) 760–772.
- [36] L.R. de Armas, S. Pallikuth, V. George, S. Rinaldi, R. Pahwa, K.L. Arheart, S. Pahwa, Reevaluation of immune activation in the era of cART and an aging HIV-infected population, *JCI Insight* 2 (20) (2017).
- [37] M. Bendenou, A. Samri, V. Avettand-Fenoel, S. Cardinaud, B. Descours, G. Carcelain, M.C. Mazon, J.F. Bergmann, A. Urrutia, A. Moris, C. Rouzioux, F. Simon, P. Andre, M. Pocard, X. Dray, T. Mourez, V. Vieillard, B. Autran, F. Barin, P. Sellier, What is the most important for elite control: genetic background of patient, genetic background of partner, both or neither? Description of complete natural history within a couple of MSM, *EBioMedicine* 27 (2018) 51–60.
- [38] S.G. Fonseca, F.A. Procopio, J.P. Goulet, B. Yassine-Diab, P. Ancuta, R.P. Sekaly, Unique features of memory T cells in HIV elite controllers: a systems biology perspective, *Curr. Opin. HIV AIDS* 6 (3) (2011) 188–196.
- [39] D.R. Kuritzkes, Hematopoietic stem cell transplantation for HIV cure, *J. Clin. Invest.* 126 (2) (2016) 432–437.
- [40] C. Liu, X. Ma, B. Liu, C. Chen, H. Zhang, HIV-1 functional cure: will the dream come true? *BMC Med.* 13 (2015) 284.
- [41] C.P. Passaes, A. Saez-Cirion, HIV cure research: advances and prospects, *Virology* 454–455 (2014) 340–352.
- [42] A.R. Cillo, J.W. Mellors, Which therapeutic strategy will achieve a cure for HIV-1? *Curr. Opin. Virol.* 18 (2016) 14–19.
- [43] L.R. Cockerham, H. Hatano, Elite control of HIV: is this the right model for a functional cure? *Trends Microbiol.* 23 (2) (2015) 71–75.
- [44] G.M. Graziani, J.B. Angel, Evaluating the efficacy of therapeutic HIV vaccines through analytical treatment interruptions, *J. Int. AIDS Soc.* 18 (2015) 20497.
- [45] S. Lam, C. Bollard, T-cell therapies for HIV, *Immunotherapy* 5 (4) (2013) 407–414.
- [46] G. Darcs, B. Van Driessche, C. Van Lint, HIV latency: should we shock or lock? *Trends Immunol.* 38 (3) (2017) 217–228.
- [47] M. Garcia, M. Gorgolas, A. Cabello, V. Estrada, J.M. Ligos, M. Fernandez-Guerrero, C. Barros, J.C. Lopez-Bernaldo, F.J. De La Hera, M. Montoya, J.M. Benito, N. Rallon, Peripheral T follicular helper cells make a difference in HIV reservoir size between elite controllers and patients on successful cART, *Sci. Rep.* 7 (1) (2017) 16799.
- [48] H. Hatano, M. Somsouk, E. Sinclair, K. Harvill, L. Gilman, M. Cohen, R. Hoh, P.W. Hunt, J.N. Martin, J.K. Wong, S.G. Deeks, S.A. Yukl, Comparison of HIV DNA and RNA in gut-associated lymphoid tissue of HIV-infected controllers and non-controllers, *AIDS* 27 (14) (2013) 2255–2260.
- [49] A.R. Hersperger, J.N. Martin, L.Y. Shin, P.M. Sheth, C.M. Kovacs, G.L. Cosma, G. Makedonas, F. Pereyra, B.D. Walker, R. Kaul, S.G. Deeks, M.R. Betts, Increased HIV-specific CD8+ T-cell cytotoxic potential in HIV elite controllers is associated with T-bet expression, *Blood* 117 (14) (2011) 3799–3808.
- [50] A.R. Hersperger, F. Pereyra, M. Nason, K. Demers, P. Sheth, L.Y. Shin, C.M. Kovacs, B. Rodriguez, S.F. Sieg, L. Teixeira-Johnson, D. Gudonis, P.A. Goepfert, M.M. Lederman, I. Frank, G. Makedonas, R. Kaul, B.D. Walker, M.R. Betts, Perforin expression directly ex vivo by HIV-specific CD8 T-cells is a correlate of HIV elite control, *PLoS Pathog.* 6 (5) (2010) e1000917.
- [51] J. Yan, S. Sabbaj, A. Bansal, N. Amatya, J.J. Shacka, P.A. Goepfert, S.L. Heath, HIV-specific CD8+ T cells from elite controllers are primed for survival, *J. Virol.* 87 (9) (2013) 5170–5181.
- [52] B. Mothe, A. Llano, J. Ibarrondo, J. Zamarreno, M. Schiaulini, C. Miranda, M. Ruiz-Riol, C.T. Berger, M.J. Herrero, E. Palou, M. Plana, M. Rolland, A. Khatri, D. Heckerman, F. Pereyra, B.D. Walker, D. Weiner, R. Paredes, B. Clotet, B.K. Felber, G.N. Pavlakis, J.I. Mullins, C. Brander, CTL responses of high functional avidity and broad variant cross-reactivity are associated with HIV control, *PLoS One* 7 (1) (2012) e29717.
- [53] S.J. Westrop, A.T.H. Cocker, A. Boasso, A.K. Sullivan, M.R. Nelson, N. Imami, Enrichment of HLA types and single-nucleotide polymorphism associated with non-progression in a strictly defined cohort of HIV-1 controllers, *Front. Immunol.* 8 (2017) 746.
- [54] K. Zipperlen, M. Gallant, S. Stapleton, J. Heath, L. Barrett, M. Grant, Protective genotypes in HIV infection reflect superior function of KIR3DS1+ over KIR3DL1+ CD8+ T cells, *Immunol. Cell Biol.* 93 (1) (2015) 67–76.
- [55] A. Bandera, E. Colella, G. Rizzardini, A. Gori, M. Clerici, Strategies to limit



- immune-activation in HIV patients, *Expert Rev. Anti Infect. Ther.* 15 (1) (2017) 43–54.
- [56] G. d'Ettorre, G. Rossi, C. Scagnolari, M. Andreotti, N. Giustini, S. Serafino, I. Schietroma, G.C. Scheri, S.N. Fard, V. Trinchieri, P. Mastromarino, C. Selvaggi, S. Scarpona, G. Fanello, F. Fiocca, G. Ceccarelli, G. Antonelli, J.M. Brenchley, V. Vullo, Probiotic supplementation promotes a reduction in T-cell activation, an increase in Th17 frequencies, and a recovery of intestinal epithelium integrity and mitochondrial morphology in ART-treated HIV-1-positive patients, *Immun. Inflamm. Dis.* 5 (3) (2017) 244–260.
- [57] W.L.A. Koay, L.V. Siems, D. Persaud, The microbiome and HIV persistence: implications for viral remission and cure, *Curr. Opin. HIV AIDS* 13 (1) (2018) 61–68.
- [58] M. El-Far, P. Kouassi, M. Sylla, Y. Zhang, A. Fouda, T. Fabre, J.P. Goulet, J. van Grevenynghe, T. Lee, J. Singer, M. Harris, J.G. Baril, B. Trottier, P. Ancuta, J.P. Routy, N. Bernard, C.L. Tremblay, Investigators of the Canadian HIV + Slow Progressor Cohort, Proinflammatory isoforms of IL-32 as novel and robust biomarkers for control failure in HIV-infected slow progressors, *Sci. Rep.* 6 (2016) 22902.
- [59] M. Pernas, L. Tarancon-Diez, E. Rodriguez-Gallego, J. Gomez, J.G. Prado, C. Casado, B. Dominguez-Molina, I. Olivares, M. Coiras, A. Leon, C. Rodriguez, J.M. Benito, N. Rallon, M. Plana, O. Martinez-Madrid, M. Dapena, J.A. Iribarren, J. Del Romero, F. Garcia, J. Alcami, M.A. Munoz-Fernandez, F. Vidal, M. Leal, C. Lopez-Galindez, E. Ruiz-Mateos, Ezequiel Ruiz-Mateos on behalf of ECRIS integrated in the Spanish AIDS Research Network, Factors leading to the loss of natural elite control of HIV-1 infection, *J. Virol.* 92 (5) (2018) e01805-17.
- [60] T.A. Crowell, K.A. Gebo, J.N. Blankson, P.T. Korthuis, B.R. Yehia, R.M. Rutstein, R.D. Moore, V. Sharp, A.E. Nijhawan, W.C. Mathews, L.H. Hanau, R.B. Corales, R. Beil, C. Somboonwit, H. Edelstein, S.L. Allen, S.A. Berry for the HIV Research Network, Hospitalization rates and reasons among HIV elite controllers and persons with medically controlled HIV infection, *J. Infect. Dis.* 211 (11) (2015) 1692–1702.
- [61] S. Krishnan, E.M. Wilson, V. Sheikh, A. Rupert, D. Mendoza, J. Yang, R. Lempicki, S.A. Migueles, I. Sereti, Evidence for innate immune system activation in HIV type 1-infected elite controllers, *J. Infect. Dis.* 209 (6) (2014) 931–939.
- [62] J.Z. Li, K.B. Arnold, J. Lo, A.S. Dugast, J. Plants, H.J. Ribaudou, K. Cesa, A. Heisey, D.R. Kuritzkes, D.A. Lauffenburger, G. Alter, A. Landay, S. Grinspoon, F. Pereyra, Differential levels of soluble inflammatory markers by human immunodeficiency virus controller status and demographics, *Open Forum Infect. Dis.* 2 (1) (2015) ofu117.
- [63] F. Pereyra, J. Lo, V.A. Triant, J. Wei, M.J. Buzon, K.V. Fitch, J. Hwang, J.H. Campbell, T.H. Burdo, K.C. Williams, S. Abbara, S.K. Grinspoon, Increased coronary atherosclerosis and immune activation in HIV-1 elite controllers, *AIDS* 26 (18) (2012) 2409–2412.
- [64] B. Dominguez-Molina, L. Tarancon-Diez, S. Hua, C. Abad-Molina, E. Rodriguez-Gallego, K. Machmach, F. Vidal, C. Tural, S. Moreno, J.M. Goni, E. Ramirez de Arellano, M. Del Val, M.F. Gonzalez-Escribano, J. Del Romero, C. Rodriguez, L. Capa, P. Viciana, J. Alcami, X.G. Yu, B.D. Walker, M. Leal, M. Lichterfeld, E. Ruiz-Mateos on behalf of ECRIS integrated in the Spanish AIDS Research Network, HLA-B\*57 and IFNL4-related polymorphisms are associated with protection against HIV-1 disease progression in controllers, *Clin. Infect. Dis.* 64 (5) (2017) 621–628.
- [65] W. Lu, S. Chen, C. Lai, M. Lai, H. Fang, H. Dao, J. Kang, J. Fan, W. Guo, L. Fu, J.M. Andrieu, Suppression of HIV replication by CD8(+) regulatory T-Cells in elite controllers, *Front. Immunol.* 7 (2016) 134.
- [66] O.T. Akinkunju, A. Bansal, S. Sabbaj, S.L. Heath, P.A. Goepfert, Interleukin-2 production by polyfunctional HIV-1-specific CD8 T cells is associated with enhanced viral suppression, *J. Acquir. Immune Defic. Syndr.* 58 (2) (2011) 132–140.
- [67] C.M. Card, Y. Keynan, J. Lajoie, C.P. Bell, M. Dawood, M. Becker, K. Kasper, K.R. Fowke, HIV controllers are distinguished by chemokine expression profile and HIV-specific T-cell proliferative potential, *JAIDS J. Acquir. Immune Defic. Syndr.* 59 (5) (2012) 427–437.
- [68] Z.M. Ndhlovu, J. Proudfoot, K. Cesa, D.M. Alvino, A. McMullen, S. Vine, E. Stampoulouglou, A. Piechocka-Trocha, B.D. Walker, F. Pereyra, Elite controllers with low to absent effector CD8+ T cell responses maintain highly functional, broadly directed central memory responses, *J. Virol.* 86 (12) (2012) 6959–6969.
- [69] D. Shasha, D. Karel, O. Angiuli, A. Greenblatt, M. Ghebremichael, X. Yu, F. Porichis, B.D. Walker, Elite controller CD8+ T cells exhibit comparable viral inhibition capacity, but better sustained effector properties compared to chronic progressors, *J. Leukoc. Biol.* 100 (6) (2016) 1425–1433.
- [70] L.D. Williams, A. Bansal, S. Sabbaj, S.L. Heath, W. Song, J. Tang, A.J. Zajac, P.A. Goepfert, Interleukin-21-producing HIV-1-specific CD8 T cells are preferentially seen in elite controllers, *J. Virol.* 85 (5) (2011) 2316–2324.
- [71] J. Tauriainen, L. Scharf, J. Fredericks, A. Najji, H.G. Ljunggren, A. Sonnerborg, O. Lund, G. Reyes-Teran, F.M. Hecht, S.G. Deeks, M.R. Betts, M. Buggert, A.C. Karlsson, Perturbed CD8(+) T cell TIGIT/CD226/PVR axis despite early initiation of antiretroviral treatment in HIV infected individuals, *Sci. Rep.* 7 (2017) 40354.
- [72] J. van Grevenynghe, F.A. Procopio, Z. He, N. Chomont, C. Riou, Y. Zhang, S. Gimmig, G. Boucher, P. Wilkinson, Y. Shi, B. Yassine-Diab, E.A. Said, L. Trautmann, M. El Far, R.S. Balderas, M.R. Boulassel, J.P. Routy, E.K. Haddad, R.P. Sekaly, Transcription factor FOXO3a controls the persistence of memory CD4(+) T cells during HIV infection, *Nat. Med.* 14 (3) (2008) 266–274.
- [73] S.J. Potter, C. Lacabaratz, O. Lambotte, S. Perez-Patrigone, B. Vingert, M. Sinet, J.H. Colle, A. Urrutia, D. Scott-Algara, F. Boufassa, J.F. Delfraissy, J. Theze, A. Venet, L.A. Chakrabarti, Preserved central memory and activated effector memory CD4+ T-cell subsets in human immunodeficiency virus controllers: an ANRS EP36 study, *J. Virol.* 81 (24) (2007) 13904–13915.
- [74] C. Riou, B. Yassine-Diab, J. Van grevenynghe, R. Somogyi, L.D. Greller, D. Gagnon, S. Gimmig, P. Wilkinson, Y. Shi, M.J. Cameron, R. Campos-Gonzalez, R.S. Balderas, D. Kelvin, R.P. Sekaly, E.K. Haddad, Convergence of TCR and cytokine signaling leads to FOXO3a phosphorylation and drives the survival of CD4+ central memory T cells, *J. Exp. Med.* 204 (1) (2007) 79–91.
- [75] D. Benati, M. Galperin, O. Lambotte, S. Gras, A. Lim, M. Mukhopadhyay, A. Nouel, K.A. Campbell, B. Lemerrier, M. Claireaux, S. Hendo, P. Lechat, P. de Truchis, F. Boufassa, J. Rossjohn, J.F. Delfraissy, F. Arenzana-Seisdedos, L.A. Chakrabarti, Public T cell receptors confer high-avidity CD4 responses to HIV controllers, *J. Clin. Invest.* 126 (6) (2016) 2093–2108.
- [76] S. Buranapraditkun, F. Pissani, J.E. Teigler, B.T. Schultz, G. Alter, M. Marovich, M.L. Robb, M.A. Eller, J. Martin, S. Deeks, Preservation of peripheral T follicular helper cell function in HIV controllers, *J. Virol.* 91 (14) (2017) e00497–e00517.
- [77] M. Locci, C. Havenar-Daughton, E. Landais, J. Wu, M.A. Kroenke, C.L. Arlehamn, L.F. Su, R. Cubas, M.M. Davis, A. Sette, E.K. Haddad, International AIDS Vaccine Initiative Protocol C Principal Investigators, P. Poignard, S. Crotty, Human circulating PD-1 + CXCR3-CXCR5 + memory Tfh cells are highly functional and correlate with broadly neutralizing HIV antibody responses, *Immunity* 39 (4) (2013) 758–769.
- [78] E. Martin-Gayo, J. Cronin, T. Hickman, Z. Ouyang, M. Lindqvist, K.E. Kolb, J. Schulze Zur Wiesch, R. Cubas, F. Porichis, A.K. Shalek, J. van Lunzen, E.K. Haddad, B.D. Walker, D.E. Kaufmann, M. Lichterfeld, X.G. Yu, Circulating CXCR5(+)/CXCR3(+)/PD-1(lo) Tfh-like cells in HIV-1 controllers with neutralizing antibody breadth, *JCI Insight* 2 (2) (2017) e89574.
- [79] R. Cubas, J. van Grevenynghe, S. Willis, L. Kardava, B.H. Santich, C.M. Buckner, R. Muir, V. Tardif, C. Nichols, F. Procopio, Z. He, T. Metcalf, K. Ghneim, M. Locci, P. Ancuta, J.P. Routy, L. Trautmann, Y. Li, A.B. McDermott, R.A. Koup, C. Petrovas, S.A. Migueles, M. Connors, G.D. Tomaras, S. Moir, S. Crotty, E.K. Haddad, Reversible reprogramming of circulating memory T follicular helper cell function during chronic HIV infection, *J. Immunol.* 195 (12) (2015) 5625–5636.
- [80] A. Iannello, M.R. Boulassel, S. Samarani, O. Debbeche, C. Tremblay, E. Toma, J.P. Routy, A. Ahmad, Dynamics and consequences of IL-21 production in HIV-infected individuals: a longitudinal and cross-sectional study, *J. Immunol.* 184 (1) (2010) 114–126.
- [81] F. Vigneault, M. Woods, M.J. Buzon, C. Li, F. Pereyra, S.D. Crosby, J. Rychert, G. Church, J. Martinez-Picado, E.S. Rosenberg, A. Telenti, X.G. Yu, M. Lichterfeld, Transcriptional profiling of CD4 T cells identifies distinct subgroups of HIV-1 elite controllers, *J. Virol.* 85 (6) (2011) 3015–3019.
- [82] K. Titanji, A. De Milito, A. Cagigi, R. Thorstenson, S. Grutzmeier, A. Atlas, B. Hejdeman, F.P. Kroon, L. Lopalco, A. Nilsson, F. Chiodi, Loss of memory B cells impairs maintenance of long-term serologic memory during HIV-1 infection, *Blood* 108 (5) (2006) 1580–1587.
- [83] C.M. Buckner, L. Kardava, X. Zhang, K. Gittens, J.S. Justement, C. Kovacs, A.B. McDermott, Y. Li, M.M. Sajadi, T.W. Chun, A.S. Fauci, S. Moir, Maintenance of hiv-specific memory B-cell responses in elite controllers despite low viral burdens, *J. Infect. Dis.* 214 (3) (2016) 390–398.
- [84] J. van Grevenynghe, R.A. Cubas, A. Noto, S. DaFonseca, Z. He, Y. Peretz, A. Filali-Mouhim, F.P. Dupuy, F.A. Procopio, N. Chomont, R.S. Balderas, E.A. Said, M.R. Boulassel, C.L. Tremblay, J.P. Routy, R.P. Sekaly, E.K. Haddad, Loss of memory B cells during chronic HIV infection is driven by Foxo3a- and TRAIL-mediated apoptosis, *J. Clin. Invest.* 121 (10) (2011) 3877–3888.
- [85] M.E. Ackerman, A. Mikhailova, E.P. Brown, K.G. Dowell, B.D. Walker, C. Bailey-Kellogg, T.J. Suscovich, G. Alter, Polyfunctional HIV-specific antibody responses are associated with spontaneous HIV control, *PLoS Pathog.* 12 (1) (2016) e1005315.
- [86] A. Rouers, J. Klingler, B. Su, A. Samri, G. Laumond, S. Even, V. Avettand-Fenoel, C. Richetta, N. Paul, F. Boufassa, L. Hocqueloux, H. Mouquet, C. Rouzioux, O. Lambotte, B. Autran, S. Graff-Dubois, C. Moog, A. Moris, A.C. Cohort, HIV-specific B cell frequency correlates with neutralization breadth in patients naturally controlling HIV-infection, *EBioMedicine* 21 (2017) 158–169.
- [87] L. Kuri-Cervantes, G.S. de Oca, S. Avila-Rios, R. Hernandez-Juan, G. Reyes-Teran, Activation of NK cells is associated with HIV-1 disease progression, *J. Leukoc. Biol.* 96 (1) (2014) 7–16.
- [88] R. Song, I. Lisovsky, B. Lebouche, J.P. Routy, J. Bruneau, N.F. Bernard, HIV protective KIR3DL1/S1-HLA-B genotypes influence NK cell-mediated inhibition of HIV replication in autologous CD4 targets, *PLoS Pathog.* 10 (1) (2014) e1003867.
- [89] C. Tomescu, F.M. Duh, R. Hoh, A. Viviani, K. Harvill, M.P. Martin, M. Carrington, S.G. Deeks, L.J. Montaner, Impact of protective killer inhibitory receptor/human leukocyte antigen genotypes on natural killer cell and T-cell function in HIV-1-infected controllers, *AIDS* 26 (15) (2012) 1869–1878.
- [90] K. Machmach, M. Leal, C. Gras, P. Viciana, M. Genebat, E. Franco, F. Boufassa, O. Lambotte, J.P. Herbeval, E. Ruiz-Mateos, Plasmacytoid dendritic cells reduce HIV production in elite controllers, *J. Virol.* 86 (8) (2012) 4245–4252.
- [91] M. Aounallah, X. Dagenais-Lussier, M. El-Far, V. Mehraj, M.A. Jenabian, J.P. Routy, J. van Grevenynghe, Current topics in HIV pathogenesis, part 2: inflammation drives a Warburg-like effect on the metabolism of HIV-infected subjects, *Cytokine Growth Factor Rev.* 28 (2016) 1–10.
- [92] J.P. Routy, V. Mehraj, Potential contribution of gut microbiota and systemic inflammation on HIV vaccine effectiveness and vaccine design, *AIDS Res. Ther.* 14 (1) (2017) 48.
- [93] J. Vesterbacka, J. Rivera, K. Noyan, M. Parera, U. Neogi, M. Calle, R. Paredes, A. Sonnerborg, M. Noguera-Julian, P. Nowak, Richer gut microbiota with distinct metabolic profile in HIV infected elite controllers, *Sci. Rep.* 7 (1) (2017) 6269.
- [94] S.X. Li, A. Armstrong, C.P. Neff, M. Shaffer, C.A. Lozupone, B.E. Palmer, Complexities of gut microbiome dysbiosis in the context of HIV infection and

- antiretroviral therapy, *Clin. Pharmacol. Ther.* 99 (6) (2016) 600–611.
- [95] I. Vujkovic-Cvijin, R.M. Dunham, S. Iwai, M.C. Maher, R.G. Albright, M.J. Broadhurst, R.D. Hernandez, M.M. Lederman, Y. Huang, M. Somsouk, S.G. Deeks, P.W. Hunt, S.V. Lynch, J.M. McCune, Dysbiosis of the gut microbiota is associated with HIV disease progression and tryptophan catabolism, *Sci. Transl. Med.* 5 (193) (2013) 193ra.
- [96] J. Chen, J. Shao, R. Cai, Y. Shen, R. Zhang, L. Liu, T. Qi, H. Lu, Anti-retroviral therapy decreases but does not normalize indoleamine 2,3-dioxygenase activity in HIV-infected patients, *PLoS One* 9 (7) (2014) e100446.
- [97] R. Zangerle, B. Widner, G. Quirchmair, G. Neurauder, M. Sarcletti, D. Fuchs, Effective antiretroviral therapy reduces degradation of tryptophan in patients with HIV-1 infection, *Clin. Immunol.* 104 (3) (2002) 242–247.
- [98] G. Marchetti, C. Tincati, G. Silvestri, Microbial translocation in the pathogenesis of HIV infection and AIDS, *Clin. Microbiol. Rev.* 26 (1) (2013) 2–18.
- [99] C.J. Kim, C. Kovacs, T.W. Chun, G. Kandel, B.J. Osborne, S. Huibner, K. Shahabi, F.Y. Yue, E. Benko, M. Ostowski, R. Kaul, Antiretroviral therapy in HIV-infected elite controllers: impact on gut immunology, microbial translocation, and biomarkers of serious non-AIDS conditions, *J. Acquir. Immune Defic. Syndr.* 67 (5) (2014) 514–518.
- [100] S. Sankaran, M. Guadalupe, E. Reay, M.D. George, J. Flamm, T. Prindiville, S. Dandekar, Gut mucosal T cell responses and gene expression correlate with protection against disease in long-term HIV-1-infected nonprogressors, *Proc. Natl. Acad. Sci. U. S. A.* 102 (28) (2005) 9860–9865.
- [101] D. Paquin-Proulx, C. Ching, I. Vujkovic-Cvijin, D. Fadrosch, L. Loh, Y. Huang, M. Somsouk, S.V. Lynch, P.W. Hunt, D.F. Nixon, D. SenGupta, Bacteroides are associated with GALT iNKT cell function and reduction of microbial translocation in HIV-1 infection, *Mucosal Immunol.* 10 (1) (2017) 69–78.
- [102] R. Nardacci, A. Amendola, F. Ciccosanti, M. Corazzari, V. Esposito, C. Vlassi, C. Taibi, G.M. Fimia, F. Del Nonno, G. Ippolito, G. D'Offizi, M. Piacentini, Autophagy plays an important role in the containment of HIV-1 in nonprogressor-infected patients, *Autophagy* 10 (7) (2014) 1167–1178.
- [103] R. Nardacci, F. Ciccosanti, C. Marsella, G. Ippolito, M. Piacentini, G.M. Fimia, Role of autophagy in HIV infection and pathogenesis, *J. Intern. Med.* 281 (5) (2017) 422–432.



**Hamza Loucif (first author).** Hamza Loucif is a Ph.D. student at the INRS-Institut Armand Frappier (Laval, Quebec) under the supervision of Dr. Julien Van Grevenynghe. He obtained his B.Sc. in Applied and Fundamental Biochemistry (2015) followed by a Master in Biotechnology and Molecular Pathology (2017) at the University of Science and Technology of Algiers (USTHB, Algeria). He concluded his Master's internship at the Department of Human Virology, HIV/AIDS National Reference Laboratory of Institut Pasteur d'Algérie, studying the role of Nitric Oxide (NO) in HIV-1 immuno-pathogenesis. He will be studying the role of autophagy process as a novel immune correlate exhibited by HIV-1-specific CD8 T cells in

“Elite Controllers”, a unique subset of individuals known to possess the ability to naturally co-exist with the virus for a long term without progressing to the AIDS stage.



**Steven Gouard.** Steven Gouard is a trainee under the supervision of Dr. Van Grevenynghe at the INRS-Institut Armand Frappier (Laval, Quebec) in order to complete his Master in Biochemistry at the University of La Rochelle (Nouvelle-Aquitaine, France). Future Ph.D. student in Dr. Julien Van Grevenynghe's laboratory, Steven Gouard will study the role of heat shock proteins in Elite controllers as well as the role of these proteins in the generation and maintenance of CD4 + T cell memory.



**Xavier Dagenais-Lussier, B.Sc.** Xavier Dagenais-Lussier is a junior Ph.D. student under the supervision of Dr. van Grevenynghe at the INRS-Institut Armand Frappier (Laval, Quebec). He recently graduated for his Master (2016), and obtained his B.Sc. in Microbiology at the University of Sherbrooke (Quebec) in 2014. He recently published a study showing that increased production of the tryptophan-related catabolite, kynurenine, participates to memory CD4 T-cell loss during the early phase of HIV-1 primary infection, by interfering with IL-2 signalling (*Journal of Virology*, 2016). Currently, Xavier Dagenais-Lussier is studying the impact of sustained interferon type I during persistent HIV-1 infection.



**Armstrong Murira, Ph.D.** Armstrong Murira is a post doctorate fellow at INRS-Institut Armand Frappier (Laval, Quebec). He is a molecular immunologist specializing in infectious diseases with a focus on Chronic Viral Infections. He graduated from Simon Fraser University, Burnaby, BC in 2014 with a doctorate in HIV-1 vaccine research. He has a wide range of experience using Bioinformatics methods to analyze cellular phenotypic and transcriptomic features of immune effector cells (mainly B cells) in both humans and murine chronic infections models. His current work is in Hepatitis C vaccine research that spans identifying IFN signatures that drive immuno-pathogenesis in chronic infections. In this regard, he has also worked with the murine LCMV model. He is a current holder of a CanHepC post -doctorate fellowship and has published in various journals including *Nature Nanotechnology*, *Viruses* and *Frontiers in Immunology*.



**Simona Stäger, D.V.M.-Ph.D.** Simona Stäger obtained her D.V.M. (1994) and her Ph.D. (1997) from the Faculty of Veterinary Medicine of the University of Berne (Switzerland). She is currently an Associate Professor at the INRS-Institut Armand-Frappier (Canada). Her lab is focused on understanding the generation and maintenance of adaptive immunity during chronic infections.



**Cécile Tremblay, Ph.D.** Cécile Tremblay is an infectious diseases/medical microbiologist specialist at the University of Montréal. She is full professor in the Department of Microbiology, Immunology, and Infectious Diseases at University of Montreal and a researcher at CR-CHUM. She obtained her M.D. at University of Montreal in 1992. She is the founder and director of a pan-Canadian cohort of HIV-infected subjects with slow disease progression, which is a collaborative effort by Canadian researchers to better understand HIV immunopathology. She is also coordinating a research initiative on premature aging and cardiovascular disease in HIV in Canada. From 2012 to 2015, she served as Director of the Quebec Public Health Laboratory. During her mandate, she developed a research program on HIV epidemiology in Québec and was responsible for the coordination of the laboratory response to biological threats and emerging infectious diseases. She has led research efforts on several infectious diseases. Today, she is also director of the *AIDS and Infectious Diseases* network, which is financed by the FRQ-S and allow many laboratory to have access to unique cohorts of HIV-1-infected subjects including long-term non progressors and HIV-1 controllers.



**Julien van Grevenynghe, Ph.D. (corresponding author)** Dr. van Grevenynghe is an assistant professor in the INRS-Institut Armand Frappier (Laval, Quebec) since February 2015. Dr. van Grevenynghe obtained his Ph.D. from INSERM U456 and University of Rennes 1 (Bretagne, France). Then, he joined Dr. Rafick Sekaly's team (CR-CHUM in Montreal and VGTI in Florida) where he focused on the characterization of the transcriptional factor Foxo3a in the long-term maintenance of memory CD4 T-cells during chronic HIV-1 infection. Today, Dr. van Grevenynghe is an expert on viral pathogenesis where his laboratory studies (i) new molecular mechanisms associated with natural immune protection in elite controllers and (ii) the involvement of metabolism by-products such as oxidative stress that occurs since HIV-1 primary-infection on memory CD4 T-cell impairments. His last publication as senior research authors were accepted in significant peer-to-peer journals including *Cell Host and Microbe*, *PLOS Pathogen* and *Journal of Virology*.



Contents lists available at [ScienceDirect](https://www.sciencedirect.com)

### Cytokine and Growth Factor Reviews

journal homepage: [www.elsevier.com/locate/cytogfr](http://www.elsevier.com/locate/cytogfr)



## Plasticity in T-cell mitochondrial metabolism: A necessary peacekeeper during the troubled times of persistent HIV-1 infection



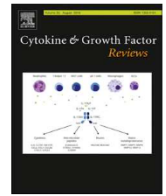
Hamza Loucif<sup>a</sup>, Xavier Dagenais-Lussier<sup>a</sup>, Cherifa Beji<sup>a</sup>, Roman Telittchenko<sup>a</sup>, Jean-Pierre Routy<sup>b</sup>, Julien van Grevenynghe<sup>a,\*</sup>

<sup>a</sup> Institut National la Recherche Scientifique (INRS)-Institut Armand-Frappier, 531 Boulevard des Prairies, Laval, H7V 1B7 QC, Canada

<sup>b</sup> Chronic Viral Illness Service and Division of Hematology, McGill University Health Centre, Glen site, Montréal, QC, Canada

---





## Plasticity in T-cell mitochondrial metabolism: A necessary peacekeeper during the troubled times of persistent HIV-1 infection

Hamza Loucif<sup>a</sup>, Xavier Dagenais-Lussier<sup>a</sup>, Cherifa Beji<sup>a</sup>, Roman Telittchenko<sup>a</sup>, Jean-Pierre Routy<sup>b</sup>, Julien van Grevenynghe<sup>a,\*</sup>

<sup>a</sup> Institut National la Recherche Scientifique (INRS)-Institut Armand-Frappier, 531 Boulevard des Prairies, Laval, H7V 1B7 QC, Canada

<sup>b</sup> Chronic Viral Illness Service and Division of Hematology, McGill University Health Centre, Glen site, Montréal, QC, Canada



### ARTICLE INFO

#### Keywords:

Immuno-metabolism  
Mitochondria  
Metabolic plasticity  
Glucose dependency  
HIV-1 control  
T-cell immunity  
Inflammation  
ART  
Metabolism-targeted therapy

### ABSTRACT

The notion of immuno-metabolism refers to the crosstalk between key metabolic pathways and the development/maintenance of protective immunity in the context of physiological processes and anti-microbial defenses. Enthusiasm for immuno-metabolism in the context of HIV-1 infection, especially among T-cell lineages, continues to grow over time as science opens new therapeutic perspectives to limit viral pathogenesis and to boost anti-viral responses. The idea of "metabolism as a therapeutic target" is called metabolic reprogramming and is based on the use of specific metabolism-targeting drugs that are currently available for cancer therapy. In this review, we will focus on the evidence that shows the key role of mitochondria, the cell's powerhouses, and their ability to use diverse metabolic resources (referred to as metabolic plasticity) in providing optimal immune T-cell protection among HIV-1-infected patients. Conversely, we highlight observations indicating that mitochondria metabolic dysfunction associated with excessive glucose dependency, a phenomenon reported as "Warburg effect", results in the inability to mount and maintain effective T-cell-dependent immunity during persistent HIV-1 infection. Therefore, helping mitochondria to regain the metabolic plasticity and allow specific T-cells to adapt and thrive under unfavorable environmental conditions during HIV-1 infection may represent the next generation of combinatory treatment options for patients.

### 1. The necessity in T-cells to diversify carbon fuel sources to cover their specific needs

It is well-acknowledged that mitochondria play a key role in energy release among eukaryotes [1,2]. Under different physiological conditions, when cells require energy for their own agenda to sustain diverse immune activity, it is believed that mitochondria produce up to 95 % of energy in the form of ATP molecules through cellular respiration [2,3]. Cellular respiration, also called mitochondrial oxidative phosphorylation (OxPhoS), allows the controlled release of free energy from diverse sources of carbon-based molecules such as carbohydrates, fat and protein energy substrates (Fig. 1). Cellular respiration consists of three related series of biochemical reactions that include: **a.** several upstream catabolic reactions that break-down molecules into smaller units, which result in the formation of acetyl coenzyme A (acetyl-CoA) and reducing equivalents. In this regard, cells are capable of metabolizing a variety of carbon substrates including glucose (through glycolysis), fatty acids (through fatty acid oxidation or FAO), ketone bodies and amino acids. **b.** The mitochondrial Krebs cycle (also called

tricarboxylic acid cycle or TCA) that incorporates AcetylCoA and reducing equivalents to generate additional reducing equivalents. **c.** The cellular respiration *per se*, where the shuttling of electrons, generated from reducing equivalents, leads to ATP release.

Glucose is one of the main nutrients from which cells extract energy [1]. However, it is now well-admitted that healthy mitochondrial metabolism should be regarded as a plastic and highly dynamic determinant of a wide range of cellular specific functions [4]. "Metabolic plasticity" is illustrated by the cellular ability to use additional carbon sources other than glucose. This ability of the cells to fuel mitochondrial metabolism also enables necessary adaptation to stress conditions, especially in conditions where there are changes in nutrient availability [4–6]. It is particularly the case with T-cells where plasticity among mitochondrial metabolism dictates all aspects of adaptive immunity [7,8] (Table 1). In fact, several research works, including those from Dr. E. L. Pearce, give a good introduction for the profound impact of the engagement of specific catabolic reactions on T-cell activation, differentiation, quiescence and function [9–12]. For instance, in their quiescent state, naïve T-cells preferentially use mitochondrial OxPhoS

\* Corresponding author.

E-mail address: [julien.vangrevenynghe@iaf.inrs.ca](mailto:julien.vangrevenynghe@iaf.inrs.ca) (J. van Grevenynghe).

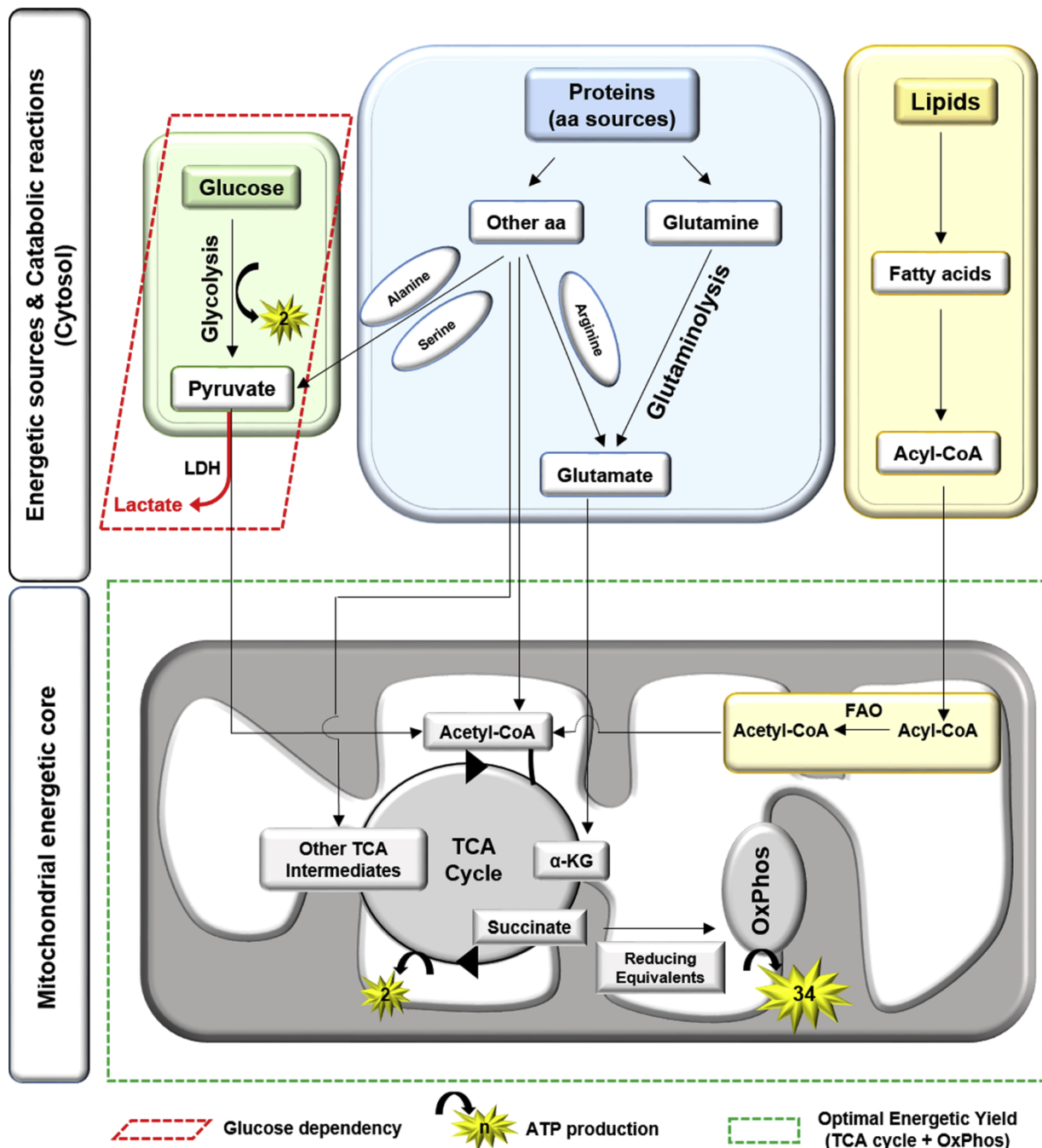























Fig. 1. Schematic representation of key carbon-based substrates and their catabolic pathways that fuel the mitochondrial respiration. Abbreviations: Acetyl-CoA, acetyl coenzyme A; Acyl-CoA, acyl-coenzyme A; Aa, amino acids; ATP, adenosine triphosphate;  $\alpha$ -KG,  $\alpha$ -ketoglutarate; FAO, fatty acid oxidation; OxPhos, oxidative phosphorylation; TCA, tricarboxylic acid.

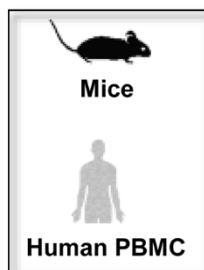
for energy generation [13]. In fact, as T-cell activation is metabolically demanding, to exit quiescence, cells switch their metabolic programming to glycolysis [12,14–16]. Glycolysis has selective advantages over mitochondrial OxPhos, which ensures a rapid and high rate of energy production during T-cell activation [13,16,17]. Although glycolysis produces less ATP molecules per cycle than OxPhos [2 ATP *versus* 36 ATP, respectively], it has a much higher ATP generation rate [2–3 seconds *versus* few hours, respectively]. Glycolysis can also be functional under hostile conditions, including hypoxia, which is characterized by the increased Hypoxia Induced Factor 1  $\alpha$  (HIF-1 $\alpha$ ). Although activated lymphocytes primarily rely on glucose uptake, additional studies show that they are able to use other environmental nutrients such as glutamine, leucine, serine, alanine and arginine as shown in

Table 1 in blue [18–22]. For instance, enriched media with L-arginine seems to support long term memory survival in specific CD4 and CD8 T cells from immunized mice with OVA<sub>257–264</sub> and HA<sub>110–119</sub> peptides. The authors found that L-arginine favors the metabolic switch from glycolysis to OxPhos that is illustrated by increased oxygen consumption and spare respiratory capacity [18]. In addition, other studies show that depriving T-cells of other non-essential amino acids such as serine [20] and alanine [21] limit their growth and effector functions. This metabolic plasticity during T-cell activation allows the cells to cover their energetic needs for proliferation and cell division even in the context of glucose restriction. Additionally, metabolic plasticity among activated T-cells is critical in laying the foundation for proper cell survival and differentiation, as well as effector function and Th<sub>17</sub>



**Table 1**  
List of immune T-cell features that are controlled by different catabolic pathways including glycolysis, glutaminolysis and mitochondrial FAO.

Metabolic/Catabolic player	T-cell phenotype	Experimental Model	Ref(s)
Glycolysis	Lck-dependent T-cell activation		[16]
	Polyfunctionality (IFN- $\gamma$ <sup>+</sup> TNF- $\alpha$ <sup>+</sup> )		[14, 15 ]
	Effector memory CD8 T-cells functionality, Cytolytic activity & proliferation		
	Up-regulation of IFN- $\gamma$ , GM-CSF, Granzyme B, Cyclin D2		[17]
	Increased Naive CD8 T-cells CD69 <sup>+</sup> frequency		
Increased Effector memory CD8 T-cells CD45RA <sup>+</sup> CD62L <sup>-</sup> IFN- $\gamma$ production		[13]	
Naive CD4 T-cell; IL-2 Production Akt Lck-dependent		[13]	
Glutaminolysis	Enhanced Th1 polarisation & less Th17 Differentiation IL-17 <sup>+</sup> RoRyt <sup>+</sup> Foxp <sup>+</sup>		[19]
	CTL potential CD8 T-cells IFN- $\gamma$ <sup>+</sup> IL-2 <sup>+</sup> Granzyme B <sup>+</sup> Perforin <sup>+</sup> Low expression of KLRG1 and inhibitory receptors PD-1, Tim3, and Lag3		
Alamine	Naive CD4 T-cell IL-2 Production STAT5 Lck-dependent		[13]
Serine	Exit from quiescence for: Naive T-cell activation & Memory re-stimulation IFN- $\gamma$ , IL-6, IL17 secretion		[21]
	Enhanced effector CD8 T-cell response IFN- $\gamma$ <sup>+</sup> CD44 <sup>+</sup> T-cells proliferation		[20]
Arginine	Naive CD8 & CD4 T cells survival & proliferation CD45RA <sup>+</sup> CCR7 <sup>+</sup> IFN- $\gamma$ production		[18]
	CD44 <sup>high</sup> CD4 T-cells generation		
	Naive CD44 <sup>low</sup> & CD4 T-cells survival under OVA257–264 peptide immunization		
OxPhos/FAO	CD8 T-cell long-term memory survival		[25]
	Memory T-cell IL-15 induced generation		[9]
	Prevent proinflammatory CD4 differentiation		[23]
	Naive CD4 T cell IL-2 Production STAT5 Lck-dependent		[13]
	effector CD4 T cell IFN- $\gamma$ <sup>+</sup> & Treg differentiation High Foxp3 expression & AMPK phosphorylation, low Glut1 expression		[26, 27]
	enhanced memory CD8 T cell TRAF <sup>+</sup> Bcl-2 <sup>low</sup> Cpt1 <sup>high</sup>		[29, 31]
	Down-regulation of effector CD8 T-cells response IFN- $\gamma$ <sup>+</sup>		
	Memory CD8 <sup>+</sup> T-cell development IL-1 <sup>high</sup>		[28]



promotion, which is reliant on glutamine metabolism [18–20,23]. It is interesting to note that interfering with different steps of glutamine metabolism impact cell population differently. Absence of glutamine prevents the proliferation of Th1 and Th17, whereas a deficiency in

glutaminase, which converts glutamine to glutamate, favors Th1 differentiation compared to Th17 [19,24]. Evidence further shows that the generation of long-lasting memory T-cells and regulatory T-cell (T<sub>reg</sub>) subsets require distinct metabolic programming that is characterized by

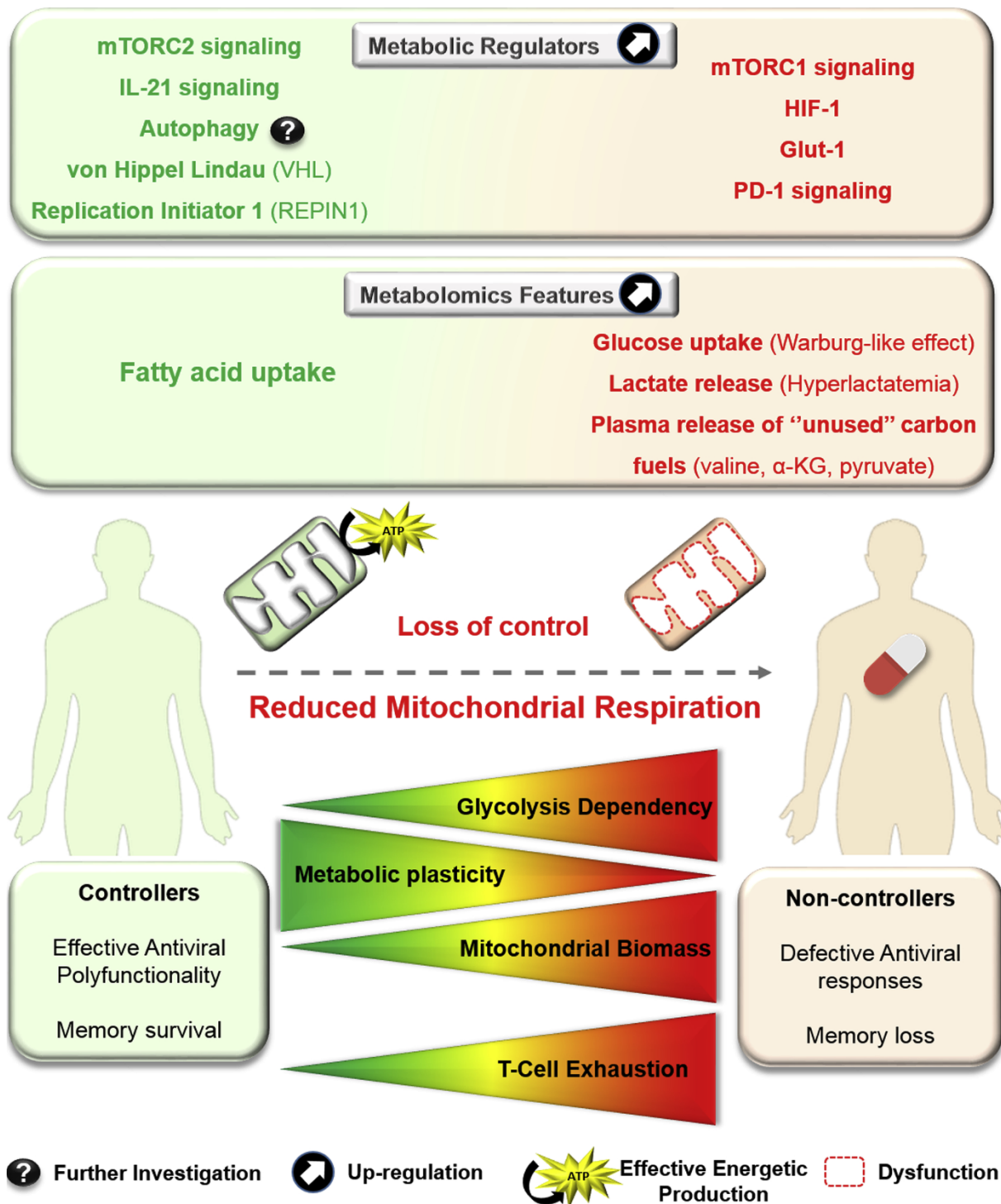


Fig. 2. Up-regulated metabolites and key metabolic regulators that may confer better antiviral immunity in HIV-1 controllers (in green) when compared to non-controllers patients (in red). Abbreviations: ATP, adenosine triphosphate;  $\alpha$ -KG,  $\alpha$ -ketoglutarate; Glut-1, glucose Transporter type 1; HIF-1 $\alpha$ , hypoxia-inducible factor 1-alpha; OxPhoS, oxidative phosphorylation; PD-1, programmed cell death 1; REPIN1, Replication Initiator 1; VHL: von Hippel Lindau.

enhanced mitochondrial FAO [25–31]. Interestingly, carnitine palmitoyltransferase 1A, which is essential for the beta-oxidation of long-chain fatty acids, seems to be critical in IFN- $\gamma$  production and, thus, for proper memory T-cell response [32]. Furthermore, Jones et al. have indicated that there is a differential metabolic response among CD4 T cells subsets. In this study they also showed that pyruvate oxidation is elevated in memory compared to naïve subsets, which indicates that glycolysis derived products such as pyruvate are beneficial to fueling mitochondria. In addition, quiescent memory subsets showed higher

OxPhoS compared to naïve subset explained by the high mitochondrial mass presented in memory subsets. This suggests that the metabolic responsiveness in human naïve and memory T-cells are distinct [13,33].

In summary, glycolysis, amino-acid, fatty acid and mitochondrial metabolism are now recognized as key metabolic and inter-connected players in T-cell activation and differentiation. Lastly, the plasticity of those metabolic networks is critical for the proper development of T helper cell lineages.

## 2. T-cell metabolic plasticity in cancer, maybe some lessons to learn for HIV-1

In healthy conditions, there is no doubt about the beneficial outcome of T-cells being able to diversify their carbon sources to ensure optimal mitochondrial use when necessary. The main reason why metabolic plasticity is a good outcome in healthy T-cells is that their mitochondria are highly dynamic organelles that respond to a multiplicity of signals in order to finely adjust their fluctuating metabolic needs (Fig. 1). Now, to think that T-cell metabolic plasticity in the context of diseases is a good thing as well, because it allows cells to adapt to any hostile environment, may also be true [5]. This also seems to be true for cancer. In order to sustain high proliferation rates, cancer cells preferentially use glycolysis even in the presence of oxygen and functional mitochondria, a phenomenon called the "Warburg effect" [34] (Fig. 1). Therefore, within the tumor environment, effector T-cells must compete with cancer cells for glucose availability, which in turn limits T-cell function and favors tumor progression [11,35–37].

The idea of manipulating other pathways that regulate the use of alternative substrates to glucose in an attempt to enhance T-cell immunity through mitochondrial respiration is compelling. Inhibiting glycolysis in immune CD8 T-cells and favoring mitochondrial metabolism enhances their memory formation and anti-tumor activity [38]. In addition, Qiu J. et al. have shown that manipulation of the short-chain fatty acid acetate-handling pathways enhance effector functions of tumor-infiltrating CD8 T-cells in the context of glucose restriction [39]. Not only do tumor cells compete with immune T-cells for glucose, but they also compete for other carbon sources such as glutamine and acetate [40–42]. In fact, data show that the diverse metabolic fuel sources that can be produced by autophagy, a lysosomal-dependent catabolic process, provide tumors with metabolic plasticity [43–45]. Although the role of macro-autophagy in T-cell homeostasis and immunity is well characterized, Hubbard and colleagues also showed the intricacy of this key process in accommodating the necessary energetic needs in activated T-cells [46]. Metabolomics analysis also reveals the importance of autophagy in the production of the lipid substrates for mitochondrial FAO and the fueling of oxidative phosphorylation in activated CD8 T cells [46,47]. This is the reason why balancing tumor inhibition and induction of immune T-cell activity with metabolism-targeting drugs will be challenging and requires more knowledge on the basics of plastic T-cell metabolism [48]. It will be even more challenging if we consider the fact that anti-tumor T-cells are chronically stimulated by persistent antigen exposure and become progressively dysfunctional, a state referred as "cell exhaustion" [49–51]. Exhausted T-cells, within the tumor environment, are characterized by many dysfunctions, including impaired mitochondrial respiration capacity, as well as reduced mitochondrial biogenesis and smaller ATP reserve [52].

In conclusion, since specific anti-tumor and anti-HIV-1 T-cells display some similarities of metabolic features due to hyper-immune activation, it is reasonable to think that information collected on cancer metabolism may give rise to new therapeutic avenues for HIV-1 treatment.

## 3. Persistent HIV-1 infection leads to increased glycolysis and mitochondria dysfunction

Similarly to cancer, immune T-cells specific for HIV-1 are subjected to constant cell-stimulation due to persistent inflammation and antigen exposure [53,54]. This persistent immune activation places a high metabolic demand on T-cells in HIV-1-infected patients and their cellular metabolic activity is increased in response to this imposed challenge. It is worth noting that, although current anti-retroviral therapy (ART) is successful at suppressing viral replication within the bloodstream, it fails to completely eliminate the virus in tissues and the systemic inflammation that comes with it [55–57]. Taking this into account, it is not surprising that T-cells from HIV-1-infected patients

display increases of glycolysis, expression of glucose transporter 1 (Glut-1) and lactate release, even after years of suppressive ART [58–60] (Fig. 2). In fact, anti-HIV-1 CD8 T-cells from infected patients display not only increased glycolysis, but also rely on strict glucose dependency to fuel their prolonged effector functions [58]. In the same study, the authors further show that glucose dependency is associated with reduced respiratory capacity and lower fatty acid uptake.

Finally, during persistent HIV-1 infection, hyper-immune activated T-cells become progressively exhausted [61,62]. Exhausted T-cells are defective cells, characterized by lower proliferation and cytokine production and high expression of the inhibitory receptor programmed death-1 (PD-1) [62,63]. During persistent HIV-1 infection, exhausted T-cells are known to display reduced mitochondrial mass and membrane potential that could in part be mediated by PD-1 signaling [64–66]. Briefly, Korenca et al. show that PD-1<sup>+</sup>CD4 T-cells from patients, which are persistently infected with HIV-1 in the presence or absence of ART, display both reduced basal and maximal mitochondrial respiration when compared to uninfected control donors [65]. Ogando et al. have demonstrated, as far as they are concerned, that PD-1 stimulation of CD8 T-cells reduces the extracellular acidification rate (ECAR) as well as basal and stimulated O<sub>2</sub> consumption rates (OCR) [66]. This indicates that PD-1 engagement may dysregulate both glycolytic and mitochondrial energetics in exhausted cells during persistent HIV-1 infection.

In summary, persistent HIV-1 infection is associated with altered plasticity of T-cell mitochondrial metabolism that is unfortunately not targeted by the current treatments.

## 4. Metabolic plasticity, another powerful tool in the hand of natural controllers

The natural or elite controllers (EC) represent a small group of infected individuals who are able to maintain undetectable levels of HIV-1 replication without ART for long periods of time [67–69]. As reviewed in our previous 2018 publication, natural controllers are living proof of sustained T-cell-mediated immune control for HIV-1 that could be possible if we decipher the molecular and metabolic mechanisms responsible for it [70]. These high-quality anti-HIV-1 CD8 T-cell protection in EC are known to possess a variety of molecular advantages in comparison to other patients such as protective HLA type I alleles (B27/57) and particular killer-cell immunoglobulin-like receptors (KIR) [70]. However, other immuno-metabolic features that are independent of their protective genetic polymorphism have also been identified. The T-cell-mediated immune control for HIV-1 in EC is foremost symbolized by highly protective anti-HIV-1 CD8 T-cells that produce multiple cytokines (perforin, granzymes A and B, IFN- $\gamma$ , IL-2, IL-21, TNF- $\alpha$ , and MIP-1 $\alpha/\beta$ ) [71,72]. The ability of CD8 T-cells to secrete multiple cytokines by each individual cell is called polyfunctionality. Interestingly, Angin et al. have recently shown that CD8 T-cells in EC, in contrast to patients under ART, preserve a potent polyfunctionality in glucose-deprived media [58]. The authors show that, although CD8 T-cells in EC do not rely on exclusive glucose dependency, they surely require proper use of mitochondria. Indeed, CD8 T-cells in EC, that are treated with the mitochondrial depolarizing agent menadione, display a reduction of their CTL activity. The authors hypothesize that CD8 T-cells in EC are able to rely on other metabolic sources, such as fatty acids. The increased use of fatty acids in cells from EC was confirmed by a lipid uptake assay. Overall, These observations indicate that CD8 T cells from EC bare metabolic plasticity features to sustain effective mitochondrial respiration [58]. The authors have similar observations with Simian Immunodeficiency Virus (SIV) infection controller and viremic macaques. In this regard, the authors find that CD8 T cells from controllers, that are collected from blood and spleen, are able to target SIV<sub>mac251</sub>-infected CD4 T-cells, regardless of glucose presence. Furthermore, their transcriptomic analyses show that CD8 T-cells from patients under ART display upregulation of genes linked to the activation of mammalian



target of rapamycin complex 1 (mTORC1) such as CD8A, HIF-1, KLRD1, CD69 and IRF-1) [58]. mTORC1 complex is known to positively regulate glycolysis as well as to keep up with the energy requirements of activation [73,74]. In contrast, CD8 T-cells from EC have a metabolic programming governed by mTORC2, which is also confirmed by the phosphorylation of AKT at both serine 450 and 473 residues. This could favor metabolic plasticity and has been linked to cell survival [58,75]. Cells from EC display upregulated mRNA levels of several negative regulators of glycolysis. Those include von Hippel-Lindau (VHL), which counteracts HIF-1-mediated upregulation of glycolysis, and Replication initiator 1 (REPIN1), which counteracts HIF-1-mediated upregulation of glycolysis and is involved in down-regulation of glucose transport respectively [58] (Fig. 2). Of note, previous observations indicated that cells from EC showed an increased autophagy associated with viral containment [76]. A study from Xu *et al.* indicated that autophagy may contribute to their metabolic plasticity during chronic viral infection by providing antigen-specific CD8 T cells with other energetic sources such as lipid substrates [47]. These observations need further investigations to define the role of autophagy in providing other carbon sources.

Finally, the loss of natural immune control that occurs in approximately 25 % of EC has been recently associated with specific metabolic changes [77,78]. The authors show that, before losing control, the plasma levels of valine and other related catabolic intermediates, including  $\alpha$ -ketoglutarate ( $\alpha$ -KG), known to be a part of the mitochondrial Krebs cycle, are potentially elevated due to a switch from OxPhoS to a glycolytic program [78]. This study places those metabolites as potential therapeutic targets to maintain an efficient HIV-1 specific antiviral immunity.

In summary, these new informative leads imply that metabolic plasticity, as opposed to strict glucose dependency, may contribute to the enhanced antiviral immune response in EC thanks to optimal mitochondrial respiration.

## 5. Challenges in T-cell metabolic reprogramming for HIV-1 treatment

With the accumulating evidence showing the critical needs to maintain plasticity in T-cell mitochondrial metabolism, in opposition to strict glucose dependency, during cancer and persistent viral infections such as HBV and HIV-1, we are living a time of renaissance in metabolism research [38,39,58,78–81]. Indeed, the concept of T-cell reprogramming in these infectious diseases, by using metabolism-targeting drugs in combination with chemotherapy (ART) and/or immuno-therapy (cytokine treatments), raises great interest within the international scientific community. This concept is reinforced if we consider the fact that IL-15 has been found to reinvigorate anti-HIV-1 CD8 T-cells in ART-treated patients through the promotion of fatty acid use for energy [58]. Indeed, IL-15 pre-treatment not only increased the frequency of HIV-specific CD8 T-cells following HIV-Gag stimulation, it also increased their capacity to block HIV-1 infection of autologous CD4 T-cells *in vitro*. In cancer, IL-21 is also able to shift immune CD8 T-cells towards a fatty-acid oxidation-dependent mitochondrial metabolism [82]. The authors show that IL-21-mediated metabolic reprogramming results in increased CD8 T-cell survivability mainly due to a higher resistance to ROS-induced cell death and an increased expression of the anti-apoptotic protein Bcl-2. Additionally, Loschinski *et al.* posit that the reduced expression of CD57 and PD-1, respectively markers of senescence and exhaustion, as well as an increase in central-memory T-cell frequency following IL-21 treatment could enhance anti-tumor protection.

In order to design proper T-cell metabolic reprogramming strategies in HIV-1-infected patients, it is critical to consider other parameters that could impede the safety and the clinical success of such treatments (Fig. 3). These parameters include the following:

### 5.1. Metabolic plasticity is also used by HIV-1 for its own agenda

Firstly, it appears that re-educating T-cells during HIV-1 infection, by ablating their glucose dependency and enhancing their metabolic plasticity, may be a good idea to directly counteract viral replication. Like any virus, HIV-1 relies on cellular metabolic resources for the completion of the viral replication cycle and the production of virions. It is now established that HIV-1 selectively infects and replicates efficiently in activated CD4 T-cells, which are primarily characterized by elevated glycolysis [83]. In fact, the replication of HIV-1 itself causes an increase of glycolytic flux in *de novo* infected CD4 T-cells [59,84,85]. Glycolysis is particularly required for virion production and is critical for the early steps of HIV-1 infection in CD4 T-cells, including HIV-1 membrane fusion and viral reverse-transcription [84,86,87]. Unfortunately, nothing in HIV-1 infection functions in a simple manner as recent evidence indicates that “wiring” CD4 T-cell metabolism to OxPhoS also augments their susceptibility to HIV-1 infection [86]. Clerc *et al.* came to this conclusion by first demonstrating that CD4 T-cell mitochondrial biomass was related to their oxygen consumption. They then showed that the CD4 T-cell with the highest mitochondrial biomass had higher percentage of infected cells following HIV-1 virion exposure. To conclude, the authors determine that glutaminolysis, one of the major catabolic pathways that fuels mitochondrial OxPhoS, is required for optimal viral infection.

Secondly, a major challenge, in fully curing HIV-1 infection, is the generation of latent viral reservoirs in different tissues that are refractory to ART [88]. HIV-1 reservoirs correspond to long-lived infected and resting cells that are able to persist for long periods. Previous data show that HIV-1 reservoirs are mainly located in memory CD4 T-cell pools that are driven by cell survival and homeostatic proliferation [89,90]. Since resting memory CD4 T-cells preferentially use mitochondrial FAO to meet their energetic demands [30], it is reasonable to hypothesize that therapeutic strategies aiming at helping T-cells using carbon sources other than glucose, such as fatty acids, may be detrimental for the host by maintaining HIV-1 reservoirs. Lastly, non-dividing and latently HIV-1-infected macrophages representing another viral reservoir in tissues use glutamine/glutamate as a major energy source, which is not the case for uninfected macrophages. Additionally, by using a combination of inhibitors, it is possible to force macrophages to use a single fuel source and assess their ability to shift one source to another. Castellano *et al.* found that the capacity of HIV-1-infected macrophages to use fatty acid, glutamine, or glucose, when it is the only available metabolic fuel was significantly higher than uninfected controls [91].

In summary, although it is easy to postulate the beneficial impact in reducing the use of glycolysis, data also indicate that other carbon sources, such as fatty acids and glutamine, may help in maintaining HIV-1 reservoirs.

### 5.2. Metabolic plasticity may allow for the maintenance of exhausted T-cells

Mediated by prolonged over-stimulation, T-cell exhaustion is a phenomenon of dysfunction or physical elimination of antigen-specific T-cells that has been largely documented in context of persistent HIV-1 infection [61,62,92]. Despite our increasing understanding of the molecular mechanisms associated with the transcriptional regulation of T-cell exhaustion, such as the dominant role of PD-1 signaling [62,93,94], it also is imperative to explore the metabolic mechanisms that control their altered nature. While activated T-cells preferentially use glycolysis for their energy demands, some evidence indicates that long-term antigen exposure modifies their metabolic requirements. Indeed, Bettonville M. *et al.* have recently shown that T-cells, when chronically stimulated, appear to rely on FAO and OxPhoS for energy production, similarly to long-lasting memory cells [95]. The reliance on FAO from chronically stimulated T-cells (T-cells<sub>CS</sub>) is mainly confirmed from two

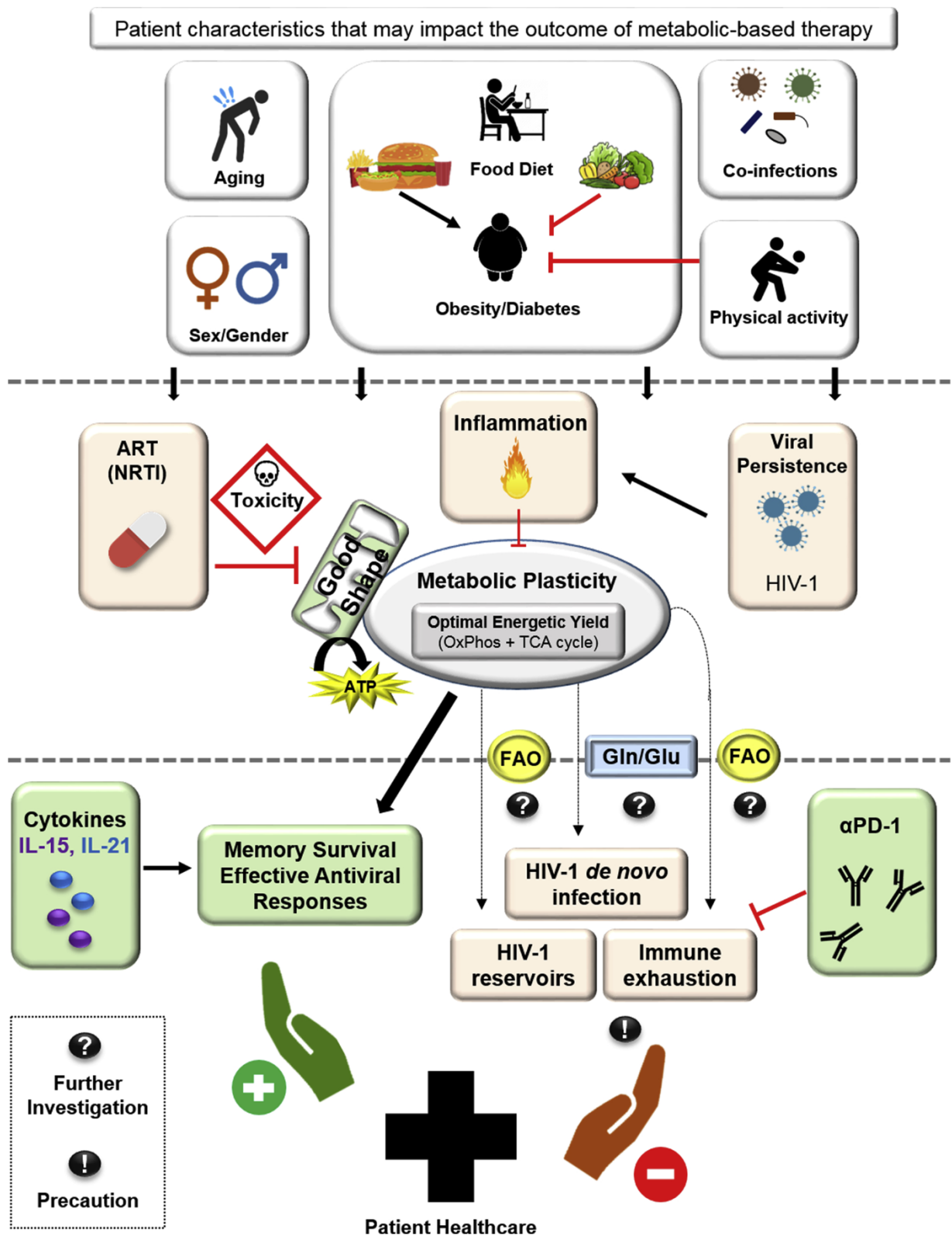


Fig. 3. Schematic representation of the complexity of designing therapeutic strategies for T-cell metabolic reprogramming during HIV-1 infection. Many factors may contribute or, conversely, prevent successful metabolic reprogramming in specific anti-HIV-1 T-cells. In some instances, patient conditions such as aging or obesity, and ART toxicity may impact mitochondria integrity and prevent an effective metabolic reprogramming in patients. On the other hand, promoting metabolic plasticity in T-cells may enhance HIV-1 reservoir seeding and exhausted cell maintenance. Abbreviations: ART, antiretroviral therapy; ATP, adenosine triphosphate;  $\alpha$ PD-1, neutralizing anti-programmed cell death 1 antibodies; FAO, Fatty acid oxidation; Gln/Glu, glutamine/glutamate; NRTI, nucleoside reverse transcriptase inhibitor; OxPhoS, oxidative phosphorylation; TCA, tricarboxylic acid.



complementary observations. Firstly, T-cells<sub>CS</sub> have a higher capacity to uptake fatty acids when compared to early effector T cells. Secondly, a treatment with etomoxir, the inhibitor of the fatty acid transporter CPT-1A, inhibits IFN- $\gamma$  production in T-cells<sub>CS</sub>, but not early effector T-cells. [95]. Another study indicates that PD-1 signaling is responsible for inhibiting glycolysis and glutamine metabolism while promoting FAO in exhausted T-cells [96]. Once again, CPT-1A is central to this conclusion, as Patsoukis et al. demonstrate that PD-L1 treatments upregulate its expression on CD4 T-cells leading to the increased oxidation of palmitate [96].

In summary, the enhancement of fatty acid use may be responsible for the survival and maintenance of exhausted T-cells in patients during persistent HIV-1 infection.

### 5.3. ART may lead to mitochondria damage in patients

In order to ensure a positive outcome from strategies that aim at promoting T-cell plasticity of mitochondrial metabolism, it is logical to postulate that infected patients have to keep functional mitochondria even after years of ART. Today, ART is systematically administered to people as early as they are diagnosed with HIV-1, regardless of the fact of if they are natural controllers or not [70]. ART reduces morbidity and mortality among HIV-1-infected patients and, as such, can be considered as a therapeutic success. However, the administration of chemical regimens in infected patients is associated with long-term adverse effects that include mitochondria toxicity. For example, mitochondria toxicity appears to be an underlying mechanism for several long-term adverse effects that are related to ART, especially treatments that include nucleoside reverse transcriptase inhibitors (NRTI) in their regimen [97–100]. Mitochondria toxicity mediated by NRTI has also been described with lower ATP production, reactive oxygen species production, inhibition of electron transport chain complexes, impairment of FAO, and altered membrane potential [101]. Maagaard A. et al. have confirmed that HIV-1-infected subjects exposed to NRTI display mitochondrial DNA loss in both CD4 and CD8 T-cells [102]. Interestingly, Angin M et al. have recently provided a table that summarizes several drug regimens and NRTI mitochondria toxicity index which may be helpful in designing safer ART administration to patients [58]. Additionally, this data may also provide the initial step in our efforts to reduce to a minimum of ART mediated mitochondria toxicity in HIV1-infected patients.

Altogether, these data indicate that some classes of chemical regimens, which are usually administered to patients, may impair proper mitochondria functioning and interfere with therapeutic success of metabolism-targeted strategies.

## 6. Concluding remarks

Thanks to the newly available experimental platforms such as the live-cell metabolic assay Seahorse device that can measure key parameters of mitochondrial function, researchers begin to realize that the maintenance of highly functional anti-HIV-1 T-cells is associated with their ability to use diverse metabolic resources. Therefore, it is tempting to believe that we are therapeutically close to be able to boost anti-viral immunity in patients by developing new combinatory strategies employing metabolism-targeting chemical tools.

However, to use such combinatory treatments to help cure the infected population, it will first be necessary to consider all parameters that are affected by such treatments and to ultimately confirm, by the use of *in vivo* models, that such treatments provide more benefits for the host rather than for the virus.

## Declaration of Competing Interest

The authors declare no conflict of financial and personal interests

## References

- [1] C. Rio Bartulos, M.B. Rogers, T.A. Williams, E. Gentekaki, H. Brinkmann, R. Cerff, M.F. Liaud, A.B. Hehl, N.R. Yarlett, A. Gruber, P.G. Kroth, M. van der Giezen, Mitochondrial glycolysis in a major lineage of eukaryotes, *Genome Biol. Evol.* 10 (9) (2018) 2310–2325.
- [2] J.B. Spinelli, M.C. Haigis, The multifaceted contributions of mitochondria to cellular metabolism, *Nat. Cell Biol.* 20 (7) (2018) 745–754.
- [3] C.N.S. Breda, G.G. Davanzo, P.J. Basso, N.O. Saraiva Camara, P.M.M. Moraes-Vieira, Mitochondria as central hub of the immune system, *Redox Biol.* 26 (2019) 101255.
- [4] I.A. Stanley, S.M. Ribeiro, A. Gimenez-Cassina, E. Norberg, N.N. Daniai, Changing appetites: the adaptive advantages of fuel choice, *Trends Cell Biol.* 24 (2) (2014) 118–127.
- [5] B.H. Goodpaster, L.M. Sparks, Metabolic flexibility in health and disease, *Cell Metab.* 25 (5) (2017) 1027–1036.
- [6] A.S. Rambold, E.L. Pearce, Mitochondrial dynamics at the interface of immune cell metabolism and function, *Trends Immunol.* 39 (1) (2018) 6–18.
- [7] G. Desdin-Mico, G. Soto-Heredero, M. Mittelbrunn, Mitochondrial activity in T cells, *Mitochondrion* 41 (2018) 51–57.
- [8] R.K. Goltink, R.L. Kyle, E.L. Pearce, Unraveling the complex interplay between T cell metabolism and function, *Annu. Rev. Immunol.* 36 (2018) 461–488.
- [9] M.D. Buck, D. O'Sullivan, R.I. Klein Goltink, J.D. Curtis, C.H. Chang, D.E. Sanin, J. Qiu, O. Kretz, D. Braas, G.J. van der Windt, Q. Chen, S.C. Huang, C.M. O'Neill, B.T. Edelson, E.J. Pearce, H. Sesaki, T.B. Huber, A.S. Rambold, E.L. Pearce, Mitochondrial dynamics controls T cell fate through metabolic programming, *Cell* 166 (1) (2016) 63–76.
- [10] M.D. Buck, D. O'Sullivan, E.L. Pearce, T cell metabolism drives immunity, *J. Exp. Med.* 212 (9) (2015) 1345–1360.
- [11] C.H. Chang, E.L. Pearce, Emerging concepts of T cell metabolism as a target of immunotherapy, *Nat. Immunol.* 17 (4) (2016) 364–368.
- [12] N.M. Chapman, M.R. Boothby, H. Chi, Metabolic coordination of T cell quiescence and activation, *Nat. Rev. Immunol.* (2019).
- [13] N. Jones, E.E. Vincent, J.G. Cronin, S. Panetti, M. Chambers, S.R. Holm, S.E. Owens, N.J. Francis, D.K. Finlay, C.A. Thornton, Akt and STAT5 mediate naive human CD4+ T-cell early metabolic response to TCR stimulation, *Nat. Commun.* 10 (1) (2019) 2042.
- [14] C.M. Cham, G. Driessens, J.P. O'Keefe, T.F. Gajewski, Glucose deprivation inhibits multiple key gene expression events and effector functions in CD8+ T cells, *Eur. J. Immunol.* 38 (9) (2008) 2438–2450.
- [15] S.R. Jacobs, C.E. Herman, N.J. Maciver, J.A. Wofford, H.L. Wieman, J.J. Hammen, J.C. Rathmell, Glucose uptake is limiting in T cell activation and requires CD28-mediated Akt-dependent and independent pathways, *J. Immunol.* 180 (7) (2008) 4476–4486.
- [16] A.V. Menk, N.E. Scharping, R.S. Moreci, X. Zeng, C. Guy, S. Salvatore, H. Bae, J. Xie, H.A. Young, S.G. Wendell, G.M. Delgoffe, Early TCR signaling induces rapid aerobic glycolysis enabling distinct acute T cell effector functions, *Cell Rep.* 22 (6) (2018) 1509–1521.
- [17] P.M. Gubser, G.R. Bantug, L. Razik, M. Fischer, S. Dimeloe, G. Hoenger, B. Durovic, A. Jauch, C. Hess, Rapid effector function of memory CD8+ T cells requires an immediate-early glycolytic switch, *Nat. Immunol.* 14 (10) (2013) 1064–1072.
- [18] R. Geiger, J.C. Rieckmann, T. Wolf, C. Basso, Y. Feng, T. Fuhrer, M. Kogadeeva, P. Picotti, F. Meissner, M. Mann, N. Zamboni, F. Sallusto, A. Lanzavecchia, L-Arginine modulates T cell metabolism and enhances survival and anti-tumor activity, *Cell* 167 (3) (2016) 829–842 e13.
- [19] M.O. Johnson, M.M. Wolf, M.Z. Madden, G. Andrejeva, A. Sugiura, D.C. Contreras, D. Maseda, M.V. Liberti, K. Paz, R.J. Kishton, M.E. Johnson, A.A. de Cubas, P. Wu, G. Li, Y. Zhang, D.C. Newcomb, A.D. Wells, N.P. Restifo, W.K. Rathmell, J.W. Locasale, M.L. Davila, B.R. Blazar, J.C. Rathmell, Distinct regulation of Th17 and Th1 cell differentiation by glutaminase-dependent metabolism, *Cell* 175 (7) (2018) 1780–1795 e19.
- [20] E.H. Ma, G. Bantug, T. Griss, S. Condotta, R.M. Johnson, B. Samborska, N. Mainolfi, V. Suri, H. Guak, M.L. Balmer, M.J. Verway, T.C. Raissi, H. Tsui, G. Boukhaled, S. Henriques da Costa, C. Frezza, C.M. Krawczyk, A. Friedman, M. Manfredi, M.J. Richer, C. Hess, R.G. Jones, Serine is an essential metabolite for effector T cell expansion, *Cell Metab.* 25 (2) (2017) 482.
- [21] N. Ron-Harel, J.M. Ghergurovich, G. Notarangelo, M.W. LaFleur, Y. Tsubosaka, A.H. Sharpe, J.D. Rabinowitz, M.C. Haigis, T cell activation depends on extracellular alanine, *Cell Rep.* 28 (12) (2019) 3011–3021 e4.
- [22] N. Ron-Harel, D. Santos, J.M. Ghergurovich, P.T. Sage, A. Reddy, S.B. Lovitch, N. Dephore, F.K. Satterstrom, M. Sheffer, J.B. Spinelli, S. Gygi, J.D. Rabinowitz, A.H. Sharpe, M.C. Haigis, Mitochondrial biogenesis and proteome remodeling promote one-carbon metabolism for T cell activation, *Cell Metab.* 24 (1) (2016) 104–117.

- [23] F. Baixauli, R. Acin-Perez, C. Villarroya-Beltri, C. Mazzeo, N. Nunez-Andrade, E. Gabande-Rodriguez, M.D. Ledesma, A. Blazquez, M.A. Martin, J.M. Falcon-Perez, J.M. Redondo, J.A. Enriquez, M. Mittelbrunn, Mitochondrial respiration controls lysosomal function during inflammatory T cell responses, *Cell Metab.* 22 (3) (2015) 485–498.
- [24] M. Nakaya, Y. Xiao, X. Zhou, J.H. Chang, M. Chang, X. Cheng, M. Blonska, X. Lin, S.C. Sun, Inflammatory T cell responses rely on amino acid transporter ASCT2 facilitation of glutamine uptake and mTORC1 kinase activation, *Immunity* 40 (5) (2014) 692–705.
- [25] A. Bachem, C. Makhlof, K.J. Binger, D.P. de Souza, D. Tull, K. Hochheiser, P.G. Whitney, D. Fernandez-Ruiz, S. Dahling, W. Kastenmuller, J. Jonsson, E. Gressier, A.M. Lew, C. Perdomo, A. Kupz, W. Figgett, F. Mackay, M. Oleshansky, B.E. Russ, I.A. Parish, A. Kallies, M.J. McConville, S.J. Turner, T. Gebhardt, S. Bedoui, Microbiota-derived short-chain fatty acids promote the memory potential of antigen-activated CD8(+) T cells, *Immunity* 51 (2) (2019) 285–297 e5.
- [26] L. Berod, C. Friedrich, A. Nandan, J. Freitag, S. Hagemann, K. Harmrolfs, A. Sandouk, C. Hesse, C.N. Castro, H. Bahre, S.K. Tschirner, N. Gorinski, M. Gohmert, C.T. Mayer, J. Huehn, E. Ponimaskin, W.R. Abraham, R. Muller, M. Lochner, T. Sparwasser, De novo fatty acid synthesis controls the fate between regulatory T and T helper 17 cells, *Nat. Med.* 20 (11) (2014) 1327–1333.
- [27] R.D. Michalek, V.A. Gerriets, S.R. Jacobs, A.N. Macintyre, N.J. MacIver, E.F. Mason, S.A. Sullivan, A.G. Nichols, J.C. Rathmell, Cutting edge: distinct glycolytic and lipid oxidative metabolic programs are essential for effector and regulatory CD4+ T cell subsets, *J. Immunol.* 186 (6) (2011) 3299–3303.
- [28] D. O'Sullivan, G.J. van der Windt, S.C. Huang, J.D. Curtis, C.H. Chang, M.D. Buck, J. Qiu, A.M. Smith, W.Y. Lam, L.M. DiPlato, F.F. Hsu, M.J. Birnbaum, E.J. Pearce, E.L. Pearce, Memory CD8(+) T cells use cell-intrinsic lipolysis to support the metabolic programming necessary for development, *Immunity* 41 (1) (2014) 75–88.
- [29] E.L. Pearce, M.C. Walsh, P.J. Cejas, G.M. Harms, H. Shen, L.S. Wang, R.G. Jones, Y. Choi, Enhancing CD8 T-cell memory by modulating fatty acid metabolism, *Nature* 460 (7251) (2009) 103–107.
- [30] D.D. Taub, C.S. Hesdorffer, L. Ferrucci, K. Madara, J.B. Schwartz, E.J. Goetzl, Distinct energy requirements for human memory CD4 T-cell homeostatic functions, *FASEB J.* 27 (1) (2013) 342–349.
- [31] G.J. van der Windt, B. Everts, C.H. Chang, J.D. Curtis, T.C. Freitas, A. Amiel, E.J. Pearce, E.L. Pearce, Mitochondrial respiratory capacity is a critical regulator of CD8+ T cell memory development, *Immunity* 36 (1) (2012) 68–78.
- [32] R.I. Klein Geltink, D. O'Sullivan, M. Corrado, A. Bremser, M.D. Buck, J.M. Buescher, E. Firat, X. Zhu, G. Niedermann, G. Caputa, B. Kelly, U. Warthorst, A. Rensing-Ehl, R.L. Kyle, L. Vandersarren, J.D. Curtis, A.E. Patterson, S. Lawless, K. Grzes, J. Qiu, D.E. Sanin, O. Kretz, T.B. Huber, S. Janssens, B.N. Lambrecht, A.S. Rambold, E.J. Pearce, E.L. Pearce, Mitochondrial priming by CD28, *Cell* 171 (2) (2017) 385–397 e11.
- [33] G.R. Bantug, M. Fischer, J. Grahlert, M.L. Balmer, G. Unterstab, L. Develioglu, R. Steiner, L. Zhang, A.S.H. Costa, P.M. Gubser, A.V. Burgener, U. Sauder, J. Loliger, R. Belle, S. Dimeloe, J. Lotscher, A. Jauch, M. Recher, G. Honger, M.N. Hall, P. Romero, C. Frezza, C. Hess, Mitochondria-endoplasmic reticulum contact sites function as immunometabolic hubs that orchestrate the rapid recall response of memory CD8(+) T cells, *Immunity* 48 (3) (2018) 542–555 e6.
- [34] K.E. Beckermann, S.O. Dudzinski, J.C. Rathmell, Dysfunctional T cell metabolism in the tumor microenvironment, *Cytokine Growth Factor Rev.* 35 (2017) 7–14.
- [35] C.H. Chang, J. Qiu, D. O'Sullivan, M.D. Buck, T. Noguchi, J.D. Curtis, Q. Chen, M. Gindin, M.M. Gubin, G.J. van der Windt, E. Tonc, R.D. Schreiber, E.J. Pearce, E.L. Pearce, Metabolic competition in the tumor microenvironment is a driver of cancer progression, *Cell* 162 (6) (2015) 1229–1241.
- [36] W.C. Cheng, P.C. Ho, Metabolic tug-of-war in tumors results in diminished T cell antitumor immunity, *Oncotarget* 5 (4) (2016) e1119355.
- [37] P.C. Ho, J.D. Bihuniak, A.N. Macintyre, M. Staron, X. Liu, R. Amezquita, Y.C. Tsui, G. Cui, G. Micevic, J.C. Perales, S.H. Kleinstein, E.D. Abel, K.L. Inogna, S. Peske, J.W. Locasale, M.W. Bosenberg, J.C. Rathmell, S.M. Kaech, Phosphoenolpyruvate is a metabolic checkpoint of anti-tumor T cell responses, *Cell* 162 (6) (2015) 1217–1228.
- [38] M. Sukumar, J. Liu, Y. Ji, M. Subramanian, J.G. Crompton, Z. Yu, R. Roychoudhuri, D.C. Palmer, P. Muranski, E.D. Karoly, R.P. Mohney, C.A. Klebanoff, A. Lal, T. Finkel, N.P. Restifo, L. Gattinoni, Inhibiting glycolytic metabolism enhances CD8+ T cell memory and antitumor function, *J. Clin. Invest.* 123 (10) (2013) 4479–4488.
- [39] J. Qiu, M. Villa, D.E. Sanin, M.D. Buck, D. O'Sullivan, R. Ching, M. Matsushita, K.M. Grzes, F. Winkler, C.H. Chang, J.D. Curtis, R.L. Kyle, N. Van Teijlingen Bakker, M. Corrado, F. Haessler, F. Alfei, J. Edwards-Hicks, L.B. Maggi Jr., D. Zehn, T. Egawa, B. Bengsch, R.I. Klein Geltink, T. Jenuwein, E.J. Pearce, E.L. Pearce, Acetate promotes T cell effector function during glucose restriction, *Cell Rep.* 27 (7) (2019) 2063–2074 e5.
- [40] S.A. Comerford, Z. Huang, X. Du, Y. Wang, L. Cai, A.K. Witkiewicz, H. Walters, M.N. Tantawy, A. Fu, H.C. Manning, J.D. Horton, R.E. Hammer, S.L. McKnight, B.P. Tu, Acetate dependence of tumors, *Cell* 159 (7) (2014) 1591–1602.
- [41] C.A. Lyssiotis, L.C. Cantley, Acetate fuels the cancer engine, *Cell* 159 (7) (2014) 1492–1494.
- [42] T. Mashimo, K. Pichumani, V. Vemireddy, K.J. Hatanpaa, D.K. Singh, S. Sirasanagandla, S. Nannepaga, S.G. Piccirillo, Z. Kovacs, C. Foong, Z. Huang, S. Barnett, B.E. Mickey, R.J. DeBerardinis, B.P. Tu, E.A. Maher, R.M. Bachoo, Acetate is a bioenergetic substrate for human glioblastoma and brain metastases, *Cell* 159 (7) (2014) 1603–1614.
- [43] J.Y. Guo, B. Xia, E. White, Autophagy-mediated tumor promotion, *Cell* 155 (6) (2013) 1216–1219.
- [44] R.M. Perera, S. Stoykova, B.N. Nicolay, K.N. Ross, J. Fitamant, M. Boukhali, J. Lengrand, V. Deshpande, M.K. Selig, C.R. Ferrone, J. Settleman, G. Stephanopoulos, N.J. Dyson, R. Zoncu, S. Ramaswamy, W. Haas, N. Bardeesy, Transcriptional control of autophagy-lysosome function drives pancreatic cancer metabolism, *Nature* 524 (7565) (2015) 361–365.
- [45] A.M. Strohecker, J.Y. Guo, G. Karshi-Uzunbas, S.M. Price, G.J. Chen, R. Mathew, M. McMahon, E. White, Autophagy sustains mitochondrial glutamine metabolism and growth of BrafV600E-driven lung tumors, *Cancer Discov.* 3 (11) (2013) 1272–1285.
- [46] V.M. Hubbard, R. Valdor, B. Patel, R. Singh, A.M. Cuervo, F. Macian, Macroautophagy regulates energy metabolism during effector T cell activation, *J. Immunol.* 185 (12) (2010) 7349–7357.
- [47] X. Xu, K. Araki, S. Li, J.H. Han, L. Ye, W.G. Tan, B.T. Konieczny, M.W. Bruinsma, J. Martinez, E.L. Pearce, D.R. Green, D.P. Jones, H.W. Virgin, R. Ahmed, Autophagy is essential for effector CD8(+) T cell survival and memory formation, *Nat. Immunol.* 15 (12) (2014) 1152–1161.
- [48] Z. Yin, L. Bai, W. Li, T. Zeng, H. Tian, J. Cui, Targeting T cell metabolism in the tumor microenvironment: an anti-cancer therapeutic strategy, *J. Exp. Clin. Cancer Res.* 38 (1) (2019) 403.
- [49] E. Allahmoradi, S. Taghilo, M. Tehrani, H. Hossein-Nattaj, G. Janabaei, R. Shekarriz, H. Asgarian-Omran, CD4+ T cells are exhausted and show functional defects in chronic lymphocytic leukemia, *Iran. J. Immunol.* 14 (4) (2017) 257–269.
- [50] L. Baitsch, P. Baumgaertner, E. Devevre, S.K. Raghav, A. Legat, L. Barba, S. Wiekowski, H. Bouzourene, B. Deplancke, P. Romero, N. Rufer, D.E. Speiser, Exhaustion of tumor-specific CD8(+) T cells in metastases from melanoma patients, *J. Clin. Invest.* 121 (6) (2011) 2350–2360.
- [51] A. Schietinger, M. Philip, V.E. Krisnawan, E.Y. Chiu, J.J. Delrow, R.S. Basom, P. Lauer, D.G. Brockstedt, S.E. Knoblauch, G.J. Hammerling, T.D. Schell, N. Garbi, P.D. Greenberg, Tumor-specific T cell dysfunction is a dynamic antigen-driven differentiation program initiated early during Tumorigenesis, *Immunity* 45 (2) (2016) 389–401.
- [52] N.E. Scharping, A.V. Menk, R.S. Moreci, R.D. Whetstone, R.E. Dadey, S.C. Watkins, R.L. Ferris, G.M. Delgoffe, The tumor microenvironment represses T cell mitochondrial biogenesis to drive intratumoral T cell metabolic insufficiency and dysfunction, *Immunity* 45 (2) (2016) 374–388.
- [53] L.R. Cockerham, J.D. Siliciano, E. Sinclair, U. O'Doherty, S. Palmer, S.A. Yukl, M.C. Strain, N. Chomont, F.M. Hecht, R.F. Siliciano, D.D. Richman, S.G. Deeks, CD4+ and CD8+ T cell activation are associated with HIV DNA in resting CD4+ T cells, *PLoS One* 9 (10) (2014) e110731.
- [54] A. Haas, K. Zimmermann, A. Oxenius, Antigen-dependent and -independent mechanisms of T and B cell hyperactivation during chronic HIV-1 infection, *J. Virol.* 85 (23) (2011) 12102–12113.
- [55] J.M. Brenchley, D.A. Price, T.W. Schacker, T.E. Asher, G. Silvestri, S. Rao, Z. Kazzaz, E. Bornstein, O. Lambotte, D. Altmann, B.R. Blazar, B. Rodriguez, L. Teixeira-Johnson, A. Landay, J.N. Martin, F.M. Hecht, L.J. Picker, M.M. Lederman, S.G. Deeks, D.C. Douek, Microbial translocation is a cause of systemic immune activation in chronic HIV infection, *Nat. Med.* 12 (12) (2006) 1365–1371.
- [56] V. Jain, W. Hartogensis, P. Bacchetti, P.W. Hunt, H. Hatano, E. Sinclair, L. Epling, T.H. Lee, M.P. Busch, J.M. McCune, C.D. Pilcher, F.M. Hecht, S.G. Deeks, Antiretroviral therapy initiated within 6 months of HIV infection is associated with lower T-cell activation and smaller HIV reservoir size, *J. Infect. Dis.* 208 (8) (2013) 1202–1211.
- [57] N.I. Wada, L.P. Jacobson, J.B. Margolick, E.C. Breen, B. Macatangay, S. Penugonda, O. Martinez-Maza, J.H. Bream, The effect of HAART-induced HIV suppression on circulating markers of inflammation and immune activation, *AIDS* 29 (4) (2015) 463–471.
- [58] M. Angin, S. Volant, C. Passaes, C. Lecroux, V. Monceaux, M.-A. Dillies, J.C. Valle-Casuso, G. Pancino, B. Vaslin, R. Le Grand, L. Weiss, C. Goujard, L. Meyer, F. Boufassa, M. Müller-Trutwin, O. Lambotte, A. Sáez-Cirión, Metabolic plasticity of HIV-specific CD8+ T cells is associated with enhanced antiviral potential and natural control of HIV-1 infection, *Nature Metabolism* 1 (7) (2019) 704–716.
- [59] J.A. Hollenbaugh, J. Munger, B. Kim, Metabolite profiles of human immunodeficiency virus infected CD4+ T cells and macrophages using LC-MS/MS analysis, *Virology* 415 (2) (2011) 153–159.
- [60] C.S. Palmer, M. Ostrowski, M. Gouillou, L. Tsai, D. Yu, J. Zhou, D.C. Henstridge, A. Maisa, A.C. Hearps, S.R. Lewin, A. Landay, A. Jaworowski, J.M. McCune, S.M. Crowe, Increased glucose metabolic activity is associated with CD4+ T-cell activation and depletion during chronic HIV infection, *AIDS* 28 (3) (2014) 297–309.
- [61] C.L. Day, D.E. Kaufmann, P. Kiepiela, J.A. Brown, E.S. Moodley, S. Reddy, E.W. Mackey, J.D. Miller, A.J. Leslie, C. DePierres, Z. Mncube, J. Duraiswamy, B. Zhu, Q. Eichbaum, M. Altfeld, E.J. Wherry, H.M. Coovadia, P.J. Goulder, P. Klennerman, R. Ahmed, G.J. Freeman, B.D. Walker, PD-1 expression on HIV-specific T cells is associated with T-cell exhaustion and disease progression, *Nature* 443 (7109) (2006) 350–354.
- [62] L. Trautmann, L. Janbazian, N. Chomont, E.A. Said, S. Gimmig, B. Bessette, M.R. Boulassel, E. Delwart, H. Sepulveda, R.S. Balderas, J.P. Routy, E.K. Haddad,



- R.P. Sekaly, Upregulation of PD-1 expression on HIV-specific CD8+ T cells leads to reversible immune dysfunction, *Nat. Med.* 12 (10) (2006) 1198–1202.
- [63] L.R. Cockerham, V. Jain, E. Sinclair, D.V. Glidden, W. Hartogenesis, H. Hatano, P.W. Hunt, J.N. Martin, C.D. Pilcher, R. Sekaly, J.M. McCune, F.M. Hecht, S.G. Deeks, Programmed death-1 expression on CD4(+) and CD8(+) T cells in treated and untreated HIV disease, *AIDS* 28 (12) (2014) 1749–1758.
- [64] C.D.T. Deguit, M. Hough, R. Hoh, M. Krone, C.D. Pilcher, J.N. Martin, S.G. Deeks, J.M. McCune, P.W. Hunt, R.L. Rutishauser, Some aspects of CD8+ T-Cell exhaustion are associated with altered T-Cell mitochondrial features and ROS content in HIV infection, *JAIDS Journal of Acquired Immune Deficiency Syndromes* 82 (2) (2019) 211–219.
- [65] M. Korenca, M. Byrne, E. Richter, B.T. Schultz, P. Juszczak, J.A. Ake, A. Ganesan, J.F. Okulicz, M.L. Robb, B. de Los Reyes, S. Winning, J. Fandrey, T.H. Burgess, S. Esser, N.L. Michael, B.K. Agan, H. Streck, Effect of HIV infection and antiretroviral therapy on immune cellular functions, *JCI Insight* 4 (12) (2019).
- [66] J. Ogando, M.E. Saez, J. Santos, C. Nuevo-Tapiolas, M. Gut, A. Esteve-Codina, S. Heath, A. Gonzalez-Perez, J.M. Cuevas, R.A. Lallace, S. Manes, PD-1 signaling affects cristae morphology and leads to mitochondrial dysfunction in human CD8(+) T lymphocytes, *J. Immunother. Cancer* 7 (1) (2019) 151.
- [67] Y. Cao, L. Qin, L. Zhang, J. Safrit, D.D. Ho, Virologic and immunologic characterization of long-term survivors of human immunodeficiency virus type 1 infection, *N. Engl. J. Med.* 332 (4) (1995) 201–208.
- [68] J. van Grevenynghe, R.A. Cubas, A. Noto, S. DaFonseca, Z. He, Y. Peretz, A. Filali-Mouhim, F.P. Dupuy, F.A. Procopio, N. Chomont, R.S. Balderas, E.A. Said, M.R. Boulassel, C.L. Tremblay, J.P. Routy, R.P. Sekaly, E.K. Haddad, Loss of memory B cells during chronic HIV infection is driven by Foxo3a- and TRAIL-mediated apoptosis, *J. Clin. Invest.* 121 (10) (2011) 3877–3888.
- [69] J. van Grevenynghe, F.A. Procopio, Z. He, N. Chomont, C. Riou, Y. Zhang, S. Gimmig, G. Boucher, P. Wilkinson, Y. Shi, B. Yassine-Diab, E.A. Said, L. Trautmann, M. El Far, R.S. Balderas, M.R. Boulassel, J.P. Routy, E.K. Haddad, R.P. Sekaly, Transcription factor FOXO3a controls the persistence of memory CD4(+) T cells during HIV infection, *Nat. Med.* 14 (3) (2008) 266–274.
- [70] H. Loucif, S. Gouard, X. Dagenais-Lussier, A. Murira, S. Stager, C. Tremblay, J. Van Grevenynghe, Deciphering natural control of HIV-1: a valuable strategy to achieve antiretroviral therapy termination, *Cytokine Growth Factor Rev.* 40 (2018) 90–98.
- [71] S. Ferrando-Martinez, J.P. Casazza, M. Leal, K. Machmach, M.A. Munoz-Fernandez, P. Viciana, R.A. Koup, E. Ruiz-Mateos, Differential glycolytic polyfunctional T cell maturation patterns in HIV-1 elite controllers, *J. Virol.* 86 (7) (2012) 3667–3674.
- [72] A. Saez-Cirion, M. Sinet, S.Y. Shin, A. Urrutia, P. Versmisse, C. Lacabartz, F. Boufassa, V. Avettand-Fenoel, C. Rouzioux, J.F. Delfraissy, F. Barre-Sinoussi, O. Lambotte, A. Venet, G. Pancino, A.E.H.C.S. Group, Heterogeneity in HIV suppression by CD8 T cells from HIV controllers: association with Gag-specific CD8 T cell responses, *J. Immunol.* 182 (12) (2009) 7828–7837.
- [73] K.N. Pollizzi, C.H. Patel, I.H. Sun, M.H. Oh, A.T. Waickman, J. Wen, G.M. Delgoffe, J.D. Powell, mTORC1 and mTORC2 selectively regulate CD8(+) T cell differentiation, *J. Clin. Invest.* 125 (5) (2015) 2090–2108.
- [74] K.N. Pollizzi, I.H. Sun, C.H. Patel, Y.C. Lo, M.H. Oh, A.T. Waickman, A.J. Tam, R.L. Blosser, J. Wen, G.M. Delgoffe, J.D. Powell, Asymmetric inheritance of mTORC1 kinase activity during division dictates CD8(+) T cell differentiation, *Nat. Immunol.* 17 (6) (2016) 704–711.
- [75] F.Z. Chowdhury, Z. Ouyang, M. Buzon, B.D. Walker, M. Lichterfeld, X.G. Yu, Metabolic pathway activation distinguishes transcriptional signatures of CD8+ T cells from HIV-1 elite controllers, *AIDS* 32 (18) (2018) 2669–2677.
- [76] R. Nardacci, A. Amendola, F. Ciccosanti, M. Corazzari, V. Esposito, C. Vlassi, C. Taibi, G.M. Fimia, F. Del Nonno, G. Ippolito, G. D’Offizi, M. Piacentini, Autophagy plays an important role in the containment of HIV-1 in nonprogressor-infected patients, *Autophagy* 10 (7) (2014) 1167–1178.
- [77] J.P. Routy, S. Isnard, R. Ramendra, Following the elite: targeting immunometabolism to limit HIV pathogenesis, *EBioMedicine* 42 (2019) 8–9.
- [78] L. Tarancon-Diez, E. Rodriguez-Gallego, A. Rull, J. Peraire, C. Vilades, I. Portilla, M.R. Jimenez-Leon, V. Alba, P. Herrero, M. Leal, E. Ruiz-Mateos, F. Vidal, On behalf of ECRIS integrated in the Spanish AIDS Research Network, Immunometabolism is a key factor for the persistent spontaneous elite control of HIV-1 infection, *EBioMedicine* 42 (2019) 86–96.
- [79] C. Ferrari, C. Boni, M. Rossi, A. Vecchi, V. Barili, D. Laccabue, P. Fiscaro, G. Missale, T cell regulation in HBV-related chronic liver disease, *J. Hepatol.* 66 (5) (2017) 1096–1098.
- [80] P. Fiscaro, V. Barili, B. Montanini, G. Acerbi, M. Ferracin, F. Guerrieri, D. Salerno, C. Boni, M. Massari, M.C. Cavallo, G. Grossi, T. Giuberti, P. Lampertico, G. Missale, M. Leverro, S. Ottonello, C. Ferrari, Targeting mitochondrial dysfunction can restore antiviral activity of exhausted HBV-specific CD8 T cells in chronic hepatitis B, *Nat. Med.* 23 (3) (2017) 327–336.
- [81] A. Schurich, L.J. Pallett, D. Jajbhay, J. Wijngaarden, I. Otano, U.S. Gill, N. Hansi, P.T. Kennedy, E. Nastouli, R. Gilson, C. Frezza, S.M. Henson, M.K. Maini, Distinct metabolic requirements of exhausted and functional virus-specific CD8 T cells in the same host, *Cell Rep.* 16 (5) (2016) 1243–1252.
- [82] R. Loschinski, M. Bottcher, A. Stoll, H. Bruns, A. Mackensen, D. Mougiakakos, IL-21 modulates memory and exhaustion phenotype of T-cells in a fatty acid oxidation-dependent manner, *Oncotarget* 9 (17) (2018) 13125–13138.
- [83] J.C. Valle-Casuso, M. Angin, S. Volant, C. Passaes, V. Monceaux, A. Mikhailova, K. Bourdic, V. Avettand-Fenoel, F. Boufassa, M. Sitbon, O. Lambotte, M.I. Thoulouze, M. Muller-Trutwin, N. Chomont, A. Saez-Cirion, Cellular metabolism is a major determinant of HIV-1 reservoir seeding in CD4(+) T cells and offers an opportunity to tackle infection, *Cell Metab.* 29 (3) (2019) 611–626 e5.
- [84] A. Hagedus, M. Kavanagh Williamson, H. Huthoff, HIV-1 pathogenicity and virion production are dependent on the metabolic phenotype of activated CD4+ T cells, *Retrovirology* 11 (2014) 98.
- [85] S. Loisel-Meyer, L. Swainson, M. Craveiro, L. Oburoglu, C. Mongellaz, C. Costa, M. Martinez, F.L. Cosset, J.L. Bhattini, L.A. Herzenberg, L.A. Herzenberg, K.R. Atkuri, M. Sitbon, S. Kinet, E. Verhoeyen, N. Taylor, Glut1-mediated glucose transport regulates HIV infection, *Proc Natl Acad Sci U S A* 109 (7) (2012) 2549–2554.
- [86] I. Clerc, D. Abba Moussa, Z. Vahlas, S. Tardito, L. Oburoglu, T.J. Hope, M. Sitbon, V. Dardalhon, C. Mongellaz, N. Taylor, Entry of glucose- and glutamine-derived carbons into the citric acid cycle supports early steps of HIV-1 infection in CD4 T cells, *Nature Metabolism* 1 (7) (2019) 717–730.
- [87] C.A. Coomer, I. Carlon-Andre, M. Iliopoulou, M.L. Dustin, E.B. Compeer, A.A. Compton, S. Padilla-Parra, Single-cell glycolytic activity regulates membrane tension and HIV-1 fusion, *BioRxiv* (2019).
- [88] T.J. Cory, The importance of targeting HIV reservoirs: preclinical insights on current and potential therapeutic opportunities, *Expert Opin. Ther. Targets* 23 (12) (2019) 987–989.
- [89] N. Chomont, M. El-Far, P. Ancuta, L. Trautmann, F.A. Procopio, B. Yassine-Diab, G. Boucher, M.R. Boulassel, G. Ghattas, J.M. Brenchley, T.W. Schacker, B.J. Hill, D.C. Douek, J.P. Routy, E.K. Haddad, R.P. Sekaly, HIV reservoir size and persistence are driven by T cell survival and homeostatic proliferation, *Nat. Med.* 15 (8) (2009) 893–900.
- [90] E. Lee, P. Bacchetti, J. Milush, W. Shao, E. Boritz, D. Douek, R. Fromentin, T. Liegler, R. Hoh, S.G. Deeks, F.M. Hecht, N. Chomont, S. Palmer, Memory CD4 + T-Cells expressing HLA-DR contribute to HIV persistence during prolonged antiretroviral therapy, *Front. Microbiol.* 10 (2019) 2214.
- [91] P. Castellano, L. Prevedel, S. Valdebenito, E.A. Eugenin, HIV infection and latency induce a unique metabolic signature in human macrophages, *Sci. Rep.* 9 (1) (2019) 3941.
- [92] M. El-Far, R. Halwani, E. Said, L. Trautmann, M. Doroudchi, L. Janbazian, S. Fonseca, J. van Grevenynghe, B. Yassine-Diab, R.P. Sekaly, E.K. Haddad, T-cell exhaustion in HIV infection, *Curr. HIV/AIDS Rep.* 5 (1) (2008) 13–19.
- [93] C. Petrovas, J.P. Casazza, J.M. Brenchley, D.A. Price, E. Gostick, W.C. Adams, M.L. Precozio, T. Schacker, M. Roederer, D.C. Douek, R.A. Koup, PD-1 is a regulator of virus-specific CD8+ T cell survival in HIV infection, *J. Exp. Med.* 203 (10) (2006) 2281–2292.
- [94] V. Velu, K. Titanji, B. Zhu, S. Husain, A. Pladevega, L. Lai, T.H. Vanderford, L. Chennareddi, G. Silvestri, G.J. Freeman, R. Ahmed, R.R. Amara, Enhancing HIV-specific immunity in vivo by PD-1 blockade, *Nature* 458 (7235) (2009) 206–210.
- [95] M. Bettonville, S. d’Aria, K. Weatherly, P.E. Porporato, J. Zhang, S. Bousbata, P. Sonveaux, M.Y. Braun, Long-term antides exposure irreversibly modifies metabolic requirements for T cell function, *Elife* 7 (2018).
- [96] N. Patsoukis, K. Bardhan, P. Chatterjee, D. Sari, B. Liu, L.N. Bell, E.D. Karoly, G.J. Freeman, V. Petkova, P. Seth, L. Li, V.A. Boussiotis, PD-1 alters T-cell metabolic reprogramming by inhibiting glycolysis and promoting lipolysis and fatty acid oxidation, *Nat. Commun.* 6 (2015) 6692.
- [97] W. Lewis, B.J. Day, W.C. Copeland, Mitochondrial toxicity of NRTI antiviral drugs: an integrated cellular perspective, *Nat. Rev. Drug Discov.* 2 (10) (2003) 812–822.
- [98] B.A. Payne, I.J. Wilson, C.A. Hately, R. Horvath, M. Santibanez-Koref, D.C. Samuels, D.A. Price, P.F. Chinnery, Mitochondrial aging is accelerated by anti-retroviral therapy through the clonal expansion of mtDNA mutations, *Nat. Genet.* 43 (8) (2011) 806–810.
- [99] S. Selvaraj, M. Ghebremichael, M. Li, Y. Foli, A. Langs-Barlow, A. Ogbuagu, L. Barakat, E. Tubridy, R. Edifor, W. Lam, Y.C. Cheng, E. Paintsil, Antiretroviral therapy-induced mitochondrial toxicity: potential mechanisms beyond polymerase-gamma inhibition, *Clin. Pharmacol. Ther.* 96 (1) (2014) 110–120.
- [100] R.L. Smith, J.M.E. Tan, M.J. Jonker, A. Jongejan, T. Buisson, S. Veldhuijzen, A.H.C. van Kampen, S. Brul, H. van der Spek, Beyond the polymerase-gamma theory: production of ROS as a mode of NRTI-induced mitochondrial toxicity, *PLoS One* 12 (11) (2017) e0187424.
- [101] N. Apostolova, A. Blas-Garcia, J.V. Esplugues, Mitochondrial toxicity in HAART: an overview of in vitro evidence, *Curr. Pharm. Des.* 17 (20) (2011) 2130–2144.
- [102] A. Maagaard, M. Holberg-Petersen, G. Lovgarden, M. Holm, F.O. Pettersen, D. Kvale, Distinct mechanisms for mitochondrial DNA loss in T and B lymphocytes from HIV-infected patients exposed to nucleoside reverse-transcriptase inhibitors and those naive to antiretroviral treatment, *J. Infect. Dis.* 198 (10) (2008) 1474–1481.



Hamza Loucif. Hamza Loucif is a Ph.D. student at the INRS-Institut Armand Frappier (Laval, Quebec) under the supervision of Dr. Julien Van Grevenynghe. He obtained his B.Sc. in Applied and Fundamental Biochemistry (2015) followed by a Master in Biotechnology and Molecular Pathology (2017) at the University of Science and Technology of Algiers (USTHB, Algeria). He concluded his Master's internship at the department of human virology, HIV/AIDS national reference laboratory of Institut Pasteur d'Algérie, studying the role of Nitric Oxide (NO) in HIV-1 immuno-pathogenesis. He is currently studying the role of autophagy process as a novel immune correlate exhibited by HIV-1-specific CD8 T cells in "Elite Controllers", a unique subset of individuals known to possess the ability to naturally co-exist with the virus for a long term without progressing to the AIDS stage.

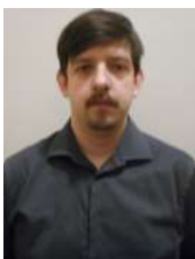




**Xavier Dagenais-Lussier, Ph.D.** Xavier Dagenais-Lussier is a Ph.D. student under the supervision of Dr. van Grevenynghe at the INRS-Institut Armand Frappier (Laval, Quebec). He graduated for his Master in 2016, and previously obtained his B.Sc. in Microbiology at the University of Sherbrooke (Quebec) in 2014. He recently published a study showing that increased expression of the interferon stimulated gene USP18 participates to defective memory CD4 T-cell survival during the early phase of HIV-1 primary infection (*PLOS Pathogens*, 2019). Currently, Xavier Dagenais-Lussier is studying the metabolic plasticity in CD4 T-cell subsets during HIV-1 infection.



**Cherifa Beji, M.Sc.** Cherifa Beji is a Master's student at the INRS-Institut Armand Frappier under the supervision of Dr. Julien Van Grevenynghe. She obtained her engineering degree in biology from the National Institute of Applied Sciences and Technology (Tunisia). She did her end of studies internship at Queen's University Cancer Research Institute, where she used R programming to expound on the use of DNA methylation as a biomarker for aggressive prostate cancer. She is currently working on the immunomodulatory effect of tetrahydrocannabinol (THC) during HIV-1 infection.



**Roman Telittchenko, B.Sc.** Roman Telittchenko is a master student under the supervision of Albert Descoteaux at the "Institut Armand Frappier-INRS". He has received his B.Sc. in the Microbiology and Immunology program at McGill University (Montreal, Québec, Canada) in 2017. Today, Roman Telittchenko is studying the *Leishmania* parasite. Specifically, he is studying whether genetic exchanges take place between two *Leishmania amazonensis* parasites in a communal vacuole in the context of an infected host cell.



**Dr. Jean-Pierre Routy, M.D.**, is an attending physician in the Division of Hematology and Chronic Viral Illness Service at the McGill University Health Centre (Glen site, Montreal). Additionally, he is a tenured professor in the department of Medicine at McGill University. Dr. Routy received his medical degree and completed his residency in Hematology-Oncology in 1986 at the University of Aix-Marseille (France). Today, his main focus is on understanding HIV-1 pathogenesis and restoring the immune system of individuals infected with HIV-1. He is also the principle investigator of a national cohort of patients recently infected with HIV, which aims to understand the natural history of HIV infection, concentrating on its effect in the gut.



**Julien van Grevenynghe, Ph.D.** Dr. van Grevenynghe is an assistant professor in the INRS-Institut Armand Frappier (Laval, Quebec) since February 2015. Dr. van Grevenynghe obtained his Ph.D. from INSERM U456 and University of Rennes 1 (Bretagne, France). Then, he joined Dr. Rafick Sekaly's team (CR-CHUM in Montreal and VGTI in Florida) where he focused on the characterization of the transcriptional factor Foxo3a in the long-term maintenance of memory CD4 T-cells during chronic HIV-1 infection. Today, Dr. van Grevenynghe is an expert on viral pathogenesis where his laboratory studies (i) new molecular and metabolic mechanisms associated with natural immune protection in elite controllers and (ii) the involvement of metabolism by-products such as oxidative stress that occurs since HIV-1 primary-infection on memory CD4 T-cell impairments. His last publication as senior research authors were accepted in significant peer-to-peer journals including *PLOS Pathogen*, *Journal of Virology* and *Cell Reports*.

Dr. van Grevenynghe is an expert on viral pathogenesis where his laboratory studies (i) new molecular and metabolic mechanisms associated with natural immune protection in elite controllers and (ii) the involvement of metabolism by-products such as oxidative stress that occurs since HIV-1 primary-infection on memory CD4 T-cell impairments. His last publication as senior research authors were accepted in significant peer-to-peer journals including *PLOS Pathogen*, *Journal of Virology* and *Cell Reports*.

RESEARCH ARTICLE

# USP18 is a significant driver of memory CD4 T-cell reduced viability caused by type I IFN signaling during primary HIV-1 infection

Xavier Dagenais-Lussier<sup>1</sup>, Hamza Loucif<sup>1</sup>, Hugo Cadorel<sup>1</sup>, Juliette Blumberger<sup>1</sup>, Stéphane Isnard<sup>2</sup>, Mariana Gé Bego<sup>3</sup>, Éric A. Cohen<sup>3,4</sup>, Jean-Pierre Routy<sup>2</sup>, Julien van Grevenynghe<sup>1\*</sup>, for the Montreal Primary Infection Study Group<sup>1</sup>

**1** Institut national de la recherche scientifique (INRS)-Institut Armand-Frappier, 531 boulevard des Prairies, Laval, QC, Canada, **2** Chronic Viral Illness Service and Division of Hematology, McGill University Health Centre, Glen site, Montréal, Québec, Canada, **3** Institut de recherches cliniques de Montréal (IRCM), Montréal, QC, Canada, **4** Department of Microbiology, Infectiology and Immunology, Université de Montréal, Montreal, QC, Canada

<sup>†</sup> Membership of the Montreal Primary Infection Study Group is listed in the Acknowledgments.

\* [julien.vangrevenynghe@iaf.inrs.ca](mailto:julien.vangrevenynghe@iaf.inrs.ca)





RESEARCH ARTICLE

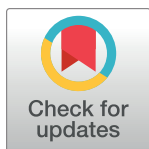
# USP18 is a significant driver of memory CD4 T-cell reduced viability caused by type I IFN signaling during primary HIV-1 infection

Xavier Dagenais-Lussier<sup>1</sup>, Hamza Loucif<sup>1</sup>, Hugo Cadorel<sup>1</sup>, Juliette Blumberger<sup>1</sup>, Stéphane Isnard<sup>2</sup>, Mariana Gé Bego<sup>3</sup>, Éric A. Cohen<sup>3,4</sup>, Jean-Pierre Routy<sup>2</sup>, Julien van Grevenynghe<sup>1\*</sup>, for the Montreal Primary Infection Study Group<sup>†</sup>

**1** Institut national de la recherche scientifique (INRS)-Institut Armand-Frappier, 531 boulevard des Prairies, Laval, QC, Canada, **2** Chronic Viral Illness Service and Division of Hematology, McGill University Health Centre, Glen site, Montréal, Québec, Canada, **3** Institut de recherches cliniques de Montréal (IRCM), Montréal, QC, Canada, **4** Department of Microbiology, Infectiology and Immunology, Université de Montréal, Montreal, QC, Canada

<sup>†</sup> Membership of the Montreal Primary Infection Study Group is listed in the Acknowledgments.

\* [julien.vangrevenynghe@iaf.inrs.ca](mailto:julien.vangrevenynghe@iaf.inrs.ca)



 OPEN ACCESS

**Citation:** Dagenais-Lussier X, Loucif H, Cadorel H, Blumberger J, Isnard S, Bego MG, et al. (2019) USP18 is a significant driver of memory CD4 T-cell reduced viability caused by type I IFN signaling during primary HIV-1 infection. *PLoS Pathog* 15 (10): e1008060. <https://doi.org/10.1371/journal.ppat.1008060>

**Editor:** Daniel C. Douek, Vaccine Research Center, UNITED STATES

**Received:** May 15, 2019

**Accepted:** August 31, 2019

**Published:** October 28, 2019

**Copyright:** © 2019 Dagenais-Lussier et al. This is an open access article distributed under the terms of the [Creative Commons Attribution License](https://creativecommons.org/licenses/by/4.0/), which permits unrestricted use, distribution, and reproduction in any medium, provided the original author and source are credited.

**Data Availability Statement:** All relevant data are within the manuscript and its Supporting Information files.

**Funding:** This study was supported by FRQ-S (grant number: 261098 to XDL), Banting Research Foundation, and the Natural Sciences and Engineering Research Council of Canada (NSERC). The funders had no role in study design, data collection and analysis, decision to publish, or preparation of the manuscript.

## Abstract

The loss of Memory CD4 T-cells (Mem) is a major hallmark of HIV-1 immuno-pathogenesis and occurs early during the first months of primary infection. A lot of effort has been put into understanding the molecular mechanisms behind this loss, yet they still have not been fully identified. In this study, we unveil the unreported role of USP18 in the deleterious effects of sustained type I IFN signaling on Mem, including HIV-1-specific CD4 T-cells. We find that interfering with IFN-I signaling pathway in infected patients, notably by targeting the interferon-stimulated gene USP18, resulted in reduced PTEN expression similar to those observed in uninfected control donors. We show that AKT activation in response to cytokine treatment, T-cell receptor (TcR) triggering, as well as HIV-1 Gag stimulation was significantly improved in infected patients when PTEN or USP18 were inhibited. Finally, our data demonstrate that higher USP18 in Mem from infected patients prevent proper cell survival and long-lasting maintenance in an AKT-dependent manner. Altogether, we establish a direct role for type I IFN/USP18 signaling in the maintenance of total and virus-specific Mem and provide a new mechanism for the reduced survival of these populations during primary HIV-1 infection.

## Author summary

In this study, we expand our knowledge of how type I interferons (IFN-I) leads to memory CD4 T-cell defective survival by unveiling the molecular mechanism behind such impairments, placing USP18 at its center. Our data further deciphers the specific USP18-related mechanism that is responsible for such impairments by implicating AKT inhibition in a PTEN-dependent manner. Our findings also point to a potential use of neutralizing anti-interferon  $\alpha/\beta$  receptor antibodies to rescue the defective memory CD4 T-cell survival

**Competing interests:** The authors have declared that no competing interests exist.

during HIV-1 infection, even in HIV-1 specific CD4 T-cell. To conclude, our findings provide the characterization of the molecular pathway leading to disturbances caused by sustained IFN-I signaling which occurs early during primary HIV-1 infection, complementing current knowledge which placed sustained IFN-I signaling as detrimental to the host during this infection.

## Introduction

The maintenance of memory CD4 T-cells (Mem) represents a key component for long-lasting immune protection during persistent infections with human immunodeficiency virus type 1 (HIV-1) and simian immunodeficiency virus (SIV) [1–4]. In this context, the elite controllers, who naturally control HIV-1 infection for decades in the absence of anti-retroviral therapy (ART), display the ability to maintain a large pool of Mem [4, 5]. For the other infected patients, loss of Mem occurs in the first months of HIV-1 infection, which exacerbates viral progression [6]. This loss depends on multiple molecular mechanisms, including metabolic disturbances, and is driven by prolonged inflammation alongside viral persistence [6–9]. Recently, our group identified a critical metabolic disturbance in the form of increased kynurenine levels in Mem from HIV-1-infected patients leading to higher production of reactive oxygen species and reducing cell responsiveness to IL-2 cytokine [6]. However, our knowledge of the different molecular mechanisms responsible for these immune defects remains incomplete as a full normalization of those defects is still unachieved. Therefore, we need to identify new factors responsible for these impairments and, more importantly, we need to establish an overall network regarding the relations between such impairments. Shedding light on such a network will enable better treatment, since individual factors are not enough to understand the full clinical picture of the disease.

Type I interferons (IFN-I) are necessary in establishing an efficient adaptive and acquired immune response, especially in acute viral infections, and are largely produced by plasmacytoid dendritic cells (pDC) following their stimulation [10, 11]. After binding the interferon $_{\alpha/\beta}$  receptor (IFNAR), IFN-I trigger the activation of interferon-stimulated genes (ISG) through the Janus kinase/STAT signaling pathway. These ISG include various intrinsic restriction factors, cytokines, chemokines, and co-stimulatory molecules [10, 12–14]. During acute viral infections, IFN-I expression is subject to negative regulation, which controls cytokine levels upon viral clearance [10]. However, in the case of persistent viral infections, such as HIV-1, sustained production of IFN- $\alpha$  is observed and is mainly driven by viremia and systemic inflammation [15–20]. Increasing evidence shows that the sustained IFN-I production during persistent viral infections can be detrimental for the host and directly participates in immune impairments [21–27]. Such impairments include the expression of inhibitory factors that reduce antiviral immunity, T-cell hyper activation and cell exhaustion as well as HIV-specific T-cell dysfunctions [17, 21, 22, 27–29]. However, it remains unknown to what extent and by which molecular mechanisms sustained IFN-I signaling affects the survival of Mem and contributes to the loss of this population during primary HIV-1 infection.

As such, we investigated whether sustained IFN-I signaling during the early and later stages of HIV-1 infection impairs Mem survival and by which mechanisms these perturbations might occur. Our data show that Mem from infected patients display increased expression of the ISG ubiquitin specific peptidase 18 (USP18), also known as UBP43. In the past two decades, several functions of USP18 have been discovered: this protein is not only an isopeptidase, but also a major regulator of IFN-I signaling [30]. Under specific circumstances, USP18

binds to IFNAR2, one the subunit of the IFNAR dimer, and compete with JAK preventing proper activation of the pathway [31]. Therefore, USP18 functions as a maestro of many biological pathways in various cell types. However, no information are available regarding the contribution of USP18 on HIV-1 immuno-pathogenesis, we investigated its impact on Mem survival and function in infected subjects. Our study identified a critical role of USP18 in the loss of Mem including HIV-1-specific cells during HIV-1 infection. Our findings also demonstrate our ability to rescue Mem from apoptosis in a PTEN- and AKT-dependent manner when USP18 is specifically targeted.

Altogether, this study puts USP18/PTEN/AKT at the center of the molecular pathway by which sustained IFN-I signaling leads to Mem impairments during HIV-1 infection.

## Results

### Mem from HIV-1-infected subjects display higher USP18 expression, which can be normalized by IFNAR blockade

Despite indications of an IFN-I signature in HIV-1 infection [22, 32–34], the status of IFN-I signaling intrinsic to Mem and how it may impair cell survival in infected subjects are unknown. First, we compared the plasma levels of IFN- $\alpha$  from primary-infected (PHI) and chronically-infected (CHI) subjects to age-matched uninfected donor controls (HIV<sup>free</sup>). [S1 Table](#) summarizes the clinical and virological data for all selected PHI and CHI subjects including viral loads (VL) and CD4 counts. Similarly to others, we found higher IFN- $\alpha$  levels in plasma from HIV-1-infected subjects compared to uninfected controls ([Fig 1A](#)) [15–20]. We also found that the subjects with high plasma IFN- $\alpha$  levels were the ones with the highest VL (correlation between the two parameters:  $P = 0.0187$ ,  $r = 0.5334$ ;  $n = 19$ ) ([S1 Fig](#)).

To assess the IFN-I signaling intrinsic to Mem, we next measured in PHI, CHI and HIV<sup>free</sup> subjects the constitutive phosphorylation levels of STAT1 and IRF7, two IFN-I-induced transcription factors, in *ex vivo* Mem by PhosFlow. Here, by using a multicolor-parameter flow cytometric analysis as previously described, we investigated IFN-I signaling on all Mem subsets classified by three surface markers, CD45RA, CD27 and CCR7 [35, 36]. Total Mem were defined by a CD3<sup>+</sup>CD4<sup>+</sup>CD45RA<sup>neg</sup> phenotype ([S2A Fig](#)). Our data showed increased constitutive levels for STAT1 pY701, STAT1 pS727 and IRF7 pS477/S479 in Mem from PHI and CHI subjects when compared to HIV<sup>free</sup> donors ([Fig 1B](#), [S2B Fig](#) and [S3A Fig](#)). The increased levels of the three phospho-proteins during HIV-1 infection were observed across all memory subsets that are determined by differential expression of CD27 and CCR7 markers. In this context, memory subsets include the long-lasting CD27<sup>+</sup>CCR7<sup>+</sup> central memory CD4 T-cells (T<sub>CM</sub>) as well as CD27<sup>neg</sup>CCR7<sup>neg</sup> effector memory CD4 T-cells (T<sub>EM</sub>) ([Fig 1B](#) and [S3A Fig](#)). Although CD45RA<sup>+</sup> CD4 T-cells also displayed higher phospho-protein levels in HIV-1-infected subjects when compared to uninfected controls, their levels did not correlate with the cell frequencies unlike Mem ([S2B and S2C Fig](#)). Increased IFN-I signaling in Mem from infected subjects was further confirmed by assessing the mRNA expression of several ISGs such as restriction factors (MxA, OAS.1 and SAMHD1), transcription regulators (IRF1 and IRF7), ISG<sub>15</sub>, ISG<sub>56</sub> and USP18 ([Fig 1C](#)). Of note, we found similar mRNA expression of STAT1 in Mem for all study groups ([Fig 1C](#), last lane).

Considering the lack of literature surrounding USP18 expression during HIV-1 infection, we next compared its protein levels in the three groups of subjects. We found increased constitutive USP18 expression in Mem from PHI and CHI compared to HIV<sup>free</sup> subjects ( $P = 0.0001$  and  $P = 0.002$ , respectively for PHI and CHI subjects;  $n = 10$  [MFI]) ([Fig 1D](#)). Percentages of USP18<sup>+</sup> Mem were also higher in PHI and CHI subjects when compared to uninfected controls ( $36.2 \pm 15.3$  [PHI],  $29.8 \pm 12.3$  [CHI] and  $7.9 \pm 4$  [HIV<sup>free</sup>];  $P < 0.0001$  and  $P = 0.0014$ ,

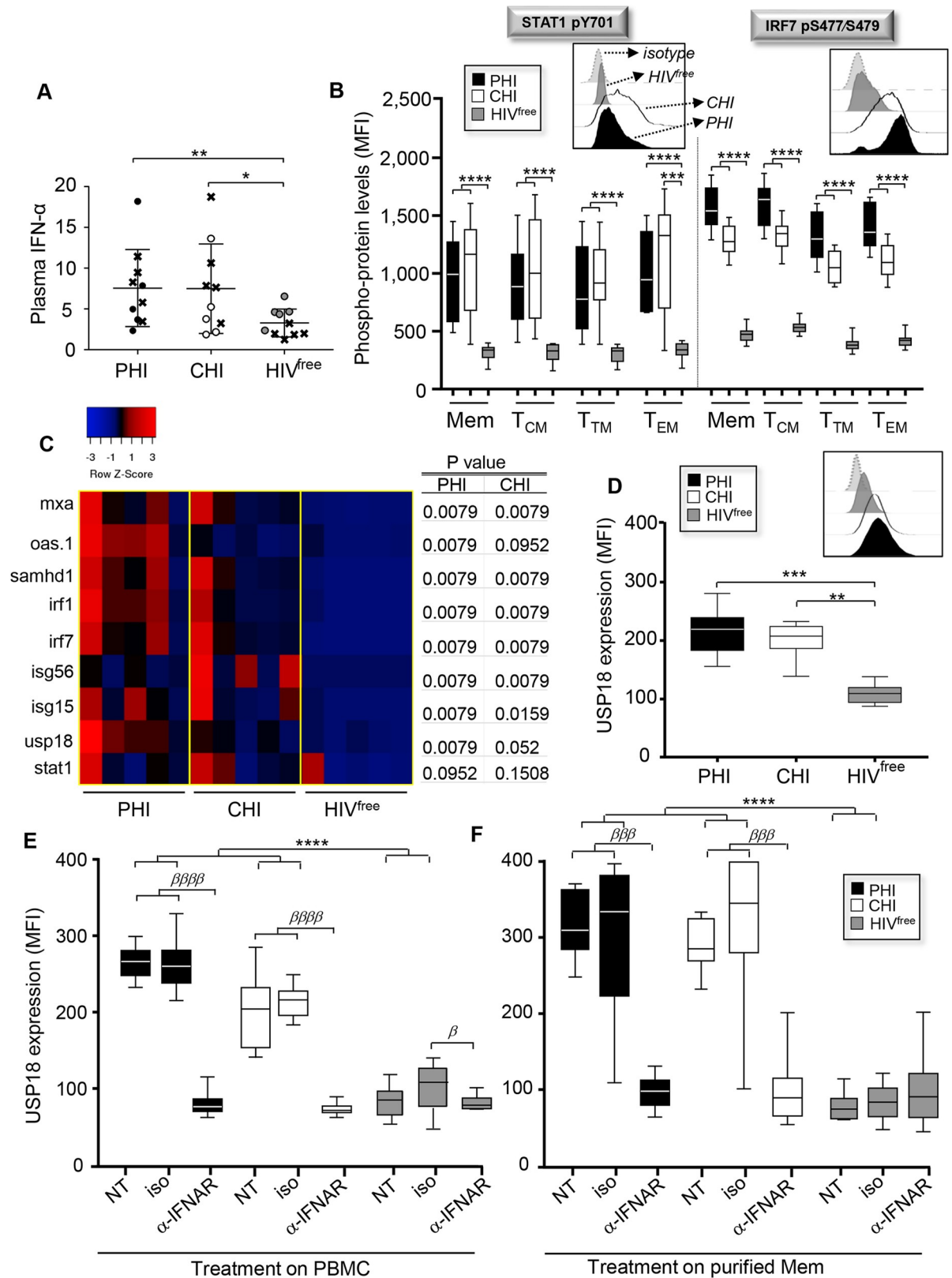


**Fig 1. Mem from PHI and CHI display higher expression levels of USP18.** (A) Plasma concentration of IFN- $\alpha$  in pg/mL for PHI, CHI and HIV<sup>free</sup> subjects. Crosses represent subjects used in C. (n = 10). (B) Levels of STAT1 pY701 and IRF7 pS477/479 on



7-AAD<sup>neg</sup>CD3<sup>+</sup>CD4<sup>+</sup>CD45RA<sup>neg</sup> Mem, as well as CD27<sup>+</sup>CCR7<sup>+</sup> central memory (T<sub>CM</sub>), CD27<sup>+</sup>CCR7<sup>neg</sup> transitional memory (T<sub>TM</sub>), and CD27<sup>neg</sup>CCR7<sup>neg</sup> effector memory (T<sub>EM</sub>) subsets (MFI, mean fluorescence intensity) (n = 10). Representative histograms including isotype control are shown above. (C) Heat map representation of gene expression related to IFN-I signaling determined by real time RT-PCR on *ex vivo* Mem. The Z-score is the number of standard deviations from the mean data point. Reds are higher than the mean, blacks close to it and blues under it. Table shows P values of PHI or CHI compared to HIV<sup>free</sup> (n = 5). (D) Expression of USP18 in *ex vivo* Mem from PHI, CHI and HIV<sup>free</sup> (MFI) (n = 10). Representative histograms are also shown above. (E,F) Expression levels of USP18 in Mem after 24 hours of neutralizing  $\alpha$ -IFNAR treatment (MFI) (n = 10). (E)  $\alpha$ -IFNAR, its respective isotype control or no treatment (NT) have been administrated either on total PBMC or (F) directly on purified Mem. The error bars indicate standard deviations from the means.  $\beta$ , symbol used for paired t test (comparison between treated Mem and control). \*, symbol used for Mann-Whitney test (comparison between study groups).

<https://doi.org/10.1371/journal.ppat.1008060.g001>

respectively for PHI and CHI) (S4A Fig). We confirmed increased USP18 expression in purified Mem from PHI and CHI subjects when compared to HIV<sup>free</sup> controls by western blot (S4B and S4C Fig). Unsurprisingly, antiviral therapy (ART), when administrated early during the first months of infection and for approximately 2.5 years, led to viral suppression alongside a full normalization of both plasma IFN- $\alpha$  levels and intrinsic USP18 expressions in Mem (S1 Table and S5A and S5B Fig). To assess whether increased USP18 expression levels in Mem from viremic subjects were associated with higher expression of IFN <sub>$\alpha/\beta$</sub>  receptors (IFNAR), we looked at the surface levels of both IFNAR1 and IFNAR2 in PHI, CHI and HIV<sup>free</sup> subjects. Not only our data did not show increased expression of IFNAR in infected subjects, but we even found reduced constitutive expression of IFNAR1 in PHI when compared to uninfected controls (S6A and S6B Fig). Similarly, increased USP18 expression levels during HIV-1 infection could not be explained by different ratios of Mem subsets as no significant differences were found between the study groups (S6C Fig). Finally, to test our ability to interfere with USP18 expression by blocking IFN-I signaling, peripheral blood mononuclear cells (PBMC) or purified Mem for all groups were cultured with neutralizing antibodies against the IFN <sub>$\alpha/\beta$</sub>  receptor ( $\alpha$ -IFNAR) or respective isotype Ig control for 24 hours before assessing USP18 levels. Our data showed that the  $\alpha$ -IFNAR treatment normalized USP18 levels in Mem from PHI and CHI subjects (Fig 1E and 1F). Of note, the presence of Ig controls did not impact USP18 levels as compared to untreated Mem (Fig 1E and 1F).

Altogether, our results show increases of USP18 expression in Mem from HIV-1-infected subjects and confirm the efficacy of IFNAR blockade in normalizing their USP18 levels at 24 post-treatment in the range of those from uninfected controls.

### Higher USP18 expression in Mem from HIV-1-infected subjects prevents optimal AKT activation in response to cytokine stimulation in a PTEN-dependent manner

Recently, data collected on lung cancer cell lines established USP18 as a potential regulator of PTEN protein levels and stability (41). To investigate whether higher USP18 expression may regulate PTEN expression in Mem during HIV-1 infection, we first assessed the constitutive *ex vivo* levels of PTEN in PHI, CHI, ART<sup>+</sup> and HIV<sup>free</sup> subjects. We found that PHI and CHI subjects displayed higher levels of PTEN compared to uninfected controls ( $P < 0.0001$ ; n = 10 [MFI]) (Fig 2A). Similarly, the percentages of PTEN<sup>+</sup> Mem were higher in PHI and CHI subjects when compared to HIV<sup>free</sup> donors ( $63.3 \pm 17.9$  [PHI],  $53.8 \pm 16.2$  [CHI] and  $9.9 \pm 7.3$  [HIV<sup>free</sup>];  $P < 0.0001$ ) (S7A Fig). Of note, Mem from ART<sup>+</sup> subjects displayed similar expression of PTEN than those from HIV<sup>free</sup> controls (S5C Fig). We found highly significant correlation between USP18 and PTEN expression levels in Mem for all tested subjects ( $P < 0.0001$ ,  $r = 0.9511$ ; n = 30) (Fig 2B).

Next, we aimed to investigate whether interfering with USP18 levels impacts PTEN expression in Mem from HIV-1-infected subjects. PBMC from PHI, CHI and HIV<sup>free</sup> subjects were



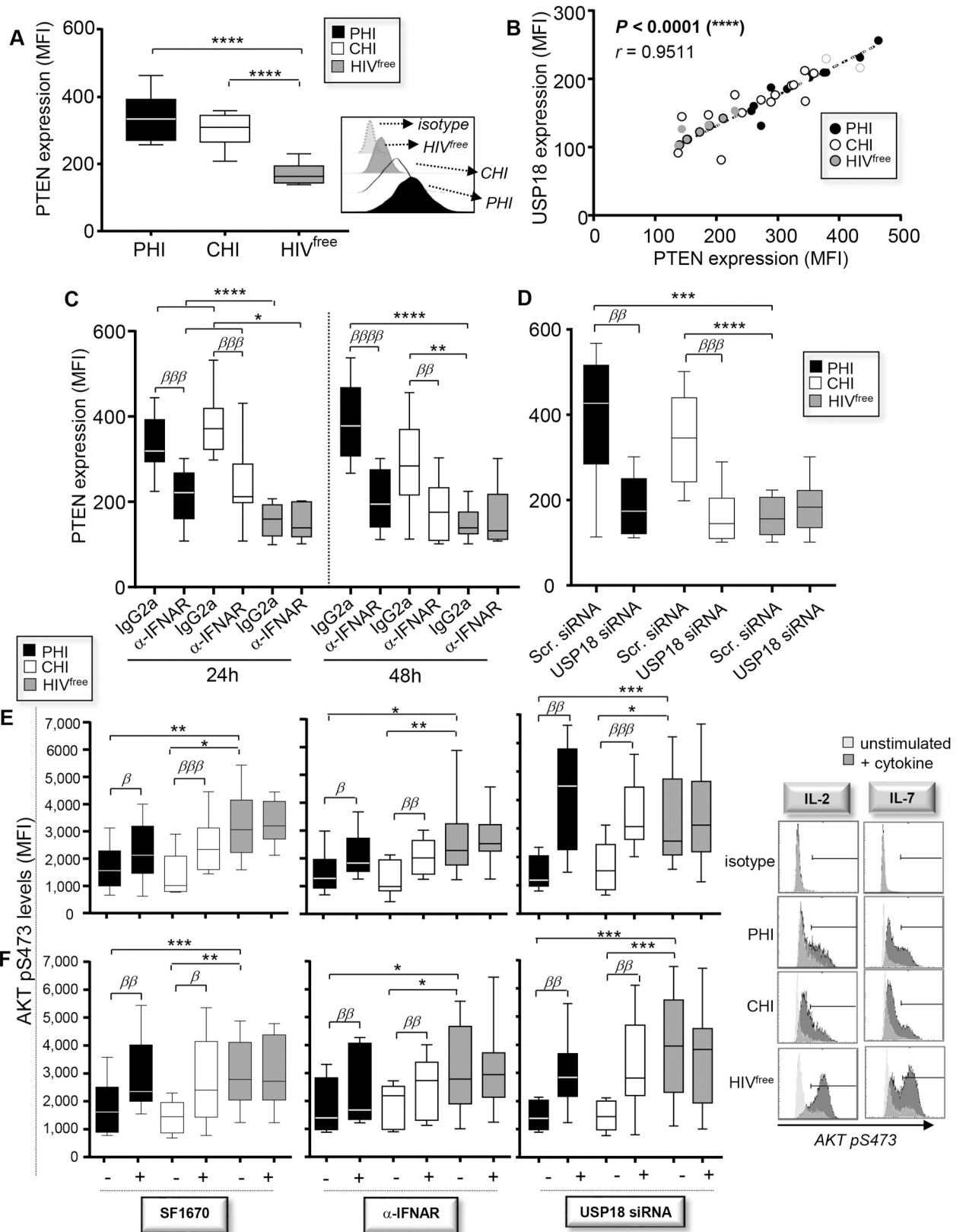


**Fig 2. High USP18 expression in Mem from PHI and CHI impairs AKT activation.** (A) *Ex vivo* PTEN expression levels in Mem from PHI, CHI and HIV<sup>free</sup> subjects (MFI) (n = 10). Representative histograms including isotype control are also shown above. (B) Correlations between USP18

expression and PTEN expression in Mem for all subjects (n = 30). (C) PTEN expression levels in Mem that have been treated for 24 or 48 hours with  $\alpha$ -IFNAR or its respective isotype control (n = 10). (D) Expression of PTEN in Mem that have been transfected with siRNA specific for USP18 or with scrambled siRNA (n = 10). (E, F) Levels of AKT pS473 following 15 minutes of IL-2 (E) or IL-7 (F) stimulation in Mem that have been pre-treated 48 hours with SF1670 (left),  $\alpha$ -IFNAR or its respective isotype control (middle), or transfected or not for 48 hours with specific USP18 siRNA (right) (n = 10). Representative histograms for AKT p473 expression in cytokine-stimulated Mem for all groups of subjects including isotype control are also shown on the right side. The error bars indicate standard deviations from the means.  $\beta$ , symbol used for paired *t* test (comparison between treated Mem and control). \*, symbol used for Mann-Whitney test (comparison between study groups).

<https://doi.org/10.1371/journal.ppat.1008060.g002>

first cultured with  $\alpha$ -IFNAR or isotype control for 24 and 48 hours. Intracellular levels of PTEN were then determined on Mem by flow cytometry. Our data showed that a 24h-long treatment with  $\alpha$ -IFNAR significantly reduced the levels of PTEN in PHI and CHI, yet it did not bring them down to the levels found in the HIV<sup>free</sup> group (Fig 2C). By prolonging the  $\alpha$ -IFNAR treatment to 48h, we found that the levels of PTEN in PHI and CHI were comparable to those found in HIV<sup>free</sup> subjects. To further confirm that USP18 was the ISG responsible for regulating PTEN expression in Mem during HIV-1 infection, we specifically inhibited USP18 expression in Mem using small interfering RNAs (siRNA) silencing. Briefly, purified Mem from PHI, CHI and HIV<sup>free</sup> subjects were either electroporated or transfected with siRNA specific for USP18 or with respective negative control siRNA for 2 hours, washed twice and then cultured with their autologous CD4-depleted PBMC (ratio Mem/PBMC = 1/4). Both levels of USP18 and PTEN were finally determined by flow cytometry in transfected Mem for all groups at 48 hours post-transfection. Electroporation alone or transfection with negative siRNA did not affect USP18 expression when compared to Mem that were not electroporated. In contrast, Mem from infected subjects that were transfected with USP18 siRNA displayed an average of 79.4% and 82.4% reductions in USP18 expression, respectively for PHI and CHI subjects (S7B Fig). Same as for  $\alpha$ -IFNAR treatments, USP18 silencing in Mem led to significant reductions of PTEN expression in PHI and CHI to levels comparable to the uninfected controls (Fig 2D). Of note, PTEN levels were similar between Mem that were electroporated alone and transfected with scrambled siRNA (S7C Fig).

Since PTEN is a negative regulator of PI3K/AKT signaling [37], we finally explored whether our HIV-1-infected groups had reduced AKT activation in response to IL-2 or IL-7 stimulations. We also assessed if we could rescue those activation levels by using either PTEN inhibitor SF1670,  $\alpha$ -IFNAR or USP18 siRNA. In this context, we first pre-treated PBMC for all groups with or without SF1670, neutralizing  $\alpha$ -IFNAR or its isotype control for 48 hours, and then stimulated the cells with cytokines for another round of 15 minutes before assessing AKT pS473 levels in Mem by PhosFlow. We also transfected purified Mem with USP18 siRNA or negative siRNA, cultured them with their autologous CD4-depleted PBMC for 48 hours and then added cytokines in cultures for 15 minutes before the FACS analysis. As expected, our data confirmed that Mem from PHI and CHI subjects displayed lower AKT activation in response to cytokine stimulations when compared to HIV<sup>free</sup> controls (Fig 2E and 2F and S8A Fig). Basal levels of AKT pS473 determined in Mem that were not stimulated were similar between all tested groups (S8A and S8B Fig). Transcriptional analyses performed on purified Mem that have been stimulated or not with IL-2 or IL-7 showed similar mRNA expression of AKT except in the case of IL-7 stimulated Mem from CHI subjects (S3B Fig). Interestingly, our data showed that all pre-treatments, including USP18 silencing, led to significant improvements of cytokine-induced AKT activation in Mem from PHI and CHI in the range of uninfected controls (Fig 2E and 2F). Of note, levels of cytokine-induced AKT activations were similar between Mem that were electroporated alone and transfected with scrambled siRNA. Although we confirmed reduced IL-2-induced STAT5 pY694 levels in Mem from PHI and CHI subjects as previously reported [6], pre-treatments with  $\alpha$ -IFNAR did not rescue STAT5

activation unlike AKT (S8C Fig). Finally, our data showed no significant differences for both basal and cytokine-induced AKT pS473 levels in Mem between ART<sup>+</sup> subjects and uninfected controls (S5D Fig).

Overall, our data show that interfering with USP18 expression during HIV-1 infection leads to better AKT activation in a PTEN-dependent manner.

### Higher USP18 expression in infected subjects impairs Mem protection against Fas-induced apoptosis

Since IL-2 and IL-7 play a critical role in regulating Mem survival [6, 38, 39], we next investigated their efficacy to protect Mem from Fas-induced apoptosis. To trigger Fas-induced apoptosis, we used the anti-Fas antibody (clone CH11), which activates the Fas signaling pathway in cultured cells [4, 6]. Briefly, PBMC from PHI, CHI and HIV<sup>free</sup> subjects were treated or not for 24 hours with CH11 antibody in the presence or absence of IL-2 or IL-7 stimulations. At 24 hours of culture, we assessed the numbers of apoptotic cells and apoptosis levels in Mem using Annexin-V staining for all conditions (for the constitutive or basal, and Fas-induced apoptosis). We calculated the numbers (N) of Fas-induced apoptotic Mem as determined by the formula: N of apoptotic Mem with CH11—N of apoptotic Mem without CH11. Although we found a trend to higher numbers of Annexin-V<sup>+</sup> Mem for the constitutive apoptosis in PHI and CHI when compared to HIV<sup>free</sup> controls (10,020 ± 2,473; 10,484 ± 3,785; and 7,865 ± 3,785, respectively), our data show no significant differences between the study groups (Fig 3A, left side). However, in the absence of cytokine stimulation, we found significant higher numbers of Fas-induced apoptotic Mem from PHI and CHI subjects when compared to HIV<sup>free</sup> subjects ( $P < 0.0001$ ) (Fig 3A [right side] and S9A Fig). Similar results were found when using percentages of apoptosis instead of absolute numbers of Mem (S9B Fig). We found that the stimulations with IL-2 and IL-7 led to lower numbers of Fas-induced apoptotic Mem for all tested groups. In the same sets of experiments, we further decided to evaluate the levels of Mem protection against Fas-induced apoptosis when the cells are stimulated by cytokines. The levels of Mem protection with cytokine stimulation in fold changes (FC) were determined by the formula: N of Fas-induced apoptotic Mem without cytokine / N of Fas-induced apoptotic Mem with cytokine. We found that the levels of cytokine-mediated Mem protection were significantly lower in PHI and CHI subjects when compared to HIV<sup>free</sup> controls (2.0 ± 0.5 [PHI], 2.1 ± 0.6 [CHI] and 4.3 ± 2.4 [HIV<sup>free</sup>]; 1.9 ± 0.5 [PHI], 1.6 ± 0.5 [CHI] and 4.9 ± 2.8 [HIV<sup>free</sup>], respectively for IL-2 and IL-7 stimulations;  $P \leq 0.0016$ ) (Fig 3B).

We next investigated whether cell pre-treatments with SF1670,  $\alpha$ -IFNAR, or USP18 siRNA improve cytokine-mediated Mem protection in PHI and CHI subjects. Briefly, PBMC were pre-treated with or without SF1670,  $\alpha$ -IFNAR or isotype control for 48 hours. As described below, pre-treated cells were then cultured for 24 hours in the presence or absence of CH11 antibodies and cytokines. Similarly, purified Mem were transfected with USP18 or scrambled siRNA and then cultured with their autologous CD4-depleted PBMC for 48 hours before assessing cytokine-mediated Mem protection. Not only did all pre-treatments significantly increase cytokine-mediated Mem protection in HIV-1-infected subjects, but specific USP18 silencing also brought the cell protection to levels comparable to the HIV<sup>free</sup> group (Fig 3C and 3D). We found that the increased Mem resistance to apoptosis driven by USP18 gene silencing was not associated with a reduction of Fas receptor expression (S10 Fig). Finally, we calculated the increases of cytokine-mediated Mem protection in the context of USP18 silencing for all tested groups. The increases determined in fold changes (FC) were obtained using the formula: cytokine-mediated Mem protection with USP18 siRNA / cytokine-mediated Mem protection with scrambled siRNA. Our data showed that targeting USP18 expression in

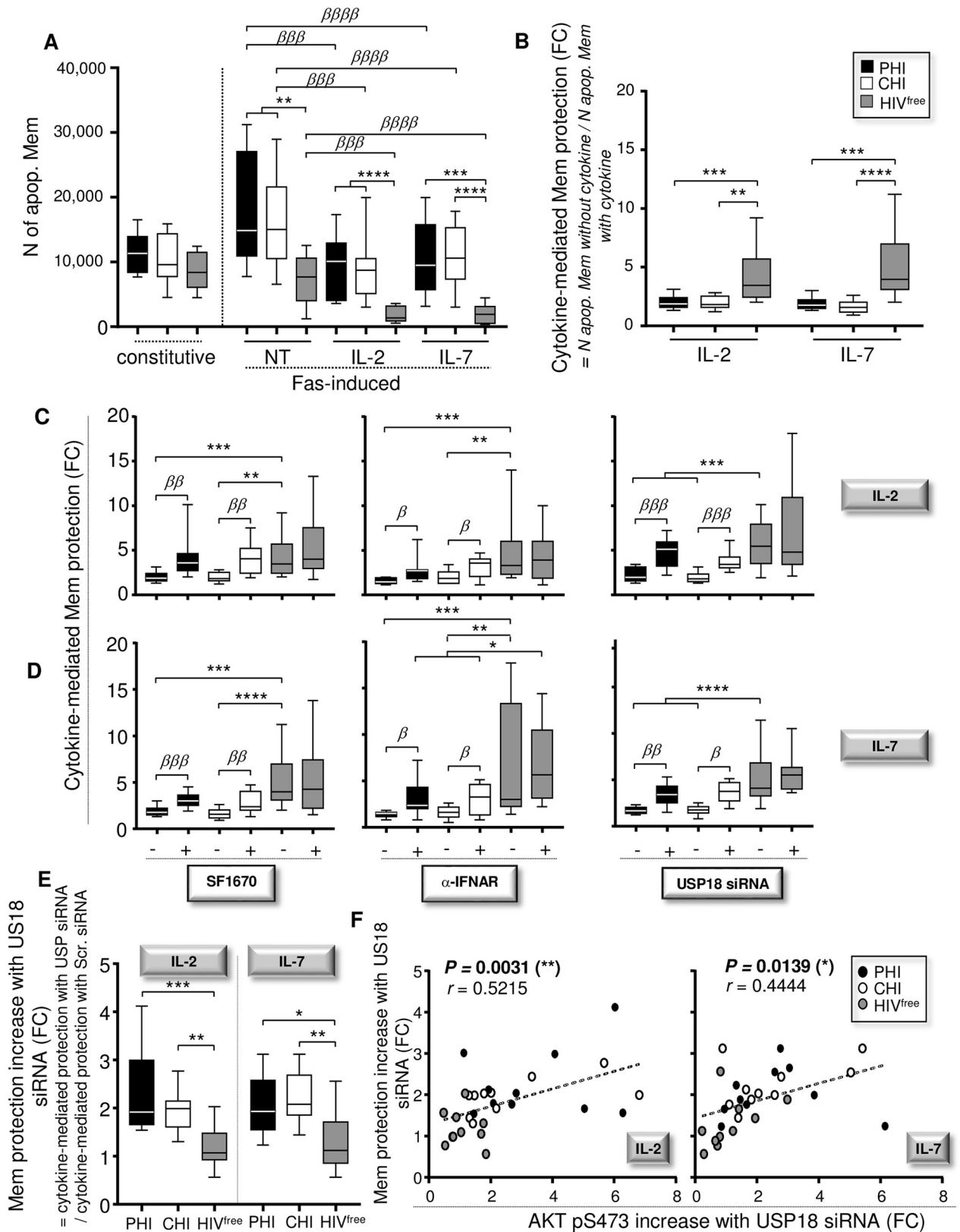


**Fig 3. Interfering with USP18 in Mem from PHI and CHI improves cytokine responses and cell resistance to apoptosis.** (A) Numbers (N) of constitutive apoptotic Mem (without any treatment) and Fas-induced apoptotic Mem in the presence or absence of IL-2 or IL-7 stimulation. N of

Fas-induced apoptotic Mem were calculated according the formula: N of apoptotic Mem with CH11 –N of apoptotic Mem without CH11 (n = 10). (B) Cytokine-mediated Mem protection are shown in fold changes (FC). Cytokine-mediated Mem protection were determined by the formula: Number of Fas-induced apoptotic Mem without cytokine / Number of Fas-induced apoptotic Mem with cytokine (n = 10). (C,D) Fold changes of IL-2- (C) or IL-7 (D)-mediated Mem protection in cells that have been pre-treated for 48h with SF1670 (left),  $\alpha$ -IFNAR or its respective isotype control (middle), or pre-transfected or not for 48 hours with USP18 siRNA (right) (n = 10). (E) Increases of Mem protection with USP18 siRNA determined in fold changes (FC). We calculated the increases of Mem protection in the context of USP18 targeting with the formula: cytokine-mediated Mem protection with USP18 siRNA / cytokine-mediated protection with scrambled siRNA. (F) Correlations between the increases of Mem protection and AKT activation after USP18 siRNA transfection in both IL-2- and IL-7-stimulated Mem (FC, fold change; n = 30). The error bars indicate standard deviations from the means.  $\beta$ , symbol used for paired *t* test (comparison between treated Mem and control). \*, symbol used for Mann-Whitney test (comparison between study groups).

<https://doi.org/10.1371/journal.ppat.1008060.g003>

PHI and CHI subjects led to significant increases of cytokine-mediated Mem protection (Fig 3E). We found highly significant correlations between the increases of Mem protection against Fas-induced apoptosis and AKT activation in both IL-2- and IL-7-stimulated Mem in the context of USP18 gene silencing ( $P = 0.0031$ ,  $r = 0.5215$  and  $P = 0.0139$ ,  $r = 0.4444$  respectively; n = 30) (Fig 3F).

In summary, we show that interfering with USP18 during primary HIV-1 infection protects Mem from apoptosis in a PTEN and AKT-dependent manner and decreases the numbers of apoptotic Mem.

### Interfering with USP18 expression in HIV-1-infected subjects improves long-lasting Mem maintenance in an AKT-dependent manner

Since the TcR triggering results in rapid activation of PI3K/AKT signaling [39, 40], we decided to investigate if this activation was lower in Mem from the PHI and CHI groups compared to the HIV<sup>free</sup> group and if interfering with PTEN, IFN-I signaling or specifically with USP18 would rescue this activation. First, PBMC from the three study groups were pre-treated or not with SF1670,  $\alpha$ -IFNAR or isotype control for 48 hours, before being stimulated with anti-CD3 and anti-CD28 antibodies (Abs) for an additional 15 minutes. Levels of AKT pS473 were finally determined in activated Mem by PhosFlow for all conditions of cultures. We also activated purified Mem with anti-CD3 and anti-CD28 Abs, transduced them with lentiviral CRISPR/Cas9 vectors mediating USP18 gene editing (lentiviral vectors for USP18 knock-out; LV<sub>USP18 KO</sub>) or control lentiviral vectors (LV<sub>Ctrl</sub>) for 4 hours, washed them twice and cultured them for 48 hours with their autologous CD4-depleted PBMC. At 48 hours post-transduction, cells were subjected to another 15-minute-long round of TcR activation before assessing AKT activation levels. Although the basal levels of AKT pS473 were similar in un-activated Mem from all tested groups, our data showed that AKT activation in response to TcR triggering was systematically lower in Mem from PHI and CHI subjects when compared to HIV<sup>free</sup> donors (Fig 4A). Both pre-treatments of Mem with SF1670 or  $\alpha$ -IFNAR led to significant improvements of AKT activation in response to TcR triggering to levels comparable to those in the HIV<sup>free</sup> group (Fig 4A, left and middle panels). We found that a 48 hour-long Mem transduction with lentiviral CRISPR/Cas9 vectors mediated USP18 gene editing resulted in more than 87% inhibition of protein levels (S11A Fig). Of note, Mem that were transduced with control lentiviral vectors displayed similar USP18 expression when compared to uninfected Mem. Similarly to cell pre-treatments, we found that specifically interfering with USP18 expression in activated Mem led to significant improvements of AKT activation to levels comparable to those of the HIV<sup>free</sup> group (Fig 4A, right panels).

Considering that Mem are first and foremost defined by their long-lasting maintenance, we next assessed the ability of Mem from PHI, CHI, and HIV<sup>free</sup> subjects to persist up to 28 days of culture in response to multiple rounds of TcR triggering as previously done [4, 41]. Briefly, purified Mem were first stimulated with anti-CD3 and anti-CD28 antibodies in the presence



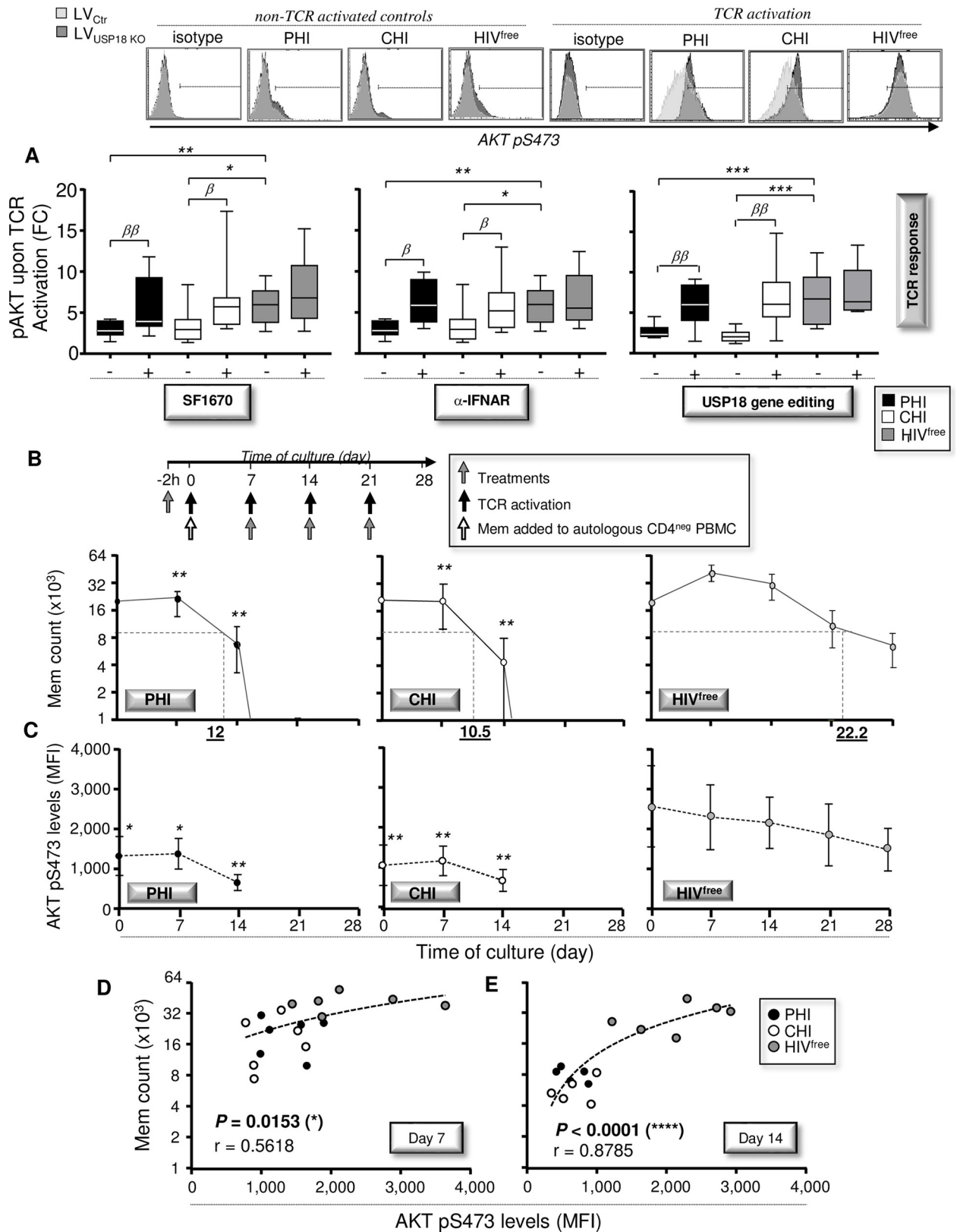


**Fig 4. Reduced pAKT S473 after TcR triggering in PHI and CHI affects long-lasting Mem maintenance.** (A) Levels of AKT pS473 following TcR activation for 30 minutes in Mem that have been pre-treated for 48h with SF1670 (left),  $\alpha$ -IFNAR or its respective isotype control (middle).

Levels of AKT pS473 in response to a 30 minute-long TcR activation have also been assessed in Mem that have been pre-transduced or not with LV<sub>USP18 KO</sub> for 48 hours (right) (n = 10). Representative histograms for AKT pS473 expression for all conditions including the non-TCR activated and isotype controls are also shown in the upper side. (B) Mem counts from PHI, CHI, and HIV<sup>free</sup> following TcR activation every 7 days for 28 days. Results are expressed as the average of six independent experiments ± SD in log<sub>2</sub> scale. Dashed lines represent Mem half-lives for each group of subjects. (C) Levels of AKT pS473 following TcR activation every 7 days for 28 days. (D,E) Correlations between cell counts and AKT pS473 levels in Mem at 7 (D) and 14 (E) days of culture (FC, fold change; n = 18). The error bars indicate standard deviations from the means. β, symbol used for paired *t* test (comparison between treated Mem and control). \*, symbol used for Mann-Whitney test (comparison between study groups).

<https://doi.org/10.1371/journal.ppat.1008060.g004>

or absence of SF1670, α-IFNAR or isotype control for 2 hours, washed twice and then cultured with their autologous CD4-depleted PBMC. Cultured cells were then re-stimulated at day 7, 14 and 21 of culture with or without the specific inhibitors. Once again, to specifically interfere with USP18 expression, we purified Mem at day 0 of cultures, transduced them with LV<sub>USP18 KO</sub> or LV<sub>Ctrl</sub> for 4 hours, washed them twice and cultured them with their autologous CD4-depleted PBMC for 7 days. Cells were then re-stimulated at day 7, 14 and 21 of cultures. At day 7, 14, 21 and 28, total numbers of viable Mem were counted, and the half-lives of these cells were estimated for each study groups. We also determined in Mem the levels of apoptosis using Annexin-V staining and the expressions of USP18 and AKT pS473 by flow cytometry. We also assessed by ELISA the levels of both IFN-α and virus productions in supernatants during the time course of culture.

As expected, USP18 gene editing led to sustained inhibition of the elevated levels of USP18 expression in Mem from PHI and CHI subjects (S11B Fig). The elevated USP18 expression in Mem from viremic subjects could be explained by sustained IFN-α production during the time course of culture (S12A Fig). Our data showed that Mem from PHI and CHI subjects were not able to persist in culture, unlike Mem from HIV<sup>free</sup> donors (Fig 4B). Total counts of viable Mem from HIV<sup>free</sup> subjects were approximately 2.1-fold higher at day 7 and 5.3-fold higher at day 14 than those obtained from HIV-1-infected subjects ( $P \leq 0.0043$ ; n = 6). Strikingly, almost all Mem from HIV-1-infected subjects died by day 21, whereas Mem from uninfected controls continued to survive for at least 28 days after four rounds of activation. The half-lives of gated Mem obtained from PHI, CHI and HIV<sup>free</sup> subjects were 12, 10.5, and 22.2 days, respectively (Fig 4B). Interestingly, the reduced ability of Mem from infected subjects to persist was associated with lower expression levels of AKT pS473 during the time course of culture (Fig 4C). In addition, we found positive correlations between the counts of viable Mem and expression levels of AKT pS473 at day 7 and day 14 of cultures ( $P = 0.0153$ ,  $r = 0.5618$  and  $P < 0.0001$ ,  $r = 0.8785$  respectively; n = 18) (Fig 4D and 4E).

Treatments with SF1670, α-IFNAR or USP18 gene editing resulted in significant improvement of cell counts and half-lives in Mem from infected subjects from day 7 of culture (Fig 5A and 5B). Although all treatments significantly increased the numbers of viable Mem in PHI and CHI subjects during the cultures and allowed even some Mem to persist up to 21 days, they did not reach Mem counts found in cultures from HIV<sup>free</sup> controls. In addition, although we systematically found HIV-1 production in cultures from infected subjects, USP18 interference did not impact the viral production (S12B Fig). This seemed to indicate that improvements of Mem survival, especially when USP18 was targeted, were not associated with reduced viral production in cultures. In contrast, all treatments led to significant increases of AKT pS473 levels intrinsic to Mem from PHI and CHI subjects (Fig 5C). We also found significant correlations between the increases of cell counts and AKT pS473 levels with USP KO in Mem at 7 and 14 days of treatment ( $P = 0.001$ ,  $r = 0.7083$  and  $P = 0.0005$ ,  $r = 0.7380$  respectively; n = 18) (Fig 5D and 5E).

Overall, our data confirm the efficacy of PTEN and USP18 interferences in improving long-lasting Mem maintenance in an AKT-dependent manner.

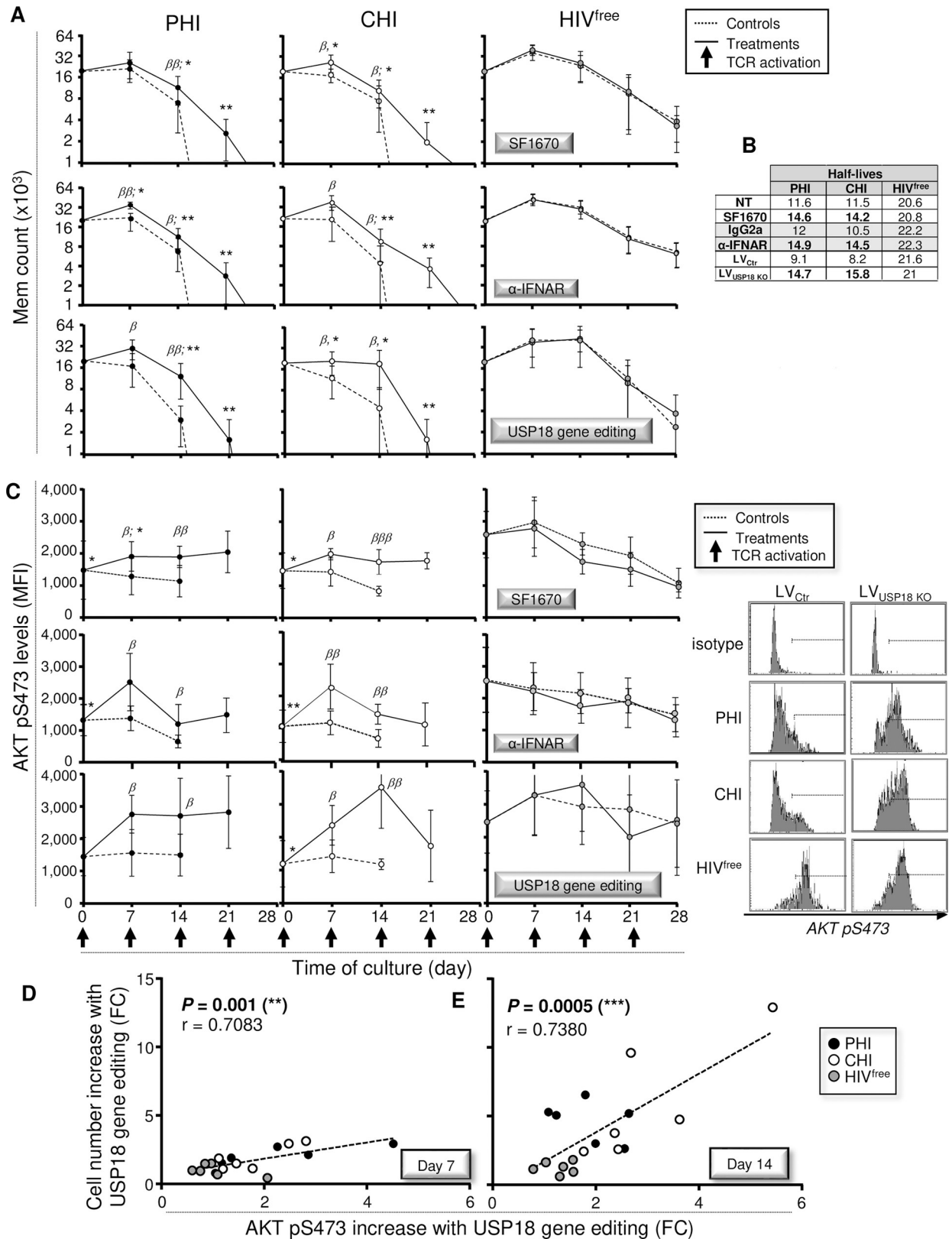


**Fig 5. Targeting USP18 in PHI and CHI results in improved Mem maintenance in an AKT-dependent manner.** (A) Mem counts from PHI, CHI, and HIV<sup>free</sup> following Tcr activation every 7 days for 28 days with or without SF1670 (top),  $\alpha$ -IFNAR or its respective isotype control



(middle), or CRISPR/Cas9 mediated USP18 gene editing (bottom) treatments. Results are expressed as the average of six independent experiments  $\pm$  SD in  $\log_2$  scale. (B) Half-lives were also determined for all study groups of subjects in the presence or absence of specific treatments. (C) Levels of AKT pS473 following TcR activation every 7 days for 28 days with or without SF1670 (top),  $\alpha$ -IFNAR (middle), or CRISPR/Cas9 mediated USP18 gene editing (bottom) treatments. Representative histograms are also shown on the right side. (D,E) Correlations between the increases of cell counts and AKT pS473 levels after CRISPR/Cas9 mediated USP18 gene editing in Mem at 7 (D) and 14 (E) days of treatment (FC, fold change;  $n = 18$ ). The error bars indicate standard deviations from the means.  $\beta$ , symbol used for paired  $t$  test (comparison between treated Mem and control). \*, symbol used for Mann-Whitney test (comparison between study groups).

<https://doi.org/10.1371/journal.ppat.1008060.g005>

## Defective long-lasting Mem maintenance in HIV-1-infected subjects is explained by increased cell death

We next aim to identify the main cause of reduced Mem counts in HIV-1-infected subjects at day 7 of culture. To investigate whether reduced numbers of Mem may be explained by lower proliferation rates, we stained purified Mem with carboxyfluorescein succinimidyl ester (CFSE) at day 0. Our data showed comparable percentages of proliferating CFSE<sup>low</sup> Mem in cultures from PHI, CHI and HIV<sup>free</sup> subjects (Fig 6A). Similarly, reduced numbers of Mem in cultures from HIV-1-infected subjects at day 7 could not be explained by different cell distribution pattern when compared to HIV<sup>free</sup> donors. Indeed, we found similar cell distribution among Mem for all study groups as determined by the percentages of T<sub>CM</sub>, T<sub>TM</sub> and shorted-lived T<sub>EM</sub> cells [39] (Fig 6B). Although the targeted USP18 editing in HIV-1-infected subjects led to significant increases of Mem at day 7 of culture, it did not impact their levels of proliferation or cell distribution patterns (Fig 6A and 6B). Put together, these results demonstrated that proliferation and cell differentiation did not play a significant role in long-lasting Mem maintenance.

In contrast, we found higher levels of apoptosis in Mem from PHI and CHI subjects compared to HIV<sup>free</sup> donors at day 7 of culture ( $38.6 \pm 8.4$  [PHI],  $49.2 \pm 11.2$  [CHI] and  $13.8 \pm 5.5$  [HIV<sup>free</sup>]) (Fig 6C). Treatments with SF1670,  $\alpha$ -IFNAR, and LV<sub>USP18 KO</sub> also led to significant reduction of Mem apoptosis in PHI and CHI subjects, although percentages of apoptotic Mem in culture from uninfected controls were systematically lower. Finally, we found a positive correlation between the reductions of Mem apoptosis and the increases of AKT pS473 levels after USP18 gene editing in Mem at day 7 of culture ( $P = 0.0311$ ,  $r = 0.5088$ ;  $n = 18$ ) (Fig 6D). The reduction of Mem apoptosis following USP18 gene editing also correlated with the increases of cell counts ( $P = 0.0081$ ,  $r = 0.6028$ ;  $n = 18$ ) (Fig 6E).

In summary, our data indicate that Mem apoptosis regulates the cell numbers in our long-term culture assay rather than proliferation or cell differentiation.

## Interfering with USP18 expression in primary-infected subjects also rescues HIV-1-specific cells from apoptosis and involves increased AKT pS473 levels

Since evidence show that HIV-1-specific CD4 T-cells display enhanced apoptotic potential that the other Ag-experienced cells [42], we decided to assess if interfering with PTEN or USP18 could also reduce the apoptosis of those cells. First, PBMC from PHI, CHI, and ART<sup>+</sup> subjects were stimulated with HIV-1 Gag p55 antigens and anti-CD28 Abs for 18 hours in the presence or absence of SF1670 inhibitor. We added the antiviral AZT in cultures from ART<sup>+</sup> subjects to maintain medical pressure and prevent *de novo* infections and viral replication. The efficacy of AZT treatment was confirmed by the absence of detectable p24 levels in supernatants from ART<sup>+</sup>'s cultures. We also inhibited USP18 expression in Mem from all groups of HIV-1-infected subjects before assessing the Gag-specific stimulation. Briefly, we transduced purified CD4 T-cells with LV<sub>USP18 KO</sub> or LV<sub>Ctrl</sub> for 4 hours, washed the cells twice, and cultured

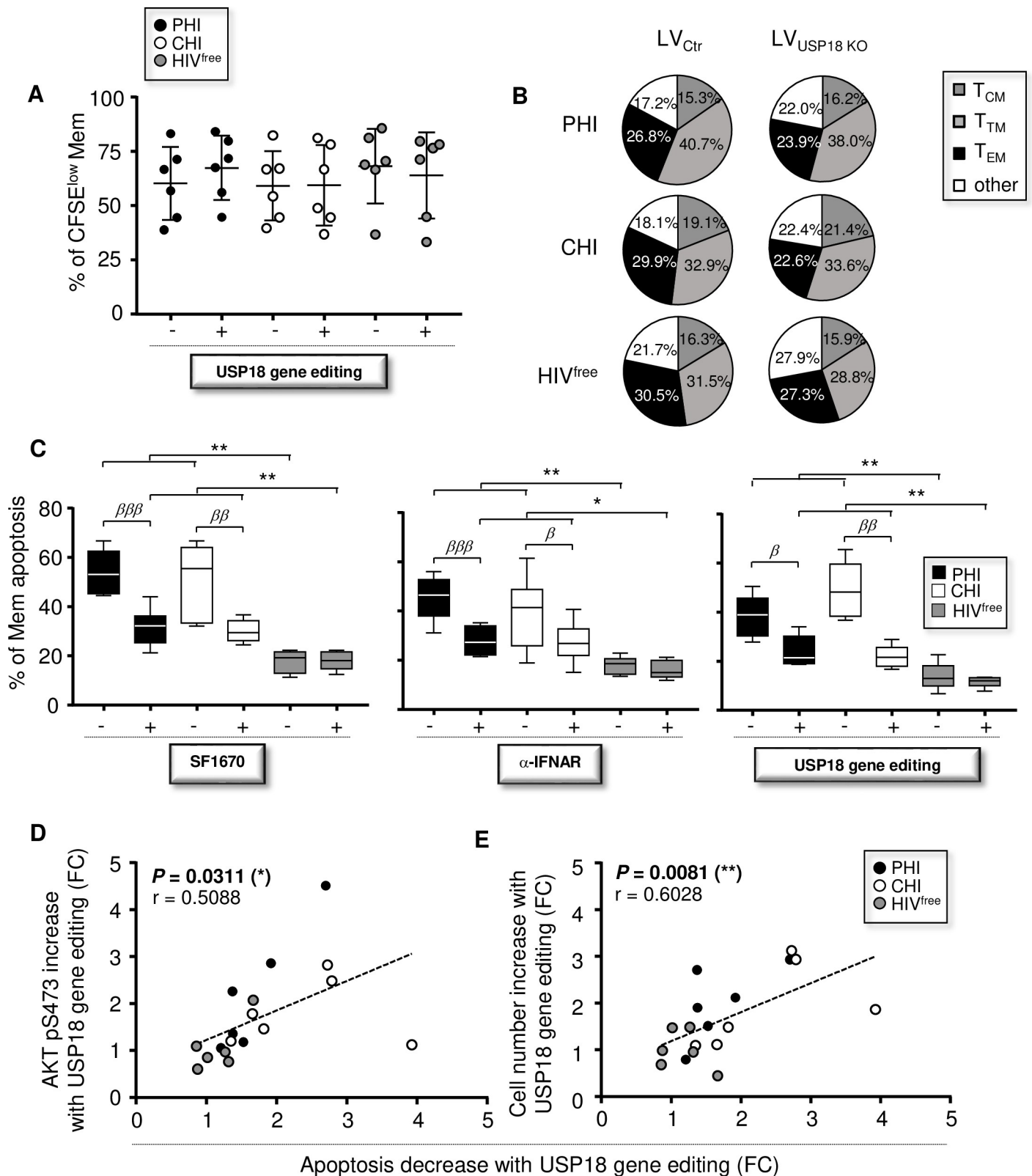


**Fig 6. Improvements of Mem maintenance in PHI and CHI with USP18 gene editing are associated with lower cell death.** (A) Levels of proliferation determined at day 7 of culture by the percentages of viable CFSE<sup>low</sup> Mem with or without CRISPR/Cas9 mediated USP18 gene editing (n = 6). (B) Distribution of Mem subsets at day 7 of culture with or without CRISPR/Cas9 mediated USP18 gene editing (n = 6). (C) Percentages of apoptotic Mem on day 7 with or without SF1670 (left), α-

IFNAR or its respective isotype control (middle), or CRISPR/Cas9 mediated USP18 gene editing (right) ( $n = 6$ ). Levels of apoptosis were determined using Annexin-V staining. (D) Correlation between the reductions of Mem apoptosis and the increases of AKT pS473 levels after USP18 gene editing in Mem at day 7 of culture (FC, fold change;  $n = 18$ ). (E) Correlation between the reductions of Mem apoptosis and the increases of cell counts after USP18 gene editing treatment at day 7 (FC, fold change;  $n = 18$ ). The error bars indicate standard deviations from the means.  $\beta$ , symbol used for paired  $t$  test (comparison between treated Mem and control). \*, symbol used for Mann-Whitney test (comparison between study groups).

<https://doi.org/10.1371/journal.ppat.1008060.g006>

them for 48 hours with their autologous CD4-depleted PBMC (ratio CD4/PBMC =  $\frac{1}{4}$ ). Finally, transduced cells were stimulated for an additional 18 hours with Gag antigens and anti-CD28 Abs. At 18 hours post-stimulation with Gag, we collected cells and assessed the expression of USP18, IFN- $\gamma$  and AKT pS473 as well as the percentages of apoptotic cells by Annexin-V staining within the HIV-1-specific CD4 T-cells. HIV-1-specific CD4 T-cells from infected subjects were determined by their positive staining for IFN- $\gamma$  following Gag stimulation (Fig 7A). Of note, we included HIV<sup>free</sup> donors as negative controls for HIV-1-specific stimulations. Uninfected controls were used for setting gating regions and discerning negative from positive cells (HIV<sup>free</sup>:  $0.08 \pm 0.12\%$  of IFN- $\gamma^+$ CD4 T-cells at 18 hours Gag post-stimulation; Fig 7B). Our data showed that PHI displayed lower proportion of HIV-1-specific CD4 T-cells when compared to ART-suppressed subjects after Gag stimulation ( $P = 0.0476$ ,  $n = 6$ ) (Fig 7B). Although it did not reach significance, we also found a trend to reduced proportion of HIV-1-specific cells in CHI when compared to ART<sup>+</sup> subjects ( $0.77 \pm 0.23\%$  and  $1.32 \pm 0.56\%$ , respectively). We confirmed increased USP18 expression in HIV-1-specific CD4 T-cells from PHI and CHI subjects when compared to those from ART<sup>+</sup> (S13 Fig; cells with no transduction or transduced with LV<sub>Ctrl</sub>). We also confirmed approximately 81.2% and 83% inhibitions of USP18 expression in HIV-1-specific CD4 T-cells from PHI and CHI subjects when their purified CD4 T-cells were pre-transduced with LV<sub>USP18 KO</sub> (S13 Fig). In this context, our results showed that treatment with SF1670 and USP18 gene editing with PHI and CHI subjects led to significant increases of proportion of HIV-1-specific cells (Fig 7B).

Our data further showed increased percentages of apoptotic Annexin-V<sup>+</sup> HIV-1-specific CD4 T-cells in PHI and CHI subjects when compared to patients under ART ( $36.8 \pm 6.1$ ,  $42 \pm 10.9$  and  $16.2 \pm 5.9$ , respectively;  $P = 0.0022$ ) (Fig 7C). As expected, interfering with PTEN or with USP18 expression in viremic subjects led to significant reduction of apoptosis in Gag-specific cells, although levels of apoptosis in PHI and CHI subjects were still higher compared to those of ART<sup>+</sup> subjects (Fig 7C). We also found reduced expression levels of AKT pS473 in HIV-1-specific CD4 T-cells from viremic subjects compared to ART<sup>+</sup> patients ( $P = 0.0022$  and  $P = 0.0173$ , respectively;  $n = 6$ ) (Fig 7D). SF1670 treatment or USP18 gene editing led to increases of AKT activation in PHI and CHI subjects (Fig 7D). Finally, we found a significant correlation between the reductions of apoptosis and increases of AKT pS473 levels in HIV-1-specific CD4 T-cells with USP18 gene editing ( $P = 0.0040$ ,  $r = 0.6427$ ;  $n = 18$ ) (Fig 7E).

Overall, our results show that interfering with PTEN or USP18 during primary HIV-1 infection not only improves Mem survival, but also protects HIV-1-specific cells as well.

## Discussion

Type I interferons (IFN-I) are central to the innate immune response against viral infections including HIV-1 [10, 12, 43]. In recent years however, the notion that IFN-I have detrimental effects if they are produced for long periods of time, as is the case during persistent viral infections, has become more evident [22, 43, 44]. Similarly to others [16–21], we found elevated IFN- $\alpha$  levels in plasma during the early and later stages of HIV-1 infection, which correlated with viral loads (Fig 1A and S1 Fig). We also found sustained production of IFN- $\alpha$  and viruses

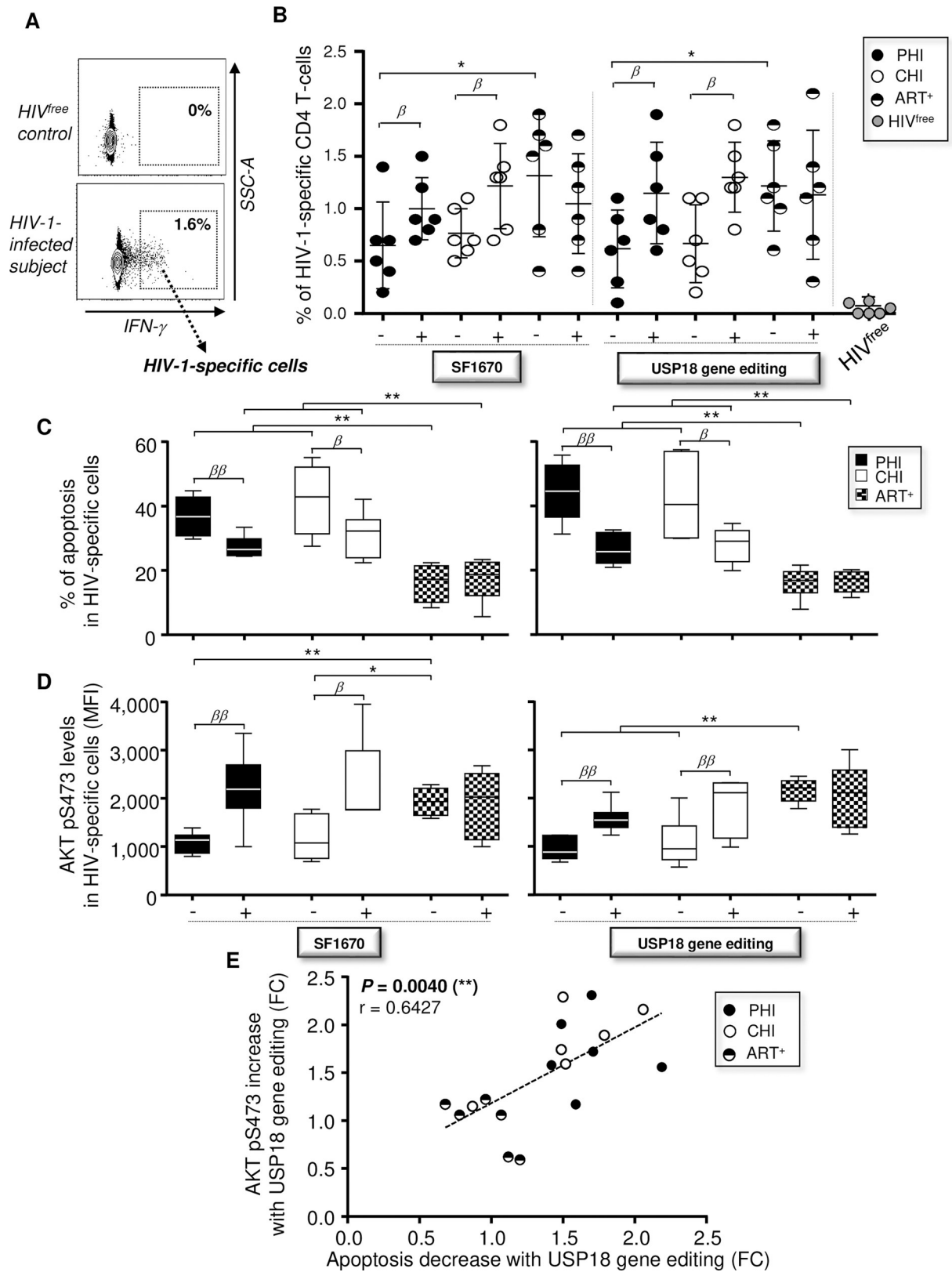


**Fig 7. Interfering with USP18 reduces apoptosis of HIV-1-specific CD4 T-cells in an AKT-dependent manner.** (A) Gating strategy for HIV-1-specific CD4 T-cells following Gag stimulation for 18 hours. HIV-1-specific clones were determined by IFN- $\gamma$  expression. (B)

Percentages of HIV-1-specific CD4 T-cells (on total CD4) in CHI, PHI, ART<sup>+</sup> and HIV<sup>free</sup> subjects after Gag stimulation in the presence or absence of SF1670. Percentages of HIV-1-specific cells were also determined in culture after 18 hours of Gag stimulation when CD4 T-cells have been pre-transduced or not for 48 hours with LV<sub>USP18 KO</sub>. HIV<sup>free</sup> donors were included as negative control for HIV-1 stimulation (n = 6). (C,D) Levels of apoptosis assessed by Annexin-V staining (C) and AKT pS473 expression (D) in HIV-1-specific CD4 T-cells at 18 hours post-stimulation in the presence of absence of SF1670 (left) or CRISPR/Cas9 mediated USP18 gene editing (right) (n = 6). (E) Correlation between the reductions of apoptosis and increases of AKT pS473 levels in HIV-1-specific CD4 T-cells after USP18 gene editing (FC, fold change; n = 18). The error bars indicate standard deviations from the means.  $\beta$ , symbol used for paired *t* test (comparison between treated Mem and control). \*, symbol used for Mann-Whitney test (comparison between study groups).

<https://doi.org/10.1371/journal.ppat.1008060.g007>

in supernatants in PHI and CHI subjects up to 21 days of our *in vitro* cultures (S12 Fig). However, despite indications of an IFN-I signature in HIV-1 infection [22, 32–34], the molecular mechanisms by which sustained IFN-I signaling negatively impacts the immune system, especially Mem, which are a major target during primary infection, are still unclear.

Here, we provide a molecular mechanism related to the elevated IFN-I signaling in Mem during primary HIV-1 infection that is clearly responsible for their defective cell survival (S14 Fig). In this context, our data reveal that IFNAR blockade in Mem during HIV-1 infection normalized the high expression of the down-stream interferon-induced gene, USP18, in the range of those from uninfected controls (Fig 1D–1F). Our data further shows that PTEN expression was reduced following either IFNAR blockade or specific USP18 gene silencing (Fig 2C and 2D). Similarly, it was previously shown that engineered gain of USP18 expression in human lung cancer cell lines stabilized PTEN protein by preventing its ISGylation post-translational modification pathway [45]. Interfering with PTEN activity or specifically with USP18 expression during HIV-1 infection led to significant improvements of Mem survival in an AKT-dependent manner (Fig 3–6). These improvements were illustrated by increased long-lasting cell maintenance, cell response to  $\gamma$ -chain cytokines and resistance to Fas-induced apoptosis (Figs 2–5) [46]. Other observations have shown that IFNAR blockade also inhibited TRAIL-induced apoptosis in CD4 T-cells during *in vitro* infection, and was associated with reduced frequencies of TRAIL<sup>+</sup> and apoptotic cells in infected subjects [18, 24, 47]. Although a previous report has indicated that prolonged IFN- $\alpha$  treatment could impair cytokine-induced AKT activation [48], we show the beneficial impact of blocking this signaling in Mem and HIV-1 specific CD4 T-cells and, for what we believe is the first time, we present an explanation on the molecular mechanism involved in this signaling.

Although our findings lead to a straightforward mechanism behind the deleterious effects of sustained IFN-I signaling on the survival of Mem (S14 Fig), there are still other factors to consider if we want to thoroughly map the molecular network involved during this signaling as well as its full impact. (i) One such aspect, is the extent at which increased USP18 expression is found. Other populations, such as CD3<sup>+</sup>CD4<sup>neg</sup>, CD3<sup>neg</sup>CD4<sup>neg</sup>, and monocytes, from PHI and CHI also showed increased USP18 expression compared to the uninfected control group (S15 Fig). This places USP18 as a potential key component of the immune system critical function as it could affect a broad spectrum of cell populations during HIV-1 infection. (ii) Another factor to consider is the fact that, USP18 is not only an isopeptidase that stabilizes PTEN expression, but also a negative regulator of IFN-I signaling [31, 49]. In the case of this study however, HIV-1-infected subjects displayed elevated IFN-I signaling despite an increase in USP18 expression. It is important to note that the isopeptidase activity of USP18 is independent of its IFN-I regulatory functions [50]. This might explain how high USP18 expression in Mem during HIV-1 infection could stabilize PTEN expression and be concomitantly associated with sustained IFN-I signaling. Of note, the IFN-I regulatory functions of USP18 depend on its capacity to bind IFNAR2 and inhibit JAK/STAT signaling and involves other factors. Through direct interaction with USP18, the insulin receptor substrate-4 was shown to



counteract its inhibitory effect on JAK/STAT signaling [51]. Conversely, STAT2 was shown to be a crucial component of the USP18-mediated suppression of IFN-I signaling [52]. Therefore, it would be interesting to investigate how USP18 impacts IFN-I signaling regulation during HIV-1 infection, and whether STAT2 and/or IRS-4 are involved. (iii) An additional aspect to consider in the case of sustained IFN-I signaling, aside from Mem survival, is that of their defective function which appears during the early stage of primary HIV-1 infection. In this regard, HIV-1-infected patients display hyper-activated and exhausted CD4 T-cells that are characterized by poor effector functions and high expression of multiple inhibitory receptors such as programmed cell death 1 [53]. Interestingly, recent data collected by Crawford A. *et al* have shown that CD4 T-cell defective function during HIV-1 infection was associated with an elevated IFN-I-induced transcriptional program. Further experiments are however warranted to know whether we could also counteract CD4 T-cell defective function during HIV-1 infection by specifically interfering with USP18 expression. Although we confirmed reduced effector functions illustrated by decreased cell ability to secrete cytokines and polyfunctionality (i.e. ability to secrete multiple cytokines), a 24 hour-long IFNAR blockade did not rescue these immune defects (S16 Fig). However, the critical role of PI3K/AKT signaling pathway in regulating T-cell function is now well established [54]. Therefore, we cannot exclude the possibility that longer IFNAR blockade or specific targeting of USP18, which are acting through AKT-dependent mechanisms, might improve cell functions during persistent HIV-1 infection as well. (iv) The elevated IFN-I signaling and USP18 expression in Mem from HIV-1-infected subjects can be explained by their sustained IFN- $\alpha$  and virus production in the environment (S12A and S12B Fig). Therefore, it is not surprising that long-term ART when administrated early during the first months of primary HIV-1 infection was effective in normalizing both IFN- $\alpha$  production and USP18 expression intrinsic to Mem (S5 Fig). Interfering with IFN-I signaling or specifically with USP18 expression may still be a therapeutic approach to consider in some cases of treated patients. Despite effective control of HIV-1 replication with ART, a minority of treated patients called immune non-responders (INR) fails to show increased CD4 T-cell counts to the level observed in uninfected control donors [55, 56]. INR remain at greater risk for health complications and non-AIDS diseases including cardiovascular disease, liver disease, renal disease, and malignancies when compared to immune responders (IRs) in whom the CD4 T-cell counts are properly restored [57, 58]. Although the molecular mechanisms that are responsible for the lack of CD4 T-cell recovery in INR are still unclear, several pieces of observations have indicated that their CD4 T-cell recovery may be adversely affected by the sustained expression of several ISG [59–61]. (v) The effect of USP18 modulation on HIV-1 infectivity remains to be fully explored, especially in humanized mice infected with HIV-1 where IFNAR blockade is associated with reduced T-cell activation [32–34]. It is well-established that CD4 T-cell activation is a key factor in facilitating HIV-1 infection and cell depletion [62, 63]. Therefore, we cannot rule out a potential effect of reduced infectivity to contribute to some of the cell survival as the USP18 targeting should be reducing inflammatory/ISG driven activation as well. In the context of our experiments, the relative short time of treatments enables higher AKT activation and cell survival seemingly independently of viral reinfection as maintaining exogenous IFN- $\alpha$  in culture in the presence of fusion inhibitor T20 did not significantly reduce Mem apoptosis compared to untreated Mem (S12C Fig). However, longer treatments might reduce viral infectivity to a significant degree, thus reducing Mem cell death to even greater extents.

As mentioned earlier, although our group has recently provided evidence that the increased production of tryptophan-related catabolite kynurenine during primary HIV-1 infection affected IL-2-induced STAT5 activation in Mem, interfering with this disturbance was not sufficient to restore proper cell survival [6]. Here, we found that blocking IFN-I signaling or

directly interfering with USP18 expression also led to significant improvements of Mem survival during primary HIV-1 infection. The molecular mechanisms described in this study did not seem to involve STAT5 activation since we found that IFNAR blockade in Mem from infected subjects had no effect on IL-2-mediated defective STAT5 phosphorylation (S3B and S8C Figs). In contrast, targeting the increased IFN-I signaling, especially the high USP18 expression in Mem from infected subjects, led to significant increase of AKT activation in a PTEN-dependent manner. Although interfering with IFN-I or specifically with USP18 expression during primary HIV-1 infection significantly improved Mem survival in an AKT-dependent manner, it did not reach the levels that were observable in uninfected controls (Figs 2–5). Similarly, although treatments of HIV-1-specific CD4 T-cells from PHI subjects with USP18 gene editing led to reduced apoptosis levels, these levels were higher compared to those from ART<sup>+</sup> subjects (Fig 7C). These observations indicate that defective Mem survival during primary HIV-1 infection is a complex mechanism, which may involve independent, but synergistic molecular disturbances such as sustained IFN-I signaling and high kynurenine production among others. Of note, the catabolism of tryptophan into kynurenine is known to be mediated by the indoleamine 2,3-dioxygenase (IDO), whose protein expression and activity are found increased during HIV-1 infection [64, 65]. Since previous results showed positive correlation between increased ISG expression and IDO levels in HIV-1-infected subjects [66, 67], we cannot exclude the fact that IFN-I blockade may also be effective in counteracting the heightened production of kynurenines during HIV-1 infection. Assessing whether targeting IFN-I and kynurenine-related pathways simultaneously might have a synergistic effect on Mem survival improvement during HIV-1 infection is also warranted.

Although those results are preliminary, USP18 gene editing in cells extracted from one spleen of an HIV-1-infected patient did confirm our observations with PBMC. Indeed, inhibiting USP18 reduced Mem apoptosis even in HIV-1-specific cells (S17 Fig). It remains important to confirm the role of USP18 in tissues with a great number of patients or by using *in vivo* models, such as humanized mice or non-human primate. Taking this into consideration, it is likely that USP18 plays a role in Mem numbers in lymphoid tissue, although its effect might be dwarfed by other mechanisms, such as pyroptosis, more present in those locations compared to peripheral blood [9, 68].

In summary, our data indicates that the interference of sustained IFN-I in human HIV-1-infected subjects, which leads to a better control of USP18 and PTEN, is a valuable tool to consider for Mem recovery and survival via AKT activation. We acknowledge the fact that proposing such therapeutic strategies to fight HIV-1 infection may also bring some concerns, since they could also be detrimental to the patients by protecting their HIV-1-infected cells and sustaining the latent HIV-1 reservoir [69, 70]. Finally, if such treatments have to be considered one day, great consideration should be given to the timing and duration of the IFNAR blockade in patients, especially when taking into account that this blockade accelerated CD4 T-cell depletion in an acute SIV model [71]. However, our data points to USP18 as an important driver for the detrimental phenotypes observed in Mem from HIV-1-infected subjects. Targeting USP18, specifically its isopeptidase activity, could bypass those unintended consequences, as there are fewer pathways impacted when compared to those regulated by IFN-I signaling.

## Materials and methods

### Ethics statement

All infected patients were participants in the Montreal HIV infection study that received approval from the McGill University Health Centre Ethical Review Board (ethic reference

number SL-00.069 [blood] and 2019–5170 [spleen]). All subjects provided an informed and written consent for participation.

### Study population

PBMC and plasma were collected from primary infected patients (PHI), untreated ART-naïve and chronically infected subjects (CHI) and patients under ART (ART<sup>+</sup>) who displayed both viral suppression and full CD4 recovery (> 400 CD4/μl blood post-treatments). Each group of HIV-1-infected patients included in the overall study was homogeneously selected and displayed similar clinical data. Clinical information of all infected patients including viral loads and CD4 counts is summarized in [S1 Table](#). We also selected age-matched uninfected control donors as negative control for HIV-1 infection.

### Products

RPMI-1640 media, FBS, antibiotics and PBS were obtained from Wisent Inc. Recombinant IL-2 and IL-7 cytokines as well as the PTEN inhibitor SF1670 were provided from Sigma Aldrich. Anti-Fas CH11 antibody is from MBL International Corporation. We purchased all antibodies and reagents for flow cytometry from BD Biosciences, except for the antibody to CD45RA-ECD, IFNAR2, IRF7 pS477/479 and USP18, which were from Beckman Coulter, Miltenyi Biotec and Santa Cruz Biotechnology respectively (Table S3). 7-aminoactinomycin D (7-AAD) came from ThermoFisher Neutralizing anti-IFNAR antibody (α-IFNAR; clone MMHAR-2) and respective isotype control were obtained from EMD Millipore. Concentrations of SF1670, α-IFNAR and isotype controls used in our study were 3 μM, 5 μg/mL and 5 μg/mL respectively. Concentration for IL-2 and IL-7 were 25 IU/mL and 0.3 ng/mL, respectively. The fusion inhibitor T20 was purchased from Sigma Aldrich.

### ELISA assay

Plasma and culture supernatant levels of IFN-α were measured by ELISA according to the manufacturer's instructions (high sensitivity human IFN alpha ELISA kit; PBL Assay Science). We also used the sensitive HIV-1 p24 ELISA kit (Abcam) to determine HIV-1 production in cell cultures.

### Purification of Mem

Mem were purified using the untouched memory CD4 isolation kit (EasySep human memory CD4<sup>+</sup> T-cell Enrichment Kit; StemCell Technologies) allowing for more than 94.6% purification without any cell stimulation and apoptosis.

### Real-time reverse-transcription (RT)-PCR analysis

Total RNA was isolated from purified Mem using an RNeasy kit according to the manufacturer's instructions (Qiagen). RNA was then reverse transcribed with oligo(dT) primers and SuperScript II reverse transcriptase (Life Technologies). PCR was performed using Taq polymerase (GE Health-care) using set of primers to evaluate ISG expression. The summary of all primers used in this study is presented in [S2 Table](#). All data are presented as relative quantifications with efficiency correction based on the relative expression of target genes versus the *gapdh* gene as the reference gene. cDNA was amplified using SyBR Green I OPCR master mix (Applied Biosystems), and all data were collected using the Rotor-Gene RG-3000 (Corbet Research) and analysed by the comparative threshold cycle (CT) method using the Rotor Gene Q serie software 2.3.1.



## Western blots

Purified Mem from all groups were subjected to SDS-PAGE and Western blot analysis to assess USP18 expression as previously described [4, 72]. Of note, results are expressed as densitometric quantification of specific bands performed using ImageJ software. The levels of expression of USP18 were normalized to  $\beta$ -actin and were later expressed as the ratio of densitometric values of protein of interest divided by densitometric values of actin within the same blot.

## Transfection and siRNA assays

We first purified  $5.10^6$  Mem from all tested groups and electroporated them using Nucleofector II technology according to the Amaxa Biosystems manufacturer's protocol. Specific USP18 siRNA and Silencer negative control siRNA were obtained from ThermoFisher Scientific. Of note, 5  $\mu$ g of siRNA were transfected or not for each condition for 2 hours without antibiotics. Purified Mem were thereafter washed twice to remove dead necrotic cells, counted and cultured until 48 hours with their autologous CD4-depleted PBMC (at ratio Mem/PBMC = 1/4). At 48 hours post-transfection, some cells were kept to measure USP18 and PTEN protein levels by flow cytometry.

## PhosFlow assays

PhosFlow assays were performed to assess the intracellular expression levels of STAT1 pY701, IRF7 pS477/479, STAT5 pY694, and AKT pS473. Briefly, cellular fixation was done using 4% PFA for 10 minutes at 36°C followed by surface staining for 10 minutes at 4°C. Afterwards, the cellular permeabilization was done using 90% ice cold methanol for 30 minutes at 4°C followed by 30 minutes of intracellular staining in PBS+2% FBS at room temperature. Of note, we systematically titrated all antibodies and washed the cells three times at the end of the protocol to ensure that all background fluorescences were at an appropriately low position on the fluorescence scale. The viability marker 7-AAD was used to exclude dead cells from analyses. BD LSRII Fortessa flow cytometer (BD) was used to collect the data which were analyzed using the DIVA software.

## Intracellular staining assays

Staining assays were performed to assess the intracellular expression levels of PTEN and USP18. The cellular permeabilization was done using 0.25% (W/V) saponine in PBS for 30 minutes at room temperature. The following multi-parameter antibody cocktail was used: anti-CD3-BB515, anti-CD4-BV605, anti-CD45RA-APC-Cy7, anti-PTEN-APC and anti-USP18-Alexa Fluor700. Of note, anti-USP18 IgG<sub>1</sub> Abs was conjugated to Alexa700 dye using the Zenon mouse IgG<sub>1</sub> labeling kit (Life Technologies Inc.) according to the manufacturer's protocol. The viability marker 7-AAD was used to exclude dead cells from analyses. BD LSRII Fortessa flow cytometer (BD) was used to collect the data which were analyzed using the DIVA software. Once again, we titrated all antibodies and washed the cells multiple times during the staining protocol to minimize all background fluorescences.

## Fas-induced apoptosis and cytokine-mediated Mem protection

We first cultured  $10^6$  PBMC with either SF1670, IFNAR or its respective isotype control (rat anti-mouse IgG2a Abs) for 48 hours. We also transfected or not Mem with USP18 siRNA or negative control siRNA for 48 hours. Cells were then treated or not with 1.25  $\mu$ g/mL of anti-Fas CH11 Abs in the presence or absence of cytokines (IL-2 or IL-7) for an additional 24

hours. We determined in Mem for all tested groups in all conditions both the numbers (N) and percentages of constitutive apoptosis (without any treatments), Fas-induced apoptosis and the cytokine-mediated Mem protections when the cells were stimulated with IL-2 or IL-7. Number of Fas-induced apoptotic Mem were determined by the formula: N of apoptotic Mem with CH11 – N of apoptotic Mem without CH11. Similarly to cell numbers, % of Fas-induced apoptosis were determined by the formula: % of apoptosis in Mem with CH11 – % of apoptosis in Mem without CH11. As a reminder, cytokine-mediated Mem protections were calculated in fold change (FC) with the formula: Number of Fas-induced apoptotic Mem without cytokine / Number of Fas-induced apoptotic Mem with cytokine.

### Production of lentiviral vectors and Mem transduction

To produce lentiviral vectors, we used the packaging plasmid psPAX2 and envelope plasmid pMD2G as previously done [4]. As transfer vector, we used either USP18 CRISPR/Cas9 KO plasmid or its respective negative control plasmid (Santa Cruz Biotechnology; sc-402259 and sc-418922, respectively). Briefly, the recombinant virion particles were produced by transient polyethylenimine co-transfection of  $10^7$  293T cells in 175 cm<sup>3</sup> flasks using 50 µg transfer vector (USP18 CRISPR/Cas9 KO plasmid or control CRISPR/Cas9 plasmid), 200 µg of psPAX2, and 200 µg of pMD2G. The transfection medium was replaced after 24 hr with fresh serum free DMEM medium (Sigma Aldrich). Viral supernatants were collected at 6 days post-transfection, filtered through a 0.45-mm filter and concentrated 150-fold by centrifuging through filtration columns (Centricon Plus-20, molecular weight cutoff 100 kDa; Millipore) at 3000g at 4°C. The concentrated recombinant virus were stored in -80°C for further usage. Viral titers (ng/mL) were assessed by using HIV-1 p24 ELISA. Of note, we used 100 ng of lentiviral vectors (LV) per  $1.10^6$  purified Mem for 4 hours, washed the cells twice and cultured them until 48 hours with their autologous CD4-depleted PBMC (ratio Mem/PBMC = ¼) to achieve significant USP18 inhibition.

### Long-lasting Mem maintenance assays

$2.10^4$  purified Mem were first activated with 0.5 µg/mL anti-CD3 and 1 µg/mL anti-CD28 Abs in the presence or absence of ST1670, anti-IFNAR or its respective isotype control for 2 hours. Mem were then washed twice, counted and cultured with  $8.10^4$  autologous CD4-depleted PBMC. Cultured cells were re-stimulated with anti-CD3 and anti-CD28 Abs with or without the specific inhibitors at days 7, 14 and 21. To interfere with USP18 expression during the long-term culture, we also purified Mem from all groups, transduced them with LV<sub>USP18 KO</sub> or LV<sub>Ctrl</sub> for 4 hours. At 4 hours post-transduction, we counted the cells and cultured  $2.10^4$  of them with  $8.10^4$  autologous CD4-depleted PBMC. Cultured cells were re-stimulated with anti-CD3 and anti-CD28 Abs at days 7, 14 and 21. Total numbers of viable Mem were counted, and the half-lives of these cells were estimated for each study groups at days 7, 14, 21 and 28 of culture. We also determined in gated Mem the levels of apoptosis using Annexin-V staining and the expressions of USP18 and AKT pS473 by flow cytometry. We also assessed by ELISA the levels of both IFN-α and virus productions in supernatants during the time course of culture. Finally, we also determined at day 7 of culture the levels of cell proliferation, differentiation and apoptosis in Mem for all donors as previously done [4].

### HIV-1-specific stimulation

PBMC were specifically stimulated for 18 hours with 5 µg/mL HIV-1 p55 Gag antigens (Austral Biologicals) and 1 µg/mL anti-CD28 Abs in the presence of GolgiPlug and GolgiStop (BD Biosciences). HIV-1-specific stimulations were performed with or without SF1670. We also

pre-transduced for 48 hours purified CD4 T-cells from HIV-1-infected subjects before the HIV-1 Gag stimulation. Of note, we added 10  $\mu$ M AZT (Sigma Aldrich) in cultures from ART<sup>+</sup> subjects to prevent *de novo* infections (confirmed by HIV-1 p24 ELISA in culture supernatants). Finally, we assessed by flow cytometry the levels of apoptosis using Annexin-V staining and AKT pS473 in responsive IFN- $\gamma$ <sup>+</sup> HIV-1-specific CD4 T-cells. Of note, we included HIV<sup>free</sup> donors as negative controls for HIV-1-specific stimulations. Uninfected controls were used for setting gating regions and discerning positive from negative cells. BD LSRII Fortessa flow cytometer (BD) was used to collect the data which were analyzed using the DIVA software.

### Spleen processing and cell isolation

Spleen tissue was processed within 30 min of surgery (patient info: 47 year old, VL = 3.21 Log copies/ml, CD4 count = 611 cells/ $\mu$ l and CD8 = 1513 cells/ $\mu$ l, 10 years of infection). Blocks were cut into small pieces and forced through a 70 $\mu$ m sterile filter using the plunger of a syringe. Filtrate was kept at 4°C for 2 hours until further processing. Unfiltered tissue was dissociated enzymatically by digestion with Liberase DL (Roche, Laval, QC, Canada) at 0.1 mg/ml for 1h at 37°C. The digestion material was diluted 3 fold with PBS containing 2% fetal bovine serum (FBS). Mononuclear cells were then isolated from splenocyte filtrate or tissue suspension by centrifugation over ficoll (Wisent, Saint-Jean-Baptiste, QC Canada). Splenocytes were then counted using 0.2% trypan blue to evaluate viability (around 85%), and finally frozen in FBS containing 10% DMSO for further use.

### Statistical analysis

We used the non-parametric Mann-Whitney *U* test that assumes independent samples for all statistical analyses between study groups of subjects (\* symbol). On the other hand, statistical analyses between two different *in vitro* conditions were performed using two-sided Student paired *t* test. Spearman's correlation test was used to identify association among study clinical and immunological variables ( $\beta$  symbol). *P* values of less than 0.05 were considered significant. Of note, several symbols were used depending the statistical analyses. One symbol, 0.05 > *P* > 0.01; two symbols, 0.01 > *P* > 0.001; three symbols, 0.001 > *P* > 0.0001; and four symbols, *P* < 0.0001.

### Supporting information

**S1 Table. Clinical and immunological data of all selected HIV-1-infected subjects including viral loads and absolute numbers of CD4 counts for 10 PHI, 10 CHI and 10 ART+ subjects.**

(TIF)

**S2 Table. Primers used for the real time RT-PCR.**

(TIF)

**S3 Table. List of all antibodies used (including information about the vendor, clone IDs and fluorophore).**

(TIF)

**S1 Fig. Increased plasma IFN- $\alpha$  in HIV-1-infected subjects correlates with viral load. (A)**

Correlation between viral load (VL; Log<sub>10</sub>) and plasma IFN- $\alpha$  (pg/mL) levels in HIV-1-infected subjects. (n = 19)

(TIF)

**S2 Fig. Increased levels of IFN-I signaling in CD45RA<sup>+</sup> CD4 T-cells during HIV-1 infection are not associated with cell loss.** (A) Gating strategy to define total Mem, T<sub>CM</sub>, T<sub>TM</sub> and T<sub>EM</sub> subsets. (B) % of STAT1 pY701<sup>+</sup> (left) or IRF7 pS477/S479<sup>+</sup> (right) cells on total, CD45RA<sup>+</sup> and Mem CD4 T-cells in PHI, CHI and HIV<sup>free</sup> subjects determined by PhosFlow (n = 10). (C) Correlations between phospho-protein levels (MFI) and cell percentages in total, CD45RA<sup>+</sup> and Mem CD4 T-cells (n = 30). The error bars indicate standard deviations from the means. \*, symbol used for Mann-Whitney test (comparison between study groups). (TIF)

**S3 Fig. Mem from all study groups of subjects displayed similar expression levels for total STAT1 and IRF-7 expression.** (A) Expression of STAT1 pS727 including representative histograms in Mem from PHI, CHI and HIV<sup>free</sup> subjects. (B) mRNA expression of STAT5 and AKT in unstimulated and cytokine-stimulated Mem. N = 10. The error bars indicate standard deviations from the means. \*, symbol used for Mann-Whitney test (comparison between study groups). (TIF)

**S4 Fig. Western blot analyses confirmed increased constitutive expression of USP18 in Mem from PHI and CHI subjects when compared to HIV<sup>free</sup> controls.** (A) % of *ex vivo* USP18<sup>+</sup> Mem in PHI, CHI and HIV<sup>free</sup> (n = 10). (B, C) USP18 expression determined in *ex vivo* Mem by western blot (n = 4). (B) Representative blots for USP18 and β-actin (sampling n2). (C) Densitometric quantification of USP18 expression with four sampling (PHI, CHI and HIV<sup>free</sup> control). Results shown represent the USP18 relative expression after β-actin normalization in each sampling. \*, symbol used for Mann-Whitney test (comparison between study groups). (TIF)

**S5 Fig. ART when administrated early and after years of treatment normalizes IFN-α production and IFN-I signaling intrinsic to Mem.** (A) Plasma concentration of IFN-α in ART<sup>+</sup> and HIV<sup>free</sup> subjects determined by ELISA (pg/mL). (B) Expression levels of USP18 on *ex vivo* Mem from ART<sup>+</sup> and HIV<sup>free</sup> subjects in MFI (i) or percentages of USP18<sup>+</sup> Mem (ii). (C) Expression levels of PTEN on *ex vivo* Mem from ART<sup>+</sup> and HIV<sup>free</sup> subjects in MFI (i) or percentages of USP18<sup>+</sup> Mem (ii). (D) *In vitro* AKT pS473 expression levels in Mem in the presence or absence of cytokine stimulations in MFI (i) or percentages of USP18<sup>+</sup> Mem (ii). (A-D) (n = 10). The error bars indicate standard deviations from the means. \*, symbol used for Mann-Whitney test (comparison between study groups). (TIF)

**S6 Fig. *Ex vivo* Mem from PHI, CHI and HIV<sup>free</sup> subjects display similar IFNAR expression and subset distribution.** (A,B) *Ex vivo* IFNAR1 and IFNAR2 surface expression in Mem determined as percentages of positive cells (A) and mean fluorescence intensities or MFI (B). (C) *Ex vivo* distribution of Mem subsets. Representative pie charts for each study group of subjects are shown above. (A-C) (n = 10). The error bars indicate standard deviations from the means. \*, symbol used for Mann-Whitney test (comparison between study groups). (TIF)

**S7 Fig. Specific USP18 gene silencing led to significant inhibition of its protein expression in Mem from HIV-1-infected subjects.** (A) % of *ex vivo* PTEN<sup>+</sup> Mem in PHI, CHI and HIV<sup>free</sup>. (B) USP18 Expression levels in Mem following 48 hours of specific USP18 siRNA transfection in PHI, CHI and HIV<sup>free</sup> subjects (MFI). Representative histograms including isotype control and transfected Mem for one PHI are also shown on the right side (MFI and % of positive cells). (C) PTEN expression in Mem that have been electroporated alone or

transfected with scrambled siRNA. (A-C) (n = 10). The error bars indicate standard deviations from the means.  $\beta$ , symbol used for paired *t* test (comparison between treated Mem and control). \*, symbol used for Mann-Whitney test (comparison between study groups).

(TIF)

**S8 Fig. Interfering with IFN-I signaling in Mem does not improve IL-2-mediated STAT5 activation.** (A,B) Expression levels of STAT5 pY694 and AKT pS473 on Mem following 15 minutes of IL-2 or IL-7 stimulation determined as (A) percentages of positive cells and (B) mean fluorescence intensities or MFI. (C) PBMC were first incubated overnight with  $\alpha$ -IFNAR or respective isotype control, and then stimulated with IL-2 for another 15 minutes before assessing STAT5 activation levels by PhosFlow (MFI). (A-C) (n = 10). The error bars indicate standard deviations from the means. \*, symbol used for Mann-Whitney test (comparison between study groups).

(TIF)

**S9 Fig. Interfering with USP18 in Mem from PHI and CHI improves cell resistance to apoptosis as determined by the percentages of apoptosis.** (A) Percentage of Fas-induced apoptosis in Mem in the presence or absence of IL-2 or IL-7 stimulation. Fas-induced apoptosis was calculated according the formula: % of apoptosis in Mem with CH11 – % of apoptosis in Mem without CH11 (n = 10). (B) Number of Fas-induced apoptotic Mem in the presence or absence of IL-2 or IL-7 stimulation in Mem that have been pre-treated for 48h with SF1670 (i),  $\alpha$ -IFNAR or its respective isotype control (ii), or pre-transfected or not for 48 hours with USP18 siRNA (iii). Number of Fas-induced apoptotic Mem was calculated according the formula: N of apoptotic Mem with CH11 – Number of apoptotic Mem without CH11 (n = 10). The error bars indicate standard deviations from the means.  $\beta$ , symbol used for paired *t* test (comparison between treated Mem and control). \*, symbol used for Mann-Whitney test (comparison between study groups).

(TIF)

**S10 Fig. USP18 siRNA transfection in Mem does not impact their CD95 expression levels.** (A,B) Expression levels of CD95 in Mem that have been pre-transfected 48 hours with specific USP18 siRNA or scramble control. Results are expressed as (A) mean fluorescence intensities and (B) percentages of positive cells. (A,B) (n = 10). The error bars indicate standard deviations from the means.

(TIF)

**S11 Fig. CRISPR/Cas9 mediated USP18 gene editing in Mem results in significant and sustained inhibition of USP18 expression.** (A) USP18 expression in Mem that have been transduced or not for 48 hours with lentiviral CRISPR/Cas9 vectors mediating USP18 gene editing (lentiviral vectors for USP18 knock-out or LV<sub>USP18 KO</sub>) or control lentiviral vectors (LV<sub>Ctrl</sub>) in PHI, CHI and HIV<sup>free</sup> subjects (MFI; n = 10). Representative histograms including isotype control are also shown on the right side for one PHI subjects. (B) USP18 expression in Mem from PHI, CHI and HIV<sup>free</sup> subjects following Mem TcR activation every 7 days for 28 days in the presence or absence of CRISPR/Cas9 mediated USP18 gene editing (n = 6). The error bars indicate standard deviations from the means.  $\beta$ , symbol used for paired *t* test (comparison between treated Mem and control). \*, symbol used for Mann-Whitney test (comparison between study groups).

(TIF)

**S12 Fig. Specifically interfering with USP18 expression in Mem does not impact IFN- $\alpha$  secretion or virus production during long-lasting *in vitro* assay.** (A) IFN- $\alpha$  and (B) p24

levels in culture medium from PHI and CHI subjects at day 7, 14 and 21 days of culture when Mem have been transduced or not at day 0 with LV<sub>USP18 KO</sub>. Results are expressed in pg/mL (n = 6). (C) Apoptosis levels in Mem from PHI and CHI at day 7 of culture when treated or not with two antiretrovirals (ARV) (n = 6). In this context, we used 10 μM AZT and one fusion inhibitor to prevent any *de novo* infection (100 nM T20). We also added or not at day 0 of cultures 150 IU/ml IFN-α to sustain IFN-I signaling in the absence of virus. The levels of HIV-1 p24 in pg/ml assessed at day 7 in supernatants are also indicated in bold for all conditions (Und., undetectable levels). The error bars indicate standard deviations from the means. β, symbol used for paired *t* test (comparison with no treatment or NT).

(TIF)

**S13 Fig. Significant inhibition of USP18 expression levels in HIV-1-specific CD4 T-cells with CRISPR/Cas9 mediated USP18 gene editing.** USP18 expression levels (MFI) in IFNγ<sup>+</sup> HIV-1-specific CD4 T-cells following 18 hours of Gag stimulation when cells have been pre-transduced or not with LV<sub>USP18 KO</sub>. Representative histograms including isotype control are also shown on the right side for one PHI. (n = 10). The error bars indicate standard deviations from the means. β, symbol used for paired *t* test (comparison between treated Mem and control). \*, symbol used for Mann-Whitney test (comparison between study groups).

(TIF)

**S14 Fig. Interplay between sustained IFN-I signaling, USP18 expression and reduced AKT activation in memory CD4 T-cells during HIV-1 infection.**

(TIF)

**S15 Fig. USP18 expression is increased in other cell populations during HIV-1 infection.**

Constitutive expression of UPS18 is higher in CD3<sup>+</sup>CD4<sup>neg</sup>, CD3<sup>neg</sup>CD4<sup>neg</sup> and monocytes from PHI and CHI when compared to HIV<sup>free</sup> subjects as determined with MFI values (left) and percentages of positive cells (right) (n = 10). Representative histograms including isotype control are also shown below. The error bars indicate standard deviations from the means. \*, symbol used for Mann-Whitney test (comparison between study groups).

(TIF)

**S16 Fig. Functional defects observed in viremic HIV-1-infected subjects are not rescued by IFNAR blockade.** (A) Results are shown as the increases in FC (Fold change) of TCR-induced secreting Mem in the presence or absence of IFNAR blockade. Secreting cells are defined as producing either IFN-γ, TNF-α, IL-2, or combinations of multiple of them. No statistical differences were observed in the percentage of secreting Mem in the absence of TCR activation for all study groups of subjects. (B) Results shown are the increases in FC of TCR-induced IFN-γ producing Mem in the presence or absence of IFNAR blockade. (C) Percentages of PD-1 positive cells in Mem in the presence or absence of IFNAR blockade. (D) Representative distribution of secreting PD-1 positive Mem in the presence or absence of IFNAR blockade. (A-D) N = 10. The error bars indicate standard deviations from the means. β, symbol used for paired *t* test (comparison between Mem treated α-IFNAR and IgG2a controls). \*, symbol used for Mann-Whitney test (comparison with HIV<sup>free</sup> controls).

(TIF)

**S17 Fig. Targeting USP18 expression in spleen CD4 T-cells from an HIV-1-infected subject results in reduced apoptosis.** Briefly, spleen cells were collected and transduced for 48 hours with LV<sub>Ctrl</sub> or LV<sub>USP18 KO</sub>. Transduced cells were then activated or not using anti-CD3 and anti-CD28 Abs (TCR stimulation), or p55 Gag and anti-CD28 Abs (HIV stimulation). (A) Gating strategy to detect the virus-specific CD4 T-cells at 18 hours of HIV-1 stimulation using



IFN- $\gamma$  expression. (B) USP18 expression in gated Mem after 48 hours of cell transduction. Iso-type control is also shown in grey. (C) Levels of apoptosis on transduced CD4 T-cells after cell activation. Representative histograms show the apoptosis in Mem and IFN- $\gamma$ <sup>+</sup> virus-specific cells for TCR and HIV stimulation, respectively. (TIF)

## Acknowledgments

We are grateful to the patients participating in the Canadian Cohort of HIV-1-infected subjects, their physicians and attending staff members. We would also like to thank Drs. S. Stäger, professor at the IAF-INRS as well as R. Telittchenko for critically reviewing the manuscript.

**Members of Montreal Primary Infection Study Group;** *Director.* Dre. C. Tremblay; *Administrative staff members.* M. Legault, D. Albert, A. Massicotte, N. Cotta-Grand; *Regular members.* Drs J-P. Routy, N. Chomont, A. Finzy, P. Ancuta, N. Bernard, J. van Grevenynghe.

## Author Contributions

**Conceptualization:** Xavier Dagenais-Lussier, Jean-Pierre Routy, Julien van Grevenynghe.

**Data curation:** Xavier Dagenais-Lussier, Hamza Loucif, Hugo Cadorel, Juliette Blumberger, Mariana Gé Bego.

**Formal analysis:** Xavier Dagenais-Lussier, Hamza Loucif, Hugo Cadorel, Juliette Blumberger, Mariana Gé Bego, Julien van Grevenynghe.

**Funding acquisition:** Julien van Grevenynghe.

**Methodology:** Xavier Dagenais-Lussier, Stéphane Isnard, Julien van Grevenynghe.

**Project administration:** Julien van Grevenynghe.

**Resources:** Éric A. Cohen, Jean-Pierre Routy.

**Supervision:** Éric A. Cohen, Jean-Pierre Routy, Julien van Grevenynghe.

**Writing – original draft:** Xavier Dagenais-Lussier, Julien van Grevenynghe.

**Writing – review & editing:** Xavier Dagenais-Lussier, Hamza Loucif, Éric A. Cohen, Jean-Pierre Routy, Julien van Grevenynghe.

## References

1. Bostik P, Noble ES, Mayne AE, Gargano L, Villinger F, Ansari AA. Central memory CD4 T cells are the predominant cell subset resistant to anergy in SIV disease resistant sooty mangabeys. *AIDS*. 2006; 20(2):181–8. <https://doi.org/10.1097/01.aids.0000198092.77948.8a> PMID: 16511410.
2. Letvin NL, Mascola JR, Sun Y, Gorgone DA, Buzby AP, Xu L, et al. Preserved CD4<sup>+</sup> central memory T cells and survival in vaccinated SIV-challenged monkeys. *Science*. 2006; 312(5779):1530–3. <https://doi.org/10.1126/science.1124226> PMID: 16763152; PubMed Central PMCID: PMC2365913.
3. Mattapallil JJ, Douek DC, Buckler-White A, Montefiori D, Letvin NL, Nabel GJ, et al. Vaccination preserves CD4 memory T cells during acute simian immunodeficiency virus challenge. *J Exp Med*. 2006; 203(6):1533–41. <https://doi.org/10.1084/jem.20060657> PMID: 16735692; PubMed Central PMCID: PMC2118314.
4. van Grevenynghe J, Procopio FA, He Z, Chomont N, Riou C, Zhang Y, et al. Transcription factor FOXO3a controls the persistence of memory CD4(+) T cells during HIV infection. *Nat Med*. 2008; 14(3):266–74. <https://doi.org/10.1038/nm1728> PMID: 18311149.
5. van Grevenynghe J, Halwani R, Chomont N, Ancuta P, Peretz Y, Tanel A, et al. Lymph node architecture collapse and consequent modulation of FOXO3a pathway on memory T- and B-cells during HIV infection. *Semin Immunol*. 2008; 20(3):196–203. <https://doi.org/10.1016/j.smim.2008.07.008> PMID: 18757210.

6. Dagenais-Lussier X, Aounallah M, Mehraj V, El-Far M, Tremblay C, Sekaly RP, et al. Kynurenine Reduces Memory CD4 T-Cell Survival by Interfering with Interleukin-2 Signaling Early during HIV-1 Infection. *J Virol*. 2016; 90(17):7967–79. <https://doi.org/10.1128/JVI.00994-16> PMID: 27356894; PubMed Central PMCID: PMC4988137.
7. Aounallah M, Dagenais-Lussier X, El-Far M, Mehraj V, Jenabian MA, Routy JP, et al. Current topics in HIV pathogenesis, part 2: Inflammation drives a Warburg-like effect on the metabolism of HIV-infected subjects. *Cytokine Growth Factor Rev*. 2016; 28:1–10. <https://doi.org/10.1016/j.cytogfr.2016.01.001> PMID: 26851985.
8. Dagenais-Lussier X, Mouna A, Routy JP, Tremblay C, Sekaly RP, El-Far M, et al. Current topics in HIV-1 pathogenesis: The emergence of deregulated immuno-metabolism in HIV-infected subjects. *Cytokine Growth Factor Rev*. 2015; 26(6):603–13. <https://doi.org/10.1016/j.cytogfr.2015.09.001> PMID: 26409789.
9. Doitsh G, Galloway NL, Geng X, Yang Z, Monroe KM, Zepeda O, et al. Cell death by pyroptosis drives CD4 T-cell depletion in HIV-1 infection. *Nature*. 2014; 505(7484):509–14. <https://doi.org/10.1038/nature12940> PMID: 24356306; PubMed Central PMCID: PMC4047036.
10. Borden EC, Sen GC, Uze G, Silverman RH, Ransohoff RM, Foster GR, et al. Interferons at age 50: past, current and future impact on biomedicine. *Nat Rev Drug Discov*. 2007; 6(12):975–90. <https://doi.org/10.1038/nrd2422> PMID: 18049472.
11. Teijaro JR. Type I interferons in viral control and immune regulation. *Curr Opin Virol*. 2016; 16:31–40. <https://doi.org/10.1016/j.coviro.2016.01.001> PMID: 26812607; PubMed Central PMCID: PMC4821698.
12. Achioni C, Marsili G, Perrotti E, Remoli AL, Sgarbanti M, Battistini A. Type I IFN—a blunt spear in fighting HIV-1 infection. *Cytokine Growth Factor Rev*. 2015; 26(2):143–58. <https://doi.org/10.1016/j.cytogfr.2014.10.004> PMID: 25466629.
13. Schoggins JW, Rice CM. Interferon-stimulated genes and their antiviral effector functions. *Curr Opin Virol*. 2011; 1(6):519–25. <https://doi.org/10.1016/j.coviro.2011.10.008> PMID: 22328912; PubMed Central PMCID: PMC3274382.
14. Schoggins JW, Wilson SJ, Panis M, Murphy MY, Jones CT, Bieniasz P, et al. A diverse range of gene products are effectors of the type I interferon antiviral response. *Nature*. 2011; 472(7344):481–5. <https://doi.org/10.1038/nature09907> PMID: 21478870; PubMed Central PMCID: PMC3409588.
15. Boasso A, Shearer GM. Chronic innate immune activation as a cause of HIV-1 immunopathogenesis. *Clin Immunol*. 2008; 126(3):235–42. <https://doi.org/10.1016/j.clim.2007.08.015> PMID: 17916442; PubMed Central PMCID: PMC2275778.
16. d'Ettorre G, Paiardini M, Ceccarelli G, Silvestri G, Vullo V. HIV-associated immune activation: from bench to bedside. *AIDS Res Hum Retroviruses*. 2011; 27(4):355–64. <https://doi.org/10.1089/aid.2010.0342> PMID: 21309730.
17. Hardy GA, Sieg S, Rodriguez B, Anthony D, Asaad R, Jiang W, et al. Interferon-alpha is the primary plasma type-I IFN in HIV-1 infection and correlates with immune activation and disease markers. *PLoS One*. 2013; 8(2):e56527. <https://doi.org/10.1371/journal.pone.0056527> PMID: 23437155; PubMed Central PMCID: PMC3577907.
18. Herbeuval JP, Hardy AW, Boasso A, Anderson SA, Dolan MJ, Dy M, et al. Regulation of TNF-related apoptosis-inducing ligand on primary CD4+ T cells by HIV-1: role of type I IFN-producing plasmacytoid dendritic cells. *Proc Natl Acad Sci U S A*. 2005; 102(39):13974–9. <https://doi.org/10.1073/pnas.0505251102> PMID: 16174727; PubMed Central PMCID: PMC1224361.
19. Lehmann C, Harper JM, Taubert D, Hartmann P, Fatkenheuer G, Jung N, et al. Increased interferon alpha expression in circulating plasmacytoid dendritic cells of HIV-1-infected patients. *J Acquir Immune Defic Syndr*. 2008; 48(5):522–30. <https://doi.org/10.1097/QAI.0b013e31817f97cf> PMID: 18645522.
20. von Sydow M, Sonnerborg A, Gaines H, Strannegard O. Interferon-alpha and tumor necrosis factor-alpha in serum of patients in various stages of HIV-1 infection. *AIDS Res Hum Retroviruses*. 1991; 7(4):375–80. <https://doi.org/10.1089/aid.1991.7.375> PMID: 1906289.
21. Boasso A, Hardy AW, Anderson SA, Dolan MJ, Shearer GM. HIV-induced type I interferon and tryptophan catabolism drive T cell dysfunction despite phenotypic activation. *PLoS One*. 2008; 3(8):e2961. <https://doi.org/10.1371/journal.pone.0002961> PMID: 18698365; PubMed Central PMCID: PMC2491901.
22. Dagenais-Lussier X, Loucif H, Murira A, Laulhe X, Stager S, Lamarre A, et al. Sustained IFN-I Expression during Established Persistent Viral Infection: A "Bad Seed" for Protective Immunity. *Viruses*. 2017; 10(1). <https://doi.org/10.3390/v10010012> PMID: 29301196; PubMed Central PMCID: PMC5795425.
23. Daugan M, Murira A, Mindt BC, Germain A, Tarrab E, Lapiere P, et al. Type I Interferon Impairs Specific Antibody Responses Early during Establishment of LCMV Infection. *Front Immunol*. 2016; 7:564. <https://doi.org/10.3389/fimmu.2016.00564> PMID: 27994594; PubMed Central PMCID: PMC5136549.










24. Herbeuval JP, Nilsson J, Boasso A, Hardy AW, Kruhlak MJ, Anderson SA, et al. Differential expression of IFN-alpha and TRAIL/DR5 in lymphoid tissue of progressor versus nonprogressor HIV-1-infected patients. *Proc Natl Acad Sci U S A*. 2006; 103(18):7000–5. <https://doi.org/10.1073/pnas.0600363103> PMID: 16632604; PubMed Central PMCID: PMC1444883.
25. Osokine I, Snell LM, Cunningham CR, Yamada DH, Wilson EB, Elsaesser HJ, et al. Type I interferon suppresses de novo virus-specific CD4 Th1 immunity during an established persistent viral infection. *Proc Natl Acad Sci U S A*. 2014; 111(20):7409–14. <https://doi.org/10.1073/pnas.1401662111> PMID: 24799699; PubMed Central PMCID: PMC4034239.
26. Teijaro JR. Too much of a good thing: Sustained type 1 interferon signaling limits humoral responses to secondary viral infection. *Eur J Immunol*. 2016; 46(2):300–2. <https://doi.org/10.1002/eji.201546224> PMID: 26783074; PubMed Central PMCID: PMC5113021.
27. Teijaro JR, Ng C, Lee AM, Sullivan BM, Sheehan KC, Welch M, et al. Persistent LCMV infection is controlled by blockade of type I interferon signaling. *Science*. 2013; 340(6129):207–11. <https://doi.org/10.1126/science.1235214> PMID: 23580529; PubMed Central PMCID: PMC3640797.
28. Wilson EB, Brooks DG. Interfering with type I interferon: a novel approach to purge persistent viral infection. *Cell Cycle*. 2013; 12(18):2919–20. <https://doi.org/10.4161/cc.26175> PMID: 23974094; PubMed Central PMCID: PMC3875659.
29. Wilson EB, Yamada DH, Elsaesser H, Herskovitz J, Deng J, Cheng G, et al. Blockade of chronic type I interferon signaling to control persistent LCMV infection. *Science*. 2013; 340(6129):202–7. <https://doi.org/10.1126/science.1235208> PMID: 23580528; PubMed Central PMCID: PMC3704950.
30. Honke N, Shaabani N, Zhang DE, Hardt C, Lang KS. Multiple functions of USP18. *Cell Death Dis*. 2016; 7(11):e2444. <https://doi.org/10.1038/cddis.2016.326> PMID: 27809302; PubMed Central PMCID: PMC5260889.
31. Basters A, Knobloch KP, Fritz G. USP18—a multifunctional component in the interferon response. *Biosci Rep*. 2018; 38(6). <https://doi.org/10.1042/BSR20180250> PMID: 30126853; PubMed Central PMCID: PMC6240716.
32. Cheng L, Ma J, Li J, Li D, Li G, Li F, et al. Blocking type I interferon signaling enhances T cell recovery and reduces HIV-1 reservoirs. *J Clin Invest*. 2017; 127(1):269–79. <https://doi.org/10.1172/JCI90745> PMID: 27941247; PubMed Central PMCID: PMC5199717.
33. Cheng L, Yu H, Li G, Li F, Ma J, Li J, et al. Type I interferons suppress viral replication but contribute to T cell depletion and dysfunction during chronic HIV-1 infection. *JCI Insight*. 2017; 2(12). <https://doi.org/10.1172/jci.insight.94366> PMID: 28614789; PubMed Central PMCID: PMC5470878.
34. Zhen A, Rezek V, Youn C, Lam B, Chang N, Rick J, et al. Targeting type I interferon-mediated activation restores immune function in chronic HIV infection. *J Clin Invest*. 2017; 127(1):260–8. <https://doi.org/10.1172/JCI89488> PMID: 27941243; PubMed Central PMCID: PMC5199686.
35. Fritsch RD, Shen X, Sims GP, Hathcock KS, Hodes RJ, Lipsky PE. Stepwise differentiation of CD4 memory T cells defined by expression of CCR7 and CD27. *J Immunol*. 2005; 175(10):6489–97. <https://doi.org/10.4049/jimmunol.175.10.6489> PMID: 16272303.
36. Okada R, Kondo T, Matsuki F, Takata H, Takiguchi M. Phenotypic classification of human CD4+ T cell subsets and their differentiation. *Int Immunol*. 2008; 20(9):1189–99. <https://doi.org/10.1093/intimm/dxn075> PMID: 18635582.
37. Molinari F, Frattini M. Functions and Regulation of the PTEN Gene in Colorectal Cancer. *Front Oncol*. 2013; 3:326. <https://doi.org/10.3389/fonc.2013.00326> PMID: 24475377; PubMed Central PMCID: PMC3893597.
38. Jaleco S, Swainson L, Dardalhon V, Burjanadze M, Kinet S, Taylor N. Homeostasis of naive and memory CD4+ T cells: IL-2 and IL-7 differentially regulate the balance between proliferation and Fas-mediated apoptosis. *J Immunol*. 2003; 171(1):61–8. <https://doi.org/10.4049/jimmunol.171.1.61> PMID: 12816983.
39. Riou C, Yassine-Diab B, Van grevenynghe J, Somogyi R, Greller LD, Gagnon D, et al. Convergence of TCR and cytokine signaling leads to FOXO3a phosphorylation and drives the survival of CD4+ central memory T cells. *J Exp Med*. 2007; 204(1):79–91. <https://doi.org/10.1084/jem.20061681> PMID: 17190839; PubMed Central PMCID: PMC2118424.
40. Kane LP, Weiss A. The PI-3 kinase/Akt pathway and T cell activation: pleiotropic pathways downstream of PIP3. *Immunol Rev*. 2003; 192:7–20. <https://doi.org/10.1034/j.1600-065x.2003.00008.x> PMID: 12670391.
41. Olganier D, Sze A, Bel Hadj S, Chiang C, Steel C, Han X, et al. HTLV-1 Tax-mediated inhibition of FOXO3a activity is critical for the persistence of terminally differentiated CD4+ T cells. *PLoS Pathog*. 2014; 10(12):e1004575. <https://doi.org/10.1371/journal.ppat.1004575> PMID: 25521510; PubMed Central PMCID: PMC4270795.

42. Yue FY, Kovacs CM, Dimayuga RC, Gu XX, Parks P, Kaul R, et al. Preferential apoptosis of HIV-1-specific CD4+ T cells. *J Immunol*. 2005; 174(4):2196–204. <https://doi.org/10.4049/jimmunol.174.4.2196> PMID: 15699152.
43. Wilson EB, Brooks DG. Decoding the complexity of type I interferon to treat persistent viral infections. *Trends Microbiol*. 2013; 21(12):634–40. <https://doi.org/10.1016/j.tim.2013.10.003> PMID: 24216022; PubMed Central PMCID: PMC3864553.
44. Snell LM, McGaha TL, Brooks DG. Type I Interferon in Chronic Virus Infection and Cancer. *Trends Immunol*. 2017; 38(8):542–57. <https://doi.org/10.1016/j.it.2017.05.005> PMID: 28579323.
45. Mustachio LM, Kawakami M, Lu Y, Rodriguez-Canales J, Mino B, Behrens C, et al. The ISG15-specific protease USP18 regulates stability of PTEN. *Oncotarget*. 2017; 8(1):3–14. <https://doi.org/10.18632/oncotarget.13914> PMID: 27980214; PubMed Central PMCID: PMC5352120.
46. Fraietta JA, Mueller YM, Yang G, Boesteanu AC, Gracias DT, Do DH, et al. Type I interferon upregulates Bak and contributes to T cell loss during human immunodeficiency virus (HIV) infection. *PLoS Pathog*. 2013; 9(10):e1003658. <https://doi.org/10.1371/journal.ppat.1003658> PMID: 24130482; PubMed Central PMCID: PMC3795023.
47. Herbeuval JP, Grivel JC, Boasso A, Hardy AW, Chougnet C, Dolan MJ, et al. CD4+ T-cell death induced by infectious and noninfectious HIV-1: role of type 1 interferon-dependent, TRAIL/DR5-mediated apoptosis. *Blood*. 2005; 106(10):3524–31. <https://doi.org/10.1182/blood-2005-03-1243> PMID: 16046522; PubMed Central PMCID: PMC1895067.
48. Nguyen TP, Bazdar DA, Mudd JC, Lederman MM, Harding CV, Hardy GA, et al. Interferon-alpha inhibits CD4 T cell responses to interleukin-7 and interleukin-2 and selectively interferes with Akt signaling. *J Leukoc Biol*. 2015; 97(6):1139–46. <https://doi.org/10.1189/jlb.4A0714-345RR> PMID: 25784743; PubMed Central PMCID: PMC4438745.
49. Honke N, Shaabani N, Merches K, Gassa A, Kraft A, Ehrhardt K, et al. Immunoactivation induced by chronic viral infection inhibits viral replication and drives immunosuppression through sustained IFN-I responses. *Eur J Immunol*. 2016; 46(2):372–80. <https://doi.org/10.1002/eji.201545765> PMID: 26507703; PubMed Central PMCID: PMC5063111.
50. Malakhova OA, Kim KI, Luo JK, Zou W, Kumar KG, Fuchs SY, et al. UBP43 is a novel regulator of interferon signaling independent of its ISG15 isopeptidase activity. *EMBO J*. 2006; 25(11):2358–67. <https://doi.org/10.1038/sj.emboj.7601149> PMID: 16710296; PubMed Central PMCID: PMC1478183.
51. Jiao B, Shi X, Chen Y, Ye H, Yao M, Hong W, et al. Insulin receptor substrate-4 interacts with ubiquitin-specific protease 18 to activate the Jak/STAT signaling pathway. *Oncotarget*. 2017; 8(62):105923–35. <https://doi.org/10.18632/oncotarget.22510> PMID: 29285303; PubMed Central PMCID: PMC5739690.
52. Arimoto KI, Lochte S, Stoner SA, Burkart C, Zhang Y, Miyauchi S, et al. STAT2 is an essential adaptor in USP18-mediated suppression of type I interferon signaling. *Nat Struct Mol Biol*. 2017; 24(3):279–89. <https://doi.org/10.1038/nsmb.3378> PMID: 28165510; PubMed Central PMCID: PMC5365074.
53. Rallon N, Garcia M, Garcia-Samaniego J, Cabello A, Alvarez B, Restrepo C, et al. Expression of PD-1 and Tim-3 markers of T-cell exhaustion is associated with CD4 dynamics during the course of untreated and treated HIV infection. *PLoS One*. 2018; 13(3):e0193829. <https://doi.org/10.1371/journal.pone.0193829> PMID: 29518102; PubMed Central PMCID: PMC5843247.
54. Pompura SL, Dominguez-Villar M. The PI3K/AKT signaling pathway in regulatory T-cell development, stability, and function. *J Leukoc Biol*. 2018. <https://doi.org/10.1002/JLB.2MIR0817-349R> PMID: 29357116.
55. Lederman MM, Calabrese L, Funderburg NT, Clagett B, Medvik K, Bonilla H, et al. Immunologic failure despite suppressive antiretroviral therapy is related to activation and turnover of memory CD4 cells. *J Infect Dis*. 2011; 204(8):1217–26. <https://doi.org/10.1093/infdis/jir507> PMID: 21917895; PubMed Central PMCID: PMC3218674.
56. Piconi S, Trabattoni D, Gori A, Parisotto S, Magni C, Meraviglia P, et al. Immune activation, apoptosis, and Treg activity are associated with persistently reduced CD4+ T-cell counts during antiretroviral therapy. *AIDS*. 2010; 24(13):1991–2000. <https://doi.org/10.1097/QAD.0b013e32833c933ce> PMID: 20651586.
57. Baker JV, Peng G, Rapkin J, Krason D, Reilly C, Cavert WP, et al. Poor initial CD4+ recovery with antiretroviral therapy prolongs immune depletion and increases risk for AIDS and non-AIDS diseases. *J Acquir Immune Defic Syndr*. 2008; 48(5):541–6. <https://doi.org/10.1097/QAI.0b013e31817bebb3> PMID: 18645520; PubMed Central PMCID: PMC3617548.
58. Lewden C, Chene G, Morlat P, Raffi F, Dupon M, Dellamonica P, et al. HIV-infected adults with a CD4 cell count greater than 500 cells/mm<sup>3</sup> on long-term combination antiretroviral therapy reach same mortality rates as the general population. *J Acquir Immune Defic Syndr*. 2007; 46(1):72–7. <https://doi.org/10.1097/QAI.0b013e318134257a> PMID: 17621240.

59. Cha L, de Jong E, French MA, Fernandez S. IFN-alpha exerts opposing effects on activation-induced and IL-7-induced proliferation of T cells that may impair homeostatic maintenance of CD4+ T cell numbers in treated HIV infection. *J Immunol*. 2014; 193(5):2178–86. <https://doi.org/10.4049/jimmunol.1302536> PMID: 25063872.
60. Fernandez S, Tanaskovic S, Helbig K, Rajasuriar R, Kramski M, Murray JM, et al. CD4+ T-cell deficiency in HIV patients responding to antiretroviral therapy is associated with increased expression of interferon-stimulated genes in CD4+ T cells. *J Infect Dis*. 2011; 204(12):1927–35. <https://doi.org/10.1093/infdis/jir659> PMID: 22006994.
61. Younes SA, Talla A, Pereira Ribeiro S, Saidakova EV, Korolevskaya LB, Shmagel KV, et al. Cycling CD4+ T cells in HIV-infected immune nonresponders have mitochondrial dysfunction. *J Clin Invest*. 2018; 128(11):5083–94. <https://doi.org/10.1172/JCI120245> PMID: 30320604; PubMed Central PMCID: PMC6205369.
62. Biancotto A, Iglehart SJ, Vanpouille C, Condack CE, Lisco A, Ruecker E, et al. HIV-1 induced activation of CD4+ T cells creates new targets for HIV-1 infection in human lymphoid tissue ex vivo. *Blood*. 2008; 111(2):699–704. <https://doi.org/10.1182/blood-2007-05-088435> PMID: 17909079; PubMed Central PMCID: PMC2200839.
63. Stevenson M, Stanwick TL, Dempsey MP, Lamonica CA. HIV-1 replication is controlled at the level of T cell activation and proviral integration. *EMBO J*. 1990; 9(5):1551–60. PMID: 2184033; PubMed Central PMCID: PMC551849.
64. Jenabian MA, El-Far M, Vyboh K, Kema I, Costiniuk CT, Thomas R, et al. Immunosuppressive Tryptophan Catabolism and Gut Mucosal Dysfunction Following Early HIV Infection. *J Infect Dis*. 2015; 212(3):355–66. <https://doi.org/10.1093/infdis/jiv037> PMID: 25616404.
65. Maneglier B, Malleret B, Guillemin GJ, Spreux-Varoquaux O, Devillier P, Rogez-Kreuz C, et al. Modulation of indoleamine-2,3-dioxygenase expression and activity by HIV-1 in human macrophages. *Fundam Clin Pharmacol*. 2009; 23(5):573–81. <https://doi.org/10.1111/j.1472-8206.2009.00703.x> PMID: 19656212.
66. Mellor AL, Lemos H, Huang L. Indoleamine 2,3-Dioxygenase and Tolerance: Where Are We Now? *Front Immunol*. 2017; 8:1360. <https://doi.org/10.3389/fimmu.2017.01360> PMID: 29163470; PubMed Central PMCID: PMC5663846.
67. Scagnolari C, Monteleone K, Selvaggi C, Pierangeli A, D'Ettoire G, Mezzaroma I, et al. ISG15 expression correlates with HIV-1 viral load and with factors regulating T cell response. *Immunobiology*. 2016; 221(2):282–90. <https://doi.org/10.1016/j.imbio.2015.10.007> PMID: 26563749.
68. Doitsh G, Greene WC. Dissecting How CD4 T Cells Are Lost During HIV Infection. *Cell Host Microbe*. 2016; 19(3):280–91. <https://doi.org/10.1016/j.chom.2016.02.012> PMID: 26962940; PubMed Central PMCID: PMC4835240.
69. Chomont N, DaFonseca S, Vandergeeten C, Ancuta P, Sekaly RP. Maintenance of CD4+ T-cell memory and HIV persistence: keeping memory, keeping HIV. *Curr Opin HIV AIDS*. 2011; 6(1):30–6. <https://doi.org/10.1097/COH.0b013e3283413775> PMID: 21242891.
70. Chomont N, El-Far M, Ancuta P, Trautmann L, Procopio FA, Yassine-Diab B, et al. HIV reservoir size and persistence are driven by T cell survival and homeostatic proliferation. *Nat Med*. 2009; 15(8):893–900. <https://doi.org/10.1038/nm.1972> PMID: 19543283; PubMed Central PMCID: PMC2859814.
71. Sandler NG, Bosinger SE, Estes JD, Zhu RT, Tharp GK, Boritz E, et al. Type I interferon responses in rhesus macaques prevent SIV infection and slow disease progression. *Nature*. 2014; 511(7511):601–5. <https://doi.org/10.1038/nature13554> PMID: 25043006; PubMed Central PMCID: PMC4418221.
72. van Grevenynghe J, Cubas RA, Noto A, DaFonseca S, He Z, Peretz Y, et al. Loss of memory B cells during chronic HIV infection is driven by Foxo3a- and TRAIL-mediated apoptosis. *J Clin Invest*. 2011; 121(10):3877–88. <https://doi.org/10.1172/JCI59211> PMID: 21926463; PubMed Central PMCID: PMC3195482.

RESEARCH ARTICLE

## The RyfA small RNA regulates oxidative and osmotic stress responses and virulence in uropathogenic *Escherichia coli*

Hicham Bessaiah <sup>1,2</sup>, Pravil Pokharel <sup>1,2</sup>, Hamza Loucif <sup>1</sup>, Merve Kulbay <sup>1</sup>, Charles Sasseville<sup>3</sup>, Hajer Habouria<sup>1,2</sup>, Sébastien Houle <sup>1,2</sup>, Jacques Bernier <sup>1</sup>, Éric Massé <sup>3</sup>, Julien Van Grevenynghe<sup>1</sup>, Charles M. Dozois<sup>1,2\*</sup>

1 INRS-Centre Armand-Frappier Santé Biotechnologie, Laval, Québec, Canada, 2 CRIPA-Centre de recherche en infectiologie porcine et avicole, Saint-Hyacinthe, Québec, Canada, 3 Department of Biochemistry, RNA Group, Université de Sherbrooke, Sherbrooke, Quebec, Canada

\* [charles.dozois@inrs.ca](mailto:charles.dozois@inrs.ca)



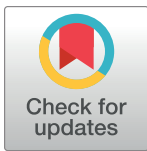
## RESEARCH ARTICLE

# The RyfA small RNA regulates oxidative and osmotic stress responses and virulence in uropathogenic *Escherichia coli*

Hicham Bessaiah<sup>1,2</sup>, Pravil Pokharel<sup>1,2</sup>, Hamza Loucif<sup>1</sup>, Merve Kulbay<sup>1</sup>, Charles Sasseville<sup>3</sup>, Hajer Habouria<sup>1,2</sup>, Sébastien Houle<sup>1,2</sup>, Jacques Bernier<sup>1</sup>, Éric Massé<sup>3</sup>, Julien Van Grevenynghe<sup>1</sup>, Charles M. Dozois<sup>1,2\*</sup>

**1** INRS-Centre Armand-Frappier Santé Biotechnologie, Laval, Québec, Canada, **2** CRIPA-Centre de recherche en infectiologie porcine et avicole, Saint-Hyacinthe, Québec, Canada, **3** Department of Biochemistry, RNA Group, Université de Sherbrooke, Sherbrooke, Quebec, Canada

\* [charles.dozois@inrs.ca](mailto:charles.dozois@inrs.ca)



## OPEN ACCESS

**Citation:** Bessaiah H, Pokharel P, Loucif H, Kulbay M, Sasseville C, Habouria H, et al. (2021) The RyfA small RNA regulates oxidative and osmotic stress responses and virulence in uropathogenic *Escherichia coli*. *PLoS Pathog* 17(5): e1009617. <https://doi.org/10.1371/journal.ppat.1009617>

**Editor:** Eric Oswald, INSERM U1220, FRANCE

**Received:** November 3, 2020

**Accepted:** May 5, 2021

**Published:** May 27, 2021

**Copyright:** © 2021 Bessaiah et al. This is an open access article distributed under the terms of the [Creative Commons Attribution License](https://creativecommons.org/licenses/by/4.0/), which permits unrestricted use, distribution, and reproduction in any medium, provided the original author and source are credited.

**Data Availability Statement:** All relevant data are within the manuscript and its [Supporting Information](#) files.

**Funding:** This work was funded through Natural Science and Engineering Research Council of Canada (NSERC) (<https://www.nserc-crsng.gc.ca>) (Discovery program, project 2019-06642) to C.M.D. We acknowledge collaborators research: É.M. (supported by an operating grant from the Canadian Institutes of Health Research (CIHR) <https://cihr-irsc.gc.ca>) and J.V.G. (Appel d'offre du Réseau SIDA/MI (FRQS <http://www.frqs.gouv.qc>).

## Abstract

Urinary tract infections (UTIs) are a common bacterial infectious disease in humans, and strains of uropathogenic *Escherichia coli* (UPEC) are the most frequent cause of UTIs. During infection, UPEC must cope with a variety of stressful conditions in the urinary tract. Here, we demonstrate that the small RNA (sRNA) RyfA of UPEC strains is required for resistance to oxidative and osmotic stresses. Transcriptomic analysis of the *ryfA* mutant showed changes in expression of genes associated with general stress responses, metabolism, biofilm formation and genes coding for cell surface proteins. Inactivation of *ryfA* in UPEC strain CFT073 decreased urinary tract colonization in mice and the *ryfA* mutant also had reduced production of type 1 and P fimbriae (pili), adhesins which are known to be important for UTI. Furthermore, loss of *ryfA* also reduced UPEC survival in human macrophages. Thus, *ryfA* plays a key regulatory role in UPEC adaptation to stress, which contributes to UTI and survival in macrophages.

## Author summary

Small regulatory RNAs play a critical role in bacterial adaptation, physiology, and metabolism. We investigated the role of the small RNA *ryfA* in uropathogenic *E. coli*, by using genetic, molecular and cell culture approaches, and mouse infection models. We demonstrate that RyfA is important for resistance to oxidative and osmotic stresses and affects the global transcription of multiple responses to stress. Deletion of *ryfA* also reduced production of type 1 and P fimbriae (pili) and increased swimming motility. RyfA also plays an important role in urinary tract infection (UTI) in the mouse model and for survival in human primary macrophages and cell lines. Elucidating a role for RyfA in adaptation to stress response and virulence provides insight into new regulatory mechanisms important for virulence in pathogenic *E. coli* and likely other Enterobacteria that may lead to development of targeted therapeutic or prophylactic approaches against these pathogens.



ca/en/) 2019-2020 and NSERC RPGPIN-2018-05272). H.B. received a PhD Fellowship from CRIPA-Programme des Regroupements stratégiques du Fonds de recherche du Québec - Nature et technologies (FRQNT) (<https://www.cripa.center/home-1>) 2020-RS4-265142. The funders had no role in study design, data collection and analysis, decision to publish, or preparation of the manuscript.

**Competing interests:** The authors have declared that no competing interest exist.

## Introduction

Urinary tract infections (UTIs) are one of the most prevalent bacterial infections, affecting millions of people each year [1]. UTIs primarily affect women, and up to 50% of adult women have experienced at least one UTI episode during their lifetime. Recurrent UTIs are observed in a quarter of women within 6 months of initial diagnosis and in half of the women within one year of a UTI episode even after antimicrobial treatment [2]. Uropathogenic *Escherichia coli* (UPEC) remains, by far, the primary causative agent of uncomplicated UTIs [1]. To establish, maintain, and to circumvent host defenses during an infection, UPEC are equipped with specialized virulence factors. Well-documented examples include adhesins (type 1, P, F1C, and S fimbriae), flagella, iron acquisition systems, a polysaccharide capsule and toxins such as hemolysin [3,4].

Bacterial adherence to host cells is critical for initiating pathogenesis and persistence during a UTI. Fimbrial adhesins (type 1, P, F1C, S, and Dr) and nonfimbrial adhesins (TosA) mediate binding to cells lining the urinary tract mucosal surfaces [5,6]. Type 1 fimbriae encoded by the *fimAICDFGH* (*fim*) operon are critical for colonization and invasion of bladder epithelial cells. They aid in formation of biofilm-like intracellular bacterial communities (IBCs) that contain large numbers of bacteria which may persist as reservoirs and may lead to recurring infections [7]. UPEC type 1 fimbriae bind to mannosylated uroplakin proteins enriched on the apical surface of the bladder [8]. *fimA* encodes the major subunit of type 1 fimbriae and *fimH* encodes the mannose-specific adhesin. The promoter region regulating *fim* expression (*fimS*) is located on a 314-bp invertible element flanked by two 9-bp inverted repeats, and the orientation of *fimS* provides a mechanism of phase variation wherein a bacterial cell produces type 1 fimbriae, *fimS* in the ON orientation, or does not produce, *fimS* in the OFF orientation [9]. FimB and FimE are site-specific recombinases involved in phase variation (flipping) of *fimS*. FimB mediates the ON-to-OFF or OFF-to-ON inversions of *fimS*, and FimE preferentially mediates the ON-to-OFF inversion of *fimS* [10]. In addition, in UPEC strain CFT073 there are three additional tyrosine recombinases, IpbA, IpuA, and IpuB, which are also capable of catalyzing inversion of *fimS* [11]. Numerous mechanisms of regulation of the *fimS* switch and expression of type 1 fimbriae have been described. Regulatory proteins such as integration host factor (IHF), leucine responsive protein (LRP), and histone-like nucleoid structuring (H-NS) affect *fim* expression [12]. Other factors have also been shown to affect type 1 fimbriae expression, including cross-talk with genes from other fimbriae [13] and environmental conditions such as pH, osmolarity, temperature, metabolite availability and oxygen levels [14,15].

As with all infectious agents, UPEC must circumvent, suppress, or resist a variety of stressful conditions and host defenses during the course of an infection. In the urinary tract, UPEC may encounter neutrophils and macrophages which produce antimicrobial factors, such as reactive oxygen species (ROS) and reactive nitrogen species (RNS) [16]. ROS and RNS can cause damage and physiological stress with pleiotropic effects on bacterial cells. These products can damage the bacterial membrane and DNA, alter enzyme activity by damaging iron-sulfur clusters in enzymes and cause oxidation of proteins and lipids [17,18]. Indeed, UPEC need to overcome environmental stresses that can be encountered during infection by a variety of mechanisms, and it is thought that resistance to ROS may be important for UPEC pathogenesis.

Bacterial small RNAs (sRNAs) are known regulators of many physiological processes [19]. Several sRNAs play key roles in bacterial adaptation to changing environmental conditions and stress responses, including responses to nutrient availability, envelope and osmotic stresses, oxidative stress, iron deficiency, and pH stress [20–22]. *ryfA* encodes a sRNA [23] and had been implicated in biofilm formation [24,25] and swarming motility [25] in *E. coli* and

pathogenesis in *Shigella dysenteriae* [26]. A toxic peptide TimP (for toxic inner membrane protein), identified when the *ryfA* paralog in *Salmonella enterica* was highly expressed, was recently reported [27].

The purpose of this research was to investigate the role of the sRNA RyfA for gene regulation in UPEC and its importance for adaptation to stress and colonization during UTI. Here, we show that RyfA contributes to resistance to oxidative and osmotic stresses in UPEC strain CFT073. In both *in vitro* and *in vivo* experiments, deletion of *ryfA* resulted in important differences in expression of genes that contribute to protection against environmental stresses, and that are known to regulate fimbrial adhesins, cellular processes, and metabolism. These regulatory changes are likely to contribute to attenuation of UPEC and its decreased capacity to survive within macrophages. These data support the hypothesis that RyfA is involved in resistance to oxidative stress in UPEC and that RyfA can also influence type 1 fimbriae expression, thereby attenuating UPEC virulence. Understanding the link between the RyfA small RNA and its connection between stress responses, and expression of type 1 fimbriae will better elucidate the signals that control UPEC virulence, and may lead to the development of therapeutics that could potentially inhibit the establishment of UTI and thereby reduce the occurrence of this highly prevalent infection.

## Results

### The *ryfA* gene is involved in resistance to osmotic stress

We previously generated a transposon (Tn) library in UPEC reference strain CFT073 [28]. The library was subjected to osmotic and oxidative stresses as a selection for potentially decreased fitness in an environment in which the bacteria encounter host-derived stresses including osmolarity in urine and interactions with host immune cells. We screened this Tn library for mutants that exhibited reduced tolerance to osmotic and oxidative stress in order to identify genes that may play a role in UPEC stress tolerance. One mutant that exhibited reduced tolerance to osmotic and oxidative stress carried a transposon insertion adjacent to the *ryfA* gene. To confirm the direct role of *ryfA* in phenotypes of decreased tolerance to stress, we generated a site-directed deletion to create a  $\Delta ryfA$  mutant of UPEC strain CFT073. To determine whether *ryfA* contributes to resistance to osmotic stress, the WT parental strain,  $\Delta ryfA$ , and a complemented  $\Delta ryfA$  strain were subjected independently to osmotic stress (0.6 M Urea) and salt stress (0.6 M NaCl), on modified LB agar. The WT and the complemented mutant were able to grow on LB agar containing NaCl or urea (Fig 1A). By contrast, on LB agar with 0.6 M urea or 0.6 M NaCl, the capacity of the *ryfA* mutant to grow was significantly reduced (Fig 1A). In LB agar, there was no growth difference between CFT073 and CFT073  $\Delta ryfA$  (S1A Fig). This result suggests that RyfA could play a role in resistance to osmotic stress caused by NaCl and urea.

### Loss of *ryfA* increases sensitivity to ROI-generating compounds

To determine if *ryfA* influences UPEC resistance to oxidative stress, bacterial survival after exposure to oxidative stress was tested using different reactive oxygen intermediate (ROI)-generating agents. We used H<sub>2</sub>O<sub>2</sub> and various superoxide generators such as plumbagin and paraquat, during growth on either rich (LB) or minimal (M9-glucose) medium. Sensitivity to these compounds was determined with wild-type UPEC strains CFT073 and 536 and corresponding  $\Delta ryfA$  mutants. On LB medium, the CFT073  $\Delta ryfA$  strain was more sensitive to the ROI-generating compounds H<sub>2</sub>O<sub>2</sub> ( $p = 0.0022$ ) and plumbagin ( $p < 0.0001$ ) when compared to parental strain CFT073 (Fig 1B). The UPEC 536  $\Delta ryfA$  mutant was only more sensitive to H<sub>2</sub>O<sub>2</sub> ( $p = 0.0065$ ) when compared to strain 536 (S1B Fig). On minimal medium, both UPEC *ryfA*

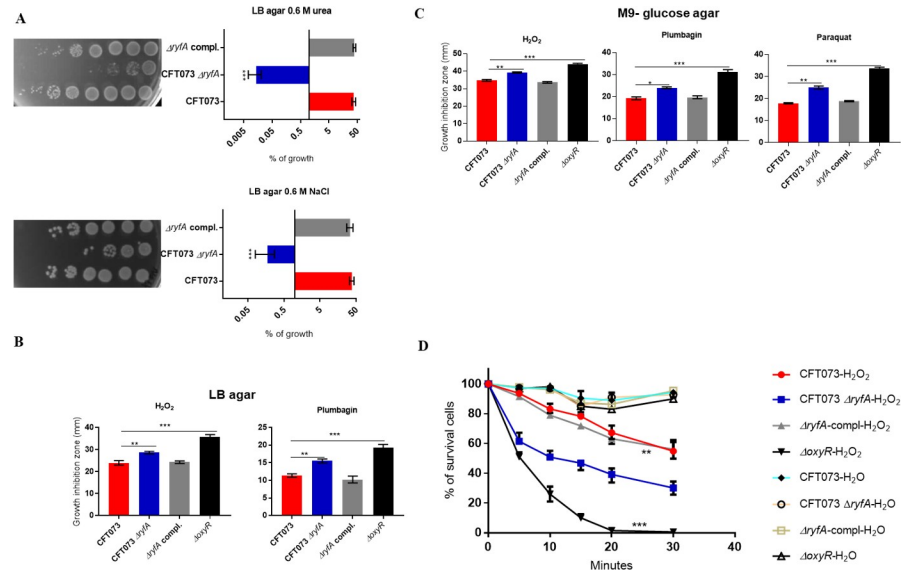


**Fig 1. Role of RyfA in osmotic and oxidative stress resistance.** (A) Growth under conditions of osmotic stress. Strains were grown shaking in LB medium until mid-log phase (O.D.<sub>600</sub>, 0.6) and plated on LB agar and LB agar with 0.6 M NaCl and 0.6 M urea (see [Methods](#)). (B) Growth inhibition zones (mm) of UPEC CFT073, *ryfA* mutant and complemented strains to oxidative stress generating compounds. Strains were grown on either LB agar or (C) M9-glucose agar. ROI-generating compounds tested were 30% hydrogen peroxide (H<sub>2</sub>O<sub>2</sub>), 53 mM plumbagin, or 40 mM paraquat. (D) Resistance to hydrogen peroxide in LB broth. WT CFT073 and *ryfA* mutant strains were examined in LB medium containing 5mM H<sub>2</sub>O<sub>2</sub> or an equivalent volume of Milli-Q water (H<sub>2</sub>O). Samples were collected every 5 minutes, diluted, and plated on LB agar to determine CFUs. The CFT073 *ΔoxyR* strain was used as a sensitive control strain. The results represent the means of replicate experiments for a minimum of three samples. Vertical bars represent the standard errors of the means. Statistical significance was calculated by one-way ANOVA (A to D): (\*,  $P < 0.05$ ; \*\*,  $P < 0.005$ ; \*\*\*,  $P < 0.0001$ ).

<https://doi.org/10.1371/journal.ppat.1009617.g001>

mutants were more sensitive to H<sub>2</sub>O<sub>2</sub>, plumbagin, and paraquat (Figs 1C and S1B). In addition, in LB broth the CFT073 *ΔryfA* mutant was killed more readily compared to wild-type CFT073 ( $p = 0.0057$ ) after exposure to 5 mM hydrogen peroxide (Fig 1D). Complementation of the *ΔryfA* mutant with a single-copy of *ryfA* on the chromosome restored resistance to ROI-generating compounds (Figs 1B, 1C and 1D). These results show that loss of the *ryfA* sRNA reduces bacterial resistance to oxidative stress, and that RyfA may contribute to regulation of genes implicated in the oxidative stress response.

### RyfA is produced in logarithmic phase

*ryfA* was originally identified by *in silico*-based genomic analyses designed to identify genes encoding previously uncharacterized sRNA molecules [23]. *In silico* analyses revealed that *ryfA* is chromosomally located between *sseA* and *sseB* (S2A Fig). Using BLAST searches, we identified *ryfA* homologues in other species of *Escherichia*, *Salmonella*, *Shigella*, *Klebsiella*, *Enterobacter*, *Serratia* and *Citrobacter* (S2A Fig). *ryfA* from CFT073 shares 98% identity at the nucleic acid level with the non-pathogenic K-12 strain MG1655 (S2B Fig), and has greater than 90% sequence identity to *ryfA* sequences from other intestinal and extraintestinal pathogenic *E. coli* and *Shigella* spp. (S2A Fig).

To determine under what conditions CFT073 produces RyfA, we performed Northern blotting under laboratory conditions. Bacteria were grown in LB medium at 37°C until the culture O.D. of 0.2 to 2.9. Northern blot analysis showed that RyfA was expressed starting at mid-log phase and reached maximal production in late exponential phase (~ 0.9 to 2.3) (Fig 2A). By



using quantitative real-time PCR (qRT-PCR) analysis we confirmed that RyfA is produced by wild-type CFT073 under the same conditions (Fig 2B). We did not detect any signal in the  $\Delta ryfA$  strain, confirming the absence of RyfA in the mutant strain (Fig 2A).

*ryfA* is predicted to be 305 nt in length (S2B Fig). The expression of *ryfA* was placed under the control of an arabinose inducible promoter and the size of the *ryfA* transcript was confirmed by radiolabeled *ryfA*-specific antisense RNA probe. A single band of approximately 300 nt was detected by northern blot in RNA samples obtained from strain CFT073 and using the inducible promoter construct (Fig 2C). The secondary structure of RyfA was predicted using the Vienna RNA websuite program [29], and its predicted secondary structure is comprised of multi-stem loops (S2C Fig).

### Transcriptomic analysis of the effect of loss of *ryfA* on UPEC gene expression

Our *in vitro* experiments revealed an important role for RyfA in response to stresses. We reasoned that the greater sensitivity of the *ryfA* mutant could be due to numerous changes in gene expression that occur in the absence of this regulatory RNA. To examine the role of RyfA, we performed RNA-Seq to compare RNA profiles between wild-type *E. coli* CFT073 and the CFT073  $\Delta ryfA$  mutant. Bacteria were cultured in triplicate at 37°C in LB with aeration to mid-logarithmic growth (O.D. 0.6), mRNAs were extracted and RNA-Seq was performed. In total, the deletion of *ryfA* significantly altered the expression of 484 genes (120 were upregulated and 364 were downregulated) with a log<sub>2</sub> fold-change (FC) greater than or equal to  $\pm 1.7$  (S1 Table). The genes that were most highly affected in response to loss of *ryfA* are listed in Fig 3. Functional analysis revealed that the genes belonging to the categories “metabolism” and “stress response” were by far the most markedly affected. Indeed, increased sensitivity to stresses is likely a consequence of altered gene expression and defective regulation of the stress response.

**Loss of *ryfA* alters expression of genes regulated by the RpoH ( $\sigma^{32}$ ) (heat shock response) regulon.** *rpoH* encodes  $\sigma^{32}$ , the primary sigma factor controlling the heat shock

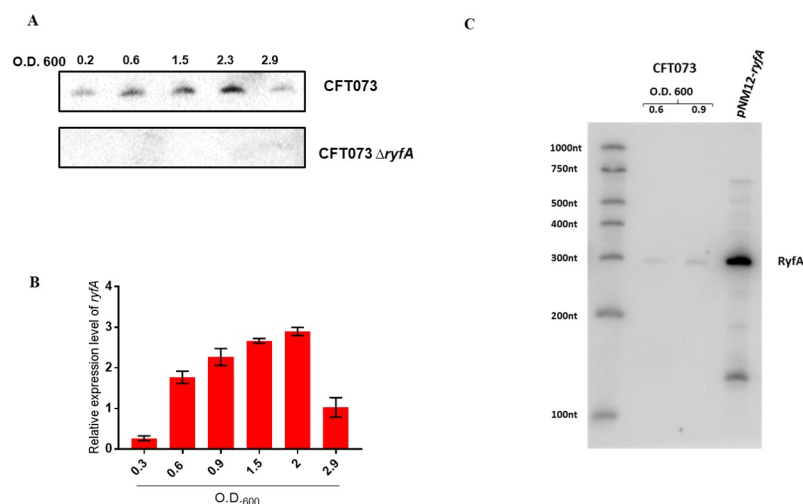


**Fig 2. CFT073 produces RyfA in mid-logarithmic phase.** (A) Northern blot analysis using 10 mg of total RNA isolated from WT CFT073 following growth in LB medium at 37°C. Lack of signal in  $\Delta ryfA$  strain confirms absence of RyfA in the  $\Delta ryfA$  strain. (B) Quantitative real-time PCR (qRT-PCR) analysis demonstrating that RyfA is produced by wild-type CFT073 under the conditions tested. (C) Northern blot showing RyfA expression in a strain overexpressing RyfA.

<https://doi.org/10.1371/journal.ppat.1009617.g002>

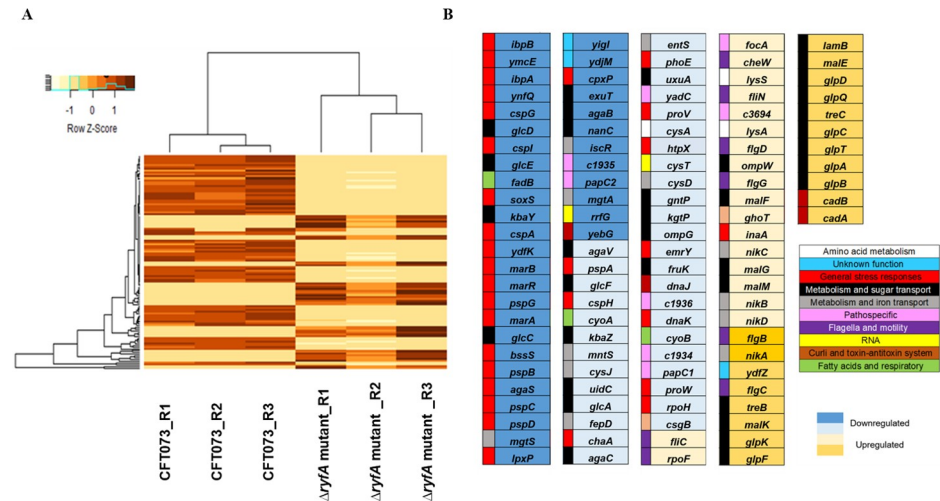


**Fig 3. Genes significantly affected by deletion of *ryfA*.** RNA-seq analysis was performed on RNA samples (in triplicate) from strain CFT073 and CFT073  $\Delta ryfA$  grown in LB at mid-log phase of growth (O.D. 0.6). (A) Heatmap of the entire data set ( $n = 6$ ) of CFT073 and  $\Delta ryfA$  mutant. Each row of the heatmap represents the  $\log_2$  fold values transformed with Z-score of 121 differentially expressed genes (upregulation, red, downregulation, yellow). Hierarchical grouping of differentially expressed genes shows clustering. Z-scores are computed on a gene-by-gene basis by subtracting the mean and then dividing by the standard deviation. Specific genes and changes are presented in Fig 3B. (B) Genes classified in different categories based on  $\log_2$  fold-change difference. Genes upregulated (yellow rectangles) and downregulated (blue rectangles) by at least 1.7-fold were considered significant with  $P < 0.05$ . Dark blue is greater or equal ( $\geq$ ) a 3-fold decrease. Light blue is a decrease from 3-fold to 1.7-fold. Light yellow is an increase from 1.7-fold to 3-fold. Dark yellow is a greater or equal ( $\geq$ ) 3-fold increase. Genes are classified in different categories with colored squares: General stress responses in red, metabolism and sugar transport in black, metabolism and iron transport in grey, patho-specific in pink, flagella and motility in purple, fatty acids and respiratory chain in green, amino acid metabolism in white, curli and toxin-antitoxin system in orange, RNA in yellow and unknown function in azure. Specific values fold-changes are presented in S1 Table (see supplementary data).

<https://doi.org/10.1371/journal.ppat.1009617.g003>

response during log-phase growth. It is subjected to tight control via a multivalent regulatory system that responds to temperature and the abundance of misfolded proteins within the cell [30]. During exponential growth, in the *ryfA* mutant, *rpoH* gene expression was down-regulated (-1.76-fold) (Fig 3). The heat shock regulon mediated by  $\sigma^{32}$  controls a major stress response to cope with heat and other stresses in *Escherichia coli* [31]. The heat-shock response is a protective mechanism that is crucial for bacterial survival and adaptation to hostile environmental conditions. The most down-regulated genes in the *ryfA* mutant were genes encoding both cold shock and heat shock proteins (Fig 3B). These included genes encoding chaperones involved in protein fate, such as those responding to heat shock: *ibpB* (-7.70-fold), *ibpA* (-5.96-fold), *dnaKJ* (-2.20-fold), *htpX* (-2.28-fold) and *cpxP* (-3.37-fold). CpxP functions as both a chaperone and a repressor of the Cpx response. This system is involved in many cytoplasmic events, such as folding of nascent polypeptide chains, rescue of misfolded proteins and assembly and disassembly of protein complexes [32,33].

**Alteration of expression of genes involved in the general stress response.** Several genes that are involved in defense against oxidative stress were also down-regulated including *soxS*, which encodes the transcriptional regulator that responds to superoxide-generating species (-5.03-fold) (Fig 3B and S1 Table). The four cold shock genes *cspG*, *cspI*, *cspA* *cspH* were also down-regulated. Other genes associated with cold-shock were downregulated such as *ymcE* (-6.39-fold) and *ydfK* (-4.07-fold), as well as genes in the *pspABCDG* operon coding for phage shock proteins. The Psp system protects proteins from aggregation and helps maintain the proton motive force (PMF) to counteract stress conditions (such as filamentous phage

infection, extreme temperatures, osmolarity changes, and the mislocalization of secretin proteins) [34]. The genes *yebG* and *ydjM*, which are induced during stress involving DNA-damage and the SOS response were also downregulated. In addition, *emrY* (-2.22-fold), encoding a multidrug resistance secretion protein and also known to reduce the lethal effects of stress was downregulated (S1 Table).

Further, other genes that contribute to resistance to antimicrobials, toxic compounds and oxidative stress were also downregulated in the *ryfA* mutant. These include the *marR* (-4.01-fold) gene encoding the multiple antibiotic resistance regulator and *marAB* (-3.92- to -4.01-fold) encoding multiple antibiotic resistance proteins. Interestingly, *proVW*, encoding systems for the transport of the osmoprotectants proline and glycine betaine were also downregulated (-1.94 and -2.29-fold, respectively) (Fig 3B). The downregulation of stress response genes corresponds to the increased sensitivity to oxidative and osmotic stress that was determined (Fig 1).

**Loss of *ryfA* altered expression of genes encoding fimbriae and required for flagella synthesis and motility.** RNA-Seq results indicated that deletion of *ryfA* altered expression of genes encoding different types of fimbriae. We observed significant downregulation of the *papC* genes, which encode the usher protein required for biogenesis of P fimbriae. The CFT073 genome harbors two copies of the *pap* operon, designated *pap1* and *pap2*, and both *papC1* and *papC2* genes were repressed (-2.02 and -3.16-fold, respectively) (Fig 3B and S1 Table). The *f9* genes, encoding F9 fimbriae (ORFs *c1931-c1936*), showed decreased expression (-3.18 to -1.61-fold). The *yadC* gene (*c0166*), encoding a putative fimbrial adhesin protein, was also down-regulated (-2.3-fold). In contrast, *focA* (*c1239*) encoding the F1C fimbrial major subunit protein was increased (1.81-fold) (Fig 3B and S1 Table). While we identified some differentially regulated fimbria-encoding genes within the *yeh*, *yqi*, and *yfc* operons, most genes within these operons were either not differentially regulated or were excluded due to having mapped reads below the cutoff value.

The gene encoding the sigma factor 28 ( $\sigma^{28}$ ), which is responsible for initiation of transcription of a number of genes involved in motility and flagellar synthesis was up-regulated (1.73-fold). In agreement with this, some flagellar biosynthesis and motility genes were also up-regulated (*flgCBGD*) (2.18 to 3.48-fold), the *fliC* gene encoding flagellin (1.60-fold), and *cheW* (1.90-fold), which encodes a positive regulator of chemotaxis (Fig 3 and S1 Table).

Some genes that are involved in biofilm formation were also downregulated, including, genes important for cellulose synthesis (*bssS*) (-3.79-fold), thin aggregative curli fiber production (*csgB*) (-1,76-fold) and lipid A biosynthesis (*lpxP*) (-3,51-fold) (Fig 3B). We were unable to determine if *csgA*, *csgD*, *csgE*, and *csgF* were differentially expressed, as their expression levels were too low under the test conditions that were used and were excluded from the final RNA-Seq analysis. Taken together, deletion of *ryfA* altered expression of multiple operons encoding fimbriae, downregulated some genes important for biofilm formation and upregulated genes required for flagellar assembly and motility.

## Validation of differentially expressed genes

To validate some of the data obtained from the RNA-Seq results, we performed qRT-PCR using primers specific to a series of genes that were differentially expressed: *soxS*, *ibpA*, *cspA*, *marA*, *bssS*, *rpoH*, *cadA*, *malE* and *treC* to compare log<sub>2</sub> fold change in gene expression between CFT073  $\Delta$ *ryfA* and the CFT073 wild-type strains. Strains were cultured under conditions identical to our RNA-Seq experiment. We observed highly similar differences in gene expression as compared to our RNA-Seq results. Specifically, we observed downregulation of *soxS*, *ibpA*, *cspA*, *marA*, *bssS*, *rpoH* and upregulation of *cadA*, and *treC* (S3A Fig).

### Inactivation of RyfA reduces production of type 1 fimbriae *in vitro*

Since the *ryfA* mutant is more sensitive to oxidative and osmotic stresses and given that type 1 fimbriae play an important role for colonization in the murine UTI model [5], the effect of the *ryfA* mutation on production of type 1 fimbriae was investigated. Production of type 1 fimbriae was determined by yeast agglutination at the mid-log phase of growth in LB medium (O.D. 0.6) and human urine (O.D. 0.4) and in static conditions. Following mid-log growth with shaking in LB broth, and overnight growth in human urine with shaking, the agglutination titer of CFT073  $\Delta$ *ryfA* was significantly reduced ( $p < 0.0001$  and  $p = 0.0062$ , respectively) as compared to parent strain CFT073 (Fig 4A). When cultured statically, agglutination titers were significantly reduced in the CFT073  $\Delta$ *ryfA* mutant compared to the WT strain in LB, human urine (Fig 4A) or minimal M9-glucose broth (S4A Fig). The yeast agglutination titer was also significantly reduced in both UPEC  $\Delta$ *ryfA* strains compared to wild-type UTI89 and 536 parent strains after mid-log phase in LB and human urine (S4B Fig). Yeast agglutination by the *ryfA* complemented mutant regained titers similar to that of the WT strain (Figs 4A and S4A and S4B). Western blotting against the type 1 fimbrial major subunit FimA confirmed a sharp reduction of FimA production by the  $\Delta$ *ryfA* mutant compared to WT strain CFT073 and the *ryfA* complemented strain (Fig 4B). Surprisingly, although production of type 1 fimbriae was reduced in the *ryfA* mutant, we did not observe significant differences in the RNA-seq data for *fim* genes under growth conditions tested. This could be explained by the fact that at O.D. 0.6, only 4% of the cell population expresses type 1 fimbriae, as previously reported [35]. However, by comparing expression of *fimA* in LB and human urine at mid-log phase and after static growth, by RT-PCR, we observed a significant decrease in *fimA* RNA levels in the

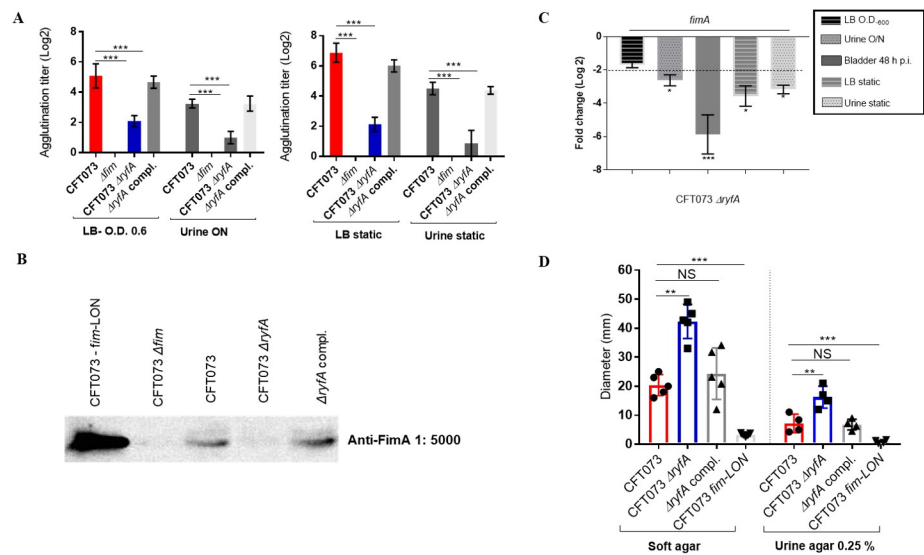


**Fig 4. Effect of deletion of *ryfA* on type 1 fimbriae (pili) production and motility.** (A) Yeast agglutination titer demonstrating level of production of type 1 fimbriae in strains cultured to the mid-log phase and after overnight static growth in LB broth and in human urine. The  $\Delta$ *fim* strain was used as a negative control and showed no agglutination. (B) Western blot of fimbrial extracts of strains cultured to the mid-log phase of growth in LB broth. The CFT073 *fim*-locked ON strain was used as a positive control. (C) Expression of *fimA* gene by qRT-PCR in the  $\Delta$ *ryfA* strain compared to the WT CFT073 strain in LB, human urine and infected bladders. (D) Motility of CFT073, *ryfA* mutant and complemented strain on 0.25% soft or urine agar. Each box and scatter dot plot (min to max) represents the mean diameter of the motility zone. Results are the mean values and standard deviations for at least three biological experiments. Statistical significance was calculated by the Student t test (A, C, D): \*,  $P < 0.05$ ; \*\*,  $P < 0.005$ ; \*\*\*,  $P < 0.0001$ . NS, not significant.

<https://doi.org/10.1371/journal.ppat.1009617.g004>

*ryfA* mutant (Fig 4C). These results indicate that deletion of the *ryfA* sRNA caused a substantial decrease in the levels of type 1 fimbriae production and *fimA* gene expression.

### Loss of RyfA increases swimming motility

The effect of *ryfA* deletion on motility was determined, since motility contributes to colonization and persistence in the urinary tract [36]. We compared the motility of the *ryfA* mutant in 0.25% soft and urine agar. We reasoned that since the deletion of *ryfA* decreased expression of type 1 fimbriae (Fig 4A), motility of the *ryfA* mutants may potentially be increased. There was a clear and significant increase in motility of the  $\Delta$ *ryfA* strain compared to wild-type CFT073 parent strain in soft agar and urine agar plates (Fig 4D). Interestingly, the upregulation of flagellar and motility genes also corresponds to the increased swimming motility that was observed on motility agar (Fig 3).

### Deletion of *ryfA* decreased the expression of P fimbriae and increased expression of F1C fimbriae

It has been observed that deletion of the *fim* operon results in increased expression of other types of fimbriae [13,35]. Since UPEC strains adhere to bladder epithelial cells and epithelial cell adherence is mediated predominantly by type 1 fimbriae, we therefore hypothesized that the *ryfA* mutant may demonstrate reduced adherence to bladder epithelial cells. To test this possibility, adhesion assays using 5637 human bladder epithelial cells (ATCC HTB-9) were performed. The *ryfA* mutant adhered to human bladder cells as well as the WT strain (Fig 5A). As expected, addition of 1.5%  $\alpha$ -d-mannopyranose, which inhibits type 1 fimbriae mediated

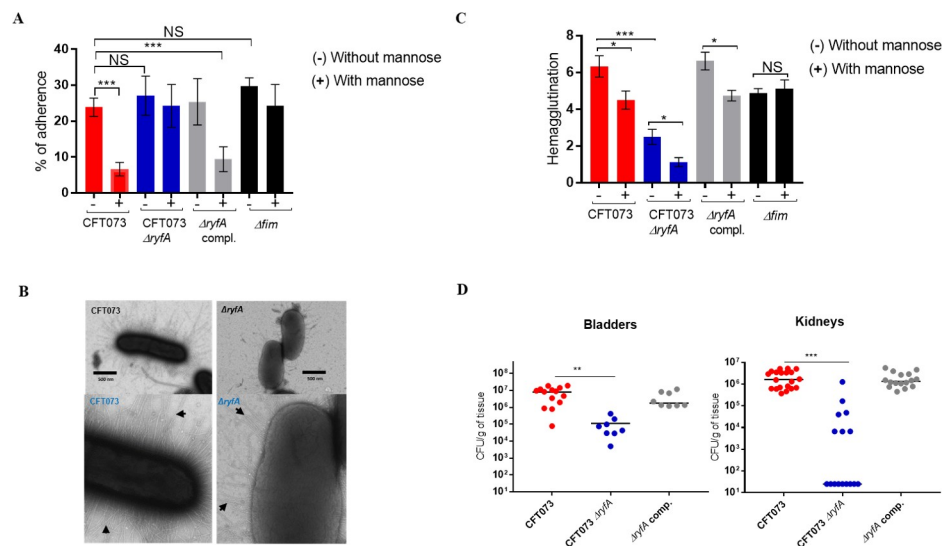


**Fig 5. Role of *ryfA* in the murine model of ascending UTI and in P fimbriae (pili) production.** (A) Adherence of strain CFT073 and its derivatives to human 5637 bladder epithelial cells in the presence or absence of 2.5%  $\alpha$ -d-mannopyranose was determined. (B) Electron microscopy of CFT073 and the  $\Delta$ *ryfA* mutant. Arrows show fimbriae on cell surfaces. (C) Production of Pap fimbriae by hemagglutination assay. Results are the mean values and standard deviations for four biological experiments. (D) Single-strain infections to compare wild-type strain CFT073 to  $\Delta$ *ryfA* mutant. Results are presented as the log<sub>10</sub> CFU g<sup>-1</sup>. Each data point represents a sample from an individual mouse, and horizontal bars indicate the medians. Two independent series of infections were performed: i (CFT073 WT and CFT073  $\Delta$ *ryfA*) and ii (CFT073 WT and the complemented mutant). The  $\Delta$ *ryfA* mutant was attenuated 146-fold in bladder and 10,000-fold in kidneys compared to the WT parent strain. Data are means  $\pm$  standard errors of the means of 10 mice. Statistical significance was calculated by one-way ANOVA (A and C) or Mann–Whitney Test (D): \*,  $P < 0.05$ ; \*\*,  $P < 0.005$ ; \*\*\*,  $P < 0.0001$ . NS, not significant.

<https://doi.org/10.1371/journal.ppat.1009617.g005>



binding, greatly decreased adherence of the WT (mean decrease of 17.2%) and complemented strain (mean decrease of 15.9%) (Fig 5A). By contrast, addition of mannopyranose only slightly reduced adherence of the  $\Delta ryfA$  (mean decrease of 2.8%) and  $\Delta fim$  (mean decrease of 5.4%) mutants, to 5637 bladder cells (Fig 5A). In line with these findings, *fimA* expression was also down-regulated by 4.8-fold in the *ryfA* mutant, during adherence to 5637 bladder cells (S4C Fig).

These results suggest that other adhesins such as the *foc*-encoded F1C fimbriae, which were upregulated in the *ryfA* mutant (Fig 3B), could potentially mediate adherence to the bladder epithelial cells. Further, electron microscopy images demonstrate that the type of fimbriae at the surface of cells of the *ryfA* mutant differ from those produced by the CFT073 wild-type strain and that fimbriae are also somewhat reduced in numbers compared to the WT parent strain (Fig 5B). As such, adherence of the *ryfA* mutant to bladder cells is largely independent of type 1 fimbriae and is mediated by other adhesins present at the cell surface. We also investigated production of Pap fimbriae by mannose-resistant hemagglutination (MRHA) of human erythrocytes of strains cultured in LB broth. Interestingly, the MRHA titer of the *ryfA* mutant was significantly reduced compared to parent strain CFT073 (Fig 5C). This supports the hypothesis that P fimbriae production is also reduced in the *ryfA* mutant. In line with these results, expression of both *papA1* and *papA2* was reduced by 3.5-fold and 6.3-fold, respectively (S4C Fig). These results demonstrate that the mannose-resistant adherence of the *ryfA* mutant to bladder epithelial cells is not attributed to increased production of Pap fimbriae, but could be due to increased production of other adhesins such as F1C fimbriae. It was also previously shown that expression of F1C fimbriae increased considerably in a strain lacking the *fim* and *pap* gene clusters [37]. Thereby, we investigated by qRT-PCR and Western blotting whether expression of F1C fimbriae was increased in this background. As shown in S4C and S4D Fig, F1C fimbriae were upregulated 7.9-fold in the *ryfA* mutant. Therefore, upregulation of F1C fimbriae in the *ryfA* mutant could potentially contribute to the *in vitro* adherence of the *ryfA* mutant to bladder cells.

We analyzed the adherence and intracellular bacterial survival of the cystitis isolate UTI89 by using imaging flow cytometry-based assays. The GFP-tagged UTI89 and its derivative strains were allowed to adhere to monolayers of the bladder epithelial cell line 5637 for 2 h (T0), after which extracellular bacteria were killed by addition of the host cell-impermeable antibiotic gentamicin. Following a 4 h (T4) incubation in the continued presence of gentamicin, infected monolayers were washed and intracellular bacterial survival (T4) was quantitatively determined by the percentage of GFP<sup>high</sup> 5637 cells. Representative images that correspond to single GFP<sup>+</sup>LAMP1<sup>+</sup> 5637 cells at T0 and T4 are shown in S5 Fig. Interestingly, the percentages of total cell-associated bacteria for  $\Delta ryfA$  and  $\Delta fim$  mutants were significantly reduced (5.03% and 4.5%, respectively) when compared to the WT parent strain (24.36%) ( $p < 0.0001$ ). At 4 h post-infection, results showed a significantly higher percentage of UTI89 GFP<sup>high</sup> labeled WT bacteria within intracellular compartments compared to either the  $\Delta ryfA$  or  $\Delta fim$  mutants (S5 Fig).

Previous studies showed that the  $\Delta fim$  or  $\Delta fimH$  UTI89 mutant strains were deficient in binding to 5637 cultured bladder epithelial cells *in vitro* and were unable to colonize and invade bladder epithelium by 6 h p.i. relative to the isogenic WT UTI89 control strain [38,39]. The UTI89  $\Delta ryfA$  mutant also produced less type 1 fimbriae compared to the WT parent strain *in vitro* (S4B Fig). These data suggest that deletion of *ryfA* affects type 1 production in UTI89 and that the adherence to 5637 cells in the absence of the type 1 fimbriae is not sufficient to trigger bacterial internalization into bladder epithelial cells.

## Loss of RyfA reduces virulence and expression of type 1 fimbriae in the murine urinary tract

Based upon increased sensitivity of the  $\Delta ryfA$  mutant to environmental stresses, we hypothesized that the impaired osmotic and oxidative stress response could result in a fitness defect during infection of the urinary tract. In the mouse infection model, the  $\Delta ryfA$  strain showed a marked decrease in bacterial numbers in both bladders (146-fold decrease) ( $P = 0.0021$ ) and the kidneys (10,000-fold decrease) ( $P < 0.0001$ ) compared to the wild-type strain CFT073 (Fig 5D). The *ryfA* complemented mutant colonized the mouse urinary tract as well as wild-type strain CFT073 (Fig 5D). Likewise, *fimA* transcription was downregulated 5.8-fold in the bladder (Fig 4C). This reduction in colonization from inactivation of *ryfA* could be due in part to the decrease in expression of *fimA* and reduced production of type 1 fimbriae, which was also observed *in vitro* (Fig 4A and 4C). However, it is likely that additional factors including decreased resistance to cellular stresses due to loss of *ryfA* contribute to the strong attenuation and decreased bacterial numbers observed during infection with the  $\Delta ryfA$  mutant, particularly in the kidneys.

In addition, we performed a co-infection of  $\Delta ryfA$  mutant with the virulent CFT073  $\Delta lac$  strain in the CBA/J murine model. The CFT073  $\Delta lac$  strain has been shown to colonize the urinary tract as well as the CFT073 wild-type parent and presented no statistical difference in a murine UTI model [40]. Interestingly, the  $\Delta ryfA$  mutant was significantly outcompeted by the CFT073  $\Delta lac$  strain with a mean of 124-fold in the bladders ( $p < 0.0001$ ) and 13-fold ( $p < 0.0001$ ) in the kidneys (S6A Fig). In contrast to the fitness decrease identified for the  $\Delta ryfA$  strain during UTI, there was no growth difference between CFT073 and CFT073  $\Delta ryfA$  when grown *in vitro* in either LB broth or in filtered human urine. The latter represents an *ex vivo* condition that may reflect nutrient availability and environmental conditions encountered in the bladder (S6B and S6C Fig). The growth of the  $\Delta ryfA$  mutant was altered in LB supplemented with 0.6 M urea or 0.6 M NaCl, but not in human urine. Interestingly, concentration ranges of urea (150 mM to 350 mM) and sodium (40 mM to a maximum of 275 mM) in human urine are considerably lower than the concentrations that were inhibitory to the *ryfA* mutant [41–43]. Thus, the competitive defect of the *ryfA* mutant during UTI was not due to a general fitness defect, and that during standard *in vitro* culture conditions, *ryfA* was dispensable. Overall, these results confirm an important role for the RyfA sRNA during colonization and infection of the urinary tract by strain CFT073.

## RyfA contributes to increased uptake and survival of UPEC in professional phagocytes

During infection, inflammatory cells produce a variety of antimicrobial factors. A primary antimicrobial agent in this repertoire is superoxide, which reacts with other molecules to form ROS. The primary source of bactericidal ROS during infection is provided by phagocyte oxidase. We next sought to assess the potential role of *ryfA* for protection from the host-generated oxidative environment during UTI by testing bacterial interaction with human macrophages. To evaluate bacterial uptake, survival and proliferation within macrophages, primary human monocyte-derived macrophages (HMDMs) and human cultured macrophage-like THP-1 cells were infected with the wild-type strain and the isogenic mutants using a gentamicin protection assay (at a multiplicity of infection (MOI) of 20). The number of bacteria present at different times was determined by viable counts. We also assessed intramacrophage survival of an *oxyR* mutant for comparison as a sensitive control. The uptake of the *ryfA* mutant was significantly reduced in HMDMs when compared with uptake of the wild-type strain (Figs 6A and 7). However, for the THP-1 macrophages, similar bacterial loads for the different strains were observed

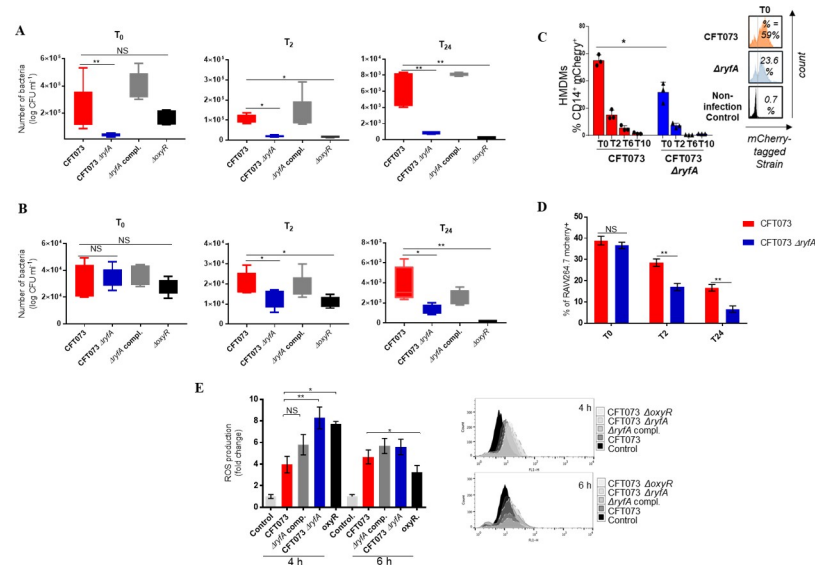


**Fig 6. Role of RyfA during interaction with professional phagocytes.** Phagocytic cells were infected with CFT073 wild-type strain, *ΔryfA* or *ΔoxyR* isogenic mutants or the *ΔryfA*-complemented strain. (A) *in vitro* differentiated human monocyte-derived macrophages (HMDMs) and (B) THP-1 human macrophages were infected with different strains for 1 h, followed by gentamicin treatment. Cells were lysed and intracellular bacterial counts (CFU ml<sup>-1</sup>) were determined at different times post-infection (pi). Infection assessment of mCherry tagged CFT073 strains via flow cytometry in (C) HMDMs and (D) RAW264.7 cells. (E) Reactive oxygen species (ROS) production in RAW264.7 cells. RAW264.7 cells were infected at an MOI of 20 and intracellular generation of ROS was measured at 4 h and 6 h post-infection by using H<sub>2</sub>DCFDA. Cells were stained with 10 μM H<sub>2</sub>DCFDA. All assays were conducted in triplicate and repeated independently at least three times. The results are expressed as the means ± sem. Significant differences between mutant, WT and complemented mutant strains were determined using One-way ANOVA. \*, *P* < 0.05; \*\*, *P* < 0.005; \*\*\*, *P* < 0.0001. NS, not significant.

<https://doi.org/10.1371/journal.ppat.1009617.g006>

(Fig 6B). In contrast to wild-type strain CFT073, for both the *ryfA* and *oxyR* mutants, viable bacteria decreased at 2 h p.i. in all types of macrophages (Figs 6A, 6B and 7). Furthermore, both mutants decreased in the intracellular compartment of macrophages at 24 h p.i. and were unable to reach the number of intracellular bacterial cells observed for the wild-type parent strain. We also obtained similar results by using multi-parameter and imaging flow cytometry (Figs 6D and 7). We monitored the uptake of mCherry-tagged CFT073 wild-type and *ryfA* mutant strains in CD14<sup>+</sup> HMDMs, which represent a classic phenotype for HMDMs. Results showed a major drop in survival of the *ryfA* mutant in HMDMs compared to the wild-type strain at all-time points (2h, 6 h and 10 h p.i.) (Fig 6C). Furthermore, we confirmed this assessment of the same GFP-tagged CFT073 strains including the *ryfA*-complemented strain via imaging flow cytometry. Representative images were also generated at 2 h p.i. for GFP<sup>high</sup> labeled strains within intracellular compartments (Fig 7). Interestingly, the *ΔryfA fim* locked-ON mutant showed a very high internalization level in HMDM compared to the WT CFT073 strain (Fig 7B). This strain also did not present any survival defect at 2 h p.i. (Fig 7B). Previous studies have suggested that fimbriae-mediated adhesion to macrophages helps *E. coli* to avoid clearance by the innate immune system [44,45]. In addition, *E. coli* overexpressing type 1 fimbriae showed increased intracellular survival in macrophages [46]. Of note, we did not observe a significant difference in the uptake of mCherry-labelled CFT073 and *ryfA* mutant by RAW264.7 macrophages (Fig 6D). However, the *ryfA* mutant survived significantly less than the parent wild-type strain at 2 h and 24 h p.i. in these cells (Fig 6D). These observations demonstrate that loss of *ryfA* can contribute to decreased virulence and clearance during extra-intestinal infections such as UTI, since cells lacking *ryfA* are more susceptible to host



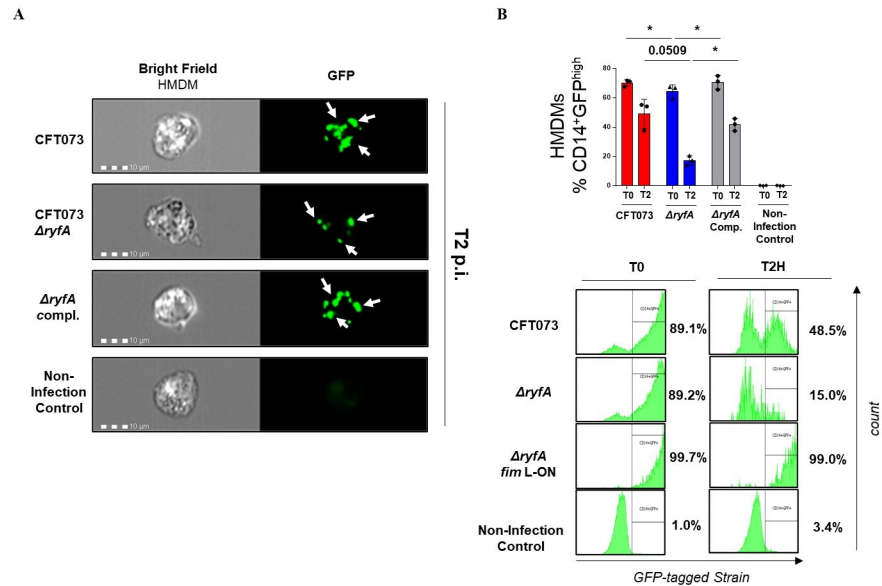


**Fig 7. Role of RyfA during interaction with human macrophage cells.** Imaging flow cytometry analysis of human monocyte-derived macrophages (HMDMs) that were infected with CFT073 wild-type strain,  $\Delta ryfA$  mutant, the  $\Delta ryfA$  complemented strain and the  $\Delta ryfA$  *fim* L-ON strain at 2 h post-infection. (A) Representative images of HMDM singlets CD14<sup>+</sup>GFP<sup>high</sup> at 2h post-infection. (B) Infection assessment for double positive percentages of CD14<sup>+</sup>GFP<sup>high</sup> HMDMs. Below, representative flow cytometric histograms for an independent experiment. Results are expressed as the means  $\pm$  sem of the replicate experiments. Significant differences between mutants, WT, and complemented mutant strain were determined using a paired Student *t*-test. \*,  $P < 0.05$ .

<https://doi.org/10.1371/journal.ppat.1009617.g007>

phagocytic cells such as macrophages. Importantly, the complemented mutant regained uptake and survival capacity in macrophages similar to wild-type parental strain CFT073 (Figs 6A, 6B and 7). It is of further interest that loss of *ryfA* also resulted in a reduced level of bacterial uptake by phagocytes, suggesting that some of the changes in expression that occur on the bacterial cell surface led to a reduced initial level of phagocytosis by macrophages. This defect of uptake by macrophages by the *ryfA* mutant also is not likely to be linked to increased sensitivity to oxidative stress, since the ROS-sensitive *oxyR* mutant did not demonstrate any differences in uptake by macrophages (Fig 6A and 6B). These results support an important role for the *ryfA* regulatory RNA in interactions with the host cellular response by contributing to uptake, survival, and replication of UPEC CFT073 inside human macrophages.

### The *ryfA* mutant generates increased ROS production in RAW264.7 murine macrophage-like cells

The phagocyte NADPH oxidase and ROS production play a key role in the elimination of bacteria following phagocytosis. To measure intracellular ROS levels, RAW264.7 macrophages infected with CFT073, the  $\Delta ryfA$ ,  $\Delta oxyR$  isogenic mutant, or the  $\Delta ryfA$  complemented strain were incubated for 4 h and 6 h with the membrane-permeant fluorescent probe H<sub>2</sub>DCFDA. The cells were then stained with a viability marker (propidium iodide) and H<sub>2</sub>DCFDA fluorescence was quantified in viable cells. Four hours later, the level of intracellular ROS after interaction with WT strain CFT073 was 3.9-fold higher when compared to uninfected control cells ( $p = 0.0026$ ) (Fig 6E). The level of intracellular ROS was 25% ( $p = 0.0093$ ) and 20% ( $p = 0.0006$ ) higher in cells infected with the  $\Delta ryfA$  and  $\Delta oxyR$  mutants respectively than in cells infected with the WT parent strain. ROS levels remained high (4-fold higher above basal level) up to 6 h p.i. in cells infected with UPEC CFT073 (Fig 6E). The ROS levels were reduced by

3-fold for the *ryfA* mutant and by half for the *oxyR* mutant after 6 h p.i. (Fig 6E), suggesting that both mutants are killed at a faster rate by ROS activity than the wild-type parent. By contrast, no significant difference was observed between the *ryfA* complemented mutant and the WT parent strain in ROS generation. These results also support the likelihood that attenuation of the *ryfA* mutant in the bladder and kidneys during UTI in the mouse model may also be due to a greater sensitivity to killing by host phagocytic cells and an increased generation of ROS within these cells.

### Effects due to loss of *ryfA* in UPEC are independent of a predicted small peptide sequence

The mechanisms of interaction of *ryfA* and its specific role in the adaptive response of pathogenic *E. coli* to resist environmental stresses and infect the urinary tract remain to be elucidated. A recent study identified that the *ryfA* gene from *Salmonella enterica* serovar Typhimurium can encode a small toxic inner membrane protein, called TimP, upon overexpression [27]. Alignment of the *ryfA* sequence of UPEC CFT073 also identified an open reading frame (ORF) spanning nt +135 to +270 (S7A Fig). This ORF is predicted to be translated into a 45-amino-acid small protein (S7B Fig). We also identified a putative Sec-dependent secretion signal using two different prediction tools: SignalP-5.0 [47] and Phobius [48] and both programs predicted a Sec translocase signal sequence spanning amino acids 1 to 22 (S7B Fig). In order to determine if such a peptide could potentially contribute to some of the regulatory changes observed due to deletion of *ryfA*, we introduced different point mutations that would eliminate the potential production of such a peptide. Three different variants of *ryfA* wherein the *E. coli* ORF predicted to encode a paralog of TimP was disrupted were generated, since some nucleotide changes could potentially affect the secondary structure of the RNA (S8 Fig). We then introduced these variants in single copy into the chromosome to complement the *ryfA* mutant of strain CFT073. Complementation of the  $\Delta$ *ryfA* mutant with any of the 3 variants of RyfA restored production of type 1 fimbriae (S7C Fig), reduced motility (S7D Fig) to wild-type levels, led to a regain in resistance to oxidative stress (S7E Fig) and survival in THP-1 macrophages (S7F Fig). These results suggest that the effects observed due to deletion of *ryfA* in UPEC do not involve the loss of a peptide that it may encode, but are more likely to be linked to the RyfA sRNA.

## Discussion

Given the importance of sRNAs for bacterial physiology and virulence, we investigated the role of the RyfA sRNA for resistance to stresses and its importance during urinary tract infection in a murine model, as well as for adherence to bladder epithelial cells, and survival in human macrophages. RyfA was shown to contribute to resistance to oxidative and osmotic stresses (Figs 1 and S1), virulence in the urinary tract of mice, and survival in host cells. Attenuation of the *ryfA* mutant could be attributed in part to increased sensitivity to osmotic and oxidative stresses, both of which are likely to be encountered during UTI. Further, downregulation of type 1 fimbriae in the *ryfA* mutant may also contribute to reduced colonization during UTI. Deletion of *ryfA* decreased production of type 1 fimbriae or *fim* gene expression *in vitro* and *in vivo* (Figs 4A and 4C and S4A). It is interesting that there is a link between sensitivity to oxidative stress and altered expression of type 1 fimbriae. Previous studies reported that mutations in other genes, including *yeaR*, *rpoS*, *ibeA* and *yqhG*, increased sensitivity to oxidative stress and concomitantly decreased expression of type 1 fimbriae [28,49–51]. Importantly, assembly of type 1 fimbriae is dependent on the oxidative state of subunit proteins in the periplasm and involves the coordinated folding of subunits through action of the

oxidoreductase DsbA and the chaperone FimC, underscoring the potential effects of oxidative imbalances on fimbrial biogenesis [52]. Collectively, these results suggest that one consequence of loss of *ryfA* may be the reduced expression of type 1 fimbriae due to increased sensitivity of UPEC to oxidative stress.

Based on the RNA-seq data obtained during growth *in vitro*, the *ryfA* mutant may be subjected to increased oxidative stress, because it is less able to deploy mechanisms to mediate a global stress response, which may also explain why it is less able to cope with additional stresses from exogenous ROI-generating compounds. The general stress response regulon under control of *rpoH*, the oxidative stress transcriptional factor *soxS*, and genes responding to heat shock and envelope stress were all repressed in the *ryfA* mutant (S1 Table). SoxS and MarA are transcription factors that contribute to adaptive responses to many stimuli, such as pH, antibiotics, oxidative stress, and host innate immune responses [53,54]. Furthermore, a triple knockout of a UPEC strain lacking *marA*, *soxS* and *rob* was unable to effectively colonize the kidney in a mouse model [55]. Since oxidative stress is increased during infection of the host, a decreased capacity to resist ROS could explain, at least in part, the attenuation of the *ryfA* mutant.

In the urinary tract, UPEC must be able to cope with transient exposure to both high osmolality and the denaturing effects of urea. RyfA contributed to resistance to osmotic stress induced by NaCl or urea (Fig 1A). Indeed, genes involved in the osmotic stress response, the glycine betaine and proline transporter *proVW*, were downregulated in the *ryfA* mutant (Fig 3). The *proVW* genes are induced in response to osmotic stress with NaCl [56] and during urinary tract infection [37] in the mouse model. Loss of *ryfA* may increase sensitivity to osmotic stress due to reduced expression of the *proVW* system. Other genes such as molecular chaperones encoding *ibpA*, *ibpB*, *cspF*, and *cspH*, which are induced in response to osmotic stress [56], were also repressed in the *ryfA* mutant. Interestingly, it was previously reported that *cspC* and *ibpB* genes were highly expressed in UPEC CFT073 isolated from mouse urine [57]. Further, *cspA*, *cspG*, *cspH*, *ibpA* and *ibpB* were among the most highly upregulated genes in asymptomatic bacteriuria (ABU) strains during static growth in human urine [58]. Moreover, the two cold-shock-associated genes *cspA* and *deaD*, were upregulated in human urine samples [59], by UPEC in murine bladders [37] and in a ABU strain in the human urinary tract [37,60]. Taken together, the decreased capacity of the *ryfA* mutant to express these stress coping chaperones and osmotic stress systems is likely to contribute to its reduced survival during UTI. Genes belonging to the Cys regulon, *soxS* and *ibpA* were reported to contribute to potassium tellurite ( $K_2TeO_3$ ) resistance [61]. Interestingly, the *ryfA* mutants of UPEC strains were more sensitive to  $K_2TeO_3$  (S1C Fig). The oxidative damage attributed to potassium tellurite is due to the intracellular generation of superoxide radicals.

UPEC strain CFT073 contains 12 distinct fimbrial gene clusters and multiple nonfimbrial adhesins [62]. However, one type of fimbria is predominantly expressed at a time, and phase variation of different adhesins involves crosstalk between fimbrial systems that limits production of fimbriae to a single type for each bacterial cell [63]. Based on gene expression data and immune-based detection, we determined that F1C fimbrial production was increased in the *ryfA* mutant (S4C and S4D Fig). Since F1C fimbriae mediate adhesion to bladder and kidney epithelial cells [64], this likely explains the mannose-resistant adherence demonstrated by the *ryfA* mutant (Fig 5A). Increased expression of F1C fimbrial genes was also observed in a  $\Delta fim \Delta pap$  mutant of UPEC CFT073 [13]. Indeed, in UPEC, the inactivation or constitutive expression of one fimbrial system can alter the expression of other adhesins [13]. Thus, it is not surprising that loss of *ryfA* in UPEC CFT073, which caused a decreased expression of type 1 and P fimbriae, has resulted in greater expression of another type of fimbrial adhesin. Taken together, these results demonstrate that *ryfA* also plays an important role in regulation and the hierarchy of cross-talk of expression of different fimbrial systems in *E. coli*.

The CFT073  $\Delta ryfA$  mutant adhered to human bladder cells as well as the WT strain. However, in contrast to the WT strain, which adhered mainly due to mannose-specific type 1 fimbriae, adherence of the *ryfA* mutant was mediated by mannose-resistant adhesins (Fig 5A). Electron microscopy demonstrated a difference in the type of fimbriae present at the cell surface of the *ryfA* mutant compared to the WT strain (Fig 5B), indicating that other adhesins are expressed at the bacterial cell surface and could mediate adherence to bladder epithelial cells. Further, the *ryfA* mutant had reduced MRHA compared to the WT strain (Fig 5C), and the expression of both *papA* genes was decreased during adhesion to bladder cells (S4C Fig). Interestingly, *ryfA* inactivation in the highly invasive cystitis strain UTI89 also significantly decreased the adherence and invasion capacity of the mutant to 5637 bladder epithelial cells (S5 Fig). Type 1 fimbriae production was also decreased in the UTI89 *ryfA* mutant (S4B Fig).

Bacterial virulence factors are often secreted or associated with the cell envelope. In the *ryfA* mutant, many genes encoding cell envelope associated proteins demonstrated significant changes in expression. We observed significant up-regulation of genes encoding flagellar biosynthesis (*flgCBGD* and *fliC*) and chemotaxis (*cheW*) (Fig 3 and S1 Table) and other genes under the control of  $\sigma^{28}$ , encoded by FliA (RpoF) which controls transcription of a number of genes involved in flagellar assembly and swimming motility. Down-regulation of *fim*, *pap*, *f9* and *yad* fimbrial transcription could also be linked to an increase in flagellar gene expression, since the *ryfA* mutant demonstrated increased swimming motility (Fig 4D), and also decreased expression of P and type 1 fimbriae (Figs 4A and 5C). The production of P fimbriae is coordinated with the repression of swimming motility [65]. Furthermore, Luterbach and Mobley [65] have demonstrated that PapX, a MarR-like protein encoded by the *pap* operon, repressed *flhD* transcription and the  $\Delta papX$  mutant was hypermotile. Taken together, these observations indicate that type 1, P, and F1C fimbriae, along with motility, can be regulated in some coordinated fashion through a mixture of transcriptional and posttranscriptional mechanisms. Of note, motility in the urinary tract can be important for the translocation of bacteria from bladder to kidneys. In contrast to our results, a previous report on an extraintestinal pathogenic *E. coli* (ExPEC) strain isolated from an ocular infection (L-1216/2010) demonstrated reduced swimming motility compared to the parent strain [24].

In the current work, the *ryfA* mutants of CFT073 and 536 exhibited a significant decrease in biofilm formation in M9 supplemented with glucose at different temperatures and in LB (at 37 and 42°C for CFT073  $\Delta ryfA$  and at 30 and 37°C for 536  $\Delta ryfA$ ) (S9 Fig). Accordingly, we also noted a statistically significant downregulation of some of the genes involved in biofilm formation, including, genes important for cellulose synthesis (*bcsS*), curli fiber production (*csgB*) and lipid A biosynthesis (*lpxP*). Further, *ibpA* and *ibpB* genes encoding small heat shock chaperone proteins which were downregulated in our mutant, were found to be induced during biofilm formation [66], and *ibpB* was also highly expressed by UPEC CFT073 isolated from mouse urine [57]. Therefore, these heat shock proteins may also promote resistance to stress by contributing to biofilm formation.

Macrophages employ ROS and RNS, that can contribute to bacterial killing [67]. In this study, the *ryfA* mutant showed significantly reduced uptake by human monocyte derived-macrophages (HMDMs) (Figs 6A and 7) as well as decreased survival rates in HMDMs, THP-1 and RAW264.7 cell lines when compared to the WT strain at all time points (Figs 6 and 7). These results indicate that RyfA plays an important role for survival in macrophages. The decreased survival inside macrophages could be explained by the numerous defects of the *ryfA* mutant, such as increased sensitivity to oxidative stress. Interestingly, the *ryfA* mutant induced high levels of intracellular ROS in RAW264.7 macrophages at 4 h p.i compared to WT strain CFT073 (Fig 6E), which may explain why the *ryfA* mutant survives less inside macrophages. Thus, a common mechanism used by bacterial pathogens to avoid host innate immune

pathways is to employ defense mechanisms against oxidative stress [68]. Interestingly, genes associated with intramacrophage survival including chaperones (*ibpA*, *ibpB*), *trxC*, *phoH* and *soxS* were downregulated in the *ryfA* mutant. Further, genes that were highly expressed and which were shown to be important for persistence of UPEC strain UTI89 within murine macrophages [69] including sigma factor H (*rpoH*), the phage shock proteins (*pspACDE*), DNA damage inducible protein (*yebG*), and small heat shock protein (*ibpB*), and biofilm formation regulatory protein (*bssS*) were all repressed in the *ryfA* mutant. The Psp system senses membrane stress and stabilizes the bacterial cell membrane under stress conditions [70]. This system is induced in *Shigella flexneri* infecting macrophage [71]. Interestingly, we found that *pspA*, *rpoH*, *ibpA* and *soxS* were all significantly downregulated in the *ryfA* mutant after 6 h p. i. in HMDM (S10 Fig). A previous study showed that *S. dysenteriae* harbors two copies of RyfA that contribute to multiplication of *S. dysenteriae* in host cells. Specifically, the overexpression of RyfA1 negatively impacted the virulence-associated process of cell-to-cell spread by elimination of *ompC* mRNA that encodes the major outer membrane protein C [26]. We report here that deletion of *ryfA* did not affect the growth of the mutant in LB broth or in human urine (S6B and S6C Fig). This lends support to our assertion that the observed defect in colonization by the *ryfA* mutant is likely due to an increased sensitivity to certain environmental stresses and changes in metabolic functions that could lead to alterations in production of fimbriae/flagella and reduced survival during infection.

Interestingly, *ryfA* RNA was significantly higher in mouse bladder after 48 h p.i. (4.82-fold) and after static growth in LB (2.44-fold) and human urine (2.03-fold) (S3B Fig). By analyzing the transcriptome profile of a UTI strain isolated directly from patients, *ryfA* was also shown to be upregulated in *E. coli* asymptomatic bacteriuria ABU strain 83972 by 1.5 to 8.9-fold compared to bacteria grown in MOPS or urine *in vitro* [60]. The ABU strain is an excellent colonizer of the human urinary tract, where it causes long-term bladder colonization.

Although, many sRNAs have been shown to mediate regulation at the RNA level through pairing with other RNA transcripts, it deserves mention that some bacterial sRNAs may code for small peptides. There are several examples of sRNAs which code for validated functional small proteins: *E. coli* SgrS encodes the protein SgrT [72], *S. aureus* RNAlII encodes a 26 amino acid  $\delta$ -hemolysin peptide [73] and *B. subtilis* SR1 encodes 39 amino acid peptide SR1P [74]. A recent study also identified that the *ryfA* gene from *Salmonella enterica* serovar Typhimurium can encode a small toxic inner membrane protein, called TimP, upon overexpression [27]. The authors also suggested a potential ORF paralog in other Enterobacteria including *E. coli* [27]. To investigate if such a peptide contributed to the phenotypes observed in the *ryfA* mutant, we derived variants of the *ryfA* allele wherein this ORF predicted to encode such a peptide was eliminated. Introduction of any of these variant alleles in the  $\Delta$ *ryfA* mutant fully complemented the mutant phenotypes (S7 Fig). As such, these experiments indicated that the potential peptide that could be encoded by *ryfA* in *E. coli* did not play an appreciable role in the regulatory effects observed due to loss of the *ryfA* gene. In the experiments presented in [27], these researchers reported effects on *Salmonella* due to artificially induced or high-level expression, and it is unknown under what natural conditions in the bacterial cell, this TimP peptide might be expressed. Notably, Fris et al. [26] investigated the characterization of *ryfA* in *Shigella dysenteriae* and attempted to identify putative peptides that might be encoded by *ryfA* and did not demonstrate production of any potential small protein under conditions tested.

Taken together, several lines of evidence suggest that inactivation of *ryfA* could attenuate pathogenic *E. coli* by altering regulatory pathways leading to changes in metabolism and decreased adaptation to environmental stresses or may potentially generate an altered response to membrane-associated stress, leading to repression of production of surface structures, including adhesins required for colonization of host tissues. Based on the important number



of adaptive and virulence associated genes that are under the control of the RyfA sRNA, it should be considered as a potential target for therapeutic interventions or preventative measures against UPEC and potentially other enterobacterial pathogens.

## Methods

### Ethics statement

This study was performed in accordance with the ethical standards of the University of Quebec, INRS. A protocol for obtaining biological samples from human donors was reviewed and approved by the ethics committee—*Comité d'éthique en recherche* of INRS (CER 19–507, approved November 19, 2019). Formal written consent was obtained by the donors.

### Bacterial strains, growth conditions and plasmids

*E. coli* strains and plasmids used in this study are listed in [S2 Table](#). *E. coli* CFT073 was initially isolated from the blood and urine of a patient with acute pyelonephritis [75]. Bacteria were grown in lysogeny broth (LB) (Alpha Bioscience, Baltimore, MD) at 37°C and in human urine. Urine was collected from healthy female volunteers that were from 20 to 40 years old and who had no history of UTI or antibiotic use in the prior 2 months. Each urine sample was immediately filter sterilized (0.2- $\mu$ m pore size), pooled, and frozen at –80°C and was used within 2 weeks. Antibiotics and reagents were added as required at the following concentrations: kanamycin, 50  $\mu$ g/ml; ampicillin, 100  $\mu$ g/ml; chloramphenicol 30  $\mu$ g/ml.

### Construction of site-directed mutants and complementation of strains

All mutants were generated by the procedure described by Datsenko and Wanner using plasmids pKD3 and pKD4 as the template for chloramphenicol and kanamycin resistance cassettes, respectively [76]. Primers used are listed in [S3 Table](#) in the supplemental material. Antibiotic resistance cassettes flanked by FLP recombination target (FRT) sequences were removed by transforming the mutant strains with pCP20 expressing the FLP recombinase [77].

### Growth under conditions of osmotic stress

Strains were tested for the capacity to grow under conditions of osmotic stress caused by NaCl or urea. Strains were inoculated 1:100 from an overnight pre-culture grown in LB and grown until mid-log phase with shaking. They were serially diluted and plated on LB agar alone and LB agar supplemented with 0.6 M NaCl or 0.6 M urea. Colonies were counted, and growth under each condition was compared to growth on LB agar.

### Sensitivity of *E. coli* strains to reactive oxygen intermediate (ROI)-generating agents

Sensitivity to oxidative stress generating agents was determined by an agar overlay diffusion method on LB plates (1.5% agar) as described by Sabri *et al.* [78]. Briefly, overnight-grown cultures were used to inoculate (1/100) fresh LB medium without antibiotics, and the resulting cultures were incubated until the O.D.<sub>600</sub> was 0.6. Then, 100  $\mu$ l of each culture were mixed with 3 ml molten top agar and poured onto an LB agar or M9- glucose plate. Whatman filter disks saturated with 10  $\mu$ l of hydrogen peroxide (30%), plumbagin (53 mM) or paraquat (40 mM) were spotted onto the disks. The plates were then incubated overnight at 37°C. Following growth, the diameters of inhibition zones were measured.

For sensitivity of bacterial cultures to H<sub>2</sub>O<sub>2</sub>, bacteria were grown at 37°C in LB broth and approximately 2.5 × 10<sup>8</sup> CFU/ml of wild-type CFT073 or mutant was inoculated into PBS containing either 5 mM H<sub>2</sub>O<sub>2</sub> and or H<sub>2</sub>O. The test was carried out under static conditions at 37°C and samples were collected at various time points post-inoculation. Samples were diluted and plated on LB agar to determine bacterial counts.

### Experimental UTI in CBA/J mice

Experimental infections were carried out using either competitive coinfection or single-strain infection models as described previously [40]. Prior to inoculation, strains were grown for 16 h at 37°C with shaking (250 rpm) in 55 ml of LB medium. For coinfection, cultures were centrifuged and pellets of a *lac*-negative derivative of the wild-type (WT) and mutant or complemented strains were mixed 1:1. Six-week-old CBA/J female mice were transurethrally inoculated with 20 μl of the 1:1 mixture containing 2 × 10<sup>9</sup> CFU of the UPEC CFT073  $\Delta$ *lacZYA* strain (QT1081) and 5 × 10<sup>8</sup> CFU of either the CFT073  $\Delta$ *ryfA* (QT5255) strain or its complemented derivative (QT5309). At 48 h p.i., mice were euthanized; bladders and kidneys were aseptically removed, homogenized, diluted, and plated on MacConkey agar to determine bacterial counts. In the single-strain experimental UTI model, mice were infected as described above but with only a single strain (10<sup>9</sup> CFU), and 48 h p.i., bacterial counts were determined from the bladders and kidneys. Bladders were dissected; one half was used to determine bacterial counts and the other half was resuspended in TRIzol reagent (Invitrogen) for RNA extraction and subsequent analysis of bacterial gene expression.

### RNA extraction and quantification of gene expression

Bacterial cultures were grown in triplicate in LB broth or human urine. RNAprotect (Qiagen, Toronto, ON, Canada) was added to cultures and RNA extracted using the RNeasy mini kit (Qiagen, Toronto, ON, Canada). Ambion Turbo DNase (Thermo Fisher Scientific, St. Laurent, QC, Canada) was used to remove contaminating DNA. RNA integrity was assessed using a Nanodrop (ND-1000). RNA was also extracted from infected bladders at 48 h p.i. with TRIzol reagent (Thermo Fisher Scientific, St. Laurent, QC, Canada), followed by DNase 1 treatment. Total RNAs were then reverse-transcribed to cDNAs using TransScript All-in-One First-Strand cDNA Synthesis SuperMix Kit (TransGen, Haidian District, Beijing, China). The resulting cDNA was used for qRT-PCR with EvaGreen according to the manufacturer's instructions (TransGen, Haidian District, Beijing, China). The *rpoD* gene was used as housekeeping control. Each qRT-PCR run was done in triplicate, and for each reaction the calculated threshold cycle ( $C_T$ ) was normalized to the  $C_T$  of the *rpoD* gene amplified from the corresponding sample. The fold change was calculated using the  $2^{-\Delta\Delta CT}$  method [79]. Genes with a fold-change above or below the defined threshold of 2 were considered as differentially expressed. Primers used for qRT-PCR analysis are listed in S3 Table in the supplemental material.

### RNA sequencing, mapping and analyses

Cultures were grown in triplicate as described above, and total RNA was isolated using the Qiagen RNeasy Protect Bacteria Mini kit. RNA-seq was performed at Génome Québec Innovation Centre, McGill University. Total RNA was quantified using a NanoDrop Spectrophotometer ND-1000 (NanoDrop Technologies, Inc.) and its integrity was assessed on a 2100 Bioanalyzer (Agilent Technologies, St. Laurent, QC, Canada). rRNA were depleted from 250 ng of total RNA using Ribo-Zero rRNA removal kit specific for bacterial RNA (Illumina). Residual RNA was cleaned up using the Agencourt RNA Clean XP Kit (Beckman Coulter) and

eluted in water. cDNA synthesis was achieved with the NEB Next RNA First Strand Synthesis and NEBNext Ultra Directional RNA Second Strand Synthesis Modules (New England BioLabs, Whitby, ON, Canada). The remaining steps of library preparation were done using and the NEBNext Ultra II DNA Library Prep Kit for Illumina (New England BioLabs, Whitby, ON, Canada). Adapters and PCR primers were purchased from New England BioLabs, Whitby, ON, Canada. Libraries were quantified using the Quant-iT PicoGreen dsDNA Assay Kit (Thermo Fisher Scientific, St. Laurent, QC, Canada) and the Kapa Illumina GA with Revised Primers-SYBR Fast Universal kit (Kapa Biosystems, Wilmington, MA, USA). Average size fragment was determined using a LabChip GX (PerkinElmer, Woodbridge, ON, Canada) instrument (G enome Qu ebec).

Reads were checked for quality using the FASTQC tool (Galaxy Version 0.72+galaxy1), poor quality reads by Trimmomatic (Galaxy Version 0.38.0) were converted to FastQ format, or “groomed” for downstream analysis using the FastQ Groomer tool (Galaxy Version 1.1.5). Bowtie (Galaxy Version 2.3.4.3+galaxy0) was used to align RNA-seq reads to the genome of *E. coli* CFT073 (GenBank accession no. AE014075.1 with default parameters. Finally, the number of reads mapping to each annotated feature was obtained with HTSeq (Galaxy Version 0.9.1). Differential expression between WT CFT073 and the *ryfA* mutant was analyzed using Degust v4.1.1 (DOI: [10.5281/zenodo.3258932](https://doi.org/10.5281/zenodo.3258932)). Transcripts were considered significant if passing the following cut-offs: adjusted p-value of < 0.05 and log<sub>2</sub> fold change of >1.7 and <-1.7. All processing steps were performed using the Galaxy platform (<https://usegalaxy.org/>).

RNA-seq data have been deposited in the GEO database, accession number GSE157450 (<https://www.ncbi.nlm.nih.gov/geo/query/acc.cgi?acc=GSE157450>).

### Verification of RNA-seq results (validation of RNA-seq results by qPCR)

RNA samples were obtained and prepared as described above for RNA-seq. qRT-PCR was performed to verify the RNA levels of 8 genes selected for validation (*soxS*, *ibpA*, *cspA*, *marA*, *bssS*, *rpoH*, *cadA* and *treC*).

### Northern blot analysis

The hot phenol method was used to extract total RNA [80]. A sample of 10 µg of total RNA was loaded on a 5% acrylamide (29:1)/8M urea gel. RNA was electro-transferred to a Hybond-XL membrane (Amersham Biosciences) and UV-crosslinked (1200J). Prehybridization was done in 50% formamide, 5× SSC, 5× Denhardt reagent, 1% SDS, and 100 µg/ml sheared salmon sperm DNA for 4 h at 60°C. The radiolabeled RNA probe was added and incubated overnight. Three 15 minutes washes of the membranes were made with 1× SSC/0.1% SDS followed by a final wash with 0.1× SSC/0.1% SDS at 65°C.

### RNA probe radio-labeling

The RNA probe antisense to the RyfA sRNA was synthesized *in vitro* using the T7 RNA polymerase. Oligos EM4969B and EM4970 were used to generate the transcription template. Transcription was carried out in the T7 transcription buffer (40 mM Tris-HCL at pH 8.0, 6 mM MgCl<sub>2</sub>, 10 mM dithiothreitol, 2 mM spermidine), 400 µM NTPs (A, C and G), 10 µM UTP, 3 µl of α-<sup>32</sup>P-UTP (3000 Ci/mmol), 20 U RNA guard, 20 U T7 RNA polymerase and 0.5 µg DNA template. After 2 h of incubation at 37°C, the mixture was treated with 2 U of Turbo DNase (Ambion) for 15 minutes. The radio-labeled probe was then purified on a G50-Sephadex column before hybridization.



## Evaluation of type 1 and P fimbriae production

The level of production of type 1 fimbriae was determined by a yeast agglutination assay [35]. Briefly, the strains were cultured at 37°C / 250 rpm in LB broth or human urine to mid-log phase (conditions which were used for transcriptional analyses), or static in LB broth, M9-glucose or human urine overnight. Following centrifugation, 40 µl of an initial suspension of approximately  $2 \times 10^{11}$  cells ml<sup>-1</sup> in PBS was transferred and serially diluted 2-fold in microtiter wells containing equal volumes of a 3% commercial yeast suspension in PBS. After 30 min of incubation on ice, yeast aggregation was monitored visually. The agglutination titer was defined as the most diluted sample showing agglutination.

The mannose-resistant hemagglutination (MRHA) assay was determined using human type O<sup>+</sup> and A<sup>+</sup> erythrocytes to determine HA that could be mediated by P fimbriae. Bacterial strains were grown to mid-log phase or passaged six times on LB agar at 37°C, after which a bacterial sample was transferred to a well containing 50 µl of 3% (vol/vol) human red blood cells. To inhibit type 1 fimbriae-dependent hemagglutination, a final concentration of 2.5% α-d-mannopyranose was added to samples.

## Preparation of fimbrial extracts and Western blotting

Preparation of fimbrial extracts and Western blotting were performed as described previously [81], with anti-FimA serum from *E. coli* strain B<sub>AM</sub> and F1C fimbriae-specific (anti-F165<sub>2</sub>) antiserum [82].

## Adherence and gentamicin protection (invasion) assays

5637 human bladder cells (ATCC HTB-9) were grown in RPMI 1640 medium (Wisent Bioproducts) supplemented with 10% fetal bovine serum, 2 mM l-glutamine, 10 mM HEPES, 1 mM sodium pyruvate, 4.5 g/liter glucose, and 1.5 g/liter sodium bicarbonate. 5637 cells were grown to confluency in RPMI 1640 and  $2 \times 10^5$  cells/well were distributed in 24-well plates. UPEC CFT073 and its derivative strains were grown in LB medium at 37°C to the mid-log phase of growth (O.D. 0.6). Immediately before infection, cultures were washed once with PBS to remove dead cells, returned to the infection medium, and infected at an estimated MOI of 10 CFU per cell. The bacterial cells were centrifuged, washed twice with PBS, resuspended in RPMI 1640 medium (Wisent Biocenter, St-Bruno, Canada) supplemented with 10% fetal bovine serum at  $10^6$  CFU ml<sup>-1</sup>, and added to each well. Bacterium-host cell contact was enhanced by a 5-min centrifugation at 600 × g. After 2 h, cells were washed three times and lysed with PBS–0.1% sodium deoxycholate (DOC), serially diluted, and plated on LB agar plates. Quantification of cell-associated bacteria was performed. To block adherence mediated by type 1 fimbriae, 2.5% α-d-mannopyranose was added to culture medium.

For GFP-tagged UTI89, bacteria were grown at 37°C in LB broth supplemented with ampicillin to O.D. 0.6. Cells were infected with UTI89 using a MOI of 10 bacteria per host cell. After a 2 h incubation at 37°C, samples were washed three times with PBS to remove any non-adherent bacteria. Triplicate samples were used to calculate the total number of the associated bacteria present both intra- and extracellularly. To determine invasion frequencies, after the initial 2 h incubation, additional sets of wells were washed three times with PBS and then incubated for another 2 h in medium containing 100 µg/ml membrane-impermeable bactericidal antibiotic gentamicin to kill any extracellular bacteria. Following additional washes with PBS, fresh medium containing a lower concentration of gentamicin (10 µg/ml) was added, and incubations were continued for another 2 h. This submaximal concentration of gentamicin was used to prevent extracellular growth of UPEC while limiting possible leaching of the antibiotic into the host cells during longer incubations. Monolayers were then washed with PBS

and the positivity percentage of GFP-tagged bacteria present within the cells were measured by using ImageStream-based assay.

### Electron microscopy

Cells for electron microscopy were grown as described above for agglutination assay experiments. A glow-discharged Formvar-coated copper grid was placed under a drop of bacterial culture for 15 min to allow cells to adsorb. Excess liquid was removed using filter paper, just before a drop of 1% phosphotungstic acid (negative stain) was placed onto the grid for 15 sec. Samples were left to air dry and viewed using a Hitachi H-7100 transmission electron microscope.

### Swimming motility assay

Motility assays were done using UPEC strains CFT073 and 536 and its mutant derivatives as previously described [28,36] with modifications. Following overnight growth at 37°C, strains were cultured at 37°C in LB broth to mid-log phase. Soft agar (1% tryptone, 0.5% NaCl, 0.25% agar) or urine agar, were stabbed in the center of the plate using an inoculating needle. Care was taken not to touch the bottom of the plate during inoculation to ensure only swimming motility was assessed. After 16 h (soft agar) or 22 h (urine agar) of incubation at 37°C, the motility diameters were measured for each strain. Wild-type *E. coli* CFT073 was always included as a reference, and five independent motility experiments for each mutant were performed. *E. coli* CFT073 *fim* L-ON was used as a negative control. Results were analyzed using a paired t-test.

### Infection of human cultured macrophage-like cell line THP-1

The human monocyte cell line THP-1 (ATCC TIB-202) was maintained in RPMI 1640 (Wisent, Saint-Jean-Baptiste, QC, Canada) containing 10% (v/v) heat-inactivated FBS (Wisent, Saint-Jean-Baptiste, QC, Canada), 1 mM sodium pyruvate (Wisent, Saint-Jean-Baptiste, QC, Canada) and 1% modified Eagle's medium with non-essential amino acids (Wisent). A stock culture was maintained as monocyte-like, non-adherent cells at 37°C in an atmosphere containing 5% (v/v) CO<sub>2</sub>. The bacterial strains were cultured at 37°C in LB broth to mid-log phase. Bacterial cells were pelleted, washed with phosphate buffer saline and added to the cell monolayer at a MOI of 20, and plates were centrifuged for 5 min at 800 ×g to synchronize bacterial uptake. After 60 min of incubation at 37°C, extracellular bacteria were removed by washing cells three times with prewarmed PBS, and the infected monolayers were either lysed with PBS-DOC (T0) or incubated for 2 h or 24 h with medium containing 100 µg gentamicin ml<sup>-1</sup> (Wisent) to kill remaining extracellular bacteria, and then with 12 µg gentamicin ml<sup>-1</sup> for the remainder of the experiment. Surviving bacteria were determined (CFU) by plating on LB agar. Results are expressed as the mean ± SEM of at least three experiments performed in duplicate. One-way ANOVA was used for statistical analysis.

### Human monocyte-derived macrophage cultures

Peripheral blood mononuclear cells (PBMC) were obtained from leukaphereses of healthy donors. All participants of the study received approval from the McGill University Health Centre Ethical Review Board (ethic reference number SL-00.069). At least a purity of 96% of human monocytes was obtained using the Human Monocyte Enrichment Kit (Stem Cell Technologies, Vancouver, BC). Afterwards, purified human monocytes were seeded in RPMI 1640 medium supplemented with 2mM glutamine, antibiotics, and 10% FBS in the presence of 50

ng/ml of Human recombinant Macrophage colony-stimulating factor (M-CSF). After 6 days, human monocyte-derived macrophages (HMDMs) were used for infection assays. Differentiation follow-up during 6 days was assessed by flow cytometry analysis.

### Multiparametric and imaging flow cytometry analyses

To assess bacterial infection in macrophages, HMDMs were harvested after adding non-enzymatic cell dissociation solution (Sigma-Aldrich, Oakville, ON, Canada) for 30 mins at room temperature. Cells were washed with PBS and prepared in FACS tubes. For surface staining, we used the following specific monoclonal antibodies provided from BD Biosciences for phenotypic analysis of human HMDMs: anti-CD3 (BV605), anti-CD14 (BV650), anti-CD80 (PE Cy7), anti-CD209 (PE) and anti-CD64 (PE). Finally, the viability marker 7-aminoactinomycin D or 7-AAD (ThermoFisher Scientific, St. Laurent, QC, Canada) was used to exclude dead cells from analyses. Afterwards, cells were fixed with 4% paraformaldehyde solution and then washed. For data analysis, samples were analyzed by flow cytometry with a BD LSRII Fortessa flow cytometer and DIVA software (BD). Viable gated cell singlets were analyzed for each sample and the percentages of mCherry<sup>high</sup> CFT073 containing CD14<sup>+</sup> HMDMs were determined. For Imaging flow cytometry, the same procedures were applied while cells were prepared in Eppendorf tubes. For surface staining, we used CD14-V450 and CD80-APC H7 for phenotypic gating of HMDMs. Samples were acquired using the Image Stream X MKII flow cytometer and analyzed with IDEAS software (Amnis) and representative images of singlets CD14<sup>+</sup> HMDMs were generated expressing GFP<sup>high</sup> CFT073 bacterial cells.

### Measurement of ROS production

RAW264.7 cells were infected at an MOI 20:1 in complete DMEM medium in 24-well plates. The same conditions as for infection of THP-1 cells were used. After 60 min of incubation at 37°C, extracellular bacteria were removed by washing cells three times with prewarmed PBS, and the cells were then incubated for 4 h or 6 h with medium containing 100 µg gentamicin ml<sup>-1</sup> to kill extracellular bacteria. The fluorescent probe 2', 7'-dichlorodihydrofluorescein diacetate (H<sub>2</sub>DCF-DA) (ThermoFisher Scientific, St. Laurent, QC, Canada), was solubilized at 5 mM in dimethyl sulfoxide (DMSO) (Sigma). Infected or uninfected cells were incubated with 10 µM H<sub>2</sub>DCFDA for 45 min at 37°C, and then washed once with PBS 1X. Cells were then trypsin treated, washed once with PBS 1X and cell pellets were suspended in a 1 µg/ml propidium iodide solution (ThermoFisher Scientific, St. Laurent, QC, Canada). The flow cytometer FACSCalibur (Becton Dickinson) was used to measure the fluorescence of the oxidized product dichlorofluorescein at a λ of 488 nm with excitation at 530 nm. The fluorescence of propidium iodide was measured at a λ of 585 nm with an excitation at 542 nm. A total of 10 000 viable cells were analyzed by sample. For all points, experiments were performed in replicates. Statistical differences between different conditions were determined with a two-tailed Student's *t* test on the indicated number (*n*) of experiments.

### Biofilm assay

Biofilm formation on polystyrene surfaces was assessed in 96-well plates. Strains were grown at various temperatures (25°C, 30°C, 37°C, and 42°C) for 48 h under static conditions in LB and M9 supplemented with 0.2% glucose. Wells were washed and stained with 0.1% crystal violet (Millipore Sigma) for 15 min, then 200 µl of ethanol-acetone (80:20) solution was added, followed by measuring at an optical density at OD<sub>595</sub>.

### Site-directed mutagenesis to generate *ryfA* variants containing point mutations

Site-directed mutagenesis was performed using the Q5EvaGreen Site-Directed Mutagenesis kit as specified by the manufacturer (New England Biolabs). pIJ546 was used as a template for the construction of the RyfA variants with specific mutations pIJ588, pIJ589 and pIJ590 at 25 to 50 ng per reaction with 10 pmol of each of the complementary primers. Primers used to generate the point mutations were CMD 2712 and CMD2713 for pIJ588 (variant 1), CMD 2715 and CMD2716 for pIJ589 (variant 2) and CMD2718 and CMD2719 for pIJ590 (variant 3). Following mutagenesis, all constructs were verified by PCR and by sequencing.

### Statistical analyses

Statistical analyses were performed using the Prism 7.04 software package (GraphPad Software). Statistically significant differences between two groups were established by unpaired t-test and comparisons among three or more groups was done by one-way analysis of variance (ANOVA). For the independent infections, comparisons of the CFU mL<sup>-1</sup> or CFU g<sup>-1</sup> distributions were analyzed using the Mann–Whitney test. A Wilcoxon signed-rank test (two-tailed;  $P \leq 0.05$ ) was used to determine statistical significance for comparison of bacterial numbers in coinfection experiments.

### Supporting information

**S1 Fig. Role of RyfA in stress resistance.** (A) Comparison of growth characteristics of CFT073,  $\Delta ryfA$  mutant and  $\Delta ryfA$  complemented strain diluted and plated on LB agar after growth in LB at 37°C to a O.D 0.6. (B) Growth inhibition zones (mm) of UPEC 536 and the *ryfA* mutant to ROI-generating compounds on LB and M9-glucose agar. (C) Sensitivities of UPEC strains CFT073 and 536 and their derivative strains to potassium tellurite on LB agar plates. Tests were performed as described in Methods. The results represent the means of replicate experiments for a minimum of three samples. Vertical bars represent the standard errors of the means. Statistical significance was calculated by one-way ANOVA (B and C): \*,  $P < 0.05$ ; \*\*,  $P < 0.005$ ; \*\*\*,  $P < 0.0001$ . (TIF)

**S2 Fig. RyfA predicted structure and sequence.** (A) Schematic depicting the chromosomal location of *ryfA* in *E. coli* CFT073 and other species. (B) Clustal Alignment of RyfA alleles from *E. coli* K-12 and 3 UPEC strains. The 304 nucleotide sequence is based on the *E. coli* K-12 MG1655 reference allele. Overall, 21 variable nucleotides were present, and the *E. coli* K-12 allele had one gap at nucleotide 290 compared to the UPEC strains. UPEC CFT073 was more similar to MG1655 as these alleles only varied at 6 sites (including the gap). UTI89 and 536 were highly similar to each other with only 3 differences. Alignment generated using MEGAX software (<https://www.megasoftware.net>). (C) The Vienna RNA websuite was used to predict the secondary structure of RyfA from CFT073. The structure is colored by base-pairing probabilities. (TIF)

**S3 Fig. *ryfA* expression at different conditions and genes affected by the absence of *ryfA* in vitro.** (A) Validation of RNA-seq data by qRT-PCR. RNA was isolated from UPEC CFT073 and the  $\Delta ryfA$  mutant in mid-log growth (O.D. 0.6) in LB at 37°C and qRT-PCR analysis was performed. Genes either upregulated or downregulated by at least 2-fold were considered significant. (B) Expression of *ryfA* gene in the WT CFT073 strain in infected bladders and after static growth in LB broth or human urine compared to RNA levels compared to expression

when grown to mid-log growth (O.D. 0.6) in LB at 37°C. qPCR data represent means of relative expression  $\pm$  range ( $n = 3$ ) of three biological replicates (\*  $p < 0.05$ , \*\* $p < 0.01$ , \*\*\* $p < 0.001$  using one-way ANOVA).

(TIF)

**S4 Fig. Effect of inactivation of *ryfA* on production of type 1 fimbriae (pili) and expression of Pap and F1C fimbriae (pili).** Type 1 fimbriae production determined by yeast agglutination. The level of type 1 fimbriae production in UPEC strains. (A) CFT073 grown static overnight in M9 medium containing 0.2% glucose, (B) 536, UTI89, and derivatives after mid-log growth in LB or overnight in human urine. (C) qRT-PCR analysis of *fimA* (Type 1), *papA* (*papA1* and *papA2-P* fimbriae) and *focA* (F1C fimbriae) genes from CFT073  $\Delta$ *ryfA* mutant adhering to 5637 bladder cells compared to levels for WT strain. The dashed line corresponds to the cutoff for a significant difference in expression. All results shown are the mean values and standard deviations for four biological experiments. Statistical significance was calculated by the one-way ANOVA (A, B and C): \*,  $P < 0.05$ ; \*\*,  $P < 0.005$ ; \*\*\*,  $P < 0.0001$ . (D) Western blot of fimbrial extracts using F1C-specific (anti-F165<sub>2</sub>) antiserum. The *fim*-negative *E. coli* K-12 strain ORN172 carrying the plasmid pYVAN which expresses F1C (F165<sub>2</sub>) fimbriae was used as positive control. Bands are from a representative gel.

(TIF)

**S5 Fig. Effect of loss of *ryfA* on adherence and intracellular bacterial survival of UPEC strain UTI89.** 5637 bladder epithelial cell monolayers were infected for 2 h with UPEC UTI89 and its derivatives strains (MOI: 10) using ImageStream-based assay. After 2 h p.i (T0), cells were then washed four times with PBS and total cell-associated bacteria were determined. After 2 h p.i., 5637 bladder epithelial cell monolayers infected with UTI89 were incubated for 4 h in medium containing gentamicin to prevent extracellular bacterial growth and to allow time for the establishment of UPEC within the host bladder cells (T4). We included non-infected cells as a negative experimental control. (A) Representative images of single GFP<sup>+</sup>LAMP1<sup>+</sup> 5637 cells at T0 and T4. (B) UPEC infection measurement was determined by the percentage of GFP<sup>high</sup> 5637 cells at different time points p.i. LAMP1, Lysosomal-associated membrane protein 1. Data represent the mean results  $\pm$  SEM from three or more independent assays performed in triplicate. Statistical significance was calculated by one-way ANOVA (A, B and C): \*,  $P < 0.05$ ; \*\*,  $P < 0.005$ ; \*\*\*,  $P < 0.0001$ .

(TIF)

**S6 Fig. Inactivation of *ryfA* in uropathogenic *E. coli* CFT073 reduces competitive colonization of the mouse urinary tract.** (A) Co-infection experiments between a CFT073  $\Delta$ *lac* and  $\Delta$ *ryfA* mutant. Data are means  $\pm$  standard errors of the means of 10 mice (B) Growth curves of CFT073 and *ryfA* mutant in LB broth (C) Comparison of growth characteristics of CFT073 or CFT073  $\Delta$ *lac* and *ryfA* mutant in human urine in monoculture and coculture. There were no significant differences in growth between CFT073 and *ryfA* mutant in all conditions tested. Error bars represent the SEM.  $P < 0.05$ ; \*\*,  $P < 0.005$ ; \*\*\*,  $P < 0.000$  Mann-Whitney Test.

(TIF)

**S7 Fig. The predicted TimP paralog in the *E. coli ryfA* gene does not contribute to phenotypes observed in the *ryfA* mutant.** (A) DNA sequence of the *ryfA* CFT073 predicted ORF corresponding to TimP is indicated with a green arrow. (B) The predicted small protein from RyfA carries a putative Sec system signal sequence in CFT073 (shown in red). (C) Type 1 fimbriae production determined by yeast agglutination in strains cultured to the mid-log phase of growth in LB broth and O/N in urine and (D) Motility in 0.25% soft agar of CFT073, isogenic *ryfA* mutant and the different variant complemented mutants. (E) Growth inhibition zones (mm) of CFT073 and its derivative strains to oxidative stress generating compounds (30%

H<sub>2</sub>O<sub>2</sub>) on LB agar. (F) THP-1 human macrophages were infected (MOI: 20) with different strains for 1 h, followed by gentamicin treatment. Cells were lysed and intracellular bacterial counts (CFU ml<sup>-1</sup>) were determined at 2 h p.i. Data represent the averages of at least three separate experiments. Error bars represent the SEM. Statistical significance was calculated by one-way ANOVA: \*,  $P < 0.05$ ; \*\*,  $P < 0.005$ ; \*\*\*,  $P < 0.0001$ . NS, not significant.

(TIF)

**S8 Fig. *ryfA* alleles with point mutations introduced to eliminate the potential TimP *E. coli* paralog peptide.** (A) The predicted peptide potentially associated with the RyfA RNA from CFT073. Native ORF present in *E. coli* CFT073 (B) Variant *ryfA* alleles wherein small sequence changes would eliminate or alter the ORF through introduction of stop codons or frame-shifts. These three variants of *ryfA* would not contain the predicted ORF and could not produce such a peptide.

(TIF)

**S9 Fig. Biofilm formation in UPEC strains CFT073 and 536 and respective *ryfA* mutants.** UPEC and *Serratia liquefaciens* strain were grown at different temperatures (30°C, 37°C, and 42°C) in LB and minimal M9 medium containing 0.2% glucose in polystyrene plate wells for 48 h and then stained with crystal violet. Remaining crystal violet after washing with acetone was measured as absorbance at 595 nm. Data are the means of three independent experiments, and error bars represent standard errors of the means. The *Serratia liquefaciens* strain was used as positive control for biofilm formation. \*,  $P < 0.05$ ; \*\*,  $P < 0.005$ ; \*\*\*,  $P < 0.0001$  compared to CFT073 or 536 using one-way ANOVA.

(TIF)

**S10 Fig. Genes whose expression is reduced in the absence of *ryfA* during infection of human macrophages.** UPEC genes associated with intramacrophage survival. HMDMs were infected at an MOI of 20. Intracellular bacterial survival was assessed at 6 h post-infection and the relative quantity of mRNA of specific genes were determined by qRT-PCR. qPCR data represent means of relative expression  $\pm$  range ( $n = 3$ ) of three biological replicates (\*  $p < 0.05$ , \*\*  $p < 0.01$ , \*\*\*  $p < 0.001$  using one-way ANOVA). Results were normalized against the steady state RNA levels of *rpoD* (see [Methods](#) for experimental details).

(TIF)

**S1 Table. Examination of transcriptome of CFT073 vs  $\Delta$ *ryfA* mutant in LB at O.D 0.6.**

Strains were inoculated in triplicate 1:100 from an overnight pre-culture grown in LB and grown until mid-log phase with shaking (250 rpm).

(PDF)

**S2 Table. Bacterial strains and plasmids used in this study.**

(DOCX)

**S3 Table. Primers used in this study.**

(PDF)

## Acknowledgments

We would like to acknowledge Hani Jrade (Ottawa Hospital Research Institute, Regenerative Medicine Program, Ottawa, ON, Canada) for the technical support in ImageStream apparatus.

## Author Contributions

**Conceptualization:** Hicham Bessaiah, Charles M. Dozois.



**Data curation:** Hicham Bessaiah.

**Formal analysis:** Hicham Bessaiah, Pravil Pokharel, Hamza Loucif, Merve Kulbay, Charles Sasseville, Sébastien Houle, Charles M. Dozois.

**Funding acquisition:** Jacques Bernier, Éric Massé, Julien Van Grevenynghe, Charles M. Dozois.

**Investigation:** Hicham Bessaiah.

**Methodology:** Hicham Bessaiah, Pravil Pokharel, Hamza Loucif, Merve Kulbay, Charles Sasseville, Hajer Habouria, Charles M. Dozois.

**Project administration:** Hicham Bessaiah, Éric Massé, Julien Van Grevenynghe, Charles M. Dozois.

**Resources:** Jacques Bernier, Julien Van Grevenynghe, Charles M. Dozois.

**Supervision:** Éric Massé, Julien Van Grevenynghe, Charles M. Dozois.

**Validation:** Hicham Bessaiah, Éric Massé, Julien Van Grevenynghe, Charles M. Dozois.

**Writing – original draft:** Hicham Bessaiah.

**Writing – review & editing:** Hicham Bessaiah, Pravil Pokharel, Charles M. Dozois.

## References

1. Foxman B. The epidemiology of urinary tract infection. *Nature Reviews Urology*. 2010; 7(12):653. <https://doi.org/10.1038/nrurol.2010.190> PMID: 21139641
2. Foxman B. Recurring urinary tract infection: incidence and risk factors. *American journal of public health*. 1990; 80(3):331–3. <https://doi.org/10.2105/ajph.80.3.331> PMID: 2305919
3. Wiles TJ, Kulesus RR, Mulvey MA. Origins and virulence mechanisms of uropathogenic *Escherichia coli*. *Exp Mol Pathol*. 2008; 85(1):11–9. Epub 2008/05/17. <https://doi.org/10.1016/j.yexmp.2008.03.007> PMID: 18482721; PubMed Central PMCID: PMC2595135.
4. Subashchandrabose S, Smith SN, Spurbeck RR, Kole MM, Mobley HL. Genome-wide detection of fitness genes in uropathogenic *Escherichia coli* during systemic infection. *PLoS Pathog*. 2013; 9(12): e1003788. Epub 2013/12/18. <https://doi.org/10.1371/journal.ppat.1003788> PMID: 24339777; PubMed Central PMCID: PMC3855560.
5. Nielubowicz GR, Mobley HL. Host–pathogen interactions in urinary tract infection. *Nature Reviews Urology*. 2010; 7(8):430. <https://doi.org/10.1038/nrurol.2010.101> PMID: 20647992
6. Vigil PD, Stapleton AE, Johnson JR, Hooton TM, Hodges AP, He Y, et al. Presence of putative repeat-in-toxin gene *tosA* in *Escherichia coli* predicts successful colonization of the urinary tract. *MBio*. 2011; 2(3):e00066–11. <https://doi.org/10.1128/mBio.00066-11> PMID: 21540363
7. Mysorekar IU, Hultgren SJ. Mechanisms of uropathogenic *Escherichia coli* persistence and eradication from the urinary tract. *Proceedings of the National Academy of Sciences*. 2006; 103(38):14170–5. <https://doi.org/10.1073/pnas.0602136103> PMID: 16968784
8. Zhou G, Mo W-J, Sebbel P, Min G, Neubert TA, Glockshuber R, et al. Uroplakin Ia is the urothelial receptor for uropathogenic *Escherichia coli*: evidence from in vitro FimH binding. *Journal of cell science*. 2001; 114(22):4095–103. PMID: 11739641
9. Abraham JM, Freitag CS, Clements JR, Eisenstein BI. An invertible element of DNA controls phase variation of type 1 fimbriae of *Escherichia coli*. *Proc Natl Acad Sci U S A*. 1985; 82(17):5724–7. Epub 1985/09/01. <https://doi.org/10.1073/pnas.82.17.5724> PMID: 2863818; PubMed Central PMCID: PMC390624.
10. Klemm P. Two regulatory *fim* genes, *fimB* and *fimE*, control the phase variation of type 1 fimbriae in *Escherichia coli*. *EMBO J*. 1986; 5(6):1389–93. Epub 1986/06/01. PMID: 2874022; PubMed Central PMCID: PMC1166953.
11. Bryan A, Roesch P, Davis L, Moritz R, Pellett S, Welch RA. Regulation of type 1 fimbriae by unlinked FimB- and FimE-like recombinases in uropathogenic *Escherichia coli* strain CFT073. *Infect Immun*. 2006; 74(2):1072–83. Epub 2006/01/24. <https://doi.org/10.1128/IAI.74.2.1072-1083.2006> PMID: 16428754; PubMed Central PMCID: PMC1360361.

12. Corcoran CP, Dorman CJ. DNA relaxation-dependent phase biasing of the *fim* genetic switch in *Escherichia coli* depends on the interplay of H-NS, IHF and LRP. *Molecular microbiology*. 2009; 74(5):1071–82. <https://doi.org/10.1111/j.1365-2958.2009.06919.x> PMID: 19889099
13. Snyder JA, Haugen BJ, Lockett CV, Maroncle N, Hagan EC, Johnson DE, et al. Coordinate expression of fimbriae in uropathogenic *Escherichia coli*. *Infect Immun*. 2005; 73(11):7588–96. Epub 2005/10/22. <https://doi.org/10.1128/IAI.73.11.7588-7596.2005> PMID: 16239562; PubMed Central PMCID: PMC1273908.
14. Schwan WR, Lee JL, Lenard FA, Matthews BT, Beck MT. Osmolarity and pH growth conditions regulate *fim* gene transcription and type 1 pilus expression in uropathogenic *Escherichia coli*. *Infect Immun*. 2002; 70(3):1391–402. Epub 2002/02/21. <https://doi.org/10.1128/iai.70.3.1391-1402.2002> PMID: 11854225; PubMed Central PMCID: PMC127777.
15. Müller CM, Åberg A, Strasevičienė J, Emödy L, Uhlin BE, Balsalobre C. Type 1 fimbriae, a colonization factor of uropathogenic *Escherichia coli*, are controlled by the metabolic sensor CRP-cAMP. *PLoS pathogens*. 2009; 5(2). <https://doi.org/10.1371/journal.ppat.1000303> PMID: 19229313
16. Babior BM. Phagocytes and oxidative stress. *The American journal of medicine*. 2000; 109(1):33–44. [https://doi.org/10.1016/s0002-9343\(00\)00481-2](https://doi.org/10.1016/s0002-9343(00)00481-2) PMID: 10936476
17. Nathan C, Shiloh MU. Reactive oxygen and nitrogen intermediates in the relationship between mammalian hosts and microbial pathogens. *Proceedings of the National Academy of Sciences*. 2000; 97(16):8841–8. <https://doi.org/10.1073/pnas.97.16.8841> PMID: 10922044
18. Storz G, Imlayt JA. Oxidative stress. *Current opinion in microbiology*. 1999; 2(2):188–94. [https://doi.org/10.1016/s1369-5274\(99\)80033-2](https://doi.org/10.1016/s1369-5274(99)80033-2) PMID: 10322176
19. Waters LS, Storz G. Regulatory RNAs in bacteria. *Cell*. 2009; 136(4):615–28. <https://doi.org/10.1016/j.cell.2009.01.043> PMID: 19239884
20. Altuvia S, Weinstein-Fischer D, Zhang A, Postow L, Storz G. A small, stable RNA induced by oxidative stress: role as a pleiotropic regulator and antimutator. *Cell*. 1997; 90(1):43–53. [https://doi.org/10.1016/s0092-8674\(00\)80312-8](https://doi.org/10.1016/s0092-8674(00)80312-8) PMID: 9230301
21. Massé E, Gottesman S. A small RNA regulates the expression of genes involved in iron metabolism in *Escherichia coli*. *Proceedings of the National Academy of Sciences*. 2002; 99(7):4620–5. <https://doi.org/10.1073/pnas.032066599> PMID: 11917098
22. Guillier M, Gottesman S. Remodelling of the *Escherichia coli* outer membrane by two small regulatory RNAs. *Molecular microbiology*. 2006; 59(1):231–47. <https://doi.org/10.1111/j.1365-2958.2005.04929.x> PMID: 16359331
23. Rivas E, Klein RJ, Jones TA, Eddy SR. Computational identification of noncoding RNAs in *E. coli* by comparative genomics. *Current biology*. 2001; 11(17):1369–73. [https://doi.org/10.1016/s0960-9822\(01\)00401-8](https://doi.org/10.1016/s0960-9822(01)00401-8) PMID: 11553332
24. Shivaji S, Konduri R, Ramchiary J, Jogadhenu PS, Arunasri K, Savitri S. Gene targets in ocular pathogenic *Escherichia coli* for mitigation of biofilm formation to overcome antibiotic resistance. *Frontiers in Microbiology*. 2019; 10:1308. <https://doi.org/10.3389/fmicb.2019.01308> PMID: 31293528
25. Bak G, Lee J, Suk S, Kim D, Lee JY, Kim K-s, et al. Identification of novel sRNAs involved in biofilm formation, motility, and fimbriae formation in *Escherichia coli*. *Scientific reports*. 2015; 5:15287. <https://doi.org/10.1038/srep15287> PMID: 26469694
26. Fris ME, Broach WH, Klim SE, Coschigano PW, Carroll RK, Caswell CC, et al. Sibling sRNA RyfA1 influences *Shigella dysenteriae* pathogenesis. *Genes*. 2017; 8(2):50. <https://doi.org/10.3390/genes8020050> PMID: 28134784
27. Andresen L, Martínez-Burgo Y, Zangelin JN, Rizvanovic A, Holmqvist E. The Small Toxic *Salmonella* Protein TimP Targets the Cytoplasmic Membrane and Is Repressed by the Small RNA TimR. *Mbio*. 2020; 11(6). <https://doi.org/10.1128/mBio.01659-20> PMID: 33172998
28. Bessaiah H, Pokharel P, Habouria H, Houle S, Dozois CM. *yqhG* Contributes to Oxidative Stress Resistance and Virulence of Uropathogenic *Escherichia coli* and Identification of Other Genes Altering Expression of Type 1 Fimbriae. *Frontiers in cellular and infection microbiology*. 2019; 9:312. <https://doi.org/10.3389/fcimb.2019.00312> PMID: 31555608
29. Lorenz A, Bernhart S, Neubock R, Hofacker I. The vienna RNA websuite. *Nucleic Acids Res*. 2008; 36(Suppl 2):W70–W4. <https://doi.org/10.1093/nar/gkn188> PMID: 18424795
30. Zhao K, Liu M, Burgess RR. The global transcriptional response of *Escherichia coli* to induced  $\sigma_{32}$  protein involves  $\sigma_{32}$  regulon activation followed by inactivation and degradation of  $\sigma_{32}$  *in vivo*. *Journal of Biological Chemistry*. 2005; 280(18):17758–68.
31. Morimoto RI, editor *The heat shock response: systems biology of proteotoxic stress in aging and disease*. Cold Spring Harbor symposia on quantitative biology; 2011: Cold Spring Harbor Laboratory Press.



32. Bukau B, Horwich AL. The Hsp70 and Hsp60 chaperone machines. *Cell*. 1998; 92(3):351–66. [https://doi.org/10.1016/s0092-8674\(00\)80928-9](https://doi.org/10.1016/s0092-8674(00)80928-9) PMID: 9476895
33. Mogk A, Deuerling E, Vorderwülbecke S, Vierling E, Bukau B. Small heat shock proteins, ClpB and the DnaK system form a functional triade in reversing protein aggregation. *Molecular microbiology*. 2003; 50(2):585–95. <https://doi.org/10.1046/j.1365-2958.2003.03710.x> PMID: 14617181
34. Flores-Kim J, Darwin AJ. Activity of a bacterial cell envelope stress response is controlled by the interaction of a protein binding domain with different partners. *Journal of Biological Chemistry*. 2015; 290(18):11417–30. <https://doi.org/10.1074/jbc.M114.614107> PMID: 25802329
35. Crepin S, Houle S, Charbonneau ME, Mourez M, Harel J, Dozois CM. Decreased expression of type 1 fimbriae by a pst mutant of uropathogenic *Escherichia coli* reduces urinary tract infection. *Infect Immun*. 2012; 80(8):2802–15. Epub 2012/06/06. <https://doi.org/10.1128/IAI.00162-12> PMID: 22665376; PubMed Central PMCID: PMC3434566.
36. Lane MC, Lockett V, Monterosso G, Lamphier D, Weinert J, Hebel JR, et al. Role of motility in the colonization of uropathogenic *Escherichia coli* in the urinary tract. *Infection and immunity*. 2005; 73(11):7644–56. <https://doi.org/10.1128/IAI.73.11.7644-7656.2005> PMID: 16239569
37. Snyder JA, Haugen BJ, Buckles EL, Lockett CV, Johnson DE, Donnenberg MS, et al. Transcriptome of uropathogenic *Escherichia coli* during urinary tract infection. *Infect Immun*. 2004; 72(11):6373–81. Epub 2004/10/27. <https://doi.org/10.1128/IAI.72.11.6373-6381.2004> PMID: 15501767; PubMed Central PMCID: PMC523057.
38. Wright KJ, Seed PC, Hultgren SJ. Development of intracellular bacterial communities of uropathogenic *Escherichia coli* depends on type 1 pili. *Cellular microbiology*. 2007; 9(9):2230–41. <https://doi.org/10.1111/j.1462-5822.2007.00952.x> PMID: 17490405
39. Mulvey MA, Schilling JD, Hultgren SJ. Establishment of a persistent *Escherichia coli* reservoir during the acute phase of a bladder infection. *Infection and immunity*. 2001; 69(7):4572–9. <https://doi.org/10.1128/IAI.69.7.4572-4579.2001> PMID: 11402001
40. Sabri M, Houle S, Dozois CM. Roles of the extraintestinal pathogenic *Escherichia coli* ZnuACB and ZupT zinc transporters during urinary tract infection. *Infection and immunity*. 2009; 77(3):1155–64. <https://doi.org/10.1128/IAI.01082-08> PMID: 19103764
41. Liu L, Mo H, Wei S, Raftery D. Quantitative analysis of urea in human urine and serum by <sup>1</sup>H nuclear magnetic resonance. *Analyst*. 2012; 137(3):595–600. <https://doi.org/10.1039/c2an15780b> PMID: 22179722
42. Shaykhtudinov RA, MacInnis GD, Dowlatabadi R, Weljie AM, Vogel HJ. Quantitative analysis of metabolite concentrations in human urine samples using <sup>13</sup>C {<sup>1</sup>H} NMR spectroscopy. *Metabolomics*. 2009; 5(3):307–17.
43. Plough IC, Baker EM. Maximum physiological concentration of sodium in human urine. *Journal of applied physiology*. 1959; 14(6):1036–8. <https://doi.org/10.1152/jappl.1959.14.6.1036> PMID: 14433526
44. Baorto DM, Gao Z, Malaviya R, Dustin ML, van der Merwe A, Lublin DM, et al. Survival of FimH-expressing enterobacteria in macrophages relies on glycolipid traffic. *Nature*. 1997; 389(6651):636–9. <https://doi.org/10.1038/39376> PMID: 9335508
45. Malaviya R, Gao Z, Thankavel K, van der Merwe PA, Abraham SN. The mast cell tumor necrosis factor  $\alpha$  response to FimH-expressing *Escherichia coli* is mediated by the glycosylphosphatidylinositol-anchored molecule CD48. *Proceedings of the National Academy of Sciences*. 1999; 96(14):8110–5. <https://doi.org/10.1073/pnas.96.14.8110> PMID: 10393956
46. Vizcarra IA, Hosseini V, Kollmannsberger P, Meier S, Weber SS, Arnoldini M, et al. How type 1 fimbriae help *Escherichia coli* to evade extracellular antibiotics. *Scientific reports*. 2016; 6(1):1–13. <https://doi.org/10.1038/s41598-016-0001-8> PMID: 28442746
47. Armenteros JJA, Tsirigos KD, Sønderby CK, Petersen TN, Winther O, Brunak S, et al. SignalP 5.0 improves signal peptide predictions using deep neural networks. *Nature biotechnology*. 2019; 37(4):420–3. <https://doi.org/10.1038/s41587-019-0036-z> PMID: 30778233
48. Käll L, Krogh A, Sonnhammer EL. Advantages of combined transmembrane topology and signal peptide prediction—the Phobius web server. *Nucleic acids research*. 2007; 35(suppl\_2):W429–W32. <https://doi.org/10.1093/nar/gkm256> PMID: 17483518
49. Dove S, Smith S, Dorman C. Control of *Escherichia coli* type 1 fimbrial gene expression in stationary phase: a negative role for RpoS. *Molecular and General Genetics MGG*. 1997; 254(1):13–20. <https://doi.org/10.1007/s004380050385> PMID: 9108285
50. Flécharde M, Cortes MA, Répérant M, Germon P. New role for the ibeA gene in H<sub>2</sub>O<sub>2</sub> stress resistance of *Escherichia coli*. *Journal of bacteriology*. 2012; 194(17):4550–60. <https://doi.org/10.1128/JB.00089-12> PMID: 22730120

51. Conover MS, Hadjifrangiskou M, Palermo JJ, Hibbing ME, Dodson KW, Hultgren SJ. Metabolic requirements of *Escherichia coli* in intracellular bacterial communities during urinary tract infection pathogenesis. *MBio*. 2016; 7(2):e00104–16. <https://doi.org/10.1128/mBio.00104-16> PMID: 27073089
52. Crespo MD, Puorger C, Schärer MA, Eidam O, Grütter MG, Capitani G, et al. Quality control of disulfide bond formation in pilus subunits by the chaperone FimC. *Nature chemical biology*. 2012; 8(8):707. <https://doi.org/10.1038/nchembio.1019> PMID: 22772153
53. Ruiz C, Levy SB. Many chromosomal genes modulate MarA-mediated multidrug resistance in *Escherichia coli*. *Antimicrobial agents and chemotherapy*. 2010; 54(5):2125–34. <https://doi.org/10.1128/AAC.01420-09> PMID: 20211899
54. Ruiz C, McMurry LM, Levy SB. Role of the multidrug resistance regulator MarA in global regulation of the hdeAB acid resistance operon in *Escherichia coli*. *Journal of bacteriology*. 2008; 190(4):1290–7. <https://doi.org/10.1128/JB.01729-07> PMID: 18083817
55. Casaz P, Garrity-Ryan LK, McKenney D, Jackson C, Levy SB, Tanaka SK, et al. MarA, SoxS and Rob function as virulence factors in an *Escherichia coli* murine model of ascending pyelonephritis. *Microbiology*. 2006; 152(12):3643–50.
56. Withman B, Gunasekera TS, Beesetty P, Agans R, Paliy O. Transcriptional responses of uropathogenic *Escherichia coli* to increased environmental osmolality caused by salt or urea. *Infection and immunity*. 2013; 81(1):80–9. <https://doi.org/10.1128/IAI.01049-12> PMID: 23090957
57. Haugen BJ, Pellett S, Redford P, Hamilton HL, Roesch PL, Welch RA. *In vivo* gene expression analysis identifies genes required for enhanced colonization of the mouse urinary tract by uropathogenic *Escherichia coli* strain CFT073 *dsdA*. *Infection and immunity*. 2007; 75(1):278–89. <https://doi.org/10.1128/IAI.01319-06> PMID: 17074858
58. Hancock V, Klemm P. Global gene expression profiling of asymptomatic bacteriuria *Escherichia coli* during biofilm growth in human urine. *Infection and immunity*. 2007; 75(2):966–76. <https://doi.org/10.1128/IAI.01748-06> PMID: 17145952
59. Hagan EC, Lloyd AL, Rasko DA, Faerber GJ, Mobley HL. *Escherichia coli* global gene expression in urine from women with urinary tract infection. *PLoS pathogens*. 2010; 6(11). <https://doi.org/10.1371/journal.ppat.1001187> PMID: 21085611
60. Roos V, Klemm P. Global gene expression profiling of the asymptomatic bacteriuria *Escherichia coli* strain 83972 in the human urinary tract. *Infection and immunity*. 2006; 74(6):3565–75. <https://doi.org/10.1128/IAI.01959-05> PMID: 16714589
61. Pérez JM, Calderón IL, Arenas FA, Fuentes DE, Pradenas GA, Fuentes EL, et al. Bacterial toxicity of potassium tellurite: unveiling an ancient enigma. *PloS one*. 2007; 2(2):e211. <https://doi.org/10.1371/journal.pone.0000211> PMID: 17299591
62. Welch RA, Burland V, Plunkett G 3rd, Redford P, Roesch P, Rasko D, et al. Extensive mosaic structure revealed by the complete genome sequence of uropathogenic *Escherichia coli*. *Proc Natl Acad Sci U S A*. 2002; 99(26):17020–4. Epub 2002/12/10. <https://doi.org/10.1073/pnas.252529799> PMID: 12471157; PubMed Central PMCID: PMC139262.
63. Hultgren SJ, Porter TN, Schaeffer AJ, Duncan JL. Role of type 1 pili and effects of phase variation on lower urinary tract infections produced by *Escherichia coli*. *Infection and immunity*. 1985; 50(2):370–7. <https://doi.org/10.1128/IAI.50.2.370-377.1985> PMID: 2865209
64. Khan AS, Kniep B, Oelschlaeger TA, Van Die I, Korhonen T, Hacker J. Receptor structure for F1C fimbriae of uropathogenic *Escherichia coli*. *Infection and immunity*. 2000; 68(6):3541–7. <https://doi.org/10.1128/iai.68.6.3541-3547.2000> PMID: 10816509
65. Luterbach CL, Mobley HL. Cross talk between MarR-like transcription factors coordinates the regulation of motility in uropathogenic *Escherichia coli*. *Infection and immunity*. 2018; 86(12):e00338–18. <https://doi.org/10.1128/IAI.00338-18> PMID: 30275009
66. Ren D, Bedzyk L, Thomas S, Ye R, Wood TK. Gene expression in *Escherichia coli* biofilms. *Applied microbiology and biotechnology*. 2004; 64(4):515–24. <https://doi.org/10.1007/s00253-003-1517-y> PMID: 14727089
67. Flannagan RS, Cosío G, Grinstein S. Antimicrobial mechanisms of phagocytes and bacterial evasion strategies. *Nature Reviews Microbiology*. 2009; 7(5):355–66. <https://doi.org/10.1038/nrmicro2128> PMID: 19369951
68. Imlay JA. The molecular mechanisms and physiological consequences of oxidative stress: lessons from a model bacterium. *Nature Reviews Microbiology*. 2013; 11(7):443–54. <https://doi.org/10.1038/nrmicro3032> PMID: 23712352
69. Mavromatis C, Bokil NJ, Totsika M, Kakkanat A, Schaale K, Cannistraci CV, et al. The co-transcriptome of uropathogenic *Escherichia coli*-infected mouse macrophages reveals new insights into host–pathogen interactions. *Cellular microbiology*. 2015; 17(5):730–46. <https://doi.org/10.1111/cmi.12397> PMID: 25410299

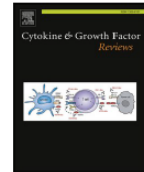
70. Maxson ME, Darwin AJ. Identification of inducers of the *Yersinia enterocolitica* phage shock protein system and comparison to the regulation of the RpoE and Cpx extracytoplasmic stress responses. *Journal of bacteriology*. 2004; 186(13):4199–208. <https://doi.org/10.1128/JB.186.13.4199-4208.2004> PMID: 15205422
71. Lucchini S, Liu H, Jin Q, Hinton JC, Yu J. Transcriptional adaptation of *Shigella flexneri* during infection of macrophages and epithelial cells: insights into the strategies of a cytosolic bacterial pathogen. *Infection and immunity*. 2005; 73(1):88–102. <https://doi.org/10.1128/IAI.73.1.88-102.2005> PMID: 15618144
72. Wadler CS, Vanderpool CK. A dual function for a bacterial small RNA: SgrS performs base pairing-dependent regulation and encodes a functional polypeptide. *Proceedings of the National Academy of Sciences*. 2007; 104(51):20454–9. <https://doi.org/10.1073/pnas.0708102104> PMID: 18042713
73. Boisset S, Geissmann T, Huntzinger E, Fechter P, Bendridi N, Possedko M, et al. *Staphylococcus aureus* RNAlII coordinately represses the synthesis of virulence factors and the transcription regulator Rot by an antisense mechanism. *Genes & development*. 2007; 21(11):1353–66. <https://doi.org/10.1101/gad.423507> PMID: 17545468
74. Gimpel M, Heidrich N, Mäder U, Krügel H, Brantl S. A dual-function sRNA from *B. subtilis*: SR1 acts as a peptide encoding mRNA on the gapA operon. *Molecular microbiology*. 2010; 76(4):990–1009. <https://doi.org/10.1111/j.1365-2958.2010.07158.x> PMID: 20444087
75. Mobley H, Green D, Trifillis A, Johnson D, Chippendale G, Lockatell C, et al. Pyelonephritogenic *Escherichia coli* and killing of cultured human renal proximal tubular epithelial cells: role of hemolysin in some strains. *Infection and immunity*. 1990; 58(5):1281–9. <https://doi.org/10.1128/IAI.58.5.1281-1289.1990> PMID: 2182540
76. Datsenko KA, Wanner BL. One-step inactivation of chromosomal genes in *Escherichia coli* K-12 using PCR products. *Proceedings of the National Academy of Sciences*. 2000; 97(12):6640–5. <https://doi.org/10.1073/pnas.120163297> PMID: 10829079
77. Cherepanov PP, Wackernagel W. Gene disruption in *Escherichia coli*: TcR and KmR cassettes with the option of Flp-catalyzed excision of the antibiotic-resistance determinant. *Gene*. 1995; 158(1):9–14. [https://doi.org/10.1016/0378-1119\(95\)00193-a](https://doi.org/10.1016/0378-1119(95)00193-a) PMID: 7789817
78. Sabri M, Caza M, Proulx J, Lymberopoulos MH, Brée A, Moulin-Schouleur M, et al. Contribution of the SitABCD, MntH, and FeoB metal transporters to the virulence of avian pathogenic *Escherichia coli* O78 strain  $\chi$ 7122. *Infection and immunity*. 2008; 76(2):601–11. <https://doi.org/10.1128/IAI.00789-07> PMID: 18025097
79. Livak KJ, Schmittgen TD. Analysis of relative gene expression data using real-time quantitative PCR and the  $2^{-\Delta\Delta CT}$  method. *Methods*. 2001; 25(4):402–8. <https://doi.org/10.1006/meth.2001.1262> PMID: 11846609
80. Aiba H, Adhya S, de Crombrugge B. Evidence for two functional gal promoters in intact *Escherichia coli* cells. *Journal of Biological Chemistry*. 1981; 256(22):11905–10. PMID: 6271763
81. Crépin S, Lamarche MG, Garneau P, Séguin J, Proulx J, Dozois CM, et al. Genome-wide transcriptional response of an avian pathogenic *Escherichia coli* (APEC) pst mutant. *BMC genomics*. 2008; 9(1):568. <https://doi.org/10.1186/1471-2164-9-568> PMID: 19038054
82. Harel J, Jacques M, Fairbrother JM, Bossé M, Forget C. Cloning of determinants encoding F1652 fimbriae from porcine septicaemic *Escherichia coli* confirms their identity as F1C fimbriae. *Microbiology*. 1995; 141(1):221–8.



Contents lists available at [ScienceDirect](#)

### Cytokine and Growth Factor Reviews

journal homepage: [www.elsevier.com/locate/cytogfr](http://www.elsevier.com/locate/cytogfr)



## Latest developments in tryptophan metabolism: Understanding its role in B cell immunity

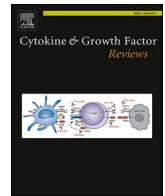


Xavier Dagenais-Lussier<sup>a</sup>, Hamza Loucif<sup>a</sup>, Cherifa Beji<sup>a</sup>, Roman Telittchenko<sup>a</sup>,  
Jean-Pierre Routy<sup>b</sup>, Julien van Grevenynghe<sup>a,\*</sup>

<sup>a</sup> Institut National de la Recherche Scientifique (INRS)-Armand-Frappier Santé Biotechnologie, 531 Boulevard des Prairies, Laval, H7V 1B7, QC, Canada

<sup>b</sup> Chronic Viral Illness Service and Division of Hematology, McGill University Health Centre, Glen site, Montréal, Québec, Canada

---



## Latest developments in tryptophan metabolism: Understanding its role in B cell immunity

Xavier Dagenais-Lussier<sup>a</sup>, Hamza Loucif<sup>a</sup>, Cherifa Beji<sup>a</sup>, Roman Telittchenko<sup>a</sup>,  
Jean-Pierre Routy<sup>b</sup>, Julien van Grevenynghe<sup>a,\*</sup>

<sup>a</sup> Institut National de la Recherche Scientifique (INRS)-Armand-Frappier Santé Biotechnologie, 531 Boulevard des Prairies, Laval, H7V 1B7, QC, Canada

<sup>b</sup> Chronic Viral Illness Service and Division of Hematology, McGill University Health Centre, Glen site, Montréal, Québec, Canada

### ARTICLE INFO

#### Keywords:

Tryptophan  
Kynurenine  
Indoleamine 2,3-dioxygenase (IDO)  
Immunosuppression  
B cells  
Autoimmunity  
Viral infection

### ABSTRACT

One of the most essential and important building blocks of life is the tryptophan amino acid. As such, the pathways surrounding its metabolism are often crucial for the maintenance of proper cell activity and homeostasis. The ratios of tryptophan to kynurenine, mainly mediated by indoleamine 2,3-dioxygenase activity, is a key parameter in the inflammation as well as immunomodulation of both aseptic and septic diseases. As a result, several studies have been published to better understand the mechanisms by which the tryptophan pathways lead to such outcomes. Many have focused on gut health and cells associated with the given environment, the majority of which constitute regulatory T cells and T helper 17 cells. However, recent studies have highlighted the role of this molecular pathway on its capacity to modulate B cells functions and humoral immunity. Accordingly, the focus of this short review is to examine the key tryptophan pathways and their impact on B cells demonstrated by those studies. A better understanding of the role of tryptophan and its metabolites is crucial for its use in disease prevention and treatments.

### 1. Introduction

Tryptophan (Trp) is metabolized via two major pathways: the kynurenine (Kyn) pathway which leads to the production of NAD<sup>+</sup> and the serotonin pathway which eventually leads to melatonin synthesis [1, 2]. Both the fact that the majority of Trp is catabolized through the Kyn pathway which is mediated by the indoleamine 2,3-dioxygenase (IDO) and that many pathologies are linked to dysregulations of the said pathway led to a focus on its impact on both septic and aseptic diseases. Regarding infections, a lot of work has been done on the increased Trp catabolism present during HIV-1 infections and how it's associated with proinflammatory molecules like IL-6, soluble CD40, gamma interferon-inducible protein 10 [3–6]; as well as with CD4 T-cell loss [7–10]. Additionally, some studies showed that the excessive Trp metabolism that occurs during such infections is associated with increased immune dysfunction. This is characterized by the decrease in Trp availability and the increased production of the immunosuppressive metabolite Kyn. Increased Kyn/Trp ratios lead to the loss of T helper 17 cells (Th17), which play a key protective role in the gut against microbial threats and the generation of regulatory T cells (Treg) [11,12]. In

the context of aseptic diseases, an altered distribution of Trp metabolites has been identified in numerous autoimmune complications such as lupus erythematosus and rheumatoid arthritis [13–20]. Although IDO activity is considered immunosuppressive, its exact role in autoimmunity remains poorly understood. Lupus erythematosus and rheumatoid arthritis patients show a skewed distribution of Trp metabolites, characterized by an elevated Kyn/Trp ratios in the serum and urine. In addition, disease activity and clinical manifestations have been positively correlated with depleted Trp and increased Kyn [13,15,16,19]. Currently, many studies as well as reviews address the effects of Trp metabolism on inflammation via T cell functions, such as Treg and Th17 [6,11,12,21–30]. However, in the last years a number of studies emerged linking Trp metabolism with B cell activity. In conjunction with this, it is now well established that B cells are critical components of autoimmune diseases, cancer, and of course viral infections [31–37]. In this short review, we will focus on covering available information on the effects that Trp metabolism has on the development of B cells, autoimmunity, viral infections, and the gut microbiota. Although it is not the focus of this review, an overview of Trp metabolism and its impact on immune functions mentioned here can be found in Fig. 1.

\* Corresponding author.

E-mail address: [julien.vangrevenynghe@inrs.ca](mailto:julien.vangrevenynghe@inrs.ca) (J. van Grevenynghe).

<https://doi.org/10.1016/j.cytogfr.2021.02.003>

Received 24 December 2020; Received in revised form 20 February 2021; Accepted 22 February 2021

Available online 24 February 2021

1359-6101/© 2021 Elsevier Ltd. All rights reserved.



## 2. Tryptophan metabolism in B cell immunity

### 2.1. Aryl hydrocarbon receptor in B cell development

The capacity of B cells to proliferate and switch their immunoglobulin isotype (class switch-recombination; CSR) is crucial for their effector functions as both are necessary for optimal humoral responses [38]. B cell proliferation is important to sustain the affinity maturation process which allows the generation of high-affinity antibodies, whereas maintaining proper Ig isotype pool is necessary for proper activation and responses [39]. Although a direct role of Trp metabolism on B cell differentiation and proliferation remains to be identified, evidence of the important role of the Aryl hydrocarbon receptor (AhR) activation, a receptor that responds to Kyn and Trp metabolite ligands, are being brought forward by two studies. The first one implicates AhR in B cell proliferation by identifying its role following B cell receptor (BcR) activation [40]. Firstly, to confirm that the AhR pathway is functional in B cells Villa et al. looked at its translocation to the nucleus following antigen-specific BcR activation in mice. This led to the expression of cytochrome P450 1A1, which is associated with cellular proliferation in breast cancer [41]. Additionally, B cells from AhR deficient mice had impaired proliferation following antigenic challenges [40]. The second study uncovers the importance of AhR in B cell CSR capacity [42]. Using AhR deficient mice as well as 2,3,7,8-Tetrachlorodibenzo-p-dioxin (TCDD), an AhR agonist, they found that AhR activation acts as a repressor of activation-induced cytidine deaminase (AID). Repression of AID, a molecule essential for CSR [43,44], led to decreased class switching to IgG3 and IgA in B cells. Taken together, this information could add to our knowledge of how AhR activation may mediate immunosuppression in the gut given the importance of IgA in mucosal

immunity [45]. To conclude, these two studies implicate AhR in B cell development, but do not look at how endogenous or microbial metabolite could mediate similar effect. Such studies will be crucial in understanding the full scope of Trp-AhR pathways in modulating B cell development.

### 2.2. Tryptophan metabolism in B cells during autoimmune diseases

Given the important role of Trp metabolism in many chronic inflammatory syndromes, the general impact of IDO on autoimmune diseases has been explored previously [46,47]. One of the first reported effect of the Trp molecular pathway on B cells stems from a study by Scott and colleagues in which they use a murine model of rheumatoid arthritis to elucidate the role of IDO in this disease [48]. Using 1-Methyltryptophan (1-MT), an inhibitor of IDO, they showed that the disease outcome could be alleviated through a diminished autoreactive B cell response which led to decreased autoantibody titers and reduced levels of inflammatory cytokines [48]. Another early report of the effect of this molecular pathway on B cells functions comes from Shinde et al. in 2015. Here, they demonstrate that IDO1 is a key feedback mechanism in limiting B cell proliferation and antibody response. They come to this conclusion by using adoptive transfer of IDO KO B cells in B cell deficient mice. They further report that IDO1 negatively regulates B cell proliferation while promoting apoptosis following LPS stimulation [49]. Following these reports, few studies have explored the relevance of Trp metabolism in mediating B cell functions until recently. Firstly, Merlo and colleagues placed IDO2 in the context of autoimmune diseases by transferring IDO2 expressing B cells into IDO2 KO mice. This led to an increase in development of arthritis compared to controls [50]. Following that, they explored the potential to target IDO2 as a form of

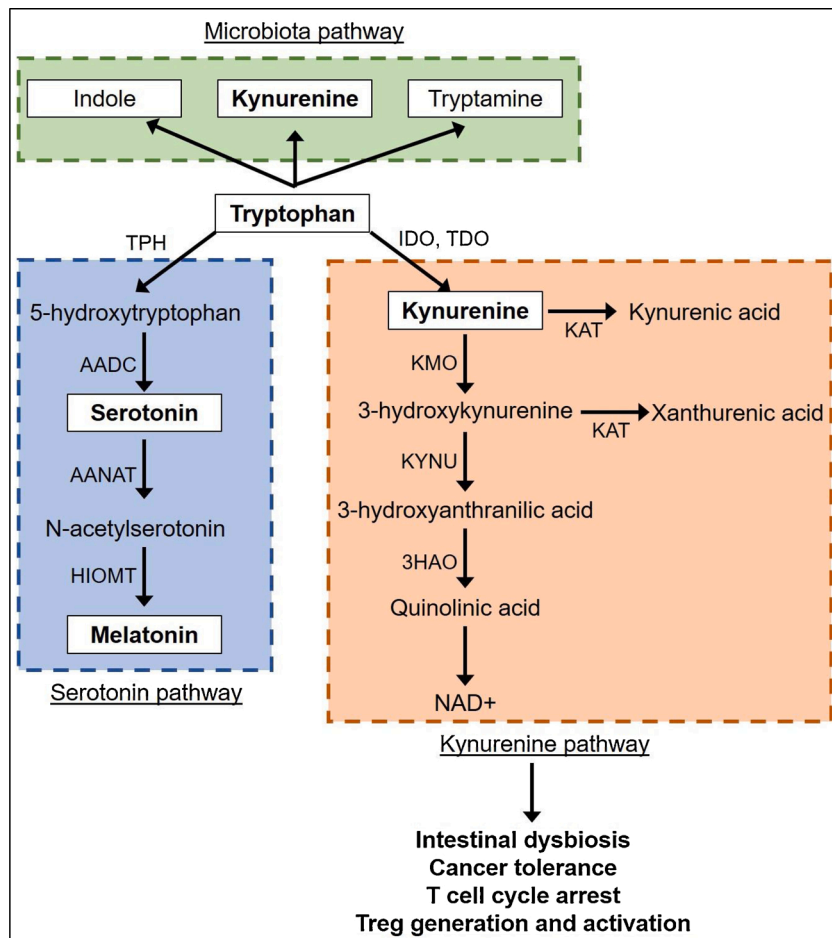


**Fig. 1.** Overview of tryptophan metabolism highlighting its impact on immune functions. 3HAO; 3-hydroxyanthranilate oxidase, AADC; aromatic amino acid decarboxylase, AANAT; aralkylamine N-acetyltransferase, HIOMT; hydroxyindole-O-methyltransferase, IDO; indoleamine 2,3-dioxygenase, KAT; kynurenine aminotransferase, KMO; kynurenine 3-monooxygenase, KYNU; kynureninase, NAD; nicotinamide adenine dinucleotide, TDO; tryptophan 2,3-dioxygenase, TPH; tryptophan hydroxylase.

treatment against autoimmune arthritis. To achieve this, they devised an elegant strategy to specifically target IDO2 within the B cell population. By using a 3DNA nanocarrier that specifically targets B cells to deliver a therapeutic dose of anti-IDO2 siRNA into autoimmune arthritis mice models, they delayed the onset of joint swelling and reduced total arthritis severity [51]. Their more recent work tries to distinguish more precisely the functions between IDO1 and IDO2 in autoimmune diseases. Using IDO1 and IDO2 KO mice as well as double KO, they conclude that IDO2 seems to be the dominant player in many B cell-mediated immune pathologies such as autoimmune arthritis [52].

However, it is interesting to note that in contrast to Merlo et al. findings, there is also a report on the beneficial effect of the AhR activation in regulatory B cells (Breg) related to the production of the anti-inflammatory cytokine IL-10. In this study, Piper et al. show, by using AhR KO mice, that this receptor is necessary for the differentiation and function of IL-10 producing Breg. In fact, not only did AhR KO B cells display reduced IL-10 production, but they also showed increased production of IL-2, IL-6, and TNF $\alpha$ ; three cytokines linked to immune activation [53]. In addition to the works of Piper et al., there are two studies which corroborate the link between IDO and immunosuppression in B cells. In the first one, they link IDO activity of Myeloid-derived suppressor cells (MDSC), a population of immature myeloid cells that possess potent suppressive capacities, to the reduced proliferation of B cells [54]. The second one looks at B cells in the context of multiple sclerosis (MS), a disease known to be related to their activity [32,55]. In this study, they show that treating experimental autoimmune encephalomyelitis in mice, a murine model of MS, with mesenchymal stromal cells increased the frequency of Breg and improved clinical symptoms [56]. Those outcomes were then reversed by using 1-MT. It is important to consider that these studies placed the Trp metabolism outside of the context of the seemingly opposite functions of IDO1 and IDO2 by either looking at AhR directly [53] or simply by not distinguishing between the two using a non-specific inhibitor [54,56]. Overall, the roles of IDO1 and IDO2 in autoimmune diseases are becoming increasingly clear with IDO1 seemingly skewing B cells functions towards immune regulation, whereas IDO2 pushes them towards immune responsiveness. However, further research is required to assess whether some of the observed phenotypes fit in this model or if it's even more nuanced than that.

### 2.3. Tryptophan metabolism in B cells during viral infections

Going outside of the context of autoimmunity, IDO is a key component of viral responses considering its induction following IFN- $\gamma$  or TNF- $\alpha$  stimulation [57,58]. The main effect associated with IDO activity during viral infection is its promotion of immunological tolerance by increasing the proliferation of Treg [59]. However, understanding the role of IDO and Trp on B cells during viral infections is still in its infancy. In this context, Bonezi et al. have reported the role of Trp metabolism in B cell differentiation during Dengue virus infection. In their work, they demonstrate that the Dengue virus infection is associated with an increased expression of IDO1 and IDO2 [60]. Additionally, the Trp and Kyn concentrations were directly correlated to the magnitude of the antibody secretion response. This suggests that IDO activity can play a role in the fine tuning of antibody responses during this infection. In contrast, other flaviviruses, such as Zika and Yellow fever virus, whose potential to induce strong antibody secreting B cells responses is lower, had lower Kyn concentrations following in vitro culture. Taken together, these results point towards the fact that Trp metabolism activation could be used as a biomarker to identify Dengue virus-mediated antigen secreting B cells responses [60]. Interestingly, this is the first reported effect of viral infections on B cell functions mediated through Trp metabolism. In addition to this, Merlo et al. also reported the importance of IDO2 in antibody production following influenza infection. In this experiment, they demonstrate that IDO2 KO mice had consistently lower antibody titers against influenza following an infection [52]. Taking this into account, it is reasonable to believe that B cells functions might be

altered in other infections that are known to affect Trp metabolism such as in the case with HIV-1 infections. This is consequential considering that viral infections are known to dysregulate Trp:Kyn ratios leading to abnormal Treg and Th17 ratios which are linked to dysbiosis. To conclude, IDO2 activity is again associated with increased immune responsiveness resulting in greater antibody titer against influenza and Dengue virus. For an overview of the virus covered in this section refer to Table 1.

### 2.4. Tryptophan metabolism in B cell and the gut microbiota

The vital role of gut microbiota on immune homeostasis and the intestinal immune response is now well acknowledged [61–64]. Recent studies have highlighted that changes in the microbiota modulate the hosts' immune system through the modulation of Trp metabolism. As such, microbial Trp catabolites are associated with antimicrobial activity [65–69], hormonal secretion [70,71], as well as being considered as AhR ligands [72–75]. As such, the role of the microbiota and their metabolism of Trp in mediating T cell immunity is well established [76,77]. Interestingly, the importance of microbiota on Breg function has previously been established [78]. Succinctly, they show that the gut microbiota promotes the differentiation of Breg in mice while antibiotic-mediated perturbation reduces their number. However, the link between the Trp metabolism of microbiota and Breg has only recently been shown. Indeed, the only reported impact of microbiota activity on B cells is a recent study by Rosser and colleagues [79]. In their research, they unravel the importance of butyrate supplementation in Breg-mediated arthritis suppression. To do so, Rosser et al. show that supplementing mice with butyrate led to an increase in microbiota produced 5-hydroxyindole-3-acetic acid and kynurenic acid; two AhR ligands associated with Trp metabolism, which ultimately increased IL-10 transcription in B cells. This regulatory phenotype of B cells was associated with a reduction in pro-arthritis stimuli [79]. Finally, by using AhR knockout mice, Rosser et al. demonstrated the role of this receptor in the butyrate-mediated promotion of Breg and the associated suppression of arthritis. Despite these findings, the impact of the gut microbiota on B cells remains to be fully explored. However, given the role of Trp and its metabolites on T cells, its impact on B cells is surely important for our full understanding of their functions in a wide array of diseases.

In conclusion, although some studies seem to point towards an immunosuppressive role of the Trp-IDO molecular pathway, it seems that the Trp-Kyn-AhR pathway mediated by IDO is still complex, not fully understood and requires some fine-tuning in order to maintain proper B cell responses. This is due to the fact that IDO1 and IDO2 can be respectively associated with an immunosuppressive or pro-inflammatory role. In this context, it is important to consider where we wish to target potential treatments in the Trp metabolism pathway and how specific they need to be to improve patients' health. Finally, we provide a schematization of the reported impact of Trp metabolism on B

**Table 1**

Role of tryptophan metabolism on B cell functions during viral infections. \* Although Yellow fever and Zika virus infection led to low Kyn concentration in culture, no correlation was found between Kyn concentration and number of antibody secreting cells. The role of Trp metabolism in B cell function during those infections remains to be explored.

Virus	Implicated molecule/metabolite	Effect of B cell functions	Ref
Dengue	High Trp consumption, High Kyn accumulation	Increased in antibody secreting cells	[60]
Yellow fever*	Low Kyn accumulation	Low antibody secreting cell response	[60]
Zika*	Low Kyn accumulation	Low antibody secreting cell response	[60]
Influenza	IDO2	Increase in antibody titer	[52]

cell functions that are currently available to our knowledge (Fig. 2).

### 3. Concluding remarks

To conclude, it is now a well-known fact that Trp metabolism is linked to autoimmunity as well as gut health through Treg:Th17 ratios. With emerging new evidence, its role in mediating different B cell properties is now only starting to come to light. As an example, one potential aspect of this pathway that remains unexplored is its role in energy production, since the Kyn pathway leads to NAD<sup>+</sup> production and impacts mitochondrial functions. Considering the pivotal role of the impact of that this pathway played on T cell functions, deepening our understanding of its role on B cells responses is a clear path that should be investigated. An increasing number of trials are underway to harness this knowledge in order for us to treat a slew of disease such as cancer, HIV-1, and autoimmune disorders [21–24,27,80–82]. In the context of Trp metabolism, there are two main approaches for treatment that currently exist. The first one is based on modulating the gut microbiota [21,82], considering its important role in Trp metabolism as seen previously. The second one aims to tamper with the metabolism directly. The most common way to do so is to use the IDO inhibitor 1-MT. The

main drawback of 1-MT is the fact that it targets both forms of IDO [83]. Considering the seemingly opposite role they play; this could lead to diminished efficacy of proposed treatments. Another aspect to consider for these medical approaches is that the affinities of Trp metabolites for the AhR differ between rodents and humans [75,84]. This is especially important to consider since predictions about AhR-ligand interactions in humans are often extrapolated from rodent studies. Although it is increasingly clear that using the Trp metabolism as a successful form of treatment will come in conjunction with other more established medical procedure as well as potential lifestyle changes, considering the role of Trp metabolism in viral infections and in B cell functions is crucial for the deepening of our understanding of different pathways involved in these processes. This is especially true in the current context of the global Coronavirus pandemic where a huge part of our success in overcoming this threat hinges on good antibody production following vaccination as well as understanding of the viral modulation of the immune system following infection. The latter might be used to identify treatments to lighten the disease outcome. The relevance of this is staggeringly evident when one considers the number of recent studies that demonstrate the role that Trp metabolism could play during SARS-CoV-2 infection [85–89]. Reports are revealing that there is a high

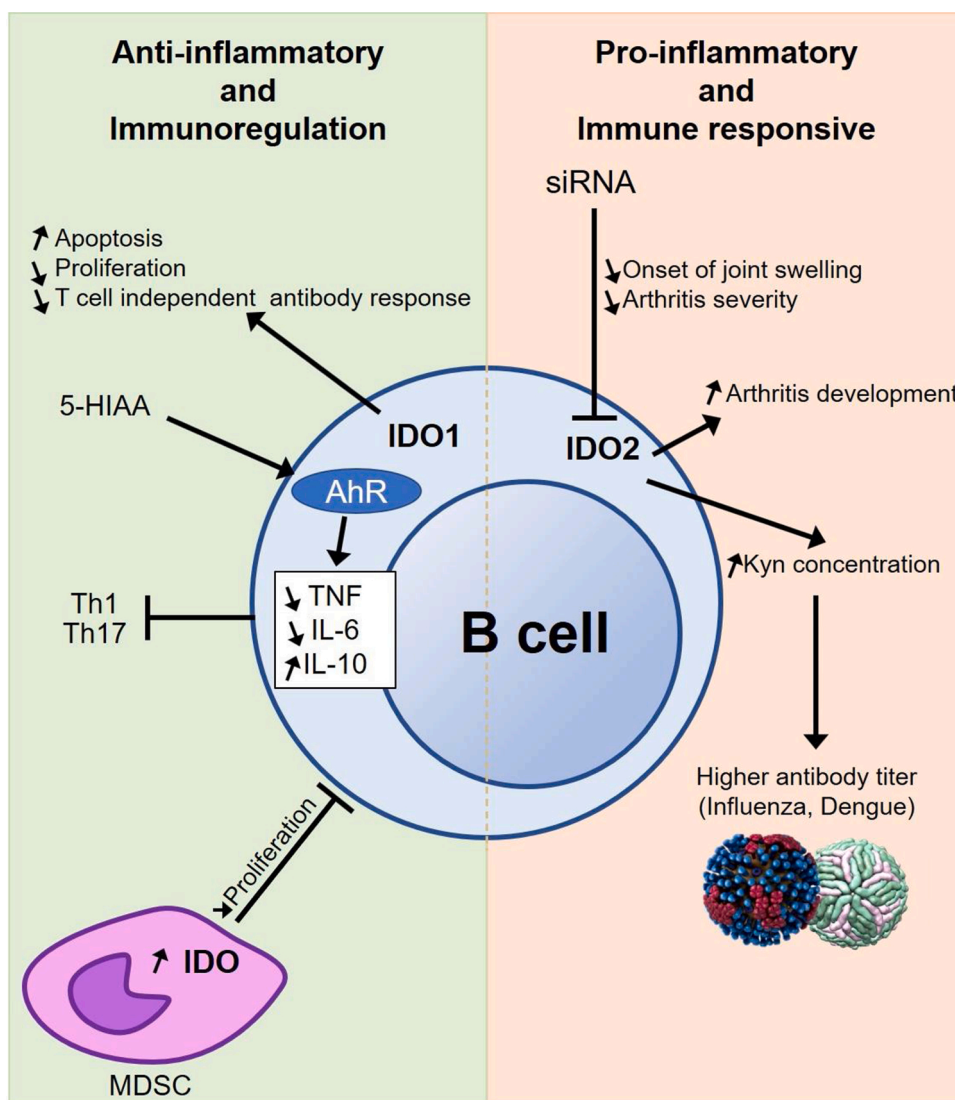


Fig. 2. Impact of tryptophan metabolism on B cell functions highlighting the seemingly paradoxical function of IDO1 and IDO2 on B cell immunomodulation. Arrows pointing up or down respectively represent an increase in the phenotype/expression or a reduction. 5-HIAA; 5-hydroxyindole-3-acetic acid, MDSC; myeloid-derived-suppressor cells.



dyregulation of Trp metabolism during this infection such as increased kynurenine/tryptophan ratios [90,91]. With this information, there are already efforts being made to maximize the treatment potential against COVID-19 [92]. In summary, not only will our understanding of the impact of Trp metabolism be useful to tackle the current pandemic, but it will surely also be required for future global health challenges.

#### CRedit authorship contribution statement

**Xavier Dagenais-Lussier:** Conceptualization, Writing - original draft, Supervision. **Hamza Loucif:** Conceptualization, Investigation, Writing - original draft, Visualization. **Cherifa Beji:** Writing - review & editing. **Roman Telittchenko:** Writing - review & editing. **Jean-Pierre Routy:** Writing - review & editing. **Julien van Grevenynghe:** Conceptualization, Supervision, Project administration, Funding acquisition.

#### Declaration of Competing Interest

The authors declare that they have no known competing financial interests or personal relationships that could have appeared to influence the work reported in this paper.

#### References

- J.R. Moffett, M.A. Nambodiri, Tryptophan and the immune response, *Immunol. Cell Biol.* 81 (2003) 247–265, <https://doi.org/10.1046/j.1440-1711.2003.t01-1-01177.x>.
- J.M. Gostner, S. Geisler, M. Stonig, L. Mair, B. Sperner-Unterwieser, D. Fuchs, Tryptophan metabolism and related pathways in psychoneuroimmunology: the impact of nutrition and lifestyle, *Neuropsychobiology* 79 (2020) 89–99, <https://doi.org/10.1159/000496293>.
- D. Fuchs, A.A. Möller, G. Reibnegger, E.R. Werner, G. Werner-Felmayer, M. P. Dierich, H. Wachter, Increased endogenous interferon-gamma and neopterin correlate with increased degradation of tryptophan in human immunodeficiency virus type 1 infection, *Immunol. Lett.* 28 (1991) 207–211, [https://doi.org/10.1016/0165-2478\(91\)90005-u](https://doi.org/10.1016/0165-2478(91)90005-u).
- D. Favre, J. Mold, P.W. Hunt, B. Kanwar, P. Loke, L. Seu, J.D. Barbour, M.M. Lowe, A. Jayawardene, F. Aweeka, Y. Huang, D.C. Douek, J.M. Brenchley, J.N. Martin, F. M. Hecht, S.G. Deeks, J.M. McCune, Tryptophan catabolism by indoleamine 2,3-dioxygenase 1 alters the balance of TH17 to regulatory T cells in HIV disease, *Sci. Transl. Med.* 2 (2010), 32ra36, <https://doi.org/10.1126/scitranslmed.3000632>.
- M.-A. Jenabian, M. Patel, I. Kema, K. Vyboh, C. Kanagaratham, D. Radzioch, P. Thébault, R. Lapointe, N. Gilmore, P. Ancuta, C. Tremblay, J.-P. Routy, Soluble CD40-ligand (sCD40L, sCD154) plays an immunosuppressive role via regulatory T cell expansion in HIV infection, *Clin. Exp. Immunol.* 178 (2014) 102–111, <https://doi.org/10.1111/cei.12396>.
- M.-A. Jenabian, M. El-Far, K. Vyboh, I. Kema, C.T. Costiniuk, R. Thomas, J.-G. Baril, R. LeBlanc, C. Kanagaratham, D. Radzioch, O. Allam, A. Ahmad, B. Lebouché, C. Tremblay, P. Ancuta, J.-P. Routy, Montreal primary infection and slow progressor study groups, immunosuppressive tryptophan catabolism and gut mucosal dysfunction following early HIV infection, *J. Infect. Dis.* 212 (2015) 355–366, <https://doi.org/10.1093/infdis/jiv037>.
- J. Chen, J. Shao, R. Cai, Y. Shen, R. Zhang, L. Liu, T. Qi, H. Lu, Anti-retroviral therapy decreases but does not normalize indoleamine 2,3-dioxygenase activity in HIV-infected patients, *PLoS One* 9 (2014), e100446, <https://doi.org/10.1371/journal.pone.0100446>.
- J.-C. Gaardbo, M. Trøsd, B. Stiksrud, Ø. Midttun, P.M. Ueland, H. Ullum, S. D. Nielsen, Increased tryptophan catabolism is associated with increased frequency of CD161+Tc17/MAIT cells and lower CD4+ T-Cell count in HIV-1 infected patients on cART after 2 years of follow-up, *J. Acquir. Immune Defic. Syndr.* 1999 70 (2015) 228–235, <https://doi.org/10.1097/QAI.0000000000000758>.
- P. Bipath, P.F. Levay, M. Viljoen, The kynurenine pathway activities in a sub-Saharan HIV/AIDS population, *BMC Infect. Dis.* 15 (2015) 346, <https://doi.org/10.1186/s12879-015-1087-5>.
- X. Dagenais-Lussier, M. Aounallah, V. Mehraj, M. El-Far, C. Tremblay, R.-P. Sekaly, J.-P. Routy, J. van Grevenynghe, Kynurenine reduces memory CD4 T-Cell survival by interfering with interleukin-2 signaling early during HIV-1 infection, *J. Virol.* 90 (2016) 7967–7979, <https://doi.org/10.1128/JVI.00994-16>.
- A. Boasso, J.-P. Herbeuval, A.W. Hardy, S.A. Anderson, M.J. Dolan, D. Fuchs, G. M. Shearer, HIV inhibits CD4+ T-cell proliferation by inducing indoleamine 2,3-dioxygenase in plasmacytoid dendritic cells, *Blood* 109 (2007) 3351–3359, <https://doi.org/10.1182/blood-2006-07-034785>.
- R. Planès, E. Bahraoui, HIV-1 Tat protein induces the production of IDO in human monocyte derived-dendritic cells through a direct mechanism: effect on T cells proliferation, *PLoS One* 8 (2013), e74551, <https://doi.org/10.1371/journal.pone.0074551>.
- B. Widner, N. Sepp, E. Kowald, U. Ortner, B. Wirleitner, P. Fritsch, G. Baier-Bitterlich, D. Fuchs, Enhanced tryptophan degradation in systemic lupus erythematosus, *Immunobiology* 201 (2000) 621–630, [https://doi.org/10.1016/S0171-2985\(00\)80079-0](https://doi.org/10.1016/S0171-2985(00)80079-0).
- K. Schroeksnadel, S. Kaser, M. Ledochowski, G. Neurauter, E. Mur, M. Herold, D. Fuchs, Increased degradation of tryptophan in blood of patients with rheumatoid arthritis, *J. Rheumatol.* 30 (2003) 1935–1939.
- M. Pertovaara, T. Hasan, A. Raitala, S.S. Oja, U. Yli-Kerttula, M. Korpela, M. Hurme, Indoleamine 2,3-dioxygenase activity is increased in patients with systemic lupus erythematosus and predicts disease activation in the sunny season, *Clin. Exp. Immunol.* 150 (2007) 274–278, <https://doi.org/10.1111/j.1365-2249.2007.03480.x>.
- A. Perl, R. Hanczko, Z.-W. Lai, Z. Oaks, R. Kelly, R. Borsuk, J.M. Asara, P. E. Phillips, Comprehensive metabolome analyses reveal N-acetylcysteine-responsive accumulation of kynurenine in systemic lupus erythematosus: implications for activation of the mechanistic target of rapamycin, *Metabolomics Off. J. Metabolomic Soc.* 11 (2015) 1157–1174, <https://doi.org/10.1007/s11306-015-0772-0>.
- S. Ainehband, P. Brenner, S. Ståhl, M. Bhat, M.D. Fidock, M. Khademi, T. Olsson, G. Engberg, J. Jokinen, S. Erhardt, F. Piehl, Cerebrospinal fluid kynurenines in multiple sclerosis; relation to disease course and neurocognitive symptoms, *Brain Behav. Immun.* 51 (2016) 47–55, <https://doi.org/10.1016/j.bbi.2015.07.016>.
- C.K. Lim, A. Bilgin, D.B. Lovejoy, V. Tan, S. Bustamante, B.V. Taylor, A. Bessedé, B. J. Brew, G.J. Guillemin, Kynurenine pathway metabolomics predicts and provides mechanistic insight into multiple sclerosis progression, *Sci. Rep.* 7 (2017) 41473, <https://doi.org/10.1038/srep41473>.
- K. Åkesson, S. Pettersson, S. Ståhl, I. Surowiec, M. Hedenström, S. Eketjäll, J. Trygg, P.-J. Jakobsson, I. Gunnarsson, E. Svenungsson, H. Idborg, Kynurenine pathway is altered in patients with SLE and associated with severe fatigue, *Lupus Sci. Med.* 5 (2018), e000254, <https://doi.org/10.1136/lupus-2017-000254>.
- L. Gaetani, F. Boscaro, G. Pieraccini, P. Calabresi, L. Romani, M. Di Filippo, T. Zelante, Host and microbial tryptophan metabolic profiling in multiple sclerosis, *Front. Immunol.* 11 (2020) 157, <https://doi.org/10.3389/fimmu.2020.00157>.
- K. Vyboh, M.-A. Jenabian, V. Mehraj, J.-P. Routy, HIV and the gut microbiota, *partners in crime: breaking the vicious cycle to unearth new therapeutic targets*, *J. Immunol. Res.* (2015) 9.
- A. Amobi, F. Qian, A.A. Lugade, K. Odunsi, Tryptophan catabolism and cancer immunotherapy targeting IDO mediated immune suppression, in: P. Kalinski (Ed.), *Tumor Immune Microenviron. Cancer Progress*. Cancer Ther., Springer International Publishing, Cham, 2017, pp. 129–144, [https://doi.org/10.1007/978-3-319-67577-0\\_9](https://doi.org/10.1007/978-3-319-67577-0_9).
- G.C. Prendergast, W.J. Malachowski, A. Mondal, P. Scherle, A.J. Muller, Indoleamine 2,3-dioxygenase and its therapeutic inhibition in cancer, *Int. Rev. Cell Mol. Biol.*, Elsevier, 2018, pp. 175–203, <https://doi.org/10.1016/b.ircmb.2017.07.004>.
- Y. Ohue, H. Nishikawa, Regulatory T (Treg) cells in cancer: can Treg cells be a new therapeutic target? *Cancer Sci.* 110 (2019) 2080–2089, <https://doi.org/10.1111/cas.14069>.
- F.M. Benavente, J.A. Soto, M.S. Pizarro-Ortega, K. Bohmwald, P.A. González, S. M. Bueno, A.M. Kalergis, Contribution of IDO to human respiratory syncytial virus infection, *J. Leukoc. Biol.* 106 (2019) 933–942, <https://doi.org/10.1002/JLB.4RU0219-051RR>.
- Ritprajak, Kaewraemruan, Hirankarn, Current paradigms of tolerogenic dendritic cells and clinical implications for systemic lupus erythematosus, *Cells* 8 (2019) 1291, <https://doi.org/10.3390/cells8101291>.
- L. Zhai, A. Bell, E. Ladomersky, K.L. Lauing, L. Bollu, J.A. Sosman, B. Zhang, J. D. Wu, S.D. Miller, J.J. Meeks, R.V. Lukas, E. Wyatt, L. Doglio, G.E. Schiltz, R. H. McCusker, D.A. Wainwright, Immunosuppressive IDO in cancer: mechanisms of action, animal models, and targeting strategies, *Front. Immunol.* 11 (2020) 1185, <https://doi.org/10.3389/fimmu.2020.01185>.
- J. Brown, B. Robusto, L. Morel, Intestinal dysbiosis and tryptophan metabolism in autoimmunity, *Front. Immunol.* 11 (2020) 1741, <https://doi.org/10.3389/fimmu.2020.01741>.
- A. Meireson, M. Devos, L. Brochez, IDO expression in cancer: different compartment, different functionality? *Front. Immunol.* 11 (2020), 531491 <https://doi.org/10.3389/fimmu.2020.531491>.
- M.-A. Jenabian, M. Patel, I. Kema, C. Kanagaratham, D. Radzioch, P. Thébault, R. Lapointe, C. Tremblay, N. Gilmore, P. Ancuta, J.-P. Routy, Distinct tryptophan catabolism and Th17/Treg balance in HIV progressors and elite controllers, *PLoS One* 8 (2013), e78146, <https://doi.org/10.1371/journal.pone.0078146>.
- J.L. Barnas, R.J. Looney, J.H. Anolik, B cell targeted therapies in autoimmune disease, *Curr. Opin. Immunol.* 61 (2019) 92–99, <https://doi.org/10.1016/j.coi.2019.09.004>.
- H. Wekerle, B cells in multiple sclerosis, *Autoimmunity* 50 (2017) 57–60, <https://doi.org/10.1080/08916934.2017.1281914>.
- A. Sarvaria, J.A. Madrigal, A. Saudemont, B cell regulation in cancer and anti-tumor immunity, *Cell. Mol. Immunol.* 14 (2017) 662–674, <https://doi.org/10.1038/cmi.2017.35>.
- A. Largeot, G. Pagano, S. Gonder, E. Moussay, J. Paggetti, The B-side of cancer immunity: the underrated tune, *Cells* 8 (2019), <https://doi.org/10.3390/cells8050449>.
- T. Inoue, I. Moran, R. Shinnakasu, T.G. Phan, T. Kurosaki, Generation of memory B cells and their reactivation, *Immunol. Rev.* 283 (2018) 138–149, <https://doi.org/10.1111/imr.12640>.
- S. Moir, A.S. Fauci, B-cell responses to HIV infection, *Immunol. Rev.* 275 (2017) 33–48, <https://doi.org/10.1111/imr.12502>.

- [37] P. Shen, S. Fillatreau, Suppressive functions of B cells in infectious diseases, *Int. Immunol.* 27 (2015) 513–519, <https://doi.org/10.1093/intimm/dxv037>.
- [38] Y. Wang, J. Liu, P.D. Burrows, J.-Y. Wang, B cell development and maturation, *Adv. Exp. Med. Biol.* 1254 (2020) 1–22, [https://doi.org/10.1007/978-981-15-3532-1\\_1](https://doi.org/10.1007/978-981-15-3532-1_1).
- [39] J. Liu, Y. Wang, Q. Min, E. Xiong, B. Heyman, J.-Y. Wang, Regulation of humoral immune responses and B cell tolerance by the IgM fc receptor (FcμR), *Adv. Exp. Med. Biol.* 1254 (2020) 75–86, [https://doi.org/10.1007/978-981-15-3532-1\\_7](https://doi.org/10.1007/978-981-15-3532-1_7).
- [40] M. Villa, M. Gialitakis, M. Tolaini, H. Ahlfors, C.J. Henderson, C.R. Wolf, R. Brink, B. Stockinger, Aryl hydrocarbon receptor is required for optimal B-cell proliferation, *EMBO J.* 36 (2017) 116–128, <https://doi.org/10.15252/embj.201695027>.
- [41] M. Rodriguez, D.A. Potter, CYP1A1 regulates breast cancer proliferation and survival, *Mol. Cancer Res. MCR.* 11 (2013) 780–792, <https://doi.org/10.1158/1541-7786.MCR-12-0675>.
- [42] B. Vaidyanathan, A. Chaudhry, W.T. Yewdell, D. Angeletti, W.-F. Yen, A. K. Wheatley, C.A. Bradfield, A.B. McDermott, J.W. Yewdell, A.Y. Rudensky, J. Chaudhuri, The aryl hydrocarbon receptor controls cell-fate decisions in B cells, *J. Exp. Med.* 214 (2017) 197–208, <https://doi.org/10.1084/jem.20160789>.
- [43] M. Muramatsu, K. Kinoshita, S. Fagarasan, S. Yamada, Y. Shinkai, T. Honjo, Class switch recombination and hypermutation require activation-induced cytidine deaminase (AID), a potential RNA editing enzyme, *Cell* 102 (2000) 553–563, [https://doi.org/10.1016/S0092-8674\(00\)00078-7](https://doi.org/10.1016/S0092-8674(00)00078-7).
- [44] P. Revy, T. Muto, Y. Levy, F. Geissmann, A. Plebani, O. Sanal, N. Catalan, M. Forveille, R. Dufourcq-Lagelouse, A. Gennery, I. Tezcan, F. Ersoy, H. Kayserili, A.G. Ugazio, N. Brousse, M. Muramatsu, L.D. Notarangelo, K. Kinoshita, T. Honjo, A. Fischer, A. Durandy, Activation-induced cytidine deaminase (AID) deficiency causes the autosomal recessive form of the Hyper-IgM syndrome (HIGM2), *Cell* 102 (2000) 565–575, [https://doi.org/10.1016/S0092-8674\(00\)00079-9](https://doi.org/10.1016/S0092-8674(00)00079-9).
- [45] S. Fagarasan, T. Honjo, Intestinal IgA synthesis: regulation of front-line body defences, *Nat. Rev. Immunol.* 3 (2003) 63–72, <https://doi.org/10.1038/nri982>.
- [46] D.H. Munn, A.L. Mellor, Indoleamine 2,3-dioxygenase and metabolic control of immune responses, *Trends Immunol.* 34 (2013) 137–143, <https://doi.org/10.1016/j.it.2012.10.001>.
- [47] A.L. Mellor, H. Lemos, L. Huang, Indoleamine 2,3-dioxygenase and tolerance: where are we now? *Front. Immunol.* 8 (2017) <https://doi.org/10.3389/fimmu.2017.01360>.
- [48] G.N. Scott, J. DuHadaway, E. Pigott, N. Ridge, G.C. Prendergast, A.J. Muller, L. Mandik-Nayak, The immunoregulatory enzyme IDO paradoxically drives B cell-mediated autoimmunity, *J. Immunol.* 182 (2009) 7509–7517, <https://doi.org/10.4049/jimmunol.0804328>.
- [49] R. Shinde, M. Shimoda, K. Chaudhary, H. Liu, E. Mohamed, J. Bradley, S. Kandala, X. Li, K. Liu, T.L. McGaha, B cell-intrinsic IDO1 regulates humoral immunity to cell-independent antigens, *J. Immunol.* 195 (2015) 2374–2382, <https://doi.org/10.4049/jimmunol.1402854>.
- [50] L.M.F. Merlo, J.B. DuHadaway, S. Grabler, G.C. Prendergast, A.J. Muller, L. Mandik-Nayak, IDO2 Modulates T Cell-dependent Autoimmune Responses Through a B Cell-Intrinsic Mechanism, 2017, p. 25.
- [51] L.M. Merlo, J. Bowers, T. Stefanoni, R. Getts, L. Mandik-Nayak, B-cell-Targeted 3DNA nanotherapy against indoleamine 2,3-dioxygenase 2 (IDO2) ameliorates autoimmune arthritis in a preclinical model, *Clin. Pathol.* 13 (2020), 2632010X2095181, <https://doi.org/10.1177/2632010X20951812>.
- [52] L.M.F. Merlo, J.B. DuHadaway, J.D. Montgomery, W.-D. Peng, P.J. Murray, G.C. Prendergast, A.J. Caton, A.J. Muller, L. Mandik-Nayak, Differential roles of IDO1 and IDO2 in T and B cell inflammatory immune responses, *Front. Immunol.* 11 (2020) 1861, <https://doi.org/10.3389/fimmu.2020.01861>.
- [53] C.J.M. Piper, E.C. Rosser, K. Oleinika, K. Nistala, T. Krausgruber, A.F. Rendeiro, A. Banos, I. Drozdov, M. Villa, S. Thomson, G. Xanthou, C. Bock, B. Stockinger, C. Mauri, Aryl hydrocarbon receptor contributes to the transcriptional program of IL-10-producing regulatory B cells, *Cell Rep.* 29 (2019) 1878–1892, <https://doi.org/10.1016/j.celrep.2019.10.018>, e7.
- [54] J. Jauffmann, F.J.N. Lelis, A.C. Teschner, K. Fromm, N. Rieber, D. Hartl, S. Beer-Hammer, Human monocyte myeloid-derived suppressor cells impair B-cell phenotype and function in vitro, *Eur. J. Immunol.* (2019) 16.
- [55] B.M. Arneth, Impact of B cells to the pathophysiology of multiple sclerosis, *J. Neuroinflammation* 16 (2019) 128, <https://doi.org/10.1186/s12974-019-1517-1>.
- [56] H. Li, Y. Deng, J. Liang, F. Huang, W. Qiu, M. Zhang, Y. Long, X. Hu, Z. Lu, W. Liu, S.G. Zheng, Mesenchymal stromal cells attenuate multiple sclerosis via IDO-dependent increasing the suppressive proportion of CD5+ IL-10+ B cells, *Am. J. Transl. Res.* 11 (2019) 5673–5688.
- [57] M. van Wissen, M. Snoek, B. Smids, H.M. Jansen, R. Lutter, IFN- $\gamma$  amplifies IL-6 and IL-8 responses by airway epithelial-like cells via indoleamine 2,3-dioxygenase, *J. Immunol.* 169 (2002) 7039–7044, <https://doi.org/10.4049/jimmunol.169.12.7039>.
- [58] G.J. Guillemin, G. Smythe, O. Takikawa, B.J. Brew, Expression of indoleamine 2,3-dioxygenase and production of quinolinic acid by human microglia, astrocytes, and neurons, *Glia* 49 (2005) 15–23, <https://doi.org/10.1002/glia.20090>.
- [59] V. Mehraj, J.-P. Routy, Tryptophan catabolism in chronic viral infections: handling uninvited guests, *Int. J. Tryptophan Res. IJTR* 8 (2015) 41–48, <https://doi.org/10.4137/IJTR.S26862>.
- [60] V. Bonezi, A.H.D. Cataneo, M.S.F. Branquinho, M.B.B. Silva, P. Gonzalez-Dias, S. S. Pereira, L.C. de S. Ferreira, H.I. Nakaya, A. Campa, P.F. Wovk, E.L.V. Silveira, Flavivirus-mediating B cell differentiation into antibody-secreting cells in humans is associated with the activation of the tryptophan metabolism, *Front. Immunol.* 11 (2020) 20, <https://doi.org/10.3389/fimmu.2020.00020>.
- [61] G. Morris, M. Berk, A. Carvalho, J.R. Caso, Y. Sanz, K. Walder, M. Maes, The role of the microbial metabolites including tryptophan catabolites and short chain fatty acids in the pathophysiology of immune-inflammatory and neuroimmune disease, *Mol. Neurobiol.* 54 (2017) 4432–4451, <https://doi.org/10.1007/s12035-016-0004-2>.
- [62] J. Gao, K. Xu, H. Liu, G. Liu, M. Bai, C. Peng, T. Li, Y. Yin, Impact of the gut microbiota on intestinal immunity mediated by tryptophan metabolism, *Front. Cell. Infect. Microbiol.* 8 (2018) 13, <https://doi.org/10.3389/fcimb.2018.00013>.
- [63] M. Sun, N. Ma, T. He, L.J. Johnston, X. Ma, Tryptophan (Trp) modulates gut homeostasis via aryl hydrocarbon receptor (Ahr), *Crit. Rev. Food Sci. Nutr.* 60 (2020) 1760–1768, <https://doi.org/10.1080/10408398.2019.1598334>.
- [64] H.M. Roager, T.R. Licht, Microbial tryptophan catabolites in health and disease, *Nat. Commun.* 9 (2018) 3294, <https://doi.org/10.1038/s41467-018-05470-4>.
- [65] H. Chen, G.R. Fink, Feedback control of morphogenesis in fungi by aromatic alcohols, *Genes Dev.* 20 (2006) 1150–1161, <https://doi.org/10.1101/gad.1411806>.
- [66] L. Elleuch, M. Shaaban, S. Smaoui, L. Mellouli, I. Karray-Rebai, L. Fourati-Ben Fguira, K.A. Shaaban, H. Laatsch, Bioactive secondary metabolites from a new terrestrial Streptomyces sp. TN262, *Appl. Biochem. Biotechnol.* 162 (2010) 579–593, <https://doi.org/10.1007/s12010-009-8808-4>.
- [67] M. Jin, C. Xu, X. Zhang, The effect of tryptophan on the bacteriophage infection in high-temperature environment, *Appl. Microbiol. Biotechnol.* 99 (2015) 8101–8111, <https://doi.org/10.1007/s00253-015-6674-2>.
- [68] T.K. Narayanan, G.R. Rao, Beta-indoleethanol and beta-indolelactic acid production by Candida species: their antibacterial and autoantibiotic action, *Antimicrob. Agents Chemother.* 9 (1976) 375–380.
- [69] B. Bommarius, A. Anyanful, Y. Izrayelit, S. Bhatt, E. Cartwright, W. Wang, A. I. Swimm, G.M. Benian, F.C. Schroeder, D. Kalman, A family of indoles regulate virulence and Shiga toxin production in pathogenic E. coli, *PLoS One* 8 (2013), e54456, <https://doi.org/10.1371/journal.pone.0054456>.
- [70] J.J. Holst, The physiology of glucagon-like peptide 1, *Physiol. Rev.* 87 (2007) 1409–1439, <https://doi.org/10.1152/physrev.00034.2006>.
- [71] V.D. de Mello, J. Paananen, J. Lindström, M.A. Lankinen, L. Shi, J. Kuusisto, J. Pihlajamäki, S. Auriola, M. Lehtonen, O. Rolandsson, I.A. Bergdahl, E. Nordin, P. Ilanne-Parikka, S. Keinänen-Kiukaanniemi, R. Landberg, J.G. Eriksson, J. Tuomilehto, K. Hanhineva, M. Uusitupa, Indolepropionic acid and novel lipid metabolites are associated with a lower risk of type 2 diabetes in the Finnish Diabetes Prevention Study, *Sci. Rep.* 7 (2017) 46337, <https://doi.org/10.1038/srep46337>.
- [72] T. Zelante, R.G. Iannitti, C. Cunha, A. De Luca, G. Giovannini, G. Pieraccini, R. Zecchi, C. D'Angelo, C. Massi-Benedetti, F. Fallarino, A. Carvalho, P. Puccetti, L. Romani, Tryptophan catabolites from microbiota engage aryl hydrocarbon receptor and balance mucosal reactivity via interleukin-22, *Immunity* 39 (2013) 372–385, <https://doi.org/10.1016/j.immuni.2013.08.003>.
- [73] L. Cervantes-Barragan, J.N. Chai, M.D. Tianero, B. Di Luccia, P.P. Ahern, J. Merriman, V.S. Cortez, M.G. Caparon, M.S. Donia, S. Gillfillan, M. Cella, J. I. Gordon, C.-S. Hsieh, M. Colonna, Lactobacillus reuteri induces gut intraepithelial CD4+CD8 $\alpha\alpha$ + T cells, *Science* 357 (2017) 806–810, <https://doi.org/10.1126/science.aah5825>.
- [74] Y. Cheng, U.-H. Jin, C.D. Allred, A. Jayaraman, R.S. Chapkin, S. Safe, Aryl hydrocarbon receptor activity of tryptophan metabolites in young adult mouse colonocytes, *Drug Metab. Dispos. Biol. Fate Chem.* 43 (2015) 1536–1543, <https://doi.org/10.1124/dmd.115.063677>.
- [75] T.D. Hubbard, I.A. Murray, W.H. Bisson, T.S. Lahoti, K. Gowda, S.G. Amin, A. D. Patterson, G.H. Perdew, Adaptation of the human aryl hydrocarbon receptor to sense microbiota-derived indoles, *Sci. Rep.* 5 (2015) 12689, <https://doi.org/10.1038/srep12689>.
- [76] M.M. Lowe, J.E. Mold, B. Kanwar, Y. Huang, A. Louie, M.P. Pollastri, C. Wang, G. Patel, D.G. Franks, J. Schlezinger, D.H. Sherr, A.E. Silverstone, M.E. Hahn, J. M. McCune, Identification of cinnabaric acid as a novel endogenous aryl hydrocarbon receptor ligand that drives IL-22 production, *PLoS One* 9 (2014), e87877, <https://doi.org/10.1371/journal.pone.0087877>.
- [77] C. Schiering, E. Wincent, A. Metidji, A. Iseppon, Y. Li, A.J. Potocnik, S. Omenetti, C.J. Henderson, C.R. Wolf, D.W. Nebert, B. Stockinger, Feedback control of AHR signalling regulates intestinal immunity, *Nature* 542 (2017) 242–245, <https://doi.org/10.1038/nature21080>.
- [78] E.C. Rosser, K. Oleinika, S. Tonon, R. Doyle, A. Bosma, N.A. Carter, K.A. Harris, S. A. Jones, N. Klein, C. Mauri, Regulatory B cells are induced by gut microbiota-driven interleukin-1 $\beta$  and interleukin-6 production, *Nat. Med.* 20 (2014) 1334–1339, <https://doi.org/10.1038/nm.3680>.
- [79] E.C. Rosser, C.J.M. Piper, D.E. Matei, P.A. Blair, A.F. Rendeiro, M. Orford, D. G. Alber, T. Krausgruber, D. Catalan, N. Klein, J.J. Manson, I. Drozdov, C. Bock, L. R. Wedderburn, S. Eaton, C. Mauri, Microbiota-derived metabolites suppress arthritis by amplifying aryl-hydrocarbon receptor activation in regulatory B cells, *Cell Metab.* 31 (2020) 837–851, <https://doi.org/10.1016/j.cmet.2020.03.003>, e10.
- [80] M. Platten, E.A.A. Nollen, U.F. Röhrig, F. Fallarino, C.A. Opitz, Tryptophan metabolism as a common therapeutic target in cancer, neurodegeneration and beyond, *Nat. Rev. Drug Discov.* 18 (2019) 379–401, <https://doi.org/10.1038/s41573-019-0016-5>.
- [81] J. Le Naour, L. Galluzzi, L. Zitvogel, G. Kroemer, E. Vacchelli, Trial watch: IDO inhibitors in cancer therapy, *Oncolimmunology* 9 (2020), 1777625, <https://doi.org/10.1080/2162402X.2020.1777625>.
- [82] J. Ouyang, S. Isnard, J. Lin, B. Fombuena, X. Peng, S. Nair Parvathy, Y. Chen, M. S. Silverman, J.-P. Routy, Treating from the inside out: relevance of fecal

- microbiota transplantation to counteract gut damage in GVHD and HIV infection, *Front. Med. (Lausanne)* 7 (2020) 421, <https://doi.org/10.3389/fmed.2020.00421>.
- [83] S. Löb, A. Königsrainer, H.-G. Rammensee, G. Opelz, P. Terness, Inhibitors of indoleamine-2,3-dioxygenase for cancer therapy: can we see the wood for the trees? *Nat. Rev. Cancer* 9 (2009) 445–452, <https://doi.org/10.1038/nrc2639>.
- [84] P. Ramadoss, G.H. Perdew, Use of 2-azido-3-[125I]iodo-7,8-dibromodibenzo-p-dioxin as a probe to determine the relative ligand affinity of human versus mouse aryl hydrocarbon receptor in cultured cells, *Mol. Pharmacol.* 66 (2004) 129–136, <https://doi.org/10.1124/mol.66.1.129>.
- [85] H. Blasco, C. Bessy, L. Plantier, A. Lefevre, E. Piver, L. Bernard, J. Marlet, K. Stefic, I. Benz-de Bretagne, P. Cannet, H. Lumbu, T. Morel, P. Boulard, C.R. Andres, P. Vourc'h, O. Héroult, A. Guillon, P. Emond, The specific metabolome profiling of patients infected by SARS-COV-2 supports the key role of tryptophan-nicotinamide pathway and cytosine metabolism, *Sci. Rep.* 10 (2020) 16824, <https://doi.org/10.1038/s41598-020-73966-5>.
- [86] A.P. Bouças, J. Rheinheimer, J. Lagopoulos, Why severe COVID-19 patients are at greater risk of developing depression: a molecular perspective, *Neuroscience* (2020), 107385842096789, <https://doi.org/10.1177/1073858420967892>.
- [87] Y. Cai, D.J. Kim, T. Takahashi, D.I. Broadhurst, S. Ma, N.J.W. Rattray, A. Casanovas-Massana, B. Israelow, J. Klein, C. Lucas, T. Mao, A.J. Moore, C. M. Muenker, J. Silva, P. Wong, Yale IMPACT Research team, A.J. Ko, S.A. Khan, A. Iwasaki, C.H. Johnson, Kynurenic acid underlies sex-specific immune responses to COVID-19, *Infect. Dis. (except HIV/AIDS)* (2020), <https://doi.org/10.1101/2020.09.06.20189159>.
- [88] M.M. Essa, H. Hamdan, S.B. Chidambaram, B. Al-Balushi, G.J. Guillemin, D. M. Ojcius, M.W. Qoronfleh, Possible role of tryptophan and melatonin in COVID-19, *Int. J. Tryptophan Res.* 13 (2020), 117864692095183, <https://doi.org/10.1177/1178646920951832>.
- [89] W.A. Turski, A. Wnorowski, G.N. Turski, C.A. Turski, L. Turski, AhR and IDO1 in pathogenesis of Covid-19 and the “Systemic AhR Activation Syndrome:” a translational review and therapeutic perspectives, *Restor. Neurol. Neurosci.* 38 (2020) 343–354, <https://doi.org/10.3233/RNN-201042>.
- [90] T. Kimhofer, S. Lodge, L. Whiley, N. Gray, R.L. Loo, N.G. Lawler, P. Nitschke, S.-H. Bong, D.L. Morrison, S. Begum, T. Richards, B.B. Yeap, C. Smith, K.G.C. Smith, E. Holmes, J.K. Nicholson, Integrative modeling of quantitative plasma lipoprotein, metabolic, and amino acid data reveals a multiorgan pathological signature of SARS-CoV-2 infection, *J. Proteome Res.* 19 (2020) 4442–4454, <https://doi.org/10.1021/acs.jproteome.0c00519>.
- [91] T. Thomas, D. Stefanoni, J.A. Reisz, T. Nemkov, L. Bertolone, R.O. Francis, K. E. Hudson, J.C. Zimring, K.C. Hansen, E.A. Hod, S.L. Spitalnik, A. D'Alessandro, COVID-19 infection results in alterations of the kynurenine pathway and fatty acid metabolism that correlate with IL-6 levels and renal status, *Infect. Dis. (except HIV/AIDS)* (2020), <https://doi.org/10.1101/2020.05.14.20102491>.
- [92] M.L. Belladonna, C. Orabona, Potential benefits of tryptophan metabolism to the efficacy of Tocilizumab in COVID-19, *Front. Pharmacol.* 11 (2020) 959, <https://doi.org/10.3389/fphar.2020.00959>.



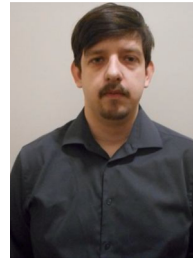
**Xavier Dagenais-Lussier, Ph.D., (first author).** Xavier Dagenais-Lussier is a Ph.D. student under the supervision of Dr. van Grevenynghe at the INRS-Institut Armand Frappier (Laval, Quebec). He graduated for his Master in 2018, and previously obtained his B.Sc. in Microbiology at the University of Sherbrooke (Quebec) in 2015. He recently published a study showing that increased expression of the interferon stimulated gene USP18 participates to defective memory CD4 T-cell survival during the early phase of HIV-1 primary infection (*PLOS Pathogens*, 2019). Currently, Xavier Dagenais-Lussier is studying the metabolic plasticity in CD4 T-cell subsets during HIV-1 infection.



**Hamza Loucif, Ph.D.** Hamza Loucif is a Ph.D. student at the INRS-Institut Armand Frappier (Laval, Quebec) under the supervision of Dr. Julien Van Grevenynghe. He obtained his B.Sc. in Applied and Fundamental Biochemistry (2015) followed by a Master in Biotechnology and Molecular Pathology (2017) at the University of Science and Technology of Algiers (USTHB, Algeria). He concluded his Master's internship at the department of human virology, HIV/AIDS national reference laboratory of Institut Pasteur d'Algérie, studying the role of Nitric Oxide (NO) in HIV-1 immuno-pathogenesis. He is currently studying the role of autophagy process as a novel immune correlate exhibited by HIV-1-specific CD8 T cells in “Elite Controllers”, a unique subset of individuals known to possess the ability to naturally co-exist with the virus for a long term without progressing to the AIDS stage.



**Cherifa Beji, M.Sc.** Cherifa Beji is a Masters student at the INRS-Institut Armand Frappier under the supervision of Dr. Julien Van Grevenynghe. She obtained her engineering degree in biology from the National Institute of Applied Sciences and Technology (Tunisia). She did her end of studies internship at Queen's University Cancer Research Institute, where she used R programming to expound on the use of DNA methylation as a biomarker for aggressive prostate cancer. She is currently working on the immunomodulatory effect of tetrahydrocannabinol (THC) on CD8 T-cells.



**Roman Telittchenko, Ph.D.** Roman Telittchenko is a PhD student under the supervision of Albert Descoteaux at the “Institut Armand Frappier-INRS”. He has received his B.Sc. in the Microbiology and Immunology program at McGill University (Montreal, Québec, Canada) in 2017. Today, Roman Telittchenko is studying the Leishmania parasite. Specifically, he is studying whether genetic exchanges take place between Leishmania parasites in the context of an infected host cell and their interaction with the LRV virus.



**Dr. Jean-Pierre Routy, M.D.,** is an attending physician in the Division of Hematology and Chronic Viral Illness Service at the McGill University Health Centre (Glen site, Montreal). Additionally, he is a tenured professor in the department of Medicine at McGill University. Dr. Routy received his medical degree and completed his residency in Hematology-Oncology in 1986 at the University of Aix-Marseille (France). Today, his main focus is on understanding HIV-1 pathogenesis and restoring the immune system of individuals infected with HIV-1. He is also the principal investigator of a national cohort of patients recently infected with HIV, which aims to understand the natural history of HIV infection, concentrating on its effect in the gut.





**Julien van Grevenynghe, Ph.D. (corresponding author)** Dr. van Grevenynghe is an assistant professor in the INRS-Institut Armand Frappier (Laval, Quebec) since February 2015. Dr. van Grevenynghe obtained his Ph.D. from INSERM U456 and University of Rennes 1 (Bretagne, France). Then, he joined Dr. Rafick Sekaly's team (CR-CHUM in Montreal and VGTI in Florida) where he focused on the characterization of the transcriptional factor Foxo3a in the long-term maintenance of memory CD4 T-cells during chronic HIV-1 infection. Today, Dr. van Grevenynghe is an expert on viral pathogenesis where his laboratory studies (i) new molecular and metabolic mechanisms associated with natural immune protection in elite controllers and (ii) the involvement of metabolism by-products such as oxidative stress that occurs since HIV-1 primary-infection on memory CD4 T-cell impairments. His last publication as senior research authors were accepted in significant peer-to-peer journals including *PLOS Pathogen*, *Journal of Virology* and *Cell Reports*.





*Review*

# Cannabinoid-Induced Immunomodulation during Viral Infections: A Focus on Mitochondria

Cherifa Beji <sup>1</sup>, Hamza Loucif <sup>1</sup> , Roman Telittchenko <sup>1</sup>, David Oलगниер <sup>2</sup>,  
Xavier Dagenais-Lussier <sup>1,\*</sup>  and Julien van Grevenynghe <sup>1,\*</sup>

<sup>1</sup> Institut National de la Recherche Scientifique (INRS)-Armand-Frappier Santé Biotechnologie, 531 Boulevard des Prairies, Laval, QC H7V 1B7, Canada; cherifa.beji@iaf.inrs.ca (C.B.); hamza.loucif@iaf.inrs.ca (H.L.); roman.telittchenko@iaf.inrs.ca (R.T.)

<sup>2</sup> Research Center for Innate Immunology, Department of Biomedicine, Aarhus University, 8000 Aarhus C, Denmark; olagnier@biomed.au.dk

\* Correspondence: xavier.dagenais@iaf.inrs.ca (X.D.-L.); julien.vangrevenynghe@iaf.inrs.ca (J.v.G.)

Received: 27 July 2020; Accepted: 7 August 2020; Published: 11 August 2020



Review

# Cannabinoid-Induced Immunomodulation during Viral Infections: A Focus on Mitochondria

Cherifa Beji <sup>1</sup>, Hamza Loucif <sup>1</sup> , Roman Telittchenko <sup>1</sup>, David Olganier <sup>2</sup>,  
Xavier Dagenais-Lussier <sup>1,\*</sup>  and Julien van Grevenynghe <sup>1,\*</sup>

<sup>1</sup> Institut National de la Recherche Scientifique (INRS)-Armand-Frappier Santé Biotechnologie, 531 Boulevard des Prairies, Laval, QC H7V 1B7, Canada; cherifa.beji@iaf.inrs.ca (C.B.); hamza.loucif@iaf.inrs.ca (H.L.); roman.telittchenko@iaf.inrs.ca (R.T.)

<sup>2</sup> Research Center for Innate Immunology, Department of Biomedicine, Aarhus University, 8000 Aarhus C, Denmark; olganier@biomed.au.dk

\* Correspondence: xavier.dagenais@iaf.inrs.ca (X.D.-L.); julien.vangrevenynghe@iaf.inrs.ca (J.v.G.)

Received: 27 July 2020; Accepted: 7 August 2020; Published: 11 August 2020



**Abstract:** This review examines the impact of cannabinoids on viral infections, as well as its effects on the mitochondria of the nervous and immune system. The paper conveys information about the beneficial and negative impacts of cannabinoids on viral infections, especially HIV-1. These include effects on the inflammatory response as well as neuroprotective effects. We also explore non-apoptotic mitochondrial pathways modulated by the activity of cannabinoids, resulting in modifications to cellular functions. As a large part of the literature derives from studies of the nervous system, we first compile the information related to mitochondrial functions in this system, particularly through the CB1 receptor. Finally, we reflect on how this knowledge could complement what has been demonstrated in the immune system, especially in the context of the CB2 receptor and Ca<sup>2+</sup> uptake. The overall conclusion of the review is that cannabinoids have the potential to affect a broad range of cell types through mitochondrial modulation, be it through receptor-specific action or not, and that this pathway has a potential implication in cases of viral infection.

**Keywords:** cannabinoid; THC; mitochondria; immunity; metabolism; inflammation; viral infection; nervous system

## 1. Introduction: Importance of Mitochondria on Immunity and Viral Control

Cells can metabolize a variety of carbon substrates including glucose, fatty acids, ketone bodies and amino acids. The cell's ability to use different carbon sources, which is done through proper mitochondrial function, is critical to their ability to adapt to stress conditions, such as changes in nutrient availability and metabolic needs [1–3]. This is especially true in the case of T-cells, where adaptive immunity is dictated by the mitochondria's capacity to use all types of carbon sources available [4,5]. As an example, naïve T-cells preferentially use oxidative phosphorylation (OXPHOS) in their quiescent state [6], while they switch to glycolysis during their activation [7–9]. Although primarily relying on glucose, activated lymphocytes can use many amino acids, such as alanine, leucine, glutamine, serine and arginine, as carbon sources [10–12]. For instance, removing alanine and leucine as carbon sources reduces T-cells effector functions and growth [11,12]. Additionally, L-arginine contributes to T-cells' long-term memory maintenance in the context of OVA immunization in mice [10]. Furthermore, increased mitochondrial fatty acid oxidation (FAO) characterizes memory and regulatory T-cells' subsets [13–15]. Which pathway the mitochondria skews towards is not only important for cell differentiation, it is also critical for proper specific anti-viral response. For example, it is known that polyfunctional anti-human immunodeficiency viruses (HIV-1) CD8 T-cells are critical to control

HIV-1 [16,17], and recent evidence shows that the capacity of CD8 T-cells to maintain polyfunctionality in glucose-deprived media might explain natural control of HIV-1 infection [18]. This was partially explained by an increase in lipid uptake. Similarly, CD8 T-cells from controller macaques can target simian immunodeficiency virus (SIV)-infected CD4 T-cells even in the absence of glucose [18]. Additionally, autophagy seems to be important for viral containment and for specific CD8 T-cells' activity by delivering lipid substrates as an additional energy source [19,20]. HIV, as well as other chronic disease patients such as cancer and sclerosis, have been known to be treated by anti-palliative substances, including cannabis. This plant has a history of being used for therapeutic purposes, namely to alleviate nausea, help calm severe pain, and stimulate the appetite to counter weight loss [21–23]. Cannabinoids are a class of compounds that can be found in the cannabis plant. These include a variety of exogenous, endogenous, and synthetic components which exhibit similar psycho-active and immune properties. With their uses in the treatment of advanced stages of illnesses as well as other therapeutic approaches, e.g., as an antidepressant, along with its appetite-stimulating properties becoming more widespread, evidence emerged showing that cannabinoids could influence viral pathogenesis and the immune system [24–28]. Currently, with the increasing number of countries and states legalizing marijuana for recreational use, its impact on health in the context of disease susceptibility is an important aspect to evaluate. The biological activity of cannabinoids is mainly mediated by cannabinoid receptors CB1 and CB2, which are predominantly expressed in cells from the nervous system and immune-derived cells, respectively [29]. When it comes to the immune system, different aspects of it are known to be affected by cannabinoids such as the level of apoptosis, suppression of cell proliferation, inhibition of pro-inflammatory cytokine and chemokine production, and the induction of anti-inflammatory cytokines and regulatory T-cells. In terms of immunomodulation, increasing evidence points towards the cannabinoids-induced effect on metabolism as a crucial player, as it induces AMP-activated protein kinase (AMPK) activation [30–32]. Considering the importance of the mitochondria and cellular metabolism for cell function and antiviral response, as mentioned earlier [33], evaluating the role of cannabinoids on both phenomena is important. As such, we wish to place the potential impact of cannabinoids on viral infections, especially in the context of HIV-1, as well as its impact on mitochondria, in the context of the function of the immune system.

## 2. Cannabinoids and Viral Infections: Potential Role of Mitochondria

The effects of cannabinoids on infections, both viral and other types, have already been thoroughly explored in past reviews [24,34,35]. In general, the effect of cannabinoids can be beneficial or detrimental depending on the concentration used, the type of infection, and, of course, which receptor is targeted. Some examples of detrimental effects include: the suppression of inflammatory myeloid cell responses by THC during the response to influenza [36] and the promotion of hepatitis C virus (HCV) replication caused by glucose metabolism disorders of hepatocytes following CB1 activation [37]. In the context of antigen-specific responses, the effects of cannabinoids are still open to question. As an example, it was reported that treatments with THC led to an earlier disease onset in the context of smallpox vaccine virus exposition in mice [38], while in the context of HIV-1, THC enhances antigen-specific immune responses [39]. This study was based on a HIV gp120-derived peptide activation of the immune system. The assessment of the modulating effect of THC was done through the evaluation of antigen-specific responses in both lymphocyte populations as well as non-lymphocyte immune cells in WT and CB1 and CB2 knocked-out mice. For T-cells, peptide-specific activation was determined by the subsequent production of interleukin (IL)-2 and interferon (IFN)- $\gamma$ , while B-cell activation was studied through the quantification of antibodies production and expression levels of activation markers. On the other hand, a slew of studies report beneficial effects for different treatment procedures such as the attenuation of CXCR4-tropic HIV infection following CB2 activation [40] as well as protection from HIV-1-Tat-mediated neuronal death [41,42] and HIV-1 gp120-mediated neural damage [43]. In this last study, Hu et al. used a human mesencephalic neuronal glial model with a composition similar to the human nervous system, then exposed it to gp120 and finally treated it

with THC in a concentration and time of exposure optimized in their previous study. A CB1 and CB2 agonist, WIN55,212-2, significantly reduced the gp120-induced apoptosis in dopaminergic neurons by controlling its subsequent ROS production in microglia. Interestingly, the beneficial effects of cannabinoids on the nervous system are not only found in the case of HIV-1 infection, but also with Theiler's virus, which is specifically used as a model of demyelination [44,45]. As mentioned earlier, cannabinoids can affect the inflammatory response, which is detrimental in the case of influenza [36]. However, considering that the inflammatory response can be detrimental in some infections [46], this effect of cannabinoids can potentially be beneficial. This is especially true in the context of HIV-1 infection, considering the lingering inflammation present in patients, even under highly active antiretroviral therapy (HAART) [47]. Reports by Henriquez et al. point toward THC as a way to control this inflammation and immune activation, as they demonstrate that treatment with THC reduces both the secretion of IFN- $\alpha$  by plasmacytoid dendritic cells (pDC) and its subsequent activation of T-cells [48,49]. This anti-inflammatory property of THC was also reported in a SIV model, where it reduced T-cell proliferation and activation in the intestine [50]. Similarly, Tahamtan et al. bring forth the important role of the endocannabinoid system in regulating the inflammatory response in the context of respiratory syncytial virus (RSV). In their studies, they demonstrate that activating either CB1 or CB2 decreased immune cell influx and cytokine production, resulting in alleviated lung pathology in a murine model [51,52]. This is particularly interesting considering that suppressing inflammation in chronic infections such as HIV-1 is expected to be beneficial in controlling the disease progression since it is mediated through prolonged dysregulation of multiple signalling pathways caused by said inflammation. However, we see how dampening the immune response can also be beneficial in more acute infections, such as RSV (see Table 1 for an overview of the reported effects). The other side of the coin is how viral infections affect the mitochondria. T-cells specific to HIV-1 are subjected to constant immune activation which creates a high energetic demand for those cells [53,54]. Considering this, CD8 T-cells from HIV-1-infected patients not only display an increase in glycolysis but are dependent on glucose for their effector function, even following successful HAART [18]. Additionally, during HIV-1 infection, T-cells become progressively exhausted [55,56], displaying reduced mitochondrial mass and membrane potential. Those phenotypes could be mediated by programmed cell death protein 1 (PD-1) stimulation, resulting in reduced mitochondrial and glycolytic activities [57]. Moreover, another aspect to consider is the effect of treatment on mitochondria health. As an example, nucleoside reverse transcriptase inhibitor (NRTI) treatments for HIV-1 infection have been associated with mitochondrial DNA loss, altered membrane potential, inhibition of electron transport chain complexes, impairment of FAO and lower ATP production [58,59]. Similarly, many reports exist of different viruses modulating the mitochondria to enhance their replication [60–62]. Mitochondrial modulations by viruses are twofold. Firstly, considering that mitochondria play a crucial role in antiviral immunity, certain viruses interfere with functions conferring that role in order to proliferate. These include the disturbance of mitochondrial dynamics such as fission and fusion, the induction of mitophagy, and the regulation of apoptotic processes [61]. Secondly, some viruses will exploit the cell's membrane transport pathways, generating organelles named viral factories. These organelles represent specialized compartments for viral replication, maturation, and export [62]. Given this fact and the role of cannabinoid signalling in modulating the mitochondria, the potential for those compounds to affect viral infections at that level are high, especially considering the reported impact of the endocannabinoid system on HCV replication through its effect on glucose metabolism [37]. However, we have to remain on the side of conjectures, as there are no direct reports on how the mitochondrial effect of cannabinoids might impact viral infections by using such mitochondrial changes. Nevertheless, in the following parts of this review, we will address the impact of cannabinoids on mitochondrial functions of cells from both the nervous and immune system. We explore this side of cannabinoids because, as we will see, they have a wide range of effects, making them strong candidates to control viral infections through mitochondrial modulation.

**Table 1.** Effects of cannabinoids on viral infections. 2-AG: 2-Arachidonoylglycerol; AEA: N-arachidonylethanolamine; CB1: Cannabinoid receptor type 1; CB2: Cannabinoid receptor type 2; CBD: Cannabidiol; HBV: hepatitis B virus; MAIDS: murine acquired immunodeficiency syndrome; THC:  $\Delta^9$ -tetrahydrocannabinol.

Virus	Treatment/Context	Model	Observations	Reference
HIV-1	THC	Human	Suppression of IFN- $\alpha$ -mediated activation of T-cells	Henriquez et al., 2018 [48]
	Inhibition of AEA hydrolysis	Murine	Reduction in HIV-Tat-mediated neuronal death and dendritic degeneration	Hermes et al., 2018 [41]
	Cannabis use in HAART treated patients	Human	Reduction in systemic inflammation and immune activation	Manuzak et al., 2018 [63]
	AEA, 2-AG	Murine	Protection of neurons from HIV-Tat excitotoxicity	Xu et al., 2017 [42]
	THC	Human	Suppression of IFN- $\alpha$ secretion by pDC	Henriquez et al., 2017 [49]
	THC	Murine	Enhancement of pVRCgp120-induced IFN- $\gamma$ production by splenic lymphocyte populations and activation of T/B cells	Chen et al., 2015 [39]
	AEA, 2-AG	Human	Suppression of pro-inflammatory and increase of anti-inflammatory cytokines, through the MAPK pathway	Krishnan and Chatterjee, 2014 [64]
	THC	Human	Reduction of cell surface HIV receptor (CD4, CCR5 and CXCR4) expression on macrophages	Williams et al., 2014 [65]
	THC, CP55940 (CB1/2 agonist)	Human	Inhibition of HIV-Tat-mediated adhesion of monocyte to extracellular matrix	Raborn et al., 2014 [66]
	JWH133, Gp1a, O-1966 (CB2 agonist)	Human	Inhibition of RT and LTR activity	Ramirez et al., 2013 [67]
WIN55,212-2 (CB1/2 agonist)	Human	Protection of human dopaminergic neurons from gp120	Hu et al., 2013 [43]	
THC, CBD	Murine	Enhancement of T-cell response after suboptimal stimulation	Chen et al., 2012 [68]	
JWH133, JWH150, 2-AG, AEA (CB2 agonists)	Human	Reduces cell-free and cell-to-cell transmission of CXCR4-tropic HIV	Constantino et al., 2012 [40]	
HIV-1	THC, 2-AG	Murine	Reduction CCR3 expression resulting in less migration of BV-2 cells towards HIV-Tat	Fraga et al., 2011 [69]
	WIN55,212-2 (CB1/2 agonist)	Murine	Inhibited gp120-induced IL-1 $\beta$ production and impairment of network functions	Kim et al., 2011 [70]
	THC, CP55940 (CB1/2 agonist)	Human	Inhibition of macrophage migration to HIV-Tat protein	Raborn and Cabral, 2010 [71]
SIV	THC	Rhesus	No upregulation of pro-inflammatory miR-21, miR-141 and miR-222 and alpha/beta defensins	Kumar et al., 2019 [50]
	THC	Rhesus	Higher expression of tight junction proteins (occludin, claudin-3), anti-inflammatory MUC13, keratin-8 (stress protection), PROM1 (epithelial proliferation)	Chandra et al., 2015 [72]
	THC	Rhesus	Upregulation of microRNA which targets proinflammatory molecules	LeCapitaine et al., 2011 [73]
	THC	Rhesus	Chronic administration increased CXCR4 expression on T-cells	Chronic administration reduced early mortality, associated with attenuation of plasma viral load and body mass retention
MAIDS	JWH015, JWH133, Gp1a (CB2 agonists)	Murine	Acute antiallodynic effects on infection-induced neuropathic pain	Molina et al., 2011 [74]
HBV	Rimonabant (CB1 inhibitor)	Human	Suppressed HBV propagation through the inhibition of hepatocyte nuclear factor 4 $\alpha$	Sheng et al., 2019 [75]
HCV	AEA	Human	Suppressed HBV propagation through the inhibition of hepatocyte nuclear factor 4 $\alpha$	Sato et al., 2020 [76]
HCV	AEA	Human	Decrease of AMPK phosphorylation, inhibition of cell surface expression of GLUT2, and suppression of cellular glucose uptake. Promotion of viral replication	Sun et al., 2014 [37]



Table 1. Cont.

Virus	Treatment/Context	Model	Observations	Reference
RSV	JZL184 (CB1 agonist)	Murine	Decreased immune cell influx and cytokine/chemokine production, and alleviated lung pathology	Tahamtan et al., 2018 (a) [51]
	JWH133 (CB2 agonist)	Murine	Decreased immune cell influx and cytokine/chemokine production, and alleviated lung pathology	Tahamtan et al., 2018 (b) [52]
Theiler's	CBD	Murine	Decreased frequency and severity of acute behavioral seizures	Patel et al., 2019 [45]
	Inhibition of 2-AG hydrolysis	Murine	Enhances remyelination	Feliu et al., 2017 [44]
	WIN55,212-2 (CB1/2 agonist)	Murine	Reduced CD4 + CD25 + Foxp3- T-cells activation in the CNS and increased regulatory CD4 + CD25 + Foxp3 + T-cell activation	Arevalo-Martin et al., 2012 [77]
	AEA	Murine	Inhibition of VCAM-1 potentially reducing neuroinflammation	Mestre et al., 2011 [78]
Influenza	THC	Murine	Suppressed DC, macrophages, monocytes, and inflammatory myeloid cell responses	Karmaus et al., 2013 [36]
Vaccinia	THC	Murine	Increased severity and duration of symptoms	Huemer et al., 2011 [38]

### 3. Cannabinoids, Mitochondria, and the Nervous System

As cannabinoids have been firstly identified as the neurotropic agents in cannabis, it comes as no surprise that a lot of early studies regarding its mechanism of action were focused on the nervous system. As such, it was discovered that the effects of cannabinoids in the brain are mainly due to the activation of the CB1 receptor. Of note, most of the information concerning the impact of cannabinoids on mitochondria comes from studies in this field of research. As such, even though the main point of this review is to consider the impact of cannabinoids on the immune system, it is necessary to place our knowledge in its initial context: the nervous system. The key element to placing CB1 and mitochondria together comes from the work of Hebert-Chatelain et al., who not only showed the presence of CB1 on the mitochondrial membrane of mouse neurons [79], but also reported its role in the regulation of cellular respiration and energy production [80]. To summarize, they demonstrated that cannabinoid signalling is necessary for PKA-dependent phosphorylation of the mitochondrial electron transport system. Thus, CB1 genetic exclusion leads to decreased cellular respiration. Although those findings came with their share of controversies [81,82], there is now a well-established link between cannabinoids, mitochondria and neuronal activity [83–85]. However, Jimenez-Blasco et al. describe in a recent study how the activation of mitochondrial CB1 actually reduces OXPHOS and hampers the metabolism of glucose in mouse astroglia [86]. In this study, they first confirmed that mitochondrial CB1 was responsible for reducing microglia oxygen consumption by comparing the effect of HU210, a CB1 agonist, with that of a cell-impermeable biotinylated version. Mitochondrial CB1 activation then leads to the destabilization of complex I. In addition to the effect on OXPHOS, mitochondrial CB1 activation also leads to a decrease in nuclear hypoxia-inducible factors 1 (HIF-1) resulting in the reduction in glycolytic activity [86]. To summarize, both complete exclusion of mitochondrial CB1 and a strong activation of this same receptor lead to reduced cellular respiration [80,86]. Interestingly, another recent study places CB1 as an important regulator of mitophagy in hippocampal neurons [87], showing that adult hippocampal CB1-KO mice displayed mitochondrial elongation and had reduced mitophagy activity compared to WT. The effect of CB1 knock-out on mitophagy was observed via the levels of Serine 65-phosphorylated ubiquitin serving as a biomarker for PTEN-induced kinase 1 (PINK1) activity. However, Kataoka et al. did not consider the localization of the CB1 to contextualize their observation. In addition to CB1-mediated mitochondrial modulation, Fisar et al. also demonstrated a non-receptor mechanism. They came to this conclusion after evaluating the effects of different cannabinoids with known receptor targets. Overall, they posit that cannabinoids can accumulate in the hydrophobic parts of the inner mitochondrial membrane, impairing the molecular interactions and assembly of the respiratory chain [88]. This comes in addition to previous reports of non-receptor specific effect of cannabinoids on mitochondria [89,90]. Interestingly, it has been shown that the CB1-mediated effect on mitochondrial dynamics is not restricted to cells of the nervous system [91]. In this study, it is shown that CB1 stimulation by the endocannabinoid, n-arachidonylethanolamine (AEA), in renal proximal tubular cells leads to dynamin-related protein 1 (DRP1) activation, with its subsequent translocation to the mitochondria that results in mitochondrial fission. Inevitably, looking at the impact of cannabinoids on the nervous system leads to having a look at the microglia. These are specialized macrophages found in the central nervous system (CNS). They are important for maintaining the health of the CNS by dealing with infections and removing damaged neurons [92]. In this context, Ma et al. found that AM1241, a CB2 agonist, mediates anti-inflammatory responses in microglia. This was observed by the upregulation of markers associated with M2 phenotypes, such as arginase 1 and brain-derived neurotrophic factor with a downregulation of the M1 markers' inducible nitric oxide synthase and tumor necrosis factor (TNF)- $\alpha$ . They suggest that this might be due to the peroxisome proliferator-activated receptor gamma coactivator 1-alpha (PGC-1 $\alpha$ ) and its association with the enhancement of mitochondria biogenesis. [93]. Both the idea that the effect of cannabinoids on mitochondria is not specific to neuronal cells as well as having a direct impact on microglia, which bridges the nervous and immune system, leads us to review the impact of cannabinoids on the mitochondria of immune cells.

#### 4. Cannabinoids, Mitochondria, and the Immune System

CB2, being abundantly present on immune cells, has made the study of cannabinoids in the context of infection a necessity. It is now well established that the activation of CB2 receptors, by endogenous or exogenous cannabinoids, is immunosuppressive [26,27]. A recent review is particularly thorough in describing the effects of cannabidiol (CBD) in regulating the immune responses [94]. In the case of T-cells, this is notable through their suppression of IL-2, IFN- $\gamma$ , and TNF- $\alpha$  [95]. Considering the crucial role that the mitochondria plays in apoptosis as well as in various intrinsic and extrinsic ways [96,97], it comes as no surprise that most studies of cannabinoids on mitochondria revolve around apoptosis [98]. One of the most recent examples of this is a study by Wu et al., who showed that CBD had a very important pro-apoptotic effect on monocytes because of its effect on mitochondrial membrane potential and cytochrome c release [99]. Although the studies indicating the non-apoptotic effect of cannabinoids on the mitochondria from immune cells remain few, some point towards a role in reactive oxygen species (ROS) production and an effect on mitochondrial respiration [95,100]. In their paper, Schultze et al. demonstrate that CBD reduces both maximal respiration and spare respiratory capacity in THP-1 monocytes [100]. Additionally, mitochondrial ROS could potentially have a role to play in LPS-induced inflammatory responses by macrophages. In this study, a 24 h treatment with CBD dramatically reduced IL-8 production by U937 monocytes [95]. Although in both studies they observed an increase in mitochondrial ROS, the effects observed were not directly linked to its production. Additional studies, with antioxidants, for example, are warranted to elucidate the role of ROS in the non-apoptotic effect of CBD on the mitochondria. As mentioned, the study of the impact of cannabinoids on the metabolism of mitochondria of immune cells is still at an early stage, especially in cells other than myeloid cells. Still, with the evidence currently at our disposition, we can see the potential importance of the cannabinoid pathway in the regulation of immune cell metabolism. Another potential non-apoptotic pathway to modulate mitochondria by cannabinoids is through calcium signalling. Indeed, ion channels, especially calcium, are known to be crucial for proper immune responses [101,102]. In this context, Olivas-Aguirre et al. found that CBD favors mitochondrial  $\text{Ca}^{2+}$  uptake on acute lymphoblastic leukemia of T lineage cells. This leads to a loss of mitochondrial membrane potential, disruption of the cristae, and ATP production, ultimately resulting in mitophagy. At sublethal concentration, they demonstrate that CBD induces a conversion of LC3-I to LC3-II, showing an activation of autophagy. [103]. This is of particular interest considering that  $\text{Ca}^{2+}$  intake is required for T-cell receptor stimulation [102,104]. Overall, the impact of cannabinoids on non-apoptotic mitochondrial pathways remains to be fully uncovered, but with the current knowledge at our disposition, we can expect it to have important ramifications for the immune system regulation, particularly in the inflammatory responses (see Figure 1 for an overview of non-apoptotic effect of cannabinoids on mitochondrial functions).

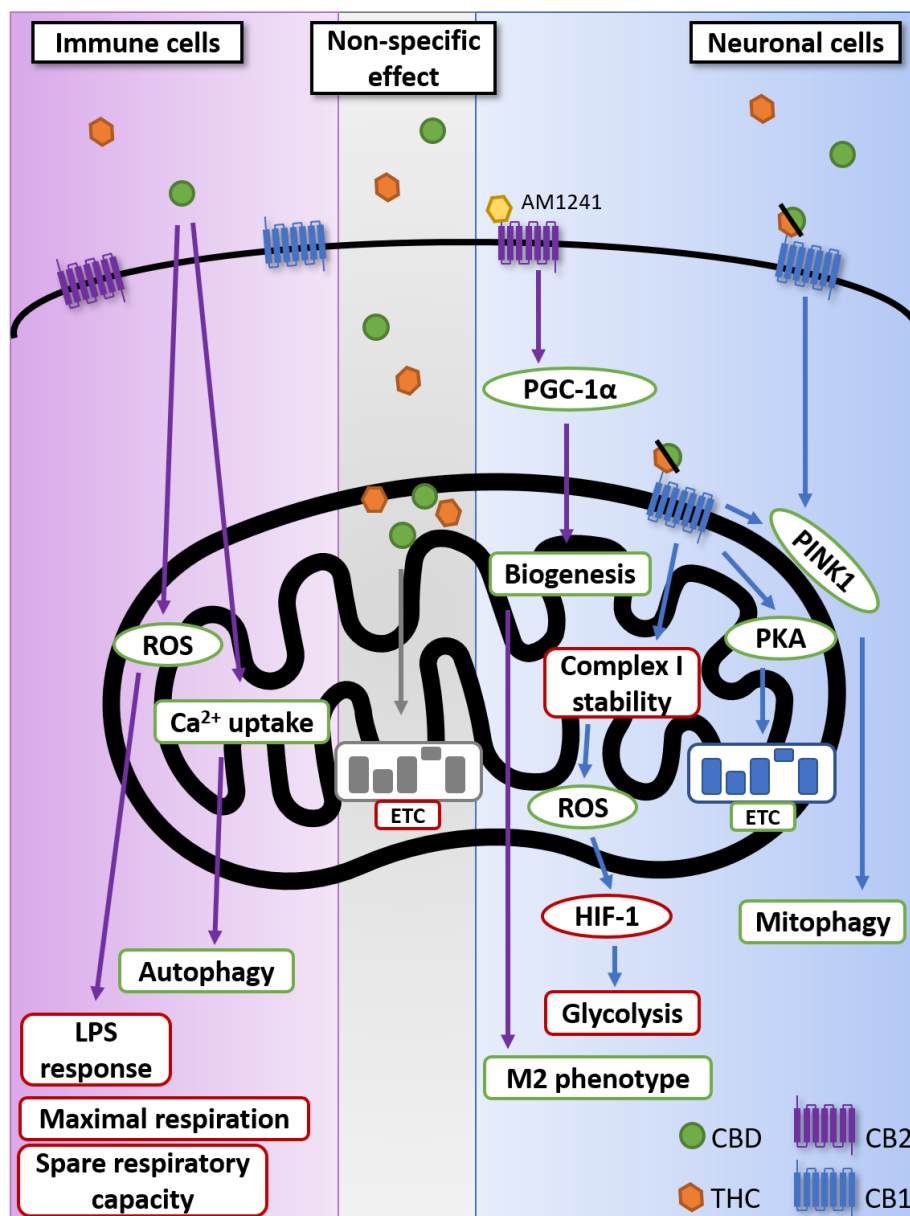


**Figure 1.** Non-apoptotic impact of cannabinoids on mitochondria. Although CB1 and CB2 are found on immune cell, the reported activity of CBD on the mitochondria of immune cells was not confirmed to be dependent on either receptor [95,100,103]. Non-specific effect represents the effect of cannabinoids on mitochondrial membrane integrity demonstrated not to be dependent on CB1 or CB2 [88–90]. It is now well established that CB1 is found on mitochondrial membrane [80,86,87,93]. Green borders represent an upregulation or increased activity; red borders represent a downregulation or reduced activity. CB1: Cannabinoid receptor type 1; CB2: Cannabinoid receptor type 2; CBD: Cannabidiol; ETC: Electron transport chain; HIF-1: hypoxia-inducible factors 1; PGC-1 $\alpha$ : peroxisome proliferator-activated receptor gamma coactivator 1-alpha; PINK1: PTEN-induced kinase 1; PKA: Protein kinase A; ROS: reactive oxygen species; THC:  $\Delta^9$ -tetrahydrocannabinol.

## 5. Conclusions

The recent legalization of marijuana in Canada, as well as in different European countries, made cannabinoids accessible as off-the-counter substances for patients in need of palliative treatment, as well as for recreational users. As such, the study of the effects of endogenous as well as exogenous cannabinoids on the immune system, be it in a resting state or in the case of viral infections,

becomes crucial. Aside from their apoptotic and non-apoptotic effects, their impact on viral infections as well as inflammation and their effect on cellular metabolism and energy uptake, and sex- and age-dependent differences, in metabolizing such substances have been pointed out. In a study by Fattore et al., although no dissimilarities were pointed out when it comes to intoxication or plasmic THC levels, male smokers showed notably higher levels in circulating THC levels and larger cardiovascular effects than female smokers, who comparatively showed higher CB1 protein expressions and more explicit hemodynamic changes [105]. In line with this study, marijuana metabolizing is also impacted by body fat levels and sexual hormones, particularly testosterone and estrogen, which, respectively, lighten and intensify THC absorption and thus impact its conversion into inactive or active metabolites such as 11-hydroxy-THC [106]. In a similar context, a recent review by Gorey et al. summarized the impact of age on cannabis use and metabolization by focusing on its effect on attention, learning and memory in youths (under 18 years old) and adults (over 18 years old) almost daily on daily smokers as well as in young and adult rats [107]. The paper showed that multiple gaps and contradictions exist in studies done on both human and rats when it comes to THC effect on neuropsychological domains, but that young smokers showed more attention deficit as well as lower prose recall compared to adults, who showed higher memory impairments. Although the effects of cannabinoids on inflammation are well established, information about how the mitochondria are involved remains limited. Considering all of the facts above, cannabinoids' metabolism, be it derived from cannabis or synthetic substances, needs to be further investigated, especially when it comes to its effect on mitochondrial plasticity in the context of viral infections and the resulting chronic inflammation. This is notable considering the growing interest in its usage during persistent infections which are associated with inflammation [34,108]. Another aspect to remember is the lipophilic nature of cannabinoids that allows them to enter cells passively. Given this property, they can potentially alter the integrity of any cellular membrane regardless of the presence of CB1/CB2 by accumulating in the hydrophobic parts, leading to impairment of molecular interactions [88]. An innovative strategy to investigate such an effect will be the use, development, and optimization of the Seahorse, which is a novel live-cell metabolic assay platform that allows the real time evaluation of cellular respiration and plasticity via the accurate measurements of mitochondrial respiration and plasticity (see Figure 2 and Table 2 for a summary of mitochondrial processes potentially affected by cannabinoids and in which cell type the effect was reported).

**Table 2.** Mitochondrial processes affected by cannabinoids in neuronal and immune cells. “+” indicates reported increase, “−” indicates reported reduction in the process. Although evidence suggests that carbon metabolism and anabolism might be affected by cannabinoids through AMPK activity, there are no direct reports of those effect [32,86,98–100,109–112].

	Neuronal	Immune
Apoptosis	−	+
Carbon metabolism	−	?
OXPHOS	+/-	−
Anabolism	?	?

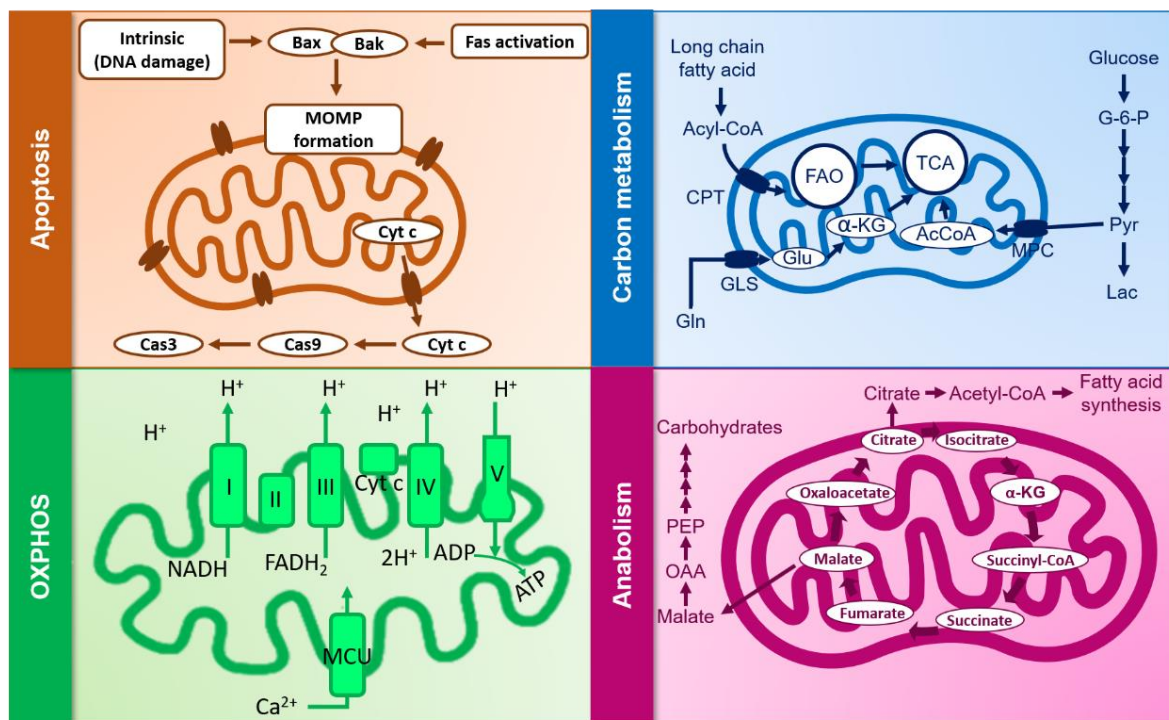


**Figure 2.** Mitochondrial processes potentially affected by cannabinoids.  $\alpha$ -KG: alpha-ketoglutarate; CPT: carnitine palmitoyltransferase; FAO: fatty acid oxidation; GLS: mitochondrial glutaminase; MOMP: mitochondrial outer membrane permeabilization; MCU: mitochondrial calcium uniporter; MPC: mitochondrial pyruvate carrier; OAA: oxaloacetate; TCA: tricarboxylic acid cycle.

**Author Contributions:** Conceptualization, C.B., X.D.-L., and J.v.G.; investigation, C.B.; writing—original draft preparation, C.B. and X.D.-L.; writing—review and editing, H.L., R.T., and D.O.; visualization, C.B.; supervision: X.D.-L., and J.v.G.; project administration: J.v.G.; funding acquisition, J.v.G. All authors have read and agreed to the published version of the manuscript.

**Funding:** The present review was conducted with funds from the Natural Sciences and Engineering Research Council of Canada and the AIDS/Infectious Diseases Network (FRQ-S; Montreal).

**Conflicts of Interest:** The authors declare no conflict of interest.

## References

1. Stanley, I.A.; Ribeiro, S.M.; Gimenez-Cassina, A.; Norberg, E.; Danial, N.N. Changing appetites: The adaptive advantages of fuel choice. *Trends Cell Biol.* **2014**, *24*, 118–127. [[CrossRef](#)]
2. Goodpaster, B.H.; Sparks, L.M. Metabolic Flexibility in Health and Disease. *Cell Metab.* **2017**, *25*, 1027–1036. [[CrossRef](#)]
3. Rambold, A.S.; Pearce, E.L. Mitochondrial Dynamics at the Interface of Immune Cell Metabolism and Function. *Trends Immunol.* **2018**, *39*, 6–18. [[CrossRef](#)]
4. Desdin-Mico, G.; Soto-Herederro, G.; Mittelbrunn, M. Mitochondrial activity in T cells. *Mitochondrion* **2018**, *41*, 51–57. [[CrossRef](#)]
5. Geltink, R.I.K.; Kyle, R.L.; Pearce, E.L. Unraveling the Complex Interplay Between T Cell Metabolism and Function. *Annu. Rev. Immunol.* **2018**, *36*, 461–488. [[CrossRef](#)]
6. Jones, N.; Vincent, E.E.; Cronin, J.G.; Panetti, S.; Chambers, M.; Holm, S.R.; Owens, S.E.; Francis, N.J.; Finlay, D.K.; Thornton, C.A. Akt and STAT5 mediate naive human CD4+ T-cell early metabolic response to TCR stimulation. *Nat. Commun.* **2019**, *10*, 2042. [[CrossRef](#)] [[PubMed](#)]
7. Chapman, N.M.; Boothby, M.R.; Chi, H. Metabolic coordination of T cell quiescence and activation. *Nat. Rev. Immunol.* **2020**, *20*, 55–70. [[CrossRef](#)]



8. Jacobs, S.R.; Herman, C.E.; Maciver, N.J.; Wofford, J.A.; Wieman, H.L.; Hammen, J.J.; Rathmell, J.C. Glucose uptake is limiting in T cell activation and requires CD28-mediated Akt-dependent and independent pathways. *J. Immunol.* **2008**, *180*, 4476–4486. [[CrossRef](#)]
9. Menk, A.V.; Scharping, N.E.; Moreci, R.S.; Zeng, X.; Guy, C.; Salvatore, S.; Bae, H.; Xie, J.; Young, H.A.; Wendell, S.G.; et al. Early TCR Signaling Induces Rapid Aerobic Glycolysis Enabling Distinct Acute T Cell Effector Functions. *Cell Rep.* **2018**, *22*, 1509–1521. [[CrossRef](#)]
10. Geiger, R.; Rieckmann, J.C.; Wolf, T.; Basso, C.; Feng, Y.; Fuhrer, T.; Kogadeeva, M.; Picotti, P.; Meissner, F.; Mann, M.; et al. L-Arginine Modulates T Cell Metabolism and Enhances Survival and Anti-tumor Activity. *Cell* **2016**, *167*, 829–842.e13. [[CrossRef](#)]
11. Ron-Harel, N.; Ghergurovich, J.M.; Notarangelo, G.; LaFleur, M.W.; Tsubosaka, Y.; Sharpe, A.H.; Rabinowitz, J.D.; Haigis, M.C. T Cell Activation Depends on Extracellular Alanine. *Cell Rep.* **2019**, *28*, 3011–3021.e4. [[CrossRef](#)]
12. Ma, E.H.; Bantug, G.; Griss, T.; Condotta, S.; Johnson, R.M.; Samborska, B.; Mainolfi, N.; Suri, V.; Guak, H.; Balmer, M.L.; et al. Serine Is an Essential Metabolite for Effector T Cell Expansion. *Cell Metab.* **2017**, *25*, 482. [[CrossRef](#)]
13. Bachem, A.; Makhoulf, C.; Binger, K.J.; de Souza, D.P.; Tull, D.; Hochheiser, K.; Whitney, P.G.; Fernandez-Ruiz, D.; Dahling, S.; Kastenmuller, W.; et al. Microbiota-Derived Short-Chain Fatty Acids Promote the Memory Potential of Antigen-Activated CD8(+) T Cells. *Immunity* **2019**, *51*, 285–297. [[CrossRef](#)]
14. Berod, L.; Friedrich, C.; Nandan, A.; Freitag, J.; Hagemann, S.; Harmrolfs, K.; Sandouk, A.; Hesse, C.; Castro, C.N.; Bahre, H.; et al. De novo fatty acid synthesis controls the fate between regulatory T and T helper 17 cells. *Nat. Med.* **2014**, *20*, 1327–1333. [[CrossRef](#)]
15. O’Sullivan, D.; van der Windt, G.J.; Huang, S.C.; Curtis, J.D.; Chang, C.H.; Buck, M.D.; Qiu, J.; Smith, A.M.; Lam, W.Y.; DiPlato, L.M.; et al. Memory CD8(+) T cells use cell-intrinsic lipolysis to support the metabolic programming necessary for development. *Immunity* **2014**, *41*, 75–88. [[CrossRef](#)]
16. Ferrando-Martinez, S.; Casazza, J.P.; Leal, M.; Machmach, K.; Munoz-Fernandez, M.A.; Viciano, P.; Koup, R.A.; Ruiz-Mateos, E. Differential Gag-specific polyfunctional T cell maturation patterns in HIV-1 elite controllers. *J. Virol.* **2012**, *86*, 3667–3674. [[CrossRef](#)]
17. Saez-Cirion, A.; Sinet, M.; Shin, S.Y.; Urrutia, A.; Versmisse, P.; Lacabaratz, C.; Boufassa, F.; Avettand-Fenoel, V.; Rouzioux, C.; Delfraissy, J.F.; et al. Heterogeneity in HIV suppression by CD8 T cells from HIV controllers: Association with Gag-specific CD8 T cell responses. *J. Immunol.* **2009**, *182*, 7828–7837. [[CrossRef](#)]
18. Angin, M.; Volant, S.; Passaes, C.; Lecroux, C.; Monceaux, V.; Dillies, M.-A.; Valle-Casuso, J.C.; Pancino, G.; Vaslin, B.; Le Grand, R.; et al. Metabolic plasticity of HIV-specific CD8+ T cells is associated with enhanced antiviral potential and natural control of HIV-1 infection. *Nat. Metab.* **2019**, *1*, 704–716. [[CrossRef](#)]
19. Nardacci, R.; Amendola, A.; Ciccocanti, F.; Corazzari, M.; Esposito, V.; Vlassi, C.; Taibi, C.; Fimia, G.M.; Del Nonno, F.; Ippolito, G.; et al. Autophagy plays an important role in the containment of HIV-1 in nonprogressor-infected patients. *Autophagy* **2014**, *10*, 1167–1178. [[CrossRef](#)]
20. Xu, X.; Araki, K.; Li, S.; Han, J.H.; Ye, L.; Tan, W.G.; Konieczny, B.T.; Bruinsma, M.W.; Martinez, J.; Pearce, E.L.; et al. Autophagy is essential for effector CD8(+) T cell survival and memory formation. *Nat. Immunol.* **2014**, *15*, 1152–1161. [[CrossRef](#)]
21. Aviram, J.; Samuelli-Leichtag, G. Efficacy of Cannabis-Based Medicines for Pain Management: A Systematic Review and Meta-Analysis of Randomized Controlled Trials. *Pain Physician* **2017**, *20*, E755–E796.
22. Mucke, M.; Phillips, T.; Radbruch, L.; Petzke, F.; Hauser, W. Cannabis-based medicines for chronic neuropathic pain in adults. *Cochrane Database Syst. Rev.* **2018**, *3*, CD012182. [[CrossRef](#)]
23. Bonini, S.A.; Premoli, M.; Tambaro, S.; Kumar, A.; Maccarinelli, G.; Memo, M.; Mastinu, A. Cannabis sativa: A comprehensive ethnopharmacological review of a medicinal plant with a long history. *J. Ethnopharmacol.* **2018**, *227*, 300–315. [[CrossRef](#)]
24. Tahamtan, A.; Tavakoli-Yaraki, M.; Rygiel, T.P.; Mokhtari-Azad, T.; Salimi, V. Effects of cannabinoids and their receptors on viral infections. *J. Med. Virol.* **2016**, *88*, 1–12. [[CrossRef](#)]
25. Acharya, N.; Penukonda, S.; Shcheglova, T.; Hagymasi, A.T.; Basu, S.; Srivastava, P.K. Endocannabinoid system acts as a regulator of immune homeostasis in the gut. *Proc. Natl. Acad. Sci. USA* **2017**, *114*, 5005–5010. [[CrossRef](#)]
26. Roth, M.D.; Baldwin, G.C.; Tashkin, D.P. Effects of delta-9-tetrahydrocannabinol on human immune function and host defense. *Chem. Phys. Lipids* **2002**, *121*, 229–239. [[CrossRef](#)]

27. Eisenstein, T.K.; Meissler, J.J. Effects of Cannabinoids on T-cell Function and Resistance to Infection. *J. Neuroimmune Pharmacol. Off. J. Soc. NeuroImmune Pharmacol.* **2015**, *10*, 204–216. [[CrossRef](#)]
28. Tanasescu, R.; Constantinescu, C.S. Cannabinoids and the immune system: An overview. *Immunobiology* **2010**, *215*, 588–597. [[CrossRef](#)]
29. Lu, H.C.; Mackie, K. An Introduction to the Endogenous Cannabinoid System. *Biol. Psychiatry* **2016**, *79*, 516–525. [[CrossRef](#)]
30. Dando, I.; Donadelli, M.; Costanzo, C.; Dalla Pozza, E.; D’Alessandro, A.; Zolla, L.; Palmieri, M. Cannabinoids inhibit energetic metabolism and induce AMPK-dependent autophagy in pancreatic cancer cells. *Cell Death Dis.* **2013**, *4*, e664. [[CrossRef](#)]
31. Liu, J.; Godlewski, G.; Jourdan, T.; Liu, Z.; Cinar, R.; Xiong, K.; Kunos, G. Cannabinoid-1 Receptor Antagonism Improves Glycemic Control and Increases Energy Expenditure Through Sirtuin-1/Mechanistic Target of Rapamycin Complex 2 and 5’ Adenosine Monophosphate-Activated Protein Kinase Signaling. *Hepatology* **2019**, *69*, 1535–1548. [[CrossRef](#)] [[PubMed](#)]
32. van Niekerk, G.; Mabin, T.; Engelbrecht, A.M. Anti-inflammatory mechanisms of cannabinoids: An immunometabolic perspective. *Inflammopharmacology* **2019**, *27*, 39–46. [[CrossRef](#)] [[PubMed](#)]
33. Loucif, H.; Dagenais-Lussier, X.; Beji, C.; Telittchenko, R.; Routy, J.P.; van Grevenynghe, J. Plasticity in T-cell mitochondrial metabolism: A necessary peacekeeper during the troubled times of persistent HIV-1 infection. *Cytokine Growth Factor Rev.* **2020**. [[CrossRef](#)] [[PubMed](#)]
34. Costiniuk, C.T.; Jenabian, M.-A. Cannabinoids and inflammation. *Aids* **2019**. [[CrossRef](#)] [[PubMed](#)]
35. Hernandez-Cervantes, R.; Mendez-Diaz, M.; Prospero-Garcia, O.; Morales-Montor, J. Immunoregulatory Role of Cannabinoids during Infectious Disease. *Neuroimmunomodulation* **2017**, *24*, 183–199. [[CrossRef](#)] [[PubMed](#)]
36. Karmaus, P.W.; Chen, W.; Crawford, R.; Kaplan, B.L.; Kaminski, N.E. Delta9-tetrahydrocannabinol impairs the inflammatory response to influenza infection: Role of antigen-presenting cells and the cannabinoid receptors 1 and 2. *Toxicol. Sci. Off. J. Soc. Toxicol.* **2013**, *131*, 419–433. [[CrossRef](#)]
37. Sun, L.J.; Yu, J.W.; Wan, L.; Zhang, X.Y.; Shi, Y.G.; Chen, M.Y. Endocannabinoid system activation contributes to glucose metabolism disorders of hepatocytes and promotes hepatitis C virus replication. *Int. J. Infect. Dis. IJID Off. Publ. Int. Soc. Infect. Dis.* **2014**, *23*, 75–81. [[CrossRef](#)]
38. Huemer, H.P.; Lassnig, C.; Bernhard, D.; Sturm, S.; Nowotny, N.; Kitchen, M.; Pavlic, M. Cannabinoids lead to enhanced virulence of the smallpox vaccine (vaccinia) virus. *Immunobiology* **2011**, *216*, 670–677. [[CrossRef](#)]
39. Chen, W.; Crawford, R.B.; Kaplan, B.L.; Kaminski, N.E. Modulation of HIVGP120 Antigen-Specific Immune Responses In Vivo by Delta9-Tetrahydrocannabinol. *J. Neuroimmune Pharmacol. official J. Soc. Neuroimmune Pharmacol.* **2015**, *10*, 344–355. [[CrossRef](#)]
40. Costantino, C.M.; Gupta, A.; Yewdall, A.W.; Dale, B.M.; Devi, L.A.; Chen, B.K. Cannabinoid receptor 2-mediated attenuation of CXCR4-tropic HIV infection in primary CD4+ T cells. *PLoS ONE* **2012**, *7*, e33961. [[CrossRef](#)]
41. Hermes, D.J.; Xu, C.; Poklis, J.L.; Niphakis, M.J.; Cravatt, B.F.; Mackie, K.; Lichtman, A.H.; Ignatowska-Jankowska, B.M.; Fitting, S. Neuroprotective effects of fatty acid amide hydrolase catabolic enzyme inhibition in a HIV-1 Tat model of neuroAIDS. *Neuropharmacology* **2018**, *141*, 55–65. [[CrossRef](#)] [[PubMed](#)]
42. Xu, C.; Hermes, D.J.; Nwanguma, B.; Jacobs, I.R.; Mackie, K.; Mukhopadhyay, S.; Lichtman, A.H.; Ignatowska-Jankowska, B.; Fitting, S. Endocannabinoids exert CB1 receptor-mediated neuroprotective effects in models of neuronal damage induced by HIV-1 Tat protein. *Mol. Cell Neurosci.* **2017**, *83*, 92–102. [[CrossRef](#)] [[PubMed](#)]
43. Hu, S.; Sheng, W.S.; Rock, R.B. CB2 receptor agonists protect human dopaminergic neurons against damage from HIV-1 gp120. *PLoS ONE* **2013**, *8*, e77577. [[CrossRef](#)] [[PubMed](#)]
44. Feliu, A.; Bonilla Del Rio, I.; Carrillo-Salinas, F.J.; Hernandez-Torres, G.; Mestre, L.; Puente, N.; Ortega-Gutierrez, S.; Lopez-Rodriguez, M.L.; Grandes, P.; Mecha, M.; et al. 2-Arachidonoylglycerol Reduces Proteoglycans and Enhances Remyelination in a Progressive Model of Demyelination. *J. Neurosci.* **2017**, *37*, 8385–8398. [[CrossRef](#)] [[PubMed](#)]
45. Patel, D.C.; Wallis, G.; Fujinami, R.S.; Wilcox, K.S.; Smith, M.D. Cannabidiol reduces seizures following CNS infection with Theiler’s murine encephalomyelitis virus. *Epilepsia Open* **2019**, *4*, 431–442. [[CrossRef](#)]



46. Dagenais-Lussier, X.; Loucif, H.; Murira, A.; Laulhe, X.; Stager, S.; Lamarre, A.; van Grevenynghe, J. Sustained IFN-I Expression during Established Persistent Viral Infection: A “Bad Seed” for Protective Immunity. *Viruses* **2017**, *10*, 12. [[CrossRef](#)]
47. Loucif, H.; Gouard, S.; Dagenais-Lussier, X.; Murira, A.; Stager, S.; Tremblay, C.; Van Grevenynghe, J. Deciphering natural control of HIV-1: A valuable strategy to achieve antiretroviral therapy termination. *Cytokine Growth Factor Rev.* **2018**, *40*, 90–98. [[CrossRef](#)]
48. Henriquez, J.E.; Rizzo, M.D.; Crawford, R.B.; Gulick, P.; Kaminski, N.E. Interferon-alpha-Mediated Activation of T Cells from Healthy and HIV-Infected Individuals Is Suppressed by Delta(9)-Tetrahydrocannabinol. *J. Pharmacol. Exp. Ther.* **2018**, *367*, 49–58. [[CrossRef](#)]
49. Henriquez, J.E.; Rizzo, M.D.; Schulz, M.A.; Crawford, R.B.; Gulick, P.; Kaminski, N.E. Delta9-Tetrahydrocannabinol Suppresses Secretion of IFNalpha by Plasmacytoid Dendritic Cells From Healthy and HIV-Infected Individuals. *J. Acquir. Immune. Defic. Syndr.* **2017**, *75*, 588–596. [[CrossRef](#)]
50. Kumar, V.; Torben, W.; Mansfield, J.; Alvarez, X.; Vande Stouwe, C.; Li, J.; Byrareddy, S.N.; Didier, P.J.; Pahar, B.; Molina, P.E.; et al. Cannabinoid Attenuation of Intestinal Inflammation in Chronic SIV-Infected Rhesus Macaques Involves T Cell Modulation and Differential Expression of Micro-RNAs and Pro-inflammatory Genes. *Front. Immunol.* **2019**, *10*, 914. [[CrossRef](#)]
51. Tahamtan, A.; Tavakoli-Yaraki, M.; Shadab, A.; Rezaei, F.; Marashi, S.M.; Shokri, F.; Mokhatri-Azad, T.; Salimi, V. The Role of Cannabinoid Receptor 1 in the Immunopathology of Respiratory Syncytial Virus. *Viral Immunol.* **2018**, *31*, 292–298. [[CrossRef](#)] [[PubMed](#)]
52. Tahamtan, A.; Samieipoor, Y.; Nayeri, F.S.; Rahbarimanesht, A.A.; Izadi, A.; Rashidi-Nezhad, A.; Tavakoli-Yaraki, M.; Farahmand, M.; Bont, L.; Shokri, F.; et al. Effects of cannabinoid receptor type 2 in respiratory syncytial virus infection in human subjects and mice. *Virulence* **2018**, *9*, 217–230. [[CrossRef](#)] [[PubMed](#)]
53. Cockerham, L.R.; Siliciano, J.D.; Sinclair, E.; O’Doherty, U.; Palmer, S.; Yukl, S.A.; Strain, M.C.; Chomont, N.; Hecht, F.M.; Siliciano, R.F.; et al. CD4+ and CD8+ T cell activation are associated with HIV DNA in resting CD4+ T cells. *PLoS ONE* **2014**, *9*, e110731. [[CrossRef](#)] [[PubMed](#)]
54. Haas, A.; Zimmermann, K.; Oxenius, A. Antigen-dependent and -independent mechanisms of T and B cell hyperactivation during chronic HIV-1 infection. *J. Virol.* **2011**, *85*, 12102–12113. [[CrossRef](#)] [[PubMed](#)]
55. Day, C.L.; Kaufmann, D.E.; Kiepiela, P.; Brown, J.A.; Moodley, E.S.; Reddy, S.; Mackey, E.W.; Miller, J.D.; Leslie, A.J.; DePierres, C.; et al. PD-1 expression on HIV-specific T cells is associated with T-cell exhaustion and disease progression. *Nature* **2006**, *443*, 350–354. [[CrossRef](#)]
56. Trautmann, L.; Janbazian, L.; Chomont, N.; Said, E.A.; Gimmig, S.; Bessette, B.; Boulassel, M.R.; Delwart, E.; Sepulveda, H.; Balderas, R.S.; et al. Upregulation of PD-1 expression on HIV-specific CD8+ T cells leads to reversible immune dysfunction. *Nat. Med.* **2006**, *12*, 1198–1202. [[CrossRef](#)]
57. Ogando, J.; Saez, M.E.; Santos, J.; Nuevo-Tapioles, C.; Gut, M.; Esteve-Codina, A.; Heath, S.; Gonzalez-Perez, A.; Cuezva, J.M.; Lacalle, R.A.; et al. PD-1 signaling affects cristae morphology and leads to mitochondrial dysfunction in human CD8(+) T lymphocytes. *J. Immunother Cancer* **2019**, *7*, 151. [[CrossRef](#)]
58. Maagaard, A.; Holberg-Petersen, M.; Lovgarden, G.; Holm, M.; Pettersen, F.O.; Kvale, D. Distinct mechanisms for mitochondrial DNA loss in T and B lymphocytes from HIV-infected patients exposed to nucleoside reverse-transcriptase inhibitors and those naive to antiretroviral treatment. *J. Infect Dis.* **2008**, *198*, 1474–1481. [[CrossRef](#)]
59. Apostolova, N.; Blas-Garcia, A.; Esplugues, J.V. Mitochondrial toxicity in HAART: An overview of in vitro evidence. *Curr. Pharm. Des.* **2011**, *17*, 2130–2144. [[CrossRef](#)]
60. Song, S.; Gong, S.; Singh, P.; Lyu, J.; Bai, Y. The interaction between mitochondria and oncoviruses. *Biochim. Biophys. Acta Mol. Basis Dis.* **2018**, *1864*, 481–487. [[CrossRef](#)]
61. Lai, J.H.; Luo, S.F.; Ho, L.J. Operation of mitochondrial machinery in viral infection-induced immune responses. *Biochem. Pharmacol.* **2018**, *156*, 348–356. [[CrossRef](#)] [[PubMed](#)]
62. de Armas-Rillo, L.; Valera, M.S.; Marrero-Hernandez, S.; Valenzuela-Fernandez, A. Membrane dynamics associated with viral infection. *Rev. Med Virol.* **2016**, *26*, 146–160. [[CrossRef](#)] [[PubMed](#)]
63. Manuzak, J.A.; Gott, T.M.; Kirkwood, J.S.; Coronado, E.; Hensley-McBain, T.; Miller, C.; Cheu, R.K.; Collier, A.C.; Funderburg, N.T.; Martin, J.N.; et al. Heavy Cannabis Use Associated With Reduction

- in Activated and Inflammatory Immune Cell Frequencies in Antiretroviral Therapy-Treated Human Immunodeficiency Virus-Infected Individuals. *Clin. Infect Dis.* **2018**, *66*, 1872–1882. [[CrossRef](#)] [[PubMed](#)]
64. Krishnan, G.; Chatterjee, N. Endocannabinoids affect innate immunity of Muller glia during HIV-1 Tat cytotoxicity. *Mol. Cell Neurosci.* **2014**, *59*, 10–23. [[CrossRef](#)] [[PubMed](#)]
65. Williams, J.C.; Appelberg, S.; Goldberger, B.A.; Klein, T.W.; Sleasman, J.W.; Goodenow, M.M. Delta(9)-Tetrahydrocannabinol treatment during human monocyte differentiation reduces macrophage susceptibility to HIV-1 infection. *J. Neuroimmune Pharmacol. Off. J. Soc. Neuroimmune Pharmacol.* **2014**, *9*, 369–379. [[CrossRef](#)]
66. Raborn, E.S.; Jamerson, M.; Marciano-Cabral, F.; Cabral, G.A. Cannabinoid inhibits HIV-1 Tat-stimulated adhesion of human monocyte-like cells to extracellular matrix proteins. *Life Sci.* **2014**, *104*, 15–23. [[CrossRef](#)]
67. Ramirez, S.H.; Reichenbach, N.L.; Fan, S.; Rom, S.; Merkel, S.F.; Wang, X.; Ho, W.Z.; Persidsky, Y. Attenuation of HIV-1 replication in macrophages by cannabinoid receptor 2 agonists. *J. Leukoc. Biol.* **2013**, *93*, 801–810. [[CrossRef](#)]
68. Chen, W.; Kaplan, B.L.; Pike, S.T.; Topper, L.A.; Lichorobiec, N.R.; Simmons, S.O.; Ramabhadran, R.; Kaminski, N.E. Magnitude of stimulation dictates the cannabinoid-mediated differential T cell response to HIVgp120. *J. Leukoc. Biol.* **2012**, *92*, 1093–1102. [[CrossRef](#)]
69. Fraga, D.; Raborn, E.S.; Ferreira, G.A.; Cabral, G.A. Cannabinoids inhibit migration of microglial-like cells to the HIV protein Tat. *J. Neuroimmune Pharmacol. Off. J. Soc. Neuroimmune Pharmacol.* **2011**, *6*, 566–577. [[CrossRef](#)]
70. Kim, H.J.; Shin, A.H.; Thayer, S.A. Activation of cannabinoid type 2 receptors inhibits HIV-1 envelope glycoprotein gp120-induced synapse loss. *Mol. Pharmacol.* **2011**, *80*, 357–366. [[CrossRef](#)]
71. Raborn, E.S.; Cabral, G.A. Cannabinoid inhibition of macrophage migration to the trans-activating (Tat) protein of HIV-1 is linked to the CB(2) cannabinoid receptor. *J. Pharmacol. Exp. Ther.* **2010**, *333*, 319–327. [[CrossRef](#)] [[PubMed](#)]
72. Chandra, L.C.; Kumar, V.; Torben, W.; Vande Stouwe, C.; Winsauer, P.; Amedee, A.; Molina, P.E.; Mohan, M. Chronic administration of Delta9-tetrahydrocannabinol induces intestinal anti-inflammatory microRNA expression during acute simian immunodeficiency virus infection of rhesus macaques. *J. Virol.* **2015**, *89*, 1168–1181. [[CrossRef](#)] [[PubMed](#)]
73. LeCapitaine, N.J.; Zhang, P.; Winsauer, P.; Walker, E.; Vande Stouwe, C.; Porretta, C.; Molina, P.E. Chronic Delta-9-tetrahydrocannabinol administration increases lymphocyte CXCR4 expression in rhesus macaques. *J. Neuroimmune Pharmacol. Off. J. Soc. Neuroimmune Pharmacol.* **2011**, *6*, 540–545. [[CrossRef](#)] [[PubMed](#)]
74. Molina, P.E.; Winsauer, P.; Zhang, P.; Walker, E.; Birke, L.; Amedee, A.; Stouwe, C.V.; Troxclair, D.; McGoey, R.; Varner, K.; et al. Cannabinoid administration attenuates the progression of simian immunodeficiency virus. *AIDS Res. Hum. Retrovir.* **2011**, *27*, 585–592. [[CrossRef](#)]
75. Sheng, W.S.; Chauhan, P.; Hu, S.; Prasad, S.; Lokensgard, J.R. Antiallodynic Effects of Cannabinoid Receptor 2 (CB2R) Agonists on Retrovirus Infection-Induced Neuropathic Pain. *Pain Res. Manag.* **2019**, *2019*, 1260353. [[CrossRef](#)]
76. Sato, A.; Ono, C.; Tamura, T.; Mori, H.; Izumi, T.; Torii, S.; Fauzyah, Y.; Yamamoto, T.; Morioka, Y.; Okuzaki, D.; et al. Rimonabant suppresses RNA transcription of hepatitis B virus by inhibiting hepatocyte nuclear factor 4alpha. *Microbiol. Immunol.* **2020**, *64*, 345–355. [[CrossRef](#)]
77. Arevalo-Martin, A.; Molina-Holgado, E.; Guaza, C. A CB(1)/CB(2) receptor agonist, WIN 55,212-2, exerts its therapeutic effect in a viral autoimmune model of multiple sclerosis by restoring self-tolerance to myelin. *Neuropharmacology* **2012**, *63*, 385–393. [[CrossRef](#)]
78. Mestre, L.; Inigo, P.M.; Mecha, M.; Correa, F.G.; Hernangomez-Herrero, M.; Loria, F.; Docagne, F.; Borrell, J.; Guaza, C. Anandamide inhibits Theiler's virus induced VCAM-1 in brain endothelial cells and reduces leukocyte transmigration in a model of blood brain barrier by activation of CB(1) receptors. *J. Neuroinflammation* **2011**, *8*, 102. [[CrossRef](#)]
79. Hebert-Chatelain, E.; Reguero, L.; Puente, N.; Lutz, B.; Chaouloff, F.; Rossignol, R.; Piazza, P.V.; Benard, G.; Grandes, P.; Marsicano, G. Cannabinoid control of brain bioenergetics: Exploring the subcellular localization of the CB1 receptor. *Mol. Metab.* **2014**, *3*, 495–504. [[CrossRef](#)]

80. Hebert-Chatelain, E.; Desprez, T.; Serrat, R.; Bellocchio, L.; Soria-Gomez, E.; Busquets-Garcia, A.; Pagano Zottola, A.C.; Delamarre, A.; Cannich, A.; Vincent, P.; et al. A cannabinoid link between mitochondria and memory. *Nature* **2016**, *539*, 555–559. [[CrossRef](#)]
81. Piomelli, D. A mighty (ochondrial) fight? *Mol. Metab.* **2014**, *3*, 345–346. [[CrossRef](#)] [[PubMed](#)]
82. Morozov, Y.M.; Dominguez, M.H.; Varela, L.; Shanabrough, M.; Koch, M.; Horvath, T.L.; Rakic, P. Antibodies to cannabinoid type 1 receptor co-react with stomatin-like protein 2 in mouse brain mitochondria. *Eur. J. Neurosci.* **2013**, *38*, 2341–2348. [[CrossRef](#)] [[PubMed](#)]
83. Djeungoue-Petga, M.A.; Hebert-Chatelain, E. Linking Mitochondria and Synaptic Transmission: The CB1 Receptor. *BioEssays News Rev. Mol. Cell. Dev. Biol.* **2017**, *39*, 1700126. [[CrossRef](#)] [[PubMed](#)]
84. Mancini, G.; Horvath, T.L. Mitochondria Bioenergetic and Cognitive Functions: The Cannabinoid Link. *Trends Cell Biol.* **2017**, *27*, 391–392. [[CrossRef](#)] [[PubMed](#)]
85. Harkany, T.; Horvath, T.L. (S)Pot on Mitochondria: Cannabinoids Disrupt Cellular Respiration to Limit Neuronal Activity. *Cell Metab.* **2017**, *25*, 8–10. [[CrossRef](#)]
86. Jimenez-Blasco, D.; Busquets-Garcia, A.; Hebert-Chatelain, E.; Serrat, R.; Vicente-Gutierrez, C.; Ioannidou, C.; Gomez-Sotres, P.; Lopez-Fabuel, I.; Resch-Beusher, M.; Resel, E.; et al. Glucose metabolism links astroglial mitochondria to cannabinoid effects. *Nature* **2020**, *583*, 603–608. [[CrossRef](#)]
87. Kataoka, K.; Bilkei-Gorzo, A.; Nozaki, C.; Togo, A.; Nakamura, K.; Ohta, K.; Zimmer, A.; Asahi, T. Age-dependent Alteration in Mitochondrial Dynamics and Autophagy in Hippocampal Neuron of Cannabinoid CB1 Receptor-deficient Mice. *Brain Res. Bull.* **2020**, *160*, 40–49. [[CrossRef](#)]
88. Fisar, Z.; Singh, N.; Hroudova, J. Cannabinoid-induced changes in respiration of brain mitochondria. *Toxicol. Lett.* **2014**, *231*, 62–71. [[CrossRef](#)]
89. Bino, T.; Chari-Bitron, A.; Shahar, A. Biochemical effects and morphological changes in rat liver mitochondria exposed to 1-tetrahydrocannabinol. *Biochim. Biophys. Acta* **1972**, *288*, 195–202. [[CrossRef](#)]
90. Mahoney, J.M.; Harris, R.A. Effect of 9-tetrahydrocannabinol on mitochondrial processes. *Biochem. Pharmacol.* **1972**, *21*, 1217–1226. [[CrossRef](#)]
91. Drori, A.; Permyakova, A.; Hadar, R.; Udi, S.; Nemirovski, A.; Tam, J. Cannabinoid-1 receptor regulates mitochondrial dynamics and function in renal proximal tubular cells. *Diabetes Obes. Metab.* **2019**, *21*, 146–159. [[CrossRef](#)] [[PubMed](#)]
92. Augusto-Oliveira, M.; Arrifano, G.P.; Lopes-Araujo, A.; Santos-Sacramento, L.; Takeda, P.Y.; Anthony, D.C.; Malva, J.O.; Crespo-Lopez, M.E. What Do Microglia Really Do in Healthy Adult Brain? *Cells* **2019**, *8*, 1293. [[CrossRef](#)] [[PubMed](#)]
93. Ma, L.; Niu, W.; Lv, J.; Jia, J.; Zhu, M.; Yang, S. PGC-1alpha-Mediated Mitochondrial Biogenesis is Involved in Cannabinoid Receptor 2 Agonist AM1241-Induced Microglial Phenotype Amelioration. *Cell. Mol. Neurobiol.* **2018**, *38*, 1529–1537. [[CrossRef](#)] [[PubMed](#)]
94. Nichols, J.M.; Kaplan, B.L.F. Immune Responses Regulated by Cannabidiol. *Cannabis Cannabinoid Res.* **2020**, *5*, 12–31. [[CrossRef](#)]
95. Muthumalage, T.; Rahman, I. Cannabidiol differentially regulates basal and LPS-induced inflammatory responses in macrophages, lung epithelial cells, and fibroblasts. *Toxicol. Appl. Pharmacol.* **2019**, *382*, 114713. [[CrossRef](#)]
96. Bock, F.J.; Tait, S.W.G. Mitochondria as multifaceted regulators of cell death. *Nat. Rev. Mol. Cell Biol.* **2020**, *21*, 85–100. [[CrossRef](#)]
97. Estaquier, J.; Vallette, F.; Vayssiere, J.L.; Mignotte, B. The mitochondrial pathways of apoptosis. *Adv. Exp. Med. Biol.* **2012**, *942*, 157–183. [[CrossRef](#)]
98. Rieder, S.A.; Chauhan, A.; Singh, U.; Nagarkatti, M.; Nagarkatti, P. Cannabinoid-induced apoptosis in immune cells as a pathway to immunosuppression. *Immunobiology* **2010**, *215*, 598–605. [[CrossRef](#)]
99. Wu, H.Y.; Huang, C.H.; Lin, Y.H.; Wang, C.C.; Jan, T.R. Cannabidiol induced apoptosis in human monocytes through mitochondrial permeability transition pore-mediated ROS production. *Free Radic. Biol. Med.* **2018**, *124*, 311–318. [[CrossRef](#)]
100. Schultze, N.; Wanka, H.; Zwicker, P.; Lindequist, U.; Haertel, B. Mitochondrial functions of THP-1 monocytes following the exposure to selected natural compounds. *Toxicology* **2017**, *377*, 57–63. [[CrossRef](#)]
101. Vaeth, M.; Feske, S. Ion channelopathies of the immune system. *Curr. Opin. Immunol.* **2018**, *52*, 39–50. [[CrossRef](#)] [[PubMed](#)]

102. Trebak, M.; Kinet, J.P. Calcium signalling in T cells. *Nat. Rev. Immunol.* **2019**, *19*, 154–169. [[CrossRef](#)] [[PubMed](#)]
103. Olivás-Aguirre, M.; Torres-Lopez, L.; Valle-Reyes, J.S.; Hernandez-Cruz, A.; Pottosin, I.; Dobrovinskaya, O. Cannabidiol directly targets mitochondria and disturbs calcium homeostasis in acute lymphoblastic leukemia. *Cell Death Dis.* **2019**, *10*, 779. [[CrossRef](#)] [[PubMed](#)]
104. Hoth, M.; Fanger, C.M.; Lewis, R.S. Mitochondrial regulation of store-operated calcium signaling in T lymphocytes. *J. Cell Biol.* **1997**, *137*, 633–648. [[CrossRef](#)]
105. Fattore, L.; Spano, M.S.; Altea, S.; Fadda, P.; Fratta, W. Drug- and cue-induced reinstatement of cannabinoid-seeking behaviour in male and female rats: Influence of ovarian hormones. *Br. J. Pharmacol.* **2010**, *160*, 724–735. [[CrossRef](#)] [[PubMed](#)]
106. Narimatsu, S.; Watanabe, K.; Yamamoto, I.; Yoshimura, H. Sex difference in the oxidative metabolism of delta 9-tetrahydrocannabinol in the rat. *Biochem. Pharmacol.* **1991**, *41*, 1187–1194. [[CrossRef](#)]
107. Gorey, C.; Kuhns, L.; Smaragdi, E.; Kroon, E.; Cousijn, J. Age-related differences in the impact of cannabis use on the brain and cognition: A systematic review. *Eur. Arch. Psychiatry Clin. Neurosci.* **2019**, *269*, 37–58. [[CrossRef](#)]
108. Costiniuk, C.T.; Saneei, Z.; Routy, J.P.; Margolese, S.; Mandarino, E.; Singer, J.; Lebouche, B.; Cox, J.; Szabo, J.; Brouillette, M.J.; et al. Oral cannabinoids in people living with HIV on effective antiretroviral therapy: CTN PT028-study protocol for a pilot randomised trial to assess safety, tolerability and effect on immune activation. *BMJ Open* **2019**, *9*, e024793. [[CrossRef](#)]
109. Fujii, M.; Sherchan, P.; Soejima, Y.; Hasegawa, Y.; Flores, J.; Doycheva, D.; Zhang, J.H. Cannabinoid receptor type 2 agonist attenuates apoptosis by activation of phosphorylated CREB-Bcl-2 pathway after subarachnoid hemorrhage in rats. *Exp. Neurol.* **2014**, *261*, 396–403. [[CrossRef](#)]
110. Nguyen, C.H.; Krewenka, C.; Radad, K.; Kranner, B.; Huber, A.; Duvigneau, J.C.; Miller, I.; Moldzio, R. THC (Delta9-Tetrahydrocannabinol) Exerts Neuroprotective Effect in Glutamate-affected Murine Primary Mesencephalic Cultures Through Restoring Mitochondrial Membrane Potential and Anti-apoptosis Involving CB1 Receptor-dependent Mechanism. *Phytother Res.* **2016**, *30*, 2044–2052. [[CrossRef](#)]
111. Viscomi, M.T.; Oddi, S.; Latini, L.; Bisicchia, E.; Maccarrone, M.; Molinari, M. The endocannabinoid system: A new entry in remote cell death mechanisms. *Exp. Neurol.* **2010**, *224*, 56–65. [[CrossRef](#)] [[PubMed](#)]
112. Xu, Z.; Lv, X.A.; Dai, Q.; Ge, Y.Q.; Xu, J. Acute upregulation of neuronal mitochondrial type-1 cannabinoid receptor and its role in metabolic defects and neuronal apoptosis after TBI. *Mol. Brain* **2016**, *9*, 75. [[CrossRef](#)] [[PubMed](#)]





© 2020 by the authors. Licensee MDPI, Basel, Switzerland. This article is an open access article distributed under the terms and conditions of the Creative Commons Attribution (CC BY) license (<http://creativecommons.org/licenses/by/4.0/>).



*Review*

## **Sustained IFN-I Expression during Established Persistent Viral Infection: A “Bad Seed” for Protective Immunity**

Xavier Dagenais-Lussier , Hamza Loucif , Armstrong Murira, Xavier Laulhé, Simona Stäger, Alain Lamarre and Julien van Grevenynghe \*

Institut National de la Recherche Scientifique (INRS)-Institut Armand-Frappier, 531 Boulevard des Prairies, Laval, H7V 1B7 QC, Canada; xavier.dagenais@iaf.inrs.ca (X.D.-L.); hamza.loucif@iaf.inrs.ca (H.L.); armstrong.murira@iaf.inrs.ca (A.M.); xavier.laulhe@iaf.inrs.ca (X.L.); simona.stager@iaf.inrs.ca (S.S.); alain.lamarre@iaf.inrs.ca (A.L.)

\* Correspondence: julien.vangrevenynghe@iaf.inrs.ca

Received: 11 December 2017; Accepted: 27 December 2017; Published: 30 December 2017



Review

# Sustained IFN-I Expression during Established Persistent Viral Infection: A “Bad Seed” for Protective Immunity

Xavier Dagenais-Lussier , Hamza Loucif , Armstrong Murira, Xavier Laulhé, Simona Stäger, Alain Lamarre and Julien van Grevenynghe \*

Institut National de la Recherche Scientifique (INRS)-Institut Armand-Frappier, 531 Boulevard des Prairies, Laval, H7V 1B7 QC, Canada; xavier.dagenais@iaf.inrs.ca (X.D.-L.); hamza.loucif@iaf.inrs.ca (H.L.); armstrong.murira@iaf.inrs.ca (A.M.); xavier.laulhe@iaf.inrs.ca (X.L.); simona.stager@iaf.inrs.ca (S.S.); alain.lamarre@iaf.inrs.ca (A.L.)

\* Correspondence: julien.vangrevenynghe@iaf.inrs.ca

Received: 11 December 2017; Accepted: 27 December 2017; Published: 30 December 2017

**Abstract:** Type I interferons (IFN-I) are one of the primary immune defenses against viruses. Similar to all other molecular mechanisms that are central to eliciting protective immune responses, IFN-I expression is subject to homeostatic controls that regulate cytokine levels upon clearing the infection. However, in the case of established persistent viral infection, sustained elevation of IFN-I expression bears deleterious effects to the host and is today considered as the major driver of inflammation and immunosuppression. In fact, numerous emerging studies place sustained IFN-I expression as a common nexus in the pathogenesis of multiple chronic diseases including persistent infections with the human immunodeficiency virus type 1 (HIV-1), simian immunodeficiency virus (SIV), as well as the rodent-borne lymphocytic choriomeningitis virus clone 13 (LCMV clone 13). In this review, we highlight recent studies illustrating the molecular dysregulation and resultant cellular dysfunction in both innate and adaptive immune responses driven by sustained IFN-I expression. Here, we place particular emphasis on the efficacy of IFN-I receptor (IFNR) blockade towards improving immune responses against viral infections given the emerging therapeutic approach of blocking IFNR using neutralizing antibodies (Abs) in chronically infected patients.

**Keywords:** sustained IFN-I expression; IFNR blockade; persistent infection; exhaustion; immune activation/inflammation; immunosuppression; cell loss

---

## 1. IFN-I and Its Beneficial Role

The type I interferon (IFN-I) system consists of five types of interferon: IFN- $\alpha$ , IFN- $\beta$ , IFN- $\omega$ , IFN- $\epsilon$ , and IFN- $\kappa$ . This is based on the structure of their respective receptors on the cell surface. Of these, only IFN- $\alpha$  is encoded by more than a single gene (13 subtypes in humans, 14 in mice). Once they bind with their receptors, they trigger the downstream induction of interferon-stimulated genes (ISGs) through the Janus kinase/signal transducers and activators of transcription signaling pathway. These ISGs include various intrinsic restriction factors, cytokines, chemokines, and co-stimulatory molecules in infected cells as well as bystander uninfected cells, all of which have been largely reviewed elsewhere [1–3]. IFN-I is considered to be the most potent autocrine and paracrine secreted “virus-induced” cytokine and is critical in establishing an efficient adaptive and acquired immune response especially in acute infections [4]. In the context of chronic infections, many studies showed a deficiency in IFN-I induced-antiviral responses. This led to the use of IFN-I as treatment for simian immunodeficiency virus (SIV), hepatitis C virus (HCV), and hepatitis B virus (HBV) infections which demonstrates its positive, although moderate, effect during the acute phase of chronic infections [2,5,6].

However, cluster of differentiation 8 (CD8) T-cell hyperactivation has been observed in HCV-infected patients that are continuously treated with IFN-I over seven months [7,8]. Considering that IFN-I signaling is crucial in controlling viral infections, the focus of this review seems counterintuitive, yet it is now well established that sustained IFN-I expression also contributes in the establishment of a persistent infection escalated by immune hyperactivation and inflammation [1,3,7].

## 2. Sustained IFN-I Expression Drives Disease Progression during Persistent Infection

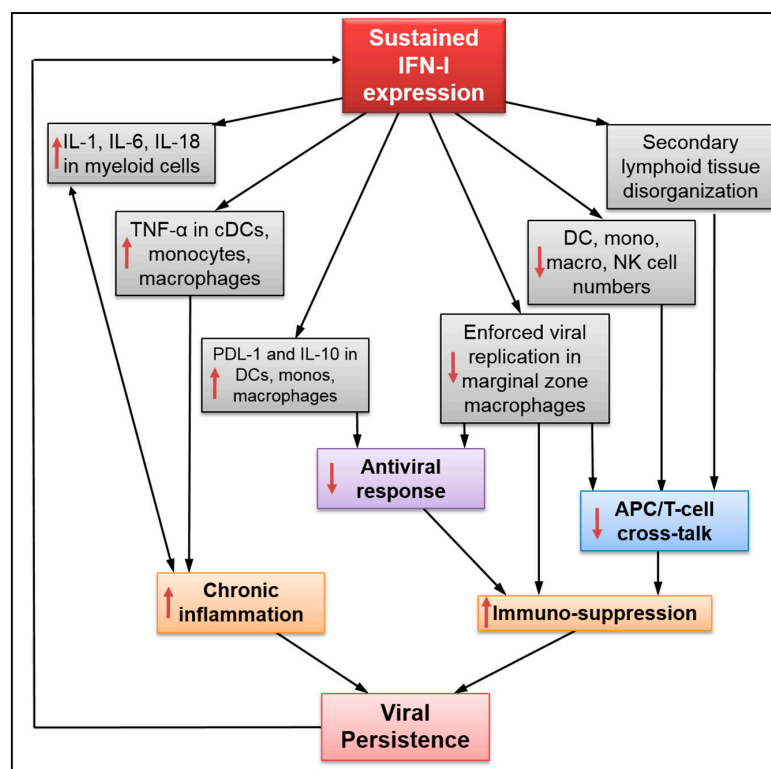
Persistent viral infections, including human immunodeficiency virus type 1 (HIV-1), are associated with prolonged dysregulation of multiple key signaling pathways, such as programmed cell death protein 1 (PD-1) and transcription factor forkhead Box O3 (FOXO3a), whose functions are critical in controlling and eliciting effective immune responses. Conversely, in the face of chronic inflammation and viral persistence, these signaling pathways drive immune dysfunction that ultimately contributes to disease progression. Importantly, these aberrancies are reversible as illustrated by the improvement in related protective immunity upon targeted blockade of the exhaustion marker, PD-1, and transcription factor, FOXO3a. Of note, both of these pathways have been found to be overexpressed in chronically HIV-1-infected patients despite induction of antiretroviral therapy (ART) wherein immune function is rescued by blockade even after years of infection [9–14]. To date, there are well-established lines of evidence placing sustained IFN-I expression as a major contributor of immune activation/inflammation and resultant disease progression during persistent viral infections such as HIV-1 and SIV [1,3,6–8,15–29]. For example, in the non-human primate model of SIV infection, natural hosts that do not progress toward acquired immune deficiency syndrome (AIDS) exhibit lower levels of IFN-I signaling and inflammation when compared to animals harbouring pathogenic infections [6,30–33]. In the context of HIV-1 infection, disease severity, reduction of CD4 T-cell counts, and poor immune restoration after ART are associated with sustained and elevated IFN-I expression [8,20,34–36]. The maintenance of IFN-I expression in patients under ART is due to the persistence of residual viral replication in tissues and local inflammation [37]. Interestingly, *in vivo* blockade of the interferon- $\alpha/\beta$  receptor (IFNR) during persistent HIV-1 infection, which reversed HIV-1-induced immune hyperactivation, also rescued anti-HIV-1 immune responses and induced the reactivation of viral reservoir in the presence of ART. More importantly, IFNR blockade reduced cell-associated virus numbers and significantly controlled HIV-1 rebound after ART cessation [18,38]. Thus, it is unsurprising that the use of humanized anti-IFNR blocking antibodies (Abs), which are currently used in a phase I trial in systemic lupus erythematosus and systemic sclerosis [39,40], are now proposed to treat persistent viral infections as a means of reducing chronic inflammation [3,27,41].

## 3. Impact of Sustained IFN-I Expression on the Innate Immune Response

Upon establishment of persistent viral infection, IFN-I is mainly produced by activated plasmacytoid dendritic cells (pDCs) and to a lesser extent by monocytes, macrophages, and conventional DCs (cDCs) by pathogen sensing [8,15,42,43]. A recent study has also shown that polyclonal Abs and Ab complexes found in HIV-1-infected subjects induced IFN-I production in pDCs [44]. As depicted in Figure 1, sustained IFN-I expression drives dysregulation at the tissue as well as cellular level within the innate immune response. For instance, IFN-I is shown to have a role in pDC loss during systemic viral infections. Using IFNR knockout mice, Swiecki and colleagues have shown that IFN-I induced the expression of several pro-apoptotic molecules such as Bim and Bax in pDCs, causing caspase activation and cell death [45]. Additionally, sustained IFN-I expression during persistent infections disrupts splenic architecture, which results in impaired immune cell interactions [26,29]. It also increases interleukin 10 (IL-10) and Programmed death-ligand 1 (PDL-1) expressions on resident immunosuppressive DCs, monocytes, and macrophages; as well as reduces total cell numbers of splenic DCs, macrophages, and natural killer cells [4,26,29,46]. This collective innate immune dysfunction is significantly rescued by IFNR blockade [26,29,46] (Table 1). Similarly, IFNR blockade in lymphocytic choriomeningitis virus clone 13 (LCMV clone 13)-infected mice reduces

the levels of pro-inflammatory cytokine IL-1 and IL-18 in plasma, and decreases the expression of active caspase-1 in DCs and macrophages [26,29]. This indicates that IFNR blockade may counteract both inflammation and inflammasome activation in innate immune cells during persistent viral infection. The progressive loss of DCs due to sustained IFN-I exposure could be explained by the downregulation of microRNA221 and resultant expression of pro-apoptotic genes such as *bim* and *foxo3a* [47]. Cunningham et al. have recently shown that, in addition to induction of IL-10 and PDL-1 in immunosuppressive DCs, sustained IFN-I expression during LCMV clone 13 infection simultaneously inhibited the generation of cDCs with T-cell stimulating capacity [48]. Furthermore, Honke and colleagues revealed that enforced viral replication in marginal zone CD169<sup>+</sup> macrophages, which is essential to ensure proper antigen synthesis, was blunted in infected mice in an IFN-I-related manner [23,49]. Interestingly, if blocking IFN-I increases viral replication, more antigen would be produced, potentially stimulating the adaptive immune response. Implementing this viral replication could be seen as a new “shock and kill” approach to current antiviral treatment. Sustained IFN-I expression during persistent viral infection promotes immunosuppression through the expansion and accumulation of Ly6C<sup>high</sup> monocytes that are functionally similar to myeloid-derived suppressor cells (MDSC) found in cancers [50,51]. Finally, findings from Rempel and colleagues show that IFN- $\alpha$  reprograms the innate immune response of monocytes and desensitizes them to normally activating microbial factors during chronic unsuppressed HIV-1 infection [52].

















Altogether, these results show that sustained IFN-I expression during persistent viral infection drives significant innate immune dysfunction, which is ultimately responsible for increased inflammation and immunosuppression, along with reduced antigen presentation. Moreover, the results strongly suggest that IFNR blockade may be effective towards improving the innate immune response during persistent viral infection.



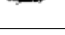


**Figure 1.** Defects mediated by sustained type I interferon (IFN-I) expression on innate immunity during persistent viral infection. APC: antigen presenting cells; TNF: tumor necrosis factor; DC: dendritic cell; cDCs: conventional dendritic cell; PDL: programmed death ligand; NK: natural killer; ↑: up-regulation; ↓: down-regulation.

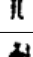


**Table 1.** List of immune dysfunctions caused by sustained type I interferon (IFN-I) signaling which are reversibly rescued by the interferon- $\alpha/\beta$  receptor (IFNR) blockade.

Phenotype Improvement(s)	Model	Virus(es)	Reference(s)
Increased cytokine producing virus-specific CD4/CD8 (IFN- $\gamma$ , TNF- $\alpha$ , IL-2); improved antiviral responses		HIV, LCMV	[12,13,23,26,34]
Reduced expression of PD-1, TIM-3, TIGIT, BATEF, CD160 on CD8 (decreased cell exhaustion)		HIV	[12,34]
Reduced KI67 <sup>+</sup> population in CD4/CD8; decrease of HIV-mediated T-cell hyperactivation		HIV	[12]
Reduced HLA-DR, CD38, CD69, CD80 expression in CD4/CD8; decrease of HIV-mediated T-cell hyperactivation		HIV	[12,34,41*,53*]
Decrease of caspase-3-dependent apoptosis in total and specific CD4 T-cells		HIV, LCMV	[13,54,55*]
Accelerating neutralizing Abs production		LCMV	[18]
Reduced PD-L1 and IL-10 expression in DCs, mono and macro. Decreased IL-10 levels in plasma/sera		HIV, LCMV	[23,26,41*]
Reduced IL-1 and IL-18 levels, and inflammasome activation in DCs and monos; decreased CD80 expression in monos		HIV, LCMV	[23,26,41*]
Increase of splenocyte cell numbers (DCs, macrophages, CD4, CD8, B and natural killers)		LCMV	[23,26,52]
Proper splenic architecture organization		LCMV	[23,26]
Decreased CXCR4 expression on GC B Increased levels of specific Ab production and specific ASCs		LCMV	[52]
Decreased caspase-3 <sup>+</sup> apoptotic virus-specific GC B (by counteracting plasmablast differentiation); B expansion		LCMV	[54]
Increased virus-specific B number; Decreased CTL CD8-mediated kill of specific B		LCMV	[56]
Reduced TRAIL/DR5-mediated apoptosis in CD4		HIV	[55*]
Decreased % of TRAIL <sup>+</sup> and apoptotic CD4		HIV	[57]
Increased Fas-mediated apoptosis in CD4 and CD8 T-cells		HIV	[58*]
Increased expression of BTLA on CD4 T-cells; reduced hyper-immune activation		HIV	[59*]
Increased Th1 differentiation in late primed virus-specific CD4		LCMV	[60]



 : Humanized mice;  ; Mice; \*: in vitro viral infection; ASC: antibody-secreting cells; CD: cluster of Differentiation; TNF: tumor Necrosis Factor; IL: interleukin; PD: programmed Death Protein; TIM: T-cell Immunoglobulin and Mucin; TIGIT: T-cell Ig and ITIM domain; BATEF: basic leucine zipper transcription factor ATF-like; LCMV: Lymphocytic choriomeningitis virus; KI: proliferation Marker, Ki-67 is a prototype monoclonal Ab and was first produced in Kiel, Germany; HLA-DR: human leukocyte antigen—antigen D related; DCs: dendritic cells; CXCR: C-X-C motif chemokine receptor; GC: germinal center; ASCs: antibody secreting cells; CTL: cytotoxic T lymphocytes; TRAIL: TNF-related apoptosis inducing ligand; Th1: Type I T helper cells; BTLA: B and T lymphocyte attenuator.

#### 4. Detrimental Role of Sustained IFN-I Expression on the Humoral Immune Response

Persistent viral infections, including HIV-1, are associated with progressive and profound perturbation of humoral immune response as characterized by: (i) progressive depletion of memory and virus-specific B-cells; (ii) impaired vaccine response; (iii) polyclonal activation of B-cells resulting in heightened production of total and non-specific Abs (aka. hypergammaglobulinemia; HGG); (iv) abnormal distribution of B-cell subpopulations; and (v) delayed appearance of neutralizing Abs [13,54,56,61,62].

Recent evidence in LCMV clone 13-infected mice that were co-immunized with the 4-hydroxy-3-nitrophenylacetic (NP) hapten showed that sustained IFN-I expression was responsible for HGG as well as reduced production of NP-specific Abs [63]. In this study, Daugan et al. also observed the delayed appearance of LCMV-specific neutralizing Abs along with disrupted B-cell follicle structure and high expression of chemokine receptor CXCR4 in germinal center (GC) B-cells [63] (Figure 2). It is important to note that aberrant expression of this receptor affects the homing of B-cells within the follicles, which resultantly impacts the architecture of this microstructure. Hence the disrupted phenotype described above. Although IFNR blockade has no effect on HGG, the treatment resulted in significant restoration of the NP-specific response that was illustrated by higher levels of specific Abs and Ab-secreting cells (ASC), along with reduction of B-cell C-X-C motif chemokine receptor 4 (CXCR4) expression and partial recovery of B-cell follicles (Table 1). Taken together, these findings suggest that, in addition to improving antigen-specific Abs responses, IFNR blockade may likely prevent atypical B-cell trafficking and localization outside of follicles. Furthermore, the authors showed that the effects of IFN-I were observed in a B-cell intrinsic manner whereby prolonged exposure to the cytokine bore direct effects on the B-cells. As such, IFNR deficiency in B-cells accelerated the development of LCMV-specific neutralizing Abs. The control of LCMV infection by IFNR blockade has also been associated with increased number of splenic B-cells [26]. Finally, three recent studies have demonstrated the detrimental role of sustained IFN-I expression on the survival of specific B-cells, the generation of short-lived plasmablasts, and neutralizing Abs in LCMV clone 13-infected mice [55,57,58]. In these studies, defective humoral immune responses were not directly attributed to B-cell-intrinsic IFN-I sensing, but rather due to reduced antiviral B-cell immune response ascribed to other effectors such as cytotoxic T-lymphocyte CD8 T-cells (CTL), IL-10<sup>+</sup> myeloid cells, and inflammatory monocytes via nitric oxide production [55,57,58]. Of note, despite the difference in direct versus indirect effect on B-cells, virus-specific humoral responses in the latter setting were rescued using IFNR blockade [55,57].

Overall, these data indicate that both direct and indirect effects of sustained IFN-I expression in B-cells contribute towards humoral dysfunction during persistent viral infection and can be counteracted by IFNR blockade.

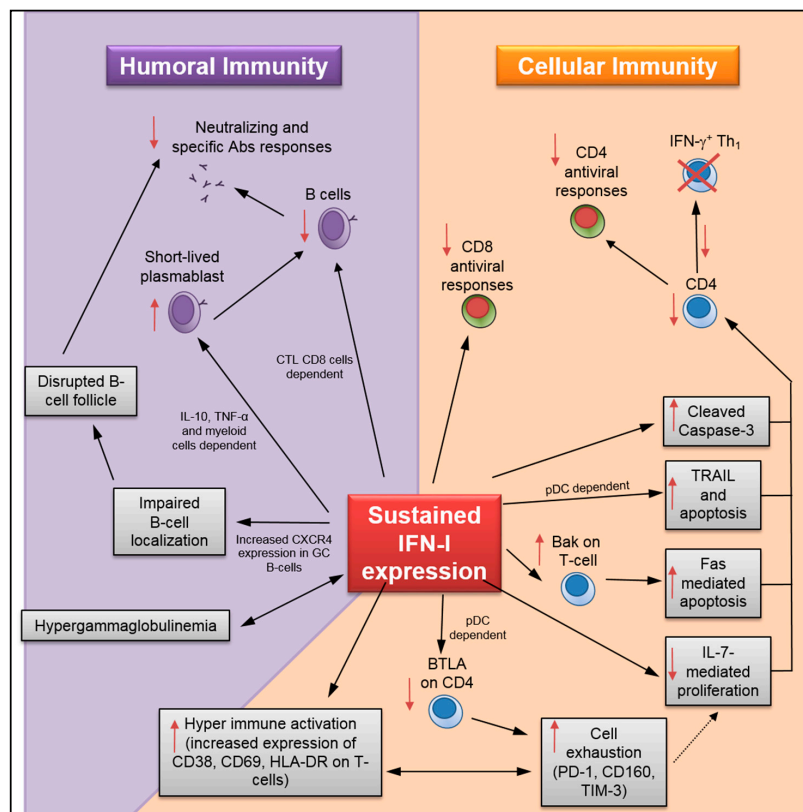


**Figure 2.** Detrimental effects of sustained IFN-I expression on humoral and cellular antiviral immunity. ↑: up-regulation; ↓: down-regulation; ◀▶: impact on both sides.

## 5. Impact of Sustained IFN-I on T-Cell Maintenance and Antiviral Response

Chronic inflammation is a major hallmark of disease progression during persistent viral infection and, in the case of HIV-1 infection, is also observed in patients undergoing ART. This ultimately results in: (i) increased sensitivity to apoptosis and cell loss in CD4 population; (ii) T-cell hyperactivation; and (iii) exhaustion along with defective antiviral response [10,11,14,64,65].

- (i) T-cell loss: Although IFN- $\alpha$  administration initially prevents systemic SIV infection in rhesus macaques, prolonged treatment accelerates CD4 T-cell loss [6]. A recent study by Chen and colleagues has shown that sustained IFN-I expression increased HIV-1-induced apoptosis and caspase-3 activity in CD4 T-cells [19] (Figure 2). Importantly, INFR blockade rescued HIV-specific T-cell and total T-cell numbers during persistent infection, as well as reduced the apoptosis in CD4 T-cells (Table 1). Herbeuval and colleagues have shown that IFNR blockade results in decreased TRAIL/DR5-mediated apoptosis and caspase-3 activity in CD4 T-cells using an in vitro HIV-1 infection model [53]. In a separate study, they also reported a lower frequency of TRAIL<sup>+</sup> and apoptotic CD4 T-cells in HIV-1-infected human samples after treatment with anti-IFN $\alpha/\beta$  neutralizing Abs [59]. In addition, it has also been shown that IFNR blockade causes downregulation of cell-death signal cascades by the reduction in Bak expression and Fas-mediated apoptosis in CD4 T-cells using an in vitro HIV-1 infection model [66]. IFNR blockade also increases total splenic T-lymphocyte and antiviral specific CD4 T-cell numbers during LCMV<sub>CL13</sub> infection [26,29,63]. Finally, data collected by Cha and colleagues indicates that sustained IFN-I expression in HIV-1-infected patients undergoing ART may promote T-cell loss by accelerating cell turnover and activation-induced cell death while decreasing T-cell homeostasis mediated by IL-7 [7,60]. Similarly, prolonged exposure to IFN-I in mice under lymphopenic conditions has been found to alter CD4 T-cell homeostasis [67].

- (ii) T-cell hyperactivation: Elevated expression of T-cell activation/proliferation markers such as CD38, HLA-DR, and Ki67, which correlates with sustained IFN-I expression during persistent HIV-1 infection [8], is significantly reduced by IFNR blockade [18,38]. Similarly, INFR blockade reduces HIV-induced CD80 expression in CCR5<sup>+</sup> T-cells, and CD69 and CD38 in T-cells during in vitro infection [46,68]. HIV-1-induced BTLA downregulation in T-cells, which may also contribute to hyperactivation, can be prevented by IFNR blockade [69].
- (iii) T-cell exhaustion: During chronic HIV-1 infection, the IFN-I pathway is associated with CD4 T-cell exhaustion [70]. Recent results in humanized mice infected with HIV-1 have shown that IFNR blockade resulted in reduced expression of several exhaustion markers in CD8 T-cells—including PD-1, CD160, and TIM-3—along with enhanced IFN- $\gamma$  and IL-2 production in virus-specific T-cells [18,19,38]. Relatedly, IFNR blockade in LCMV<sub>CL13</sub>-infected mice enhances virus-specific CD4 T-cell response [26,29]. Finally, sustained IFN-I expression during LCMV<sub>CL13</sub> infection also suppresses de novo Th<sub>1</sub> differentiation in late primed virus-specific CD4 [71]. In this study, the authors have shown that, although reduced Th<sub>1</sub> differentiation was not mediated through direct IFN-I sensing by CD4 T-cells, it could be rescued by IFNR blockade.
- (iv) Impact on immunosuppressive Treg: Although the effect of IFN-I signaling on hyperactivation and cell exhaustion is evident, its impact on regulatory T cells (Treg) during viral infections remains unclear [3]. In the case of acute LCMV infection, studies provide contradicting information showing either no effect of IFN-I on Treg [72], or a direct effect in reducing their numbers resulting in lower viral load [73]. Moreover, the effect of Treg depletion during chronic LCMV infection failed to increase viral clearance due to PD-L1 expression on infected cells despite an increase in virus-specific CD8 T-cell activity [74].

In summary, IFNR blockade during persistent viral infection decreases T-cell apoptosis, hyperactivation, and exhaustion, as well as improves antiviral immune response and cell maintenance.

## 6. Concluding Remarks

Overall, an increasing amount of evidence using human and in vivo models potentiates the beneficial outcomes of blocking IFN-I signaling during the chronic phase of viral infection once the viral persistence, chronic inflammation, and elevated IFN-I signatures are established in patients (Table 1). It is important to consider the complexity of the factors to ensure the safety and the clinical success for blocking IFN-I signaling-based therapy [3,28]. Namely, the timing of such treatment is critical considering that early administration of exogenous IFN-I is usually beneficial for the host and prevents the establishment of persistent infection [6,27,75] and, in the case of SIV, early IFNR blockade results in accelerated disease progression leading to AIDS [6]. As such, it is crucial to increase our knowledge on how sustained IFN-I signaling and timing of IFNR blockade precisely impacts molecular networks and immune cell phenotypes during persistent viral infections. This information will facilitate the translation of this therapeutic concept into successful treatment.

**Conflicts of Interest:** The authors declare no conflict of interest.

## References

1. Acchioni, C.; Marsili, G.; Perrotti, E.; Remoli, A.L.; Sgarbanti, M.; Battistini, A. Type I IFN—A blunt spear in fighting HIV-1 infection. *Cytokine Growth Factor Rev.* **2015**, *26*, 143–158. [[CrossRef](#)] [[PubMed](#)]
2. Borden, E.C.; Sen, G.C.; Uze, G.; Silverman, R.H.; Ransohoff, R.M.; Foster, G.R.; Stark, G.R. Interferons at age 50: Past, current and future impact on biomedicine. *Nat. Rev. Drug Discov.* **2007**, *6*, 975–990. [[CrossRef](#)] [[PubMed](#)]
3. Snell, L.M.; McGaha, T.L.; Brooks, D.G. Type I interferon in chronic virus infection and cancer. *Trends Immunol.* **2017**, *38*, 542–557. [[CrossRef](#)] [[PubMed](#)]
4. Teijaro, J.R. Type I interferons in viral control and immune regulation. *Curr. Opin. Virol.* **2016**, *16*, 31–40. [[CrossRef](#)] [[PubMed](#)]

5. Gonzalez, S.A.; Keeffe, E.B. Chronic viral hepatitis: Epidemiology, molecular biology, and antiviral therapy. *Front. Biosci.* **2011**, *16*, 225–250. [[CrossRef](#)]
6. Sandler, N.G.; Bosinger, S.E.; Estes, J.D.; Zhu, R.T.; Tharp, G.K.; Boritz, E.; Levin, D.; Wijeyesinghe, S.; Makamdop, K.N.; del Prete, G.Q.; et al. Type I interferon responses in rhesus macaques prevent SIV infection and slow disease progression. *Nature* **2014**, *511*, 601–605. [[CrossRef](#)] [[PubMed](#)]
7. Cha, L.; Berry, C.M.; Nolan, D.; Castley, A.; Fernandez, S.; French, M.A. Interferon- $\alpha$ , immune activation and immune dysfunction in treated HIV infection. *Clin. Transl. Immunol.* **2014**, *3*, e10. [[CrossRef](#)] [[PubMed](#)]
8. Hardy, G.A.; Sieg, S.; Rodriguez, B.; Anthony, D.; Asaad, R.; Jiang, W.; Mudd, J.; Schacker, T.; Funderburg, N.T.; Pilch-Cooper, H.A.; et al. Interferon- $\alpha$  is the primary plasma type-I IFN in HIV-1 infection and correlates with immune activation and disease markers. *PLoS ONE* **2013**, *8*, e56527. [[CrossRef](#)] [[PubMed](#)]
9. Said, E.A.; Dupuy, F.P.; Trautmann, L.; Zhang, Y.; Shi, Y.; El-Far, M.; Hill, B.J.; Noto, A.; Ancuta, P.; Peretz, Y.; et al. Programmed death-1-induced interleukin-10 production by monocytes impairs CD4+ T cell activation during HIV infection. *Nat. Med.* **2010**, *16*, 452–459. [[CrossRef](#)] [[PubMed](#)]
10. Trautmann, L.; Janbazian, L.; Chomont, N.; Said, E.A.; Gimmig, S.; Bessette, B.; Boulassel, M.R.; Delwart, E.; Sepulveda, H.; Balderas, R.S.; et al. Up regulation of PD-1 expression on HIV-specific CD8+ T cells leads to reversible immune dysfunction. *Nat. Med.* **2006**, *12*, 1198–1202. [[CrossRef](#)] [[PubMed](#)]
11. Trautmann, L.; Said, E.A.; Halwani, R.; Janbazian, L.; Chomont, N.; El-Far, M.; Breton, G.; Haddad, E.K.; Sekaly, R.P. Programmed death 1: A critical regulator of T-cell function and a strong target for immunotherapies for chronic viral infections. *Curr. Opin. HIV AIDS* **2007**, *2*, 219–227. [[CrossRef](#)] [[PubMed](#)]
12. Van Grevenynghe, J.; Cubas, R.A.; DaFonseca, S.; Metcalf, T.; Tremblay, C.L.; Trautmann, L.; Sekaly, R.P.; Schatzle, J.; Haddad, E.K. Foxo3a: An integrator of immune dysfunction during HIV infection. *Cytokine Growth Factor Rev.* **2012**, *23*, 215–221. [[CrossRef](#)] [[PubMed](#)]
13. Van Grevenynghe, J.; Cubas, R.A.; Noto, A.; DaFonseca, S.; He, Z.; Peretz, Y.; Filali-Mouhim, A.; Dupuy, F.P.; Procopio, F.A.; Chomont, N.; et al. Loss of memory B cells during chronic HIV infection is driven by Foxo3a and TRAIL-mediated apoptosis. *J. Clin. Investig.* **2011**, *121*, 3877–3888. [[CrossRef](#)] [[PubMed](#)]
14. Van Grevenynghe, J.; Procopio, F.A.; He, Z.; Chomont, N.; Riou, C.; Zhang, Y.; Gimmig, S.; Boucher, G.; Wilkinson, P.; Shi, Y.; et al. Transcription factor Foxo3a controls the persistence of memory CD4(+) T cells during hiv infection. *Nat. Med.* **2008**, *14*, 266–274. [[CrossRef](#)] [[PubMed](#)]
15. Beltra, J.C.; Decaluwe, H. Cytokines and persistent viral infections. *Cytokine* **2016**, *82*, 4–15. [[CrossRef](#)] [[PubMed](#)]
16. Bolen, C.R.; Robek, M.D.; Brodsky, L.; Schulz, V.; Lim, J.K.; Taylor, M.W.; Kleinstein, S.H. The blood transcriptional signature of chronic hepatitis C virus is consistent with an ongoing interferon-mediated antiviral response. *J. Interferon Cytokine Res.* **2013**, *33*, 15–23. [[CrossRef](#)] [[PubMed](#)]
17. Bosinger, S.E.; Utay, N.S. Type I interferon: Understanding its role in HIV pathogenesis and therapy. *Curr. HIV/AIDS Rep.* **2015**, *12*, 41–53. [[CrossRef](#)] [[PubMed](#)]
18. Cheng, L.; Ma, J.; Li, J.; Li, D.; Li, G.; Li, F.; Zhang, Q.; Yu, H.; Yasui, F.; Ye, C.; et al. Blocking type I interferon signaling enhances T cell recovery and reduces HIV-1 reservoirs. *J. Clin. Investig.* **2017**, *127*, 269–279. [[CrossRef](#)] [[PubMed](#)]
19. Cheng, L.; Yu, H.; Li, G.; Li, F.; Ma, J.; Li, J.; Chi, L.; Zhang, L.; Su, L. Type I interferons suppress viral replication but contribute to T cell depletion and dysfunction during chronic HIV-1 infection. *JCI Insight* **2017**, *2*, e94366. [[CrossRef](#)] [[PubMed](#)]
20. Fernandez, S.; Tanaskovic, S.; Helbig, K.; Rajasuriar, R.; Kramski, M.; Murray, J.M.; Beard, M.; Purcell, D.; Lewin, S.R.; Price, P.; et al. CD4+ T-cell deficiency in HIV patients responding to antiretroviral therapy is associated with increased expression of interferon-stimulated genes in CD4+ T cells. *J. Infect. Dis.* **2011**, *204*, 1927–1935. [[CrossRef](#)] [[PubMed](#)]
21. Guidotti, L.G.; Chisari, F.V. Immunobiology and pathogenesis of viral hepatitis. *Annu. Rev. Pathol.* **2006**, *1*, 23–61. [[CrossRef](#)] [[PubMed](#)]
22. Hardy, G.A.; Sieg, S.F.; Rodriguez, B.; Jiang, W.; Asaad, R.; Lederman, M.M.; Harding, C.V. Desensitization to type I interferon in HIV-1 infection correlates with markers of immune activation and disease progression. *Blood* **2009**, *113*, 5497–5505. [[CrossRef](#)] [[PubMed](#)]
23. Honke, N.; Shaabani, N.; Merches, K.; Gassa, A.; Kraft, A.; Ehrhardt, K.; Haussinger, D.; Lohning, M.; Dittmer, U.; Hengel, H.; et al. Immunoactivation induced by chronic viral infection inhibits viral replication and drives immunosuppression through sustained IFN-I responses. *Eur. J. Immunol.* **2016**, *46*, 372–380. [[CrossRef](#)] [[PubMed](#)]



24. Marsili, G.; Remoli, A.L.; Sgarbanti, M.; Perrotti, E.; Fragale, A.; Battistini, A. HIV-1, interferon and the interferon regulatory factor system: An interplay between induction, antiviral responses and viral evasion. *Cytokine Growth Factor Rev.* **2012**, *23*, 255–270. [[CrossRef](#)] [[PubMed](#)]
25. Su, A.I.; Pezacki, J.P.; Wodicka, L.; Brideau, A.D.; Supekova, L.; Thimme, R.; Wieland, S.; Bukh, J.; Purcell, R.H.; Schultz, P.G.; et al. Genomic analysis of the host response to hepatitis C virus infection. *Proc. Natl. Acad. Sci. USA* **2002**, *99*, 15669–15674. [[CrossRef](#)] [[PubMed](#)]
26. Teijaro, J.R.; Ng, C.; Lee, A.M.; Sullivan, B.M.; Sheehan, K.C.; Welch, M.; Schreiber, R.D.; de la Torre, J.C.; Oldstone, M.B. Persistent LCMV infection is controlled by blockade of type I interferon signaling. *Science* **2013**, *340*, 207–211. [[CrossRef](#)] [[PubMed](#)]
27. Wang, B.; Kang, W.; Zuo, J.; Kang, W.; Sun, Y. The significance of type-I interferons in the pathogenesis and therapy of human immunodeficiency virus 1 infection. *Front. Immunol.* **2017**, *8*, 1431. [[CrossRef](#)] [[PubMed](#)]
28. Wilson, E.B.; Brooks, D.G. Decoding the complexity of type I interferon to treat persistent viral infections. *Trends Microbiol.* **2013**, *21*, 634–640. [[CrossRef](#)] [[PubMed](#)]
29. Wilson, E.B.; Yamada, D.H.; Elsaesser, H.; Herskovitz, J.; Deng, J.; Cheng, G.; Aronow, B.J.; Karp, C.L.; Brooks, D.G. Blockade of chronic type I interferon signaling to control persistent LCMV infection. *Science* **2013**, *340*, 202–207. [[CrossRef](#)] [[PubMed](#)]
30. Harris, L.D.; Tabb, B.; Sodora, D.L.; Paiardini, M.; Klatt, N.R.; Douek, D.C.; Silvestri, G.; Muller-Trutwin, M.; Vasile-Pandrea, I.; Apetrei, C.; et al. Down regulation of robust acute type I interferon responses distinguishes nonpathogenic simian immunodeficiency virus (SIV) infection of natural hosts from pathogenic SIV infection of rhesus macaques. *J. Virol.* **2010**, *84*, 7886–7891. [[CrossRef](#)] [[PubMed](#)]
31. Jacquelin, B.; Mayau, V.; Targat, B.; Liovat, A.S.; Kunkel, D.; Petitjean, G.; Dillies, M.A.; Roques, P.; Butor, C.; Silvestri, G.; et al. Nonpathogenic SIV infection of african green monkeys induces a strong but rapidly controlled type I IFN response. *J. Clin. Investig.* **2009**, *119*, 3544–3555. [[CrossRef](#)] [[PubMed](#)]
32. Mandl, J.N.; Barry, A.P.; Vanderford, T.H.; Kozyr, N.; Chavan, R.; Klucking, S.; Barrat, F.J.; Coffman, R.L.; Staprans, S.I.; Feinberg, M.B. Divergent TLR7 and TLR9 signaling and type I interferon production distinguish pathogenic and nonpathogenic AIDS virus infections. *Nat. Med.* **2008**, *14*, 1077–1087. [[CrossRef](#)] [[PubMed](#)]
33. Rotger, M.; Dalmau, J.; Rauch, A.; McLaren, P.; Bosinger, S.E.; Martinez, R.; Sandler, N.G.; Roque, A.; Liebner, J.; Battegay, M.; et al. Comparative transcriptomics of extreme phenotypes of human HIV-1 infection and SIV infection in sooty mangabey and rhesus macaque. *J. Clin. Investig.* **2011**, *121*, 2391–2400. [[CrossRef](#)] [[PubMed](#)]
34. Boasso, A.; Shearer, G.M. Chronic innate immune activation as a cause of HIV-1 immunopathogenesis. *Clin. Immunol.* **2008**, *126*, 235–242. [[CrossRef](#)] [[PubMed](#)]
35. Sedaghat, A.R.; German, J.; Teslovich, T.M.; Cofrancesco, J., Jr.; Jie, C.C.; Talbot, C.C., Jr.; Siliciano, R.F. Chronic CD4+ T-cell activation and depletion in human immunodeficiency virus type 1 infection: Type I interferon-mediated disruption of T-cell dynamics. *J. Virol.* **2008**, *82*, 1870–1883. [[CrossRef](#)] [[PubMed](#)]
36. Stylianou, E.; Aukrust, P.; Bendtzen, K.; Muller, F.; Froland, S.S. Interferons and interferon (IFN)-inducible protein 10 during highly active anti-retroviral therapy (HAART)-possible immunosuppressive role of IFN-alpha in HIV infection. *Clin. Exp. Immunol.* **2000**, *119*, 479–485. [[CrossRef](#)] [[PubMed](#)]
37. Van Grevenynghe, J.; Halwani, R.; Chomont, N.; Ancuta, P.; Peretz, Y.; Tanel, A.; Procopio, F.A.; Shi, Y.; Said, E.A.; Haddad, E.K.; et al. Lymph node architecture collapse and consequent modulation of FOXO3a pathway on memory T- and B-cells during HIV infection. *Semin. Immunol.* **2008**, *20*, 196–203. [[CrossRef](#)] [[PubMed](#)]
38. Zhen, A.; Rezek, V.; Youn, C.; Lam, B.; Chang, N.; Rick, J.; Carrillo, M.; Martin, H.; Kasparian, S.; Syed, P.; et al. Targeting type I interferon-mediated activation restores immune function in chronic HIV infection. *J. Clin. Investig.* **2017**, *127*, 260–268. [[CrossRef](#)] [[PubMed](#)]
39. McBride, J.M.; Jiang, J.; Abbas, A.R.; Morimoto, A.; Li, J.; Maciuga, R.; Townsend, M.; Wallace, D.J.; Kennedy, W.P.; Drappa, J. Safety and pharmacodynamics of rontalizumab in patients with systemic lupus erythematosus: Results of a phase I, placebo-controlled, double-blind, dose-escalation study. *Arthritis Rheum.* **2012**, *64*, 3666–3676. [[CrossRef](#)] [[PubMed](#)]
40. Wang, B.; Higgs, B.W.; Chang, L.; Vainshtein, I.; Liu, Z.; Streicher, K.; Liang, M.; White, W.I.; Yoo, S.; Richman, L.; et al. Pharmacogenomics and translational simulations to bridge indications for an anti-interferon- $\alpha$  receptor antibody. *Clin. Pharmacol. Ther.* **2013**, *93*, 483–492. [[CrossRef](#)] [[PubMed](#)]
41. Wilson, E.B.; Brooks, D.G. Interfering with type I interferon: A novel approach to purge persistent viral infection. *Cell Cycle* **2013**, *12*, 2919–2920. [[CrossRef](#)] [[PubMed](#)]

42. Herbeuval, J.P.; Nilsson, J.; Boasso, A.; Hardy, A.W.; Kruhlak, M.J.; Anderson, S.A.; Dolan, M.J.; Dy, M.; Andersson, J.; Shearer, G.M. Differential expression of IFN- $\alpha$  and TRAIL/DR5 in lymphoid tissue of progressor versus nonprogressor HIV-1-infected patients. *Proc. Natl. Acad. Sci. USA* **2006**, *103*, 7000–7005. [[CrossRef](#)] [[PubMed](#)]
43. Lehmann, C.; Harper, J.M.; Taubert, D.; Hartmann, P.; Fatkenheuer, G.; Jung, N.; van Lunzen, J.; Stellbrink, H.J.; Gallo, R.C.; Romerio, F. Increased interferon  $\alpha$  expression in circulating plasmacytoid dendritic cells of HIV-1-infected patients. *J. Acquir. Immune Defic. Syndr.* **2008**, *48*, 522–530. [[CrossRef](#)] [[PubMed](#)]
44. Veenhuis, R.T.; Freeman, Z.T.; Korleski, J.; Cohen, L.K.; Massaccesi, G.; Tomasi, A.; Boesch, A.W.; Ackerman, M.E.; Margolick, J.B.; Blankson, J.N.; et al. HIV-antibody complexes enhance production of type I interferon by plasmacytoid dendritic cells. *J. Clin. Investig.* **2017**, *127*, 4352–4364. [[CrossRef](#)] [[PubMed](#)]
45. Swiecki, M.; Wang, Y.; Vermi, W.; Gilfillan, S.; Schreiber, R.D.; Colonna, M. Type I interferon negatively controls plasmacytoid dendritic cell numbers in vivo. *J. Exp. Med.* **2011**, *208*, 2367–2374. [[CrossRef](#)] [[PubMed](#)]
46. Boasso, A.; Hardy, A.W.; Landay, A.L.; Martinson, J.L.; Anderson, S.A.; Dolan, M.J.; Clerici, M.; Shearer, G.M. PDL-1 upregulation on monocytes and T cells by HIV via type I interferon: Restricted expression of type I interferon receptor by CCR5-expressing leukocytes. *Clin. Immunol.* **2008**, *129*, 132–144. [[CrossRef](#)] [[PubMed](#)]
47. Sehgal, M.; Zeremski, M.; Talal, A.H.; Ginwala, R.; Elrod, E.; Grakoui, A.; Li, Q.G.; Philip, R.; Khan, Z.K.; Jain, P. IFN- $\alpha$ -induced downregulation of miR-221 in dendritic cells: Implications for HCV pathogenesis and treatment. *J. Interferon Cytokine Res.* **2015**, *35*, 698–709. [[CrossRef](#)] [[PubMed](#)]
48. Cunningham, C.R.; Champhekar, A.; Tullius, M.V.; Dillon, B.J.; Zhen, A.; de la Fuente, J.R.; Herskovitz, J.; Elsaesser, H.; Snell, L.M.; Wilson, E.B.; et al. Type I and type II interferon coordinately regulate suppressive dendritic cell fate and function during viral persistence. *PLoS Pathog.* **2016**, *12*, e1005356. [[CrossRef](#)] [[PubMed](#)]
49. Honke, N.; Shaabani, N.; Cadeddu, G.; Sorg, U.R.; Zhang, D.E.; Trilling, M.; Klingel, K.; Sauter, M.; Kandolf, R.; Gailus, N.; et al. Enforced viral replication activates adaptive immunity and is essential for the control of a cytopathic virus. *Nat. Immunol.* **2011**, *13*, 51–57. [[CrossRef](#)] [[PubMed](#)]
50. Norris, B.A.; Uebelhoefer, L.S.; Nakaya, H.I.; Price, A.A.; Grakoui, A.; Pulendran, B. Chronic but not acute virus infection induces sustained expansion of myeloid suppressor cell numbers that inhibit viral-specific T cell immunity. *Immunity* **2013**, *38*, 309–321. [[CrossRef](#)] [[PubMed](#)]
51. Taleb, K.; Auffray, C.; Villefroy, P.; Pereira, A.; Hosmalin, A.; Gaudry, M.; Le Bon, A. Chronic type I IFN is sufficient to promote immunosuppression through accumulation of myeloid-derived suppressor cells. *J. Immunol.* **2017**, *198*, 1156–1163. [[CrossRef](#)] [[PubMed](#)]
52. Rempel, H.; Sun, B.; Calosing, C.; Pillai, S.K.; Pulliam, L. Interferon- $\alpha$  drives monocyte gene expression in chronic unsuppressed HIV-1 infection. *AIDS* **2010**, *24*, 1415–1423. [[CrossRef](#)] [[PubMed](#)]
53. Herbeuval, J.P.; Grivel, J.C.; Boasso, A.; Hardy, A.W.; Chougnet, C.; Dolan, M.J.; Yagita, H.; Lifson, J.D.; Shearer, G.M. CD4<sup>+</sup> T-cell death induced by infectious and noninfectious HIV-1: Role of type 1 interferon-dependent, TRAIL/DR5-mediated apoptosis. *Blood* **2005**, *106*, 3524–3531. [[CrossRef](#)] [[PubMed](#)]
54. Kardava, L.; Moir, S.; Shah, N.; Wang, W.; Wilson, R.; Buckner, C.M.; Santich, B.H.; Kim, L.J.; Spurlin, E.E.; Nelson, A.K.; et al. Abnormal B cell memory subsets dominate HIV-specific responses in infected individuals. *J. Clin. Investig.* **2014**, *124*, 3252–3262. [[CrossRef](#)] [[PubMed](#)]
55. Fallet, B.; Narr, K.; Ertuna, Y.I.; Remy, M.; Sommerstein, R.; Cornille, K.; Kreutzfeldt, M.; Page, N.; Zimmer, G.; Geier, F.; et al. Interferon-driven deletion of antiviral B cells at the onset of chronic infection. *Sci. Immunol.* **2016**, *1*. [[CrossRef](#)]
56. Moir, S.; Fauci, A.S. Insights into B cells and HIV-specific B-cell responses in HIV-infected individuals. *Immunol. Rev.* **2013**, *254*, 207–224. [[CrossRef](#)] [[PubMed](#)]
57. Moseman, E.A.; Wu, T.; de la Torre, J.C.; Schwartzberg, P.L.; McGavern, D.B. Type I interferon suppresses virus-specific B cell responses by modulating CD8<sup>+</sup> T cell differentiation. *Sci. Immunol.* **2016**, *1*. [[CrossRef](#)]
58. Sammicheli, S.; Kuka, M.; Di Lucia, P.; de Oya, N.J.; De Giovanni, M.; Fioravanti, J.; Cristofani, C.; Maganuco, C.G.; Fallet, B.; Ganzer, L.; et al. Inflammatory monocytes hinder antiviral B cell responses. *Sci. Immunol.* **2016**, *1*. [[CrossRef](#)]
59. Herbeuval, J.P.; Hardy, A.W.; Boasso, A.; Anderson, S.A.; Dolan, M.J.; Dy, M.; Shearer, G.M. Regulation of tnf-related apoptosis-inducing ligand on primary CD4<sup>+</sup> T cells by HIV-1: Role of type I IFN-producing plasmacytoid dendritic cells. *Proc. Natl. Acad. Sci. USA* **2005**, *102*, 13974–13979. [[CrossRef](#)] [[PubMed](#)]

60. Cha, L.; de Jong, E.; French, M.A.; Fernandez, S. IFN- $\alpha$  exerts opposing effects on activation-induced and IL-7-induced proliferation of T cells that may impair homeostatic maintenance of CD4<sup>+</sup> T cell numbers in treated HIV infection. *J. Immunol.* **2014**, *193*, 2178–2186. [[CrossRef](#)] [[PubMed](#)]
61. Moir, S.; Fauci, A.S. B-cell responses to HIV infection. *Immunol. Rev.* **2017**, *275*, 33–48. [[CrossRef](#)] [[PubMed](#)]
62. Noto, A.; Pantaleo, G. B-cell abnormalities and impact on antibody response in HIV infection. *Curr. Opin. HIV AIDS* **2017**, *12*, 203–208. [[CrossRef](#)] [[PubMed](#)]
63. Daugan, M.; Murira, A.; Mindt, B.C.; Germain, A.; Tarrab, E.; Lapierre, P.; Fritz, J.H.; Lamarre, A. Type I interferon impairs specific antibody responses early during establishment of LCMV infection. *Front. Immunol.* **2016**, *7*, 564. [[CrossRef](#)] [[PubMed](#)]
64. Aounallah, M.; Dagenais-Lussier, X.; El-Far, M.; Mehraj, V.; Jenabian, M.A.; Routy, J.P.; van Grevenynghe, J. Current topics in HIV pathogenesis, part 2: Inflammation drives a warburg-like effect on the metabolism of HIV-infected subjects. *Cytokine Growth Factor Rev.* **2016**, *28*, 1–10. [[CrossRef](#)] [[PubMed](#)]
65. El-Far, M.; Halwani, R.; Said, E.; Trautmann, L.; Doroudchi, M.; Janbazian, L.; Fonseca, S.; van Grevenynghe, J.; Yassine-Diab, B.; Sekaly, R.P.; et al. T-cell exhaustion in HIV infection. *Curr. HIV/AIDS Rep.* **2008**, *5*, 13–19. [[CrossRef](#)] [[PubMed](#)]
66. Fraietta, J.A.; Mueller, Y.M.; Yang, G.; Boesteanu, A.C.; Gracias, D.T.; Do, D.H.; Hope, J.L.; Kathuria, N.; McGettigan, S.E.; Lewis, M.G.; et al. Type I interferon upregulates bak and contributes to T cell loss during human immunodeficiency virus (HIV) infection. *PLoS Pathog.* **2013**, *9*, e1003658. [[CrossRef](#)] [[PubMed](#)]
67. Le Saout, C.; Hasley, R.B.; Imamichi, H.; Tcheung, L.; Hu, Z.; Luckey, M.A.; Park, J.H.; Durum, S.K.; Smith, M.; Rupert, A.W.; et al. Chronic exposure to type-I IFN under lymphopenic conditions alters CD4 T cell homeostasis. *PLoS Pathog.* **2014**, *10*, e1003976. [[CrossRef](#)] [[PubMed](#)]
68. Boasso, A.; Hardy, A.W.; Anderson, S.A.; Dolan, M.J.; Shearer, G.M. HIV-induced type I interferon and tryptophan catabolism drive T cell dysfunction despite phenotypic activation. *PLoS ONE* **2008**, *3*, e2961. [[CrossRef](#)] [[PubMed](#)]
69. Zhang, Z.; Xu, X.; Lu, J.; Zhang, S.; Gu, L.; Fu, J.; Jin, L.; Li, H.; Zhao, M.; Zhang, J.; et al. B and T lymphocyte attenuator down-regulation by HIV-1 depends on type I interferon and contributes to T-cell hyperactivation. *J. Infect. Dis.* **2011**, *203*, 1668–1678. [[CrossRef](#)] [[PubMed](#)]
70. Crawford, A.; Angelosanto, J.M.; Kao, C.; Doering, T.A.; Odorizzi, P.M.; Barnett, B.E.; Wherry, E.J. Molecular and transcriptional basis of CD4(+) T cell dysfunction during chronic infection. *Immunity* **2014**, *40*, 289–302. [[CrossRef](#)] [[PubMed](#)]
71. Osokine, I.; Snell, L.M.; Cunningham, C.R.; Yamada, D.H.; Wilson, E.B.; Elsaesser, H.J.; de la Torre, J.C.; Brooks, D. Type I interferon suppresses de novo virus-specific CD4 Th1 immunity during an established persistent viral infection. *Proc. Natl. Acad. Sci. USA* **2014**, *111*, 7409–7414. [[CrossRef](#)] [[PubMed](#)]
72. Che, J.W.; Kraft, A.R.; Selin, L.K.; Welsh, R.M. Regulatory T cells resist virus infection-induced apoptosis. *J. Virol.* **2015**, *89*, 2112–2120. [[CrossRef](#)] [[PubMed](#)]
73. Srivastava, S.; Koch, M.A.; Pepper, M.; Campbell, D.J. Type I interferons directly inhibit regulatory T cells to allow optimal antiviral T cell responses during acute LCMV infection. *J. Exp. Med.* **2014**, *211*, 961–974. [[CrossRef](#)] [[PubMed](#)]
74. Penaloza-MacMaster, P.; Kamphorst, A.O.; Wieland, A.; Araki, K.; Iyer, S.S.; West, E.E.; O'Mara, L.; Yang, S.; Konieczny, B.T.; Sharpe, A.H.; et al. Interplay between regulatory T cells and PD-1 in modulating T cell exhaustion and viral control during chronic LCMV infection. *J. Exp. Med.* **2014**, *211*, 1905–1918. [[CrossRef](#)] [[PubMed](#)]
75. Wang, Y.; Swiecki, M.; Cella, M.; Alber, G.; Schreiber, R.D.; Gilfillan, S.; Colonna, M. Timing and magnitude of type I interferon responses by distinct sensors impact CD8 T cell exhaustion and chronic viral infection. *Cell Host Microbe* **2012**, *11*, 631–642. [[CrossRef](#)] [[PubMed](#)]

